

Exploration of Toll-like Receptor 7 and 8 Agonists as Potential Vaccine Adjuvants

By

Euna Yoo

Submitted to the Graduate Degree program in Medicinal Chemistry

and the Graduate Faculty of the University of Kansas

in partial fulfillment of the requirements for the degree of

Doctor of Philosophy

Dissertation Committee:

Chairperson (Sunil A. David)

Michael F. Rafferty

Mario Rivera

Blake R. Peterson

Jennifer S. Laurence

Date defended: _____

The Thesis Committee for Euna Yoo certifies

that this is the approved version of the following thesis:

Exploration of Toll-like Receptor 7 and 8 Agonists as Potential Vaccine Adjuvants

Dissertation Committee:

Chairperson (Sunil A. David)

Blake R. Peterson

Michael F. Rafferty

Jennifer S. Laurence

Mario Rivera

Date approved: _____

Abstract

Toll-like receptors (TLRs)-7/8 are among pathogen recognition receptors (PRRs) present in the endosomal compartment that are activated by viral single-stranded RNA (ssRNA) as well as synthetic small molecules. TLR7/8 agonists hold promise as potential vaccine adjuvants, since they directly activate antigen-presenting cells and enhance T helper 1-driven immune responses.

A general introduction to TLRs, with an emphasis on the role of TLR7/8 activation in innate and adaptive immune responses is presented in Chapter 1.

Structure-activity relationship (SAR) studies in small molecule TLR8/7-agonistic ligands showed that thiazolo[4,5-c]quinolines display mixed TLR8/7 agonistic activities with the optimal C2-alkyl chain length being butyl (Chapter 2).

In an ongoing search toward exploring alternative chemotypes, furo[2,3-c]pyridines with pyridoxal as the aldehyde component in a one-pot multicomponent Groebke–Blackburn–Bienaymé reaction were obtained and found to exhibit TLR8-dependent NF- κ B activation and strong adjuvanticity without proinflammatory cytokine induction (Chapter 3).

Combinatorial libraries using the Groebke–Blackburn–Bienaymé reaction have also yielded TLR7/8-inactive, but antibacterial imidazo[1,2-a]pyridines (Chapter 4).

Based on the previously reported SARs on imidazoquinolines, the syntheses and biological evaluation of novel imidazo[4,5-c]pyridine analogues were undertaken, with modifications at the N4- and C6 positions, which afforded strong Type I IFN inducers in conjunction with attenuated proinflammatory profiles (Chapter 5).

With the goal of defining structural requisites governing activity and selectivity at TLR7 and/or TLR8, we undertook scaffold-hopping approach, quantum chemical calculations followed by linear discriminant analyses that permitted the classification of inactive, TLR8-active, and TLR7/8 dual-active compounds, confirming the critical role of partial charges in determining biological activity (Chapter 6).

Molecular conjugation of TLR7/8 agonists to hyaluronic acid (HA) was evaluated to enhance selective and targeted delivery of vaccine construct to draining lymph nodes while limiting systemic exposure. The superior adjuvanticity evoking affinity-matured high-avidity immunoglobulins after a single boost was observed with HA conjugate bearing dual TLR7/8 agonist (Chapter 7).

Extensive SAR investigations in several TLR7/8 agonistic scaffolds and exploration as vaccine adjuvant candidates have incrementally improved our understanding of how these molecules activate innate and adaptive immune responses and also catalyzed novel approaches to vaccine design and development.

Acknowledgements

There are a lot of people without whose help this thesis would not have been possible.

First, I would like to acknowledge and thank my advisor, Professor Sunil David, for his guidance and support during my graduate studies. He has taught me and inspired me in so many ways. His enthusiasm, encouragement, and faith in me have been extremely helpful. I owe him a debt of gratitude. I would also like to thank past and current members of the David research group, for their help and assistance. I could never have reached the heights or explored the depths without their efforts and contribution. I am particularly thankful to Dr. Diptesh Sil, Dr. Nikunj Shukla, and Dr. Deepak Salunke for their friendship and advice throughout my graduate studies.

I would like to thank my committee members – Dr. Michael Rafferty, Dr. Blake Peterson, Dr. Jennifer Laurence, and Dr. Mario Rivera for their time and effort in serving on my committee. They have been very kind to me giving valuable advice and suggestions. I am also thankful to my teachers Dr. Hea-Young Park Choo and Dr. Jae Wook Yang and the faculty members of the Department of Medicinal Chemistry and their guidance and support.

Very special thanks to my friends Gail and Philip Padden for their friendship. They and their family have shown me the hospitality, kindness and respect. I am so grateful to have them in my life.

Finally, I would like to take this opportunity to thank my parents, my two sisters Eunmi and Eunji, and my brother-in-law Jaewoo for their unconditional love, encouragement, and continuous support and prayer.

Euna Yoo

April, 16, 2015

TABLE OF CONTENTS

ACKNOWLEDGEMENTS	5
TABLE OF CONTENTS	6
ABBREVIATIONS	7
CHAPTER 1. INTRODUCTION	9
1.1. VACCINE ADJUVANTS	10
1.2. INNATE IMMUNITY AND TOLL-LIKE RECEPTORS (TLRs)	12
1.3. INTRACELLULAR TLR ACTIVATION – TLR7/8.....	15
CHAPTER 2. TLR8/7-AGONISTIC 2-ALKYLTHIAZOLO[4,5-<i>c</i>]QUINOLINES	22
2.1. INTRODUCTION.....	23
2.2. RESULTS AND DISCUSSION	24
2.3. CONCLUSION.....	36
2.4. EXPERIMENTAL	36
CHAPTER 3. TLR8-AGONISTIC 2,3-DIAMINO-FURO[2,3-<i>c</i>]PYRIDINES	74
3.1. INTRODUCTION.....	75
3.2. RESULTS AND DISCUSSION	76
3.3. CONCLUSION.....	91
3.4. EXPERIMENTAL	92
CHAPTER 4. ANTIBACTERIAL ACTIVITIES OF GROEBKE-BLACKBURN-BIENAYMÉ-DERIVED IMIDAZO[1,2-<i>a</i>]PYRIDIN-3-AMINES	112
4.1. INTRODUCTION.....	113
4.2. RESULTS AND DISCUSSION	114
4.3. CONCLUSIONS	126
4.4. EXPERIMENTAL	126
CHAPTER 5. TLR7-AGONISTIC IMIDAZO[4,5-<i>c</i>]PYRIDINES	147
5.1. INTRODUCTION.....	148
5.2. RESULTS AND DISCUSSION	151
5.3. CONCLUSIONS	162
5.4. EXPERIMENTAL	162
CHAPTER 6. DETERMINANTS OF ACTIVITY AT HUMAN TLR7 AND 8: QSAR OF DIVERSE HETEROCYCLIC SCAFFOLDS	197
6.1. INTRODUCTION.....	198
6.2. RESULTS AND DISCUSSION	200
6.3. CONCLUSION.....	215
6.4. EXPERIMENTAL	215
CHAPTER 7. HYALURONIC ACID CONJUGATION OF TLR7/8 AGONISTS FOR LYMPHOID TISSUE DELIVERY	239
7.1. INTRODUCTION.....	240
7.2. RESULTS AND DISCUSSION	243
7.3. CONCLUSION.....	257
7.4. EXPERIMENTAL	260
REFERENCES	264

Abbreviations

AIBN	azobisisobutyronitrile
APC	antigen-presenting cell
Be-1	B-effector-1-cells
CCR	chemokine receptor
cDC	conventional dendritic cell
CDMT	2-chloro-4,6-dimethoxy-1,3,5-triazine
CIK	cytokine-induced killer
CLR	C-type lectin receptor
CRP	C-reactive protein
CXCL	chemokine ligand
DC	dendritic cell
DFT	density functional theory
DIPEA	diisopropylethylamine
DMF	dimethylformamide
DMSO	dimethylsulfoxide
DS	degree of substitution
dsRNA	double stranded RNA
EC ₅₀	half maximal effective concentration
ECM	extracellular matrix
EDC	<i>N</i> -(3-dimethylaminopropyl)- <i>N'</i> -ethylcarbodiimide
ELISA	enzyme-linked immunosorbent assay
ESI	electrospray ionization
GlcNAc	<i>N</i> -acetyl glucosamine
GlcUA	glucuronic acid
HA	hyaluronic acid
HAase	hyaluronidase
HBTU	<i>N,N,N',N'</i> -Tetramethyl- <i>O</i> -(1 <i>H</i> -benzotriazol-1-yl)uronium hexafluorophosphate
HCV	hepatitis C virus
HEK	human embryonic kidney
HIV	human immunodeficiency virus
hPBMC	human peripheral blood mononuclear cell
HPV	human papilloma virus
IFN	interferon
Ig	immunoglobulin
IL	interleukin
IP	interferon gamma-induced protein
IRF	IFN regulatory factor
ITAM	immunoreceptor tyrosine-based activation motif
LC	liquid chromatography
LDH	lactate dehydrogenase
LPS	lipopolysaccharides
LRR	leucine-rich repeats

LYVE-1	lymphatic vessel endothelial hyaluronan receptor-1
MBC	minimum bactericidal concentration
MCP	monocyte chemoattractant protein
mCPBA	<i>m</i> -chloroperoxybenzoic acid
MDA	melanoma differentiation-associated protein
MES	2-(<i>N</i> -morpholino)ethanesulfonic acid
MESP	molecular electrostatic potential
MHC	major histocompatibility complex
MIC	minimum inhibitory concentration
MIP	macrophage inflammatory protein
MPL	monophosphoryl lipid A
MRSA	methicillin-resistant <i>Staphylococcus aureus</i>
MS	mass spectroscopy
MyD88	myeloid differentiation primary response gene 88
NALP	NACHT, LRR and PYD domains-containing protein
NBS	<i>N</i> -bromosuccinimide
NF- κ B	nuclear factor κ B
NK	natural killer
NLR	NOD-like receptor
NMM	<i>N</i> -methylnmorpholine
NMP	<i>N</i> -methyl-2-pyrrolidone
NMR	nuclear magnetic resonance
NOD	nucleotide oligomerization domain
ORTEP	oak ridge thermal ellipsoid plot
PAMP	pathogen-associated molecular pattern
PBS	phosphate buffer saline
pDC	plasmacytoid dendritic cell
PLVAP	plasmalemma vesicle-associated protein
PRR	pattern recognition receptor
QSAR	quantitative structure-activity relationship
RIG	retinoic acid inducible gene
RLR	RIG-I-like receptor
sAP	secreted alkaline phosphatase
SAR	structure-activity relationship
SEC	size exclusion chromatography
ssRNA	single stranded RNA
TB	tuberculosis
TBAF	tetra- <i>n</i> -butylammonium fluoride
TFA	trifluoroacetic acid
Th1	T helper 1
Th2	T helper 2
THF	tetrahydrofuran
TIR	toll/IL-1 receptor
TLR	toll-like receptor
TNF	tumor necrosis factor

Chapter 1.

Introduction



1.1. Vaccine Adjuvants

There can be no greater substantiation of Benjamin Franklin's adage, 'An ounce of prevention is worth a pound of cure' than the resounding impact that vaccines have had in preventing morbidity and mortality due to infectious diseases.¹ Vaccines have resulted in the eradication or dramatic reduction in number of cases such as smallpox, polio, and tetanus. Nevertheless, there is still a pressing need for new vaccines for diseases for which sufficiently effective vaccines do not exist, but also to replace reactogenic vaccines with safer alternatives.²

In order to achieve a high level of efficacy and safety, many newer vaccines with more defined composition that is often linked to lower immunogenicity rely on potent immunostimulants (vaccine adjuvants).³ The Food and Drug Administration (FDA) considers an adjuvant to a substance added to vaccines to enhance the immune response in vaccinated individuals. Adjuvants also serve to reduce the amount of antigen needed for the induction of a robust immune response ('dose-sparing effect') or the number of immunizations needed for protective immunity. The ability of adjuvants to broaden antibody responses could be crucial for the success of vaccines against many pathogens that display substantial antigenic drift and/or strain variations including influenza viruses, human immunodeficiency virus (HIV), human papilloma virus (HPV), and the malaria parasite.⁴ Adjuvants also help improve the efficacy of vaccines in newborns, the elderly or immunocompromised persons, or can be used as antigen delivery systems for the uptake of antigens.⁵

Several hundred natural and synthetic compounds have been identified to have adjuvantic activity (Table 1).⁵⁻⁶ Alum, principally aluminum phosphate or hydroxide, was originally identified in the 1920s and has been the most widely used human adjuvants.⁷ Studies have shown that alum enhances antigen uptake by dendritic cells (DCs), recruitment of immune-competent cells

to the injection site, and stimulation of immune cells via the inflammasome pathway,⁸ although further details and precise mechanisms need to be elucidated.⁹ A second adjuvant that could be considered a success is the MF59 squalene oil in water emulsion (O/W). MF59 is licensed in most of Europe for use with seasonal flu vaccines in the elderly. MF59 induces the recruitment of neutrophils and monocytes to the site of immunization and potentiates both cellular and humoral immune responses.¹⁰ Virosomes are liposomes that contain fusogenic viral proteins and have been licensed as a component of an influenza vaccine.¹¹ They can be classified more as delivery systems since their main function is to promote more effective delivery of vaccine antigens and immunostimulants. The most advanced of adjuvants, termed the AS series, are generally combinations of alum (or emulsions or liposomes) with immune potentiators.¹² The immune potentiator component(s) is added to increase antibody titers or to induce more potent and focused T cell responses. The more complex formulations, comprising of three or more adjuvant components, are particularly designed to induce more potent T helper 1 (Th1) cellular immune responses.¹³

Despite the impressive success of currently approved adjuvants for generating immunity to viral and bacterial infections, an understanding of the mechanism of action of vaccine adjuvants has remained rudimentary until recently, and there is a compelling need for the rational development of adjuvants that not only provide protective antibody responses, but also generate strong T cell immunity, especially in subunit vaccine constructs incorporating highly purified, recombinantly expressed proteins as immunogens.¹⁴ Adjuvants that stimulate cellular immunity (antigen-specific CD4 and CD8 responses) have been particularly important in protective immunity against intracellular pathogens, and it is worth noting that none of the currently approved adjuvants uniformly and/or sufficiently enhance cell-mediated immune responses. The availability of adjuvants with defined mechanisms of action would not only permit a greater insight into the interface between innate and adaptive immunity, but could perhaps also help

circumvent some of the potential deficiencies associated with current vaccines and catalyze the development of highly efficacious, yet safe vaccines for infectious diseases.

Table 1. Major adjuvant formulations tested in humans.

Name	Class	Receptors or Pathway	Indications
Licensed Adjuvants			
Alum	Mineral salt	NALP3, Ag delivery	Various
MF59	Oil/water emulsion	Immune cell recruitment, Ag uptake	Influenza (Fraud), Pandemic flu
Liposome	Lipid vesicle	Ag delivery	HAV, Flu
AS03	Oil/water emulsion + α -tocopherol		Pandemic flu (Pandemic)
AS04	Monophosphoryl Lipid A (MPL) + Alum	TLR4	HBV (Fendrix), HPV (Cevaxix)
Widespread Experimental Use or in Late Stage Clinical Development			
Montanide	Water/oil emulsion		Malaria, cancer
PLG	Polymeric microparticle		DNA vaccine (HIV)
Flagellin	Flagellin from <i>S. typhimurium</i>	TLR5	Flu
QS21	Saponin		Various
AS01	MPL + liposomes + QS21	TLR4	Malaria, TB
AS02	MPL + Oil/water emulsion + QS21	TLR4	Malaria
RC-529	Synthetic MPL + Alum	TLR4	HBV
ISCOMs	Saponins + cholesterol + phospholipids		Various
Poly(I:C)	Synthetic derivative of dsRNA	TLR3, MDA5	
IC31	Peptide + oligonucleotide	TLR9	TB
CpG 7909	Oligonucleotide + Alum or MF59	TLR9	HBV, malaria, HCV
ISS	Oligonucleotide Alum	TLR9	HBV
MF59 + MTP-PE	Lipidated MDP + Oil/water emulsion		HIV, Flu
Imiquimod	Imidazoquinoline derivatives	TLR7/8	
CAF01	Trehalose dimycolate	Mincle	

1.2. Innate Immunity and Toll-like Receptors (TLRs)

The human immune system can be conceived of as comprising of two mutually non-exclusive subsystems: the innate and the adaptive components; these two limbs work cooperatively to afford protection from numerous pathogenic microorganisms and toxins.¹⁵ Until recently, innate immunity was thought of as rather crude and unsophisticated first line of defense, providing non-

specific microbicidal activity and early inflammatory signals and merely allowing downstream adaptive immune responses more time to develop. However, it is now clear that the adaptive immune responses are largely predicated upon the level and specificity of the initial signals perceived by innate immune cells following infection and/or vaccination, determining whether or not specific and sustained response and protection will ensue.^{6b, 15a, 16}

Vaccine adjuvant research has expanded rapidly in the past decade and has directly benefited from our evolving understanding of immunology, beginning with the recognition of the cellular elements involved in innate immunity, and growing to encompass the elucidation of the mechanisms of recruitment of adaptive immune effector pathways. Knowledge of the molecular mechanism of innate immune activation has also afforded a large number of potential new targets for immune stimulators.¹⁷ Numerous receptors and signaling pathways in the innate immune system have been defined. Unlike adaptive immunity, the initial innate immune responses rely on a limited number of germline-encoded pattern recognition receptors (PRRs), which recognize specific molecular patterns present in molecules that are broadly shared by pathogens but are sufficiently different so as to be distinguishable from host molecules, and are collectively referred to as pathogen-associated molecular patterns (PAMPs).¹⁸ PRRs are classified according to their structural homology: Toll-like receptors (TLRs), RIG-I-like receptors (RLRs),¹⁹ NOD-like receptors (NLRs),²⁰ and C-type lectin receptors (CLRs).²¹

The TLR family is one of the well studied targets in terms of ligands, downstream signaling pathways, and functional relevance.²² There are 10 TLRs in the human genome; these are transmembrane proteins with an extracellular domain having leucine-rich repeats (LRR) and a cytosolic domain called the Toll/IL-1 receptor (TIR) domain.^{18b} The ligands for these receptors are highly conserved microbial molecules such as lipopolysaccharides (LPS) (recognized by TLR4), lipopeptides (TLR2 in combination with TLR1 or TLR6), flagellin (TLR5), single stranded

RNA (TLR7 and TLR8), double stranded RNA (TLR3), CpG motif-containing DNA (recognized by TLR9), and profilin present on uropathogenic bacteria (TLR11).²³ TLR1, -2, -4, -5, and -6 recognize extracellular stimuli, while TLR3, -7, -8 and -9 function within the endolysosomal compartment.^{18b} The activation of TLRs by their cognate ligands leads to production of inflammatory cytokines, and up-regulation of major histocompatibility complex (MHC) molecules and co-stimulatory signals in antigen-presenting cells as well as activating natural killer (NK) cells (innate immune response), in addition to priming and amplifying T-, and B-cell effector functions (adaptive immune responses).²⁴ TLR stimuli serve to link innate and adaptive immunity and therefore there is considerable interest in utilizing TLR agonists as vaccine adjuvants.²⁵

The discovery of TLRs and identification of natural TLR ligands have intensified the search for synthetic agonists that can target TLRs with greater specificity and selectivity than pathogen-derived ligands.^{24c, 26} Interestingly, many immunostimulants that had been identified previously were later found to be TLR agonists such as imidazoquinolines for TLR7/8 (*vide infra*).^{24c} Indeed, the only TLR agonist approved by the FDA as an adjuvant (3-O-desacyl-4'-monophosphoryl lipid A, derived from hydrolytic treatment of lipopolysaccharide isolated from *Salmonella Minnesota* Re595;²⁷ MPL) was indentified to be a TLR4 agonist²⁸ long after its adjuvantic properties had been established.²⁹

A detailed understanding of the structural and mechanistic bases of adjuvanticity and toxicity is pivotal in rationally developing novel adjuvants. In an effort to explore and develop strategies for the rapid and simultaneous evaluation of both adjuvantic potency and proinflammatory activities of relatively large focused libraries of compounds being generated by our group, we have examined representative members of virtually the entire compendium of known TLR agonists in a series of hierarchical assays. Of all the innate immune stimuli examined, we found that TLR2

(thioacylglycerol lipopeptide chemotype), TLR4 (LPS and MPL), TLR5 (flagellin), and TLR7 (imidazoquinoline chemotype) were immunostimulatory; the imidazoquinoline class of TLR7 agonists was found to be extraordinarily immunostimulatory, stimulating virtually all subsets of lymphocytes, and yet without inducing dominant proinflammatory cytokine responses.³⁰

1.3. Intracellular TLR Activation – TLR7/8

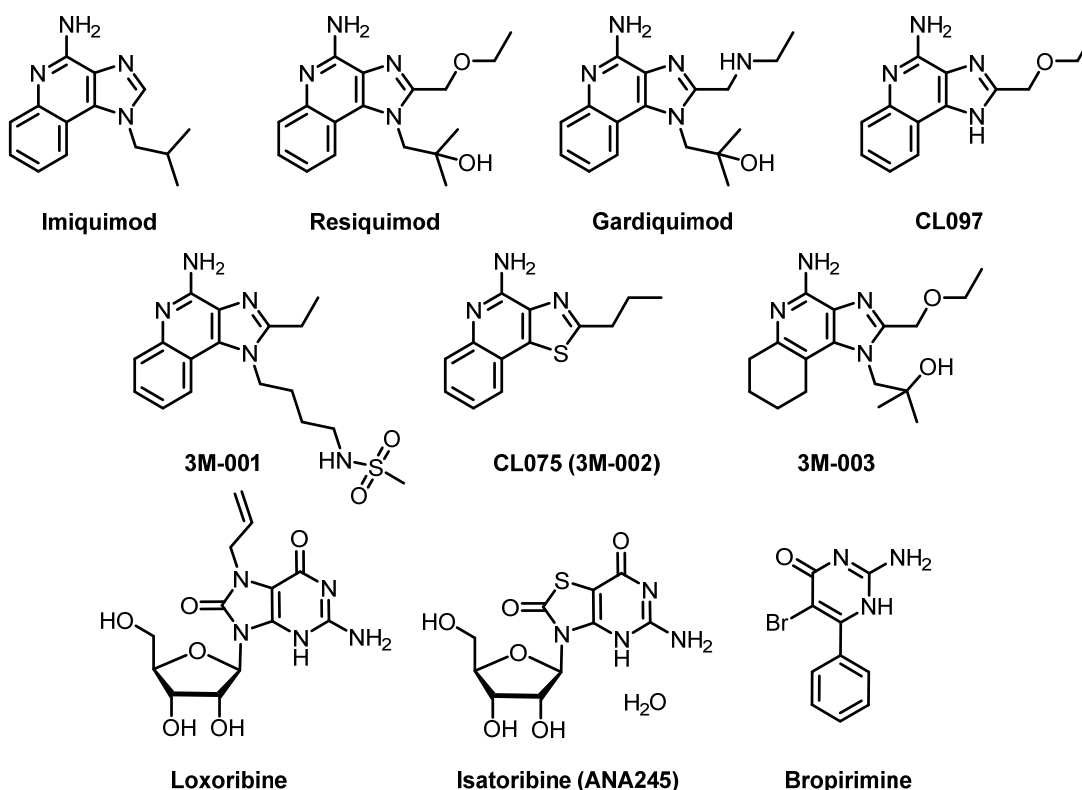
The prototypical intracellular TLRs (TLR3 and TLR7-9) are generally associated with sensing nucleic acids released within endosomal compartments. Their activation leads to the production of a variety of nuclear factor (NF)- κ B-mediated cytokines and Type I interferons (IFNs). TLR7 and TLR8 are phylogenetically and structurally related. TLR7 is expressed in plasmacytoid dendritic cells (pDC) and B cells, whereas TLR8 is mainly expressed in conventional/myeloid dendritic cells (cDCs), monocytes, macrophages, and neutrophils. Single stranded RNA (ssRNA) molecules of viral as well as nonviral origin (poly(dT); double-stranded thymidine homopolymer) induce the production of inflammatory cytokines, mediated by the recognition in the endosomal compartment by TLR7 and TLR8.³¹ TLR7 preferentially recognizes GU-rich RNA sequences and TLR8 has more affinity for AU-rich sequences.³² The activation by ssRNA induces the recruitment of the adapter protein Myeloid Differentiation primary response gene 88 (MyD88) via its TIR domain. TIR domains initiate the signaling cascade through TIR adapters, leading to downstream responses to specific pathogens. This results in the activation of NF- κ B and IFN regulatory factors (IRFs) 3 and 7, which in turn induce the production of proinflammatory cytokines such as tumor necrosis factor (TNF)- α , interleukin (IL)-1 and IL-6 and Type I IFNs, respectively.³³ TLR7 and TLR8 can also detect a variety of synthetic chemical agonists. Small molecule, non-polymeric, synthetic agonists include the imidazoquinolines

(imiquimod, resiquimod [R-848], and gardiquimod),³⁴ as well as guanosine analogues such as loxoribine³⁵ (Fig. 1).

Long before endosomal TLR7 was discovered to serve as the primary sensor for short, single-stranded, GU-rich RNA sequences (ssRNA), mainly of viral origin,^{31a-c} a number of small molecules were synthesized and evaluated in the 1970s and '80s for antiviral activities owing to their pronounced Type I interferon (IFN- α and - β) inducing properties.³⁶ Members of the 1*H*-imidazo[4,5-*c*]quinolines were found to be good Type I IFN inducers in human cell-derived assays,³⁷ and FDA approval was obtained in 1997 for Imiquimod (commercialized under the brand name Aldara™) for the treatment of basal cell carcinoma and actinic keratosis.³⁸ The drug was later discovered to be a TLR7 agonist. The induction of IFN- α , IL-6 and TNF- α by imiquimod has been observed in vitro and in both human and animal studies. Imiquimod also activates NK lymphocytes and cells of the monocyte/macrophage lineage, and induces B lymphocytes to proliferate and differentiate.³⁹ Resiquimod (R-848), another structurally similar compound, stimulates immune responses via TLR7 in mice and via TLR7 and TLR8 in humans.⁴⁰ Resiquimod also triggers significant cytokine secretion, macrophage activation, and enhancement of cellular immunity.⁴¹ Resiquimod reached Phase III clinical trials for the topical treatment of genital herpes; however, development was suspended due to lack of adequate efficacy.⁴² CL097 and 3M-003 are derivatives of resiquimod that activate both TLR7 and TLR8.⁴³ 3M-001, selective TLR7 agonist, stimulates plasmacytoid dendritic cells to produce cytokines such as IFN- α and IFN- γ inducible protein (IP)-10.⁴⁴ Gardiquimod is another agonist of human and mouse TLR7 and more potent than imiquimod. At higher concentration, it is also known to activate TLR8.^{43b} CL075 (3M-002) is a thiazoquinoline derivative that triggers TLR8 in human peripheral blood mononuclear cells (PBMCs). Agonistic activity of CL075 at TLR8 is known to activate NF- κ B and trigger secretion of TNF- α and IL-12. This compound also

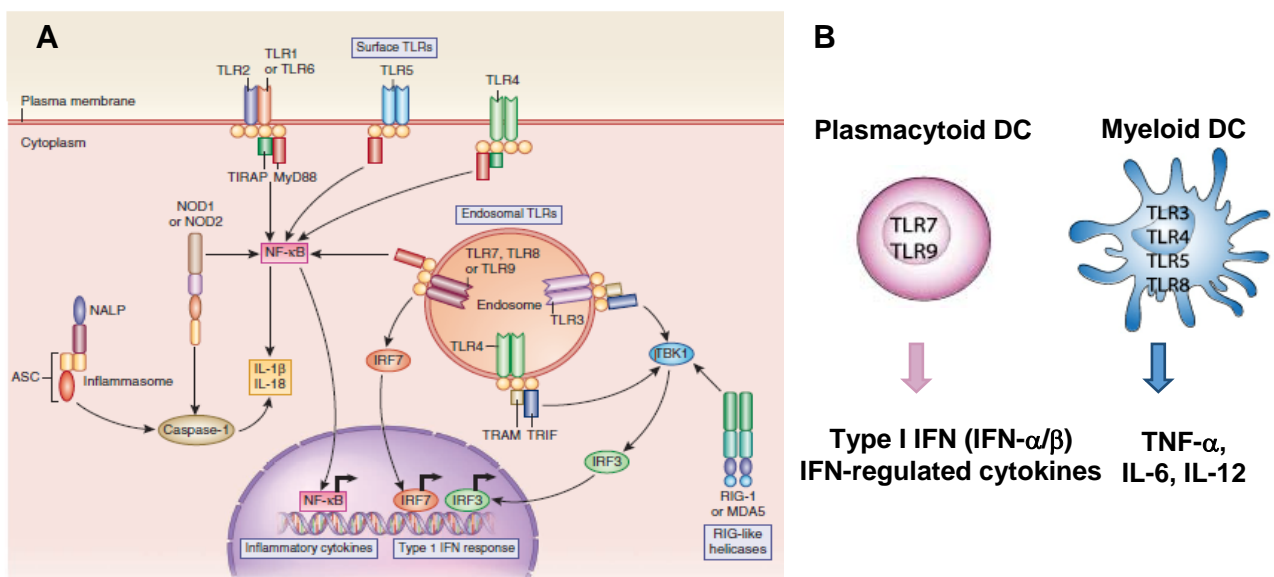
activates TLR7, however, to a lesser extent.⁴⁵ Loxoribine is a guanosine ribonucleoside analogue that activates human and mouse TLR7. This compound enhances anti-tetanus-specific IgG antibody anamnestic responses in a dose-dependent manner in human PBMCs, as well as strongly activating NK cells in IL-12-dependent manner.^{35c} Isatoribine (ANA245) and ANA975 (an oral prodrug of isatoribine) are other examples of guanosine nucleoside analogues. Isatoribine, like imiquimod, was also identified as an immune potentiator before its mechanism of action was elucidated to be through activation of TLR7. These agents were developed for treatment of HCV infection;⁴⁶ however, ANA975 has been discontinued due to unacceptable toxicity.⁴⁷ Bropirimine is an aryl pyrimidinone analogue, an antineoplastic compound that induces IFN- α and is used for treatment of carcinoma.⁴⁸ The mechanism of action of bropirimine is likely associated with direct anti-tumor effect rather than cytokine mediated anti-tumor activity.⁴⁹

Fig. 1. Chemical structures of representative synthetic TLR7/8 agonists.



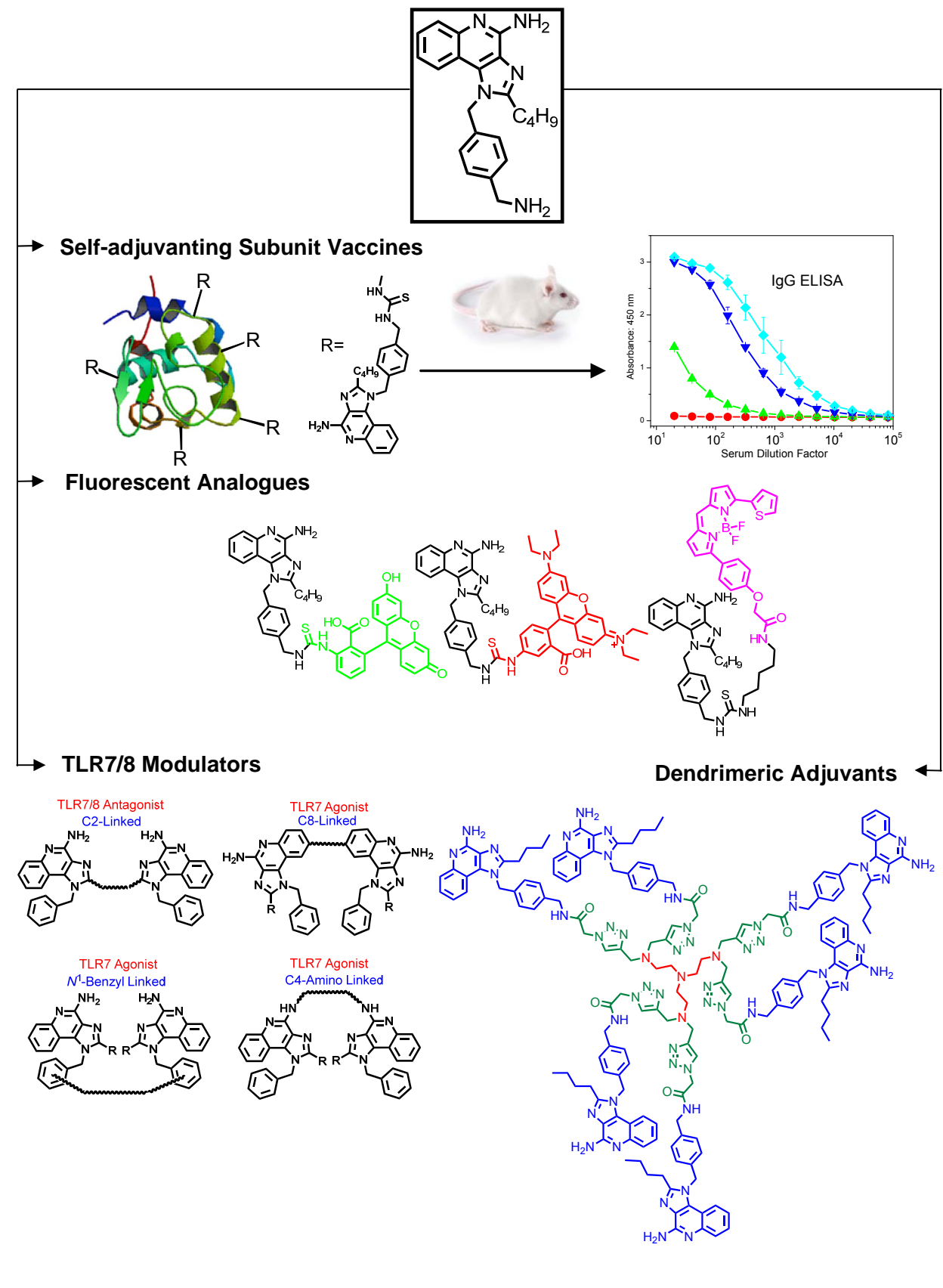
Much of what is known about the vaccine adjuvant potential of TLR7 and/or TLR8 agonists has been derived from preclinical studies in animal models using the imidazoquinolines. These compounds, as mentioned earlier, have shown to directly activate antigen-presenting cells resulting in the induction of costimulatory molecules and numerous cytokines that modulate adaptive immunity.⁵⁰ In terms of differences between human TLR7 and TLR8, TLR7-selective agonists were known to be more effective at inducing IFN- α and IFN-regulated cytokines than TLR8-selective agonists. On the other hand, TLR8 is functional in monocytes and myeloid DC, and its engagement results in the production of dominant proinflammatory cytokines such as TNF- α , IL-12, and MIP-1 α .⁴⁵ Together with IL-12, Type I IFNs appear to be required for optimal Th1 and CD8⁺ T cell responses following the administration of TLR7 and TLR8 agonists.⁵¹ Thus, TLR7 and TLR8 agonists, as well as TLR7/8 dual agonists could hold potential applications as vaccine adjuvants, especially in regard to their propensity for promoting Th1-type immune responses.

Fig. 2. A. Target receptors on APCs for adjuvants and their downstream signaling (adapted from Reed, S. G. et al, *Nature medicine* 2013, 19 (12), 1597). **B.** Expression of TLRs in human DCs and their ability to produce cytokines.



Desirous of specifically identifying chemotypes with strong Th1-biased immunostimulatory signatures, we implemented screens examining the induction of Type I and Type II IFNs (IFN- α/β and IFN- γ , respectively),⁵² IL-12,⁵³ and IL-18⁵⁴ using human PBMCs, all of which are strongly associated with dominant Th1 outcomes. These studies enabled us to determine that of all of the diverse chemotypes of our rapidly expanding libraries and identify *N*¹-(4-aminomethyl) benzyl-substituted TLR7/8 dual-agonistic imidazoquinoline (Fig. 3) that displayed a prominent Th1 bias, orders of magnitude higher than that of even lipopolysaccharide. This lead compound has been pivotal in exploring a variety of concepts such as TLR7/8 modulators and antagonists,⁵⁵ model self-adjuvanting subunit vaccine constructs,⁵⁶ a dendrimeric adjuvant,⁵⁷ and cell-permeable, endosome-localizing, fluorescent analogues that retain agonistic activity⁵⁸ (Fig. 3). The covalently coupled TLR7/TLR8 dual-agonistic imidazoquinoline to antigens using mild, nondenaturing conditions induced high antibody titers indicative of Th1 immunity.⁵⁶ The dendrimeric adjuvant consisting of six linked TLR7/8 agonists (hexamer) lost TLR8 activity but retained the TLR7 agonistic effects, and it was found to be superior to the imidazoquinoline monomer in inducing high titers of high-affinity antibodies to bovine α -lactalbumin in rabbits. Additionally, epitope mapping experiments showed that the dendrimer induced immunoreactivity to more contiguous peptide epitopes along the amino acid sequence of the model antigen.⁵⁷

Fig. 3. Utility and diversification of *N*¹-(4-aminomethyl)benzyl-substituted imidazoquinoline.

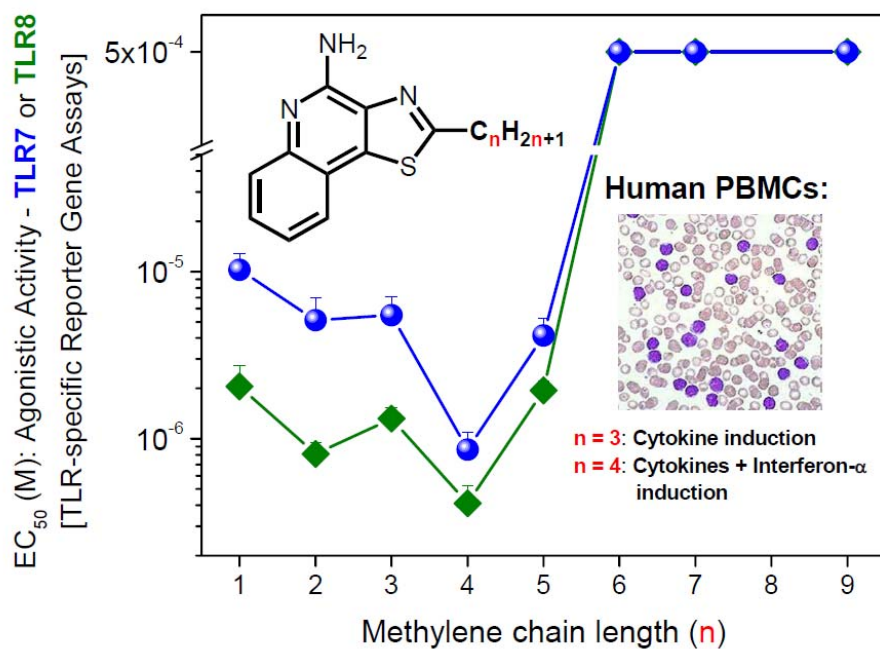


Excessive or uncontrolled innate immune responses could potentially result in reactogenicity, and even undermine subsequent adaptive immune responses, and it is of particular importance to simultaneously take into consideration aspects of immune potentiation alongside safety issues associated with local or systemic immune activation and inflammation.

The premise of this thesis is that a careful and systematic exploration of chemical space around TLR7/8 chemotypes, as well as the development of standardized panels of bioassays that permit a detailed insight into the immunopharmacology of such molecules would not only allow the determination of the structural correlates governing adjuvantic activity (Chapters 2-6), but also allow the rational exploration of novel strategies to dissociate adjuvanticity from reactogenicity (Chapter 7).

Chapter 2.

TLR8/7-agonistic 2-alkylthiazolo[4,5-*c*]quinolines



2.1. Introduction

We decided to extend our investigations toward delineating structure-activity relationships (SAR) in small-molecule agonistic ligands of TLR8 (thiazolo[4,5-c]quinolines) for the following reasons: First, the thiazoloquinolines are of interest because like the imidazoquinolines, these compounds were identified in antiviral assays long before the discovery of the endosomal TLR7 and TLR8 receptors,^{36, 59} and other than the original landmark studies performed by investigators at 3M Pharmaceuticals,⁶⁰ SAR of the thiazoloquinoline chemotype remains poorly explored; qualitative assays for TNF- α and IFN- α induction in human blood were performed in these initial studies as surrogate biomarkers of immunostimulation, and no data on TLR-7 and -8 specific agonistic activities existed in the literature. Second, TLR8 agonists, both single-stranded RNA as well as small molecule imidazoquinoline ligands such as R-848 (resiquimod, Chapter 1)⁶¹ and thiazoloquinolines such as 3M-002 (CL075, Chapter 1)^{45, 62} appear uniquely potent in activating costimulatory responses in neonatal antigen-presenting cells (APCs), inducing robust production of the Th1-polarizing cytokines TNF- α and IL-12, which are not observed upon stimulation by TLR-2, -4, or -7 agonists. Such Th1-biasing compounds are of particular interest as candidate vaccine adjuvants in the newborn.⁶³ During the first few weeks of life, newborns rely almost entirely on maternal IgG antibodies acquired by passive transplacental passage,⁶⁴ and remain susceptible to a wide range of pathogens until early infancy.⁶⁵ Neonates and infants, in whom vaccines could — and perhaps should — have the greatest impact, do not mount adequate adaptive immune responses, and therefore are most vulnerable; consequently, even the most efficacious vaccines that confer excellent protection in adults may fail to elicit strong immune responses in them.⁶⁶ There is mounting evidence pointing to significant differences between adult and infant innate immune responses.⁶⁷ The neonatal immunophenotype is characterized by decreased production of both Type I and Type II IFNs, IL-

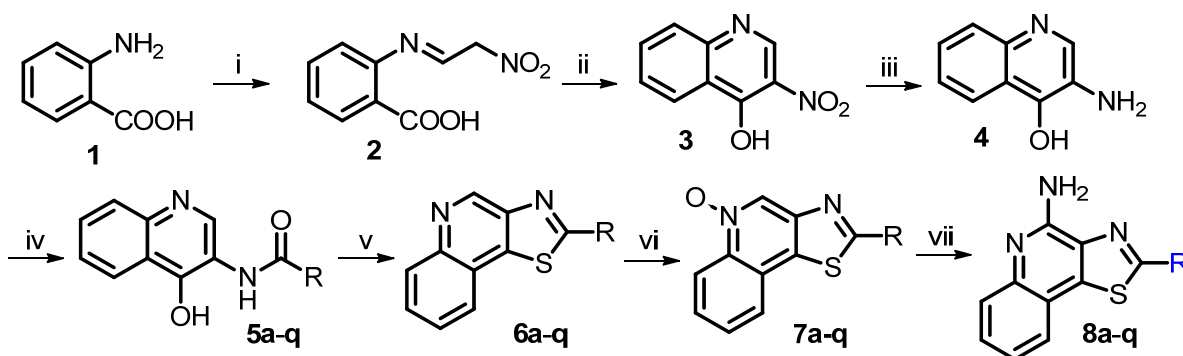
12, IL-18, IL-23 and other proinflammatory cytokines such as TNF- α , the preferential induction of memory B lymphocytes rather than immunoglobulin-secreting plasma cells, as well as a pronounced Th2 skewing of T-cell responses.^{65-66, 68} TLR8 agonists induce the production of IL-12, IL-18 and IFN- γ , and may therefore be of value in developing vaccines for the neonate. We therefore sought to explore SAR in the thiazoloquinolines (typified by CL075, **8c** in Scheme 1).

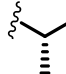
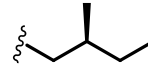
Our studies began with examining the optimal alkyl chain length at the C2 position. We found, as expected, that the C2-alkyl thiazoloquinolines exhibit mixed TLR8/7 agonistic activities in primary reporter gene assays with the optimal chain length being butyl. We observed unexpectedly strict length dependence with only the C2-butyl, but none of the other analogues, inducing IFN- α in human PBMCs. Examination of analogues with branched alkyl groups at C2 suggested poor tolerance of terminal steric bulk. We noted, however, that certain C2-branched analogues were substantially more TLR8-selective than their corresponding straight-chain analogues. Virtually all modifications at C8 led to abrogation of agonistic activity. Alkylation on the C4-amine was not tolerated, whereas *N*-acyl analogues with short acyl groups (other than acetyl) retained activity.

2.2. Results and Discussion

In our previous work on the TLR7-active imidazoquinolines, we had observed a distinct relationship between C2-alkyl chain length and TLR7-agonistic potency,⁶⁹ and we therefore thought it logical to begin our SAR studies on the thiazoloquinolines by examining analogues with C2-alkyl groups of varying chain lengths. These analogues (**8a-h**, Scheme 1) were synthesized in parallel from the 3-aminoquinolin-4-ol precursor **4**.⁶⁹

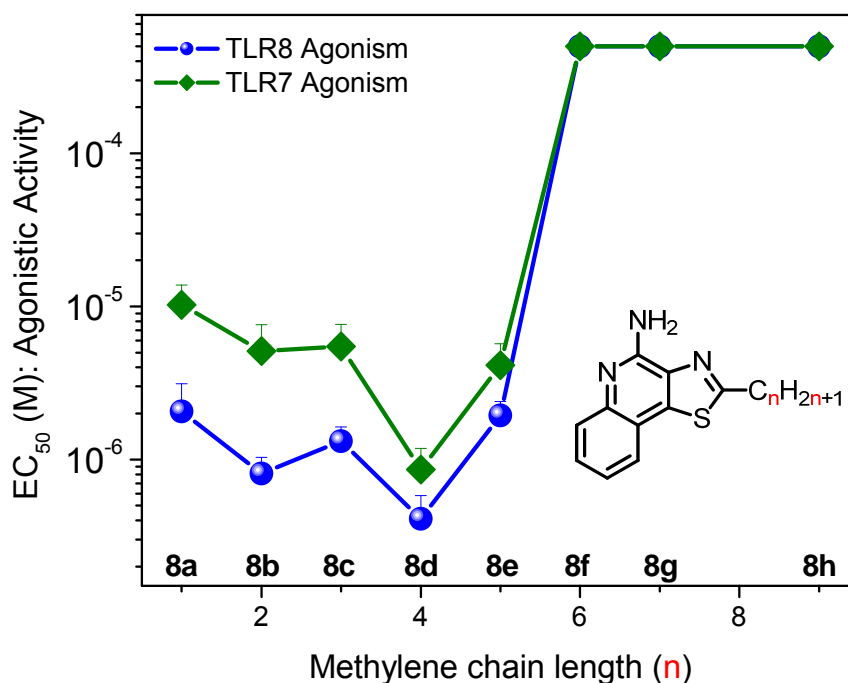
Scheme 1. Synthesis of C2-alkylthiazoloquinoline analogues.



a: R = CH₃, b: R = C₂H₅, c: R = C₃H₇, d: R = C₄H₉, e: R = C₅H₁₁, f: R = C₆H₁₃
g: R = C₇H₁₅, h: R = C₉H₁₉, i: R = CH(CH₃)₂, j: R = CH₂CH(CH₃)₂, k: R = CH₂C(CH₃)₃
l: R = C₂H₅CH(CH₃)₂, m: R = C₂H₅C(CH₃)₃, n: R = , o: R = 
p: R = C₂H₅CF₃, q: R = C₃H₇CF₃

Reagents: i. HCl, HON=CHCH₂NO₂, H₂O; ii. (CH₃CO)₂O, CH₃COOK; iii. Pt/C, H₂, DMF; iv. RCOCl, Et₃N, CH₂Cl₂: DMF = 10:1; v. P₂S₅, pyridine; vi. mCPBA, CHCl₃; vii. (a) benzoyl isocyanate, CH₂Cl₂ (b) NaOCH₃, MeOH.

Fig. 1. TLR7 and TLR8 agonistic potencies of the C2-alkyl thiazoloquinoline homologues. Data points represent means and standard deviations of EC₅₀ values derived from dose-response profiles and are computed on quadruplicates.

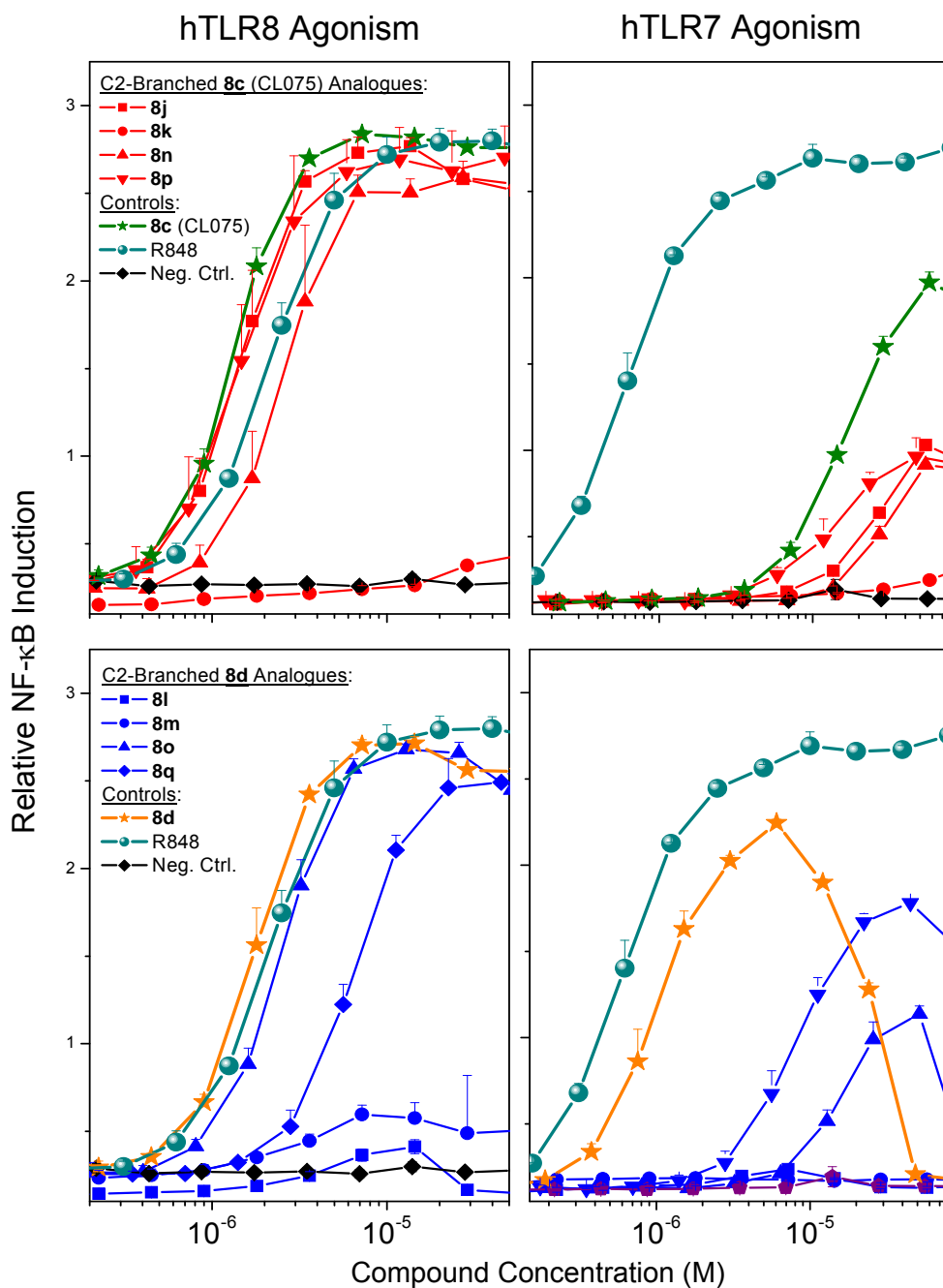


In primary screens using human TLR7 and TLR8-specific reporter gene assays, these analogues exhibited, as anticipated, mixed TLR8/TLR7 agonism; the EC₅₀ values of **8c** (CL075) were found to be 1.32 μ M and 5.48 μ M, respectively (Fig. 1, Table 1). As in our earlier SAR studies on the imidazoquinolines,⁶⁹ we observed a clear dependence of agonistic potency on the C2-alkyl chain length. The C2-methyl, -ethyl, and -propyl analogues (**8a-c**) displayed comparable potencies in the hTLR8 and hTLR7 reporter gene assays (Fig. 1). Maximal TLR8-agonistic potency was observed in the butyl analogue (**8d**). Increasing the chain length to pentyl (**8e**) led to attenuation of potency, and higher homologues (**8f-h**) showed abrogation of activity (Fig. 1, Table 1). The C2-butyl analogue **8d** appeared to exhibit substantially higher TLR7-agonistic potency than **8c** (Figs. 1 and 3), suggesting that subtle variations at C2 could modulate TLR8 versus TLR7 specificity.

We therefore synthesized several additional analogues of both **8c** (C2-n-propyl) and **8d** (C2-n-butyl) with branched alkyl groups at C2 (**8i-o**, Scheme 1) and examined their activities (Fig. 2). The introduction of an isopropyl group at C2 (**8i**) led to an approximately ten-fold reduction in TLR8-agonistic potency (Table 1), while the attenuation of its activity in TLR7-specific reporter gene assays was more modest (about two-fold). Rather dramatic differences were noted between **8j** (C2-isobutyl)/**8k** (C2-neopentyl) and **8l** (C2-isopentyl)/**8m** (C2-neohexyl) congeneric pairs. Whereas **8j** was as potent as **8c** in TLR8 agonism assays, **8k** was inactive (Fig. 2), which suggested poor tolerance of terminal steric bulk. However, **8l** and **8m** were both inactive, pointing to additional length requirements in C2-branched alkyl substituents. These results led us to evaluate analogues **8n** (2-methylpropyl substituent at C2) and **8o** (2-methylbutyl substituent). Both these compounds retained TLR8 agonistic properties readily comparable to their parent compounds **8c** and **8d**, respectively, lending support to the premise that steric bulk at the ω -position of the C2-alkyl group was not tolerated. We also evaluated bioisosteric

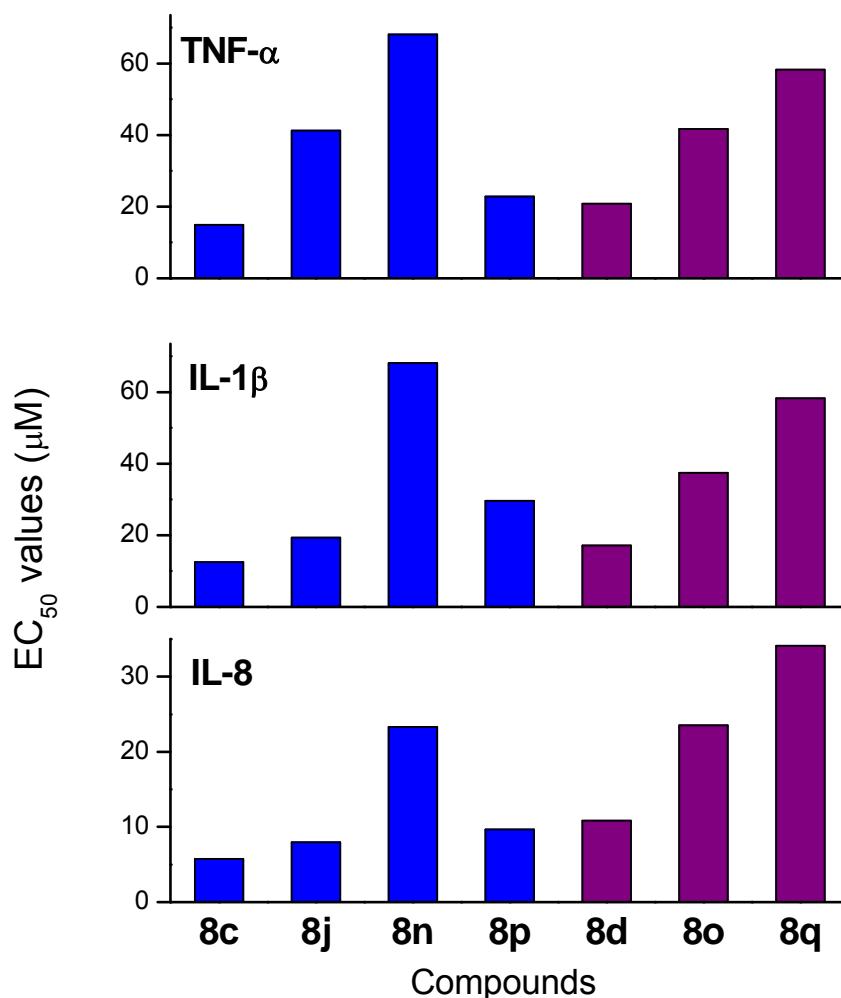
analogues **8p** and **8q** (Scheme 1) with terminal trifluoromethyl groups. A decrease in potency at TLR8 was observed in the longer homologue (**8q**). We noted that, in general, analogues with branched C2-alkyl groups of optimal chain length and bulk (such as **8j**, **8n**, and **8o**) are substantially more TLR8-selective than their corresponding straight-chain analogues (Fig. 2).

Fig. 2. TLR8- and TLR7-specific NF- κ B induction profiles of branched-chain and trifluoromethyl analogues of **8c** and **8d**. Means and SD obtained from quadruplicate samples are shown.



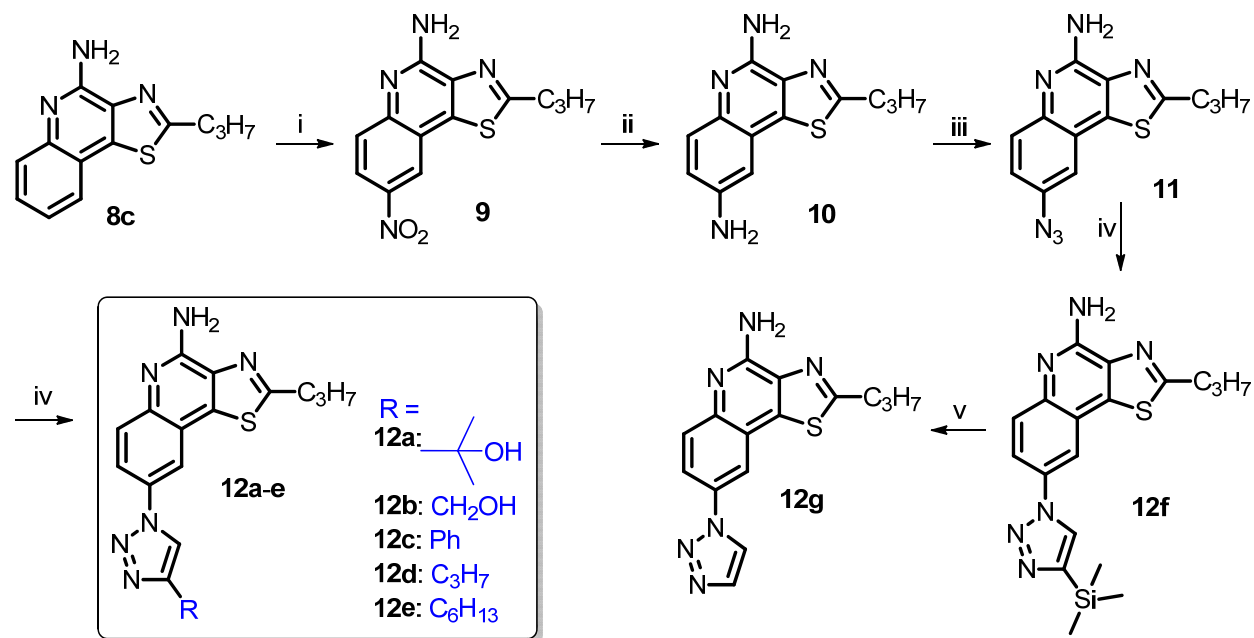
However, in secondary cytokine induction screens using human PBMCs, the branched-chain analogues behave differently in that they were neither as potent as their straight-chain parent compounds (Fig. 3), nor did they show enhanced IL-12, IL-18, and IFN- γ production (data not shown) as would be expected for TLR8-selective compounds. We do not yet understand the basis of attenuated activity of the C2-branched analogues, and we are currently exploring whether differential plasma protein binding behavior of these compounds could be contributory.⁷⁰

Fig. 3. EC_{50} values of proinflammatory cytokine induction in human PBMCs by analogues of **8c** and **8d**. Representative data from three independent experiments are shown.



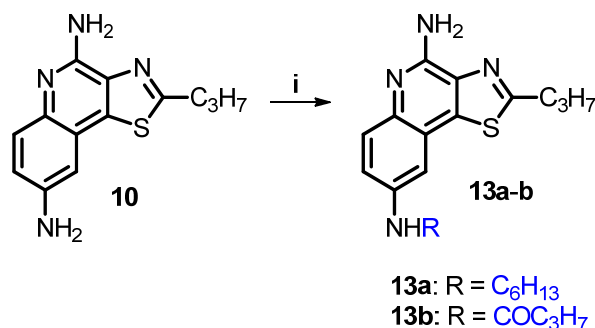
Noting that previous studies in the patent literature^{60, 71} had been performed largely on the C7 position, and C8 and C4 analogues remain unexplored. We therefore first examined substituents on the quinoline at the C8 position of **8c** (CL075). Electrophilic substitution on the quinoline ring selectively afforded the 8-nitro analogue **9** (Scheme 2), and the 8-bromo analogue **14** (Scheme 4), both of which were inactive. The 8-amino (**10**) and 8-azido (**11**) analogues were obtained from **9** (Scheme 2). Compound **10** showed attenuated activity relative to **8c**, and **11** was inactive. The triazole derivatives **12a-g** were synthesized from **11** (Scheme 2) using conventional copper-catalyzed ‘click’ chemistry; of these analogues, the triazolo analogue **12e** displayed feeble, but selective TLR8 agonism (Table 1). Selective C8 *N*-alkylation and *N*-acylation of the 8-amino analogue **10** provided analogues **13a** and **13b** (Scheme 3), both of which were inactive (Table 1).

Scheme 2. Modification at the C8 position.



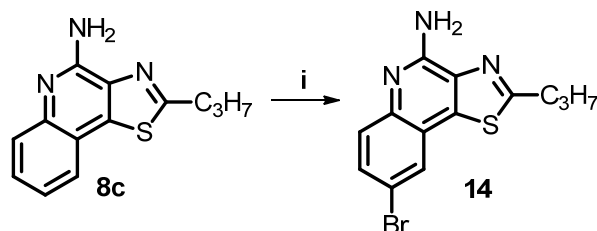
Reagents: i. HNO₃, H₂SO₄; ii. Zn, NH₄COOH, MeOH; iii. NaNO₂, CH₃COOH, NaN₃; iv. alkyne, CuSO₄, sodium ascorbate, THF, H₂O; v. TBAF, THF.

Scheme 3. Synthesis of C8 N-alkyl and N-acyl analogues.



Reagents: i. For **13a**, C₆H₁₃I, K₂CO₃, DMF; For **13b**, C₃H₇COCl, Et₃N, CH₂Cl₂.

Scheme 4. Synthesis of 8-bromothiazoloquinoline.

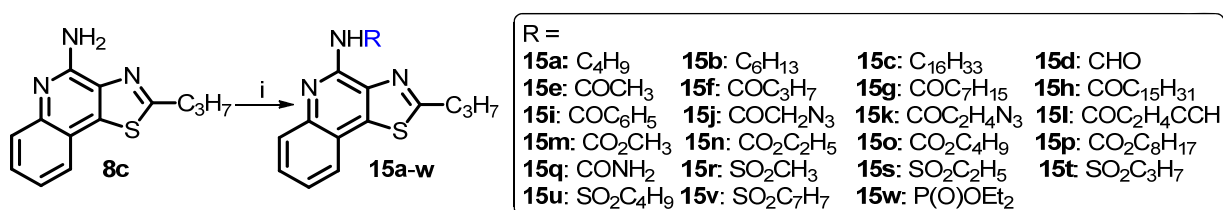


Reagents: i. NBS, NH₄OAc, CH₃CN.

Next, the C4-amine of **8c** was alkylated or acylated, yielding analogues **15a-i** (Scheme 5). The C4-N-alkylated compounds **15a** and **15b** were devoid of any agonistic activity, while some, but not all of the C4-N-acylated derivatives with short acyl groups were found to be active. Specifically, the formyl (**15d**), and butyryl (**15f**) analogues, but not the acetyl (**15e**) compound, were active. Cytokine induction profiles in hPBMCs mirrored these findings with a near-complete loss of activity for the acetyl compound **15e** (Fig. 5A). Our provisional interpretation that a stringent length requirement exists for the acyl substituents on the C4-amine was borne out in compounds **15j-l** (azidoacetamide, azidopropionamide and pentynamide analogues, respectively), which displayed weak, TLR8-selective agonistic activity (Table 1). Aromatic amides at this position appear not to be tolerated, since the benzamide analogue **15i** was entirely inactive. A series of carbamates (**15m-p**) and sulfonamides (**15r-v**) were also

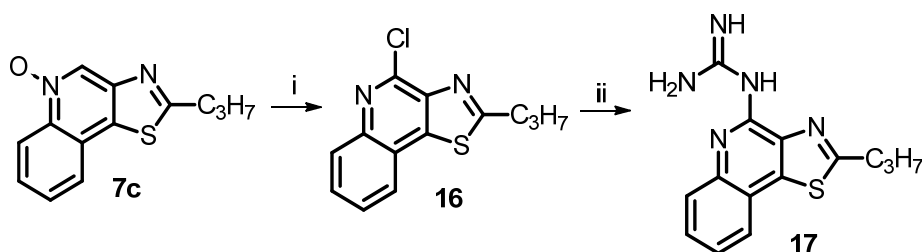
synthesized (Scheme 5). The carbamate derivatives showed feeble activity with very low area-under-curves in primary TLR8 screens, while the sulfonamide analogues were completely inactive (Table 1). Several other analogs including urea (**15q**; Scheme 5), phosphoramidate (**15w**; Scheme 5) and guanidine (**17**; Scheme 6) functional groups at C4 were also examined, but were found to be inactive.

Scheme 5. Synthesis of C4 N-alkyl and N-acyl analogues.



Reagents: i. For **15a**, **15b** and **15c**, RX, NaH, THF; For **15d**, 2,2,2-trifluoroethylformate, Et₃N; For **15e-i**, RCOCl, Py; For **15j-l**, RCO₂H, HBTU, Et₃N; For **15m-p**, ROCOCl, Et₃N, CH₂Cl₂; For **15q**, ClSO₂NCO, NaHCO₃; For **15r-v**, RSO₂Cl, CH₂Cl₂; For **15w**, ClP(O)OEt₂, CH₂Cl₂.

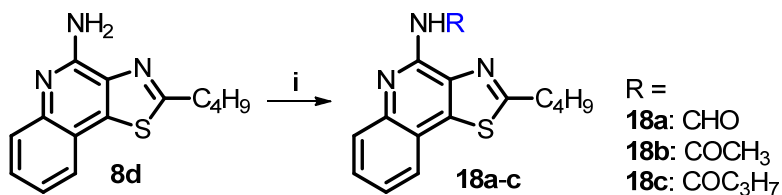
Scheme 6. Synthesis of C4 guanidino analogues.



Reagents: i. POCl₃, 100 °C; ii. guanidine hydrochloride, NaH, 1,4-dioxane.

The peculiar SAR, with only the acetamide analogue (**15e**) showing loss of activity was unexpected and, desiring to confirm this pattern, we also synthesized selected amide analogues of **8d** (**18a-c**, formamide, acetamide, and butyramide derivatives, respectively; Scheme 7). As the **8c** derivatives, a virtually identical pattern was observed, with a selective loss of activity for the acetamide analogue **18b** (Figs. 4B and 5B, Table 1).

Scheme 7. Synthesis of C4 N-alkyl and N-acyl analogues of **8d**.



Reagents: i. For **18a**, 2,2,2-trifluoroethylformate, Et₃N; For **18b** and **18c**, RCOCl, pyridine.

Fig. 4. TLR8 induction by C4-amides of **8c** (Panel A) and **8d** (Panel B). Data points represent means and standard deviations on quadruplicates.

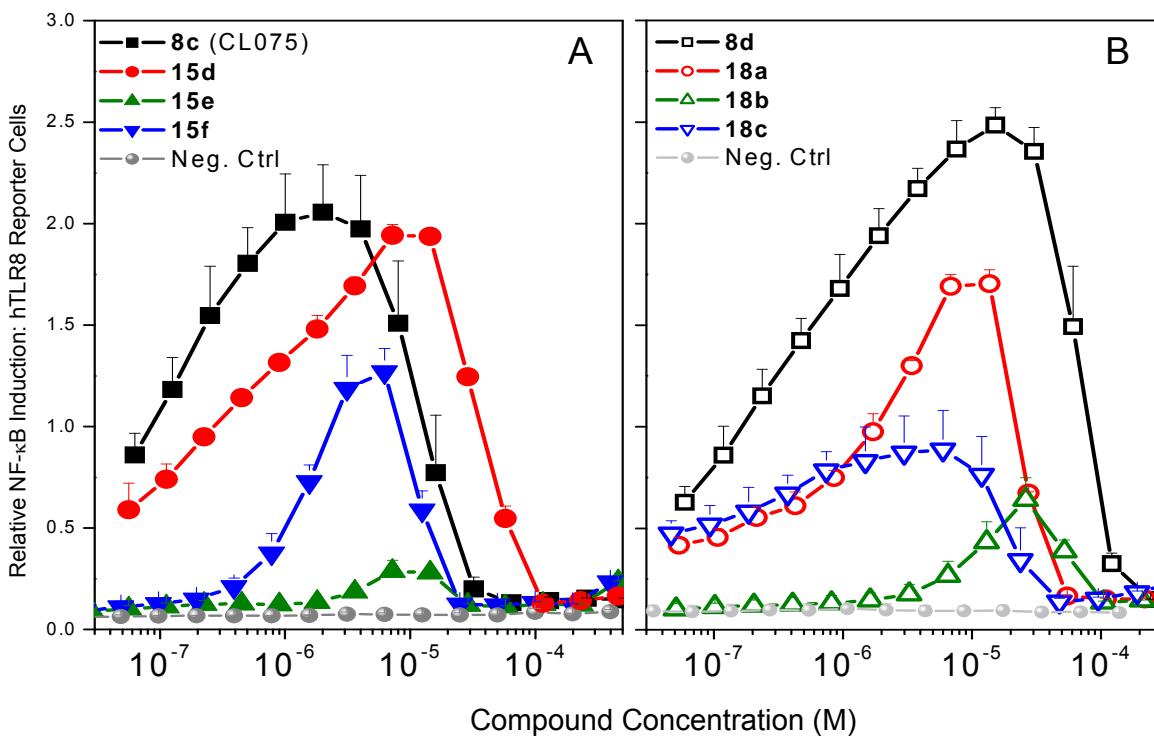
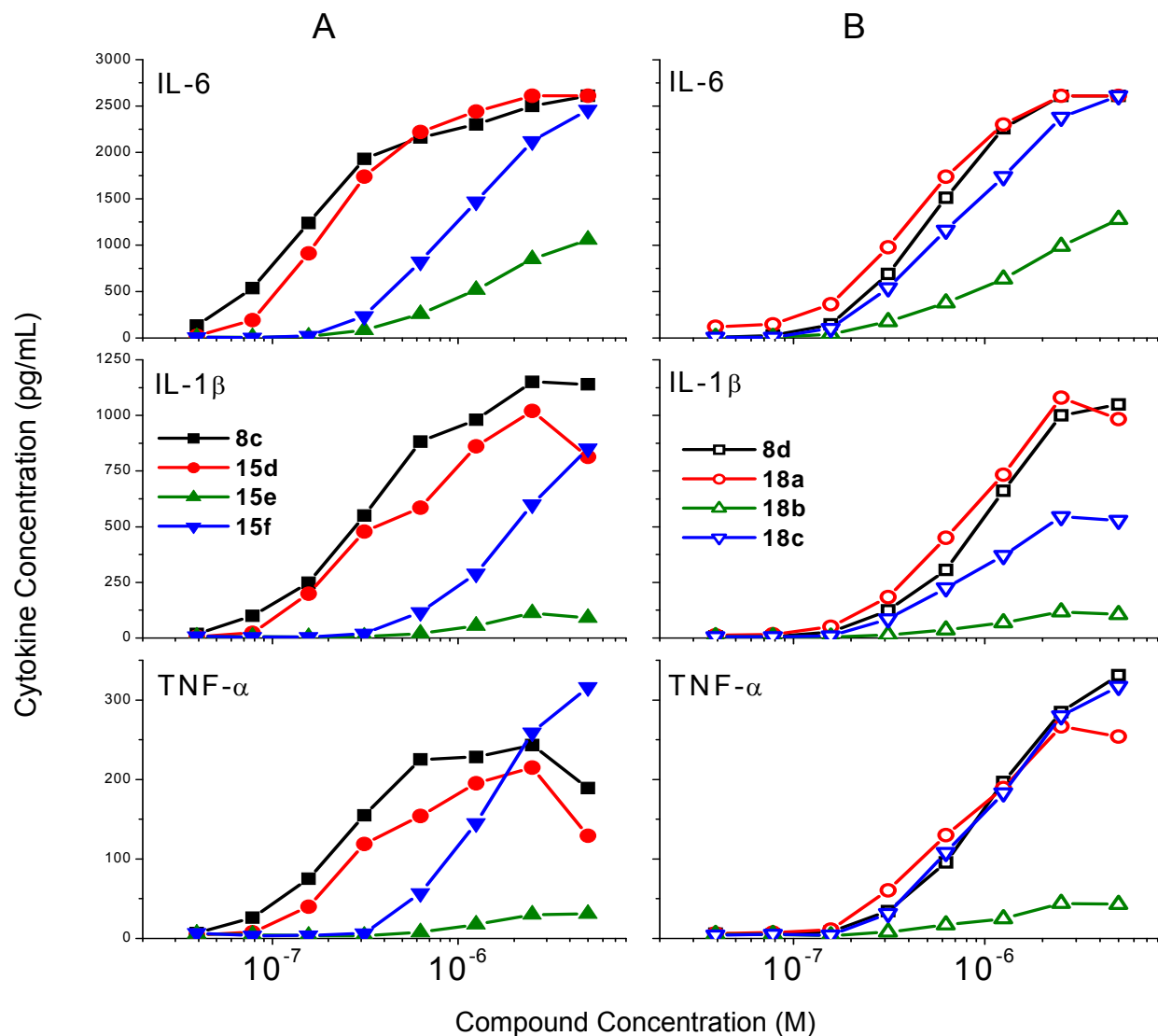


Fig. 5. Dose-response profiles of proinflammatory cytokine induction in hPBMCs by C4-amides of **8c** (Panel A) and **8d** (Panel B). Representative data from three independent experiments are presented. Vehicle controls (not shown) elicited undetectable levels of cytokines.



Our studies aimed at understanding structure-activity relationships in the thiazoloquinolines have yielded two compounds of interest: **8c** and **8d**, possessing differential TLR8/TLR7-agonistic properties. All of the other analogues were either of lower potency, or exhibited very poor aqueous solubility (such as the amide analogues **15d** and **18a**, for instance). We therefore elected to directly evaluate the adjuvantic properties of **8c** and **8d**. In light of the fact that murine

TLR8 was thought to be functionally inactive,⁷² we chose to examine the adjuvantic activities of **8c**, **8d** directly in a rabbit model using bovine α -lactalbumin as a model subunit vaccine antigen, which is a small (14 kDa), soluble protein which we have adopted as our test-antigen in ongoing humoral and cellular immune response assays.⁵⁶

We were gratified to find that both **8c** and **8d** were highly adjuvantic in evoking high antigen-specific IgG titers (Fig. 6). Importantly, no evidence of local or systemic toxicity was apparent in any of the cohorts. The data suggest that **8d**, with its dual TLR7/TLR8-agonistic properties, elicits adjuvanticity with greater consistency and uniformity, as evidenced by narrower confidence intervals of antibody titers (Fig. 6).

Fig. 6. Box-plots of anti-bovine α -lactalbumin IgG titers in cohorts of three rabbits immunized with α -lactalbumin adjuvanted with either **8c** or **8d**. Means and medians of titers are represented by \square and $-$ symbols within the box, respectively, and the X symbols indicate the 1% and 99% percentile values.

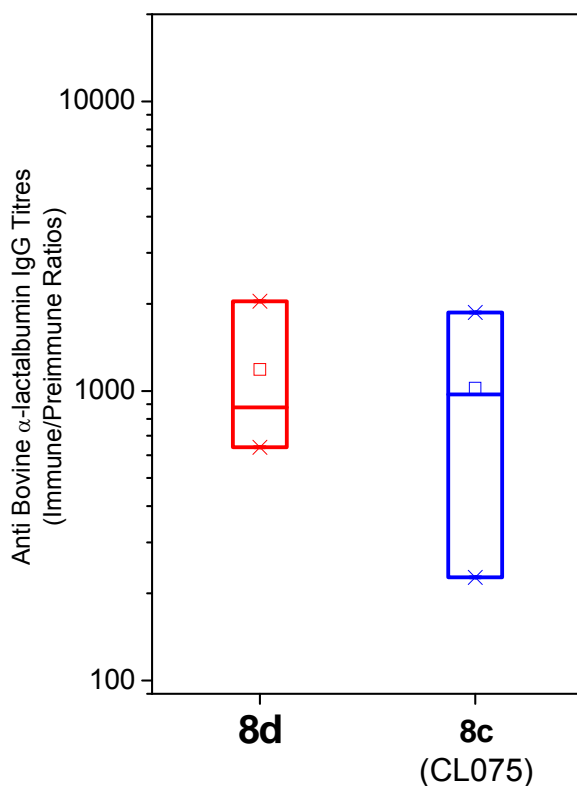
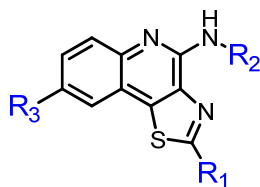
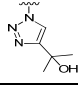
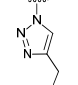
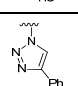
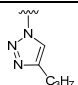
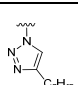
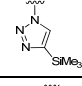
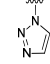


Table 1. EC_{50} values of compounds in human TLR7/8-specific reporter gene assay.



No.	R ₁	R ₂	R ₃	Agonistic Activity (μM)	
				TLR8	TLR7
8a	CH ₃	H	H	2.06	10.24
8b	C ₂ H ₅	H	H	0.81	5.12
8c	C ₃ H ₇	H	H	1.32	5.48
8d	C ₄ H ₉	H	H	0.41	0.86
8e	C ₅ H ₁₁	H	H	1.94	4.14
8f	C ₆ H ₁₃	H	H	Inactive	Inactive
8g	C ₇ H ₁₅	H	H	Inactive	Inactive
8h	C ₉ H ₁₉	H	H	Inactive	Inactive
8i	CH(CH ₃) ₂	H	H	10.85	9.67
8j	CH ₂ CH(CH ₃) ₂	H	H	1.55	6.96
8k	CH ₂ C(CH ₃) ₃	H	H	Inactive	Inactive
8l	C ₂ H ₅ CH(CH ₃) ₂	H	H	Inactive	Inactive
8m	C ₂ H ₅ C(CH ₃) ₃	H	H	Inactive	Inactive
8n	(S)-2-(sec-butyl)	H	H	2.77	8.11
8o	(S)-2-(2-methylbutyl)	H	H	2.51	4.74
8p	C ₂ H ₅ CF ₃	H	H	1.61	3.63
8q	C ₃ H ₇ CF ₃	H	H	6.29	2.25
9	C ₃ H ₇	H	NO ₂	Inactive	Inactive
10	C ₃ H ₇	H	NH ₂	3.88	8.19
11	C ₃ H ₇	H	N ₃	Inactive	Inactive
12a	C ₃ H ₇	H		Inactive	Inactive
12b	C ₃ H ₇	H		Inactive	Inactive
12c	C ₃ H ₇	H		Inactive	Inactive
12d	C ₃ H ₇	H		Inactive	Inactive
12e	C ₃ H ₇	H		Inactive	Inactive

12f	C ₃ H ₇	H		9.84	Inactive
12g	C ₃ H ₇	H		Inactive	Inactive
13a	C ₃ H ₇	H	NHC ₆ H ₁₃	Inactive	Inactive
13b	C ₃ H ₇	H	NHCOC ₃ H ₇	Inactive	Inactive
14	C ₃ H ₇	H	Br	Inactive	Inactive
15a	C ₃ H ₇	C ₄ H ₉	H	Inactive	Inactive
15b	C ₃ H ₇	C ₆ H ₁₃	H	Inactive	Inactive
15c	C ₃ H ₇	C ₁₆ H ₃₃	H	Inactive	Inactive
15d	C ₃ H ₇	CHO	H	0.88	Inactive
15e	C ₃ H ₇	COCH ₃	H	Inactive	Inactive
15f	C ₃ H ₇	COC ₃ H ₇	H	1.14	Inactive
15g	C ₃ H ₇	COC ₇ H ₁₅	H	Inactive	Inactive
15h	C ₃ H ₇	COC ₁₅ H ₃₁	H	Inactive	Inactive
15i	C ₃ H ₇	COC ₅ H ₅	H	Inactive	Inactive
15j	C ₃ H ₇	COCH ₂ N ₃	H	1.20	3.53
15k	C ₃ H ₇	COC ₂ H ₄ N ₃	H	2.23	Inactive
15l	C ₃ H ₇	COC ₂ H ₄ C≡C	H	1.20	Inactive
15m	C ₃ H ₇	CO ₂ CH ₃	H	Weak	Inactive
15n	C ₃ H ₇	CO ₂ C ₂ H ₅	H	Inactive	Inactive
15o	C ₃ H ₇	CO ₂ C ₄ H ₉	H	Inactive	Inactive
15p	C ₃ H ₇	CO ₂ C ₈ H ₁₇	H	Inactive	Inactive
15q	C ₃ H ₇	CONH ₂	H	Inactive	Inactive
15r	C ₃ H ₇	SO ₂ CH ₃	H	10.56	Inactive
15s	C ₃ H ₇	SO ₂ C ₂ H ₅	H	Inactive	Inactive
15t	C ₃ H ₇	SO ₂ C ₃ H ₇	H	Inactive	Inactive
15u	C ₃ H ₇	SO ₂ C ₄ H ₉	H	Inactive	Inactive
15v	C ₃ H ₇	SO ₂ C ₆ H ₄ CH ₃	H	Inactive	Inactive
15w	C ₃ H ₇	PO(OEt) ₂	H	Inactive	Inactive
17	C ₃ H ₇	CNHNH ₂	H	Inactive	Inactive
18a	C ₄ H ₉	CHO	H	2.31	2.54
18b	C ₄ H ₉	COCH ₃	H	Inactive	Inactive
18c	C ₄ H ₉	COC ₃ H ₇	H	0.42	0.49

2.3. Conclusion

TLR8 agonists are thought to be uniquely potent in activating adaptive immune responses by inducing robust production of T helper 1-polarizing cytokines, and may be promising candidate vaccine adjuvants, especially for neonatal vaccines. Thiazoloquinoline analogues with methyl, ethyl, propyl and butyl groups at C2 displayed comparable TLR8-agonistic potencies; however, the C2-butyl compound **8d** was unique in possessing substantial TLR7-agonistic activity. Analogues with branched alkyl groups at C2 displayed poor tolerance of terminal steric bulk. C4-*N*-acyl analogues with short acyl groups (other than acetyl) retained TLR8 agonistic activity, but were substantially less water-soluble. Immunization in rabbits with a model subunit antigen adjuvanted with the most potent TLR8 agonist showed dramatic enhancements of antigen-specific antibody titers.

2.4. Experimental

Chemistry. All of the solvents and reagents used were obtained commercially and used as such unless noted otherwise. Moisture- or air-sensitive reactions were conducted under nitrogen atmosphere in oven-dried (120 °C) glass apparatus. The solvents were removed under reduced pressure using standard rotary evaporators. Flash column chromatography was carried out using RediSep Rf 'Gold' high performance silica columns on CombiFlash Rf instrument unless otherwise mentioned, while thin-layer chromatography was carried out on silica gel (200 μm) CCM pre-coated aluminum sheets. Purity for all final compounds was confirmed to be greater than 98% by LC-MS using a Zorbax Eclipse Plus 4.6 mm × 150 mm, 5 μm analytical reverse phase C18 column with H₂O–isopropanol or H₂O–CH₃CN gradients and either an Agilent ESI-

TOF mass spectrometer (mass accuracy of 20 ppm) or an Agilent 6520 ESI-QTOF mass spectrometer (mass accuracy of <10 ppm) operating in the positive ion (or negative ion, as appropriate) acquisition mode.

Synthesis of compound 2: 2-(2-Nitroethylideneamino)benzoic acid. Nitromethane (4.32 mL, 80 mmol) was added dropwise to a solution of NaOH (9.6 g, 250 mmol) in water (10 mL) at 0 °C. The mixture was then warmed to 40 °C and nitromethane (4.32 mL, 80 mmol) was again added slowly at 40-45 °C. The temperature was maintained until a clear solution was obtained. The reaction mixture was then heated to 55 °C for 2-5 minutes, cooled to 30 °C, poured onto crushed ice and acidified with conc. HCl (11 mL). The resultant solution of methazoic acid was added immediately to a filtered solution of anthranilic acid **1** (10 g, 73 mmol) and conc. HCl (3.3 mL) in water (75 mL). The reaction mixture was allowed to stand at room temperature for 12 h. After filtration, the residue obtained was washed with water, and dried to yield compound **2** (12.94 g, 85%). ¹H NMR (400 MHz, MeOD) δ 8.14 (d, *J* = 7.7 Hz, 1H), 7.83 (d, *J* = 6.1 Hz, 1H), 7.68 – 7.59 (m, 2H), 7.22 (t, *J* = 7.4 Hz, 1H), 6.73 (d, *J* = 6.3 Hz, 1H). ¹³C NMR (101 MHz, MeOD) δ 168.6, 141.2, 136.6, 134.3, 132.0, 123.2, 116.7, 114.5, 100.0. MS (ESI) calculated for C₉H₈N₂O₄, *m/z* 208.05, found 209.06 [M+H]⁺.

Synthesis of compound 3: 3-Nitroquinolin-4-ol. A solution of compound **2** (12.94 g, 62.2 mmol) in acetic anhydride (50 mL) was placed in a 2-neck flask fitted with a reflux condenser. It was stirred and heated to 105 °C until a clear solution was obtained. Heating was then discontinued and potassium acetate (6.22 g, 63.5 mmol) was added. The mixture was then refluxed for 15 min with vigorous stirring, until a solid started to precipitate. The reaction mixture was then slowly cooled to room temperature. The residue was filtered, washed with glacial acetic acid until the washings were colorless, then suspended in water, filtered, washed with

water and dried at 110 °C to get 3-nitroquinolin-4-ol **3** (4.68 g, 40%). ¹H NMR (500 MHz, DMSO) δ 13.04 (s, 1H), 9.21 (s, 1H), 8.25 (dd, *J* = 8.1, 1.1 Hz, 1H), 7.83 – 7.77 (m, 1H), 7.74 – 7.70 (m, 1H), 7.52 (ddd, *J* = 8.1, 7.1, 1.1 Hz, 1H). ¹³C NMR (126 MHz, DMSO) δ 167.6, 142.5, 138.3, 133.2, 130.9, 128.1, 125.9, 125.8, 119.5. MS (ESI) calculated for C₉H₆N₂O₃, *m/z* 190.04, found 191.05 [M+H]⁺.

Synthesis of compound 4: 3-Aminoquinolin-4-ol. To a solution of compound **3** (1.89 g, 9.93 mmol) in DMF (25 mL), was added 5% Pt on carbon (20%, 0.38 g). The reaction mixture was allowed to react in a Parr hydrogenation apparatus at 60 psi H₂ pressure for 3.5 h with vigorous shaking. The reaction mixture was filtered through celite with several washes of methanol. The filtrate was concentrated by evaporation to get compound **4** (1.5 g, 94%). ¹H NMR (500 MHz, MeOD) δ 8.90 (d, *J* = 8.1 Hz, 1H), 8.33 (d, *J* = 5.8 Hz, 1H), 8.30 – 8.23 (m, 2H), 7.97 (ddd, *J* = 8.1, 6.0, 1.9 Hz, 1H). ¹³C NMR (126 MHz, MeOD) δ 146.9, 140.8, 138.9, 134.2, 131.2, 130.6, 128.7, 127.5. MS (ESI) calculated for C₉H₈N₂O, *m/z* 160.06, found 161.07 [M+H]⁺.

Synthesis of compound 5a: N-(4-hydroxyquinolin-3-yl)acetamide. Compound **4** (200 mg, 1.25 mmol) was dissolved in a mixture of CH₂Cl₂ (20 mL) and DMF (2 mL) and stirred at room temperature for 5 min. Acetyl chloride (133 μL, 1.875 mmol) was added to the stirring reaction mixture at 0 °C and the solution was allowed to react for 1.5 h. Solvents were removed and the crude residue was purified using silica gel column chromatography (0-10% MeOH in CH₂Cl₂) to obtain the compound **5a** (106 mg, 42%). ¹H NMR (500 MHz, CDCl₃) δ 9.20 (d, *J* = 5.5 Hz, 1H), 8.86 (s, 1H), 8.46 (s, 1H), 8.41 (dd, *J* = 8.3, 1.0 Hz, 1H), 7.62 (ddd, *J* = 8.3, 7.1, 1.3 Hz, 1H), 7.41 – 7.32 (m, 2H), 2.26 (s, 3H). ¹³C NMR (126 MHz, CDCl₃) δ 169.1, 137.9, 132.1, 126.6, 126.3, 123.6, 123.3, 122.9, 117.6, 24.6. MS (ESI) calculated for C₁₁H₁₀N₂O₂, *m/z* 202.07, found 203.08 [M+H]⁺.

Compounds **5b-5q** were synthesized similarly as compound **5a**.

5b: N-(4-hydroxyquinolin-3-yl)propionamide. 132 mg, 43%. ¹H NMR (500 MHz, CDCl₃) δ 9.29 (s, 1H), 8.71 (s, 1H), 8.42 (d, *J* = 7.7 Hz, 1H), 7.64 (t, *J* = 7.4 Hz, 1H), 7.49 (s, 1H), 7.38 (s, 1H), 2.56 (dd, *J* = 14.2, 7.0 Hz, 2H), 1.31 (t, *J* = 7.5 Hz, 3H). ¹³C NMR (126 MHz, CDCl₃) δ 137.9, 132.2, 126.1, 126.1, 124.5, 124.1, 124.0, 123.9, 118.0, 30.6, 9.9. MS (ESI) calculated for C₁₂H₁₂N₂O₂, *m/z* 216.09, found 217.10 [M+H]⁺.

5c: N-(4-hydroxyquinolin-3-yl)butyramide. ¹H NMR (500 MHz, MeOD) δ 9.02 (s, 1H), 8.28 (dd, *J* = 8.3, 1.3 Hz, 1H), 7.68 (ddd, *J* = 8.4, 7.0, 1.4 Hz, 1H), 7.57 (d, *J* = 8.4 Hz, 1H), 7.42 – 7.35 (m, 1H), 2.46 (t, *J* = 7.5 Hz, 2H), 1.74 (dd, *J* = 14.9, 7.4 Hz, 2H), 1.01 (t, *J* = 7.4 Hz, 3H). ¹³C NMR (126 MHz, MeOD) δ 174.6, 172.2, 139.7, 133.1, 131.3, 126.2, 124.8, 124.7, 122.8, 119.4, 39.6, 20.3, 14.0. MS (ESI) calculated for C₁₃H₁₄N₂O₂, *m/z* 230.11, found 231.11 [M+H]⁺.

5d: N-(4-hydroxyquinolin-3-yl)pentanamide. 155 mg, 52%. ¹H NMR (500 MHz, CDCl₃) δ 10.61 (s, 1H), 9.18 (s, 1H), 8.98 (s, 1H), 8.19 (d, *J* = 8.0 Hz, 1H), 7.72 – 7.62 (m, 2H), 7.37 – 7.30 (m, 1H), 2.44 (t, *J* = 7.4 Hz, 2H), 1.60 – 1.52 (m, 2H), 1.32 (dq, *J* = 14.7, 7.4 Hz, 2H), 0.89 (dd, *J* = 12.5, 5.1 Hz, 3H). ¹³C NMR (126 MHz, CDCl₃) δ 171.6, 168.9, 138.0, 131.4, 129.1, 124.0, 123.0, 122.9, 121.4, 118.5, 27.4, 21.9, 13.8. MS (ESI) calculated for C₁₄H₁₆N₂O₂, *m/z* 244.12, found 245.13 [M+H]⁺.

5e: N-(4-hydroxyquinolin-3-yl)hexanamide. 141 mg, 44%. ¹H NMR (500 MHz, CDCl₃) δ 9.65 (s, 1H), 8.44 (d, *J* = 8.2 Hz, 1H), 8.31 (d, *J* = 7.2 Hz, 1H), 7.88 (t, *J* = 7.4 Hz, 1H), 7.68 (t, *J* = 7.3 Hz, 1H), 2.82 (t, *J* = 6.5 Hz, 2H), 1.88 – 1.76 (m, 2H), 1.48 – 1.35 (m, 4H), 0.92 (t, *J* = 7.0 Hz,

3H). ^{13}C NMR (126 MHz, CDCl_3) δ 177.9, 137.1, 133.7, 128.0, 124.8, 122.0, 120.7, 120.1, 36.1, 31.3, 25.6, 22.5, 14.1. MS (ESI) calculated for $\text{C}_{15}\text{H}_{18}\text{N}_2\text{O}_2$, m/z 258.14, found 259.15 $[\text{M}+\text{H}]^+$.

5f: *N*-(4-hydroxyquinolin-3-yl)heptanamide. 105 mg, 31%. ^1H NMR (500 MHz, CDCl_3) δ 9.24 (d, $J = 6.3$ Hz, 1H), 8.88 (d, $J = 1.6$ Hz, 1H), 8.46 (s, 1H), 8.43 – 8.40 (m, 1H), 7.62 (ddd, $J = 8.4, 7.1, 1.4$ Hz, 1H), 7.40 – 7.33 (m, 2H), 2.49 – 2.44 (m, 2H), 1.80 – 1.72 (m, 2H), 1.44 – 1.36 (m, 2H), 1.32 (td, $J = 7.1, 3.5$ Hz, 4H), 0.89 (dd, $J = 9.7, 4.3$ Hz, 3H). ^{13}C NMR (126 MHz, CDCl_3) δ 172.3, 170.7, 138.0, 132.0, 126.5, 126.3, 123.5, 123.3, 122.8, 117.6, 37.7, 31.7, 29.1, 25.8, 22.6, 14.2. MS (ESI) calculated for $\text{C}_{16}\text{H}_{20}\text{N}_2\text{O}_2$, m/z 272.15, found 273.16 $[\text{M}+\text{H}]^+$.

5g: *N*-(4-hydroxyquinolin-3-yl)octanamide. 263 mg, 73%. ^1H NMR (500 MHz, CDCl_3) δ 9.25 (d, $J = 6.4$ Hz, 1H), 8.99 (s, 1H), 8.46 (s, 1H), 8.43 – 8.40 (m, 1H), 7.62 (ddd, $J = 8.4, 7.0, 1.4$ Hz, 1H), 7.40 – 7.33 (m, 2H), 2.49 – 2.44 (m, 2H), 1.81 – 1.73 (m, 2H), 1.41 – 1.24 (m, 8H), 0.88 (t, $J = 6.9$ Hz, 3H). ^{13}C NMR (126 MHz, CDCl_3) δ 172.3, 170.8, 138.0, 132.0, 126.6, 126.3, 123.5, 123.3, 122.8, 117.6, 37.7, 31.9, 29.4, 29.2, 25.9, 22.8, 14.2. MS (ESI) calculated for $\text{C}_{17}\text{H}_{22}\text{N}_2\text{O}_2$, m/z 286.17, found 287.18 $[\text{M}+\text{H}]^+$.

5h: *N*-(4-hydroxyquinolin-3-yl)decanamide. 231 mg, 59%. ^1H NMR (500 MHz, CDCl_3) δ 9.24 (s, 1H), 8.47 (s, 1H), 8.41 (dd, $J = 8.2, 1.0$ Hz, 1H), 7.63 – 7.58 (m, 1H), 7.40 (d, $J = 8.4$ Hz, 1H), 7.37 – 7.32 (m, 1H), 2.50 – 2.43 (m, 2H), 1.80 – 1.72 (m, 2H), 1.43 – 1.20 (m, 12H), 0.87 (t, $J = 7.0$ Hz, 3H). ^{13}C NMR (126 MHz, CDCl_3) δ 172.4, 170.8, 138.0, 132.0, 126.8, 126.2, 123.5, 123.3, 122.7, 117.7, 37.7, 32.0, 29.6, 29.5, 29.4, 29.4, 25.9, 22.8, 14.3. MS (ESI) calculated for $\text{C}_{19}\text{H}_{26}\text{N}_2\text{O}_2$, m/z 314.20, found 315.21 $[\text{M}+\text{H}]^+$.

Synthesis of compound 6a: 2-Methylthiazolo[4,5-c]quinoline. To a solution of compound **5a** (100 mg, 0.49 mmol) in pyridine (10 mL), was added phosphorous pentasulfide (109 mg, 0.49 mmol) and reaction mixture was refluxed for 2 h. The resulting solution was cooled to room temperature and pyridine was removed under reduced pressure. The residue was dissolved in water and pH was adjusted to 8 with saturated sodium bicarbonate solution and extracted in ethyl acetate. The organic layer was dried over sodium sulfate and concentrated to afford compound **6a** (64 mg, 65%). ¹H NMR (500 MHz, CDCl₃) δ 9.42 (s, 1H), 8.23 (d, *J* = 8.3 Hz, 1H), 7.94 (dd, *J* = 8.1, 0.9 Hz, 1H), 7.73 (ddd, *J* = 8.4, 7.0, 1.4 Hz, 1H), 7.62 (ddd, *J* = 8.1, 7.1, 1.1 Hz, 1H), 2.94 (s, 3H). ¹³C NMR (126 MHz, CDCl₃) δ 167.5, 148.0, 145.6, 144.3, 141.1, 130.6, 128.8, 127.6, 125.0, 123.5, 20.3. MS (ESI) calculated for C₁₁H₈N₂S, *m/z* 200.04, found 201.05 [M+H]⁺.

Compounds **6b-6q** were synthesized similarly as compound **6a**.

6b: 2-Ethylthiazolo[4,5-c]quinoline. 90 mg, 70%. ¹H NMR (500 MHz, CDCl₃) δ 9.45 (s, 1H), 8.24 (d, *J* = 8.3 Hz, 1H), 7.99 – 7.94 (m, 1H), 7.73 (ddd, *J* = 8.4, 7.0, 1.4 Hz, 1H), 7.64 (ddd, *J* = 8.1, 7.1, 1.1 Hz, 1H), 3.26 (q, *J* = 7.6 Hz, 2H), 1.54 (dd, *J* = 10.6, 4.5 Hz, 3H). ¹³C NMR (126 MHz, CDCl₃) δ 174.2, 147.9, 145.8, 144.2, 140.6, 130.6, 128.8, 127.6, 125.0, 123.6, 28.0, 14.0. MS (ESI) calculated for C₁₂H₁₀N₂S, *m/z* 214.06, found 215.08 [M+H]⁺.

6c: 2-Propylthiazolo[4,5-c]quinoline. 950 mg, 95%. ¹H NMR (400 MHz, CDCl₃) δ 9.45 (s, 1H), 8.24 (d, *J* = 8.3 Hz, 1H), 7.97 (dd, *J* = 8.1, 0.9 Hz, 1H), 7.74 (ddd, *J* = 8.4, 7.0, 1.4 Hz, 1H), 7.69 – 7.59 (m, 1H), 3.26 – 3.11 (m, 2H), 2.04 – 1.92 (m, 2H), 1.10 (t, *J* = 7.4 Hz, 3H). ¹³C NMR (126 MHz, CDCl₃) δ 172.8, 147.9, 145.8, 144.3, 140.7, 130.6, 128.8, 127.6, 125.0, 123.6, 36.4, 23.3, 13.8. MS (ESI) calculated for C₁₃H₁₂N₂S, *m/z* 228.07, found 229.08 [M+H]⁺.

6d: 2-Butylthiazolo[4,5-c]quinoline. 108 mg, 73%. ^1H NMR (500 MHz, CDCl_3) δ 9.44 (s, 1H), 8.24 (d, $J = 8.4$ Hz, 1H), 7.96 (dd, $J = 8.1, 0.9$ Hz, 1H), 7.73 (ddd, $J = 8.4, 5.4, 1.4$ Hz, 1H), 7.63 (ddd, $J = 8.1, 7.1, 1.1$ Hz, 1H), 3.25 – 3.19 (m, 2H), 1.97 – 1.89 (m, 2H), 1.55 – 1.46 (m, 2H), 1.00 (t, $J = 7.4$ Hz, 3H). ^{13}C NMR (126 MHz, CDCl_3) δ 173.0, 147.9, 145.8, 144.2, 140.6, 130.6, 128.8, 128.8, 127.6, 125.0, 123.6, 34.2, 32.0, 22.4, 13.9. MS (ESI) calculated for $\text{C}_{14}\text{H}_{14}\text{N}_2\text{S}$, m/z 242.09, found 243.10 $[\text{M}+\text{H}]^+$.

6e: 2-Pentylthiazolo[4,5-c]quinoline. 104 mg, 76%. ^1H NMR (500 MHz, CDCl_3) δ 9.45 (s, 1H), 8.24 (d, $J = 8.3$ Hz, 1H), 7.96 (dd, $J = 8.1, 0.9$ Hz, 1H), 7.73 (ddd, $J = 8.4, 7.0, 1.4$ Hz, 1H), 7.63 (ddd, $J = 8.1, 7.1, 1.1$ Hz, 1H), 3.24 – 3.17 (m, 2H), 1.95 (dt, $J = 15.3, 7.7$ Hz, 2H), 1.50 – 1.36 (m, 4H), 0.93 (t, $J = 7.2$ Hz, 3H). ^{13}C NMR (126 MHz, CDCl_3) δ 173.1, 147.9, 145.8, 144.2, 140.7, 130.6, 128.8, 127.6, 125.0, 123.6, 34.4, 31.4, 29.6, 22.5, 14.1. MS (ESI) calculated for $\text{C}_{15}\text{H}_{16}\text{N}_2\text{S}$, m/z 256.10, found 257.14 $[\text{M}+\text{H}]^+$.

6f: 2-Hexylthiazolo[4,5-c]quinoline. 93 mg, 96%. ^1H NMR (500 MHz, CDCl_3) δ 9.45 (s, 1H), 8.24 (d, $J = 8.4$ Hz, 1H), 7.97 (dd, $J = 8.1, 0.9$ Hz, 1H), 7.74 (ddd, $J = 8.4, 7.0, 1.4$ Hz, 1H), 7.66 – 7.62 (m, 1H), 3.25 – 3.19 (m, 2H), 1.98 – 1.90 (m, 2H), 1.48 (dd, $J = 10.5, 4.5$ Hz, 2H), 1.36 (ddd, $J = 16.3, 7.0, 4.9$ Hz, 4H), 0.90 (dd, $J = 9.4, 4.7$ Hz, 3H). ^{13}C NMR (126 MHz, CDCl_3) δ 173.1, 147.9, 145.8, 144.3, 140.7, 130.6, 128.8, 127.6, 125.0, 123.6, 34.5, 31.6, 29.9, 28.9, 22.6, 14.2. MS (ESI) calculated for $\text{C}_{16}\text{H}_{18}\text{N}_2\text{S}$, m/z 270.12, found 271.14 $[\text{M}+\text{H}]^+$.

6g: 2-Heptylthiazolo[4,5-c]quinoline. 108 mg, 42%. ^1H NMR (500 MHz, CDCl_3) δ 9.44 (s, 1H), 8.23 (d, $J = 8.4$ Hz, 1H), 7.96 (dd, $J = 8.1, 0.9$ Hz, 1H), 7.73 (ddd, $J = 8.4, 7.0, 1.4$ Hz, 1H), 7.65 – 7.60 (m, 1H), 3.22 – 3.17 (m, 2H), 1.94 (dt, $J = 15.3, 7.6$ Hz, 3H), 1.50 – 1.43 (m, 3H), 1.40 – 1.35 (m, 2H), 1.31 – 1.27 (m, 4H), 0.88 (t, $J = 7.0$ Hz, 3H). ^{13}C NMR (126 MHz, CDCl_3) δ 173.1,

147.9, 145.8, 144.2, 140.6, 130.6, 128.8, 127.6, 125.0, 123.6, 34.5, 31.8, 29.9, 29.2, 29.1, 22.7, 14.2. MS (ESI) calculated for C₁₇H₂₀N₂S, m/z 284.13, found 285.17 [M+H]⁺.

6h: 2-Nonylthiazolo[4,5-c]quinoline. 157 mg, 52%. ¹H NMR (500 MHz, CDCl₃) δ 9.45 (s, 1H), 8.24 (d, *J* = 8.4 Hz, 1H), 7.96 (d, *J* = 8.1 Hz, 1H), 7.73 (ddd, *J* = 8.4, 5.3, 1.4 Hz, 1H), 7.63 (t, *J* = 7.5 Hz, 1H), 3.23 – 3.18 (m, 2H), 1.94 (dt, *J* = 15.4, 7.7 Hz, 2H), 1.51 – 1.43 (m, 2H), 1.40 – 1.34 (m, 2H), 1.31 – 1.24 (m, 8H), 0.87 (t, *J* = 6.9 Hz, 3H). ¹³C NMR (126 MHz, CDCl₃) δ 173.1, 147.9, 145.8, 144.2, 130.6, 128.8, 128.7, 127.6, 125.0, 123.6, 120.3, 34.5, 32.0, 29.9, 29.5, 29.4, 29.4, 29.2, 22.8, 14.2. MS (ESI) calculated for C₁₉H₂₄N₂S, m/z 312.17, found 313.19 [M+H]⁺.

6i: 2-Isopropylthiazolo[4,5-c]quinoline. 164 mg, 83%. ¹H NMR (500 MHz, CDCl₃) δ 9.46 (s, 1H), 8.24 (d, *J* = 8.2 Hz, 1H), 8.01 – 7.96 (m, 1H), 7.73 (ddd, *J* = 8.4, 7.0, 1.4 Hz, 1H), 7.64 (ddd, *J* = 8.1, 7.0, 1.2 Hz, 1H), 3.58 – 3.48 (m, 1H), 1.56 (d, *J* = 6.9 Hz, 6H). ¹³C NMR (126 MHz, CDCl₃) δ 179.3, 147.8, 145.9, 144.2, 140.2, 130.6, 128.8, 127.6, 125.0, 123.7, 34.3, 23.1. MS (ESI) calculated for C₁₃H₁₂N₂S, m/z 228.10, found 229.08 [M+H]⁺.

6j: 2-Isobutylthiazolo[4,5-c]quinoline. 150 mg, 72%. ¹H NMR (500 MHz, MeOD) δ 9.31 (s, 1H), 8.18 (d, *J* = 8.3 Hz, 1H), 8.11 (dd, *J* = 8.1, 0.9 Hz, 1H), 7.81 (ddd, *J* = 8.4, 7.0, 1.4 Hz, 1H), 7.73 (ddd, *J* = 8.1, 7.1, 1.2 Hz, 1H), 2.30 (m, *J* = 13.7, 6.8 Hz, 1H), 1.08 (d, *J* = 6.6 Hz, 6H). ¹³C NMR (126 MHz, MeOD) δ 174.5, 148.7, 146.0, 144.7, 142.6, 130.5, 130.4, 129.3, 126.2, 124.7, 43.7, 31.1, 22.6. MS (ESI) calculated for C₁₄H₁₄N₂S, m/z 242.09, found 243.09 [M+H]⁺.

6l: 2-Isopentylthiazolo[4,5-c]quinoline. 165 mg, 75%. ¹H NMR (500 MHz, CDCl₃) δ 9.44 (s, 1H), 8.26 – 8.22 (m, 1H), 7.98 – 7.95 (m, 1H), 7.73 (ddd, *J* = 8.4, 7.0, 1.4 Hz, 1H), 7.64 (ddd, *J*

= 8.1, 7.0, 1.2 Hz, 1H), 3.26 – 3.20 (m, 2H), 1.88 – 1.82 (m, 2H), 1.75 (dd, $J = 13.3, 6.7$ Hz, 1H), 1.01 (d, $J = 6.6$ Hz, 6H). ^{13}C NMR (126 MHz, CDCl_3) δ 173.2, 147.9, 145.8, 144.3, 140.6, 130.6, 128.8, 127.6, 125.0, 123.6, 38.8, 32.5, 27.9, 22.5. MS (ESI) calculated for $\text{C}_{15}\text{H}_{16}\text{N}_2\text{S}$, m/z 256.10.10, found 257.10 $[\text{M}+\text{H}]^+$.

6o: (S)-2-(2-methylbutyl)thiazolo[4,5-c]quinoline. 170 mg, 77%. ^1H NMR (500 MHz, CDCl_3) δ 9.45 (s, 1H), 8.24 (d, $J = 8.3$ Hz, 1H), 7.96 (dd, $J = 8.1, 0.9$ Hz, 1H), 7.73 (ddd, $J = 8.4, 7.0, 1.4$ Hz, 1H), 7.63 (ddd, $J = 8.1, 7.1, 1.1$ Hz, 1H), 3.21 (dd, $J = 14.6, 6.2$ Hz, 1H), 3.01 (dd, $J = 14.6, 8.2$ Hz, 1H), 2.12 – 2.02 (m, 1H), 1.58 – 1.48 (m, 1H), 1.40 – 1.30 (m, 1H), 1.03 (d, $J = 6.7$ Hz, 3H), 0.98 (t, $J = 7.4$ Hz, 3H). ^{13}C NMR (126 MHz, CDCl_3) δ 172.1, 147.9, 145.8, 144.2, 140.8, 130.6, 128.8, 127.6, 125.0, 123.6, 41.4, 36.3, 29.4, 19.2, 11.5. MS (ESI) calculated for $\text{C}_{15}\text{H}_{16}\text{N}_2\text{S}$, m/z 256.10, found 257.10 $[\text{M}+\text{H}]^+$.

6p: 2-(3,3,3-Trifluoropropyl)thiazolo[4,5-c]quinoline. 180 mg, 74%. ^1H NMR (500 MHz, CDCl_3) δ 9.45 (s, 1H), 8.26 (d, $J = 8.4$ Hz, 1H), 7.99 – 7.95 (m, 1H), 7.76 (ddd, $J = 8.4, 7.0, 1.4$ Hz, 1H), 7.66 (ddd, $J = 8.1, 7.0, 1.2$ Hz, 1H), 3.51 – 3.45 (m, 2H), 2.91 – 2.80 (m, 2H). ^{13}C NMR (126 MHz, CDCl_3) δ 168.0, 147.7, 145.8, 144.4, 140.8, 130.7, 129.2, 127.8, 126.4 (q, $1\text{JCF} = 276.5$ Hz), 125.0, 123.4, 33.0 (q, $2\text{JCF} = 29.8$ Hz), 27.0 (q, $3\text{JCF} = 3.5$ Hz). MS (ESI) calculated for $\text{C}_{13}\text{H}_9\text{F}_3\text{N}_2\text{S}$, m/z 282.04, found 283.04 $[\text{M}+\text{H}]^+$.

6q: 2-(4,4,4-Trifluorobutyl)thiazolo[4,5-c]quinoline. 190 mg, 75%. ^1H NMR (500 MHz, CDCl_3) δ 9.46 (s, 1H), 8.26 (d, $J = 8.2$ Hz, 1H), 8.00 – 7.95 (m, 1H), 7.76 (ddd, $J = 8.4, 7.0, 1.4$ Hz, 1H), 7.66 (ddd, $J = 8.1, 7.0, 1.2$ Hz, 1H), 3.32 (t, $J = 7.2$ Hz, 2H), 2.37 – 2.22 (m, 4H). ^{13}C NMR (126 MHz, CDCl_3) δ 170.4, 147.9, 145.8, 144.4, 140.7, 130.7, 129.1, 127.8, 127.0 (q, $1\text{JCF} = 276.4$

Hz), 125.0, 123.5, 33.9 (q, $2J_{CF} = 28.9$ Hz), 33.0, 21.1 (q, $3J_{CF} = 3.0$ Hz). MS (ESI) calculated for $C_{14}H_{11}F_3N_2S$, m/z 296.05, found 297.06 $[M+H]^+$.

Synthesis of compound 7a: 2-Methylthiazolo[4,5-c]quinoline 5-oxide. To a solution of compound **6a** (57 mg, 0.28 mmol) in $CHCl_3$ (10 mL), was added *m*-chloroperoxybenzoic acid (95 mg, 0.43 mmol) and the reaction mixture was stirred at room temperature for 18 h. The solvent was then removed under reduced pressure and the crude residue was purified using silica gel column chromatography (5% MeOH/ CH_2Cl_2) to obtain compound **7a** (57 mg, 94%). 1H NMR (500 MHz, $CDCl_3$) δ 9.13 (s, 1H), 8.89 (d, $J = 8.9$ Hz, 1H), 7.94 (dd, $J = 7.9, 1.1$ Hz, 1H), 7.81 – 7.72 (m, 2H), 2.93 (s, 3H). ^{13}C NMR (126 MHz, $CDCl_3$) δ 169.7, 147.2, 139.0, 131.5, 131.1, 129.9, 129.7, 125.6, 123.8, 121.6, 20.4. MS (ESI) calculated for $C_{11}H_8N_2OS$, m/z 216.04, found 217.05 $[M+H]^+$.

Compounds **7b-7q** were synthesized similarly as compound **7a**.

7b: 2-Ethylthiazolo[4,5-c]quinoline 5-oxide. 81 mg, 88%. 1H NMR (500 MHz, $CDCl_3$) δ 9.15 (s, 1H), 8.90 (dd, $J = 8.6, 0.8$ Hz, 1H), 7.95 (dd, $J = 8.0, 1.0$ Hz, 1H), 7.82 – 7.72 (m, 2H), 3.23 (q, $J = 7.6$ Hz, 2H), 1.53 (d, $J = 15.1$ Hz, 3H). ^{13}C NMR (126 MHz, $CDCl_3$) δ 176.4, 147.1, 139.0, 131.6, 130.7, 129.9, 129.6, 125.6, 123.9, 121.6, 28.0, 13.9. MS (ESI) calculated for $C_{12}H_{10}N_2OS$, m/z 230.05, found 231.06 $[M+H]^+$.

7c: 2-Propylthiazolo[4,5-c]quinoline 5-oxide. 950 mg, 88%. 1H NMR (400 MHz, $CDCl_3$) δ 9.14 (s, 1H), 8.90 (d, $J = 8.7$ Hz, 1H), 7.95 (dd, $J = 7.9, 1.1$ Hz, 1H), 7.82 – 7.71 (m, 2H), 3.17 (t, $J = 7.6$ Hz, 2H), 1.95 (dt, $J = 14.9, 7.4$ Hz, 2H), 1.09 (t, $J = 7.4$ Hz, 3H). ^{13}C NMR (126 MHz, $CDCl_3$) δ 175.0, 147.1, 139.0, 131.6, 130.7, 129.9, 129.6, 123.9, 121.6, 36.4, 23.2, 13.8. MS (ESI) calculated for $C_{13}H_{12}N_2OS$, m/z 244.07, found 245.07 $[M+H]^+$.

7d: 2-Butylthiazolo[4,5-c]quinoline 5-oxide. 82 mg, 75%. ^1H NMR (500 MHz, CDCl_3) δ 9.13 (s, 1H), 8.90 – 8.86 (m, 1H), 7.94 (dd, $J = 7.9, 1.1$ Hz, 1H), 7.80 – 7.71 (m, 2H), 3.21 – 3.16 (m, 2H), 1.94 – 1.86 (m, 2H), 1.53 – 1.45 (m, 2H), 0.99 (t, $J = 7.4$ Hz, 3H). ^{13}C NMR (126 MHz, CDCl_3) δ 175.2, 147.1, 139.0, 131.6, 130.6, 129.9, 129.6, 125.6, 123.9, 121.6, 34.2, 31.8, 22.4, 13.9. MS (ESI) calculated for $\text{C}_{14}\text{H}_{14}\text{N}_2\text{OS}$, m/z 258.08, found 259.09 $[\text{M}+\text{H}]^+$.

7e: 2-Pentylthiazolo[4,5-c]quinoline 5-oxide. 90 mg, 87%. ^1H NMR (500 MHz, CDCl_3) δ 9.13 (s, 1H), 8.88 (d, $J = 8.1$ Hz, 1H), 7.94 (dd, $J = 8.0, 1.2$ Hz, 1H), 7.81 – 7.70 (m, 2H), 3.22 – 3.13 (m, 2H), 1.92 (dt, $J = 15.4, 7.7$ Hz, 2H), 1.48 – 1.36 (m, 4H), 0.92 (t, $J = 7.1$ Hz, 3H). ^{13}C NMR (126 MHz, CDCl_3) δ 175.3, 147.0, 138.9, 131.6, 130.7, 129.9, 129.6, 125.6, 123.9, 121.6, 34.5, 31.3, 29.5, 22.4, 14.0. MS (ESI) calculated for $\text{C}_{15}\text{H}_{16}\text{N}_2\text{OS}$, m/z 272.10, found 273.11 $[\text{M}+\text{H}]^+$.

7f: 2-Hexylthiazolo[4,5-c]quinoline 5-oxide. 65 mg, 76%. ^1H NMR (500 MHz, CDCl_3) δ 9.15 (s, 1H), 8.90 (d, $J = 8.5$ Hz, 1H), 7.96 (dd, $J = 8.0, 1.0$ Hz, 1H), 7.82 – 7.72 (m, 2H), 3.22 – 3.17 (m, 2H), 1.92 (dd, $J = 15.3, 7.7$ Hz, 2H), 1.51 – 1.44 (m, 2H), 1.40 – 1.30 (m, 4H), 0.90 (t, $J = 7.1$ Hz, 3H). ^{13}C NMR (126 MHz, CDCl_3) δ 175.3, 147.1, 139.0, 131.7, 130.8, 129.9, 129.6, 125.6, 123.9, 121.6, 34.5, 31.6, 29.8, 28.9, 22.6, 14.2. MS (ESI) calculated for $\text{C}_{16}\text{H}_{18}\text{N}_2\text{OS}$, m/z 286.11, found 287.12 $[\text{M}+\text{H}]^+$.

7g: 2-Heptylthiazolo[4,5-c]quinoline 5-oxide. 81 mg, 75%. ^1H NMR (500 MHz, CDCl_3) δ 9.13 (s, 1H), 8.88 (dd, $J = 8.7, 0.8$ Hz, 1H), 7.94 (dd, $J = 7.9, 1.1$ Hz, 1H), 7.80 – 7.71 (m, 2H), 3.21 – 3.15 (m, 2H), 1.91 (dt, $J = 15.3, 7.6$ Hz, 2H), 1.49 – 1.42 (m, 2H), 1.41 – 1.35 (m, 2H), 1.32 – 1.26 (m, 4H), 0.88 (t, $J = 7.0$ Hz, 3H). ^{13}C NMR (126 MHz, CDCl_3) δ 175.3, 147.0, 138.9, 131.6, 130.7, 129.9, 129.6, 125.6, 123.9, 121.6, 34.5, 31.7, 29.8, 29.2, 29.0, 22.7, 14.2. MS (ESI) calculated for $\text{C}_{17}\text{H}_{20}\text{N}_2\text{OS}$, m/z 300.13, found 301.14 $[\text{M}+\text{H}]^+$.

7h: 2-Nonylthiazolo[4,5-c]quinoline 5-oxide. 105 mg, 66%. ^1H NMR (500 MHz, CDCl_3) δ 9.13 (s, 1H), 8.88 (d, $J = 8.5$ Hz, 1H), 7.93 (dd, $J = 7.9, 1.1$ Hz, 1H), 7.81 – 7.69 (m, 2H), 3.19 – 3.14 (m, 2H), 1.91 (dt, $J = 15.3, 7.6$ Hz, 2H), 1.45 (dt, $J = 14.9, 7.0$ Hz, 2H), 1.35 (dd, $J = 14.2, 6.9$ Hz, 2H), 1.29 – 1.21 (m, 8H), 0.86 (t, $J = 6.9$ Hz, 3H). ^{13}C NMR (126 MHz, CDCl_3) δ 175.3, 147.0, 138.9, 131.6, 130.7, 129.8, 129.6, 125.6, 123.9, 121.5, 34.5, 31.9, 29.8, 29.5, 29.3, 29.2, 22.8, 14.2. MS (ESI) calculated for $\text{C}_{19}\text{H}_{24}\text{N}_2\text{OS}$, m/z 328.16, found 329.17 $[\text{M}+\text{H}]^+$.

7i: 2-Isopropylthiazolo[4,5-c]quinoline 5-oxide. 150 mg, 62%. ^1H NMR (500 MHz, CDCl_3) δ 9.15 (s, 1H), 8.90 (dd, $J = 8.7, 1.0$ Hz, 1H), 7.99 – 7.95 (m, 1H), 7.79 (ddd, $J = 8.6, 7.0, 1.5$ Hz, 1H), 7.77 – 7.72 (m, 1H), 3.54 – 3.45 (m, 1H), 1.54 (d, $J = 6.9$ Hz, 6H). ^{13}C NMR (126 MHz, CDCl_3) δ 181.5, 147.0, 138.9, 131.7, 130.3, 129.9, 129.6, 125.6, 124.0, 121.6, 34.4, 23.0. MS (ESI) calculated for $\text{C}_{13}\text{H}_{12}\text{N}_2\text{OS}$, m/z 244.07.10, found 245.07 $[\text{M}+\text{H}]^+$.

7j: 2-Isobutylthiazolo[4,5-c]quinoline 5-oxide. 80 mg, 75%. ^1H NMR (500 MHz, MeOD) δ 9.26 (s, 1H), 8.79 (dd, $J = 8.6, 0.9$ Hz, 1H), 8.25 – 8.21 (m, 1H), 7.95 (ddd, $J = 8.7, 7.1, 1.5$ Hz, 1H), 7.90 (ddd, $J = 8.2, 7.1, 1.4$ Hz, 1H), 3.14 (d, $J = 7.2$ Hz, 2H), 2.35 – 2.25 (m, 1H), 1.09 (d, $J = 6.6$ Hz, 6H). ^{13}C NMR (126 MHz, MeOD) δ 176.8, 147.8, 139.0, 135.3, 133.5, 131.7, 131.6, 127.2, 125.2, 121.5, 43.7, 31.0, 22.6. MS (ESI) calculated for $\text{C}_{14}\text{H}_{14}\text{N}_2\text{OS}$, m/z 258.08.10, found 259.08 $[\text{M}+\text{H}]^+$.

7k: 2-Neopentylthiazolo[4,5-c]quinoline 5-oxide. 80 mg, 75%. ^1H NMR (500 MHz, MeOD) δ 9.31 (s, 1H), 8.79 (dd, $J = 8.7, 0.9$ Hz, 1H), 8.26 – 8.22 (m, 1H), 7.99 – 7.88 (m, 2H), 3.16 (s, 2H), 1.13 (s, 9H). ^{13}C NMR (126 MHz, MeOD) δ 174.7, 147.8, 138.8, 135.9, 133.8, 131.8, 131.7, 127.3, 125.1, 121.4, 48.3, 33.2, 29.9. MS (ESI) calculated for $\text{C}_{14}\text{H}_{16}\text{N}_2\text{OS}$, m/z 272.10, found 273.10 $[\text{M}+\text{H}]^+$.

7l: 2-Isopentylthiazolo[4,5-c]quinoline 5-oxide. 110 mg, 69%. ^1H NMR (500 MHz, MeOD) δ 9.23 (s, 1H), 8.77 (dd, $J = 8.6, 0.9$ Hz, 1H), 8.21 – 8.18 (m, 1H), 7.93 (ddd, $J = 8.7, 7.0, 1.5$ Hz, 1H), 7.89 (ddd, $J = 8.2, 7.1, 1.3$ Hz, 1H), 3.27 (dd, $J = 8.4, 7.4$ Hz, 2H), 1.88 – 1.82 (m, 2H), 1.78 – 1.69 (m, 1H), 1.02 (d, $J = 6.6$ Hz, 6H). ^{13}C NMR (126 MHz, MeOD) δ 178.1, 147.7, 138.9, 135.1, 133.5, 131.6, 131.6, 127.1, 125.1, 121.5, 39.6, 33.1, 28.8, 22.6. MS (ESI) calculated for $\text{C}_{15}\text{H}_{16}\text{N}_2\text{OS}$, m/z 272.10, found 273.10 $[\text{M}+\text{H}]^+$.

7m: 2-(3,3-Dimethylbutyl)thiazolo[4,5-c]quinoline 5-oxide. 80 mg, 76%. ^1H NMR (500 MHz, MeOD) δ 9.22 (s, 1H), 8.77 (dd, $J = 8.7, 0.9$ Hz, 1H), 8.21 – 8.18 (m, 1H), 7.93 (ddd, $J = 8.7, 7.1, 1.5$ Hz, 1H), 7.89 (ddd, $J = 8.2, 7.1, 1.3$ Hz, 1H), 3.27 – 3.22 (m, 2H), 1.89 – 1.84 (m, 2H), 1.04 (s, 9H). ^{13}C NMR (126 MHz, MeOD) δ 178.7, 147.7, 138.9, 135.1, 133.4, 131.6, 131.6, 127.1, 125.1, 121.4, 44.7, 31.5, 30.9, 29.5. MS (ESI) calculated for $\text{C}_{16}\text{H}_{18}\text{N}_2\text{OS}$, m/z 286.11, found 287.11 $[\text{M}+\text{H}]^+$.

7n: (S)-2-(sec-butyl)thiazolo[4,5-c]quinoline 5-oxide. 117 mg, 78%. ^1H NMR (500 MHz, MeOD) δ 9.23 (s, 1H), 8.77 (dd, $J = 8.6, 1.0$ Hz, 1H), 8.22 – 8.18 (m, 1H), 7.93 (ddd, $J = 8.7, 7.1, 1.5$ Hz, 1H), 7.88 (ddd, $J = 8.2, 7.1, 1.4$ Hz, 1H), 3.35 (dd, $J = 13.9, 6.9$ Hz, 1H), 2.04 – 1.94 (m, 1H), 1.92 – 1.82 (m, 1H), 1.52 (d, $J = 6.9$ Hz, 3H), 1.02 (t, $J = 7.4$ Hz, 3H). ^{13}C NMR (126 MHz, MeOD) δ 183.1, 147.7, 138.9, 134.7, 133.5, 131.6, 131.6, 127.1, 125.2, 121.5, 42.3, 31.6, 20.9, 12.0. MS (ESI) calculated for $\text{C}_{14}\text{H}_{14}\text{N}_2\text{OS}$, m/z 258.09, found 259.08 $[\text{M}+\text{H}]^+$.

7o: (S)-2-(2-methylbutyl)thiazolo[4,5-c]quinoline 5-oxide. 103 mg, 74%. ^1H NMR (500 MHz, MeOD) δ 9.24 (s, 1H), 8.78 (dd, $J = 8.7, 0.8$ Hz, 1H), 8.23 – 8.19 (m, 1H), 7.94 (ddd, $J = 8.7, 7.1, 1.5$ Hz, 1H), 7.89 (dd, 1H), 3.26 (dd, $J = 14.7, 6.2$ Hz, 1H), 3.06 (dd, $J = 14.7, 8.0$ Hz, 1H), 2.14 – 2.03 (m, 1H), 1.60 – 1.50 (m, 1H), 1.44 – 1.30 (m, 1H), 1.04 (d, $J = 6.7$ Hz, 3H), 1.00 (t, J

= 7.4 Hz, 3H). ^{13}C NMR (126 MHz, MeOD) δ 177.0, 147.8, 139.0, 135.3, 133.5, 131.7, 131.6, 127.1, 125.1, 121.5, 41.8, 37.4, 30.2, 19.4, 11.6. MS (ESI) calculated for $\text{C}_{15}\text{H}_{16}\text{N}_2\text{OS}$, m/z 272.10, found 273.10 $[\text{M}+\text{H}]^+$.

7p: 2-(3,3,3-Trifluoropropyl)thiazolo[4,5-c]quinoline 5-oxide. 120 mg, 75%. ^1H NMR (500 MHz, MeOD) δ 9.24 (s, 1H), 8.76 (dd, $J = 8.8, 0.7$ Hz, 1H), 8.17 (dd, 1H), 7.93 (ddd, $J = 8.6, 7.0, 1.4$ Hz, 1H), 7.88 (ddd, $J = 8.2, 7.1, 1.3$ Hz, 1H), 3.54 (t, 2H), 2.99 – 2.87 (m, 2H). ^{13}C NMR (126 MHz, MeOD) δ 173.8, 147.6, 139.1, 135.2, 133.6, 131.8, 131.6, 128.1 (q, $1\text{JCF} = 275.6$ Hz), 127.1, 125.0, 121.5, 33.2 (q, $2\text{JCF} = 29.7$ Hz), 27.7 (q, $3\text{JCF} = 3.5$ Hz). MS (ESI) calculated for $\text{C}_{13}\text{H}_9\text{F}_3\text{N}_2\text{OS}$, m/z 298.04, found 299.04 $[\text{M}+\text{H}]^+$.

7q: 2-(4,4,4-Trifluorobutyl)thiazolo[4,5-c]quinoline 5-oxide. 128 mg, 81%. ^1H NMR (500 MHz, MeOD) δ 9.26 (s, 1H), 8.80 – 8.74 (m, 1H), 8.22 – 8.18 (m, 1H), 7.94 (ddd, $J = 8.6, 7.1, 1.5$ Hz, 1H), 7.89 (ddd, $J = 8.2, 7.1, 1.3$ Hz, 1H), 3.36 (t, $J = 7.5$ Hz, 2H), 2.48 – 2.34 (m, 2H), 2.27 – 2.17 (m, 2H). ^{13}C NMR (126 MHz, MeOD) δ 176.0, 147.8, 139.0, 135.2, 133.6, 131.7, 131.6, 128.6 (q, $1\text{JCF} = 275.4$ Hz), 127.1, 125.1, 121.5, 33.6 (q, $2\text{JCF} = 29.0$ Hz), 33.5, 22.6 (q, $3\text{JCF} = 3.2$ Hz). MS (ESI) calculated for $\text{C}_{14}\text{H}_{11}\text{F}_3\text{N}_2\text{OS}$, m/z 312.05, found 313.05 $[\text{M}+\text{H}]^+$.

Synthesis of compound 8a: 2-Methylthiazolo[4,5-c]quinolin-4-amine. Compound **7a** (50 mg, 0.23 mmol) was dissolved in anhydrous CH_2Cl_2 (5 mL). Benzoyl isocyanate (68 mg, 0.46 mmol) was added to the reaction mixture and refluxed for 30 min. The solvent was then removed under vacuum and the residue was dissolved in anhydrous methanol (5 mL). Excess of sodium methoxide was added and the reaction mixture was refluxed for 2 h. After evaporating solvents under reduced pressure, the crude residue was purified using silica gel column chromatography (0-7% MeOH in CH_2Cl_2) to obtain compound **8a** as a white solid (41 mg, 82%).

^1H NMR (400 MHz, CDCl_3) δ 7.77 (dd, $J = 8.4, 0.5$ Hz, 1H), 7.72 (dd, $J = 8.0, 1.0$ Hz, 1H), 7.55 (ddd, $J = 8.4, 7.1, 1.5$ Hz, 1H), 7.31 (ddd, $J = 8.1, 7.1, 1.2$ Hz, 1H), 5.61 (s, 2H), 2.89 (s, 3H). ^{13}C NMR (126 MHz, CDCl_3) δ 165.9, 151.5, 144.8, 141.0, 138.1, 129.1, 126.8, 124.8, 123.2, 120.1, 20.1. MS (ESI) calculated for $\text{C}_{11}\text{H}_9\text{N}_3\text{S}$, m/z 215.05, found 216.06 $[\text{M}+\text{H}]^+$.

Compounds **8b-8q** were synthesized similarly as compound **8a**.

8b: 2-Ethylthiazolo[4,5-c]quinolin-4-amine. White solid (36 mg, 47%). ^1H NMR (400 MHz, CDCl_3) δ 7.77 (dd, $J = 8.4, 0.5$ Hz, 1H), 7.74 (dd, $J = 8.0, 1.1$ Hz, 1H), 7.56 (ddd, $J = 8.4, 7.1, 1.5$ Hz, 1H), 7.31 (ddd, $J = 8.1, 7.1, 1.1$ Hz, 1H), 5.58 (s, 2H), 3.20 (q, $J = 7.6$ Hz, 2H), 1.51 (t, $J = 7.6$ Hz, 3H). ^{13}C NMR (126 MHz, CDCl_3) δ 172.6, 151.6, 144.8, 140.4, 138.0, 129.0, 126.8, 124.8, 123.2, 120.2, 27.8, 14.1. MS (ESI) calculated for $\text{C}_{12}\text{H}_{11}\text{N}_3\text{S}$, m/z 229.07, found 230.08 $[\text{M}+\text{H}]^+$.

8c: 2-Propylthiazolo[4,5-c]quinolin-4-amine. White solid (450 mg, 90%). ^1H NMR (400 MHz, CDCl_3) δ 7.77 (d, $J = 8.4$ Hz, 1H), 7.73 (dd, $J = 8.0, 1.3$ Hz, 1H), 7.55 (ddd, $J = 8.4, 7.1, 1.4$ Hz, 1H), 7.34 – 7.27 (m, 1H), 5.67 (s, 2H), 3.13 (t, $J = 7.6$ Hz, 2H), 1.94 (dd, $J = 15.0, 7.4$ Hz, 2H), 1.09 (t, $J = 7.4$ Hz, 3H). ^{13}C NMR (126 MHz, CDCl_3) δ 171.2, 151.7, 144.7, 140.5, 138.0, 129.0, 126.8, 124.8, 123.1, 120.2, 36.2, 23.4, 13.8. MS (ESI) calculated for $\text{C}_{13}\text{H}_{13}\text{N}_3\text{S}$, m/z 243.08, found 244.09 $[\text{M}+\text{H}]^+$.

8d: 2-Butylthiazolo[4,5-c]quinolin-4-amine. White solid (25 mg, 32%). ^1H NMR (400 MHz, CDCl_3) δ 7.77 (dd, $J = 8.4, 0.6$ Hz, 1H), 7.73 (dd, $J = 8.0, 1.0$ Hz, 1H), 7.56 (ddd, $J = 8.5, 7.1, 1.5$ Hz, 1H), 7.31 (ddd, $J = 8.1, 7.1, 1.2$ Hz, 1H), 5.56 (s, 2H), 3.20 – 3.13 (m, 2H), 1.90 (dt, $J = 15.3, 7.6$ Hz, 2H), 1.50 (dq, $J = 14.7, 7.4$ Hz, 2H), 1.00 (t, $J = 7.4$ Hz, 3H). ^{13}C NMR (126 MHz,

CDCl₃) δ 171.5, 151.6, 144.7, 140.5, 138.0, 129.0, 126.8, 124.8, 123.2, 120.2, 34.0, 32.0, 22.4, 13.9. MS (ESI) calculated for C₁₄H₁₅N₃S, m/z 257.10, found 258.11 [M+H]⁺.

8e: 2-Pentylthiazolo[4,5-c]quinolin-4-amine. White solid (38 mg, 45%). ¹H NMR (400 MHz, CDCl₃) δ 7.77 (d, *J* = 8.1 Hz, 1H), 7.73 (dd, *J* = 8.0, 1.1 Hz, 1H), 7.55 (ddd, *J* = 8.4, 7.1, 1.4 Hz, 1H), 7.34 – 7.29 (m, 1H), 5.59 (s, 2H), 3.18 – 3.12 (m, 2H), 1.96 – 1.86 (m, 2H), 1.50 – 1.35 (m, 4H), 0.94 (t, *J* = 7.1 Hz, 3H). ¹³C NMR (126 MHz, CDCl₃) δ 171.5, 151.6, 144.7, 140.5, 138.0, 129.0, 126.8, 124.8, 123.2, 120.2, 34.3, 31.4, 29.7, 22.5, 14.1 MS (ESI) calculated for C₁₅H₁₇N₃S, m/z 271.11, found 272.12 [M+H]⁺.

8f: 2-Hexylthiazolo[4,5-c]quinolin-4-amine. White solid (25 mg, 44%). ¹H NMR (400 MHz, CDCl₃) δ 7.77 (dd, *J* = 8.4, 0.5 Hz, 1H), 7.73 (dd, *J* = 8.0, 1.0 Hz, 1H), 7.55 (ddd, *J* = 8.4, 7.1, 1.5 Hz, 1H), 7.31 (ddd, *J* = 8.1, 7.1, 1.1 Hz, 1H), 5.56 (s, 2H), 3.21 – 3.11 (m, 2H), 1.91 (dt, *J* = 15.3, 7.5 Hz, 2H), 1.46 (dt, *J* = 9.2, 7.0 Hz, 2H), 1.39 – 1.30 (m, 4H), 0.91 (t, *J* = 7.1 Hz, 3H). ¹³C NMR (126 MHz, CDCl₃) δ 171.6, 151.6, 144.7, 140.51, 138.0, 129.1, 126.8, 124.8, 123.2, 120.2, 34.3, 31.6, 30.0, 29.0, 22.6, 14.2. MS (ESI) calculated for C₁₆H₁₉N₃S, m/z 285.13, found 286.14 [M+H]⁺.

8g: 2-Heptylthiazolo[4,5-c]quinolin-4-amine. White solid (34 mg, 42%). ¹H NMR (400 MHz, CDCl₃) δ 7.77 (dd, *J* = 8.4, 0.5 Hz, 1H), 7.73 (dd, *J* = 8.0, 1.0 Hz, 1H), 7.55 (ddd, *J* = 8.4, 7.1, 1.5 Hz, 1H), 7.31 (ddd, *J* = 8.1, 7.1, 1.2 Hz, 1H), 5.56 (s, 2H), 3.20 – 3.08 (m, 2H), 1.91 (dt, *J* = 15.3, 7.6 Hz, 2H), 1.50 – 1.42 (m, 2H), 1.38 (ddd, *J* = 14.0, 8.2, 5.2 Hz, 2H), 1.30 (dt, *J* = 11.5, 3.9 Hz, 4H), 0.89 (t, *J* = 6.9 Hz, 3H). ¹³C NMR (126 MHz, CDCl₃) δ 171.6, 151.6, 144.7, 140.5, 138.0, 129.0, 126.8, 124.8, 123.2, 120.2, 34.3, 31.8, 30.0, 29.2, 29.1, 22.8, 14.2. MS (ESI) calculated for C₁₇H₂₁N₃S, m/z 299.15, found 300.16 [M+H]⁺.

8h: 2-Nonylthiazolo[4,5-c]quinolin-4-amine. White solid (26 mg, 26%). ¹H NMR (400 MHz, CDCl₃) δ 7.77 (dd, *J* = 8.4, 0.5 Hz, 1H), 7.73 (dd, *J* = 8.0, 1.0 Hz, 1H), 7.55 (ddd, *J* = 8.5, 7.1, 1.5 Hz, 1H), 7.31 (ddd, *J* = 8.1, 7.1, 1.2 Hz, 1H), 5.57 (s, 2H), 3.21 – 3.09 (m, 2H), 1.91 (dt, *J* = 15.3, 7.6 Hz, 2H), 1.46 (ddd, *J* = 14.9, 8.7, 6.5 Hz, 2H), 1.36 (dd, *J* = 13.7, 6.7 Hz, 2H), 1.28 (s, 8H), 0.88 (t, *J* = 6.9 Hz, 3H). ¹³C NMR (126 MHz, CDCl₃) δ 171.6, 151.6, 144.7, 140.5, 138.0, 129.0, 126.8, 124.8, 123.2, 120.2, 34.3, 32.0, 30.0, 29.6, 29.4, 29.4, 29.2, 22.8, 14.3. MS (ESI) calculated for C₁₉H₂₅N₃S, *m/z* 327.18, found 328.19 [M+H]⁺.

8i: 2-Isopropylthiazolo[4,5-c]quinolin-4-amine. White solid (40 mg, 67%). ¹H NMR (500 MHz, CDCl₃) δ 7.77 (dd, *J* = 8.4, 0.5 Hz, 1H), 7.75 – 7.71 (m, 1H), 7.55 (ddd, *J* = 8.4, 7.0, 1.5 Hz, 1H), 7.31 (ddd, *J* = 8.1, 7.1, 1.2 Hz, 1H), 5.66 (s, 2H), 3.51 – 3.41 (m, 1H), 1.52 (d, *J* = 6.9 Hz, 6H). ¹³C NMR (126 MHz, CDCl₃) δ 177.7, 151.8, 144.7, 140.0, 137.9, 129.0, 126.8, 124.8, 123.1, 120.3, 34.2, 23.2. MS (ESI) calculated for C₁₃H₁₃N₃S, *m/z* 243.09.10, found 244.09 [M+H]⁺.

8j: 2-Isobutylthiazolo[4,5-c]quinolin-4-amine. White solid (38 mg, 77%). ¹H NMR (500 MHz, CDCl₃) δ 7.77 (dd, *J* = 8.4, 0.5 Hz, 1H), 7.73 (dd, *J* = 8.0, 1.0 Hz, 1H), 7.55 (ddd, *J* = 8.4, 7.1, 1.5 Hz, 1H), 7.31 (ddd, *J* = 8.1, 7.1, 1.1 Hz, 1H), 5.63 (s, 2H), 3.02 (d, *J* = 7.2 Hz, 2H), 2.30 – 2.20 (m, 1H), 1.06 (d, *J* = 6.6 Hz, 6H). ¹³C NMR (126 MHz, CDCl₃) δ 170.3, 151.7, 144.8, 140.6, 138.1, 129.1, 126.8, 124.9, 123.1, 120.2, 43.1, 30.0, 22.5. MS (ESI) calculated for C₁₄H₁₅N₃S, *m/z* 257.10, found 258.10 [M+H]⁺.

8k: 2-Neopentylthiazolo[4,5-c]quinolin-4-amine. White solid (45 mg, 76%). ¹H NMR (500 MHz, CDCl₃) δ 7.77 (dd, *J* = 8.4, 0.5 Hz, 1H), 7.74 (dd, *J* = 8.0, 1.0 Hz, 1H), 7.55 (ddd, *J* = 8.4, 5.5, 1.5 Hz, 1H), 7.31 (ddd, *J* = 8.1, 7.1, 1.1 Hz, 1H), 5.60 (s, 2H), 3.04 (s, 2H), 1.10 (s, 9H). ¹³C

NMR (126 MHz, CDCl₃) δ 168.1, 151.7, 144.8, 140.7, 138.2, 129.1, 126.8, 124.9, 123.2, 120.1, 47.8, 32.3, 29.7. MS (ESI) calculated for C₁₄H₁₇N₃S, m/z 271.11, found 272.11 [M+H]⁺.

8l: 2-Isopentylthiazolo[4,5-c]quinolin-4-amine. White solid (40 mg, 68%). ¹H NMR (500 MHz, CDCl₃) δ 7.77 (dd, *J* = 8.4, 0.5 Hz, 1H), 7.73 (dd, *J* = 8.0, 1.0 Hz, 1H), 7.55 (ddd, *J* = 8.4, 7.1, 1.5 Hz, 1H), 7.31 (ddd, *J* = 8.1, 7.1, 1.1 Hz, 1H), 5.61 (s, 2H), 3.20 – 3.13 (m, 2H), 1.84 – 1.78 (m, 2H), 1.77 – 1.69 (m, 1H), 1.00 (d, *J* = 6.5 Hz, 6H). ¹³C NMR (126 MHz, CDCl₃) δ 171.7, 151.6, 144.7, 140.5, 138.0, 129.0, 126.8, 124.8, 123.2, 120.2, 38.9, 32.3, 27.9, 22.5. MS (ESI) calculated for C₁₅H₁₆N₂OS, m/z 271.11, found 272.11 [M+H]⁺.

8m: 2-(3,3-Dimethylbutyl)thiazolo[4,5-c]quinolin-4-amine. White solid (45 mg, 65%). ¹H NMR (500 MHz, CDCl₃) δ 7.77 (dd, *J* = 8.4, 0.5 Hz, 1H), 7.74 – 7.70 (m, 1H), 7.55 (ddd, *J* = 8.4, 7.0, 1.5 Hz, 1H), 7.31 (ddd, *J* = 8.1, 7.1, 1.1 Hz, 1H), 5.64 (s, 2H), 3.17 – 3.09 (m, 2H), 1.86 – 1.79 (m, 2H), 1.02 (s, 9H). ¹³C NMR (126 MHz, CDCl₃) δ 172.2, 151.6, 144.7, 140.4, 138.0, 129.0, 126.8, 124.8, 123.1, 121.0, 44.1, 30.8, 30.1, 29.3. MS (ESI) calculated for C₁₆H₁₉N₃S, m/z 285.13, found 286.14 [M+H]⁺.

8n: (S)-2-(sec-butyl)thiazolo[4,5-c]quinolin-4-amine. White solid (45 mg, 76%). ¹H NMR (500 MHz, CDCl₃) δ 7.79 – 7.75 (m, 1H), 7.75 – 7.72 (m, 1H), 7.55 (ddd, *J* = 8.4, 7.0, 1.5 Hz, 1H), 7.31 (ddd, *J* = 8.1, 7.1, 1.2 Hz, 1H), 5.63 (s, 2H), 3.30 – 3.21 (m, 1H), 2.00 – 1.90 (m, 1H), 1.88 – 1.76 (m, 1H), 1.49 (d, *J* = 6.9 Hz, 3H), 1.00 (t, *J* = 7.4 Hz, 3H). ¹³C NMR (126 MHz, CDCl₃) δ 177.0, 151.7, 144.7, 140.0, 137.9, 129.0, 126.8, 124.8, 123.1, 120.3, 41.0, 30.9, 21.0, 11.9. MS (ESI) calculated for C₁₄H₁₅N₃S, m/z 257.10, found 258.10 [M+H]⁺.

8o: (S)-2-(2-methylbutyl)thiazolo[4,5-c]quinolin-4-amine. White solid (46 mg, 77%). ^1H NMR (500 MHz, CDCl_3) δ 7.77 (dd, $J = 8.4, 0.5$ Hz, 1H), 7.73 (dd, $J = 8.0, 1.0$ Hz, 1H), 7.55 (ddd, $J = 8.4, 7.1, 1.5$ Hz, 1H), 7.31 (ddd, $J = 8.1, 7.1, 1.1$ Hz, 1H), 5.66 (s, 2H), 3.14 (dd, $J = 14.6, 6.2$ Hz, 1H), 2.96 (dd, $J = 14.6, 8.1$ Hz, 1H), 2.08 – 1.97 (m, 1H), 1.57 – 1.47 (m, 1H), 1.38 – 1.28 (m, 1H), 1.02 (d, $J = 6.7$ Hz, 3H), 0.97 (t, $J = 7.4$ Hz, 3H). ^{13}C NMR (126 MHz, CDCl_3) δ 170.5, 151.7, 144.7, 140.6, 138.1, 129.0, 126.8, 124.8, 123.1, 120.2, 41.2, 36.3, 29.3, 19.2, 11.5. MS (ESI) calculated for $\text{C}_{15}\text{H}_{17}\text{N}_3\text{S}$, m/z 271.11, found 272.11 $[\text{M}+\text{H}]^+$.

8p: 2-(3,3,3-Trifluoropropyl)thiazolo[4,5-c]quinolin-4-amine. White solid (70 mg, 78%). ^1H NMR (500 MHz, CDCl_3) δ 7.80 – 7.76 (m, 1H), 7.73 (dd, $J = 8.0, 1.0$ Hz, 1H), 7.58 (ddd, $J = 8.4, 7.1, 1.4$ Hz, 1H), 7.35 – 7.30 (m, 1H), 5.63 (s, 2H), 3.45 – 3.39 (m, 2H), 2.87 – 2.76 (m, 2H). ^{13}C NMR (126 MHz, CDCl_3) δ 166.5, 151.6, 145.0, 140.8, 137.9, 129.4, 126.9, 126.4 (q, $1\text{JCF} = 276.5$ Hz), 124.9, 123.4, 119.9, 33.1 (q, $2\text{JCF} = 29.8$ Hz), 26.8 (q, $3\text{JCF} = 3.4$ Hz). MS (ESI) calculated for $\text{C}_{13}\text{H}_{10}\text{F}_3\text{N}_3\text{S}$, m/z 297.05, found 298.05 $[\text{M}+\text{H}]^+$.

8q: 2-(4,4,4-Trifluorobutyl)thiazolo[4,5-c]quinolin-4-amine. White solid (50 mg, 72%). ^1H NMR (500 MHz, CDCl_3) δ 7.77 (dd, $J = 8.4, 0.4$ Hz, 1H), 7.73 (dd, $J = 8.0, 1.1$ Hz, 1H), 7.57 (ddd, $J = 8.4, 7.1, 1.4$ Hz, 1H), 7.32 (ddd, $J = 8.1, 7.1, 1.1$ Hz, 1H), 5.62 (s, 2H), 3.25 (t, $J = 7.2$ Hz, 2H), 2.36 – 2.26 (m, 2H), 2.26 – 2.18 (m, 2H). ^{13}C NMR (126 MHz, CDCl_3) δ 168.8, 151.6, 144.9, 140.6, 138.1, 129.3, 127.0 (q, $1\text{JCF} = 276.4$ Hz), 126.9, 124.9, 123.3, 120.0, 33.1 (q, $2\text{JCF} = 29.7$ Hz), 32.7, 21.9 (q, $3\text{JCF} = 3.0$ Hz). MS (ESI) calculated for $\text{C}_{14}\text{H}_{12}\text{F}_3\text{N}_3\text{S}$, m/z 311.07, found 312.07 $[\text{M}+\text{H}]^+$.

Synthesis of compound 9: 8-Nitro-2-propylthiazolo[4,5-c]quinolin-4-amine. To a stirred solution of compound **8c** (200 mg, 0.82 mmol) in H_2SO_4 (0.5 mL), was added HNO_3 (0.5 mL)

and the reaction mixture was stirred at room temperature for 1 h. The reaction mixture was neutralized with 1N NaOH and extracted with EtOAc (3 × 15 mL). The combined organic layer was dried over Na₂SO₄, concentrated under reduced pressure, and the crude residue was purified using silica gel column chromatography (0-5% MeOH in CH₂Cl₂) to obtain compound **9** as a yellow solid (171 mg, 72%). ¹H NMR (400 MHz, CDCl₃) δ 8.68 (d, *J* = 2.5 Hz, 1H), 8.35 (dd, *J* = 9.2, 2.6 Hz, 1H), 7.80 (d, *J* = 9.2 Hz, 1H), 6.09 (s, 2H), 3.17 (dd, *J* = 8.7, 6.4 Hz, 2H), 1.97 (dd, *J* = 15.0, 7.5 Hz, 2H), 1.11 (t, *J* = 7.4 Hz, 3H). ¹³C NMR (126 MHz, CDCl₃) δ 173.3, 153.6, 148.3, 142.5, 141.2, 138.7, 127.3, 123.2, 121.5, 119.1, 36.2, 23.3, 13.8. MS (ESI) calculated for C₁₃H₁₂N₄O₂S, *m/z* 288.07, found 289.08 [M+H]⁺.

Synthesis of compound 10: 2-Propylthiazolo[4,5-*c*]quinoline-4,8-diamine. To a stirred solution of compound **9** (200 mg, 0.69 mmol) in methanol (5 mL), were added zinc dust (453 mg, 6.94 mmol) and ammonium formate (437 mg, 6.94 mmol), and the reaction mixture was stirred at room temperature for 30 min. The reaction mixture was then filtered through celite, the filtrate concentrated under reduced pressure, and purified over silica gel column chromatography (0-10% MeOH in CH₂Cl₂) to afford compound **10** as a yellow solid (185 mg, 88%). ¹H NMR (400 MHz, CDCl₃) δ 8.71 (s, 1H), 8.46 (s, 2H), 7.70 (d, *J* = 8.9 Hz, 1H), 7.00 (dd, *J* = 8.9, 2.5 Hz, 1H), 6.87 (d, *J* = 2.4 Hz, 1H), 3.17 – 3.09 (m, 2H), 1.99 – 1.88 (m, 2H), 1.08 (t, *J* = 7.4 Hz, 3H). ¹³C NMR (126 MHz, CDCl₃) δ 173.1, 170.3, 149.2, 143.9, 142.1, 137.1, 129.5, 121.9, 120.7, 118.7, 107.4, 36.1, 23.2, 13.8. MS (ESI) calculated for C₁₃H₁₄N₄S, *m/z* 258.09, found 259.10 [M+H]⁺.

Synthesis of compound 11: 8-Azido-2-propylthiazolo[4,5-*c*]quinolin-4-amine. To a stirred solution of compound **10** (25 mg, 0.096 mmol) in a 1:1 mixture of acetic acid and water (2 mL), was added sodium nitrite (20 mg, 0.29 mmol) and the reaction mixture was stirred at room

temperature for 1 h. Sodium azide (18.8 mg, 0.29 mmol) was then added to the reaction mixture and stirred for additional 1 h. The reaction mixture was neutralized with 1N NaOH and extracted with EtOAc (3 × 10 mL). The combined organic layer was dried over Na₂SO₄, concentrated under reduced pressure, and the crude compound was purified on silica gel column chromatography (0-5% MeOH in CH₂Cl₂) to obtain compound **11** as a brown solid (18 mg, 67%). ¹H NMR (400 MHz, CDCl₃) δ 7.76 (d, *J* = 8.9 Hz, 1H), 7.31 (d, *J* = 2.5 Hz, 1H), 7.26 – 7.23 (m, 1H), 5.60 (s, 2H), 3.17 – 3.12 (m, 2H), 2.01 – 1.90 (m, 2H), 1.09 (t, *J* = 7.4 Hz, 3H). ¹³C NMR (126 MHz, CDCl₃) δ 172.0, 151.3, 139.5, 138.5, 134.8, 128.4, 121.0, 120.8, 113.5, 36.2, 23.4, 13.8. MS (ESI) calculated for C₁₃H₁₂N₆S, *m/z* 284.08, found 285.09 [M+H]⁺.

Synthesis of compound 12a: 2-(1-(4-Amino-2-propylthiazolo[4,5-c]quinolin-8-yl)-1*H*-1,2,3-triazol-4-yl)propan-2-ol. To a stirred solution of compound **11** (12 mg, 0.042 mmol) in THF (1 mL), were added CuSO₄·5H₂O (1.3 mg, 0.005 mmol, in 0.5 mL water), sodium ascorbate (2.1 mg, 0.010 mmol, in 0.5 mL water), 2-methylbut-3-yn-2-ol (8.4 μL, 0.084 mmol) and the reaction mixture stirred at room temperature for 1 h. The reaction mixture was diluted with water and extracted with EtOAc (3 × 10 mL). The combined organic layer was dried over Na₂SO₄, concentrated under reduced pressure, and the crude residue was purified using silica gel column chromatography (0-10% MeOH in CH₂Cl₂) to obtain compound **12a** as a white solid (14 mg, 92%). ¹H NMR (400 MHz, CDCl₃) δ 8.12 (d, *J* = 2.0 Hz, 1H), 7.97 (s, 1H), 7.91 – 7.81 (m, 2H), 5.74 (s, 2H), 3.49 (s, 1H), 3.19 – 3.13 (m, 2H), 1.96 (dd, *J* = 15.0, 7.5 Hz, 2H), 1.74 (s, 6H), 1.10 (t, *J* = 7.4 Hz, 3H). ¹³C NMR (126 MHz, CDCl₃) δ 172.5, 156.5, 152.2, 144.5, 140.2, 138.7, 132.0, 128.3, 121.5, 120.3, 117.8, 116.4, 68.9, 36.2, 30.7, 23.4, 13.8. MS (ESI) calculated for C₁₈H₂₀N₆OS, *m/z* 368.14, found 369.15 [M+H]⁺.

Compounds **12b-12f** were synthesized similarly as compound **12a**.

12b: (1-(4-Amino-2-propylthiazolo[4,5-c]quinolin-8-yl)-1*H*-1,2,3-triazol-4-yl)methanol.

White solid (15 mg, 83%). ¹H NMR (500 MHz, DMSO) δ 8.84 (s, 1H), 8.33 (d, *J* = 2.5 Hz, 1H), 8.06 (dd, *J* = 9.0, 2.5 Hz, 1H), 7.76 (d, *J* = 9.0 Hz, 1H), 7.13 (s, 2H), 5.37 (t, *J* = 5.6 Hz, 1H), 4.64 (d, *J* = 5.9 Hz, 2H), 3.19 (t, *J* = 7.5 Hz, 2H), 1.88 (dt, *J* = 14.8, 7.4 Hz, 2H), 1.04 (t, *J* = 7.4 Hz, 3H). ¹³C NMR (126 MHz, DMSO) δ 171.8, 152.7, 149.2, 144.5, 139.1, 138.2, 130.8, 127.3, 121.2, 120.9, 118.9, 115.2, 55.1, 35.2, 22.8, 13.5. MS (ESI) calculated for C₁₆H₁₆N₆OS, *m/z* 340.11, found 341.11 [M+H]⁺.

12c: 8-(4-Phenyl-1*H*-1,2,3-triazol-1-yl)-2-propylthiazolo[4,5-c]quinolin-4-amine. Solid (19

mg, 93%). ¹H NMR (500 MHz, DMSO) δ 9.44 (s, 1H), 8.36 (d, *J* = 2.5 Hz, 1H), 8.12 (dd, *J* = 9.0, 2.5 Hz, 1H), 7.97 (dd, *J* = 8.2, 1.1 Hz, 2H), 7.80 (d, *J* = 9.0 Hz, 1H), 7.53 (dd, *J* = 10.6, 4.8 Hz, 2H), 7.44 – 7.37 (m, 1H), 7.17 (s, 2H), 3.21 (t, *J* = 7.5 Hz, 2H), 1.90 (dd, *J* = 14.9, 7.4 Hz, 2H), 1.04 (t, *J* = 7.4 Hz, 3H). ¹³C NMR (126 MHz, DMSO) δ 171.8, 152.8, 147.3, 144.7, 139.0, 138.2, 130.6, 130.4, 129.1, 128.3, 127.4, 125.3, 120.9, 119.8, 118.9, 115.3, 35.2, 22.8, 13.5. MS (ESI) calculated for C₂₁H₁₈N₆S, *m/z* 386.13, found 387.14 [M+H]⁺.

12d: 2-Propyl-8-(4-propyl-1*H*-1,2,3-triazol-1-yl)thiazolo[4,5-c]quinolin-4-amine. Yellow solid

(16 mg, 86%). ¹H NMR (500 MHz, DMSO) δ 8.72 (s, 1H), 8.28 (d, *J* = 2.4 Hz, 1H), 8.04 (dd, *J* = 9.0, 2.5 Hz, 1H), 7.75 (d, *J* = 9.0 Hz, 1H), 7.12 (s, 2H), 3.19 (t, *J* = 7.5 Hz, 2H), 2.71 (t, *J* = 7.5 Hz, 2H), 1.89 (dd, *J* = 14.9, 7.4 Hz, 2H), 1.72 (dd, *J* = 14.9, 7.4 Hz, 2H), 1.04 (t, *J* = 7.4 Hz, 3H), 0.98 (t, *J* = 7.4 Hz, 3H). ¹³C NMR (126 MHz, DMSO) δ 171.8, 152.7, 148.0, 144.4, 139.0, 138.2, 130.9, 127.3, 120.8, 120.3, 118.9, 115.0, 35.2, 27.1, 22.8, 22.1, 13.7, 13.5. MS (ESI) calculated for C₁₈H₂₀N₆S, *m/z* 352.15, found 353.15 [M+H]⁺.

12e: 8-(4-Pentyl-1*H*-1,2,3-triazol-1-yl)-2-propylthiazolo[4,5-*c*]quinolin-4-amine. Solid (19 mg, 91%). ¹H NMR (500 MHz, DMSO) δ 8.71 (s, 1H), 8.27 (d, *J* = 2.5 Hz, 1H), 8.04 (dd, *J* = 9.0, 2.5 Hz, 1H), 7.75 (d, *J* = 9.0 Hz, 1H), 7.12 (s, 2H), 3.19 (t, *J* = 7.5 Hz, 2H), 2.72 (t, *J* = 7.6 Hz, 2H), 1.89 (dd, *J* = 14.9, 7.4 Hz, 2H), 1.69 (dt, *J* = 15.3, 7.6 Hz, 2H), 1.42 – 1.26 (m, 6H), 1.04 (t, *J* = 7.4 Hz, 3H), 0.87 (dd, *J* = 9.2, 4.9 Hz, 3H). ¹³C NMR (126 MHz, DMSO) δ 171.8, 152.7, 148.2, 144.4, 139.0, 138.2, 130.9, 127.3, 120.8, 120.2, 118.9, 114.9, 35.2, 31.1, 28.8, 28.3, 25.1, 22.8, 22.1, 14.0, 13.5. MS (ESI) calculated for C₂₁H₂₆N₆S, *m/z* 394.19, found 395.20 [M+H]⁺.

12f: 2-Propyl-8-(4-(trimethylsilyl)-1*H*-1,2,3-triazol-1-yl)thiazolo[4,5-*c*]quinolin-4-amine. White solid (18 mg, 90%). ¹H NMR (500 MHz, DMSO) δ 8.98 (s, 1H), 8.31 (d, *J* = 2.4 Hz, 1H), 8.07 (dd, *J* = 9.0, 2.5 Hz, 1H), 7.76 (d, *J* = 9.0 Hz, 1H), 7.13 (s, 2H), 3.19 (t, *J* = 7.5 Hz, 2H), 1.89 (dd, *J* = 14.8, 7.4 Hz, 2H), 1.04 (t, *J* = 7.4 Hz, 3H), 0.36 – 0.33 (m, 9H). ¹³C NMR (126 MHz, DMSO) δ 171.8, 152.7, 146.1, 144.4, 139.1, 138.2, 130.7, 128.9, 127.3, 121.3, 118.9, 115.3, 35.2, 22.8, 13.5, -0.9. MS (ESI) calculated for C₁₈H₂₂N₆SSi, *m/z* 382.14, found 383.14 [M+H]⁺.

Synthesis of compound 12g: 2-Propyl-8-(1*H*-1,2,3-triazol-1-yl)thiazolo[4,5-*c*]quinolin-4-amine. To a stirred solution of compound **12f** (20 mg, 0.052 mmol) in THF (1 mL) was added TBAF (20 mg, 0.078 mmol), and the reaction mixture was stirred at room temperature for 10 h. The reaction mixture was then diluted with water and extracted with EtOAc (3 × 10 mL). The organic layer was dried over Na₂SO₄, concentrated under reduced pressure, and the crude material purified using silica gel column chromatography (0-5% MeOH in CH₂Cl₂) to obtain compound **12g** as a white solid (14 mg, 87%). ¹H NMR (500 MHz, DMSO) δ 8.94 (d, *J* = 1.1 Hz, 1H), 8.29 (d, *J* = 2.4 Hz, 1H), 8.04 (dd, *J* = 9.0, 2.5 Hz, 1H), 7.98 (d, *J* = 1.1 Hz, 1H), 7.75 (d, *J* =

9.0 Hz, 1H), 7.12 (s, 2H), 3.17 (t, $J = 7.5$ Hz, 2H), 1.91 – 1.83 (m, 2H), 1.02 (t, $J = 7.4$ Hz, 3H). ^{13}C NMR (126 MHz, DMSO) δ 171.7, 152.8, 144.6, 139.1, 138.2, 134.4, 130.7, 127.4, 123.4, 121.2, 118.9, 115.5, 35.23 22.8, 13.5. MS (ESI) calculated for $\text{C}_{15}\text{H}_{14}\text{N}_6\text{S}$, m/z 310.10, found 311.10 $[\text{M}+\text{H}]^+$.

Synthesis of compound 13a: *N*⁸-hexyl-2-propylthiazolo[4,5-*c*]quinoline-4,8-diamine. To a stirred solution of compound **10** (25 mg, 0.096 mmol) in DMF (2 mL) were added 1-iodohexane (20.5 mg, 0.096 mmol) and potassium carbonate (26.7 mg, 0.19 mmol), and the reaction mixture was stirred at room temperature for 4 h. The reaction mixture was diluted with water and extracted with EtOAc (3 \times 10 mL). The organic layer was dried over Na_2SO_4 , concentrated under reduced pressure, and the crude compound was purified using silica gel column chromatography (0-5% MeOH in CH_2Cl_2) to obtain **13a** as a solid (16 mg, 61%). ^1H NMR (500 MHz, CDCl_3) δ 7.69 (d, $J = 8.9$ Hz, 1H), 6.96 (dd, $J = 8.9, 2.6$ Hz, 1H), 6.67 (d, $J = 2.5$ Hz, 1H), 6.15 (s, 2H), 3.87 (s, 1H), 3.18 (t, $J = 7.1$ Hz, 2H), 3.15 – 3.11 (m, 2H), 1.99 – 1.89 (m, 2H), 1.68 (dt, $J = 14.7, 7.2$ Hz, 2H), 1.49 – 1.41 (m, 2H), 1.35 (td, $J = 7.2, 3.7$ Hz, 4H), 1.09 (t, $J = 7.4$ Hz, 3H), 0.92 (t, $J = 7.1$ Hz, 3H). ^{13}C NMR (126 MHz, CDCl_3) δ 172.1, 148.2, 145.5, 141.2, 137.4, 124.8, 120.3, 119.8, 102.9, 44.3, 36.2, 31.8, 29.4, 27.0, 23.3, 22.8, 14.2, 13.8. MS (ESI) calculated for $\text{C}_{19}\text{H}_{26}\text{N}_4\text{S}$, m/z 342.19, found 343.20 $[\text{M}+\text{H}]^+$.

Synthesis of compound 13b: *N*-(4-amino-2-propylthiazolo[4,5-*c*]quinolin-8-yl)butyramide.

To a stirred solution of compound **10** (20 mg, 0.077 mmol) in CH_2Cl_2 (2 mL) were added triethylamine (30 μL , 0.164 mmol) and butyryl chloride (8.7 μL , 0.082); the reaction mixture was stirred at room temperature for 1 h. The reaction mixture was then diluted with water and extracted with EtOAc (3 \times 10 mL). The combined organic layer was dried over Na_2SO_4 , concentrated under reduced pressure, and the crude compound was purified using silica gel

column chromatography (0-10% MeOH in CH₂Cl₂) to furnish compound **13b** as a white solid (22 mg, 87%). ¹H NMR (400 MHz, CDCl₃) δ 8.34 (d, *J* = 2.2 Hz, 1H), 7.71 (d, *J* = 8.9 Hz, 1H), 7.37 (dd, *J* = 8.9, 2.4 Hz, 2H), 5.67 (d, *J* = 1.2 Hz, 2H), 3.13 (t, *J* = 7.4 Hz, 2H), 2.41 (t, *J* = 7.4 Hz, 2H), 1.94 (dd, *J* = 15.0, 7.5 Hz, 2H), 1.85 – 1.74 (m, 2H), 1.11 – 1.02 (m, 6H). ¹³C NMR (126 MHz, CDCl₃) δ 172.0, 171.5, 150.9, 140.6, 138.2, 133.4, 126.8, 122.1, 120.2, 114.6, 39.8, 36.2, 23.3, 19.2, 13.9, 13.8. MS (ESI) calculated for C₁₇H₂₀N₄OS, *m/z* 328.14, found 329.15 [M+H]⁺.

Synthesis of compound 14: 8-Bromo-2-propylthiazolo[4,5-*c*]quinolin-4-amine. To a stirred solution of compound **8c** (50 mg, 0.205 mmol) in CH₃CN (1 mL) were added *N*-bromosuccinimide (44 mg, 0.246 mmol), ammonium acetate (1.6 mg, 0.02 mmol) and the reaction mixture was stirred at room temperature for 12 h. The reaction mixture was then diluted with water and extracted with EtOAc (3 × 10 mL). The combined organic layer was dried over Na₂SO₄, concentrated under reduced pressure, and the crude material was purified using silica gel column chromatography (0-5% MeOH in CH₂Cl₂) to obtain compound **14** as a white solid (40 mg, 67%). ¹H NMR (500 MHz, CDCl₃) δ 7.86 (dd, *J* = 2.0, 0.6 Hz, 1H), 7.61 (dd, *J* = 3.9, 1.3 Hz, 2H), 5.68 (s, 2H), 3.16 – 3.11 (m, 2H), 1.95 (dt, *J* = 15.0, 7.4 Hz, 2H), 1.09 (t, *J* = 7.4 Hz, 3H). ¹³C NMR (126 MHz, CDCl₃) δ 172.1, 151.8, 143.4, 139.3, 138.4, 132.1, 128.4, 126.9, 121.5, 115.9, 36.2, 23.4, 13.8. MS (ESI) calculated for C₁₃H₁₂BrN₃S, *m/z* 320.99, found 322.00 [M+H]⁺.

Synthesis of compound 15a: *N*-butyl-2-propylthiazolo[4,5-*c*]quinolin-4-amine. To a stirred solution of compound **8c** (50 mg, 0.205 mmol) in THF (1 mL) were added sodium hydride (10 mg, 0.41 mmol) and 1-iodobutane (35 μL, 0.308 mmol), the resulting mixture was stirred at room temperature for 6 h. The reaction mixture was then diluted with water and extracted with CH₂Cl₂ (3 × 10 mL). The organic layer was dried over Na₂SO₄, concentrated under reduced

pressure, and the crude compound was purified using silica gel column chromatography (0-5% MeOH in CH₂Cl₂) to obtain compound **15a** (45 mg, 70%). ¹H NMR (500 MHz, CDCl₃) δ 7.81 (dd, *J* = 8.3, 0.5 Hz, 1H), 7.70 – 7.66 (m, 1H), 7.51 (ddd, *J* = 8.4, 7.1, 1.5 Hz, 1H), 7.23 (ddd, *J* = 8.0, 7.1, 1.1 Hz, 1H), 5.96 (t, *J* = 4.8 Hz, 1H), 3.77 – 3.69 (m, 2H), 3.15 – 3.08 (m, 2H), 1.99 – 1.89 (m, 2H), 1.75 (ddd, *J* = 14.9, 11.1, 7.5 Hz, 2H), 1.52 (dq, *J* = 14.7, 7.4 Hz, 2H), 1.08 (t, *J* = 7.4 Hz, 3H), 1.00 (t, *J* = 7.4 Hz, 3H). ¹³C NMR (126 MHz, CDCl₃) δ 170.7, 151.2, 145.3, 138.9, 138.3, 128.6, 126.9, 124.5, 122.1, 119.3, 40.6, 36.0, 31.9, 23.3, 20.3, 14.0, 13.7. MS (ESI) calculated for C₁₇H₂₁N₃S, *m/z* 299.15, found 300.14 [M+H]⁺.

Compounds **15b** and **15c** were synthesized similarly as compound **15a**.

15b: N-hexyl-2-propylthiazolo[4,5-c]quinolin-4-amine. White solid (9.9 mg, 72%, based on starting material recovery). ¹H NMR (400 MHz, CDCl₃) δ 7.81 (d, *J* = 8.3 Hz, 1H), 7.68 (dd, *J* = 7.9, 1.1 Hz, 1H), 7.51 (ddd, *J* = 8.5, 7.1, 1.5 Hz, 1H), 7.23 (ddd, *J* = 8.1, 7.2, 1.1 Hz, 1H), 5.96 (t, *J* = 4.6 Hz, 1H), 3.71 (dt, *J* = 7.2, 5.8 Hz, 2H), 3.11 (dd, *J* = 8.7, 6.5 Hz, 2H), 1.94 (dd, *J* = 15.0, 7.5 Hz, 2H), 1.76 (t, *J* = 7.3 Hz, 2H), 1.53 – 1.44 (m, 2H), 1.36 (ddd, *J* = 6.9, 6.2, 3.3 Hz, 4H), 1.08 (t, *J* = 7.4 Hz, 3H), 0.91 (dd, *J* = 9.1, 5.1 Hz, 3H). ¹³C NMR (101 MHz, CDCl₃) δ 170.9, 151.3, 145.5, 139.1, 138.5, 128.8, 127.1, 124.6, 122.3, 119.5, 41.1, 36.2, 31.8, 29.9, 27.1, 23.5, 22.8, 14.2, 13.8. MS (ESI) calculated for C₁₉H₂₅N₃S, *m/z* 327.18, found 328.18 [M+H]⁺.

15c: N-hexadecyl-2-propylthiazolo[4,5-c]quinolin-4-amine. White solid (26 mg, 68%). ¹H NMR (400 MHz, CDCl₃) δ 7.81 (d, *J* = 7.9 Hz, 1H), 7.68 (dd, *J* = 7.9, 1.1 Hz, 1H), 7.51 (ddd, *J* = 8.5, 7.1, 1.5 Hz, 1H), 7.23 (td, *J* = 7.1, 3.6 Hz, 1H), 5.96 (s, 1H), 3.71 (dd, *J* = 12.9, 7.1 Hz, 2H), 3.11 (dd, *J* = 8.7, 6.5 Hz, 2H), 1.98 – 1.88 (m, 2H), 1.76 (dt, *J* = 14.8, 7.4 Hz, 2H), 1.51 – 1.43 (m, 2H), 1.30 – 1.21 (m, 24H), 1.08 (t, *J* = 7.4 Hz, 3H), 0.88 (t, *J* = 6.8 Hz, 3H). ¹³C NMR (126

MHz, CDCl₃) δ 170.9, 151.4, 145.5, 139.1, 138.5, 128.7, 127.1, 124.6, 122.3, 119.5, 41.1, 36.8, 36.1, 32.1, 29.9, 29.8, 29.8, 29.8, 29.8, 29.8, 29.7, 29.6, 29.5, 27.3, 24.8, 23.5, 22.8, 14.3, 13.9. MS (ESI) calculated for C₂₉H₄₅N₃S, m/z 467.33, found 468.35 [M+H]⁺.

Synthesis of compound 15d: *N*-(2-propylthiazolo[4,5-*c*]quinolin-4-yl)formamide. To a stirred solution of compound **8c** (50 mg, 0.205 mmol) in 1,4-dioxane (1 mL) were added 2,2,2-trifluoroethylformate (60 μ L, 0.616 mmol) and triethylamine (86 μ L, 0.616 mmol). The resulting mixture was stirred at 80 °C for 12 h. The reaction mixture was then diluted with water and extracted with CH₂Cl₂ (3 \times 10 mL). The combined organic layer was dried over Na₂SO₄, concentrated under reduced pressure, and the crude compound was purified using silica gel column chromatography (0-3% MeOH in CH₂Cl₂) to furnish compound **15d** as a white solid (26 mg, 46%). ¹H NMR (500 MHz, CDCl₃) δ 9.84 (d, *J* = 10.8 Hz, 1H), 8.86 (d, *J* = 10.3 Hz, 1H), 8.03 – 7.94 (m, 1H), 7.84 (ddd, *J* = 8.0, 1.4, 0.5 Hz, 1H), 7.67 (ddd, *J* = 8.5, 7.0, 1.4 Hz, 1H), 7.50 (ddd, *J* = 8.1, 7.1, 1.2 Hz, 1H), 3.24 – 3.08 (m, 2H), 2.05 – 1.87 (m, 2H), 1.09 (t, *J* = 7.4 Hz, 3H). ¹³C NMR (126 MHz, CDCl₃) δ 172.7, 162.0, 143.8, 143.2, 141.7, 137.5, 129.5, 128.8, 125.8, 124.8, 121.9, 36.2, 23.1, 13.8. MS (ESI) calculated for C₁₄H₁₃N₃OS, m/z 271.08, found 272.09 [M+H]⁺.

Synthesis of compound 15e: *N*-(2-propylthiazolo[4,5-*c*]quinolin-4-yl)acetamide. To a stirred solution of compound **8c** (20 mg, 0.082 mmol) in pyridine (1 mL) was added acetyl chloride (5.8 μ L, 0.082 mmol), the resulting mixture was stirred at room temperature for 1 h. The solvent was evaporated under reduced pressure and extracted with CH₂Cl₂ (3 \times 10 mL). The combined organic layer was dried over Na₂SO₄, concentrated under reduced pressure, and the crude compound was purified using silica gel column chromatography (0-5% MeOH in CH₂Cl₂) to furnish compound **15e** as a white solid (18 mg, 78%). ¹H NMR (500 MHz, CDCl₃) δ 8.03 (d, *J*

= 8.3 Hz, 1H), 7.88 (dd, $J = 8.1, 0.9$ Hz, 1H), 7.72 (ddd, $J = 8.4, 7.2, 1.3$ Hz, 1H), 7.59 – 7.54 (m, 1H), 3.17 (td, $J = 7.6, 2.3$ Hz, 2H), 2.77 (s, 3H), 1.96 (dd, $J = 15.0, 7.5$ Hz, 2H), 1.09 (t, $J = 7.3$ Hz, 3H). ^{13}C NMR (126 MHz, CDCl_3) δ 173.0, 144.7, 138.3, 131.6, 130.0, 127.2, 126.5, 125.9, 125.3, 125.0, 121.2, 36.2, 25.7, 23.2, 13.8. MS (ESI) calculated for $\text{C}_{15}\text{H}_{15}\text{N}_3\text{OS}$, m/z 285.09, found 286.11 $[\text{M}+\text{H}]^+$.

Compounds **15f-15i** were synthesized similarly as compound **15e**.

15f: *N*-(2-propylthiazolo[4,5-*c*]quinolin-4-yl)butyramide. White solid (20 mg, 78%). ^1H NMR (500 MHz, CDCl_3) δ 8.96 (s, 1H), 8.04 (d, $J = 8.3$ Hz, 1H), 7.82 (dd, $J = 8.0, 1.0$ Hz, 1H), 7.65 (ddd, $J = 8.4, 7.1, 1.4$ Hz, 1H), 7.49 (ddd, $J = 8.1, 7.1, 1.1$ Hz, 1H), 3.21 – 3.04 (m, 4H), 2.01 – 1.92 (m, 2H), 1.92 – 1.82 (m, 2H), 1.10 (td, $J = 7.4, 6.1$ Hz, 6H). ^{13}C NMR (126 MHz, CDCl_3) δ 172.1, 144.5, 143.5, 140.8, 138.6, 129.2, 129.2, 125.7, 124.6, 121.4, 39.9, 36.2, 23.2, 18.6, 14.1, 13.8. MS (ESI) calculated for $\text{C}_{17}\text{H}_{19}\text{N}_3\text{OS}$, m/z 313.12, found 314.13 $[\text{M}+\text{H}]^+$.

15g: *N*-(2-propylthiazolo[4,5-*c*]quinolin-4-yl)octanamide. White solid (25 mg, 83%). ^1H NMR (400 MHz, CDCl_3) δ 8.95 (s, 1H), 8.04 (d, $J = 8.3$ Hz, 1H), 7.82 (dd, $J = 8.0, 0.9$ Hz, 1H), 7.65 (ddd, $J = 8.4, 7.1, 1.4$ Hz, 1H), 7.52 – 7.44 (m, 1H), 3.15 (t, $J = 7.5$ Hz, 4H), 1.96 (dd, $J = 14.9, 7.4$ Hz, 2H), 1.83 (dd, $J = 15.2, 7.7$ Hz, 2H), 1.54 – 1.45 (m, 2H), 1.39 – 1.23 (m, 6H), 1.09 (t, $J = 7.4$ Hz, 3H), 0.89 (t, $J = 6.9$ Hz, 3H). ^{13}C NMR (126 MHz, CDCl_3) δ 172.1, 144.5, 143.5, 140.8, 138.6, 129.3, 129.2, 125.7, 124.7, 121.4, 38.1, 36.2, 31.9, 29.8, 29.6, 29.3, 25.2, 23.2, 22.8, 14.2, 13.8. MS (ESI) calculated for $\text{C}_{21}\text{H}_{27}\text{N}_3\text{OS}$, m/z 369.19, found 370.22 $[\text{M}+\text{H}]^+$.

15h: *N*-(2-propylthiazolo[4,5-*c*]quinolin-4-yl)palmitamide. Yellow solid (33 mg, 84%). ^1H NMR (500 MHz, CDCl_3) δ 8.95 (s, 1H), 8.04 (d, $J = 8.3$ Hz, 1H), 7.83 (dd, $J = 8.0, 1.0$ Hz, 1H),

7.65 (ddd, $J = 8.4, 7.1, 1.4$ Hz, 1H), 7.49 (ddd, $J = 10.4, 5.8, 2.2$ Hz, 1H), 3.20 – 3.10 (m, 4H), 2.01 – 1.91 (m, 2H), 1.84 (dt, $J = 15.2, 7.6$ Hz, 2H), 1.53 – 1.44 (m, 2H), 1.43 – 1.34 (m, 2H), 1.34 – 1.19 (m, 20H), 1.09 (t, $J = 7.4$ Hz, 3H), 0.88 (t, $J = 7.0$ Hz, 3H). ^{13}C NMR (126 MHz, CDCl_3) δ 172.1, 144.5, 143.6, 140.8, 138.6, 129.3, 129.2, 125.7, 124.7, 121.5, 38.1, 36.2, 32.1, 29.8, 29.8, 29.8, 29.7, 29.6, 29.6, 29.5, 25.2, 23.2, 22.8, 14.3, 13.8. MS (ESI) calculated for $\text{C}_{29}\text{H}_{43}\text{N}_3\text{OS}$, m/z 481.31, found 482.33 $[\text{M}+\text{H}]^+$.

15i: *N*-(2-propylthiazolo[4,5-*c*]quinolin-4-yl)benzamide. White solid (24 mg, 96%). ^1H NMR (400 MHz, CDCl_3) δ 9.70 (s, 1H), 8.24 (d, $J = 8.5$ Hz, 1H), 8.07 (d, $J = 7.4$ Hz, 2H), 7.86 (d, $J = 7.6$ Hz, 1H), 7.69 (t, $J = 7.5$ Hz, 1H), 7.62 – 7.51 (m, 4H), 3.19 (t, $J = 7.6$ Hz, 2H), 1.98 (dt, $J = 14.9, 7.5$ Hz, 2H), 1.12 (t, $J = 7.4$ Hz, 3H). ^{13}C NMR (126 MHz, CDCl_3) δ 172.4, 164.7, 144.7, 143.8, 140.9, 139.3, 135.0, 132.4, 130.1, 129.2, 129.0, 127.7, 126.1, 124.5, 121.8, 36.2, 23.4, 13.9. MS (ESI) calculated for $\text{C}_{20}\text{H}_{17}\text{N}_3\text{OS}$, m/z 347.11, found 348.12 $[\text{M}+\text{H}]^+$.

Synthesis of compound 15j: 2-Azido-*N*-(2-propylthiazolo[4,5-*c*]quinolin-4-yl)acetamide. To a stirred solution of 2-azidoacetic acid (18.6 mg, 0.123 mmol) in DMF (1 mL) were added triethylamine (23 μL , 0.164 mmol) and HBTU (46.6 mg, 0.123 mmol), and the resulting mixture was stirred at room temperature for 15 min. Compound **8c** (20 mg, 0.082 mmol) was then added, and stirring was continued for 4 h. The reaction mixture was diluted with water and extracted with CH_2Cl_2 (3 \times 10 mL). The organic layer was dried over Na_2SO_4 , concentrated under reduced pressure, and the crude residue was purified by silica gel column chromatography (0-5% MeOH in CH_2Cl_2) to obtain compound **15j** as a white solid (50 mg, 96%). ^1H NMR (500 MHz, CDCl_3) δ 9.25 (d, $J = 0.6$ Hz, 1H), 8.03 (d, $J = 8.1$ Hz, 1H), 7.84 (dd, $J = 8.0, 1.0$ Hz, 1H), 7.68 (ddd, $J = 8.4, 7.1, 1.4$ Hz, 1H), 7.52 (ddd, $J = 8.1, 7.2, 1.1$ Hz, 1H), 4.86 (s, 2H), 3.17 (t, $J = 7.5$ Hz, 2H), 2.01 – 1.92 (m, 2H), 1.10 (t, $J = 7.4$ Hz, 3H). ^{13}C NMR (126 MHz,

CDCl₃) δ 172.7, 143.6, 143.1, 141.4, 138.2, 129.5, 129.1, 126.2, 124.8, 121.6, 54.7, 36.2, 23.2, 13.8. MS (ESI) calculated for C₁₅H₁₄N₆OS, m/z 326.10, found 327.11 [M+H]⁺.

Compounds **15k-15l** were synthesized similarly as compound **15j**.

15k: 3-Azido-N-(2-propylthiazolo[4,5-c]quinolin-4-yl)propan-amide. White solid (59 mg, 85%). ¹H NMR (500 MHz, CDCl₃) δ 9.07 (s, 1H), 8.03 (d, *J* = 8.3 Hz, 1H), 7.84 (dd, *J* = 8.0, 0.9 Hz, 1H), 7.67 (ddd, *J* = 8.4, 7.1, 1.4 Hz, 1H), 7.53 – 7.48 (m, 1H), 3.82 (t, *J* = 6.6 Hz, 2H), 3.59 (s, 2H), 3.16 (t, *J* = 7.5 Hz, 2H), 2.01 – 1.91 (m, 2H), 1.09 (dd, *J* = 9.3, 5.4 Hz, 3H). ¹³C NMR (126 MHz, CDCl₃) δ 172.4, 144.1, 143.3, 141.1, 138.3, 129.4, 129.1, 125.9, 124.7, 121.5, 46.9, 37.6, 36.2, 23.2, 13.8. MS (ESI) calculated for C₁₆H₁₆N₆OS, m/z 340.11, found 341.12 [M+H]⁺.

15l: N-(2-propylthiazolo[4,5-c]quinolin-4-yl)pent-4-ynamide. White solid (60 mg, 90%). ¹H NMR (500 MHz, CDCl₃) δ 9.02 (s, 1H), 8.05 (d, *J* = 8.3 Hz, 1H), 7.82 (dd, *J* = 8.0, 0.9 Hz, 1H), 7.66 (ddd, *J* = 8.4, 7.1, 1.4 Hz, 1H), 7.49 (ddd, *J* = 8.1, 7.1, 1.1 Hz, 1H), 3.49 (s, 2H), 3.15 (dd, *J* = 8.6, 6.5 Hz, 2H), 2.75 (ddd, *J* = 9.0, 6.9, 2.7 Hz, 2H), 2.03 (t, *J* = 2.7 Hz, 1H), 2.00 – 1.90 (m, 2H), 1.09 (t, *J* = 7.4 Hz, 3H). ¹³C NMR (126 MHz, CDCl₃) δ 172.2, 144.2, 143.4, 141.0, 138.4, 129.3, 129.2, 125.8, 124.7, 121.5, 83.6, 68.9, 37.2, 36.2, 23.2, 14.3, 13.8. MS (ESI) calculated for C₁₈H₁₇N₃OS, m/z 323.11, found 324.13 [M+H]⁺.

Synthesis of compound 15m: Methyl (2-propylthiazolo[4,5-c]quinolin-4-yl)carbamate. To a stirred solution of **8c** (50 mg, 0.205 mmol) in CH₂Cl₂ (2 mL) were added triethylamine (57 μ L, 0.410 mmol) and methyl chloroformate (32 μ L, 0.3075 mmol), and the resulting mixture was stirred at room temperature for 5 h. The reaction mixture was diluted with water and extracted with CH₂Cl₂ (3 \times 10 mL). The organic layer was dried over Na₂SO₄, concentrated under reduced

pressure, and the crude residue was purified by silica gel column chromatography (0-5% MeOH in CH₂Cl₂) to obtain compound **15m** as a white solid (58 mg, 94%). ¹H NMR (500 MHz, CDCl₃) δ 8.51 (s, 1H), 8.16 (d, *J* = 8.4 Hz, 1H), 7.82 (dd, *J* = 8.0, 0.9 Hz, 1H), 7.69 – 7.63 (m, 1H), 7.52 – 7.46 (m, 1H), 3.91 (s, 3H), 3.17 – 3.11 (m, 2H), 1.95 (dt, *J* = 14.8, 7.4 Hz, 2H), 1.09 (t, *J* = 7.4 Hz, 3H). ¹³C NMR (126 MHz, CDCl₃) δ 172.2, 152.2, 144.3, 143.8, 140.8, 138.6, 129.7, 129.2, 125.7, 124.5, 121.4, 52.9, 36.2, 23.3, 13.8. MS (ESI) calculated for C₁₅H₁₅N₃O₂S, *m/z* 301.09, found 302.17 [M+H]⁺.

Compounds **15n-15p** were synthesized similarly as compound **15m**.

15n: Ethyl (2-propylthiazolo[4,5-*c*]quinolin-4-yl)carbamate. Yellow solid (50 mg, 77%). ¹H NMR (500 MHz, CDCl₃) δ 8.48 (s, 1H), 8.17 (t, *J* = 8.3 Hz, 1H), 8.17 (t, *J* = 8.3 Hz, 1H), 7.81 (dd, *J* = 8.0, 1.0 Hz, 1H), 7.81 (dd, *J* = 8.0, 1.0 Hz, 1H), 7.69 – 7.61 (m, 1H), 7.51 – 7.45 (m, 1H), 4.36 (q, *J* = 7.1 Hz, 2H), 3.18 – 3.12 (m, 2H), 2.01 – 1.90 (m, 2H), 1.39 (t, *J* = 7.1 Hz, 3H), 1.09 (t, *J* = 7.4 Hz, 3H). ¹³C NMR (126 MHz, CDCl₃) δ 172.1, 151.6, 144.5, 143.8, 140.8, 138.6, 129.8, 129.1, 125.7, 124.5, 121.3, 61.8, 36.2, 23.3, 14.7, 13.8. MS (ESI) calculated for C₁₆H₁₇N₃O₂S, *m/z* 315.10, found 316.19 [M+H]⁺.

15o: Butyl (2-propylthiazolo[4,5-*c*]quinolin-4-yl)carbamate. White solid (52 mg, 74%). ¹H NMR (500 MHz, CDCl₃) δ 8.47 (s, 1H), 8.18 – 8.13 (m, 1H), 7.81 (dd, *J* = 8.0, 0.9 Hz, 1H), 7.66 (qd, *J* = 8.5, 2.6 Hz, 1H), 7.52 – 7.45 (m, 1H), 4.31 (t, *J* = 6.7 Hz, 2H), 3.19 – 3.11 (m, 2H), 2.02 – 1.91 (m, 2H), 1.80 – 1.70 (m, 2H), 1.54 – 1.44 (m, 2H), 1.13 – 1.06 (m, 3H), 0.98 (t, *J* = 7.4 Hz, 3H). ¹³C NMR (126 MHz, CDCl₃) δ 172.1, 151.8, 144.5, 143.7, 140.8, 138.6, 129.8, 129.1, 125.7, 124.5, 121.3, 65.7, 36.2, 31.0, 23.3, 19.2, 13.9, 13.8. MS (ESI) calculated for C₁₈H₂₁N₃O₂S, *m/z* 343.14, found 344.14 [M+H]⁺.

15p: Octyl (2-propylthiazolo[4,5-c]quinolin-4-yl)carbamate. White solid (60 mg, 73%). ^1H NMR (500 MHz, CDCl_3) δ 8.47 (s, 1H), 8.17 – 8.13 (m, 1H), 7.81 (dd, $J = 8.0, 1.0$ Hz, 1H), 7.68 – 7.61 (m, 1H), 7.47 (ddd, $J = 8.1, 7.2, 1.1$ Hz, 1H), 4.30 (t, $J = 6.7$ Hz, 2H), 3.15 (dd, $J = 9.7, 5.5$ Hz, 2H), 2.02 – 1.90 (m, 3H), 1.80 – 1.71 (m, 2H), 1.51 – 1.39 (m, 3H), 1.38 – 1.22 (m, 10H), 1.09 (dd, $J = 9.0, 5.8$ Hz, 5H), 0.88 (t, $J = 7.0$ Hz, 3H). ^{13}C NMR (126 MHz, CDCl_3) δ 172.1, 151.8, 144.5, 143.9, 140.8, 138.6, 129.7, 129.1, 125.6, 124.5, 121.3, 66.0, 36.2, 31.9, 29.4, 29.4, 29.0, 26.0, 23.3, 22.8, 14.2, 13.8. MS (ESI) calculated for $\text{C}_{22}\text{H}_{29}\text{N}_3\text{O}_2\text{S}$, m/z 399.20, found 400.21 $[\text{M}+\text{H}]^+$.

Synthesis of compound 15q: 1-(2-Propylthiazolo[4,5-c]quinolin-4-yl)urea. To a stirred solution of **8c** (50 mg, 0.205 mmol) in acetonitrile (2 mL) were added NaHCO_3 (26 mg, 0.307 mmol) and chlorosulfonyl isocyanate (27 μL , 0.307 mmol), and the resulting mixture was stirred at room temperature for 1 h. Then, one more equivalent of chlorosulfonyl isocyanate (27 μL , 0.307 mmol) was added and the reaction mixture was stirred at room temperature for additional 1h. The reaction mixture was diluted with water and extracted with EtOAc (3 \times 10 mL). The organic layer was dried over Na_2SO_4 , concentrated under reduced pressure, and the crude residue was purified by silica gel column chromatography (0-5% MeOH in CH_2Cl_2) to obtain compound **15q** as a white solid (26 mg, 45% starting material was recovered). ^1H NMR (500 MHz, CDCl_3) δ 9.84 (d, $J = 10.8$ Hz, 1H), 8.86 (d, $J = 10.3$ Hz, 1H), 8.03 – 7.94 (m, 1H), 7.84 (ddd, $J = 8.0, 1.4, 0.5$ Hz, 1H), 7.67 (ddd, $J = 8.5, 7.0, 1.4$ Hz, 1H), 7.50 (ddd, $J = 8.1, 7.1, 1.2$ Hz, 1H), 3.24 – 3.08 (m, 2H), 2.05 – 1.87 (m, 2H), 1.09 (t, $J = 7.4$ Hz, 3H). ^{13}C NMR (126 MHz, CDCl_3) δ 172.7, 162.0, 143.8, 143.2, 141.7, 137.5, 129.5, 128.8, 125.8, 124.8, 121.9, 36.2, 23.1, 13.8. MS (ESI) calculated for $\text{C}_{14}\text{H}_{14}\text{N}_4\text{OS}$, m/z 286.09, found 287.09 $[\text{M}+\text{H}]^+$.

Synthesis of compound 15r: *N*-(2-propylthiazolo[4,5-*c*]quinolin-4-yl)methanesulfonamide.

To a stirred solution of **8c** (40 mg, 0.146 mmol) in dichloromethane (2 mL) was added methyl methanesulfonyl chloride (26 μ L, 0.292 mmol), and the resulting mixture was stirred at room temperature for 12 h. The reaction mixture was diluted with water and extracted with CH₂Cl₂ (3 \times 10 mL). The organic layer was dried over Na₂SO₄, concentrated under reduced pressure, and the crude residue was purified by silica gel column chromatography (0-5% MeOH in CH₂Cl₂) to obtain compound **15r** as a white solid (34 mg, 65%). ¹H NMR (500 MHz, CDCl₃) δ 11.91 (s, 1H), 7.73 (d, *J* = 7.8 Hz, 1H), 7.58 (t, *J* = 7.4 Hz, 1H), 7.40 (t, *J* = 7.6 Hz, 2H), 3.29 (s, 3H), 3.20 – 3.15 (m, 2H), 1.97 – 1.87 (m, 2H), 1.07 (t, *J* = 7.4 Hz, 3H). ¹³C NMR (126 MHz, CDCl₃) δ 173.0, 148.8, 143.4, 141.6, 133.5, 130.6, 125.4, 125.2, 117.5, 116.9, 43.2, 36.3, 23.7, 13.8. MS (ESI) calculated for C₁₄H₁₅N₃O₂S₂, *m/z* 321.06, found 322.06 [M+H]⁺.

Compounds **15s-15v** were synthesized similarly as compound **15r**.

15s: *N*-(2-propylthiazolo[4,5-*c*]quinolin-4-yl)ethanesulfonamide. White solid (35 mg, 63%).

¹H NMR (500 MHz, CDCl₃) δ 12.05 (s, 1H), 7.72 (d, *J* = 6.7 Hz, 1H), 7.58 (t, *J* = 7.1 Hz, 1H), 7.40 (d, *J* = 7.3 Hz, 2H), 3.34 (d, *J* = 5.0 Hz, 2H), 3.18 (t, *J* = 7.7 Hz, 2H), 1.99 – 1.87 (m, 2H), 1.46 (t, *J* = 7.4 Hz, 3H), 1.07 (t, *J* = 7.4 Hz, 3H). ¹³C NMR (126 MHz, CDCl₃) δ 172.9, 149.9, 143.3, 141.9, 133.5, 130.7, 125.5, 125.0, 117.7, 116.8, 49.4, 36.3, 23.8, 13.8, 8.3. MS (ESI) calculated for C₁₅H₁₇N₃O₂S₂, *m/z* 335.08, found 336.08 [M+H]⁺.

15t: *N*-(2-propylthiazolo[4,5-*c*]quinolin-4-yl)propane-1-sulfonamide. White solid (35 mg,

61%). ¹H NMR (500 MHz, CDCl₃) δ 12.05 (s, 1H), 7.72 (d, *J* = 6.7 Hz, 1H), 7.58 (t, *J* = 7.1 Hz, 1H), 7.40 (d, *J* = 7.3 Hz, 2H), 3.34 (d, *J* = 5.0 Hz, 2H), 3.18 (t, *J* = 7.7 Hz, 2H), 1.99 – 1.87 (m, 2H), 1.46 (t, *J* = 7.4 Hz, 3H), 1.07 (t, *J* = 7.4 Hz, 3H). ¹³C NMR (126 MHz, CDCl₃) δ 172.9,

149.9, 143.3, 141.9, 133.5, 130.7, 125.5, 125.0, 117.7, 116.8, 49.4, 36.3, 23.8, 13.8, 8.3. MS (ESI) calculated for C₁₆H₁₉N₃O₂S₂, m/z 349.09, found 350.09 [M+H]⁺.

15u: *N*-(2-propylthiazolo[4,5-*c*]quinolin-4-yl)butane-1-sulfonamide. White solid (37 mg, 62%). ¹H NMR (500 MHz, CDCl₃) δ 12.04 (s, 1H), 7.71 (d, *J* = 6.7 Hz, 1H), 7.57 (t, *J* = 7.0 Hz, 1H), 7.39 (d, *J* = 6.2 Hz, 2H), 3.32 (s, 2H), 3.18 (t, *J* = 7.7 Hz, 2H), 2.00 – 1.82 (m, 4H), 1.55 – 1.40 (m, 2H), 1.07 (t, *J* = 7.4 Hz, 3H), 0.94 (t, *J* = 7.4 Hz, 3H). ¹³C NMR (126 MHz, CDCl₃) δ 172.8, 149.7, 143.3, 141.9, 133.5, 130.7, 125.5, 125.0, 117.6, 116.8, 54.8, 36.3, 25.5, 23.8, 21.7, 13.8, 13.8. MS (ESI) calculated for C₁₇H₂₁N₃O₂S₂, m/z 363.11, found 364.11 [M+H]⁺.

15v: 4-Methyl-*N*-(2-propylthiazolo[4,5-*c*]quinolin-4-yl)benzenesulfonamide. White solid (40 mg, 61%). ¹H NMR (500 MHz, CDCl₃) δ 12.04 (s, 1H), 7.71 (d, *J* = 6.7 Hz, 1H), 7.57 (t, *J* = 7.0 Hz, 1H), 7.39 (d, *J* = 6.2 Hz, 2H), 3.32 (s, 2H), 3.18 (t, *J* = 7.7 Hz, 2H), 2.00 – 1.82 (m, 4H), 1.55 – 1.40 (m, 2H), 1.07 (t, *J* = 7.4 Hz, 3H), 0.94 (t, *J* = 7.4 Hz, 3H). ¹³C NMR (126 MHz, CDCl₃) δ 172.8, 149.0, 143.4, 143.0, 142.1, 139.9, 133.5, 130.7, 129.4, 126.7, 125.5, 125.1, 117.7, 117.0, 36.2, 23.67, 21.7, 13.8. MS (ESI) calculated for C₂₀H₁₉N₃O₂S₂, m/z 397.09, found 398.10 [M+H]⁺.

Synthesis of compound 15w: Diethyl (2-propylthiazolo[4,5-*c*]quinolin-4-yl)phosphoramidate. To a stirred solution of **8c** (50 mg, 0.205 mmol) in CH₂Cl₂ (2 mL) was added diethyl chlorophosphate (60 μL, 0.810 mmol), and the resulting mixture was stirred at room temperature for 12 h. The reaction mixture was diluted with water and extracted with CH₂Cl₂ (3 × 10 mL). The organic layer was dried over Na₂SO₄, concentrated under reduced pressure, and the crude residue was purified by silica gel column chromatography (0-5% MeOH in CH₂Cl₂) to obtain compound **15w** as a white solid (45 mg, 56%). ¹H NMR (500 MHz, DMSO) δ 8.41 (d, *J* =

10.1 Hz, 1H), 7.96 (d, $J = 7.8$ Hz, 1H), 7.83 (d, $J = 8.3$ Hz, 1H), 7.68 (dd, $J = 11.2, 4.0$ Hz, 1H), 7.49 (t, $J = 7.4$ Hz, 1H), 4.24 (p, $J = 7.2$ Hz, 4H), 3.20 (t, $J = 7.5$ Hz, 2H), 1.94 – 1.85 (m, 2H), 1.27 (t, $J = 7.0$ Hz, 6H), 1.02 (t, $J = 7.4$ Hz, 3H). ^{13}C NMR (126 MHz, DMSO) δ 171.9, 147.0, 143.0, 140.3, 138.0 (d, $J = 10.4$ Hz), 131.2, 129.2 (d, $J = 207.2$ Hz), 127.8 (d, $J = 94.8$ Hz), 124.9 (d, $J = 12.8$ Hz), 120.2, 63.1 (d, $J = 5.6$ Hz), 35.2, 63.1 (d, $J = 5.6$ Hz), 16.2 (d, $J = 6.8$ Hz) 13.5. MS (ESI) calculated for $\text{C}_{17}\text{H}_{22}\text{N}_3\text{O}_3\text{PS}$, m/z 379.11, found 380.12 $[\text{M}+\text{H}]^+$.

Synthesis of compound 17: 1-(2-Propylthiazolo[4,5-c]quinolin-4-yl)guanidine. Compound **7c** (100 mg, 0.411 mmol) was dissolved in POCl_3 (3 mL) and stirred at 100 °C for 1 h. POCl_3 was evaporated under reduced pressure, ice cold water was added and the residue was extracted with CH_2Cl_2 (3 \times 10 mL). The organic layer was dried over Na_2SO_4 , concentrated under reduced pressure to give crude **16** (100 mg, 93%) which was used further without purification. To a stirred solution of guanidine (62 mg, 0.615 mmol) in 1,4-dioxane (2 mL) was added NaH (12 mg, 0.492 mmol), the reaction mixture was stirred at 60 °C for 30 min. Compound **16** (30 mg, 0.123 mmol) in DMF (2 mL) was added and heating was continued at 90 °C for 12 h. The reaction mixture was diluted with water and extracted with CH_2Cl_2 (3 \times 10 mL). The organic layer was dried over Na_2SO_4 , concentrated under reduced pressure, and the crude residue was purified by silica gel column chromatography (0-10% MeOH in CH_2Cl_2) to obtain compound **17** as a yellow solid (25 mg, 71%). ^1H NMR (500 MHz, MeOD) δ 8.05 (dd, $J = 8.4, 0.5$ Hz, 1H), 8.00 – 7.96 (m, 1H), 7.75 (ddd, $J = 8.4, 7.1, 1.4$ Hz, 1H), 7.62 (ddd, $J = 8.2, 7.1, 1.2$ Hz, 1H), 3.25 (dd, $J = 8.7, 6.4$ Hz, 2H), 2.06 – 1.97 (m, 2H), 1.11 (t, $J = 7.4$ Hz, 3H). ^{13}C NMR (126 MHz, MeOD) δ 175.2, 157.5, 146.0, 143.5, 142.7, 138.9, 131.0, 129.3, 128.0, 125.9, 122.5, 36.9, 24.2, 14.0. MS (ESI) calculated for $\text{C}_{14}\text{H}_{15}\text{N}_5\text{S}$, m/z 285.10, found 286.11 $[\text{M}+\text{H}]^+$.

Compound **18a** was synthesized similarly as compound **15c**.

18a: N-(2-butylthiazolo[4,5-c]quinolin-4-yl)formamide. White solid (32 mg, 71%). ¹H NMR (500 MHz, CDCl₃) δ 9.85 (d, *J* = 10.8 Hz, 1H), 8.86 (d, *J* = 10.3 Hz, 1H), 7.99 (d, *J* = 8.4 Hz, 1H), 7.85 (dd, *J* = 8.0, 0.9 Hz, 1H), 7.67 (ddd, *J* = 8.4, 7.1, 1.4 Hz, 1H), 7.50 (ddd, *J* = 8.1, 7.1, 1.1 Hz, 1H), 3.20 – 3.16 (m, 2H), 1.91 (dt, *J* = 15.2, 7.6 Hz, 2H), 1.55 – 1.45 (m, 2H), 1.01 (t, *J* = 7.4 Hz, 3H). ¹³C NMR (126 MHz, CDCl₃) δ 172.8, 161.9, 143.7, 143.2, 141.6, 137.4, 129.4, 128.7, 125.7, 124.7, 121.8, 33.8, 31.6, 22.2, 13.8. MS (ESI) calculated for C₁₅H₁₅N₃OS, *m/z* 285.09, found 286.10 [M+H]⁺.

Compounds **18b** and **18c** were synthesized similarly as compound **15d**.

18b: N-(2-butylthiazolo[4,5-c]quinolin-4-yl)acetamide. White solid (50 mg, 85%). ¹H NMR (500 MHz, CDCl₃) δ 8.97 (s, 1H), 8.02 (d, *J* = 8.3 Hz, 1H), 7.82 (ddd, *J* = 8.0, 1.4, 0.5 Hz, 1H), 7.65 (ddd, *J* = 8.4, 7.1, 1.4 Hz, 1H), 7.49 (ddd, *J* = 8.1, 7.1, 1.2 Hz, 1H), 3.21 – 3.13 (m, 2H), 2.82 (s, 3H), 1.96 – 1.85 (m, 2H), 1.55 – 1.44 (m, 2H), 1.04 – 0.96 (m, 3H). ¹³C NMR (126 MHz, CDCl₃) δ 172.4, 144.4, 143.4, 140.9, 138.5, 129.2, 129.1, 125.7, 124.7, 121.5, 34.0, 31.8, 25.9, 22.3, 13.9. MS (ESI) calculated for C₁₆H₁₇N₃OS, *m/z* 299.11, found 300.11 [M+H]⁺.

18c: N-(2-butylthiazolo[4,5-c]quinolin-4-yl)butyramide. White solid (55 mg, 87%). ¹H NMR (500 MHz, CDCl₃) δ 8.95 (s, 1H), 8.05 (d, *J* = 8.3 Hz, 1H), 7.82 (ddd, *J* = 8.0, 1.4, 0.4 Hz, 1H), 7.65 (ddd, *J* = 8.4, 7.1, 1.4 Hz, 1H), 7.49 (ddd, *J* = 8.1, 7.1, 1.2 Hz, 1H), 3.22 – 3.06 (m, 4H), 1.95 – 1.83 (m, 4H), 1.54 – 1.45 (m, 2H), 1.10 (t, *J* = 7.4 Hz, 3H), 1.00 (t, *J* = 7.4 Hz, 3H). ¹³C NMR (126 MHz, CDCl₃) δ 172.2, 144.3, 143.4, 140.7, 138.4, 129.1, 129.0, 125.6, 124.5, 121.3, 39.8, 33.8, 31.7, 22.2, 18.5, 14.0, 13.8. MS (ESI) calculated for C₁₈H₂₁N₃OS, *m/z* 327.14, found 328.14 [M+H]⁺.

Human TLR-7/-8 reporter gene assays (NF- κ B induction). The induction of NF- κ B was quantified using HEK-Blue-7 (hTLR7-specific) and HEK-Blue-8 (hTLR8-specific) cells as previously described by us.^{30, 55b, 69} HEK293 cells stably co-transfected with human TLR7 or human TLR8 and secreted alkaline phosphatase (sAP), were maintained in HEK-Blue™ Selection medium containing zeocin and normocin. Stable expression of secreted alkaline phosphatase (sAP) under control of NF- κ B/AP-1 promoters is inducible by appropriate TLR agonists, and extracellular sAP in the supernatant is proportional to NF- κ B induction. HEK-Blue cells were incubated at a density of $\sim 10^5$ cells/ml in a volume of 80 μ l/well, in 384-well, flat-bottomed, cell culture-treated microtiter plates until confluency was achieved, and subsequently stimulated with graded concentrations of stimuli. sAP was assayed spectrophotometrically using an alkaline phosphatase-specific chromogen (present in HEK-detection medium as supplied by the vendor) at 620 nm.

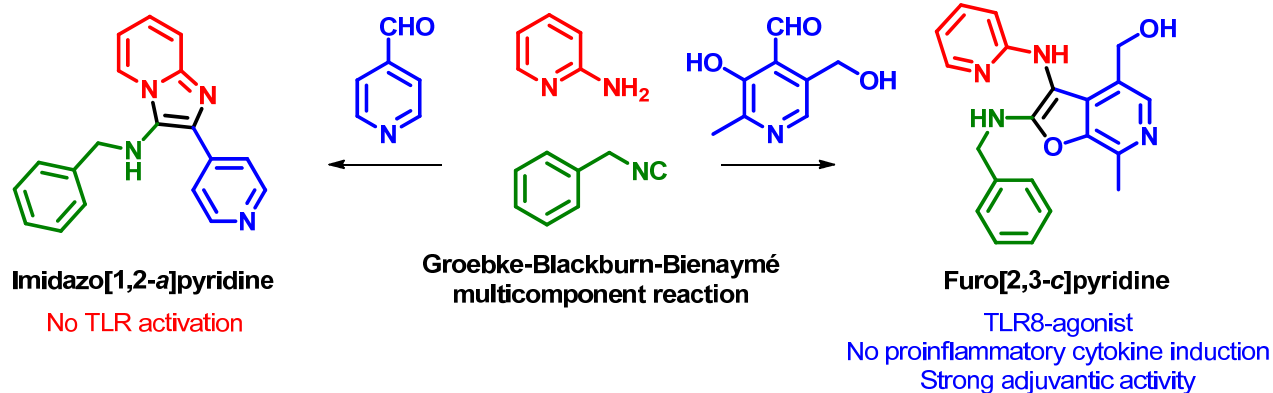
Immunoassays for Interferon (IFN)- α , IFN- γ , Interleukin (IL)-12, IL-18, and cytokines. Fresh human peripheral blood mononuclear cells (hPBMCs) were isolated from human blood obtained by venipuncture with informed consent and as per institutional guidelines on Ficoll-Hypaque gradients as described elsewhere.⁷³ Aliquots of PBMCs (10^5 cells in 100 μ L/well) were stimulated for 12 h with graded concentrations of test compounds. Supernatants were isolated by centrifugation, and were assayed in triplicates using either high-sensitivity analyte-specific ELISA kits (PBL Interferon Source, Piscataway, NJ and R&D Systems, Inc., Minneapolis, MN), or analyte-specific multiplexed cytokine/chemokine bead array assays as reported by us previously.⁶⁹ PBMC supernatants were also analyzed for 41 chemokines and cytokines (EGF, Eotaxin, FGF-2, Flt-3 ligand, Fractalkine, G-CSF, GM-CSF, GRO, IFN- α 2, IFN- γ , IL-10, IL-12 (p40), IL-12 (p70), IL-13, IL-15, IL-17, IL-1ra, IL-1 α , IL-1 β , IL-2, IL-3, IL-4, IL-5, IL-6, IL-7, IL-8, IL-9, IP-10, MCP-1, MCP-3, MDC (CCL22), MIP-1 α , MIP-1 β , PDGF-AA, PDGF-AB/BB,

RANTES, TGF α , TNF- α , TNF- β , VEGF, and sCD40L) using a magnetic bead-based multiplexed assay kit (Milliplex MAP Human Cytokine/Chemokine kit). Data were acquired and processed on a MAGPIX instrument (EMD Millipore, Billerica, MA) with intra-assay coefficients of variation ranging from 4 to 8% for the 41 analytes.

Rabbit immunization and antigen-specific ELISA. All experiments were performed at Harlan Laboratories (Indianapolis, IN) in accordance with institutional guidelines (University of Kansas IACUC permit # 119-06). Cohorts of adult female New Zealand White rabbits (n = 4 per cohort) were immunized intramuscularly in the flank region with (a) 100 μ g of bovine α -lactalbumin in 0.2 mL saline, or (b) 100 μ g of bovine α -lactalbumin plus 100 μ g of either **8c** or **8d** in 0.2 mL saline. Pre-immune test-bleeds were first obtained on Day 1 via venipuncture of the marginal vein of the ear. Animals were immunized on Days 1 and 15. A final test-bleed was performed via the marginal vein of the ear on Day 28. Sera were stored at -80 °C until used. Bovine α -lactalbumin-specific ELISAs were performed in 384-well format using automated liquid handling methods as described by us.⁷⁴

Chapter 3.

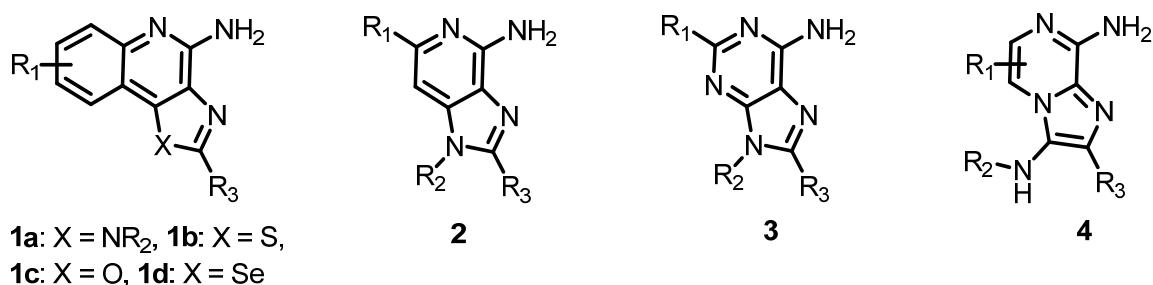
TLR8-agonistic 2,3-diamino-furo[2,3-*c*] pyridines



3.1. Introduction

As mentioned earlier, small molecule TLR7/8 activators constitute a small set of compounds occupying a very small chemical space. The identification of simpler molecules as TLR7/8 agonists may pave the way for inexpensive vaccine constructs, and we are therefore keenly interested in exploring alternative chemotypes that are synthetically less complex. A detailed structural characterization of the mode of binding of TLR7 ligands is not yet available to guide scaffold-hopping approaches.⁷⁵ We speculated that 3,8-diamino-imidazo[1,2-*a*]pyrazines **4** may bear sufficient structural similarities to the known TLR7/8 ligands (Fig. 1). These molecules are, in principle, readily accessible in two steps (one-pot synthetic process) via the Groebke-Blackburn-Bienaymé multicomponent reaction,⁷⁶ and we envisaged a rapid elaboration and screening of a library of compounds for TLR7/8 agonistic activities.

Fig. 1. TLR7/8 agonistic scaffolds. R_1 is typically alkyl or *O*-alkyl, R_2 is alkyl or benzyl, and R_3 is usually alkyl and OH in oxoadenines.



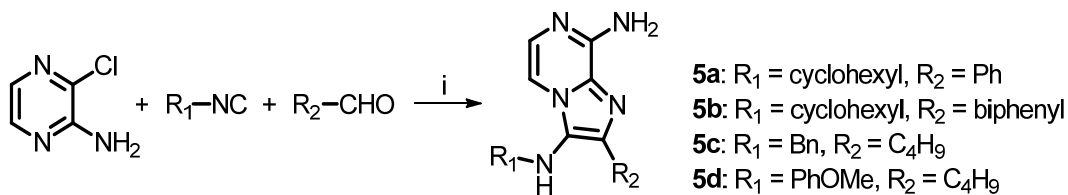
We began with the syntheses of small test-libraries of 3,8-diamino-imidazo[1,2-*a*]pyrazines as well as 3-amino-imidazo[1,2-*a*]pyridine/pyrazines (Schemes 1 and 2). Most of these compounds (**5a-d**, **6-23**) were inactive in NF- κ B reporter gene assays specific for human TLR-3, -7, -8, and -9; however compounds **26-29** obtained with pyridoxal as the aldehyde component were found to specifically activate NF- κ B signaling in TLR8-transfected HEK293 cells. Detailed spectroscopic

analyses confirmed the formation of a hitherto unknown 2,3-diamino-furo[2,3-*c*]pyridine skeleton via a non-canonical pathway, which was unambiguously confirmed by single crystal X-ray analysis. The TLR8-specific agonistic properties of this novel and unexpected chemotype warranted a systematic SAR, which is presented herein.

3.2. Results and Discussion

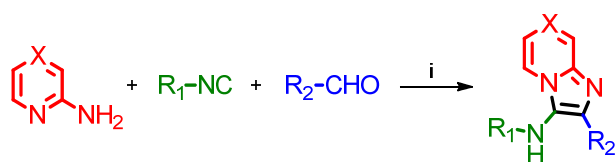
We have previously described extensive SAR on the 1,2-disubstituted-(1*H*-imidazo[4,5-*c*]quinoline-4-amines) class of compounds (**1a**, Fig. 1) as TLR7/8 agonists,^{55b, 58, 69, 77} and their application in designing self-adjuvanting vaccine constructs.⁵⁶ In our ongoing search toward identifying novel and synthetically simpler candidate vaccine adjuvants, we hypothesized that the imidazo[1,2-*a*]pyrazines **4** would possess sufficient structural similarity with the known small molecule TLR7/8 ligands such as **1-3** (Fig. 1). These molecules are readily accessible in a one-pot, two-step process using the Groebke-Blackburn-Bienaymé multicomponent reaction as a key step. An acid-catalyzed (HCl in dioxane), microwave-mediated (400 W, 110 °C, 10 min) reaction using 2-amino-3-chloropyrazine (amidine component), isocyanocyclohexane (isonitrile component) and benzaldehyde (aldehyde component) resulted, as expected, in 8-chloro-*N*-cyclohexyl-2-phenylimidazo[1,2-*a*]pyrazin-3-amine (Scheme 1). Subsequent microwave-mediated *ipso*-chloro displacement using ammonium hydroxide was unsuccessful, but conventional heating in a sealed tube (110 °C, 16 h) furnished the desired *N*³-cyclohexyl-2-phenylimidazo[1,2-*a*]pyrazine-3,8-diamine **5a** (Scheme 1) in 30% yield over two steps. Using this one-pot process, a small set of 8-amino-imidazo[1,2-*a*]pyrazines **5b-d** was synthesized by varying the aldehyde and isonitrile components (Scheme 1).

Scheme 1. A two step one-pot synthetic process.

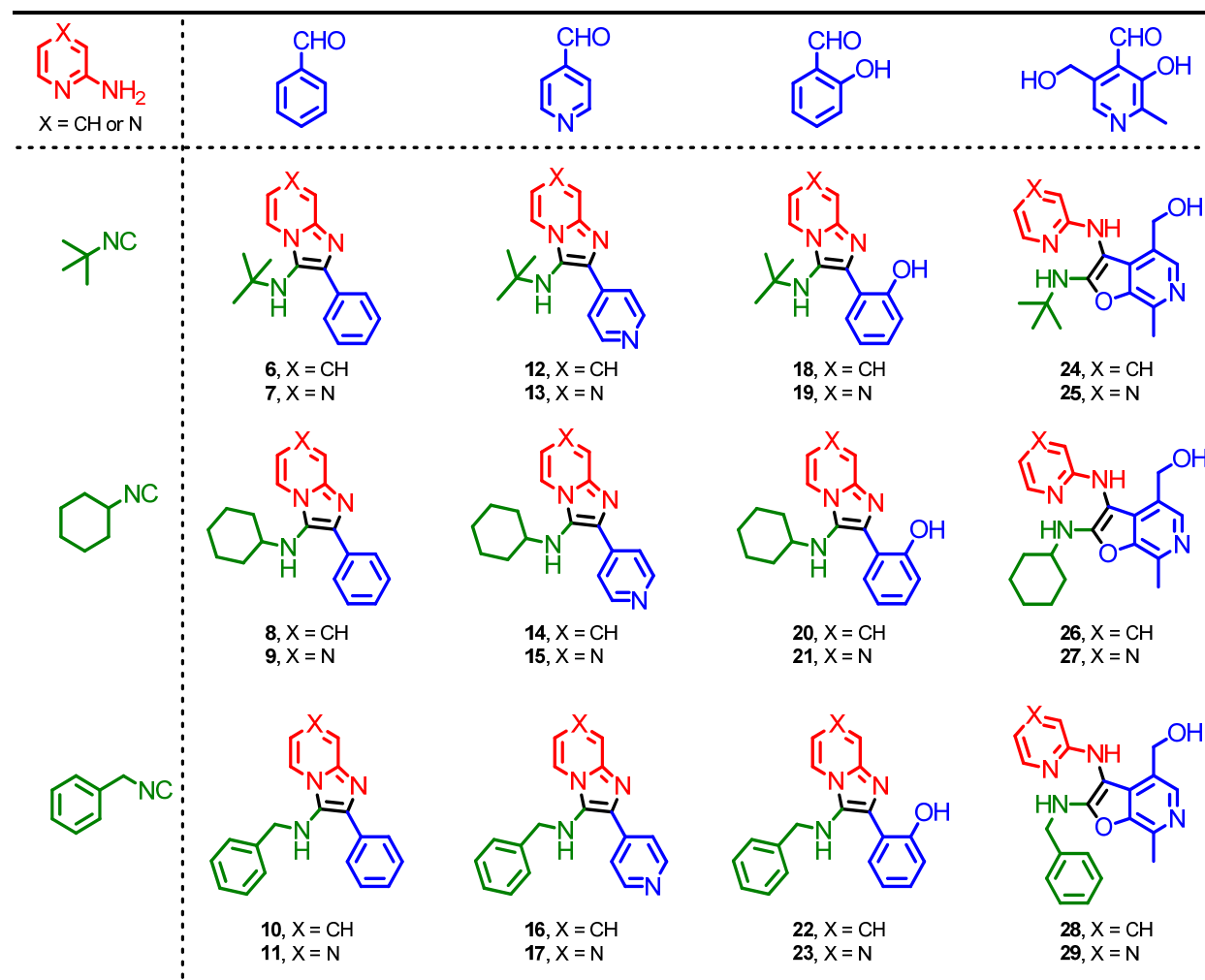


Reagents and conditions: i. (a) HCl in 1,4-dioxane, CH₃CN, MW 400W, 110 °C, 20 min (b) NH₄OH, 110 °C, 16h.

Scheme 2. Twenty-four membered diverse test-library.



Reagents and conditions: i. HCl in 1,4-dioxane, CH₃CN, MW 400W, 110 °C, 20 min.



Simultaneously, a diverse test-library comprising of twenty-four compounds was also synthesized using two amidines (2-aminopyridine and 2-aminopyrazine), three isocyanides (2-isocyano-2-methylpropane, isocyanocyclohexane, (isocyanomethyl)benzene), and four aldehydes (benzaldehyde, isonicotinaldehyde, salicylaldehyde, and pyridoxal) (Scheme 2). The syntheses of **6-23** proceeded smoothly. However, the typical Groebke reaction, carried out at 110 °C for 20 min in CH₃CN, was found to be excessively harsh for reactions using pyridoxal (**24-29**), leading to low yields and charring of reaction mixtures. Reactions for this subset of compounds progressed rapidly in 2 min under microwave conditions at 80 °C and 600 W power in CH₃CN or MeOH. We noticed that only compounds **24-29** (synthesized using pyridoxal) were fluorescent on TLC under long-wave ultraviolet radiation.

The compounds were screened in NF- κ B reporter gene assays specific for human TLR-3, -4, -5, -7, -8, and -9. The 3,8-diamino-imidazo[1,2-*a*]pyrazines **5a-d** as well as 3-amino-imidazo[1,2-*a*]pyridine/pyrazine library members **6-23** did not display any activity in these assays up to concentrations of 250 μ M. However, compounds **26-29** obtained with the use of pyridoxal as the aldehyde component, were found to specifically activate NF- κ B signaling in human TLR8-transfected HEK293 cells (Table 1, Fig. 2), but not human TLR-3, -4, -5, -7, and -9.

The NMR spectra of compounds **26-29** as well as their fluorescence properties alerted us to the possibility of the formation of a new chemical entity with a heterocyclic system other than the classical imidazo[1,2-*a*]pyridine/pyrazines during the Groebke-Blackburn-Bienaymé multi-component reaction. In ¹H NMR spectra, the aliphatic CH of the cyclohexyl group in compounds **8/9**, **14/15**, and **20/21** (Scheme 2) appeared in the range of 3.0 to 3.1 δ ppm, whereas a pronounced downfield shift of this CH proton (up to 3.85 δ ppm) was observed in compounds **26** and **27**. Similar observations were noted in another set in which the aliphatic benzylic CH₂ in

compounds **10/11**, **16/17**, and **22/23** appeared in the range of 4.2 to 4.3 δ ppm, whereas a pronounced downfield shift of this CH₂ (up to 4.76 δ ppm) was observed in compounds **28** and **29**. ¹³C NMR spectra of compounds **24-29** showed an unusual upfield shift of one of the aromatic quaternary carbons in the region (90-96 δ ppm) (Fig. 3). These observations suggested a different heterocyclic system in **24-29**. Initial efforts to crystallize these molecules were unsuccessful. Pending continuing crystallization efforts, we sought to elucidate the structures of these compounds via alternate routes.

Fig. 2. Dose-response profiles of TLR8 agonism by select 2,3-diamino-furo[2,3-*c*]pyridines. Top: TLR8 agonism by compounds derived from Schemes 2 and 5. Bottom: TLR8 agonism by compounds derived from Schemes 6 and 7.

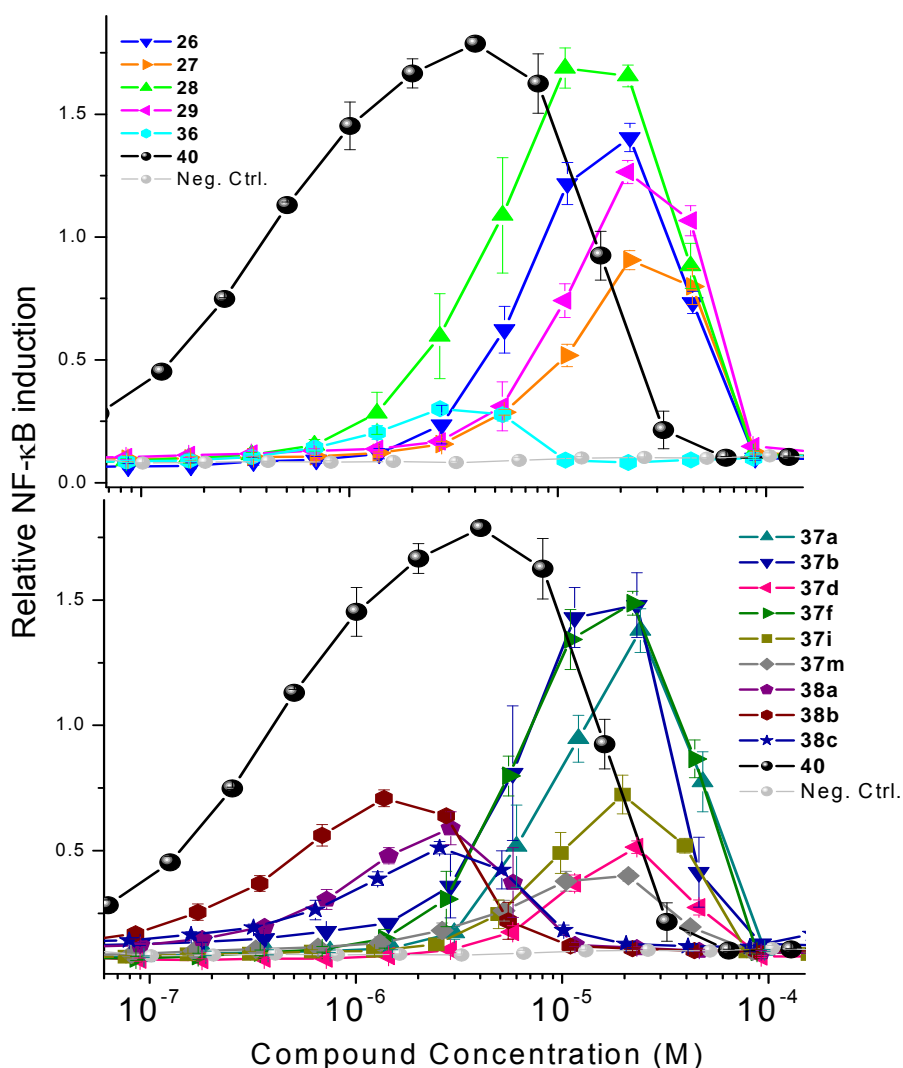
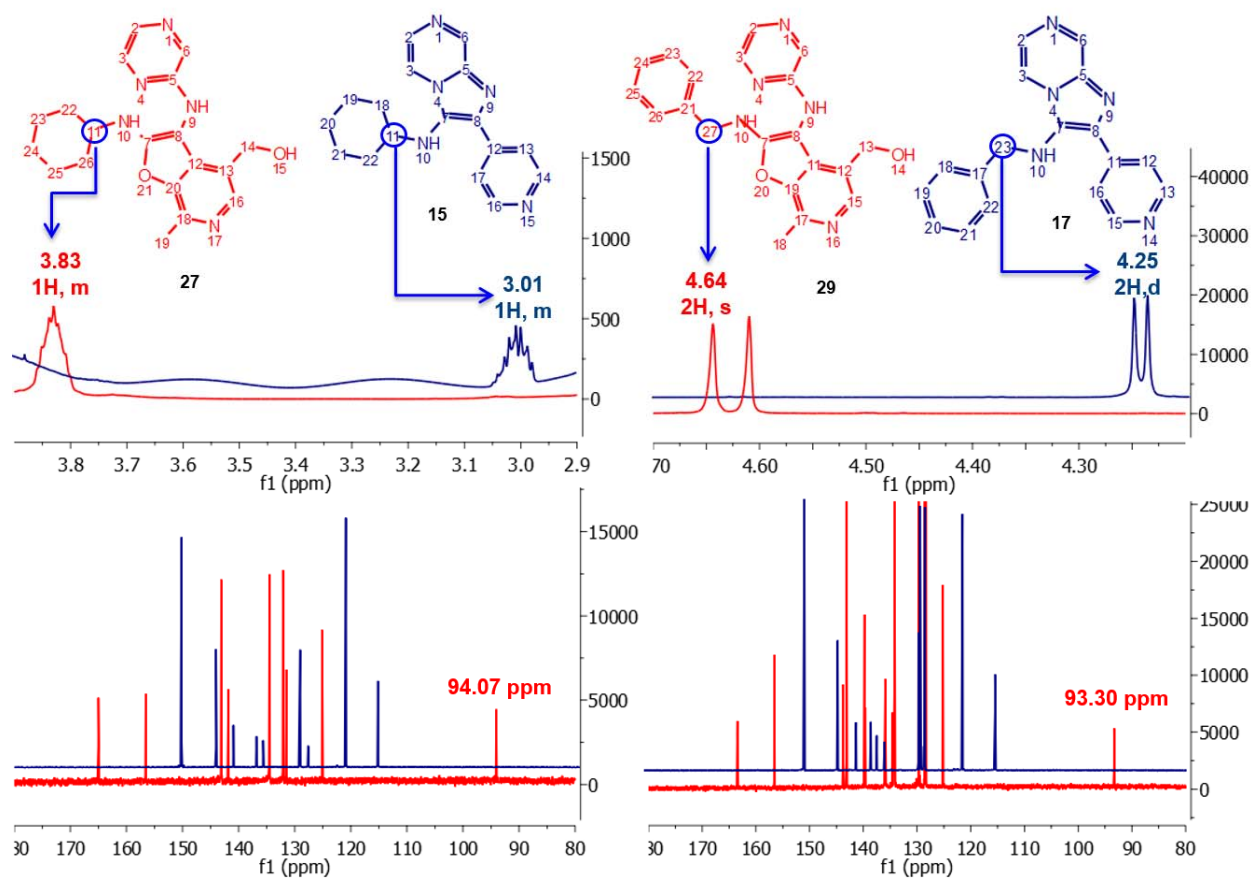


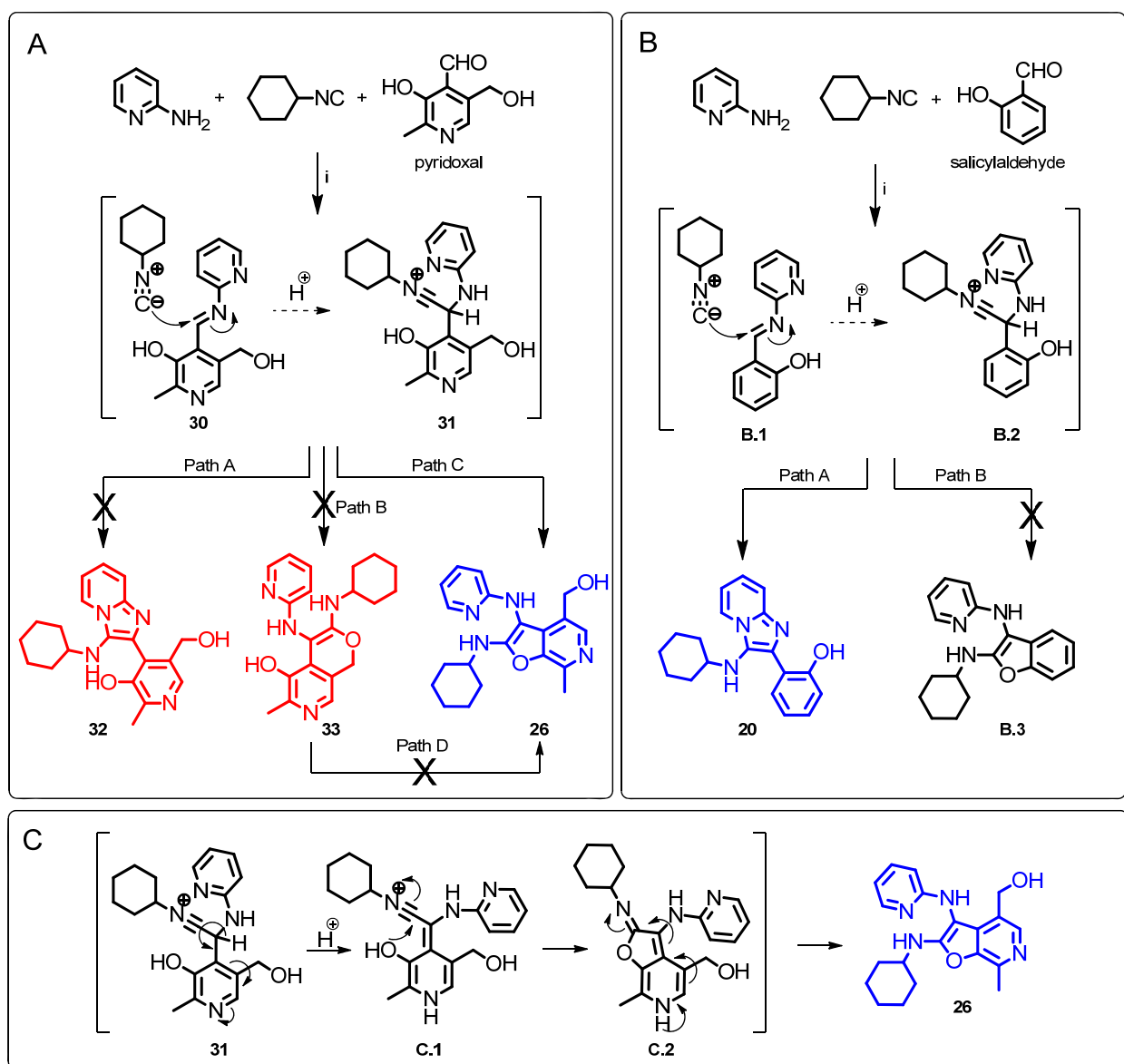
Fig. 3. ^1H and ^{13}C NMR spectra of the classic Groebke products (**15** and **17**) and non-Groebke, pyridoxal-derived furo[2,3-*c*]pyridines (**27** and **29**).



Three possible cyclization products appeared plausible in this acid-catalyzed multicomponent reaction (Panel A in Scheme 3). As mentioned earlier, NMR spectroscopic observations for compounds **24-29** were not congruent with the 4-(3-(cyclohexylamino)imidazo[1,2-*a*]pyridin-2-yl)-5-(hydroxymethyl)-2-methylpyridin-3-ol **32**, the expected product via the canonical Groebke mechanism ('Path A', Panel A in Scheme 3). In order to test whether the phenolic or benzylic hydroxyl groups of pyridoxal may be involved in an alternate pathway of cyclization, we carried out a reaction using a pyridoxal derivative **34** with its phenolic hydroxyl protected with a benzyl group (Scheme 4). This resulted in a product with a spectral signature entirely consistent with

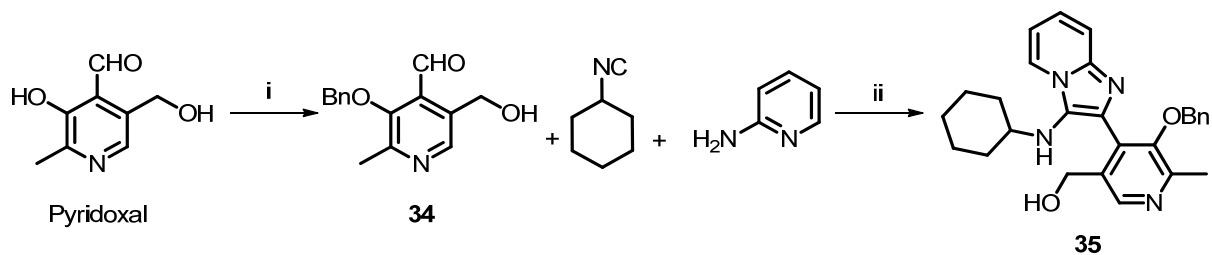
the classical Groebke product (5-(benzyloxy)-4-(3-(cyclohexylamino)imidazo[1,2-a]pyridin-2-yl)-6-methylpyridin-3-yl)methanol **35**, indirectly also ruling out the possibility of cyclization involving the benzylic hydroxyl group ('Path B', Panel A in Scheme 3). We reasoned that annulation via 'Path C' ought to lead to a furo[2,3-c]pyridine skeleton **26**, and that if this were indeed the case, this cyclization could proceed even if the amidine were to be replaced with an aniline.

Scheme 3. Possible cyclization pathways and proposed mechanism.



Reagents and conditions: *i*. HCl in 1,4-dioxane, CH₃CN or CH₃OH, MW 600W, 80 °C, 2 min.

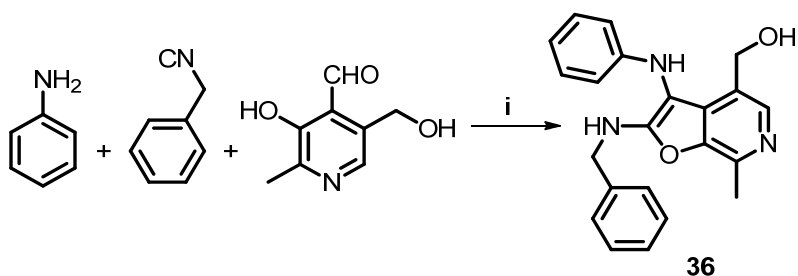
Scheme 4. Synthesis of compound **35** using a pyridoxal derivative **34** with its phenolic hydroxyl protected with a benzyl group.



Reagents and conditions: i. BnBr, K₂CO₃, DMF, 25 °C, 16h; ii. HCl in 1,4-dioxane, CH₃CN, MW 400W, 110 °C, 20 min.

We were gratified that a multicomponent reaction involving aniline, benzyl isonitrile and pyridoxal (Scheme 5) yielded the fluorescent compound **36**, which ¹H and ¹³C NMR spectra resembled those of compounds **24-29**. Interestingly, **36** was also found to be weakly active (EC₅₀ = 1.68 μM) in primary TLR8 screens (Table 1, Fig. 2). Our investigations suggested the formation of a hitherto unknown furo[2,3-*c*]pyridine structure, exclusively when pyridoxal was used as the aldehyde component in the Groebke-Blackburn-Bienaymé multicomponent reaction.

Scheme 5. Synthesis of compound **36** using aniline.



Reagents and conditions: i. HCl in 1,4-dioxane, CH₃OH, MW 600W, 80 °C, 2 min.

Although a definitive elucidation of the reaction mechanism leading to the unexpected furo[2,3-*c*]pyridine was not an immediate goal, understanding plausible mechanisms was of interest, and

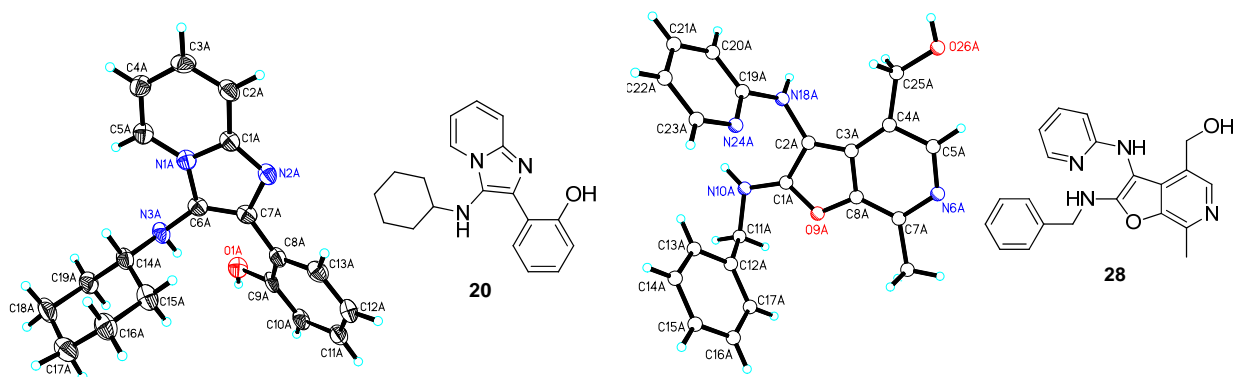
was probed in some detail. Formation of the pyrano[3,4-*c*]pyridine **33** via nucleophilic attack of the benzylic hydroxyl group, and its subsequent rearrangement to the furo[2,3-*c*]pyridine **26** (Path D, Panel A in Scheme 3) appeared improbable. Salicylaldehyde, which lacks the bulky hydroxymethylene group, yielded the classical imidazo[1,2-*a*]pyridine **20** (confirmed by single crystal X-ray analysis, see below), rather than the benzofuran derivative **B.3** (Panel B in Scheme 3). We reasoned, therefore, that the benzylic hydroxyl in the transition state **31** could assist cyclization via Path C (Panel A in Scheme 3) due to steric reasons, apposing the phenolic hydroxyl with the electrophilic carbon. In addition to the direct formation of the furo[2,3-*c*]pyridine **26** via path C, a plausible alternate mechanism for this unusual cyclization route, involving the pyridine ring system is proposed in Scheme 3 (Panel C).

After many unsuccessful attempts, a hydrochloride salt of compound **28** was crystallized as multiply-twinned bundles in acetonitrile. A multi-domain specimen of **28** was cut from one bundle which gave a set of diffracted intensities, permitting a crystal structure solution (non-centrosymmetric, triclinic P1-C1 space group with eight crystallographically-independent molecules in the asymmetric unit), but not a satisfactory refinement (Fig. 4). The structure of **28** unambiguously confirmed the furo[2,3-*c*]pyridine chemotype. The structure of compound **20** (obtained with salicylaldehyde, which also possesses a phenolic OH; Scheme 2) was also elucidated, which established the formation of a classic Groebke product 2-(3-(cyclohexylamino)imidazo[1,2-*a*]pyridin-2-yl)phenol (Fig. 4). These observations clearly emphasize the significance of the additional substituents of pyridoxal, directing the unique cyclization route leading to the furo[2,3-*c*]pyridine scaffold.

Thus, our initial attempts toward the synthesis of twenty-four membered imidazo[1,2-*a*]pyrazine/pyridine test-library unexpectedly resulted in the formation of densely substituted furo[2,3-*c*]pyridines **24-29**. Pyridoxal was found to be an indispensable component for this cyclization

reaction. Four of the six compounds obtained (**26-29**, Scheme 2) were found to be active in our primary screens using TLR8-transfected HEK293 cells, while compounds **24** and **25**, synthesized using 2-isocyano-2-methylpropane as one of the components, were found to be inactive, warranting detailed structure based activity relationship investigations for this new chemotype.

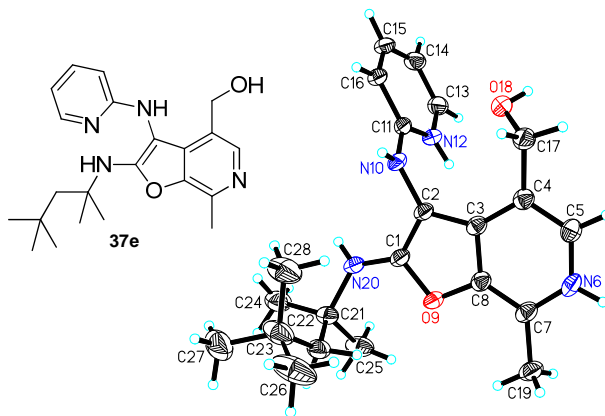
Fig. 4. Crystal structures of the salicylaldehyde-derived classic Groebke product (imidazo[1,2-*a*]pyridine, **20**), and a non-Groebke, pyridoxal-derived furo[2,3-*c*]pyridine, **28**.



Among the active compounds **26-29**, we observed that compounds **26** and **28** (derived from 2-aminopyridine) were more active than **27** and **29** (from 2-aminopyrazine; Table 1, Fig. 2). We therefore selected 2-aminopyridine and pyridoxal as the invariant components and varied the isonitrile component. We explored thirteen different isonitriles (Scheme 6), including linear aliphatic (as in **37a** and **37b**), branched aliphatic (**37c-e**), linear aliphatic with silyl (**37f**), heteroaromatic ring (**37g**), ester (**37h** and **37i**), and phosphate ester (**37j**) termini, as well as aromatic substituents (**37k-m**). Maximal activity was observed in **37b**, with a pentylene substituent on the C2 amine (Scheme 6, Fig. 2). Diminishing the chain length by one methylene unit (**37a**) decreased activity, and potency was further attenuated in compounds with alpha-

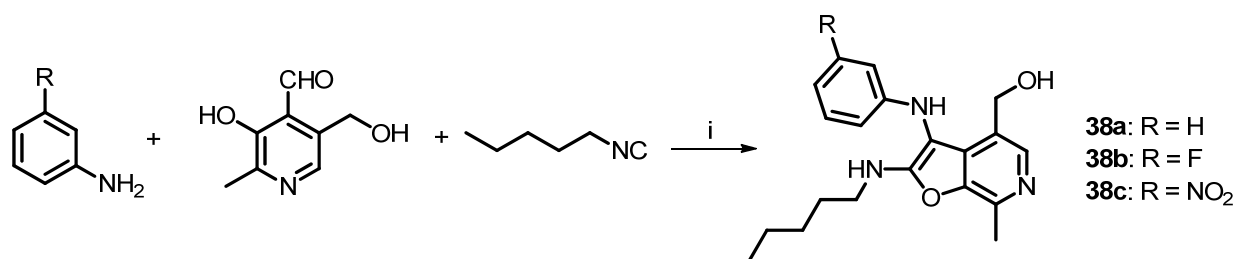
As mentioned earlier, our earlier efforts at unambiguously confirming the structure of **28** did not allow for satisfactory crystal structure refinement because of the intrinsic properties of the crystal space group. Having synthesized thirteen additional furo[2,3-*c*]pyridines (**37a-m**) for purposes of delineating SAR, a parallel crystallization of these compounds was attempted using various solvents. Suitable crystals of compound **37e** were obtained as pale yellow crystals by slow evaporation of a super-saturated solution of **37e** in CH₃CN/CH₃OH mixtures at room temperature. A single-domain specimen was selected and the X-ray diffraction data was collected. The ORTEP diagram of **37e** is shown in Fig. 5, confirming the non-Groebke furo[2,3-*c*]pyridine.

Fig. 5. Crystal structure (ORTEP view) of the non-Groebke furo[2,3-*c*]pyridine, **37e**, obtained with the use of pyridoxal as the aldehyde component.



Previous mention was made that **36** (Scheme 5) was found to be weakly active ($EC_{50} = 1.68$ μ M, Table 1, Fig. 2) relative to the lead compound **28**, suggesting that the 2-aminopyridine core could be substituted by anilines in this multicomponent reaction. Having optimized the C2 group as pentylamine (derived from 1-isocyanopentane, Scheme 6), three more furo[2,3-*c*]pyridines were synthesized using aniline **38a**, 3-fluoroaniline **38b**, and 3-nitroaniline **38c** in combination with 1-isocyanopentane and pyridoxal (Scheme 7).

Scheme 7. Synthesis of analogues using substituted anilines.

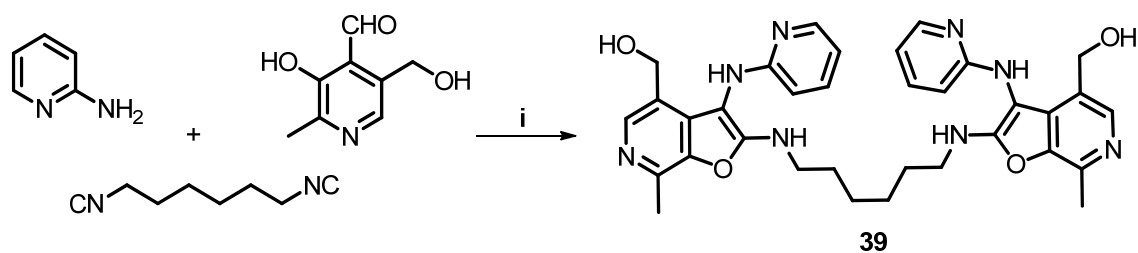


Reagents and conditions: i. HCl in 1,4-dioxane, CH₃OH, MW 600W, 80 °C, 2 min.

The C2 *N*-pentyl analogue **38a** was found to be more active than the C2 *N*-benzyl analogue **36** (Fig. 2, Table 1). The nitro derivative **38c** was found to be as potent as the parent compound **38a**, whereas substantial gain in TLR8 activity was noticed for the fluoro-substituted compound **38b** in TLR8-specific functional assays. However, these compounds exhibited a poorer dose-response profile (lower area-under the-curve, Fig. 2). It is pertinent to note that no stable product could be obtained by the replacement of 2-aminopyridine with aliphatic amines.

Several TLRs are thought to signal via ligand-induced dimerization, as evident in the crystal structures of TLRs. Therefore, the dimeric compound **39** was also synthesized using 1,6-diisocyanohexane (Scheme 8); the activity of this analogue was comparable in its TLR8-agonistic potency to the most active compounds, **28**, **37a**, **37b** and **37f** (Table 1).

Scheme 8. Synthesis of dimeric compounds **39**.



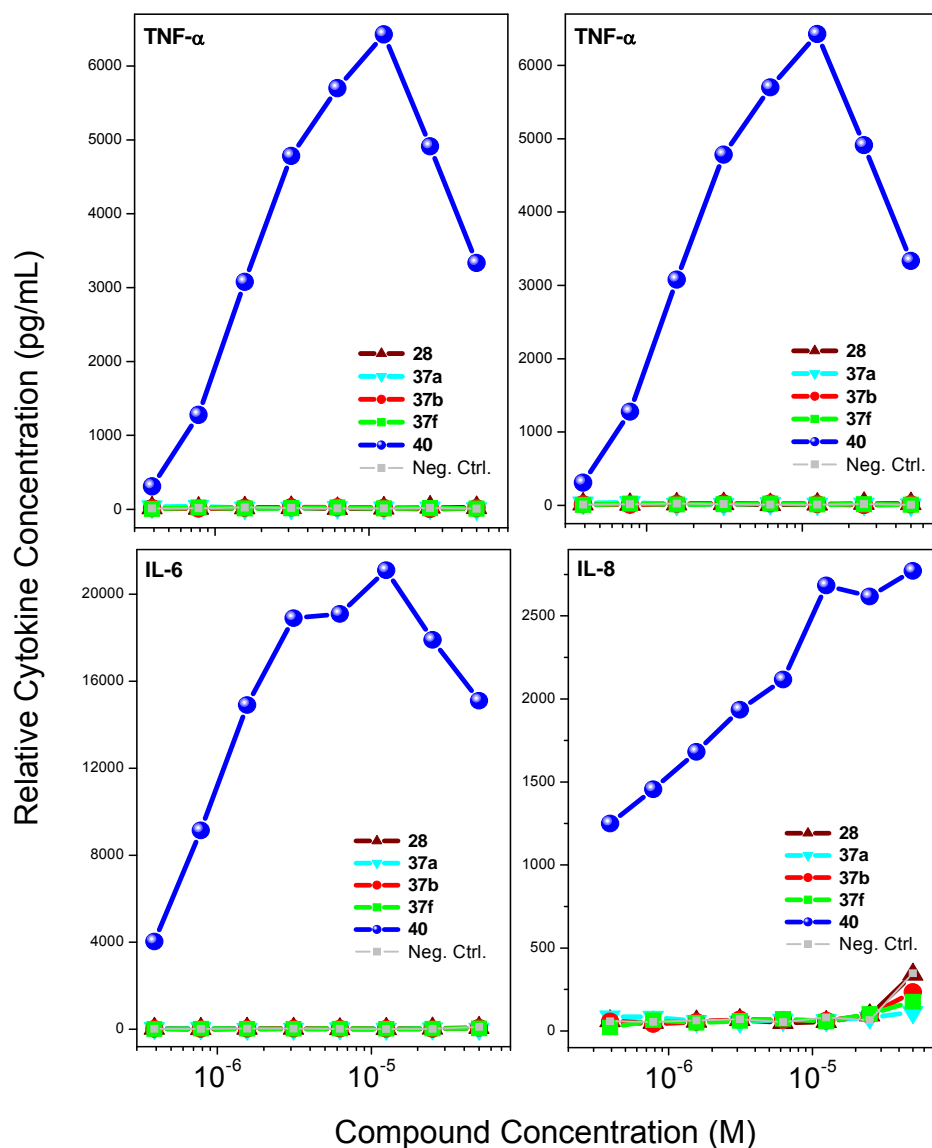
Reagents and conditions: i. HCl in 1,4-dioxane, CH₃CN, MW 600W, 80 °C, 2 min.

Table 1. EC₅₀ values of compounds in human TLR8-specific reporter gene assay.

No.	Structure	TLR8 Agonistic Activity (μM)	No.	Structure	TLR8 Agonistic Activity (μM)
24		Inactive	37f		4.99
25		Inactive	37g		Inactive
26		6.93	37h		Inactive
27		10.58	37i		7.64 Low AUC
28		4.91	37j		Inactive
29		9.79	37k		Inactive
35		Inactive	37l		Inactive
36		1.68 Very low AUC	37m		4.27 Very low AUC
37a		9.38	37n		Inactive
37b		5.81	38a		2.25 Low AUC
37c		Inactive	38b		0.37 Low AUC
37d		9.01 Low AUC	38c		0.85 Low AUC
37e		Inactive	39		3.37

We examined the cytokine-inducing properties^{25a, 30} of a subset of compounds that were maximally active (**28**, **37a**, **37b** and **37f**), all of which showed robust dose-response profiles in primary TLR8-agonistic screens (Fig. 2). We used 2-propylthiazolo[4,5-c]quinolin-4-amine **40** (CL075) as a reference TLR8 agonist,^{45, 62} which exhibited an EC₅₀ of 1.32 μM (Fig. 2). In human PBMCs, only the reference thiazoloquinoline **40**, but none of the furo[2,3-c]pyridines showed any proinflammatory cytokine induction (Fig. 6).

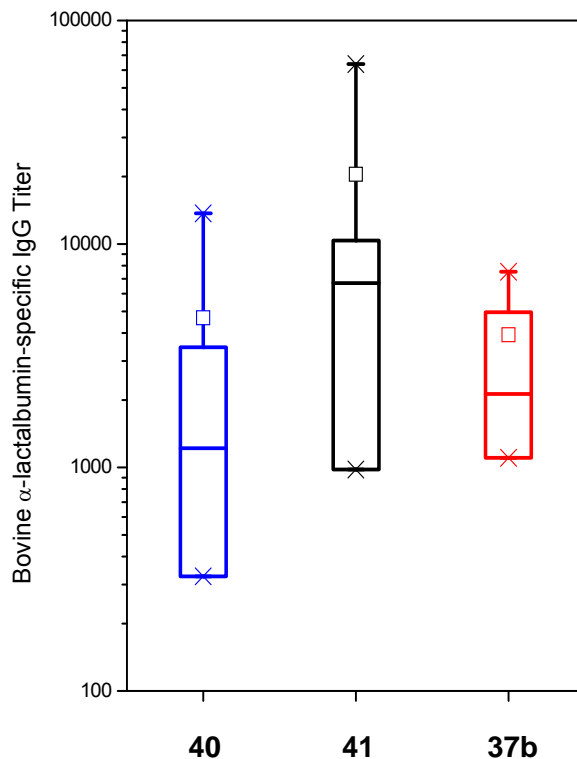
Fig. 6. Dose-response profiles of proinflammatory cytokine induction in hPBMCs by compounds 28, 37a, 37b and 37f. Representative data from three independent experiments are presented.



We do not yet know if the dissociation between TLR8-specific NF- κ B induction on the one hand, and lack of cytokine induction on the other is ascribable to a non-myeloid differentiation primary response gene 88 (MyD88)-independent mechanism.^{33a, 79} However, mindful of recent observations that proinflammatory activity is not an absolute prerequisite for adjuvant properties,⁸⁰ and because we had previously observed potent NF- κ B transactivation in a *bis*-quinoline, 7-chloro-*N*-(4-(7-chloroquinolin-4-ylamino)butyl)quinolin-4-amine **41** (RE-660)⁸¹ unaccompanied by any proinflammatory cytokine induction, we decided to examine two representative compounds (**37b** and **37f**) in transcriptomal profiling experiments. Consistent with the cytokine assays, there were no transcriptional signatures of inflammation; however, both compounds upregulated several chemokine ligand (both CXCL and CCL) genes. Although entirely bereft of any proinflammatory activity, the *bis*-quinoline compound **41** was found to be a potent adjuvant which appears to be related to its functional agonism at CCR1.⁸¹ Given some similarities in activity profiles between the furo[2,3-*c*]pyridines and **41**, we decided to evaluate and compare the adjuvant activity of **37b** alongside the reference compounds, **40** and **41**. Rabbits were immunized using bovine α -lactalbumin as a model subunit antigen.⁵⁶

Anti- α -lactalbumin IgG titers in immune sera clearly showed an adjuvant effect of **37b**, with a rise-in-titer values of >1000, comparable to the adjuvant activities of the reference compounds, **40** and **41** (Fig. 7). The complete lack of proinflammatory cytokine induction coupled with strong adjuvant activity of the novel furo[2,3-*c*]pyridines render this hitherto unknown chemotype an exceedingly attractive class of compounds which are expected to be devoid of local or systemic reactogenicity.

Fig. 7. Anti-bovine α -lactalbumin-specific IgG titers in rabbits adjuvanted with **37b**, **40**, and **41** ($n=4$, for each cohort). Box-plots of ratios of immune/pre-immune titers yielding absorbance values of 1.0 are shown for the individual samples.



3.3. Conclusion

In our ongoing search toward identifying novel and synthetically simpler candidate vaccine adjuvants, we hypothesized that the imidazo[1,2-*a*]pyrazines, readily accessible via the Groebke–Blackburn–Bienaymé multicomponent reaction, would possess sufficient structural similarity with TLR7/8-agonistic imidazoquinolines. With pyridoxal as the aldehyde component, furo[2,3-*c*]pyridines, rather than the expected imidazo[1,2-*a*]pyridines, were obtained, which were characterized by NMR spectroscopy and crystallography. Several analogues were found to activate TLR8-dependent NF- κ B signaling. In a focused library of furo[2,3-*c*]pyridines, a

distinct SAR was observed with varying substituents at C2. In human PBMCs, none of the furo[2,3-*c*]pyridines showed any proinflammatory cytokine induction but upregulated several chemokine ligand genes. In immunization studies in rabbits, the most active compound showed prominent adjuvantic effects. The complete lack of proinflammatory cytokine induction coupled with strong adjuvantic activity of the novel furo[2,3-*c*]pyridines render this hitherto unknown chemotype an attractive class of compounds which are expected to be devoid of local or systemic reactogenicity.

3.4. Experimental

Chemistry. All of the solvents and reagents used were obtained commercially and used as such unless noted otherwise. Moisture- or air-sensitive reactions were conducted under nitrogen atmosphere in oven-dried (120 °C) glass apparatus. The solvents were removed under reduced pressure using standard rotary evaporators. Flash column chromatography was carried out using RediSep Rf “Gold” high performance silica columns on a CombiFlash Rf instrument unless otherwise mentioned, while thin-layer chromatography was carried out on silica gel (200 μm) CCM precoated aluminum sheets. The purity of all final compounds was confirmed to be greater than 95% by HPLCMS using a Zorbax Eclipse Plus 4.6 mm × 150 mm, 5 μm analytical reverse phase C18 column with either H₂O–isopropanol or H₂O–CH₃CN gradients, a diode-array detector operating in the 190–500 nm range (2 nm bandpass), and an Agilent ESI-TOF mass spectrometer (integration on total ion intensity counts, with a mass accuracy of 10 ppm) operating in the positive ion acquisition mode.

Synthesis of compound 5a: *N*³-cyclohexyl-2-phenylimidazo[1,2-*a*]pyrazine-3,8-diamine.

To a solution of 2-amino-3-chloropyrazine (64 mg, 0.50 mmol) in anhydrous acetonitrile (1 mL), were added benzaldehyde (60 μL, 0.60 mmol), 4N HCl/dioxane (10 μL) and cyclohexylisocyanide (74 μL, 0.60 mmol). The reaction mixture was then heated under microwave conditions (400 W, 110 °C) in a sealed vial for 20 min. The reaction mixture was cooled to room temperature; ammonium hydroxide (NH₃ content 28-30%, 0.5 mL) was added and further heated at 110 °C in a sealed vial for overnight. After cooling the reaction mixture to room temperature, the solvents were removed and the residue was purified using column chromatography to obtain compound **5a** (47 mg, 30%). ¹H NMR (500 MHz, MeOD) δ 8.02 (dd, *J* = 8.2, 1.3 Hz, 2H), 7.64 (d, *J* = 4.8 Hz, 1H), 7.46 (dd, *J* = 10.9, 4.6 Hz, 2H), 7.39 – 7.28 (m, 1H), 7.21 (d, *J* = 4.8 Hz, 1H), 2.96 – 2.83 (m, 1H), 1.76 (d, *J* = 11.6 Hz, 2H), 1.71 – 1.62 (m, 2H), 1.57-1.51 (m, 1H), 1.31 – 1.19 (m, 2H), 1.19 – 1.03 (m, 3H). ¹³C NMR (126 MHz, MeOD) δ 151.14, 136.46, 135.17, 129.95, 129.55, 129.44, 128.67, 128.24, 128.11, 109.02, 57.87, 35.05, 26.86, 25.99. MS (ESI) calcd for C₁₈H₂₁N₅, *m/z* 307.1797, found 308.1923 [M+H]⁺.

Compounds **5b-5d** were synthesized similarly as compound **5a**.

5b: 2-([1,1'-Biphenyl]-4-yl)-*N*³-cyclohexylimidazo[1,2-*a*]pyrazine-3,8-diamine. 44 mg, 23%.

¹H NMR (500 MHz, MeOD) δ 8.13 (d, *J* = 8.2 Hz, 2H), 7.72 (d, *J* = 8.3 Hz, 2H), 7.71 – 7.67 (m, 2H), 7.64 (d, *J* = 4.8 Hz, 1H), 7.45 (t, *J* = 7.7 Hz, 2H), 7.38 – 7.31 (m, 1H), 7.22 (d, *J* = 4.8 Hz, 1H), 3.02 – 2.84 (m, 1H), 1.80 (d, *J* = 12.2 Hz, 2H), 1.69 (dd, *J* = 8.2, 5.3 Hz, 2H), 1.55 (s, 1H), 1.35 – 1.23 (m, 2H), 1.24 – 1.01 (m, 3H). ¹³C NMR (126 MHz, MeOD) δ 151.16, 141.92, 141.53, 136.10, 134.18, 130.07, 129.93, 129.56, 128.57, 128.45, 128.13, 128.02, 127.86, 109.03, 57.99, 35.12, 26.88, 26.03. MS (ESI) calcd for C₂₄H₂₅N₅, *m/z* 383.2110, found 384.2382 [M+H]⁺.

5c: *N*³-benzyl-2-butylimidazo[1,2-*a*]pyrazine-3,8-diamine. 10 mg, 7%. ¹H NMR (500 MHz, MeOD) δ 7.44 (d, *J* = 4.8 Hz, 1H), 7.29 – 7.17 (m, 5H), 7.12 (d, *J* = 4.8 Hz, 1H), 4.13 (s, 2H), 2.51 – 2.42 (m, 2H), 1.54 – 1.42 (m, 2H), 1.31 (dq, *J* = 14.8, 7.4 Hz, 2H), 0.91 (t, *J* = 7.4 Hz, 3H). ¹³C NMR (126 MHz, MeOD) δ 150.52, 141.10, 138.98, 130.14, 129.57, 129.49, 128.81, 128.40, 127.74, 108.93, 53.28, 32.76, 27.26, 23.73, 14.26. MS (ESI) calcd for C₁₇H₂₁N₅, *m/z* 295.1797, found 296.1952 [M+H]⁺.

5d: 2-Butyl-*N*³-(4-methoxyphenyl)imidazo[1,2-*a*]pyrazine-3,8-diamine. 36 mg, 23%. ¹H NMR (500 MHz, MeOD) δ 7.26 (d, *J* = 4.7 Hz, 1H), 7.16 (d, *J* = 4.7 Hz, 1H), 6.80 – 6.69 (m, 2H), 6.49 – 6.38 (m, 2H), 3.70 (s, 3H), 2.67 (t, *J* = 7.6 Hz, 2H), 1.73 – 1.62 (m, 2H), 1.41 – 1.23 (m, 2H), 0.88 (t, *J* = 7.4 Hz, 3H). ¹³C NMR (126 MHz, MeOD) δ 154.65, 150.75, 142.09, 140.98, 129.90, 128.28, 124.98, 115.97, 115.50, 109.10, 56.07, 32.40, 27.41, 23.46, 14.15. MS (ESI) calcd for C₁₇H₂₁N₅O, *m/z* 311.1746, found 312.1905 [M+H]⁺.

Synthesis of compound 6: *N*-(*tert*-butyl)-2-phenylimidazo[1,2-*a*]pyridin-3-amine. To a solution of 2-aminopyridine (24 mg, 0.25 mmol) in anhydrous acetonitrile, were added benzaldehyde (28 μL, 0.28 mmol), 4N HCl/dioxane (5 μL) and *tert*-butyl isonitrile (27 μL, 0.24 mmol). The reaction mixture was then heated under microwave conditions (400 W, 110 °C) in a sealed vial for 20 min. After cooling the reaction mixture to room temperature, the solvents were removed and the residue was purified using column chromatography to obtain compound **6** (44 mg, 70%). ¹H NMR (400 MHz, CDCl₃) δ 8.23 (dt, *J* = 6.9, 1.2 Hz, 1H), 7.90 (dt, *J* = 8.1, 1.6 Hz, 2H), 7.55 (dt, *J* = 9.0, 1.0 Hz, 1H), 7.43 (t, *J* = 7.6 Hz, 2H), 7.31 (t, *J* = 7.4 Hz, 1H), 7.13 (ddd, *J* = 9.0, 6.6, 1.3 Hz, 1H), 6.77 (td, *J* = 6.8, 1.1 Hz, 1H), 3.12 (s, 1H), 1.04 (s, 9H). ¹³C NMR (101 MHz, CDCl₃) δ 142.15, 135.42, 135.40, 128.43, 128.32, 127.52, 124.17, 123.64, 117.48,

111.46, 101.91, 56.59, 30.43. MS (ESI) calcd for C₁₇H₁₉N₃, *m/z* 265.1579, found 266.1664 [M+H]⁺.

Compounds **7-29** were synthesized similarly as compound **6**.

7: N-(tert-butyl)-2-phenylimidazo[1,2-a]pyrazin-3-amine. 47 mg, 74%. ¹H NMR (400 MHz, CDCl₃) δ 9.00 (d, *J* = 1.4 Hz, 1H), 8.14 (dd, *J* = 4.6, 1.5 Hz, 1H), 7.91 (dd, *J* = 8.3, 1.3 Hz, 2H), 7.86 (d, *J* = 4.6 Hz, 1H), 7.46 (t, *J* = 7.5 Hz, 2H), 7.37 (t, *J* = 7.4 Hz, 1H), 3.19 (s, 1H), 1.05 (s, 9H). ¹³C NMR (101 MHz, CDCl₃) δ 143.54, 142.40, 137.43, 134.38, 129.04, 128.66, 128.38, 128.33, 125.17, 116.49, 57.11, 30.45. MS (ESI) calcd for C₁₆H₁₈N₄, *m/z* 266.1531, found 267.1588 [M+H]⁺.

8: N-cyclohexyl-2-phenylimidazo[1,2-a]pyridin-3-amine. 64 mg, 86%. ¹H NMR (500 MHz, CDCl₃) δ 8.16 (d, *J* = 6.8 Hz, 1H), 8.05 (dd, *J* = 8.3, 1.2 Hz, 2H), 7.62 (d, *J* = 9.0 Hz, 1H), 7.45 (t, *J* = 7.8 Hz, 2H), 7.32 (t, *J* = 7.4 Hz, 1H), 7.17 (ddd, *J* = 8.9, 6.7, 1.2 Hz, 1H), 6.82 (td, *J* = 6.8, 0.9 Hz, 1H), 3.32 (s, 1H), 3.07 – 2.85 (m, 1H), 1.81 (d, *J* = 13.1 Hz, 2H), 1.68 (dd, *J* = 9.1, 3.6 Hz, 2H), 1.60 – 1.54 (m, 1H), 1.28 – 1.12 (m, 5H). ¹³C NMR (126 MHz, CDCl₃) δ 141.02, 135.43, 133.45, 128.74, 127.74, 127.20, 125.17, 125.04, 123.07, 116.94, 112.30, 57.02, 34.27, 25.81, 24.94. MS (ESI) calcd for C₁₉H₂₁N₃, *m/z* 291.1735, found 292.1832 [M+H]⁺.

9: N-cyclohexyl-2-phenylimidazo[1,2-a]pyrazin-3-amine. 25 mg, 36%. ¹H NMR (500 MHz, CDCl₃) δ 8.99 (d, *J* = 1.4 Hz, 1H), 8.01 (ddd, *J* = 4.6, 3.2, 1.8 Hz, 3H), 7.85 (d, *J* = 4.6 Hz, 1H), 7.48 (t, *J* = 7.7 Hz, 2H), 7.38 (t, *J* = 7.4 Hz, 1H), 3.26 (s, 1H), 3.00 (m, 1H), 2.22 (s, 1H), 1.82 (dd, *J* = 6.6, 5.4 Hz, 2H), 1.70 (dd, *J* = 9.3, 3.3 Hz, 2H), 1.62 – 1.55 (m, 1H), 1.34 – 1.07 (m, 5H). ¹³C NMR (126 MHz, CDCl₃) δ 143.37, 139.08, 136.82, 133.62, 129.01, 128.90, 128.30,

127.42, 126.70, 115.73, 57.02, 34.41, 25.69, 24.91. MS (ESI) calcd for C₁₈H₂₀N₄, *m/z* 292.1688, found 293.1775 [M+H]⁺.

10: *N*-benzyl-2-phenylimidazo[1,2-*a*]pyridin-3-amine. 62 mg, 86%. ¹H NMR (500 MHz, CDCl₃) δ 7.98 (ddt, *J* = 3.7, 3.0, 1.6 Hz, 3H), 7.57 (dt, *J* = 9.0, 1.0 Hz, 1H), 7.45 (t, *J* = 7.7 Hz, 2H), 7.39 – 7.26 (m, 6H), 7.13 (ddd, *J* = 9.0, 6.7, 1.3 Hz, 1H), 6.74 (td, *J* = 6.8, 1.1 Hz, 1H), 4.20 (d, *J* = 6.1 Hz, 2H), 3.52 (t, *J* = 6.0 Hz, 1H), 2.45 (s, 1H). ¹³C NMR (126 MHz, CDCl₃) δ 141.57, 139.06, 136.04, 134.13, 128.84, 128.30, 127.82, 127.65, 127.16, 125.77, 124.32, 122.50, 117.52, 111.94, 52.57. MS (ESI) calcd for C₂₀H₁₇N₃, *m/z* 299.1422, found 300.1490 [M+H]⁺.

11: *N*-benzyl-2-phenylimidazo[1,2-*a*]pyrazin-3-amine. 45 mg, 62%. ¹H NMR (500 MHz, CDCl₃) δ 8.98 (d, *J* = 1.3 Hz, 1H), 7.94 (dt, *J* = 8.1, 1.6 Hz, 2H), 7.82 (dd, *J* = 4.6, 1.4 Hz, 1H), 7.77 (d, *J* = 4.6 Hz, 1H), 7.47 (t, *J* = 7.6 Hz, 2H), 7.39 (t, *J* = 7.4 Hz, 1H), 7.34 – 7.27 (m, 5H), 4.23 (d, *J* = 2.4 Hz, 2H), 3.66 (s, 1H), 2.20 (s, 1H). ¹³C NMR (126 MHz, CDCl₃) δ 143.46, 138.76, 138.56, 136.79, 133.34, 129.06, 129.03, 128.99, 128.46, 128.24, 128.08, 127.42, 127.18, 115.38, 52.39. MS (ESI) calcd for C₁₉H₁₆N₄, *m/z* 300.1375, found 301.1494 [M+H]⁺.

12: *N*-(*tert*-butyl)-2-(pyridin-4-yl)imidazo[1,2-*a*]pyridin-3-amine. 50 mg, 78%. ¹H NMR (500 MHz, CDCl₃) δ 8.65 (d, *J* = 5.9 Hz, 2H), 8.20 (dt, *J* = 6.9, 1.0 Hz, 1H), 7.96 (dd, *J* = 4.7, 1.4 Hz, 2H), 7.56 (d, *J* = 9.1 Hz, 1H), 7.18 (ddd, *J* = 9.0, 6.6, 1.2 Hz, 1H), 6.81 (td, *J* = 6.8, 1.0 Hz, 1H), 3.07 (s, 1H), 1.10 (s, 9H). ¹³C NMR (126 MHz, CDCl₃) δ 149.69, 142.82, 142.39, 136.46, 124.86, 124.77, 123.38, 122.17, 117.68, 111.82, 56.78, 30.38. MS (ESI) calcd for C₁₆H₁₈N₄, *m/z* 266.1531, found 267.1747 [M+H]⁺.

13: *N*-(*tert*-butyl)-2-(pyridin-4-yl)imidazo[1,2-*a*]pyrazin-3-amine. 49 mg, 76%. ¹H NMR (500 MHz, CDCl₃) δ 9.02 (d, *J* = 1.4 Hz, 1H), 8.69 (dd, *J* = 4.5, 1.6 Hz, 2H), 8.11 (dd, *J* = 4.7, 1.5 Hz, 1H), 7.94 (dd, *J* = 4.5, 1.6 Hz, 2H), 7.88 (d, *J* = 4.7 Hz, 1H), 3.12 (s, 1H), 1.10 (s, 9H). ¹³C NMR (126 MHz, CDCl₃) δ 150.22, 144.25, 141.96, 139.25, 137.72, 129.39, 126.24, 122.42, 116.42, 57.46, 30.61. MS (ESI) calcd for C₁₅H₁₇N₅, *m/z* 267.1484, found 268.1705 [M+H]⁺.

14: *N*-cyclohexyl-2-(pyridin-4-yl)imidazo[1,2-*a*]pyridin-3-amine. 69 mg, 98%. ¹H NMR (500 MHz, CDCl₃) δ 8.64 (dd, *J* = 4.6, 1.6 Hz, 2H), 8.07 (dt, *J* = 6.9, 1.2 Hz, 1H), 8.00 (dd, *J* = 4.6, 1.6 Hz, 2H), 7.54 (dt, *J* = 9.1, 1.0 Hz, 1H), 7.17 (ddd, *J* = 9.1, 6.6, 1.3 Hz, 1H), 6.81 (td, *J* = 6.8, 1.1 Hz, 1H), 3.11 (d, *J* = 3.9 Hz, 1H), 2.98 (td, *J* = 10.3, 4.1 Hz, 1H), 1.83 (d, *J* = 10.8 Hz, 2H), 1.71 (dd, *J* = 9.4, 3.3 Hz, 2H), 1.59 (dd, *J* = 7.3, 1.4 Hz, 1H), 1.32 – 1.09 (m, 5H). ¹³C NMR (126 MHz, CDCl₃) δ 150.03, 142.26, 142.11, 133.78, 126.92, 124.92, 122.87, 121.21, 117.99, 112.31, 57.26, 34.42, 25.75, 24.97. MS (ESI) calcd for C₁₈H₂₀N₄, *m/z* 292.1688, found 293.1854 [M+H]⁺.

15: *N*-cyclohexyl-2-(pyridin-4-yl)imidazo[1,2-*a*]pyrazin-3-amine. 56 mg, 80%. ¹H NMR (500 MHz, CDCl₃) δ 9.01 (d, *J* = 1.5 Hz, 1H), 8.70 (dd, *J* = 4.5, 1.6 Hz, 2H), 8.03 – 7.93 (m, 3H), 7.88 (d, *J* = 4.6 Hz, 1H), 3.21 (d, *J* = 5.9 Hz, 1H), 3.06 – 2.97 (m, 1H), 1.84 (d, *J* = 10.5 Hz, 2H), 1.72 (dd, *J* = 9.7, 2.6 Hz, 2H), 1.63 – 1.58 (m, 1H), 1.31 – 1.14 (m, 5H). ¹³C NMR (126 MHz, CDCl₃) δ 150.42, 144.32, 141.25, 137.17, 135.99, 129.45, 128.03, 121.37, 115.69, 57.35, 34.55, 25.62, 24.93. MS (ESI) calcd for C₁₇H₁₉N₅, *m/z* 293.1640, found 294.1894 [M+H]⁺.

16: *N*-benzyl-2-(pyridin-4-yl)imidazo[1,2-*a*]pyridin-3-amine. 54 mg, 75%. ¹H NMR (500 MHz, CDCl₃) δ 8.62 (dd, *J* = 4.6, 1.6 Hz, 2H), 7.94 (dt, *J* = 6.9, 1.1 Hz, 1H), 7.90 (dd, *J* = 4.6, 1.6 Hz, 2H), 7.55 (dt, *J* = 9.1, 1.0 Hz, 1H), 7.34 – 7.27 (m, 5H), 7.17 (ddd, *J* = 9.1, 6.6, 1.3 Hz, 1H), 6.76

(td, $J = 6.8, 1.1$ Hz, 1H), 4.22 (d, $J = 6.1$ Hz, 2H), 3.52 (t, $J = 6.1$ Hz, 1H). ^{13}C NMR (126 MHz, CDCl_3) δ 150.12, 142.11, 141.94, 138.64, 133.41, 128.98, 128.31, 128.06, 127.46, 125.05, 122.50, 121.13, 118.06, 112.42, 52.64. MS (ESI) calcd for $\text{C}_{19}\text{H}_{16}\text{N}_4$, m/z 300.1375, found 301.1599 $[\text{M}+\text{H}]^+$.

17: *N*-benzyl-2-(pyridin-4-yl)imidazo[1,2-*a*]pyrazin-3-amine. 47 mg, 65%. ^1H NMR (500 MHz, CDCl_3) δ 9.01 (d, $J = 1.4$ Hz, 1H), 8.67 (dd, $J = 4.5, 1.6$ Hz, 2H), 7.87 (dd, $J = 4.5, 1.6$ Hz, 2H), 7.78 (dt, $J = 4.6, 3.0$ Hz, 2H), 7.30 (dd, $J = 5.1, 1.9$ Hz, 3H), 7.24 (dd, $J = 6.9, 2.6$ Hz, 2H), 4.25 (d, $J = 6.2$ Hz, 2H), 3.66 (t, $J = 6.2$ Hz, 1H). ^{13}C NMR (126 MHz, CDCl_3) δ 150.46, 144.33, 140.94, 138.23, 137.12, 135.70, 129.45, 129.14, 128.45, 128.32, 128.25, 121.34, 115.35, 52.59. MS (ESI) calcd for $\text{C}_{18}\text{H}_{15}\text{N}_5$, m/z 301.1327, found 302.1474 $[\text{M}+\text{H}]^+$.

18: 2-(3-(*tert*-butylamino)imidazo[1,2-*a*]pyridin-2-yl)phenol. 20 mg, 30%. ^1H NMR (500 MHz, CDCl_3) δ 12.47 (bs, 1H), 8.19 (d, $J = 6.9$ Hz, 1H), 8.12 (dd, $J = 7.8, 1.6$ Hz, 1H), 7.51 (d, $J = 9.0$ Hz, 1H), 7.24 – 7.17 (m, 2H), 7.07 – 6.97 (m, 1H), 6.95 – 6.87 (m, 1H), 6.83 (td, $J = 6.8, 0.9$ Hz, 1H), 3.16 (bs, 1H), 1.16 (s, 9H). ^{13}C NMR (126 MHz, CDCl_3) δ 157.07, 148.51, 140.76, 138.42, 134.51, 131.35, 129.43, 128.13, 124.82, 123.01, 118.69, 117.76, 116.96, 112.09, 109.94, 57.22, 30.50. MS (ESI) calcd for $\text{C}_{17}\text{H}_{19}\text{N}_3\text{O}$, m/z 281.1528, found 282.1770 $[\text{M}+\text{H}]^+$.

19: 2-(3-(*tert*-butylamino)imidazo[1,2-*a*]pyrazin-2-yl)phenol. 40 mg, 59%. ^1H NMR (500 MHz, CDCl_3) δ 11.87 (s, 1H), 8.98 (d, $J = 1.4$ Hz, 1H), 8.16 – 8.08 (m, 2H), 7.92 (d, $J = 4.6$ Hz, 1H), 7.31 – 7.24 (m, 1H), 7.05 (dd, $J = 8.2, 1.0$ Hz, 1H), 6.93 (td, $J = 7.9, 1.2$ Hz, 1H), 3.22 (bs, 1H), 1.17 (s, 9H). ^{13}C NMR (126 MHz, CDCl_3) δ 157.08, 142.79, 140.85, 135.93, 130.39, 129.72, 128.31, 123.47, 119.03, 118.04, 117.65, 115.85, 57.73, 30.54. MS (ESI) calcd for $\text{C}_{16}\text{H}_{18}\text{N}_4\text{O}$, m/z 282.1481, found 283.1690 $[\text{M}+\text{H}]^+$.

20: 2-(3-(Cyclohexylamino)imidazo[1,2-a]pyridin-2-yl)phenol. 30 mg, 41%. ¹H NMR (500 MHz, CDCl₃) δ 13.16 (s, 1H), 8.17 (d, *J* = 6.8 Hz, 1H), 8.04 (dd, *J* = 7.8, 1.3 Hz, 1H), 7.50 (dt, *J* = 9.0, 0.9 Hz, 1H), 7.25 – 7.17 (m, 2H), 7.04 (dd, *J* = 8.2, 1.1 Hz, 1H), 6.95 – 6.89 (m, 1H), 6.87 (td, *J* = 6.8, 1.0 Hz, 1H), 3.17 – 2.99 (m, 2H), 1.83 (d, *J* = 12.5 Hz, 2H), 1.72 (dd, *J* = 9.5, 3.1 Hz, 2H), 1.64 – 1.57 (m, 1H), 1.32 (dd, *J* = 22.7, 11.7 Hz, 2H), 1.26 – 1.13 (m, 3H). ¹³C NMR (126 MHz, CDCl₃) δ 157.67, 139.51, 136.00, 129.25, 126.41, 124.88, 123.55, 122.62, 118.82, 117.84, 117.40, 116.64, 112.46, 57.08, 34.19, 25.83, 24.96. MS (ESI) calcd for C₁₉H₂₁N₃O, *m/z* 307.1685, found 308.1995 [M+H]⁺.

21: 2-(3-(Cyclohexylamino)imidazo[1,2-a]pyrazin-2-yl)phenol. 54 mg, 73%. ¹H NMR (500 MHz, CDCl₃) δ 12.52 (bs, 1H), 8.96 (d, *J* = 1.4 Hz, 1H), 8.05 (ddd, *J* = 9.5, 6.2, 1.5 Hz, 2H), 7.94 (d, *J* = 4.6 Hz, 1H), 7.30 – 7.26 (m, 1H), 7.07 (dd, *J* = 8.2, 1.1 Hz, 1H), 6.94 (td, *J* = 8.0, 1.2 Hz, 1H), 3.31 – 2.99 (m, 2H), 1.83 (d, *J* = 12.3 Hz, 2H), 1.77 – 1.70 (m, 2H), 1.62 (dd, *J* = 7.5, 2.3 Hz, 1H), 1.33 (dd, *J* = 21.3, 10.5 Hz, 2H), 1.27 – 1.15 (m, 3H). ¹³C NMR (126 MHz, CDCl₃) δ 157.70, 142.41, 138.53, 134.72, 130.19, 129.97, 126.50, 125.10, 119.13, 118.09, 116.60, 115.35, 57.17, 34.34, 25.69, 24.92. MS (ESI) calcd for C₁₈H₂₀N₄O, *m/z* 308.1637, found 309.1856 [M+H]⁺.

22: 2-(3-(Benzylamino)imidazo[1,2-a]pyridin-2-yl)phenol. 10 mg, 13%. ¹H NMR (500 MHz, CDCl₃) δ 13.02 (s, 1H), 8.06 – 7.95 (m, 2H), 7.51 (d, *J* = 9.0 Hz, 1H), 7.42 – 7.29 (m, 5H), 7.25 – 7.17 (m, 2H), 7.06 (dd, *J* = 8.2, 1.0 Hz, 1H), 6.95 – 6.89 (m, 1H), 6.80 (td, *J* = 6.8, 0.9 Hz, 1H), 4.24 (bs, 2H), 3.41 (s, 1H). ¹³C NMR (126 MHz, CDCl₃) δ 157.75, 139.49, 138.91, 135.58, 129.38, 128.96, 128.43, 127.97, 125.95, 124.95, 124.41, 122.19, 119.04, 117.88, 117.21, 116.74, 112.51, 52.43. MS (ESI) calcd for C₂₀H₁₇N₃O, *m/z* 315.1372, found 316.1611 [M+H]⁺.

23: 2-(3-(Benzylamino)imidazo[1,2-a]pyrazin-2-yl)phenol. 43 mg, 57%. ¹H NMR (500 MHz, CDCl₃) δ 12.40 (bs, 1H), 8.95 (d, *J* = 1.4 Hz, 1H), 8.02 (dd, *J* = 7.9, 1.6 Hz, 1H), 7.82 (d, *J* = 4.6 Hz, 1H), 7.78 (dd, *J* = 4.6, 1.4 Hz, 1H), 7.37 – 7.27 (m, 6H), 7.09 (dd, *J* = 8.3, 1.2 Hz, 1H), 6.94 (ddd, *J* = 7.9, 7.3, 1.2 Hz, 1H), 4.26 (d, *J* = 5.1 Hz, 2H), 3.53 (s, 1H). ¹³C NMR (126 MHz, CDCl₃) δ 157.70, 142.41, 138.44, 138.07, 134.64, 130.35, 129.95, 129.12, 128.39, 128.24, 126.21, 125.76, 119.36, 118.13, 116.33, 114.97, 52.35. MS (ESI) calcd for C₁₉H₁₆N₄O, *m/z* 316.1324, found 317.1545 [M+H]⁺.

24: (2-(*tert*-butylamino)-7-methyl-3-(pyridin-2-ylamino)furo[2,3-*c*]pyridin-4-yl)methanol. 13 mg, 17%. ¹H NMR (400 MHz, MeOD) δ 7.97 (d, *J* = 4.1 Hz, 1H), 7.87 (s, 1H), 7.59 (ddd, *J* = 8.7, 7.2, 1.8 Hz, 1H), 6.75 (ddd, *J* = 7.0, 5.2, 0.7 Hz, 1H), 6.67 (d, *J* = 8.4 Hz, 1H), 4.61 (s, 2H), 2.72 (s, 3H), 1.53 (s, 9H). ¹³C NMR (126 MHz, MeOD) δ 165.65, 159.92, 147.97, 143.43, 140.55, 139.89, 132.15, 131.86, 125.53, 115.57, 110.65, 96.72, 59.04, 55.33, 30.04, 13.08. MS (ESI) calcd for C₁₈H₂₂N₄O₂, *m/z* 326.1743, found 327.1782 [M+H]⁺.

25: (2-(*tert*-butylamino)-7-methyl-3-(pyrazin-2-ylamino)furo[2,3-*c*]pyridin-4-yl)methanol. 14 mg, 18%. ¹H NMR (500 MHz, MeOD) δ 8.01 (d, *J* = 1.1 Hz, 1H), 7.88 (dd, *J* = 2.8, 1.4 Hz, 1H), 7.80 (s, 1H), 7.77 (d, *J* = 2.8 Hz, 1H), 4.56 (s, 2H), 2.65 (s, 3H), 1.43 (s, 9H). ¹³C NMR (126 MHz, MeOD) δ 165.60, 156.50, 143.30, 143.00, 140.79, 134.76, 134.39, 132.05, 131.74, 125.39, 95.43, 58.99, 55.50, 29.98, 12.92. MS (ESI) calcd for C₁₇H₂₁N₅O₂, *m/z* 327.1695, found 328.1836 [M+H]⁺.

26: (2-(Cyclohexylamino)-7-methyl-3-(pyridin-2-ylamino)furo[2,3-*c*]pyridin-4-yl)methanol. 19 mg, 22%. ¹H NMR (500 MHz, MeOD) δ 8.07 (t, *J* = 7.4 Hz, 1H), 7.96 (s, 1H), 7.90 (d, *J* = 5.9 Hz, 1H), 7.29 (d, *J* = 8.4 Hz, 1H), 7.07 (t, *J* = 6.7 Hz, 1H), 4.64 (s, 2H), 3.91 – 3.79 (m, 1H), 2.75

(s, 3H), 2.05 (d, $J = 8.8$ Hz, 2H), 1.87 – 1.77 (m, 2H), 1.68 (d, $J = 13.1$ Hz, 1H), 1.48 – 1.33 (m, 4H), 1.21 (dd, $J = 12.1, 9.2$ Hz, 1H). ^{13}C NMR (126 MHz, MeOD) δ 164.86, 155.98, 145.65, 143.70, 142.10, 137.34, 133.72, 132.85, 124.81, 115.77, 115.45, 89.79, 59.50, 54.25, 34.33, 26.28, 26.16, 12.97. MS (ESI) calcd for $\text{C}_{20}\text{H}_{24}\text{N}_4\text{O}_2$, m/z 352.1899, found 353.2023 $[\text{M}+\text{H}]^+$.

27: (2-(Cyclohexylamino)-7-methyl-3-(pyrazin-2-ylamino)furo[2,3-c]pyridin-4-yl)methanol.

24 mg, 28%. ^1H NMR (500 MHz, MeOD) δ 8.10 (s, 1H), 7.97 (d, $J = 1.4$ Hz, 1H), 7.86 (s, 2H), 4.64 (s, 2H), 3.86 – 3.78 (m, 1H), 2.71 (s, 3H), 2.03 – 1.96 (m, 2H), 1.80 (dd, $J = 5.3, 3.1$ Hz, 2H), 1.66 (d, $J = 13.0$ Hz, 1H), 1.38 (t, $J = 9.6$ Hz, 4H), 1.23 – 1.15 (m, 1H). ^{13}C NMR (126 MHz, MeOD) δ 165.01, 156.57, 143.09, 142.98, 141.82, 134.49, 132.10, 131.50, 125.12, 94.07, 58.98, 53.94, 34.42, 26.31, 26.20, 12.80. MS (ESI) calcd for $\text{C}_{19}\text{H}_{23}\text{N}_5\text{O}_2$, m/z 353.1852, found 354.1902 $[\text{M}+\text{H}]^+$.

28: (2-(Benzylamino)-7-methyl-3-(pyridin-2-ylamino)furo[2,3-c]pyridin-4-yl)methanol.

13 mg, 15%. ^1H NMR (500 MHz, MeOD) δ 8.06 – 8.01 (m, 1H), 8.00 (s, 1H), 7.89 (d, $J = 5.9$ Hz, 1H), 7.44 – 7.39 (m, 2H), 7.34 (t, $J = 7.5$ Hz, 2H), 7.28 (t, $J = 7.3$ Hz, 1H), 7.23 (d, $J = 8.6$ Hz, 1H), 7.05 (t, $J = 6.7$ Hz, 1H), 4.76 (s, 2H), 4.65 (s, 2H), 2.77 (s, 3H). ^{13}C NMR (126 MHz, MeOD) δ 165.45, 156.13, 145.31, 143.75, 142.15, 138.61, 138.18, 133.67, 133.22, 130.23, 130.00, 129.91, 128.97, 128.77, 125.32, 115.82, 115.01, 90.66, 59.42, 47.33, 12.98. MS (ESI) calcd for $\text{C}_{21}\text{H}_{20}\text{N}_4\text{O}_2$, m/z 360.1586, found 361.1830 $[\text{M}+\text{H}]^+$.

29: (2-(Benzylamino)-7-methyl-3-(pyrazin-2-ylamino)furo[2,3-c]pyridin-4-yl)methanol.

15 mg, 16%. ^1H NMR (500 MHz, MeOD) δ 7.99 (s, 1H), 7.94 (dd, $J = 2.8, 1.5$ Hz, 1H), 7.87 (s, 1H), 7.81 (d, $J = 2.8$ Hz, 1H), 7.37 – 7.32 (m, 2H), 7.29 (dd, $J = 10.3, 5.0$ Hz, 2H), 7.21 (t, $J = 7.3$ Hz, 1H), 4.64 (s, 2H), 4.61 (s, 2H), 2.61 (s, 3H). ^{13}C NMR (126 MHz, MeOD) δ 163.44, 156.59,

143.82, 143.17, 139.78, 139.64, 135.93, 134.61, 134.23, 134.16, 129.68, 128.54, 128.38, 125.19, 93.30, 59.41, 47.06, 14.34. MS (ESI) calcd for C₂₀H₁₉N₅O₂, *m/z* 361.1539, found 362.1805 [M+H]⁺.

Synthesis of compound 34: (2-(Benzylamino)-7-methyl-3-(phenylamino)furo[2,3-c]pyridin-4-yl)methanol. To a solution of aniline (45 μ L, 0.5 mmol) in anhydrous methanol, were added pyridoxal hydrochloride (112 mg, 0.55 mmol), 4N HCl/dioxane (10 μ L) and benzyl isonitrile (68 μ L, 0.55 mmol). The reaction mixture was then heated under microwave conditions (600 W, 80 $^{\circ}$ C) in a sealed vial for 2 min. After cooling the reaction mixture to room temperature, the solvents were removed and the residue was purified using column chromatography to obtain compound **34** (84 mg, 47%). ¹H NMR (500 MHz, MeOD) δ 7.88 (s, 1H), 7.34 (d, *J* = 7.8 Hz, 2H), 7.29 (t, *J* = 7.6 Hz, 2H), 7.21 (t, *J* = 7.2 Hz, 1H), 7.09 (t, *J* = 7.9 Hz, 2H), 6.66 (td, *J* = 7.3, 0.9 Hz, 1H), 6.58 – 6.51 (m, 2H), 4.57 (s, 2H), 4.52 (s, 2H), 2.54 (s, 3H). ¹³C NMR (126 MHz, MeOD) δ 160.73, 150.14, 141.35, 141.10, 138.40, 137.10, 130.29, 129.51, 128.35, 128.23, 119.02, 114.15, 94.89, 60.27, 47.02, 16.66. MS (ESI) calcd for C₂₂H₂₁N₃O₂, *m/z* 359.1634, found 360.1832 [M+H]⁺.

Synthesis of compound 35: 3-(Benzyloxy)-5-(hydroxymethyl)-2-methylisonicotin aldehyde. To a solution of pyridoxal hydrochloride (500 mg, 2.45 mmol) in anhydrous DMF, were added potassium carbonate (408 mg, 2.95 mmol), and benzyl bromide (0.35 mL, 2.95 mmol). The reaction mixture was stirred at room temperature for overnight. After the completion of reaction, water (20 mL) was added and the crude product obtained was extracted in ethyl acetate. The organic layer was washed with water, dried over anhydrous sodium sulfate and evaporated. The residue was purified using column chromatography to obtain compound **35** (100 mg, 15%). ¹H NMR (500 MHz, CDCl₃) δ 8.05 (s, 1H), 7.45 – 7.32 (m, 5H), 6.64 (d, *J* = 1.7

Hz, 1H), 5.34 (d, $J = 11.2$ Hz, 1H), 5.22 (d, $J = 12.7$ Hz, 1H), 5.19 (d, $J = 11.2$ Hz, 1H), 4.99 (d, $J = 12.7$ Hz, 1H), 2.50 (s, 3H). ^{13}C NMR (126 MHz, CDCl_3) δ 150.88, 148.63, 136.84, 136.17, 135.53, 135.42, 128.80, 128.47, 127.74, 100.10, 74.13, 69.95, 19.38. MS (ESI) calcd for $\text{C}_{15}\text{H}_{15}\text{NO}_3$, m/z 257.1052, found 258.1279 $[\text{M}+\text{H}]^+$.

Synthesis of compound 36: (5-(Benzyloxy)-4-(3-(cyclohexylamino)imidazo[1,2-a]pyridin-2-yl)-6-methylpyridin-3-yl)methanol. To a solution of 2-aminopyridine (24 mg, 0.25 mmol) in anhydrous acetonitrile, were added 3-(benzyloxy)-5-(hydroxymethyl)-2-methylisonicotinaldehyde **34** (68 mg, 0.28 mmol), 4N HCl/dioxane (5 μL) and cyclohexylisonitrile (30 μL , 0.24 mmol). The reaction mixture was then heated under microwave conditions (400 W, 110 $^\circ\text{C}$) in a sealed vial for 20 min. After cooling the reaction mixture to room temperature, the solvents were removed and the residue was purified using column chromatography to obtain compound **36** (19 mg, 17%). ^1H NMR (500 MHz, CDCl_3) δ 8.41 (s, 1H), 8.07 (d, $J = 6.9$ Hz, 1H), 7.54 (d, $J = 9.1$ Hz, 1H), 7.26 – 7.15 (m, 4H), 7.02 – 6.97 (m, 2H), 6.90 (td, $J = 6.8, 1.0$ Hz, 1H), 4.59 (bs, 1H), 4.43 (s, 2H), 4.36 (bs, 1H), 3.88 (d, $J = 7.9$ Hz, 1H), 2.61 (bs, 1H), 2.58 (s, 3H), 1.85-1.75 (m, 1H), 1.70-1.65 (m, 1H), 1.50-1.40 (m, 2H), 1.37-1.28 (m, 1H), 1.22-1.05 (s, 2H), 1.05-0.85 (m, 2H), 0.60 (bs, 1H). ^{13}C NMR (126 MHz, CDCl_3) δ 152.95, 150.53, 145.20, 141.29, 135.58, 129.62, 129.25, 128.76, 128.58, 128.57, 128.40, 126.28, 125.05, 123.16, 117.47, 112.53, 76.73, 61.64, 56.36, 34.32, 33.74, 25.60, 25.03, 24.53, 19.58. MS (ESI) calcd for $\text{C}_{27}\text{H}_{30}\text{N}_4\text{O}_2$, m/z 442.2369, found 443.2410 $[\text{M}+\text{H}]^+$.

Synthesis of compound 37a: (2-(Butylamino)-7-methyl-3-(pyridin-2-ylamino)furo[2,3-c]pyridin-4-yl)methanol. To a solution of 2-aminopyridine (24 mg, 0.25 mmol) in anhydrous acetonitrile, were added pyridoxal hydrochloride (56 mg, 0.28 mmol), 4N HCl/dioxane (5 μL) and *n*-butyl isonitrile (25 μL , 0.24 mmol). The reaction mixture was then heated under microwave

conditions (600 W, 80 °C) in a sealed vial for 2 min. After cooling the reaction mixture to room temperature, solvents were removed and the residue was purified using column chromatography to obtain compound **37a** (32 mg, 41%). ¹H NMR (500 MHz, MeOD) δ 8.06 (t, *J* = 8.0 Hz, 1H), 7.96 (s, 1H), 7.90 (d, *J* = 5.8 Hz, 1H), 7.29 (d, *J* = 8.5 Hz, 1H), 7.07 (t, *J* = 6.6 Hz, 1H), 4.65 (s, 2H), 3.56 (t, *J* = 7.1 Hz, 2H), 2.75 (s, 3H), 1.75 – 1.61 (m, 2H), 1.49 – 1.35 (m, 2H), 0.96 (t, *J* = 7.4 Hz, 3H). ¹³C NMR (126 MHz, MeOD) δ 165.68, 155.98, 145.61, 143.66, 142.08, 137.58, 133.67, 132.87, 124.84, 115.82, 115.31, 90.01, 59.50, 43.64, 32.79, 20.93, 13.99, 12.96. MS (ESI) calcd for C₁₈H₂₂N₄O₂, *m/z* 326.1743, found 327.1925 [M+H]⁺.

Compounds **37b-37m** were synthesized similarly as compound **37a**.

37b: (7-Methyl-2-(pentylamino)-3-(pyridin-2-ylamino)furo[2,3-*c*]pyridin-4-yl)methanol. 27 mg, 33%. ¹H NMR (500 MHz, MeOD) δ 8.06 (t, *J* = 8.0 Hz, 1H), 7.96 (s, 1H), 7.91 (d, *J* = 5.9 Hz, 1H), 7.28 (d, *J* = 8.5 Hz, 1H), 7.07 (t, *J* = 6.6 Hz, 1H), 4.65 (s, 2H), 3.56 (t, *J* = 7.1 Hz, 2H), 2.75 (s, 3H), 1.75 – 1.64 (m, 2H), 1.38 (d, *J* = 3.6 Hz, 4H), 0.92 (t, *J* = 6.9 Hz, 3H). ¹³C NMR (126 MHz, MeOD) δ 165.68, 156.04, 145.55, 143.66, 142.09, 137.74, 133.66, 132.85, 124.85, 115.82, 115.25, 90.09, 59.49, 43.90, 30.42, 29.98, 23.31, 14.32, 12.95. MS (ESI) calcd for C₁₉H₂₄N₄O₂, *m/z* 340.1899, found 341.2058 [M+H]⁺.

37c: (2-(Isopropylamino)-7-methyl-3-(pyridin-2-ylamino)furo[2,3-*c*]pyridin-4-yl)methanol. 20 mg, 27%. ¹H NMR (500 MHz, MeOD) δ 8.05 (t, *J* = 8.0 Hz, 1H), 7.95 (s, 1H), 7.90 (d, *J* = 5.9 Hz, 1H), 7.26 (d, *J* = 8.6 Hz, 1H), 7.05 (t, *J* = 6.7 Hz, 1H), 4.63 (s, 2H), 4.25 (dt, *J* = 13.0, 6.5 Hz, 1H), 2.74 (s, 3H), 1.33 (d, *J* = 6.5 Hz, 6H). ¹³C NMR (126 MHz, MeOD) δ 164.96, 156.16, 145.41, 143.72, 142.06, 137.79, 133.63, 132.82, 124.86, 115.77, 115.24, 90.04, 59.48, 47.16, 23.12, 12.94. MS (ESI) calcd for C₁₇H₂₀N₄O₂, *m/z* 312.1586, found 313.1740 [M+H]⁺.

37d: (7-Methyl-2-(pentan-2-ylamino)-3-(pyridin-2-ylamino)furo[2,3-c]pyridin-4-yl)methanol.

34 mg, 42%. ¹H NMR (500 MHz, MeOD) δ 7.99 (t, *J* = 8.0 Hz, 1H), 7.88 (s, 1H), 7.83 (d, *J* = 5.2 Hz, 1H), 7.20 (d, *J* = 7.3 Hz, 1H), 7.00 (t, *J* = 6.7 Hz, 1H), 4.56 (s, 2H), 4.03 (dq, *J* = 12.9, 6.5 Hz, 1H), 2.66 (s, 3H), 1.60 – 1.41 (m, 2H), 1.38 – 1.26 (m, 2H), 1.23 (d, *J* = 6.6 Hz, 3H), 0.86 (t, *J* = 7.4 Hz, 3H). ¹³C NMR (126 MHz, MeOD) δ 165.14, 155.98, 145.72, 143.66, 142.17, 137.38, 133.77, 132.84, 124.79, 115.82, 115.41, 89.73, 59.52, 51.18, 39.97, 21.53, 20.53, 14.15, 12.94. MS (ESI) calcd for C₁₉H₂₄N₄O₂, *m/z* 340.1899, found 341.2077 [M+H]⁺.

37e: (7-Methyl-3-(pyridin-2-ylamino)-2-((2,4,4-trimethylpentan-2-yl)amino)furo[2,3-c]

pyridin-4-yl)methanol. 33 mg, 36%. ¹H NMR (500 MHz, MeOD) δ 8.08 (t, *J* = 8.0 Hz, 1H), 7.99 (s, 1H), 7.90 (s, 1H), 7.27 (s, 1H), 7.08 (dd, *J* = 7.0, 6.4 Hz, 1H), 4.63 (s, 2H), 2.78 (s, 3H), 1.95 (d, *J* = 12.9 Hz, 2H), 1.60 (s, 6H), 1.00 (s, 9H). ¹³C NMR (126 MHz, MeOD) δ 165.37, 156.14, 145.64, 143.96, 141.40, 137.05, 133.87, 132.93, 124.92, 115.77, 115.62, 90.82, 59.88, 59.51, 53.31, 32.62, 31.82, 30.73, 13.06. MS (ESI) calcd for C₂₂H₃₀N₄O₂, *m/z* 382.2369, found 383.2541 [M+H]⁺.

37f: (7-Methyl-3-(pyridin-2-ylamino)-2-(((trimethylsilyl)methyl)amino)furo[2,3-c]pyridin-4-

yl)methanol. 24 mg, 28%. ¹H NMR (500 MHz, MeOD) δ 8.03 (t, *J* = 8.0 Hz, 1H), 7.91-7.90 (m, 2H), 7.24 (d, *J* = 8.7 Hz, 1H), 7.04 (t, *J* = 6.6 Hz, 1H), 4.62 (s, 2H), 3.11 (s, 2H), 2.72 (s, 3H), 0.12 (s, 9H). ¹³C NMR (126 MHz, MeOD) δ 165.66, 156.25, 145.27, 143.32, 142.02, 138.19, 133.57, 132.16, 124.28, 115.77, 115.00, 90.25, 59.52, 34.64, 12.94, -2.60. MS (ESI) calcd for C₁₈H₂₄N₄O₂Si, *m/z* 356.1669, found 357.1815 [M+H]⁺.

37g: (7-Methyl-2-((2-morpholinoethyl)amino)-3-(pyridin-2-ylamino)furo[2,3-c]pyridin-4-yl)

methanol. 9 mg, 10%. ¹H NMR (500 MHz, MeOD) δ 8.03 (s, 2H), 7.93 (d, *J* = 5.8 Hz, 1H), 7.27

(d, $J = 7.3$ Hz, 1H), 7.05 (t, $J = 6.5$ Hz, 1H), 4.66 (s, 2H), 4.06-3.95 (m, 6H), 3.54 (bs, 2H), 3.42 (bs, 4H), 2.80 (s, 3H). ^{13}C NMR (126 MHz, MeOD) δ 165.51, 156.26, 145.10, 143.92, 141.95, 138.27, 134.09, 133.62, 126.01, 115.97, 115.07, 90.35, 64.80, 59.39, 57.37, 53.45, 37.84, 13.21. MS (ESI) calcd for $\text{C}_{20}\text{H}_{25}\text{N}_5\text{O}_3$, m/z 383.1957, found 384.2132 $[\text{M}+\text{H}]^+$.

37h: Ethyl 2-((4-(hydroxymethyl)-7-methyl-3-(pyridin-2-ylamino)furo[2,3-c]pyridin-2-yl)amino)acetate. 21 mg, 25%. ^1H NMR (500 MHz, MeOD) δ 8.07 (t, $J = 8.0$ Hz, 1H), 8.03 (s, 1H), 7.91 (d, $J = 6.1$ Hz, 1H), 7.29 (d, $J = 8.9$ Hz, 1H), 7.08 (t, $J = 6.7$ Hz, 1H), 4.66 (s, 2H), 4.36 (s, 2H), 4.18 (q, $J = 7.1$ Hz, 2H), 2.74 (s, 3H), 1.25 (t, $J = 7.1$ Hz, 3H). ^{13}C NMR (126 MHz, MeOD) δ 170.68, 165.42, 155.75, 145.81, 143.87, 142.15, 137.71, 133.94, 133.89, 125.93, 115.98, 115.25, 91.02, 62.95, 59.42, 44.55, 14.48, 13.03. MS (ESI) calcd for $\text{C}_{18}\text{H}_{20}\text{N}_4\text{O}_4$, m/z 356.1485, found 357.1738 $[\text{M}+\text{H}]^+$.

37i: tert-Butyl 3-((4-(hydroxymethyl)-7-methyl-3-(pyridin-2-ylamino)furo[2,3-c]pyridin-2-yl)amino)propanoate. 20 mg, 21%. ^1H NMR (500 MHz, MeOD) δ 8.08 (t, $J = 8.0$ Hz, 1H), 8.00 (s, 1H), 7.91 (d, $J = 5.8$ Hz, 1H), 7.29 (d, $J = 7.8$ Hz, 1H), 7.08 (t, $J = 6.7$ Hz, 1H), 4.66 (s, 2H), 3.80 (t, $J = 6.4$ Hz, 2H), 2.78 (s, 3H), 2.67 (t, $J = 6.7$ Hz, 2H), 1.42 (s, 9H). ^{13}C NMR (126 MHz, MeOD) δ 171.99, 165.49, 155.86, 145.77, 143.76, 142.08, 137.49, 133.79, 133.30, 125.17, 115.86, 115.36, 90.25, 82.28, 59.49, 39.67, 36.03, 28.31, 13.02. MS (ESI) calcd for $\text{C}_{21}\text{H}_{26}\text{N}_4\text{O}_4$, m/z 398.1954, found 399.2128 $[\text{M}+\text{H}]^+$.

37j: Diethyl (((4-(hydroxymethyl)-7-methyl-3-(pyridin-2-ylamino)furo[2,3-c]pyridin-2-yl)amino)methyl)phosphonate. 13 mg, 13%. ^1H NMR (500 MHz, MeOD) δ 8.08 – 8.00 (m, 2H), 7.95 (d, $J = 5.7$ Hz, 1H), 7.23 (d, $J = 4.9$ Hz, 1H), 7.06 (t, $J = 6.5$ Hz, 1H), 4.69 (s, 2H), 4.24 – 4.16 (m, 4H), 4.09 (d, $J = 10.6$ Hz, 2H), 2.81 (s, 3H), 1.33 (t, $J = 7.0$ Hz, 6H). ^{13}C NMR (126

MHz, MeOD) δ 164.98, 156.41, 145.04, 143.68, 142.06, 139.12, 133.83, 133.71, 125.96, 115.97, 114.67, 91.93, 64.56 (d, $J = 6.9$ Hz), 59.37, 39.02 (d, $J = 158.9$ Hz), 16.78 (d, $J = 5.6$ Hz), 13.09. MS (ESI) calcd for $C_{19}H_{25}N_4O_5P$, m/z 420.1563, found 421.1672 $[M+H]^+$.

37k: (2-((4-Methoxyphenyl)amino)-7-methyl-3-(pyridin-2-ylamino)furo[2,3-c]pyridin-4-yl) methanol. 13 mg, 14%. 1H NMR (500 MHz, MeOD) δ 7.99 – 7.87 (m, 2H), 7.62 (t, $J = 7.8$ Hz, 1H), 7.33 (d, $J = 8.8$ Hz, 2H), 6.90 (d, $J = 8.8$ Hz, 2H), 6.77 (t, $J = 6.3$ Hz, 2H), 4.66 (s, 2H), 3.77 (s, 3H), 2.71 (s, 3H). ^{13}C NMR (126 MHz, MeOD) δ 162.79, 159.21, 158.92, 146.57, 143.34, 141.31, 140.61, 132.84, 132.22, 130.80, 126.51, 124.33, 115.64, 115.43, 111.46, 96.53, 62.30, 58.97, 55.97, 13.06. MS (ESI) calcd for $C_{21}H_{20}N_4O_3$, m/z 376.1535, found 377.1694 $[M+H]^+$.

37l: (2-((2-Chloro-6-methylphenyl)amino)-7-methyl-3-(pyridin-2-ylamino)furo[2,3-c]pyridin-4-yl) methanol. 27 mg, 28%. 1H NMR (500 MHz, MeOD) δ 8.10 (s, 1H), 7.90 (dd, $J = 20.4, 6.6$ Hz, 2H), 7.28 – 7.15 (m, 3H), 7.03 (t, $J = 6.6$ Hz, 1H), 6.95 (s, 1H), 4.70 (s, 2H), 2.75 (s, 3H), 2.32 (s, 3H). ^{13}C NMR (126 MHz, MeOD) δ 162.57, 155.17, 145.80, 144.21, 142.68, 139.93, 136.98, 134.45, 133.96, 133.78, 132.14, 130.74, 128.65, 126.80, 115.93, 114.82, 91.45, 59.30, 18.71, 13.11. MS (ESI) calcd for $C_{21}H_{19}ClN_4O_2$, m/z 394.1197, found 395.1349 $[M+H]^+$.

37m: (S)-(7-methyl-2-((1-phenylethyl)amino)-3-(pyridin-2-ylamino)furo[2,3-c]pyridin-4-yl) methanol. 28 mg, 31%. 1H NMR (500 MHz, MeOD) δ 7.92 (s, 1H), 7.89 (t, $J = 8.0$ Hz, 1H), 7.90 – 7.81 (m, 1H), 7.38 (d, $J = 7.6$ Hz, 2H), 7.29 (t, $J = 7.4$ Hz, 2H), 7.21 (t, $J = 7.2$ Hz, 1H), 7.05 (d, $J = 6.1$ Hz, 1H), 6.94 (t, $J = 6.4$ Hz, 1H), 5.20 (q, $J = 6.8$ Hz, 1H), 4.58 (s, 2H), 2.68 (s, 3H), 1.60 (d, $J = 6.9$ Hz, 3H). ^{13}C NMR (126 MHz, MeOD) δ 164.81, 157.13, 144.72, 143.97, 143.61, 142.11, 140.61, 133.20, 132.80, 129.92, 128.71, 126.98, 125.52, 115.70, 113.93, 91.91, 59.24, 54.49, 23.31, 12.88. MS (ESI) calcd for $C_{22}H_{22}N_4O_2$, m/z 374.1743, found 375.1931 $[M+H]^+$.

Synthesis of compound 37n: ((2-Amino-7-methyl-3-(pyridin-2-ylamino)furo[2,3-c]pyridin-4-yl)methanol. The solution of compound **37e** (95 mg, 0.25 mmol) in TFA/CH₂Cl₂ (50%, 4 mL) was stirred at room temperature for 6 h. The solvents were removed and the residue obtained was column purified to afford compound **37n** (56 mg, 84%). ¹H NMR (500 MHz, MeOD) δ 7.91 – 7.86 (m, 2H), 7.81 (t, *J* = 7.9 Hz, 1H), 6.96 (d, *J* = 8.6 Hz, 1H), 6.87 (t, *J* = 6.5 Hz, 1H), 4.61 (s, 2H), 2.66 (s, 3H). ¹³C NMR (126 MHz, MeOD) δ 167.39, 157.68, 143.36, 143.14, 142.12, 132.82, 132.44, 125.47, 115.59, 113.10, 92.54, 59.18, 12.80. MS (ESI) calcd for C₁₄H₁₄N₄O₂, *m/z* 270.1117, found 271.1310 [M+H]⁺.

Compounds **38a-38c** were synthesized similarly as compound **34**.

38a: (7-Methyl-2-(pentylamino)-3-(phenylamino)furo[2,3-c]pyridin-4-yl)methanol. 117 mg, 70%. ¹H NMR (500 MHz, MeOD) δ 7.85 (s, 1H), 7.14 (dd, *J* = 8.6, 7.4 Hz, 2H), 6.71 (tt, *J* = 7.4, 1.0 Hz, 1H), 6.60 (dd, *J* = 8.6, 1.0 Hz, 2H), 4.65 – 4.59 (m, 2H), 3.51 (t, *J* = 7.1 Hz, 2H), 2.68 (s, 3H), 1.72 – 1.57 (m, 2H), 1.41 – 1.28 (m, 4H), 0.95 – 0.84 (m, 3H). ¹³C NMR (126 MHz, MeOD) δ 165.54, 149.56, 143.22, 141.35, 133.46, 132.44, 130.44, 125.33, 119.45, 114.08, 96.74, 59.31, 43.42, 31.00, 29.94, 23.33, 14.34, 13.48. MS (ESI) calcd for C₂₀H₂₅N₃O₂, *m/z* 339.1947, found 340.2087 [M+H]⁺.

38b: (3-((3-Fluorophenyl)amino)-7-methyl-2-(pentylamino)furo[2,3-c]pyridin-4-yl)methanol. 70 mg, 82%. ¹H NMR (500 MHz, MeOD) δ 7.81 (s, 1H), 7.06 (td, *J* = 8.2, 6.7 Hz, 1H), 6.42 – 6.32 (m, 2H), 6.23 (d, *J* = 11.5 Hz, 1H), 4.60 (s, 2H), 3.46 (t, *J* = 7.1 Hz, 2H), 2.65 (s, 3H), 1.59 (p, *J* = 7.1 Hz, 2H), 1.31 – 1.23 (m, 4H), 0.83 (t, *J* = 7.0 Hz, 3H). ¹³C NMR (126 MHz, MeOD) 166.34, 165.62 (d, *J* = 242.1 Hz), 151.55 (d, *J* = 10.4 Hz), 142.79, 142.04, 131.84 (d, *J* = 10.1 Hz), 131.65, 131.28, 125.42, 110.01, 105.58 (d, *J* = 21.8 Hz), 100.74 (d, *J* = 25.8

Hz), 96.47, 58.95, 43.43, 30.83, 29.93, 23.33, 14.35, 12.79. MS (ESI) calcd for C₂₀H₂₄FN₃O₂, *m/z* 357.1853, found 358.2013 [M+H]⁺.

38c: (7-Methyl-3-((3-nitrophenyl)amino)-2-(pentylamino)furo[2,3-*c*]pyridin-4-yl)methanol.

34 mg, 37%. ¹H NMR (500 MHz, MeOD) δ 7.90 (s, 1H), 7.49 (dd, *J* = 8.1, 2.2 Hz, 1H), 7.34 (s, 1H), 7.31 (t, *J* = 8.1 Hz, 1H), 6.95 (d, *J* = 8.0 Hz, 1H), 4.54 (s, 2H), 3.41 (t, *J* = 7.0 Hz, 2H), 2.56 (s, 3H), 1.65 – 1.52 (m, 2H), 1.30 (dd, *J* = 8.5, 4.8 Hz, 4H), 0.86 (t, *J* = 6.5 Hz, 3H). ¹³C NMR (126 MHz, MeOD) δ 160.86, 151.59, 150.89, 144.93, 141.84, 138.47, 136.71, 131.12, 124.51, 120.06, 113.05, 107.81, 92.23, 60.13, 43.34, 31.50, 30.02, 23.40, 16.73, 14.35. MS (ESI) calcd for C₂₀H₂₄N₄O₄, *m/z* 384.1798, found 385.1950 [M+H]⁺.

Synthesis of compound 39: 2,2'-(Hexane-1,6-diylbis(azanediyl))bis(7-methyl-3-(pyridin-2-ylamino)furo[2,3-*c*]pyridine-4,2-diyl)dimethanol. To a solution of 2-aminopyridine (48 mg, 0.50 mmol) in anhydrous acetonitrile, were added pyridoxal hydrochloride (112 mg, 0.56 mmol), 4N HCl/dioxane (10 μL) and 1,6-diisocyanohexane (36 μL, 0.24 mmol). The reaction mixture was then heated under microwave conditions (600 W, 80 °C) in a sealed vial for 2 min. After cooling the reaction mixture to room temperature, solvent was removed and the residue was purified using column chromatography to obtain compound **39** (21 mg, 7%). ¹H NMR (500 MHz, MeOD) δ 8.07 (t, *J* = 8.0 Hz, 2H), 7.97 (s, 2H), 7.90 (d, *J* = 5.6 Hz, 2H), 7.31 (d, *J* = 5.6 Hz, 2H), 7.07 (t, *J* = 6.7 Hz, 2H), 4.64 (s, 4H), 3.57 (t, *J* = 7.0 Hz, 4H), 2.75 (s, 6H), 1.78 – 1.65 (m, 4H), 1.46 (s, 4H). ¹³C NMR (126 MHz, MeOD) δ 165.67, 155.95, 145.66, 143.71, 142.10, 137.48, 133.70, 132.91, 124.87, 115.83, 115.43, 90.05, 59.50, 43.86, 30.65, 27.48, 13.02. MS (ESI) calcd for C₃₄H₃₈N₈O₄, *m/z* 622.3016, found 623.3187 [M+H]⁺.

X-ray crystallographic structural studies of 20, 28, and 37e. Crystals for compound **28** utilize the non-centrosymmetric triclinic space group P1-C1 with eight crystallographically-independent molecules in the asymmetric unit. They also invariably form multiply-twinned bundles. After many unsuccessful attempts, a multi-domain specimen of **28** was cut from one of these bundles that gave a set of diffracted intensities that permitted a crystal structure solution but not a satisfactory refinement. Full sets of unique diffracted intensities were measured for single-domain specimens of compounds **20** and **37e** using monochromated CuK α radiation ($\lambda = 1.54178$ Å) on a Bruker Proteum Single Crystal Diffraction System equipped with Helios multilayer optics, an APEX II CCD detector and a Bruker MicroStar microfocus rotating anode x-ray source operating at 45kV and 60mA. Diffracted intensities were obtained with the Bruker program SAINT and the structures were solved using “direct methods” techniques incorporated into the Bruker SHELXTL Version 2010.3-0 software package. All stages of weighted full-matrix least-squares refinement were performed using the SHELXTL software with F_o^2 data. The final structural model for compounds **20** and **37e** incorporated anisotropic thermal parameters for all non-hydrogen atoms and isotropic thermal parameters for all hydrogen atoms. The respective asymmetric units consist of four molecules of **20**; one molecule of **37e**. All hydrogen atoms for **37e** and hydrogen atoms of **20** that are bonded to amine nitrogens (one in each molecule) were located in a difference Fourier map and included in the structural model as independent isotropic atoms whose parameters were allowed to vary in least-squares refinement cycles. All hydroxyl hydrogens for **20** were placed at idealized sp³-hybridized positions with an O-H bond length of 0.84 Å; the hydroxyl group was then allowed to rotate about its O-C bond during least squares refinement cycles. The remaining hydrogen atoms for **20** were included in the structural model as idealized atoms (assuming sp²- or sp³-hybridization of the carbon or nitrogen atoms and C-H bond lengths of 0.95 to 1.00 Å or N-H bond lengths of 0.88 Å). The isotropic thermal parameters of all idealized hydrogen atoms for **20** were fixed at values 1.2 (nonmethyl) or 1.5

(methyl) times the equivalent isotropic thermal parameter of the carbon, nitrogen or oxygen atom to which they are covalently bonded.

Human TLR-3/-4/-5/-7/-8/-9 reporter gene assays (NF- κ B induction). As described in Chapter 2.

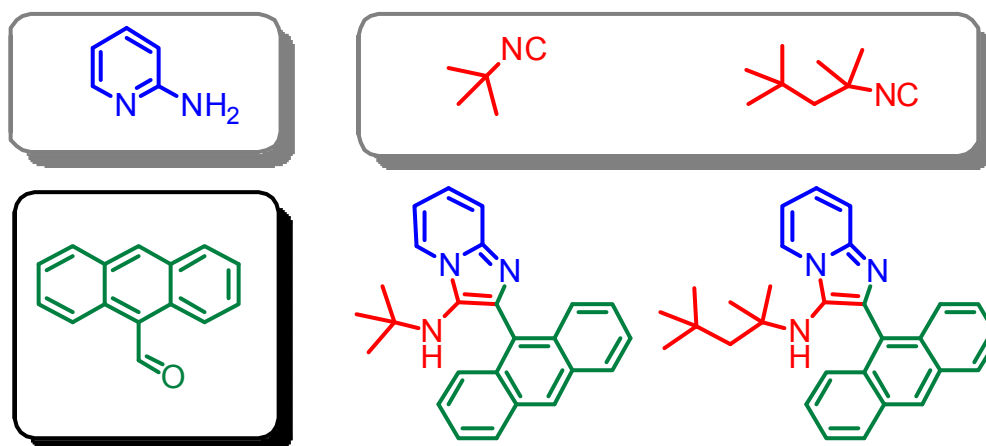
Immunoassays for cytokines. As described in Chapter 2.

Rabbit immunization and antigen-specific ELISA. As described in Chapter 2.

Transcriptomal profiling in human PBMCs. Detailed procedures for transcriptomal profiling have been described by us previously.³⁰ Briefly, fresh human PBMC samples were stimulated with 10 μ g/mL of **37b** and **37f** for two hours, and total RNA was extracted from treated and negative control blood samples with QIAamp RNA Blood Mini Kit (Qiagen). Subsequently, 160 ng of each of the RNA samples was used. The Human Genome GeneChip U133 plus 2.0 oligonucleotide array (Affymetrix, Santa Clara, CA) was employed. Established standard protocols at the KU Genomics Facility were performed on cRNA target preparation, array hybridization, washing, staining and image scanning. The microarray data was first subjected to quality assessment using the Affymetrix GeneChip Operating Software (GCOS). QC criteria included low background, low noise, detection of positive controls, and a 5'/3' ratio of < 3.0. To facilitate direct comparison of gene expression data between different samples, the GeneChip data were first subjected to preprocessing. This step involved scaling (in GCOS) data from all chips to a target intensity value of 500, and further normalizations steps in GeneSpring GX (Agilent Technologies, Santa Clara, CA). Prior to identifying target genes, genes that were detected as non-expressed in all samples, i.e., those with absence calls, were filtered out. To identify genes whose expression was changed by our compounds, a fold change threshold of 2.0 between the compound treatment and the negative control was used.

Chapter 4.

Antibacterial activities of Groebke-Blackburn- Bienaymé-derived imidazo[1,2-*a*]pyridin-3-amines



MIC: 3.91 $\mu\text{g}/\text{mL}$ (MRSA)

4.1. Introduction

The introduction of antibiotics into the therapeutic armamentarium in the early 20th century revolutionized the management of microbial infections. Once considered 'wonder drugs', antibiotics have perhaps become victims of their own success, and resistance to these drugs has almost invariably followed on the heels of their widespread use (and misuse). The incidence of methicillin-resistant *Staphylococcus aureus* (MRSA) infections continues to increase alarmingly not only in hospital-associated settings (nosocomial infections), but in recent times, also in community settings in the United States, and throughout the globe. The increase in morbidity and mortality due to *S. aureus* infections⁸² is a reflection of increased invasive procedures, indwelling devices, older age, and comorbidities, as well as the acquisition of resistance to commonly-used antimicrobial agents. Of particular concern is the emergence of multidrug-resistant strains of Gram-positive bacteria, with the loss of susceptibility to a wide range of reserve antibiotics such as vancomycin.⁸³ The need for the development of effective antibiotics is urgent, especially in the face of a diminishing pipeline of drugs for antimicrobial chemotherapy.

As mentioned in Chapter 3, some of the initial compounds that were synthesized using the one-pot multicomponent Groebke-Blackburn-Bienaymé reaction with the aim to explore new TLR7/8-modulatory chemotype were proved to be neither agonistic nor antagonistic at TLR7/8 but found to have antibacterial activity against *S. aureus* with a clear indication of possible SARs. Subsequent focused libraries of compounds were synthesized and these latter compounds, too, were not active in TLR7 and TLR8 screens, but displayed prominent bacteriostatic activity against several Gram-positive bacteria, including MRSA. To investigate the mechanism of antibacterial activity of this new chemotype, a resistant strain of *S. aureus* was generated by serially passaging the organism in escalating doses of the most active analogue. A comparison

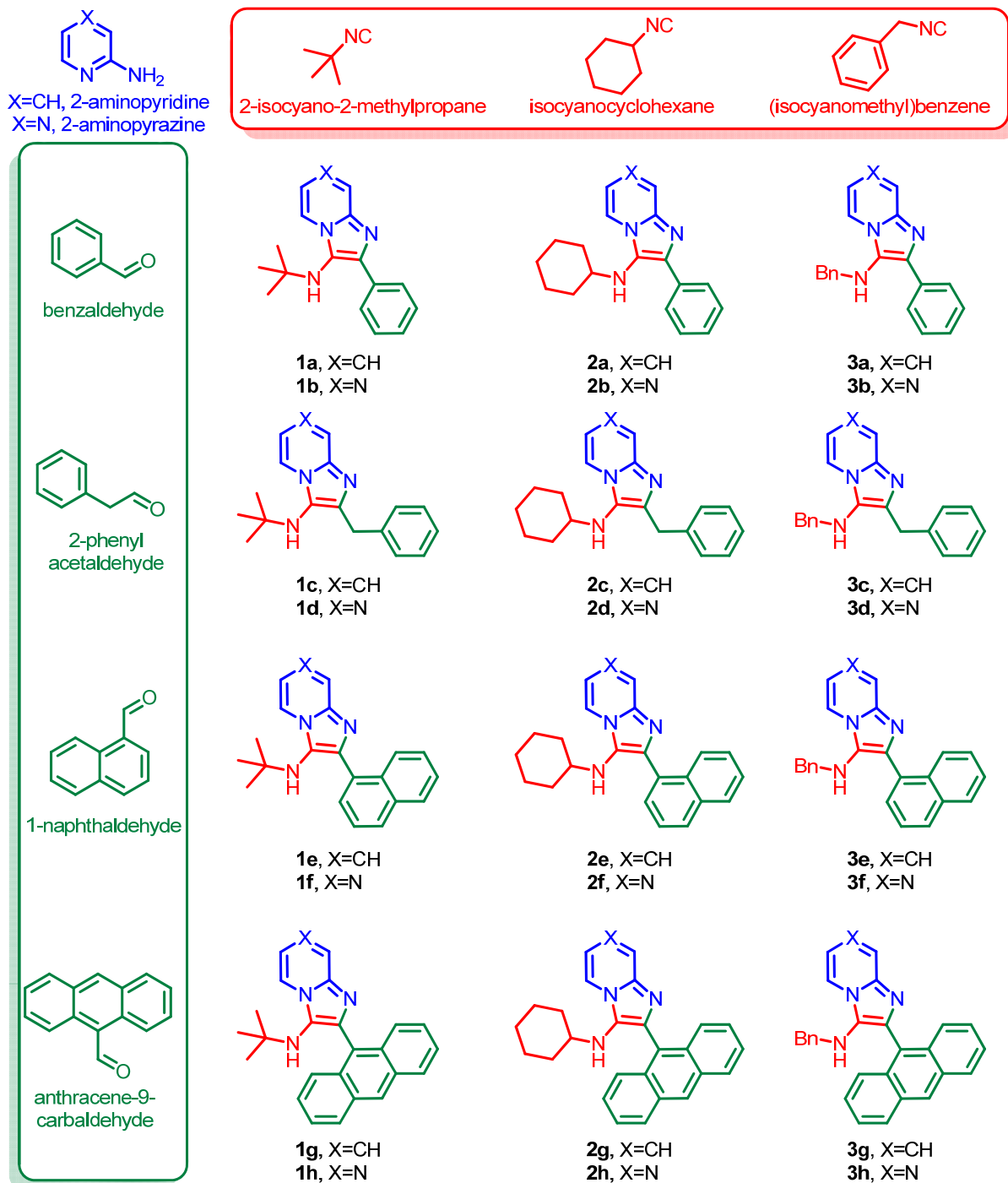
of minimum inhibitory concentrations (MICs) of known bacteriostatic agents in wild-type and resistant strains indicates a novel mechanism of action. These findings served as a point of departure for further exploration of SAR and mechanisms of bacteriostatic activity in this chemotype.

4.2. Results and Discussion

Our initial test-library comprising of twenty-four compounds was synthesized (Scheme 1) using two amidines (2-aminopyridine and 2-aminopyrazine), three isonitriles (2-isocyano-2-methylpropane, isocyanocyclohexane, (isocyanomethyl)benzene), and four aldehydes (benzaldehyde, 2-phenylacetaldehyde, 1-naphthaldehyde, anthracene-9-carbaldehyde). The syntheses of **1a-3h** (Scheme 1) proceeded smoothly. All compounds were tested in TLR7 and TLR8 agonism and antagonism assays using specific reporter gene-based cellular assays as described earlier;^{58, 77} to our disappointment, none of the compounds displayed any activity in these assays up to concentrations of 250 μ M (data not shown). The assay plates were stored in the autoclave room at room temperature prior to disposal, and, quite by accident, we observed a dose-dependent inhibition of a bacterial contaminant in such plates. We therefore decided to examine the antibacterial activities of these compounds in antibacterial screens (*E. coli* ATCC 9637 and *S. aureus* ATCC 13709) routinely employed in our laboratory.⁸⁴ Four compounds were identified to be inhibitory to *S. aureus* ATCC 13709 but not *E. coli* ATCC 9637. Maximal antibacterial activity resided in compounds derived from 2-aminopyridine, bearing either a bulky *N-tert*-butyl, or cyclohexyl groups at C3, and a large aromatic pendant group (naphthyl or anthracenyl) at C2 (**1e**, **1g**, **2e**, **2g**). The MICs of both **1g** and **2g** for *S. aureus* ATCC 13709 and

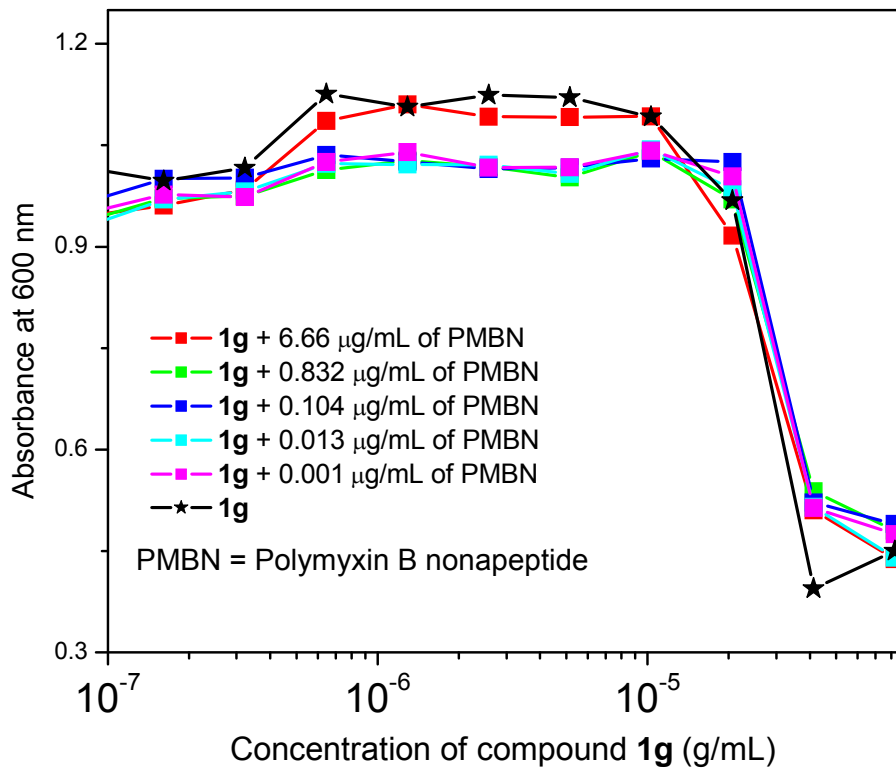
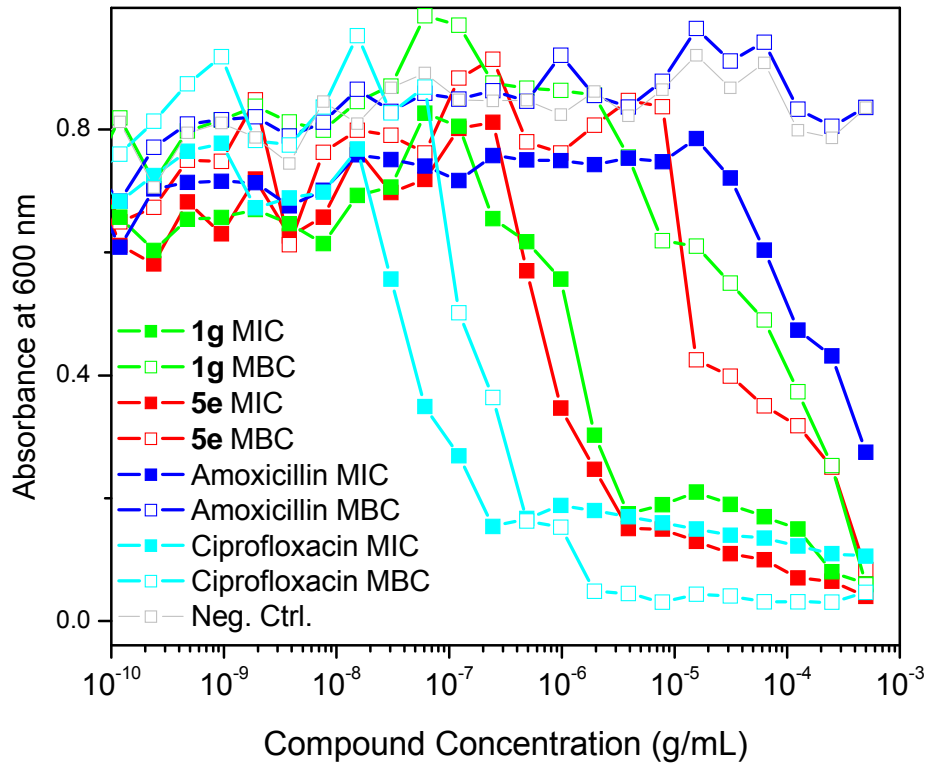
MRSA ATCC 33591 were 3.91 $\mu\text{g/mL}$ (Table 1), and 7.81 $\mu\text{g/mL}$ for coagulase-negative *S. epidermidis* ATCC 35983 (data not shown).

Scheme 1. Synthesis of a library of compounds using Groebke multicomponent reaction.



Reagents and conditions: MW, 400W, 110 $^{\circ}\text{C}$, 20 min, HCl/dioxane, CH_3CN .

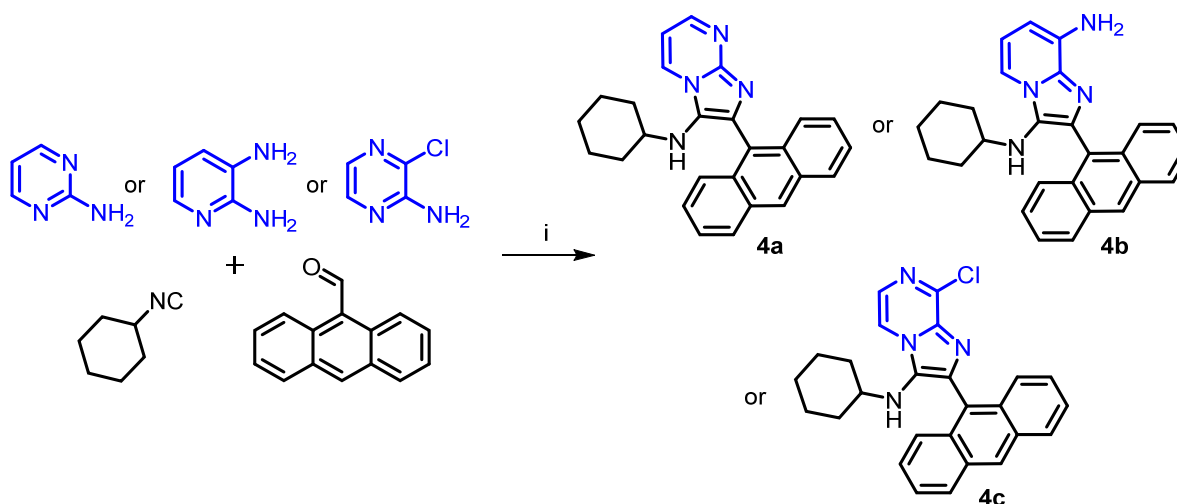
Fig. 1. Comparison of antimicrobial susceptibility of wild-type *S. aureus* ATCC 13709 (hatched bars) and 5e-resistant organism.



The active compounds listed above were all determined to be bacteriostatic rather than bactericidal by conventional microplate MBC assays.⁸⁵ The outer membrane of Gram-negative bacteria serves as a permeability barrier for hydrophobic antimicrobials,⁸⁶ and we wondered if the lack of activity of these compounds against Gram-negative bacteria could be attributable to its bulky, nonpolar nature. We therefore performed additional assays using polymyxin B nonapeptide,⁸⁷ which is commonly used to permeabilize the outer-membranes of Gram-negative bacteria, rendering the organisms susceptible to otherwise impermeable antimicrobials;⁸⁸ however, the imidazopyridines did not exert any significant antibacterial effect even at high concentrations of polymyxin B nonapeptide (Fig. 1), confirming that the antibacterial spectrum of these compounds is specific to Gram-positive organisms.

Given that **1g** and **2g** demonstrated identical potencies, we arbitrarily selected isocyanocyclohexane and anthracene-9-carbaldehyde as the invariant components, and varied the amidine component; we chose 2-aminopyrimidine, 2,3-diaminopyridine, and 2-amino-3-chloropyrazine (Scheme 2). The 2-amino-3-chloropyrazine-derived compound **4c** was inactive, while **4a** and **4b** exhibited lower activities than **1g** (Table 1).

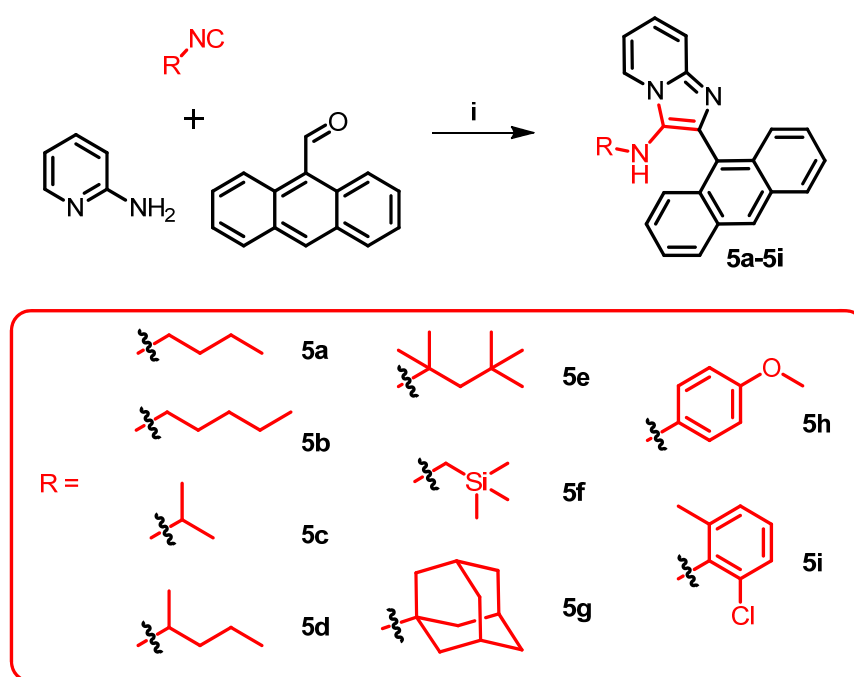
Scheme 2. Groebke reaction using different amidines.



Reagents and conditions: i. MW, 400W, 110 °C, 30 min, HCl/dioxane, CH₃CN.

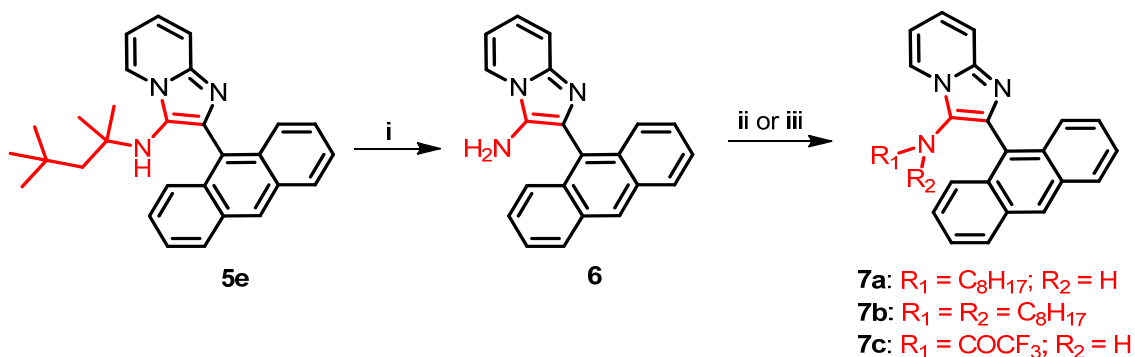
Next, we varied the isonitrile component. We explored nine different isonitriles (Scheme 3) chosen to include linear aliphatic (as in **5a** and **5b**), branched aliphatic (**5c-e**), silyl-containing (**5f**), adamantyl (**5g**), and aromatic substituents (**5h** and **5i**). We observed that the *N*-2,4,4-trimethylpentan-2-yl group of **5e**, could be dealkylated under strongly acidic conditions as has been reported recently,⁷⁸ affording the possibility of introducing alkyl or acyl substituents (represented by **7a-c**, Scheme 4) that were not accessible through commercially available isonitriles. Optimal activity profiles appeared to correspond to compounds with branched-chain substituents (**5d** and **5e**), while compounds with aromatic substituents (**5h** and **5i**) were bereft of antibacterial activity (Table 1).

Scheme 3. Groebke reaction using various isonitriles.



Reagents and conditions: i. MW, 400W, 110 °C, 20 min, HCl/dioxane, CH₃CN.

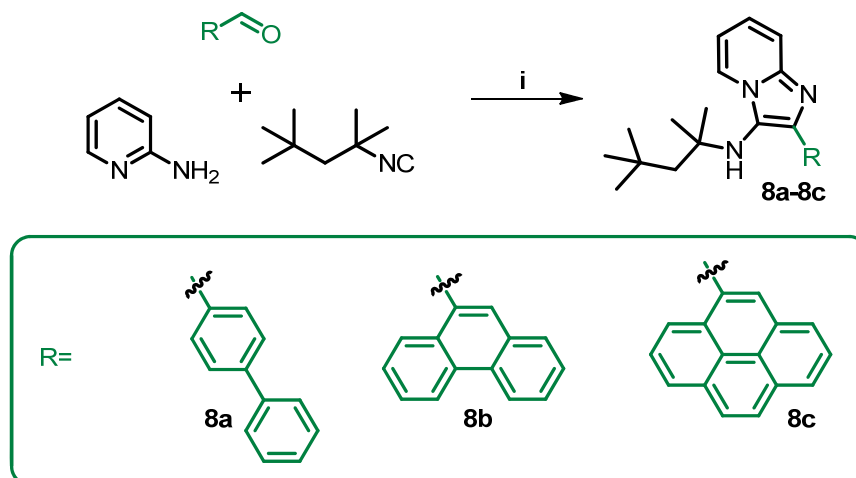
Scheme 4. Derivatization of the C3-amine.



Reagents and conditions: i. HCl/dioxane; ii. For **7a** and **7b**, $C_7H_{15}CHO$, CH_3COOH , $NaCNBH_3$, MeOH; iii. For **7c**, $(CF_3CO)_2O$, CH_2Cl_2 .

Noting that bulky, aldehyde-derived aromatic substituents at C2 corresponded to maximal activity (exemplified by the anthracenyl group in **1g**, **2g**, and **5a-g**), it was of interest to explore other similar functional groups. Compounds with biphenyl (**8a**), phenanthrenyl (**8b**), and pyrenyl (**8c**) substituents were therefore synthesized and evaluated (Scheme 5). Compounds **8b** and **8c** exhibited lower activity than the anthracenyl-bearing compound, while the biphenyl compound **8a** was inactive, pointing to the necessity of a large polycyclic, aromatic group at C2.

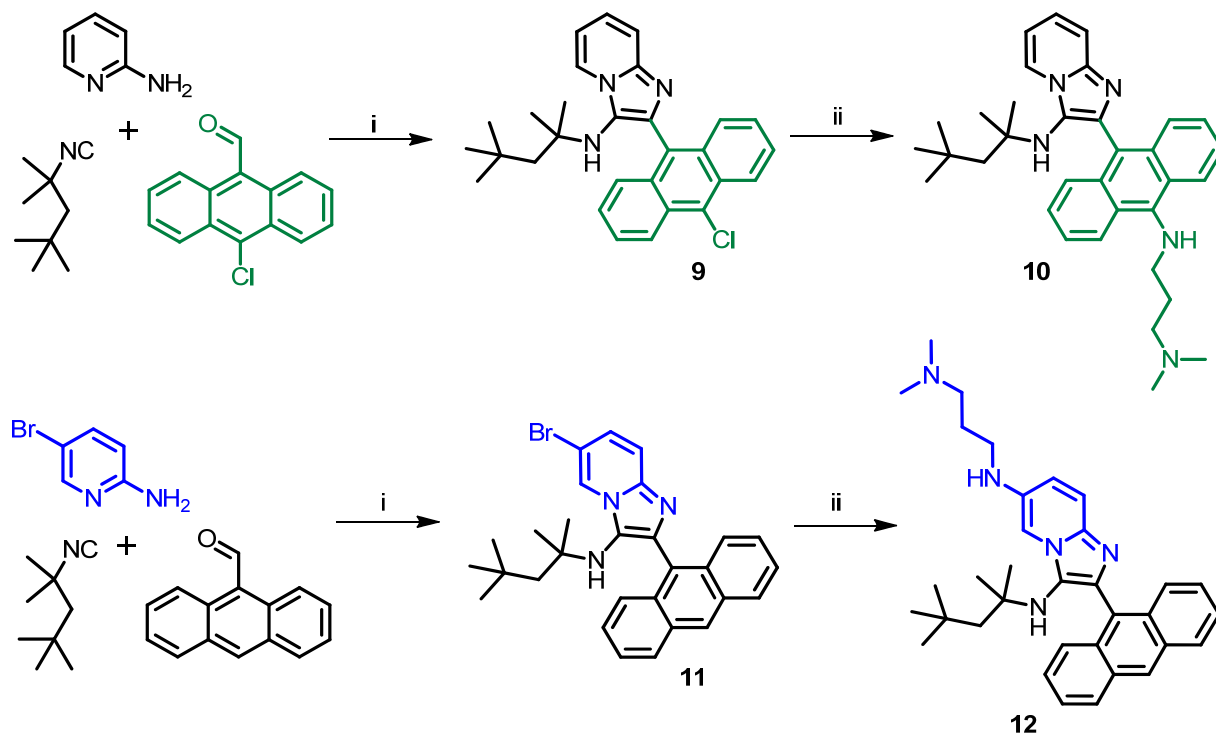
Scheme 5. Groebke reaction using various aldehydes.



Reagents and conditions: i. MW, 400W, 110 °C, 20 min, HCl/dioxane, CH_3CN .

The compound that showed maximal activity thus far was the very lipophilic **5e**, and it was desirable to explore more polar analogues for future evaluation in vivo models. We therefore attempted to introduce *N,N*-dimethylaminopropylamino groups on both the amidine- and aldehyde-derived portions of **5e**. This was achieved in a straightforward manner using appropriate halo-substituted components, followed by Buchwald-Hartwig coupling as depicted in Scheme 6. The antibacterial activities of **10** and **12** were found to be identical to that of **5e** (Table 1).

Scheme 6. Synthesis of polar derivatives of **5e**.

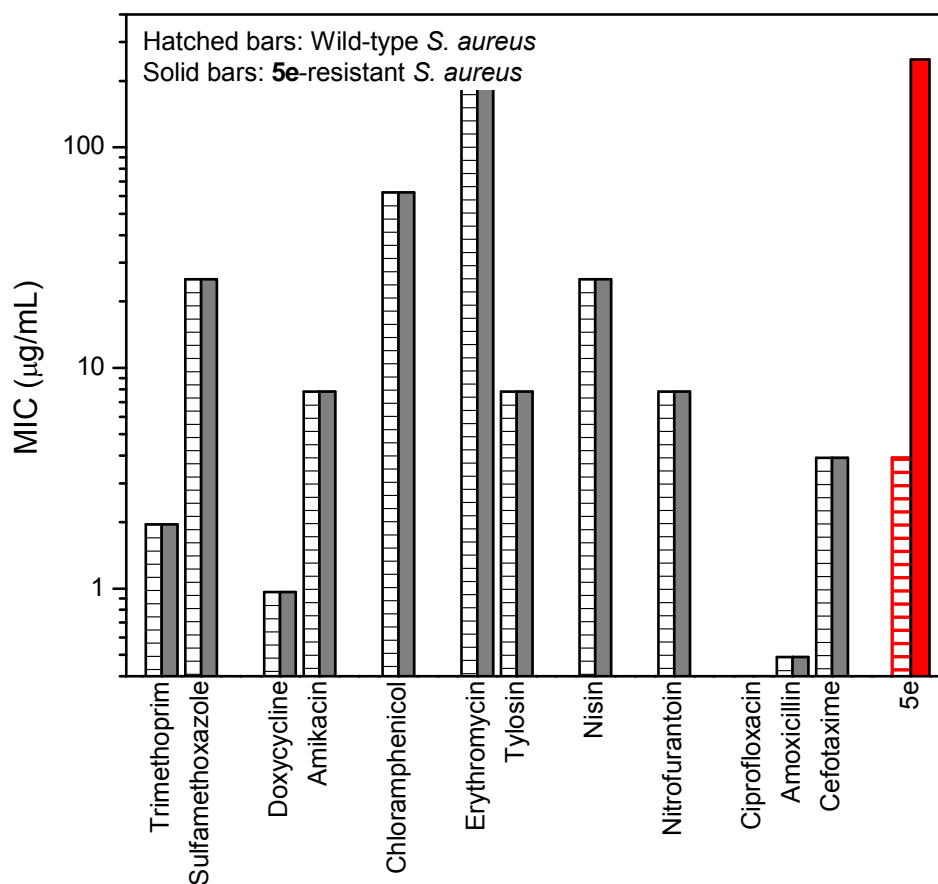


Reagents and conditions: i. MW, 400W, 110 °C, 30 min, HCl/dioxane, CH₃CN; ii. K(OtBu), Pd₂(dba)₃, DavePhos, NH₂(CH₂)₃N(CH₃)₂, dioxane, 80 °C.

Although the lead compounds of this chemotype exhibit narrow-spectrum bacteriostatic activity against Gram-positive organisms, the substantial potency against MRSA warranted an attempt at understanding the mechanism of action. Our preliminary studies have been to examine the

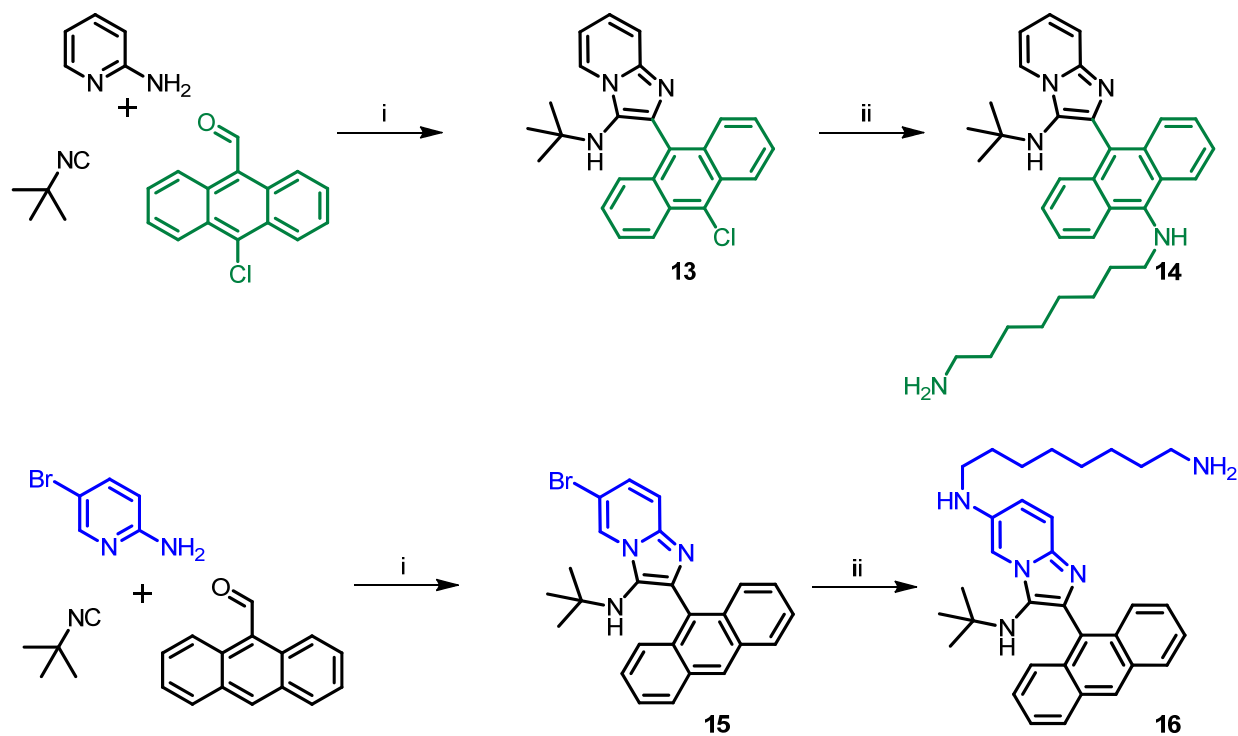
antibiograms of wild-type and **5e**-resistant *S. aureus* organisms, comparing a variety of antimicrobials with known mechanisms of action. **5e**-resistant *S. aureus* organisms were generated by exposing the bacterium to escalating doses of the compound. Within about 10 serial passages, organisms that withstood **5e** up to concentrations of 100 $\mu\text{g/mL}$ emerged. The MICs of various classes of bacteriostatic and bactericidal antibiotics were found to be identical within experimental error for both the wild-type and **5e**-resistant *S. aureus*, suggesting that the molecular target of **5e** and related compounds were distinct and unique (Fig. 2).

Fig. 2. Comparison of antimicrobial susceptibility of wild-type *S. aureus* ATCC 13709 (hatched bars) and **5e**-resistant organism (solid bars) to a range of bacteriostatic antibiotics with known mechanisms of action, and **5e**. Bacteriostatics include trimethoprim and sulfamethoxazole (dihydrofolate reductase pathway), doxycycline and amikacin (30S ribosomal subunit), chloramphenicol (23S ribosomal subunit), erythromycin and tylosin (50S ribosomal subunit), nisin (lipid II), nitrofurantoin (bacterial DNA); also included were the bactericidal controls, ciprofloxacin, amoxicillin, and cefotaxime.



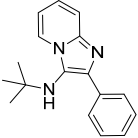
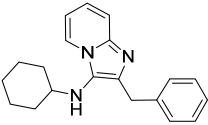
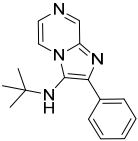
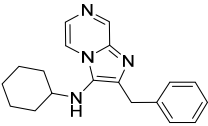
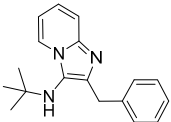
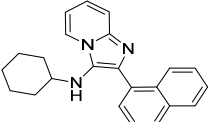
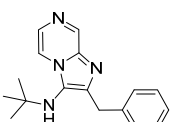
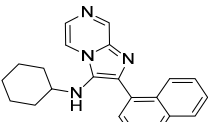
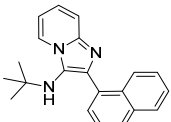
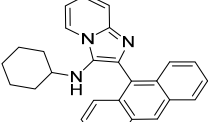
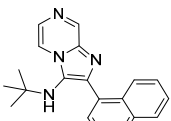
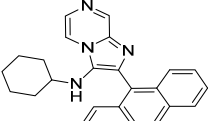
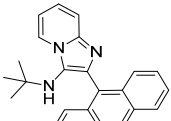
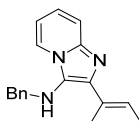
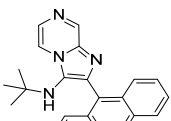
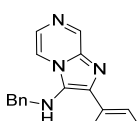
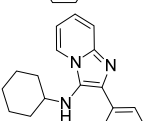
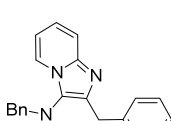
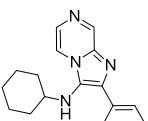
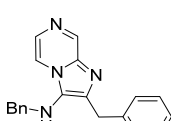
We noticed, however, that upon prolonged storage (~ 2 weeks), aqueous solutions of hydrochloride salts of both **10** and **12** were degrading gradually, giving rise to *N*-dealkylated products as was discussed earlier. Furthermore, we were desirous of introducing a functional group that would permit facile coupling of probes such as fluorophores or biotin in order to identify the possible molecular target(s) of **5e**. We elected to replace the *N*-2,4,4-trimethyl pentan-2-yl group with the more stable *tert*-butyl group, and the *N,N*-dimethylaminopropylamino group with a 1,8-diaminooctane, using the Buchwald-Hartwig coupling strategy employed earlier (Scheme 7). The introduction of the primary amine-bearing 1,8-diaminooctanyl group on either the anthracenyl or pyridinyl portions of the molecule did not result in significant attenuation of antibacterial activity relative to **1g** (Table 1), allowing the possibility of exploring the binding partners for these compounds.

Scheme 7. Synthesis of **1g** derivatives bearing terminal primary amines.



Reagents and conditions: i. MW 400W, 110 °C, 30 min, HCl/dioxane, CH₃CN; ii. (a) K(OtBu), Pd₂(dba)₃, DavePhos, NH₂(CH₂)₈NHBoc, dioxane, 80 °C (b) 4M HCl/dioxane.

Table1. Minimum Inhibitory Concentration values ($\mu\text{g/mL}$) of compounds.^a

Structure	Compound Number	MIC ($\mu\text{g/mL}$)		Structure	Compound Number	MIC ($\mu\text{g/mL}$)	
		<i>S. aureus</i>	MRSA			<i>S. aureus</i>	MRSA
	1a	ND	NT		2c	ND	NT
	1b	ND	NT		2d	ND	NT
	1c	ND	NT		2e	7.81	15.62
	1d	ND	NT		2f	ND	NT
	1e	62.5	31.25		2g	3.91	3.91
	1f	ND	NT		2h	7.81	NT
	1g	3.91	3.91		3a	ND	NT
	1h	ND	NT		3b	ND	NT
	2a	ND	NT		3c	ND	NT
	2b	ND	NT		3d	ND	NT

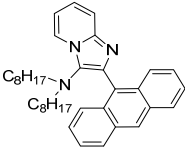
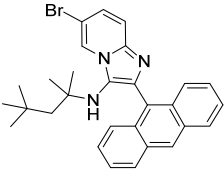
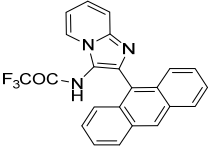
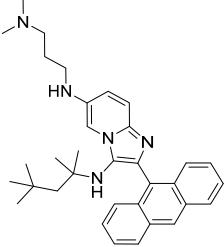
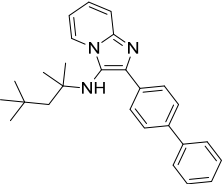
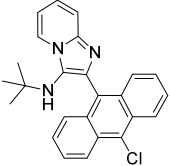
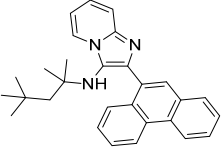
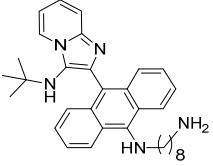
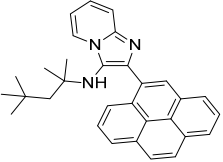
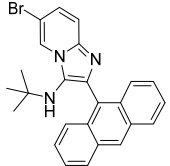
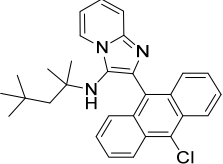
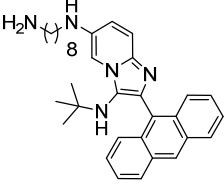
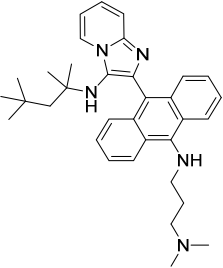
(continued on next page)

Table 1. (continued)

Structure	Compound Number	MIC ($\mu\text{g/mL}$)		Structure	Compound Number	MIC ($\mu\text{g/mL}$)	
		<i>S. aureus</i>	MRSA			<i>S. aureus</i>	MRSA
	3e	15.62	NT		5c	15.62	15.62
	3f	ND	NT		5d	7.81	3.91
	3g	ND	NT		5e	3.91	3.91
	3h	ND	NT		5f	15.62	NT
	4a	15.62	NT		5g	15.62	NT
	4b	15.62	NT		5h	ND	NT
	4c	ND	NT		5i	ND	NT
	5a	3.91	7.81		6	ND	NT
	5b	3.91	7.81		7a	7.81	NT

(continued on next page)

Table 1. (continued)

Structure	Compound Number	MIC ($\mu\text{g/mL}$)		Structure	Compound Number	MIC ($\mu\text{g/mL}$)	
		<i>S. aureus</i>	MRSA			<i>S. aureus</i>	MRSA
	7b	31.25	NT		11	15.62	NT
	7c	62.5	NT		12	3.91	NT
	8a	ND	NT		13	7.81	NT
	8b	7.81	NT		14	7.81	15.62
	8c	15.62	NT		15	15.62	NT
	9	7.81	NT		16	3.91	7.81
	10	3.91	NT				

^aND denotes no activity detected at 100 $\mu\text{g/mL}$ and NT denotes not tested.

4.3. Conclusions

Our attempts at exploring imidazo[1,2-*a*]pyridin-3-amines for TLR7 (or 8)-modulatory activities have unexpectedly led to the identification of a novel chemotype with substantial bacteriostatic activity against Gram-positive bacteria, including methicillin-resistant *S. aureus* (MRSA). Our preliminary results suggest that the mechanism of action may be distinct from known bacteriostatics. Structure-activity relationship studies have led to the identification of positions on the scaffold for additional structural modifications that should allow for the introduction of probes designed to examine cognate binding partners and molecular targets, while not significantly compromising antibacterial potency.

4.4. Experimental

Chemistry. All of the solvents and reagents used were obtained commercially and used as such unless noted otherwise. Moisture- or air-sensitive reactions were conducted under nitrogen atmosphere in oven-dried (120 °C) glass apparatus. The solvents were removed under reduced pressure using standard rotary evaporators. Flash column chromatography was carried out using RediSep Rf 'Gold' high performance silica columns on CombiFlash Rf instrument unless otherwise mentioned, while thin-layer chromatography was carried out on silica gel CCM pre-coated aluminum sheets. Microwave reactions were done in Synthos 3000 instrument (Anton Paar). IR spectra were recorded on Shimadzu 8400 series FTIR instrument and values are reported in cm^{-1} . Purity for all final compounds was confirmed to be greater than 95% by LC-MS using a Zorbax Eclipse Plus 4.6 × 150 mm, 5 μm analytical reverse phase C18 column with H₂O-isopropanol or H₂O-CH₃CN gradients and an Agilent ESI-TOF mass spectrometer (mass

accuracy of 3 ppm) operating in the positive ion acquisition mode. Unless otherwise mentioned, the compounds synthesized were obtained as yellow solids.

Synthesis of compound 1a: *N*-(*tert*-butyl)-2-phenylimidazo[1,2-*a*]pyridin-3-amine. To the solution of 2-aminopyridine (24 mg, 0.25 mmol) in anhydrous acetonitrile, were added benzaldehyde (28 μ L, 0.28 mmol), a catalytic amount of 4N HCl/dioxane (10 μ L) and *tert*-butyl isonitrile (27 μ L, 0.24 mmol). The reaction mixture was then heated under microwave conditions (400 W, 110 °C, 20 min). After the reaction mixture was cooled to room temperature, solvent was removed and the residue was purified using column chromatography to obtain compound **1a** (44 mg, 69%). ^1H NMR (400 MHz, CDCl_3) δ 8.23 (dt, J = 6.9, 1.2 Hz, 1H), 7.90 (dt, J = 8.1, 1.6 Hz, 2H), 7.55 (dt, J = 9.0, 1.0 Hz, 1H), 7.43 (t, J = 7.6 Hz, 2H), 7.31 (t, J = 7.4 Hz, 1H), 7.13 (ddd, J = 9.0, 6.6, 1.3 Hz, 1H), 6.77 (td, J = 6.8, 1.1 Hz, 1H), 3.12 (s, 1H), 1.04 (s, 9H). ^{13}C NMR (101 MHz, CDCl_3) δ 135.42, 128.43, 128.32, 127.52, 124.17, 123.64, 117.48, 111.46, 101.91, 56.59, 30.43. MS (ESI) calculated for $\text{C}_{17}\text{H}_{19}\text{N}_3$, m/z 265.16, found 266.17 $[\text{M}+\text{H}]^+$.

Compounds **1b-f**, **2a-f**, and **3a-f** were synthesized similarly as compound **1a**.

1b: *N*-(*tert*-butyl)-2-phenylimidazo[1,2-*a*]pyrazin-3-amine. 45 mg, 62%. ^1H NMR (400 MHz, CDCl_3) δ 9.00 (d, J = 1.4 Hz, 1H), 8.14 (dd, J = 4.6, 1.5 Hz, 1H), 7.91 (dd, J = 8.3, 1.3 Hz, 2H), 7.86 (d, J = 4.6 Hz, 1H), 7.46 (t, J = 7.5 Hz, 2H), 7.37 (t, J = 7.4 Hz, 1H), 3.19 (s, 1H), 1.05 (s, 9H). ^{13}C NMR (101 MHz, CDCl_3) δ 143.54, 142.40, 137.43, 134.38, 129.04, 128.66, 128.38, 128.33, 125.17, 116.49, 100.13, 57.11, 30.45. MS (ESI) calculated for $\text{C}_{16}\text{H}_{18}\text{N}_4$, m/z 266.15, found 267.16 $[\text{M}+\text{H}]^+$.

1c: 2-Benzyl-*N*-(*tert*-butyl)imidazo[1,2-*a*]pyridin-3-amine. 41 mg, 61%. ^1H NMR (400 MHz, CDCl_3) δ 8.16 (dt, J = 6.9, 1.1 Hz, 1H), 7.47 (dt, J = 9.0, 1.0 Hz, 1H), 7.28 – 7.23 (m, 4H), 7.21 –

7.14 (m, 1H), 7.08 (ddd, $J = 9.0, 6.7, 1.3$ Hz, 1H), 6.72 (td, $J = 6.8, 1.1$ Hz, 1H), 4.20 (s, 2H), 2.57 (s, 1H), 1.18 (s, 9H). ^{13}C NMR (101 MHz, CDCl_3) δ 139.83, 139.62, 128.68, 128.48, 126.06, 123.41, 123.35, 117.06, 110.93, 101.78, 98.20, 55.71, 34.36, 30.45. MS (ESI) calculated for $\text{C}_{18}\text{H}_{21}\text{N}_3$, m/z 279.17, found 280.19 $[\text{M}+\text{H}]^+$.

1d: 2-Benzyl-*N*-(*tert*-butyl)imidazo[1,2-*a*]pyrazin-3-amine. 31 mg, 43%. ^1H NMR (400 MHz, CDCl_3) δ 8.92 (d, $J = 1.4$ Hz, 1H), 8.06 (dd, $J = 4.6, 1.5$ Hz, 1H), 7.81 (d, $J = 4.6$ Hz, 1H), 7.32 – 7.27 (m, 2H), 7.25 – 7.18 (m, 3H), 4.24 (s, 2H), 2.62 (s, 1H), 1.20 (s, 9H). ^{13}C NMR (101 MHz, CDCl_3) δ 142.95, 142.78, 138.88, 137.32, 128.72, 128.67, 126.45, 116.28, 56.29, 34.39, 30.48. MS (ESI) calculated for $\text{C}_{17}\text{H}_{20}\text{N}_4$, m/z 280.17, found 281.18 $[\text{M}+\text{H}]^+$.

1e: *N*-(*tert*-butyl)-2-(naphthalen-1-yl)imidazo[1,2-*a*]pyridin-3-amine. 56 mg, 74%. ^1H NMR (400 MHz, CDCl_3) δ 8.34 (dt, $J = 6.9, 1.1$ Hz, 1H), 8.02 – 7.85 (m, 3H), 7.68 – 7.44 (m, 5H), 7.19 (ddd, $J = 9.0, 6.7, 1.3$ Hz, 1H), 6.83 (td, $J = 6.8, 1.1$ Hz, 1H), 3.00 (s, 1H), 0.78 (s, 9H). ^{13}C NMR (101 MHz, CDCl_3) δ 133.83, 132.94, 131.98, 128.48, 128.25, 128.15, 126.57, 125.73, 125.70, 125.34, 123.97, 123.64, 117.45, 111.37, 101.79, 100.00, 55.95, 29.76. MS (ESI) calculated for $\text{C}_{21}\text{H}_{21}\text{N}_3$, m/z 315.17, found 316.19 $[\text{M}+\text{H}]^+$.

1f: *N*-(*tert*-butyl)-2-(naphthalen-1-yl)imidazo[1,2-*a*]pyrazin-3-amine. 29 mg, 38%. ^1H NMR (400 MHz, CDCl_3) δ 9.07 (d, $J = 1.4$ Hz, 1H), 8.24 (dd, $J = 4.6, 1.5$ Hz, 1H), 7.97 – 7.87 (m, 4H), 7.67 – 7.42 (m, 4H), 3.08 (s, 1H), 0.80 (s, 9H). ^{13}C NMR (101 MHz, CDCl_3) δ 143.57, 141.83, 133.85, 131.76, 131.71, 128.98, 128.95, 128.67, 128.27, 126.94, 126.02, 125.31, 125.19, 116.54, 105.36, 98.21, 56.51, 29.81. MS (ESI) calculated for $\text{C}_{20}\text{H}_{20}\text{N}_4$, m/z 316.17, found 317.17 $[\text{M}+\text{H}]^+$.

1g: 2-(Anthracen-9-yl)-N-(tert-butyl)imidazo[1,2-a]pyridin-3-amine. 55 mg, 63%. IR (CHCl₃) ν_{max} (cm⁻¹): 2970, 1500, 1473, 1342, 1311. ¹H NMR (400 MHz, CDCl₃) δ 8.52 (s, 1H), 8.40 (dt, J = 6.9, 1.2 Hz, 1H), 8.09 – 8.02 (m, 2H), 7.93 – 7.86 (m, 2H), 7.66 (dt, J = 9.0, 1.1 Hz, 1H), 7.51 – 7.38 (m, 4H), 7.29 – 7.20 (m, 1H), 6.89 (td, J = 6.8, 1.1 Hz, 1H), 2.69 (s, 1H), 0.64 (s, 9H). ¹³C NMR (101 MHz, CDCl₃) δ 142.71, 131.45, 130.94, 128.75, 127.60, 126.80, 126.34, 126.19, 125.06, 124.00, 123.62, 117.57, 111.40, 101.78, 97.01, 55.59, 29.72. MS (ESI) calculated for C₂₅H₂₃N₃, m/z 365.19, found 366.20 [M+H]⁺.

1h: 2-(Anthracen-9-yl)-N-(tert-butyl)imidazo[1,2-a]pyrazin-3-amine. 50 mg, 57%. ¹H NMR (400 MHz, CDCl₃) δ 9.14 (d, J = 1.5 Hz, 1H), 8.57 (s, 1H), 8.31 (dd, J = 4.6, 1.5 Hz, 1H), 8.12 – 8.05 (m, 2H), 7.98 (d, J = 4.6 Hz, 1H), 7.83 – 7.75 (m, 2H), 7.53 – 7.42 (m, 4H), 2.75 (s, 1H), 0.65 (s, 9H). ¹³C NMR (101 MHz, CDCl₃) δ 143.65, 139.88, 138.08, 131.37, 130.86, 129.05, 128.96, 128.35, 127.48, 126.81, 125.52, 125.24, 116.55, 101.78, 56.14, 29.77. MS (ESI) calculated for C₂₄H₂₂N₄, m/z 366.18, found 367.19 [M+H]⁺ and 389.18 [M+Na]⁺.

2a: N-cyclohexyl-2-phenylimidazo[1,2-a]pyridin-3-amine. 51 mg, 73%. ¹H NMR (500 MHz, CDCl₃) δ 8.16 (d, J = 6.8 Hz, 1H), 8.05 (dd, J = 8.3, 1.2 Hz, 2H), 7.62 (d, J = 9.0 Hz, 1H), 7.45 (t, J = 7.8 Hz, 2H), 7.32 (t, J = 7.4 Hz, 1H), 7.17 (ddd, J = 8.9, 6.7, 1.2 Hz, 1H), 6.82 (td, J = 6.8, 0.9 Hz, 1H), 3.32 (s, 1H), 3.07 – 2.85 (m, 1H), 1.81 (d, J = 13.1 Hz, 2H), 1.68 (dd, J = 9.1, 3.6 Hz, 2H), 1.60 – 1.54 (m, 1H), 1.28 – 1.12 (m, 5H). ¹³C NMR (126 MHz, CDCl₃) δ 141.02, 135.43, 133.45, 128.74, 127.74, 127.20, 125.17, 125.04, 123.07, 116.94, 112.30, 57.02, 34.27, 25.81, 24.94. MS (ESI) calculated for C₁₉H₂₁N₃, m/z 291.17, found 292.18 [M+H]⁺.

2b: N-cyclohexyl-2-phenylimidazo[1,2-a]pyrazin-3-amine. 25 mg, 36%. ¹H NMR (500 MHz, CDCl₃) δ 8.99 (d, J = 1.4 Hz, 1H), 8.01 (ddd, J = 4.6, 3.2, 1.8 Hz, 3H), 7.85 (d, J = 4.6 Hz, 1H),

7.48 (t, $J = 7.7$ Hz, 2H), 7.38 (t, $J = 7.4$ Hz, 1H), 3.26 (s, 1H), 3.00 (s, 1H), 1.82 (dd, $J = 6.6, 5.4$ Hz, 2H), 1.70 (dd, $J = 9.3, 3.3$ Hz, 2H), 1.62 – 1.55 (m, 1H), 1.34 – 1.07 (m, 5H). ^{13}C NMR (126 MHz, CDCl_3) δ 143.37, 139.08, 136.82, 133.62, 129.01, 128.90, 128.30, 127.42, 126.70, 115.73, 57.02, 34.41, 25.69, 24.91. MS (ESI) calculated for $\text{C}_{18}\text{H}_{20}\text{N}_4$, m/z 292.17, found 293.18 $[\text{M}+\text{H}]^+$.

2c: 2-Benzyl-*N*-cyclohexylimidazo[1,2-*a*]pyridin-3-amine. 51 mg, 70%. ^1H NMR (500 MHz, CDCl_3) δ 8.04 (dt, $J = 6.8, 1.1$ Hz, 1H), 7.52 – 7.46 (m, 1H), 7.31 – 7.26 (m, 4H), 7.19 (qd, $J = 5.3, 2.7$ Hz, 1H), 7.10 (ddd, $J = 9.0, 6.7, 1.3$ Hz, 1H), 6.76 (td, $J = 6.8, 1.1$ Hz, 1H), 4.16 (s, 2H), 2.77 (s, 1H), 2.60 (s, 1H), 1.79 – 1.67 (m, 4H), 1.59 (s, 1H), 1.32 – 1.04 (m, 5H). ^{13}C NMR (126 MHz, CDCl_3) δ 141.11, 139.62, 137.49, 128.68, 128.53, 126.20, 125.44, 123.43, 122.59, 116.93, 111.41, 57.32, 34.17, 34.11, 25.74, 24.85. MS (ESI) calculated for $\text{C}_{20}\text{H}_{23}\text{N}_3$, m/z 305.19, found 306.20 $[\text{M}+\text{H}]^+$.

2d: 2-Benzyl-*N*-cyclohexylimidazo[1,2-*a*]pyrazin-3-amine. 37 mg, 50%. ^1H NMR (500 MHz, CDCl_3) δ 8.92 (d, $J = 1.4$ Hz, 1H), 7.93 (dd, $J = 4.6, 1.5$ Hz, 1H), 7.81 (d, $J = 4.6$ Hz, 1H), 7.33 – 7.25 (m, 4H), 7.22 (ddd, $J = 6.2, 3.3, 1.6$ Hz, 1H), 4.20 (s, 2H), 2.81 (s, 1H), 2.68 (s, 1H), 1.84 – 1.65 (m, 4H), 1.60 (d, $J = 6.1$ Hz, 1H), 1.24 – 0.95 (m, 5H). ^{13}C NMR (126 MHz, CDCl_3) δ 141.19, 139.22, 137.30, 135.01, 127.27, 127.20, 127.17, 125.71, 125.04, 114.00, 55.65, 32.84, 32.76, 24.09, 23.31. MS (ESI) calculated for $\text{C}_{19}\text{H}_{22}\text{N}_4$, m/z 306.18, found 307.20 $[\text{M}+\text{H}]^+$.

2e: *N*-cyclohexyl-2-(naphthalen-1-yl)imidazo[1,2-*a*]pyridin-3-amine. 24 mg, 29%. ^1H NMR (500 MHz, CDCl_3) δ 8.20 (d, $J = 6.8$ Hz, 1H), 7.95 – 7.88 (m, 3H), 7.72 – 7.64 (m, 2H), 7.59 – 7.54 (m, 1H), 7.53 – 7.45 (m, 2H), 7.25 – 7.20 (m, 1H), 6.90 (t, $J = 6.8$ Hz, 1H), 3.15 (s, 1H), 2.63 (t, $J = 9.6$ Hz, 1H), 1.58 (d, $J = 12.6$ Hz, 2H), 1.50 – 1.36 (m, 3H), 1.04 – 0.77 (m, 5H). ^{13}C

NMR (126 MHz, CDCl₃) δ 141.06, 133.76, 131.95, 128.57, 128.49, 128.15, 126.76, 126.65, 125.86, 125.50, 125.36, 124.30, 122.89, 117.21, 112.14, 56.32, 33.70, 25.47, 24.51. MS (ESI) calculated for C₂₃H₂₃N₃, m/z 341.19, found 342.20 [M+H]⁺.

2f: *N*-cyclohexyl-2-(naphthalen-1-yl)imidazo[1,2-*a*]pyrazin-3-amine. 50 mg, 61%. ¹H NMR (500 MHz, CDCl₃) δ 9.05 (d, *J* = 1.5 Hz, 1H), 8.05 (dd, *J* = 4.6, 1.5 Hz, 1H), 7.96 – 7.93 (m, 2H), 7.92 – 7.89 (m, 2H), 7.61 (ddd, *J* = 15.2, 7.5, 4.2 Hz, 4H), 7.55 – 7.48 (m, 1H), 3.27 (s, 1H), 2.73 (s, 1H), 1.61 (dd, *J* = 9.5, 3.2 Hz, 2H), 1.44 (ddd, *J* = 14.5, 11.6, 4.6 Hz, 3H), 1.07 – 0.82 (m, 5H). ¹³C NMR (126 MHz, CDCl₃) δ 143.40, 138.38, 136.73, 133.80, 131.90, 130.80, 129.03, 128.84, 128.58, 128.53, 128.07, 126.87, 126.08, 125.30, 125.27, 115.67, 56.12, 33.85, 25.35, 24.50. MS (ESI) calculated for C₂₂H₂₂N₄, m/z 342.18, found 343.19 [M+H]⁺ and 365.17 [M+Na]⁺.

2g: 2-(Anthracen-9-yl)-*N*-cyclohexylimidazo[1,2-*a*]pyridin-3-amine. 83 mg, 88%. ¹H NMR (500 MHz, CDCl₃) δ 8.54 (s, 1H), 8.23 (dt, *J* = 6.8, 1.2 Hz, 1H), 8.06 (d, *J* = 8.4 Hz, 2H), 7.83 (dd, *J* = 8.7, 0.8 Hz, 2H), 7.66 (dt, *J* = 9.0, 1.0 Hz, 1H), 7.49 – 7.44 (m, 2H), 7.40 (ddd, *J* = 8.6, 6.5, 1.3 Hz, 2H), 7.23 (ddd, *J* = 9.0, 6.7, 1.3 Hz, 1H), 6.90 (td, *J* = 6.8, 1.1 Hz, 1H), 2.80 (d, *J* = 7.4 Hz, 1H), 2.62 – 2.49 (m, 1H), 1.47 (d, *J* = 12.6 Hz, 2H), 1.35 – 1.24 (m, 3H), 0.89 – 0.77 (m, 3H), 0.68 (dt, *J* = 12.8, 6.6 Hz, 2H). ¹³C NMR (126 MHz, CDCl₃) δ 142.02, 134.01, 131.38, 131.20, 128.59, 128.34, 128.10, 127.64, 126.25, 126.12, 125.10, 123.40, 122.81, 117.72, 111.60, 56.18, 33.62, 25.39, 24.38. MS (ESI) calculated for C₂₇H₂₅N₃, m/z 391.20, found 392.22 [M+H]⁺.

2h: 2-(Anthracen-9-yl)-*N*-cyclohexylimidazo[1,2-*a*]pyrazin-3-amine. 17 mg, 18%. ¹H NMR (500 MHz, CDCl₃) δ 9.12 (d, *J* = 1.4 Hz, 1H), 8.59 (s, 1H), 8.13 – 8.06 (m, 3H), 7.97 (d, *J* = 4.6 Hz, 1H), 7.72 (dd, *J* = 8.7, 0.6 Hz, 2H), 7.46 (dddd, *J* = 10.0, 7.8, 6.5, 1.1 Hz, 4H), 2.91 (d, *J* =

6.2 Hz, 1H), 2.62 (s, 1H), 1.48 (d, $J = 12.6$ Hz, 2H), 1.29 (dd, $J = 24.7, 8.3$ Hz, 3H), 0.91 – 0.76 (m, 3H), 0.76 – 0.63 (m, 2H). ^{13}C NMR (126 MHz, CDCl_3) δ 142.63, 136.28, 135.36, 130.29, 130.12, 128.74, 128.01, 127.76, 127.36, 125.75, 125.54, 124.62, 124.25, 114.68, 54.95, 32.71, 24.20, 23.32. MS (ESI) calculated for $\text{C}_{26}\text{H}_{24}\text{N}_4$, m/z 392.20, found 393.20 $[\text{M}+\text{H}]^+$.

3a: *N*-benzyl-2-phenylimidazo[1,2-*a*]pyridin-3-amine. 62 mg, 86%. ^1H NMR (500 MHz, CDCl_3) δ 7.98 (ddt, $J = 3.7, 3.0, 1.6$ Hz, 3H), 7.57 (dt, $J = 9.0, 1.0$ Hz, 1H), 7.45 (t, $J = 7.7$ Hz, 2H), 7.39 – 7.26 (m, 6H), 7.13 (ddd, $J = 9.0, 6.7, 1.3$ Hz, 1H), 6.74 (td, $J = 6.8, 1.1$ Hz, 1H), 4.20 (d, $J = 6.1$ Hz, 2H), 3.52 (t, $J = 6.0$ Hz, 1H). ^{13}C NMR (126 MHz, CDCl_3) δ 141.57, 139.06, 136.04, 134.13, 128.84, 128.30, 127.82, 127.65, 127.16, 125.77, 124.32, 122.50, 117.52, 111.94, 52.57. MS (ESI) calculated for $\text{C}_{20}\text{H}_{17}\text{N}_3$, m/z 299.14, found 300.15 $[\text{M}+\text{H}]^+$.

3b: *N*-benzyl-2-phenylimidazo[1,2-*a*]pyrazin-3-amine. 45 mg, 62%. ^1H NMR (500 MHz, CDCl_3) δ 8.98 (d, $J = 1.3$ Hz, 1H), 7.94 (dt, $J = 8.1, 1.6$ Hz, 2H), 7.82 (dd, $J = 4.6, 1.4$ Hz, 1H), 7.77 (d, $J = 4.6$ Hz, 1H), 7.47 (t, $J = 7.6$ Hz, 2H), 7.39 (t, $J = 7.4$ Hz, 1H), 7.34 – 7.27 (m, 5H), 4.23 (d, $J = 2.4$ Hz, 2H), 3.66 (s, 1H). ^{13}C NMR (126 MHz, CDCl_3) δ 143.46, 138.76, 138.56, 136.79, 133.34, 129.06, 129.03, 128.99, 128.46, 128.24, 128.08, 127.42, 127.18, 115.38, 52.39. MS (ESI) calculated for $\text{C}_{19}\text{H}_{16}\text{N}_4$, m/z 300.14, found 301.15 $[\text{M}+\text{H}]^+$.

3c: *N*,2-dibenzylimidazo[1,2-*a*]pyridin-3-amine. 33 mg, 44%. ^1H NMR (500 MHz, CDCl_3) δ 7.95 (dt, $J = 6.8, 1.1$ Hz, 1H), 7.49 (dt, $J = 9.1, 0.9$ Hz, 1H), 7.38 – 7.15 (m, 10H), 7.09 (ddd, $J = 9.0, 6.7, 1.3$ Hz, 1H), 6.72 (td, $J = 6.7, 1.1$ Hz, 1H), 4.01 (s, 2H), 3.94 (d, $J = 5.5$ Hz, 2H), 2.99 (s, 1H). ^{13}C NMR (126 MHz, CDCl_3) δ 141.18, 139.68, 139.24, 137.57, 128.69, 128.62, 128.57, 128.28, 127.59, 126.25, 125.93, 123.36, 122.14, 117.15, 111.44, 52.83, 34.13. MS (ESI) calculated for $\text{C}_{21}\text{H}_{19}\text{N}_3$, m/z 313.16, found 314.18 $[\text{M}+\text{H}]^+$.

3d: N,2-dibenzylimidazo[1,2-a]pyrazin-3-amine. 19 mg, 25%. ^1H NMR (500 MHz, CDCl_3) δ 7.83 – 7.72 (m, 2H), 7.35 – 7.25 (m, 5H), 7.25 – 7.18 (m, 4H), 7.16 (dd, $J = 7.0, 2.2$ Hz, 2H), 4.03 (s, 2H), 3.96 (d, $J = 3.9$ Hz, 2H), 3.15 – 3.05 (m, 1H). ^{13}C NMR (126 MHz, CDCl_3) δ 141.87, 139.52, 137.76, 137.68, 135.44, 128.01, 127.89, 127.75, 127.71, 127.66, 127.63, 127.59, 127.56, 127.26, 127.19, 126.97, 126.84, 126.75, 125.57, 114.09, 51.49, 51.46, 33.19. MS (ESI) calculated for $\text{C}_{20}\text{H}_{18}\text{N}_4$, m/z 314.15, found 315.17 $[\text{M}+\text{H}]^+$.

3e: N-benzyl-2-(naphthalen-1-yl)imidazo[1,2-a]pyridin-3-amine. 42 mg, 50%. ^1H NMR (500 MHz, CDCl_3) δ 8.15 – 8.10 (m, 1H), 8.01 (d, $J = 8.3$ Hz, 1H), 7.94 – 7.86 (m, 2H), 7.61 (d, $J = 9.0$ Hz, 1H), 7.55 – 7.44 (m, 4H), 7.18 (ddd, $J = 9.0, 6.7, 1.3$ Hz, 1H), 7.15 – 7.11 (m, 3H), 7.02 (dd, $J = 6.5, 3.0$ Hz, 2H), 6.83 (td, $J = 6.8, 1.0$ Hz, 1H), 3.92 (d, $J = 4.9$ Hz, 2H), 3.53 (s, 1H). ^{13}C NMR (126 MHz, CDCl_3) δ 141.35, 138.75, 135.57, 133.79, 132.14, 131.50, 128.45, 128.37, 128.33, 127.88, 127.34, 127.31, 126.49, 125.88, 125.82, 125.27, 123.69, 122.50, 117.60, 111.80, 52.42. MS (ESI) calculated for $\text{C}_{24}\text{H}_{19}\text{N}_3$, m/z 349.16, found 350.18 $[\text{M}+\text{H}]^+$.

3f: N-benzyl-2-(naphthalen-1-yl)imidazo[1,2-a]pyrazin-3-amine. 12 mg, 14%. ^1H NMR (500 MHz, CDCl_3) δ 9.01 (d, $J = 1.5$ Hz, 1H), 7.97 – 7.89 (m, 4H), 7.83 (d, $J = 4.6$ Hz, 1H), 7.49 (tddd, $J = 10.0, 6.8, 3.6, 1.4$ Hz, 4H), 7.17 – 7.08 (m, 3H), 7.01 – 6.94 (m, 2H), 3.96 (d, $J = 5.8$ Hz, 2H), 3.78 (t, $J = 5.8$ Hz, 1H). ^{13}C NMR (126 MHz, CDCl_3) δ 143.50, 138.21, 137.83, 136.53, 133.78, 131.90, 130.44, 129.08, 128.95, 128.89, 128.49, 128.46, 128.02, 127.77, 127.73, 127.58, 126.78, 126.06, 125.45, 125.21, 115.35, 51.83. MS (ESI) calculated for $\text{C}_{23}\text{H}_{18}\text{N}_4$, m/z 350.15, found 351.18 $[\text{M}+\text{H}]^+$.

3g: 2-(Anthracen-9-yl)-N-benzylimidazo[1,2-a]pyridin-3-amine. 47 mg, 49%. ^1H NMR (500 MHz, CDCl_3) δ 8.55 (s, 1H), 8.18 (dt, $J = 6.9, 1.2$ Hz, 1H), 8.07 (d, $J = 8.5$ Hz, 2H), 7.82 (dd, $J =$

8.8, 0.9 Hz, 2H), 7.66 (dt, $J = 9.0, 1.1$ Hz, 1H), 7.50 – 7.43 (m, 2H), 7.39 (ddd, $J = 8.7, 6.5, 1.3$ Hz, 2H), 7.22 (ddd, $J = 9.0, 6.7, 1.3$ Hz, 1H), 7.05 – 6.95 (m, 3H), 6.90 – 6.82 (m, 3H), 3.74 (d, $J = 6.3$ Hz, 2H), 3.25 (t, $J = 6.3$ Hz, 1H). ^{13}C NMR (126 MHz, CDCl_3) δ 140.88, 137.71, 132.57, 130.36, 130.23, 127.77, 127.54, 127.15, 127.02, 126.76, 126.63, 126.10, 125.31, 125.10, 124.09, 122.54, 121.46, 116.74, 110.71, 51.19. MS (ESI) calculated for $\text{C}_{28}\text{H}_{21}\text{N}_3$, m/z 399.17, found 400.20 $[\text{M}+\text{H}]^+$.

3h: 2-(Anthracen-9-yl)-*N*-benzylimidazo[1,2-*a*]pyrazin-3-amine. 8 mg, 8%. ^1H NMR (500 MHz, CDCl_3) δ 9.09 (d, $J = 1.4$ Hz, 1H), 8.59 (s, 1H), 8.08 (d, $J = 8.5$ Hz, 2H), 8.01 (dd, $J = 4.6, 1.5$ Hz, 1H), 7.91 (d, $J = 4.6$ Hz, 1H), 7.69 (dd, $J = 8.8, 0.7$ Hz, 2H), 7.52 – 7.45 (m, 2H), 7.41 (ddd, $J = 8.6, 6.5, 1.2$ Hz, 2H), 7.06 – 6.94 (m, 3H), 6.83 – 6.77 (m, 2H), 3.78 (d, $J = 5.3$ Hz, 2H), 3.44 (s, 1H). ^{13}C NMR (126 MHz, CDCl_3) δ 143.66, 138.12, 137.10, 135.78, 131.32, 131.19, 130.28, 129.06, 128.75, 128.50, 128.33, 127.55, 127.41, 126.56, 126.53, 125.74, 125.28, 115.37, 51.61. MS (ESI) calculated for $\text{C}_{27}\text{H}_{20}\text{N}_4$, m/z 400.17, found 401.19 $[\text{M}+\text{H}]^+$.

Compounds **4a-4c** were synthesized similarly as compound **1a**.

4a: 2-(Anthracen-9-yl)-*N*-cyclohexylimidazo[1,2-*a*]pyrimidin-3-amine. 40 mg, 43%. ^1H NMR (500 MHz, CDCl_3) δ 8.61 (dd, $J = 4.1, 2.1$ Hz, 1H), 8.56 (s, 1H), 8.54 (dd, $J = 6.8, 2.1$ Hz, 1H), 8.07 (d, $J = 8.4$ Hz, 2H), 7.83 (dd, $J = 8.7, 0.8$ Hz, 2H), 7.49 – 7.44 (m, 2H), 7.41 (ddd, $J = 8.6, 6.5, 1.3$ Hz, 2H), 6.97 (dd, $J = 6.8, 4.1$ Hz, 1H), 2.83 (s, 1H), 2.47 (s, 1H), 1.43 (d, $J = 12.9$ Hz, 2H), 1.29 (d, $J = 7.4$ Hz, 3H), 0.82 (t, $J = 6.6$ Hz, 3H), 0.75 – 0.62 (m, 2H). ^{13}C NMR (126 MHz, CDCl_3) δ 148.91, 144.93, 135.89, 131.34, 131.05, 130.37, 128.66, 128.12, 127.26, 126.67, 126.29, 126.07, 125.18, 108.17, 56.46, 33.55, 25.28, 24.28. MS (ESI) calculated for $\text{C}_{26}\text{H}_{24}\text{N}_4$, m/z 392.20, found 393.22 $[\text{M}+\text{H}]^+$.

4b: 2-(Anthracen-9-yl)-N³-cyclohexylimidazo[1,2-a]pyridine-3,8-diamine. 15 mg, 15%. ¹H NMR (500 MHz, CDCl₃) δ 8.54 (s, 1H), 8.06 (d, *J* = 8.4 Hz, 2H), 7.86 (dd, *J* = 8.7, 0.7 Hz, 2H), 7.70 (dd, *J* = 6.7, 0.9 Hz, 1H), 7.49 – 7.44 (m, 2H), 7.43 – 7.37 (m, 2H), 6.74 (t, *J* = 7.0 Hz, 1H), 6.40 (dd, *J* = 7.3, 0.9 Hz, 1H), 4.57 (s, 2H), 2.77 (s, 1H), 2.56 (s, 1H), 1.49 (d, *J* = 12.4 Hz, 2H), 1.29 (d, *J* = 5.7 Hz, 3H), 0.94 – 0.75 (m, 3H), 0.75 – 0.61 (m, 2H). ¹³C NMR (126 MHz, CDCl₃) δ 135.97, 135.69, 132.06, 131.45, 131.37, 129.03, 128.57, 128.36, 127.62, 126.37, 126.06, 125.12, 113.22, 112.69, 101.65, 56.09, 33.63, 25.41, 24.41. MS (ESI) calculated for C₂₇H₂₆N₄, *m/z* 406.22, found 407.23 [M+H]⁺.

4c: 2-(Anthracen-9-yl)-8-chloro-N-cyclohexylimidazo[1,2-a]pyrazin-3-amine. 20 mg, 20%. ¹H NMR (500 MHz, CDCl₃) δ 8.59 (s, 1H), 8.10 – 8.06 (m, 3H), 7.77 (d, *J* = 4.5 Hz, 1H), 7.70 (dd, *J* = 8.7, 0.7 Hz, 2H), 7.52 – 7.47 (m, 2H), 7.46 – 7.41 (m, 2H), 2.93 (d, *J* = 6.8 Hz, 1H), 2.66 – 2.58 (m, 1H), 1.48 (d, *J* = 12.4 Hz, 2H), 1.32 (d, *J* = 6.9 Hz, 3H), 0.92 – 0.79 (m, 3H), 0.69 (dd, *J* = 22.4, 11.8 Hz, 2H). ¹³C NMR (126 MHz, CDCl₃) δ 143.61, 136.76, 134.02, 131.59, 131.27, 131.26, 128.77, 128.58, 127.43, 126.61, 126.17, 125.63, 125.29, 115.63, 56.13, 33.74, 25.16, 24.33. MS (ESI) calculated for C₂₆H₂₃ClN₄, *m/z* 426.16, found 427.17 [M+H]⁺.

Compounds **5a-5i** were synthesized similarly as compound **1a**.

5a: 2-(Anthracen-9-yl)-N-butylimidazo[1,2-a]pyridin-3-amine. 22 mg, 25%. ¹H NMR (500 MHz, CDCl₃) δ 8.55 (s, 1H), 8.19 (dt, *J* = 6.8, 1.2 Hz, 1H), 8.06 (d, *J* = 8.4 Hz, 2H), 7.84 (dd, *J* = 8.7, 0.8 Hz, 2H), 7.67 (dt, *J* = 9.1, 1.0 Hz, 1H), 7.48 – 7.44 (m, 2H), 7.40 (ddd, *J* = 8.6, 6.5, 1.3 Hz, 2H), 7.22 (ddd, *J* = 9.0, 6.7, 1.3 Hz, 1H), 6.90 (td, *J* = 6.8, 1.1 Hz, 1H), 2.89 (t, *J* = 6.1 Hz, 1H), 2.64 (q, *J* = 6.6 Hz, 2H), 1.09 – 0.97 (m, 2H), 0.86 – 0.72 (m, 2H), 0.43 (t, *J* = 7.4 Hz, 3H). ¹³C NMR (126 MHz, CDCl₃) δ 141.97, 133.07, 131.52, 131.47, 129.40, 128.68, 128.39, 127.80,

126.46, 126.21, 125.25, 123.46, 122.61, 117.92, 111.80, 47.92, 32.18, 19.67, 13.53. MS (ESI) calculated for C₂₅H₂₃N₃, m/z 365.19, found 366.20 [M+H]⁺.

5b: 2-(Anthracen-9-yl)-N-pentylimidazo[1,2-a]pyridin-3-amine. 35 mg, 38%. ¹H NMR (500 MHz, CDCl₃) δ 8.55 (s, 1H), 8.19 (dt, *J* = 6.8, 1.2 Hz, 1H), 8.06 (d, *J* = 8.4 Hz, 2H), 7.84 (dd, *J* = 8.7, 0.8 Hz, 2H), 7.67 (dt, *J* = 9.0, 1.1 Hz, 1H), 7.49 – 7.44 (m, 2H), 7.40 (ddd, *J* = 8.6, 6.5, 1.3 Hz, 2H), 7.22 (ddd, *J* = 9.0, 6.7, 1.3 Hz, 1H), 6.90 (td, *J* = 6.8, 1.1 Hz, 1H), 2.91 (t, *J* = 6.4 Hz, 1H), 2.65 (q, *J* = 6.7 Hz, 2H), 1.02 (dt, *J* = 14.3, 7.0 Hz, 2H), 0.82 – 0.65 (m, 4H), 0.52 (t, *J* = 7.1 Hz, 3H). ¹³C NMR (126 MHz, CDCl₃) δ 141.85, 132.95, 131.40, 131.34, 129.24, 128.56, 128.26, 127.67, 126.32, 126.10, 125.13, 123.31, 122.48, 117.81, 111.67, 48.05, 29.68, 28.58, 22.07, 13.70. MS (ESI) calculated for C₂₆H₂₅N₃, m/z 379.20, found 380.22 [M+H]⁺.

5c: 2-(Anthracen-9-yl)-N-isopropylimidazo[1,2-a]pyridin-3-amine. 15 mg, 18%. ¹H NMR (500 MHz, CDCl₃) δ 8.54 (s, 1H), 8.25 (dt, *J* = 6.8, 1.2 Hz, 1H), 8.08 – 8.04 (m, 2H), 7.84 (dd, *J* = 8.7, 0.9 Hz, 2H), 7.66 (dt, *J* = 9.0, 1.1 Hz, 1H), 7.49 – 7.44 (m, 2H), 7.41 (ddd, *J* = 8.6, 6.5, 1.3 Hz, 2H), 7.23 (ddd, *J* = 9.0, 6.7, 1.3 Hz, 1H), 6.90 (td, *J* = 6.8, 1.1 Hz, 1H), 2.86 (dq, *J* = 12.5, 6.3 Hz, 1H), 2.71 (d, *J* = 6.4 Hz, 1H), 0.69 (d, *J* = 6.3 Hz, 6H). ¹³C NMR (126 MHz, CDCl₃) δ 142.10, 134.36, 131.39, 131.13, 128.63, 128.31, 128.29, 127.69, 126.23, 126.17, 125.11, 123.56, 122.78, 117.69, 111.64, 49.20, 23.15. MS (ESI) calculated for C₂₄H₂₁N₃, m/z 351.17, found 352.19 [M+H]⁺.

5d: 2-(Anthracen-9-yl)-N-isopropylimidazo[1,2-a]pyridin-3-amine. 37 mg, 41%. ¹H NMR (500 MHz, CDCl₃) δ 8.54 (s, 1H), 8.23 (dd, *J* = 6.8, 1.0 Hz, 1H), 8.06 (d, *J* = 8.3 Hz, 2H), 7.89 – 7.83 (m, 2H), 7.67 (dt, *J* = 9.0, 1.0 Hz, 1H), 7.50 – 7.37 (m, 4H), 7.23 (ddd, *J* = 9.0, 6.7, 1.3 Hz, 1H), 6.90 (td, *J* = 6.8, 1.1 Hz, 1H), 2.79 – 2.61 (m, 2H), 1.12 – 0.95 (m, 2H), 0.92 – 0.82 (m,

2H), 0.79 – 0.67 (m, 1H), 0.63 (d, $J = 6.2$ Hz, 2H), 0.39 (t, $J = 7.1$ Hz, 2H), 0.29 (t, $J = 7.4$ Hz, 1H). ^{13}C NMR (126 MHz, CDCl_3) δ 142.03, 134.21, 131.41, 131.39, 131.36, 131.19, 131.13, 128.62, 128.61, 128.59, 128.36, 128.34, 127.64, 127.61, 126.26, 126.15, 126.13, 125.09, 123.45, 123.34, 122.68, 122.60, 117.74, 117.71, 111.62, 59.63, 53.06, 39.14, 26.01, 20.85, 18.53, 13.58, 9.01. MS (ESI) calculated for $\text{C}_{26}\text{H}_{25}\text{N}_3$, m/z 379.20, found 380.22 $[\text{M}+\text{H}]^+$.

5e: 2-(Anthracen-9-yl)-*N*-(2,4,4-trimethylpentan-2-yl)imidazo[1,2-*a*]pyridin-3-amine. 51 mg, 50%. IR (CHCl_3) ν_{max} (cm^{-1}): 2956, 1519, 1481, 1365, 1340. ^1H NMR (500 MHz, CDCl_3) δ 8.53 (s, 1H), 8.41 (d, $J = 6.9$ Hz, 1H), 8.05 (d, $J = 7.7$ Hz, 2H), 7.88 (d, $J = 8.5$ Hz, 2H), 7.66 (d, $J = 9.0$ Hz, 1H), 7.50 – 7.38 (m, 4H), 7.24 (ddd, $J = 8.9, 6.7, 1.2$ Hz, 1H), 6.88 (td, $J = 6.8, 1.0$ Hz, 1H), 2.89 (s, 1H), 0.97 (s, 2H), 0.68 (s, 6H), 0.52 (s, 9H). ^{13}C NMR (126 MHz, CDCl_3) δ 142.71, 137.08, 131.44, 131.01, 129.27, 128.71, 127.53, 126.78, 126.32, 126.24, 125.05, 123.94, 123.70, 117.51, 111.35, 59.61, 55.82, 31.20, 30.95, 28.61. MS (ESI) calculated for $\text{C}_{29}\text{H}_{31}\text{N}_3$, m/z 421.25, found 422.27 $[\text{M}+\text{H}]^+$.

5f: 2-(Anthracen-9-yl)-*N*-((trimethylsilyl)methyl)imidazo[1,2-*a*]pyridin-3-amine. 33 mg, 35%. ^1H NMR (500 MHz, CDCl_3) δ 8.55 (s, 1H), 8.15 (dt, $J = 6.8, 1.1$ Hz, 1H), 8.06 (d, $J = 8.4$ Hz, 2H), 7.89 (dd, $J = 8.7, 0.7$ Hz, 2H), 7.69 – 7.65 (m, 1H), 7.49 – 7.44 (m, 2H), 7.43 – 7.38 (m, 2H), 7.22 (ddd, $J = 9.0, 6.7, 1.3$ Hz, 1H), 6.91 (td, $J = 6.8, 1.0$ Hz, 1H), 2.60 (s, 1H), 2.15 (s, 2H), -0.31 (s, 9H). ^{13}C NMR (126 MHz, CDCl_3) δ 141.55, 132.06, 131.73, 131.42, 131.23, 128.58, 128.10, 127.65, 126.45, 126.02, 125.11, 123.20, 122.44, 117.79, 111.61, 38.69, -3.37. MS (ESI) calculated for $\text{C}_{25}\text{H}_{25}\text{N}_3\text{Si}$, m/z 395.18, found 396.20 $[\text{M}+\text{H}]^+$.

5g: *N*-(adamantan-1-yl)-2-(anthracen-9-yl)imidazo[1,2-*a*]pyridin-3-amine. 46 mg, 43%. ^1H NMR (500 MHz, CDCl_3) δ 8.52 (s, 1H), 8.45 (dt, $J = 6.9, 1.1$ Hz, 1H), 8.08 – 8.03 (m, 2H), 7.87

(d, $J = 8.8$ Hz, 2H), 7.65 (dt, $J = 9.0, 1.0$ Hz, 1H), 7.44 (dddd, $J = 10.0, 7.9, 6.5, 1.3$ Hz, 4H), 7.23 (ddd, $J = 9.0, 6.7, 1.3$ Hz, 1H), 6.88 (td, $J = 6.8, 1.1$ Hz, 1H), 2.66 (s, 1H), 1.65 (s, 3H), 1.34 (d, $J = 12.1$ Hz, 3H), 1.19 (d, $J = 11.4$ Hz, 3H), 1.13 (d, $J = 2.5$ Hz, 6H). ^{13}C NMR (126 MHz, CDCl_3) δ 142.80, 137.17, 131.51, 131.15, 129.27, 128.82, 127.68, 126.39, 126.35, 125.99, 125.17, 123.99, 123.87, 117.61, 111.43, 55.78, 43.30, 36.03, 29.50. MS (ESI) calculated for $\text{C}_{31}\text{H}_{29}\text{N}_3$, m/z 443.24, found 444.26 $[\text{M}+\text{H}]^+$.

5h: 2-(Anthracen-9-yl)-*N*-(4-methoxyphenyl)imidazo[1,2-*a*]pyridin-3-amine. 36 mg, 36%. ^1H NMR (500 MHz, CDCl_3) δ 8.50 (s, 1H), 8.01 (d, $J = 8.5$ Hz, 2H), 7.90 – 7.83 (m, 3H), 7.74 (d, $J = 9.1$ Hz, 1H), 7.46 – 7.39 (m, 2H), 7.38 – 7.28 (m, 3H), 6.87 (td, $J = 6.8, 1.0$ Hz, 1H), 6.61 – 6.56 (m, 2H), 6.37 – 6.29 (m, 2H), 5.29 (s, 1H), 3.63 (s, 3H). ^{13}C NMR (126 MHz, CDCl_3) δ 153.58, 142.85, 137.63, 136.25, 131.45, 131.34, 128.69, 128.04, 127.61, 126.28, 126.18, 125.19, 124.47, 123.39, 123.21, 118.11, 115.45, 114.84, 112.22, 55.69. MS (ESI) calculated for $\text{C}_{28}\text{H}_{21}\text{N}_3\text{O}$, m/z 415.17, found 416.19 $[\text{M}+\text{H}]^+$.

5i: 2-(Anthracen-9-yl)-*N*-(2-chloro-6-methylphenyl)imidazo[1,2-*a*]pyridin-3-amine. 11 mg, 11%. ^1H NMR (500 MHz, CDCl_3) δ 8.38 (s, 1H), 8.21 (dt, $J = 6.8, 1.1$ Hz, 1H), 7.94 (d, $J = 8.4$ Hz, 2H), 7.75 (ddd, $J = 15.6, 8.3, 4.8$ Hz, 3H), 7.41 – 7.35 (m, 2H), 7.34 – 7.28 (m, 3H), 6.97 (td, $J = 6.8, 1.1$ Hz, 1H), 6.61 (dd, $J = 7.9, 1.0$ Hz, 1H), 6.41 – 6.35 (m, 1H), 6.29 (t, $J = 7.7$ Hz, 1H), 5.43 (s, 1H), 1.48 (s, 3H). ^{13}C NMR (126 MHz, CDCl_3) δ 142.20, 139.32, 137.26, 131.22, 129.58, 128.96, 128.51, 127.69, 127.36, 126.96, 126.32, 125.86, 124.98, 124.43, 124.33, 122.77, 121.59, 118.07, 112.53, 18.14. MS (ESI) calculated for $\text{C}_{28}\text{H}_{20}\text{ClN}_3$, m/z 433.13, found 434.15 $[\text{M}+\text{H}]^+$.

Synthesis of compound 6: 2-(Anthracen-9-yl)imidazo[1,2-a]pyridin-3-amine. Compound **5e** (50 mg, 0.12 mmol) was stirred in a solution of 4M HCl/dioxane for 3 h, followed by removing the solvent under vacuum. The residue was then purified using column chromatography to obtain compound **6** in quantitative yield. ¹H NMR (500 MHz, CDCl₃) δ 8.55 (s, 1H), 8.12 (d, *J* = 6.8 Hz, 1H), 8.07 (d, *J* = 8.4 Hz, 2H), 7.87 (d, *J* = 8.8 Hz, 2H), 7.66 (d, *J* = 9.1 Hz, 1H), 7.49 – 7.45 (m, 2H), 7.44 – 7.38 (m, 2H), 7.23 – 7.17 (m, 1H), 6.91 (td, *J* = 6.8, 0.9 Hz, 1H), 3.07 (s, 2H). ¹³C NMR (126 MHz, CDCl₃) δ 141.49, 131.62, 131.32, 130.44, 128.77, 127.97, 127.79, 126.54, 126.32, 125.88, 125.33, 123.00, 122.10, 117.82, 111.89. MS (ESI) calculated for C₂₁H₁₅N₃, *m/z* 309.13, found 310.14 [M+H]⁺.

Syntheses of compounds 7a and 7b: To a solution of compound **6** (20 mg, 0.065 mmol) in anhydrous methanol, were added octyl aldehyde (15 μL, 0.098 mmol), 4 drops of acetic acid and sodium cyanoborohydride (6 mg, 0.098 mmol). The reaction mixture was stirred for 18h and the solvent was then removed under vacuum. The residue was purified using column chromatography to obtain compounds **7a** (0-3% MeOH in CH₂Cl₂) and **7b** (0-2% MeOH in CH₂Cl₂).

7a: 2-(Anthracen-9-yl)-*N*-octylimidazo[1,2-a]pyridin-3-amine. 10 mg, 36%. ¹H NMR (500 MHz, CDCl₃) δ 8.54 (s, 1H), 8.20 (dt, *J* = 6.8, 1.1 Hz, 1H), 8.06 (d, *J* = 8.4 Hz, 2H), 7.84 (dd, *J* = 8.7, 0.7 Hz, 2H), 7.67 (d, *J* = 9.0 Hz, 1H), 7.50 – 7.43 (m, 2H), 7.42 – 7.37 (m, 2H), 7.23 (ddd, *J* = 9.0, 6.7, 1.3 Hz, 1H), 6.91 (td, *J* = 6.8, 1.1 Hz, 1H), 2.92 (s, 1H), 2.70 – 2.61 (m, 2H), 1.21 – 1.11 (m, 2H), 0.99 (ddd, *J* = 15.6, 8.8, 7.1 Hz, 4H), 0.90 – 0.84 (m, 2H), 0.82 (t, *J* = 7.3 Hz, 3H), 0.73 – 0.66 (m, 4H). ¹³C NMR (126 MHz, CDCl₃) δ 141.95, 132.96, 131.54, 131.48, 129.37, 128.73, 128.28, 127.86, 126.44, 126.28, 125.28, 123.54, 122.65, 117.92, 111.86, 48.16, 31.79,

30.06, 29.11, 29.10, 26.56, 22.70, 14.22. MS (ESI) calculated for C₂₉H₃₁N₃, m/z 421.25, found 422.27 [M+H]⁺.

7b: 2-(Anthracen-9-yl)-N,N-dioctylimidazo[1,2-a]pyridin-3-amine. 7 mg, 20%. ¹H NMR (500 MHz, CDCl₃) δ 8.54 (s, 1H), 8.30 (d, *J* = 6.8 Hz, 1H), 8.04 (d, *J* = 8.5 Hz, 2H), 7.63 (d, *J* = 8.7 Hz, 3H), 7.46 – 7.40 (m, 2H), 7.31 (ddd, *J* = 8.6, 6.5, 1.1 Hz, 2H), 7.26 – 7.21 (m, 1H), 6.90 (td, *J* = 6.8, 1.0 Hz, 1H), 2.51 – 2.45 (m, 4H), 1.32 – 1.19 (m, 8H), 1.19 – 1.08 (m, 8H), 1.08 – 0.93 (m, 8H), 0.85 (t, *J* = 7.2 Hz, 6H). ¹³C NMR (126 MHz, CDCl₃) δ 142.02, 135.49, 132.12, 131.84, 131.45, 129.90, 128.41, 127.72, 127.10, 125.49, 125.20, 123.93, 123.19, 117.77, 111.74, 54.71, 31.92, 29.51, 29.38, 29.16, 27.09, 22.75, 14.25. MS (ESI) calculated for C₃₇H₄₇N₃, m/z 533.38, found 534.38 [M+H]⁺.

Synthesis of compound 7c: N-(2-(anthracen-9-yl)imidazo[1,2-a]pyridin-3-yl)-2,2,2-trifluoroacetamide. To a solution of compound **6** (10 mg, 0.024 mmol) in anhydrous CH₂Cl₂, was added trifluoroacetic anhydride (4 μL, 0.03 mmol) and the reaction mixture was stirred for 12 h. The solvent was then removed under vacuum and the residue was purified using column chromatography (0-3% MeOH in CH₂Cl₂) to obtain compound **7c** (10 mg, 73%). IR (CHCl₃) ν_{max} (cm⁻¹): 1730, 1494, 1355, 1315, 1240, 1195, 1157. ¹H NMR (500 MHz, MeOD) δ 8.89 (s, 1H), 8.76 (d, *J* = 6.8 Hz, 1H), 8.28 – 8.14 (m, 3H), 8.10 (d, *J* = 9.0 Hz, 1H), 7.77 (d, *J* = 8.5 Hz, 2H), 7.72 (dd, *J* = 10.0, 4.0 Hz, 1H), 7.59 (ddt, *J* = 9.9, 6.6, 3.9 Hz, 4H). ¹³C NMR (126 MHz, MeOD) δ 161.71, 161.41, 161.11, 160.82, 159.55, 159.23, 158.92, 158.61, 140.74, 135.66, 132.62, 132.61, 132.47, 130.22, 129.81, 129.06, 127.34, 127.00, 125.58, 118.91, 118.54, 113.88. MS (ESI) calculated for C₂₃H₁₄F₃N₃O, m/z 405.11, found 406.12 [M+H]⁺.

Compound **8a-8c** were synthesized similarly as compound **1a**.

8a: 2-([1,1'-Biphenyl]-4-yl)-N-(2,4,4-trimethylpentan-2-yl)imidazo[1,2-a]pyridin-3-amine. 60 mg, 63%. ¹H NMR (500 MHz, CDCl₃) δ 8.27 (d, *J* = 6.9 Hz, 1H), 7.99 – 7.95 (m, 2H), 7.71 – 7.65 (m, 4H), 7.61 (d, *J* = 9.0 Hz, 1H), 7.46 (dd, *J* = 10.5, 4.8 Hz, 2H), 7.38 – 7.33 (m, 1H), 7.21 – 7.15 (m, 1H), 6.82 (dd, *J* = 6.6, 6.2 Hz, 1H), 3.29 (s, 1H), 1.61 (s, 2H), 1.05 (s, 9H), 0.99 (s, 6H). ¹³C NMR (126 MHz, CDCl₃) δ 140.75, 140.14, 128.92, 128.78, 128.70, 127.31, 127.27, 127.26, 127.00, 126.96, 124.63, 123.66, 123.48, 117.04, 111.69, 60.86, 57.09, 31.86, 31.76, 29.02. MS (ESI) calculated for C₂₇H₃₁N₃, *m/z* 397.25, found 398.25 [M+H]⁺.

8b: 2-(Phenanthren-9-yl)-N-(2,4,4-trimethylpentan-2-yl)imidazo[1,2-a]pyridin-3-amine. 79 mg, 78%. ¹H NMR (500 MHz, CDCl₃) δ 8.78 (d, *J* = 8.2 Hz, 1H), 8.74 (d, *J* = 8.1 Hz, 1H), 8.37 (dt, *J* = 6.9, 1.1 Hz, 1H), 8.04 (dd, *J* = 8.2, 1.0 Hz, 1H), 7.92 (dd, *J* = 7.9, 1.2 Hz, 1H), 7.90 (s, 1H), 7.68 (dddd, *J* = 8.3, 6.9, 4.2, 1.4 Hz, 2H), 7.65 – 7.56 (m, 3H), 7.21 (ddd, *J* = 9.0, 6.7, 1.3 Hz, 1H), 6.86 (td, *J* = 6.8, 1.1 Hz, 1H), 3.21 (s, 1H), 1.26 (s, 2H), 0.78 (s, 6H), 0.73 (s, 9H). ¹³C NMR (126 MHz, CDCl₃) δ 142.35, 139.07, 131.88, 131.67, 131.27, 130.82, 130.44, 129.27, 128.91, 127.17, 126.89, 126.83, 126.72, 126.63, 125.55, 124.24, 123.90, 123.18, 122.72, 117.53, 111.59, 60.24, 56.39, 31.63, 31.45, 28.78. MS (ESI) calculated for C₂₉H₃₁N₃, *m/z* 421.25, found 422.26 [M+H]⁺ and 444.25 [M+Na]⁺.

8c: 2-(Pyren-4-yl)-N-(2,4,4-trimethylpentan-2-yl)imidazo[1,2-a]pyridin-3-amine. 47 mg, 44%. ¹H NMR (500 MHz, CDCl₃) δ 8.40 (dt, *J* = 6.9, 1.1 Hz, 1H), 8.28 (d, *J* = 7.8 Hz, 1H), 8.23 – 8.16 (m, 4H), 8.11 (dd, *J* = 12.1, 5.0 Hz, 3H), 8.02 (t, *J* = 7.6 Hz, 1H), 7.67 (dt, *J* = 9.0, 0.9 Hz, 1H), 7.23 (ddd, *J* = 9.0, 6.7, 1.3 Hz, 1H), 6.87 (td, *J* = 6.8, 1.1 Hz, 1H), 3.24 (s, 1H), 1.20 (s, 2H), 0.73 (s, 9H), 0.67 (s, 6H). ¹³C NMR (126 MHz, CDCl₃) δ 142.45, 139.49, 131.39, 131.00, 130.94, 130.62, 129.17, 128.39, 128.17, 127.55, 127.46, 125.92, 125.48, 125.20, 125.05,

125.01, 124.95, 124.79, 124.06, 123.77, 117.46, 111.40, 60.22, 56.27, 31.54, 31.32, 28.53. MS (ESI) calculated for C₃₁H₃₁N₃, m/z 445.25, found 446.26 [M+H]⁺ and 468.25 [M+Na]⁺.

Compound **9** was synthesized similarly as compound **1a**.

9: **2-(10-Chloroanthracen-9-yl)-N-(2,4,4-trimethylpentan-2-yl)imidazo[1,2-a]pyridin-3-amine.** 128 mg, 59%. ¹H NMR (500 MHz, CDCl₃) δ 8.60 (d, *J* = 8.8 Hz, 2H), 8.41 (d, *J* = 6.9 Hz, 1H), 7.90 (d, *J* = 8.8 Hz, 2H), 7.67 (d, *J* = 9.0 Hz, 1H), 7.62 – 7.57 (m, 2H), 7.50 – 7.45 (m, 2H), 7.28 – 7.25 (m, 1H), 6.90 (t, *J* = 6.8 Hz, 1H), 2.83 (s, 1H), 0.96 (s, 2H), 0.68 (s, 6H), 0.52 (s, 9H). ¹³C NMR (126 MHz, CDCl₃) δ 142.73, 136.53, 131.45, 129.61, 129.14, 128.64, 127.24, 127.01, 126.69, 126.58, 126.55, 125.21, 124.28, 123.73, 117.53, 111.57, 59.62, 55.90, 31.20, 31.00, 28.67. MS (ESI) calculated for C₂₉H₃₀ClN₃, m/z 455.21, found 456.23 [M+H]⁺.

Synthesis of compound 10: N¹,N¹-dimethyl-N³-(10-(3-((2,4,4-trimethylpentan-2-yl)amino)imidazo[1,2-a]pyridin-2-yl)anthracen-9-yl)propane-1,3-diamine. To a solution of compound **9** (50 mg, 0.11 mmol) in anhydrous dioxane, were added potassium *tert*-butoxide (38 mg, 0.34 mmol), N¹,N¹-dimethylpropane-1,3-diamine (69 μL, 0.55 mmol) and catalytic amounts of *tris*(dibenzylideneacetone)dipalladium [Pd₂(dba)₃] and 2-dicyclohexylphosphino-2'-(*N,N*-dimethylamino)biphenyl [DavePhos]. The reaction was heated in a sealed tube at 80 °C for 4 h. The solvent was then removed under vacuum and the residue was purified using column chromatography to obtain compound **10** (15 mg, 26%). ¹H NMR (500 MHz, MeOD) δ 8.53 (dt, *J* = 6.9, 1.0 Hz, 1H), 8.47 (d, *J* = 8.7 Hz, 2H), 7.74 (d, *J* = 8.5 Hz, 2H), 7.60 – 7.56 (m, 1H), 7.51 – 7.45 (m, 2H), 7.44 – 7.35 (m, 3H), 7.04 (td, *J* = 6.8, 1.1 Hz, 1H), 3.45 (t, *J* = 7.1 Hz, 2H), 2.57 – 2.52 (m, 2H), 2.30 (s, 6H), 2.02 – 1.91 (m, 2H), 0.95 (s, 2H), 0.74 (s, 6H), 0.45 (s, 9H). ¹³C NMR (126 MHz, MeOD) δ 144.90, 143.81, 137.83, 133.18, 128.54, 127.84, 127.32, 126.52, 126.46,

125.51, 125.31, 125.08, 124.09, 117.18, 113.25, 60.30, 58.65, 56.77, 51.56, 45.43, 44.86, 32.49, 31.81, 31.76, 29.47, 29.44. MS (ESI) calculated for C₃₄H₄₃N₅, m/z 521.35, found 522.37 [M+H]⁺.

Compound **11** was synthesized similarly as compound **1a**.

11: 2-(Anthracen-9-yl)-6-bromo-N-(2,4,4-trimethylpentan-2-yl)imidazo[1,2-a]pyridin-3-amine. 150 mg, 63%. ¹H NMR (500 MHz, CDCl₃) δ 8.54 – 8.51 (m, 2H), 8.08 – 8.04 (m, 2H), 7.82 (dd, *J* = 8.6, 0.9 Hz, 2H), 7.56 (dd, *J* = 9.4, 0.7 Hz, 1H), 7.49 – 7.41 (m, 4H), 7.30 (dd, *J* = 9.4, 1.9 Hz, 1H), 2.91 (s, 1H), 0.96 (s, 2H), 0.68 (s, 6H), 0.50 (s, 9H). ¹³C NMR (126 MHz, CDCl₃) δ 141.22, 138.24, 131.56, 131.08, 128.94, 128.70, 127.97, 127.51, 127.30, 126.66, 126.08, 125.26, 124.04, 118.41, 106.62, 59.88, 55.93, 31.31, 31.07, 28.78. MS (ESI) calculated for C₂₉H₃₀BrN₃, m/z 499.16, found 500.18 [M+H]⁺.

Compound **12** was synthesized similarly as compound **10**.

12: 2-(Anthracen-9-yl)-N⁶-(3-(dimethylamino)propyl)-N⁸-(2,4,4-trimethylpentan-2-yl)imidazo[1,2-a]pyridine-3,6-diamine. 21 mg, 40%. ¹H NMR (500 MHz, MeOD) δ 8.61 (s, 1H), 8.11 (d, *J* = 8.2 Hz, 2H), 7.83 (d, *J* = 8.6 Hz, 2H), 7.65 (d, *J* = 1.9 Hz, 1H), 7.52 – 7.42 (m, 4H), 7.39 (d, *J* = 9.5 Hz, 1H), 7.04 (dd, *J* = 9.5, 2.1 Hz, 1H), 3.18 (t, *J* = 6.8 Hz, 2H), 2.60 – 2.54 (m, 2H), 2.34 (s, 6H), 1.98 – 1.90 (m, 2H), 0.93 (s, 2H), 0.73 (s, 6H), 0.46 (s, 9H). ¹³C NMR (126 MHz, MeOD) δ 140.23, 138.50, 136.47, 133.04, 132.49, 130.41, 129.86, 128.71, 128.35, 127.41, 127.33, 126.29, 121.96, 117.07, 103.72, 60.35, 58.54, 56.85, 45.44, 43.56, 31.78, 31.70, 29.50, 27.45. MS (ESI) calculated for C₃₄H₄₃N₅, m/z 521.35, found 522.36 [M+H]⁺.

Compound **13** was synthesized similarly as compound **1a**.

13: *N*-(*tert*-butyl)-2-(10-chloroanthracen-9-yl)imidazo[1,2-*a*]pyridin-3-amine. 242 mg, 84%.

¹H NMR (500 MHz, CDCl₃) δ 8.60 (d, *J* = 8.8 Hz, 2H), 8.40 (dt, *J* = 6.9, 1.1 Hz, 1H), 7.91 (d, *J* = 8.8 Hz, 2H), 7.66 (d, *J* = 9.0 Hz, 1H), 7.60 (ddd, *J* = 8.8, 6.5, 1.1 Hz, 2H), 7.48 (ddd, *J* = 8.7, 6.5, 1.1 Hz, 2H), 7.28 – 7.23 (m, 1H), 6.90 (td, *J* = 6.8, 1.1 Hz, 1H), 2.63 (s, 1H), 0.65 (s, 9H). ¹³C NMR (126 MHz, CDCl₃) δ 142.88, 136.60, 131.47, 129.77, 129.12, 128.75, 127.13, 126.76, 126.72, 126.67, 125.36, 124.42, 123.78, 117.69, 111.71, 55.76, 29.90. MS (ESI) calculated for C₂₅H₂₂ClN₃, *m/z* 399.15, found 400.17 [M+H]⁺.

Compound **14** was synthesized similarly as compound **10**.

14: *N*'-(10-(3-(*tert*-butylamino)imidazo[1,2-*a*]pyridin-2-yl)anthracen-9-yl)octane-1,8-

diamine. 20 mg, 32%. ¹H NMR (500 MHz, MeOD) δ 9.01 (d, *J* = 6.8 Hz, 1H), 8.55 (d, *J* = 8.8 Hz, 2H), 8.15 – 8.08 (m, 1H), 7.99 (dd, *J* = 13.0, 4.8 Hz, 3H), 7.85 (dd, *J* = 8.4, 7.0 Hz, 2H), 7.80 – 7.71 (m, 2H), 7.67 (dd, *J* = 10.0, 4.0 Hz, 1H), 3.79 (dd, *J* = 16.7, 8.6 Hz, 2H), 2.94 (dd, *J* = 14.0, 6.6 Hz, 2H), 2.00 – 1.91 (m, 2H), 1.72 – 1.63 (m, 2H), 1.46 – 1.38 (m, 6H), 0.81 (s, 9H). ¹³C NMR (126 MHz, MeOD) δ 139.74, 135.47, 135.36, 132.83, 130.52, 129.36, 129.01, 128.07, 127.63, 127.26, 127.03, 125.59, 123.03, 118.21, 113.15, 56.34, 54.29, 40.75, 30.28, 30.13, 29.99, 28.55, 27.62, 27.38, 27.35. MS (ESI) calculated for C₃₃H₄₁N₅, *m/z* 507.34, found 508.35 [M+H]⁺.

Compound **15** was synthesized similarly as compound **1a**.

15: 2-(Anthracen-9-yl)-6-bromo-*N*-(*tert*-butyl)imidazo[1,2-*a*]pyridin-3-amine. 260 mg, 81%.

¹H NMR (500 MHz, CDCl₃) δ 8.54 – 8.52 (m, 2H), 8.08 – 8.04 (m, 2H), 7.83 (d, *J* = 8.6 Hz, 2H), 7.56 (dd, *J* = 9.4, 0.6 Hz, 1H), 7.49 – 7.42 (m, 4H), 7.30 (dd, *J* = 9.4, 1.9 Hz, 1H), 2.68 (s, 1H),

0.64 (s, 9H). ^{13}C NMR (126 MHz, CDCl_3) δ 141.20, 138.13, 131.52, 130.96, 128.97, 128.47, 128.04, 127.60, 127.27, 126.67, 125.99, 125.25, 123.94, 118.41, 106.67, 55.85, 29.83. MS (ESI) calculated for $\text{C}_{25}\text{H}_{22}\text{BrN}_3$, m/z 443.10, found 444.10 $[\text{M}+\text{H}]^+$.

Compound **16** was synthesized similarly as compound **10**.

16: *N*⁶-(8-aminooctyl)-2-(anthracen-9-yl)-*N*³-(*tert*-butyl)imidazo[1,2-*a*]pyridine-3,6-diamine.

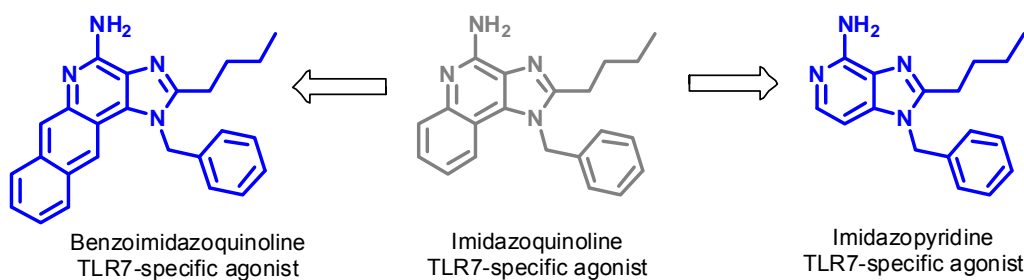
55 mg, 47%. ^1H NMR (500 MHz, MeOD) δ 8.81 (s, 1H), 8.20 (dd, $J = 6.5, 2.3$ Hz, 2H), 7.85 – 7.80 (m, 2H), 7.72 – 7.56 (m, 7H), 3.23 (t, $J = 7.0$ Hz, 2H), 2.97 – 2.90 (m, 2H), 1.80 (dt, $J = 14.5, 7.1$ Hz, 2H), 1.72 – 1.64 (m, 2H), 1.59 – 1.51 (m, 2H), 1.45 (s, 6H), 0.78 (s, 9H). ^{13}C NMR (126 MHz, MeOD) δ 141.50, 141.40, 134.23, 132.75, 132.52, 131.64, 130.29, 128.91, 128.20, 127.68, 126.85, 126.05, 121.64, 112.69, 104.55, 56.28, 45.40, 40.78, 30.46, 30.35, 30.30, 29.46, 28.65, 28.27, 27.52. MS (ESI) calculated for $\text{C}_{33}\text{H}_{41}\text{N}_5$, m/z 507.34, found 508.35 $[\text{M}+\text{H}]^+$.

Microbiological methods. MICs of the compounds were determined by broth microdilution method per CLSI (formerly NCCLS) guidelines as described earlier.⁸⁹ Mid-log phase Mueller-Hinton broth (MHB; noncation supplemented) cultures of organisms (40 μL ; optical density at 600 nm adjusted to 0.5 AU, and diluted 10-fold) were added to equal volumes of 2-fold serially diluted compounds in a 384-well microtiter plate with the help of a Biotek Precision 2000 automated microplate pipetting system. The MICs of known antibiotics were included as reference compounds for comparison of activity. The microtiter plates were sealed and incubated overnight at 37°C. The plates were read at an absorbance of 600 nm. The lowest concentration of an agent inhibiting growth of the organisms was recorded as the MIC. For MBC determinations, conventional microdilution techniques were employed wherein 0.5 μL of each of

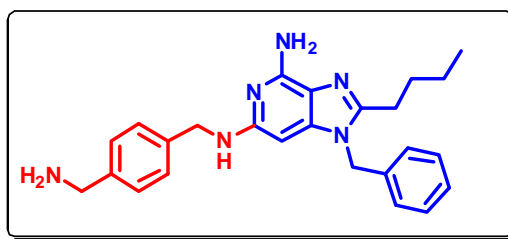
the 384 wells in the parent MIC plate was diluted into 80 μ L of fresh MHB using the Biotek Precision 2000 automated liquid handling device. The microtiter plates were incubated overnight at 37°C. The plates were read at an absorbance of 600 nm. **5e**-resistant *S. aureus* organisms were generated by exposing *S. aureus* ATCC 13709 to escalating doses of the compound. Within about 10 serial passages, organisms that withstood **5e** up to concentrations of 100 μ g/mL emerged.

Chapter 5.

TLR7-agonistic imidazo[4,5-*c*]pyridines



Potent TLR7-specific agonist ($EC_{50} = 0.26 \mu\text{M}$)
High IFN- α / Low Proinflammatory Cytokine Induction



5.1. Introduction

Occupancy of TLR7^{31b, 51a, 90} or TLR9⁹¹ in professional antigen-presenting cells (APCs), particularly plasmacytoid dendritic cells (pDCs), leads to the induction of IFN- α/β . Although the Type I IFNs are best known historically for their antiviral activities,⁹² recent studies show that they have many essential functions in the control of adaptive immunity.⁹³ First, Type I IFNs promote cross-priming through direct stimulation of DCs, leading to specific CD8⁺ lymphocytic responses to soluble antigens.⁹⁴ Second, Type I IFNs potently enhance the primary antibody responses to soluble antigens, inducing sustained and durable humoral responses with appropriate isotype switching, as well as the induction of immunological memory.⁹⁵ B lymphocytes can differentiate into two distinct types of functionally polarized effectors: B-effector-1-cells (Be-1), producing a Th1-like cytokine pattern, or Be-2, characterized by a Th2-like profile.⁹⁶ It is of particular interest that recent reports suggest that IFN- α may serve as an initial trigger for Be-1-biased differentiation pattern.⁹⁷ Third, Type I IFNs secondarily induce Type II IFN (IFN- γ) secretion, also driving Th1-biased adaptive immune responses.⁹⁸ Type I IFN-inducing TLR ligands may therefore hold promise as vaccine adjuvants.

In an effort to identify optimal immunostimulatory chemotypes, we have screened representative members of virtually the entire compendium of known TLR agonists in a series of hierarchical assays including primary TLR-reporter assays, secondary indices of immune activation such as IFN- $\alpha/\beta/\gamma$ and cytokine induction, activation of lymphocytic subsets in whole human blood, and tertiary screens characterizing transcriptomal activation patterns.³⁰ In these assays, small-molecule agonists of TLR7 were uniquely immunostimulatory; they were potent inducers of Type I IFN and, unlike TLR-4, -5, or -8 agonists,³⁰ did not evoke dominant proinflammatory cytokine responses, suggesting that they may be effective, yet safe vaccine adjuvants, a

premise that we have been actively exploring.⁵⁶ Small molecule TLR7 agonists are also being investigated as orally bioavailable, endogenous Type I IFN inducers for the management of chronic viral diseases,⁹⁹ especially hepatitis C and hepatitis B. Current therapeutic regimens for the therapy of hepatitis C and hepatitis B include parenteral IFN- α .¹⁰⁰ Clinical trials of TLR7 agonists for hematological malignancies are also currently underway.¹⁰¹

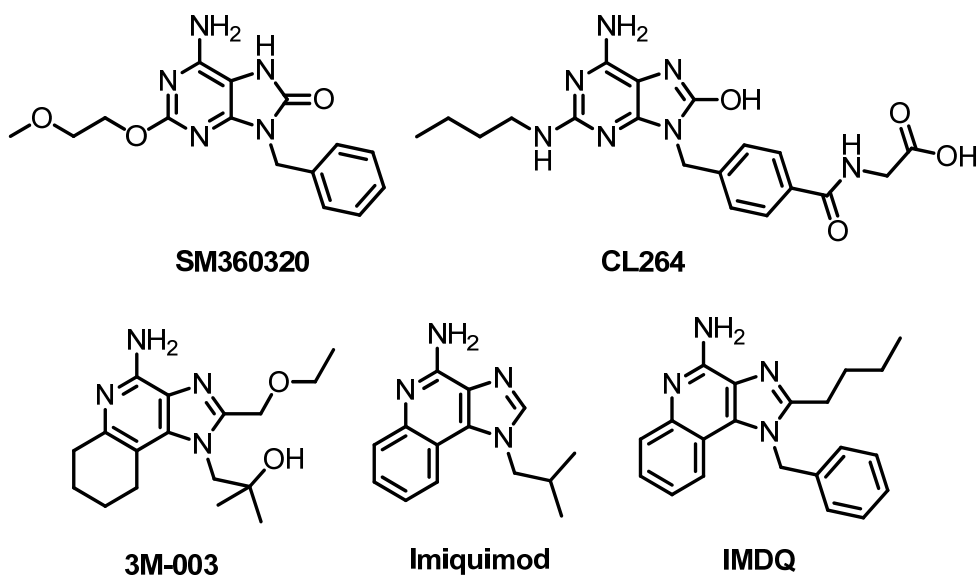
As mentioned earlier, the currently known small molecule agonists of TLR7 occupy a very small chemical space, and are represented by the 1*H*-imidazo[4,5-*c*]quinolines,³⁷ 8-hydroxy-^{76, 102} or 8-oxoadenines,¹⁰³ and guanine nucleoside analogues.^{31a, 104} We had previously reported structure-activity relationships (SAR) in the imidazoquinolines with a focus on substituents at the *N*¹, *C*², *N*³ and *N*⁴ positions,^{55b, 69} and we had observed that relatively minor structural modifications at these positions yielded compounds with widely differing immunomodulatory properties.^{55a, 56, 58, 77}

It was of interest, therefore, to extend our SAR studies to the quinoline ring system. We asked if a part-structure (imidazopyridine) or a benzologue (benzoimidazoquinoline) would alter the biological properties of the parent imidazoquinoline compound. Examination of the structures of 3M-003¹⁰⁵ and the 8-hydroxy- and 8-oxoadenines (Fig. 1) suggested that the quinoline system may be dispensable, and activity would be retained in imidazopyridines. Indeed, imidazopyridine derivatives with alkyl groups at *C*6 and *C*7 positions,¹⁰⁶ hydroxyalkyl,¹⁰⁷ oxime and hydroxylamine-bearing substituents at *C*2,¹⁰⁸ and alkylsulfonamide substituents at the *N*1 position¹⁰⁹ have been reported in the patent literature. Detailed activity profiles of these compounds, however, are not available, perhaps owing to the fact that the investigations of such compounds precede the discovery of the TLRs.

Incorporating substituents that we had previously determined to be optimal in the imidazoquinolines (*N*¹-benzyl and *C*²-butyl; IMDQ, Fig. 1), we embarked on the syntheses and biological evaluation of novel 1*H*-imidazo[4,5-*c*]pyridine analogues with modifications at the *N*4-

and C6 positions. The parent imidazopyridine compound, 1-benzyl-2-butyl-1*H*-imidazo[4,5-*c*]pyridin-4-amine, exhibited moderate TLR7-agonistic activity. *N*⁴-acyl or -alkyl substitutions abrogated activity. The majority of C6 derivatives bearing aryl groups were also inactive, but analogues with *N*⁶-benzyl substituents gained TLR7-specific activity. Particular *N*⁶ substituents were found to augment TLR7-specific agonistic potency without compromising specificity at TLR7; consistent with their pure TLR7 activity (and undetectable TLR8 agonism), these compounds potently induced IFN- α in human peripheral blood mononuclear cells (PBMCs), upregulated CD69 in lymphocytic subsets, and yet showed very weak proinflammatory cytokine-inducing activities. Strong Type I IFN inducers, especially in conjunction with attenuated proinflammatory profiles are expected to be potently adjuvantic without inducing prominent local or systemic inflammation.

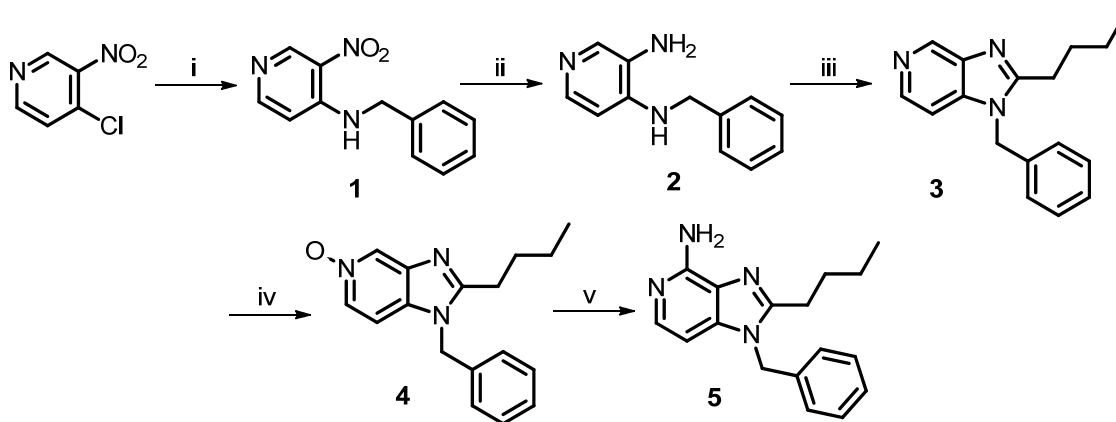
Fig. 1. Structures of small molecule agonists of TLR7 represented by the 8-oxoadenine (SM360320), 8-hydroxyadenines (CL264), 1*H*-imidazo[4,5-*c*]quinolines 3M-003, 1-isobutyl-1*H*-imidazo[4,5-*c*]quinolin-4-amine (Imiquimod) and 1-benzyl-2-butyl-1*H*-imidazo[4,5-*c*]quinolin-4-amine (IMDQ).



5.2. Results and Discussion

Our interest in exploring TLR7 agonists as vaccine adjuvants has been greatly reinforced by our observations that pure TLR7 agonists, unlike other TLR ligands, are potently immunostimulatory without prominently activating inflammatory programs in human whole blood model systems.³⁰ As mentioned earlier, the structures of 3M-003¹⁰⁵ and the 8-hydroxy- and 8-oxoadenines (Fig. 1), as well as patent literature suggested that the quinoline system may be dispensable, and activity would be retained in imidazopyridines. Our previous SAR studies on the imidazoquinolines had established that *N*¹-benzyl and *C*²-butyl substituents were optimal,⁶⁹ our point of departure in examining structure-activity relationships in the imidazopyridines consequently began with the evaluation of 1-benzyl-2-butyl-1*H*-imidazo[4,5-*c*]pyridin-4-amine (5), following the synthetic strategy described earlier (Scheme 1).^{37, 69} Compound 5, itself a novel and unprecedented structure, was found to possess TLR7-specific agonistic activity (EC₅₀: 1.57 μM, Fig. 2, Table 1), with negligible TLR8 activity. The potency of the lead TLR7-specific imidazoquinoline (1-benzyl-2-butyl-1*H*-imidazo[4,5-*c*]quinolin-4-amine, structure in Fig. 1) was 0.06 μM (Fig. 2).⁶⁹

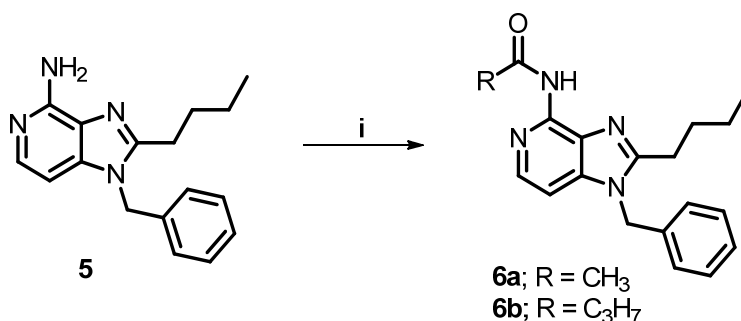
Scheme 1. Synthesis of 1-benzyl-2-butyl-1*H*-imidazo[4,5-*c*]pyridin-4-amine 5.



Reagents: i. BnNH₂, NEt₃, CH₂Cl₂; ii. Zn, HCOONH₄, MeOH; iii. (a) C₄H₉COCl, NEt₃, THF (b) NaOH, EtOH; iv. *m*CPBA, CHCl₃; v. (a) Benzoyl isocyanate, CH₂Cl₂ (b) NaOMe, MeOH.

Acylation (**6a** and **6b**, Scheme 2) of the C⁴-NH₂ resulted in complete abrogation of activity (Table 1).

Scheme 2. Synthesis of C⁴-N-acylated analogues.

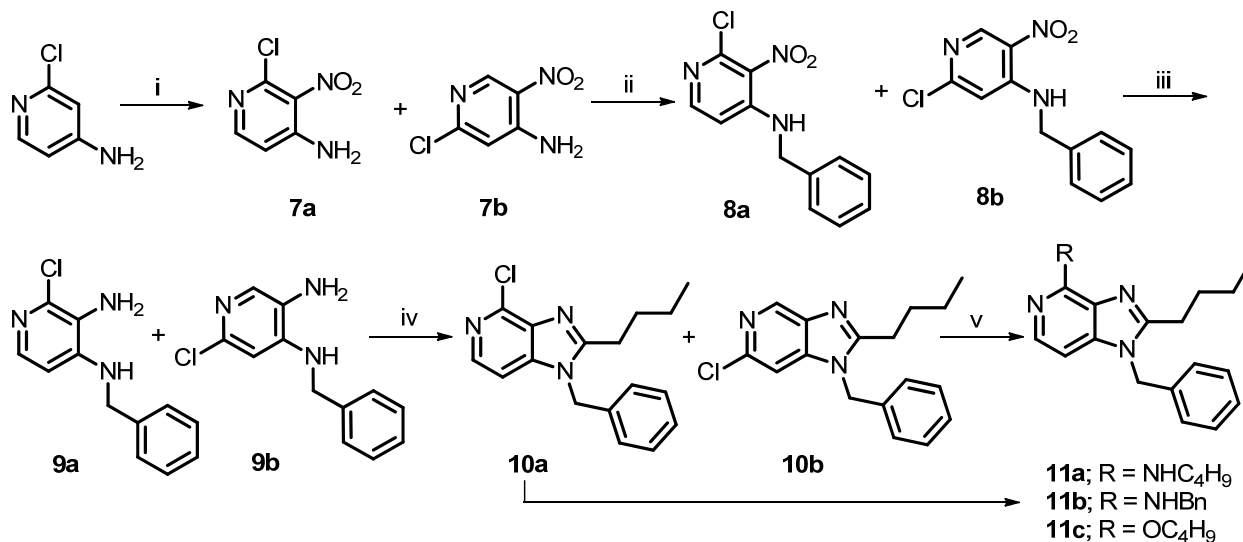


Reagents: i. RCOCl, NEt₃, CH₂Cl₂.

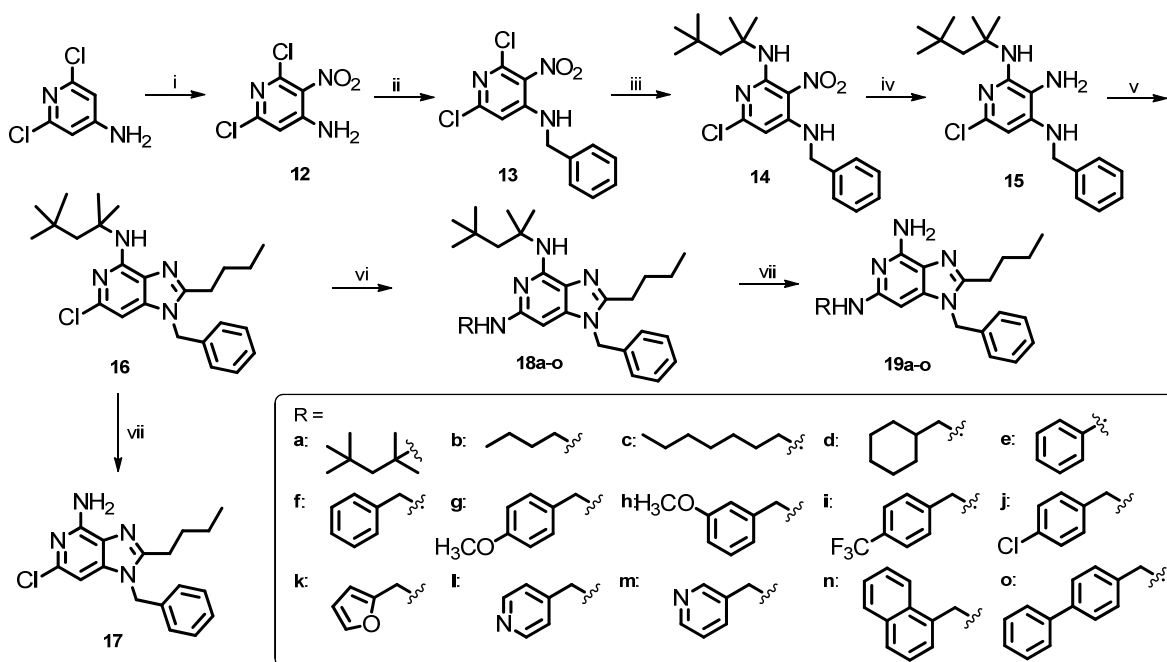
C6-modified analogues were synthesized via an alternate route. Nitration of 4-amino-2-chloropyridine resulted, as expected, in a mixture of the 3- and 5-nitro intermediates **7a** and **7b**, which were taken forward to obtain the 4- and 6-chloroimidazopyridines **10a** and **10b** (Scheme 3). Excellent chromatographic separation of these advanced intermediates was possible. Pd-catalyzed C-N cross-coupling reactions using *n*-butylamine and benzylamine from intermediate **10a** furnished the C⁴-N-alkylated analogues **11a** and **11b**, respectively (Scheme 3). A 4-butoxy analogue **11c** was also obtained by *ipso*-chloro displacement with 1-butanol. Compounds **11a-c** were, however, inactive (Table 1). We had envisaged utilizing the 6-chloroimidazopyridine intermediate **10b** for synthesizing C6-functionalized analogues. However, this intermediate exhibited unexpectedly low reactivity to displacement with nucleophiles or to Buchwald-Hartwig coupling reactions. As outlined in Scheme 4, we utilized 4-amino-2,6-dichloropyridine as the starting material and obtained **13** as a key intermediate which, upon reaction with *tert*-octylamine⁷⁸ provided exclusively the N²-alkylated intermediate **14**. The 6-chloro-N-(2,4,4-trimethylpentan-2-yl)-1*H*-imidazopyridin-4-amine intermediate **16** was obtained without difficulty,

and we were able to synthesize the N^6 -substituted analogues **19a-o** under conventional Buchwald-Hartwig conditions (Scheme 4).

Scheme 3. Synthesis of C^4 - N - and O -alkylated analogues.

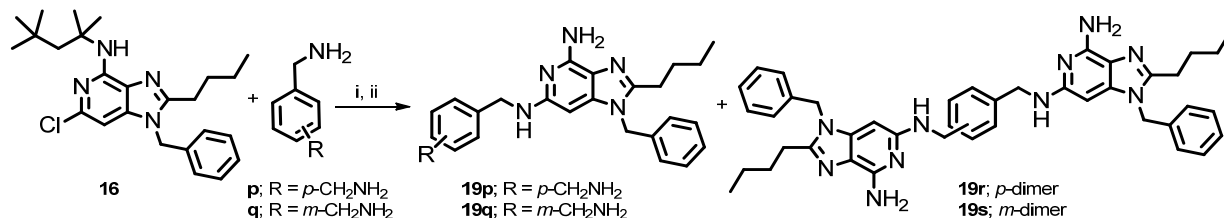


Scheme 4. Synthesis of N^6 -substituted analogues.



TLRs signal via ligand-induced dimerization, but since that the crystal structure of human TLR7 and of its ligand binding modes are as yet unknown, we utilized intermediate **16** in constructing ‘dimeric’ imidazopyridines (using *p*- and *m*-xylylenediamine, Scheme 5) to ascertain if such pre-organized dimeric ligands could yield high-potency agonists.

Scheme 5. Synthesis of dimeric compounds.



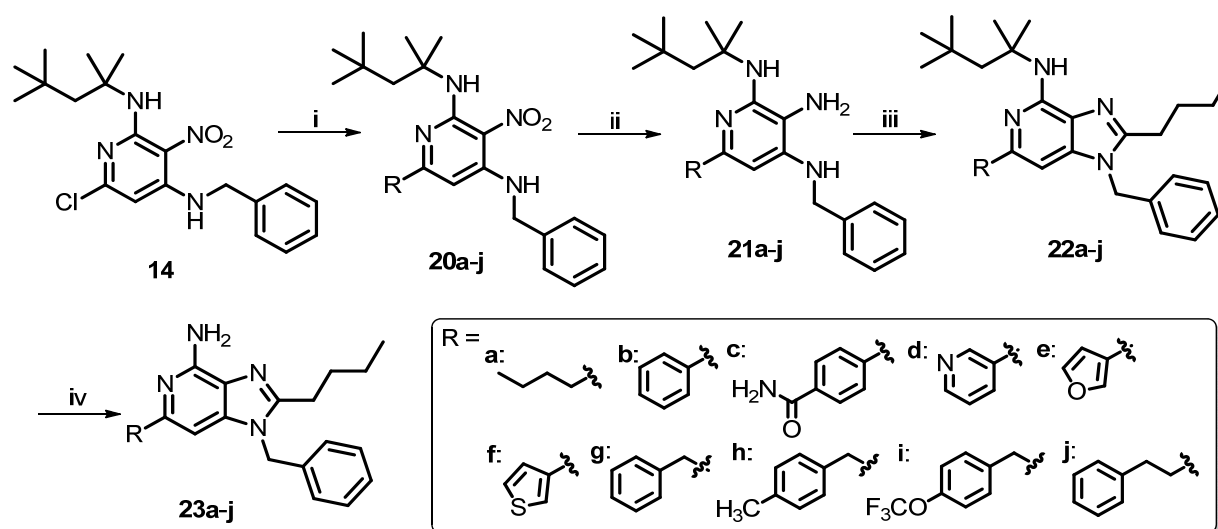
Reagents: i. Pd₂(dba)₃, DavePhos, KO^tBu, dioxane; ii. HCl.

The 6-chloroimidazopyridine **17** (Scheme 4) was inactive (Table 1). Buchwald-Hartwig-derived *N*⁶-substituted analogues **19a-q**, however, showed a distinctive SAR. Compound **19a** with a free NH₂ at C6, obtained by coupling the *tert*-octylamine and subsequent *N*-dealkylation with HCl (Scheme 4, Table 1) displayed TLR7-specific agonism with a potency comparable to that of the parent C6-unsubstituted compound **5**. Modest gains in potency were obtained in analogues with short aliphatic substituents with *N*⁶-butyl (**19b**) and *N*⁶-cyclohexylmethyl (**19d**), but potency diminished in the *N*⁶-heptyl analogue (**19c**). The *N*⁶-phenyl-substituted compound **19e** was marginally weaker than **5**; however, the potency of the *N*⁶-benzyl analogue **19f** was ~7.6 times that of **5** (Table 1, Fig. 2), triggering a detailed SAR investigation on various aryl substituents at *N*⁶. Both steric and electronic effects appear to play a role in governing TLR7-agonistic potency, since the biphenylmethyl-substituted compound **19o** was active, whereas the naphthylmethyl analogue **19n** was quiescent; to a first approximation, electron-rich *N*⁶ substituents appear to be preferred, with the methoxybenzyl derivatives (**19g** and **19h**) and the pyridinylmethyl compounds (**19l** and **19m**) being marginally more active than the trifluoromethyl- (**19i**) or chloro-

(**19j**) substituted analogues. Compounds **19p** and **19q** were also active in primary screens, with EC_{50} values of 0.26 and 0.37 μ M, respectively (Table 1).

For the C6-substituted compounds **23a-j** (Scheme 6), we observed mediocre yields in pilot Suzuki coupling reactions with the advanced intermediate **16**. We therefore exploited the electron-withdrawing resonance effect of the 3-nitro group in **14**. As expected, the classical Suzuki reaction on intermediate **14** using various aliphatic and aromatic boronic acids/boronate esters resulted in the intermediates **20a-j** (Scheme 6), which were further derivatized to obtain the desired C6 alkyl/aryl substituted imidazopyridines **23a-j**.

Scheme 6. Synthesis of C6-substituted analogues.

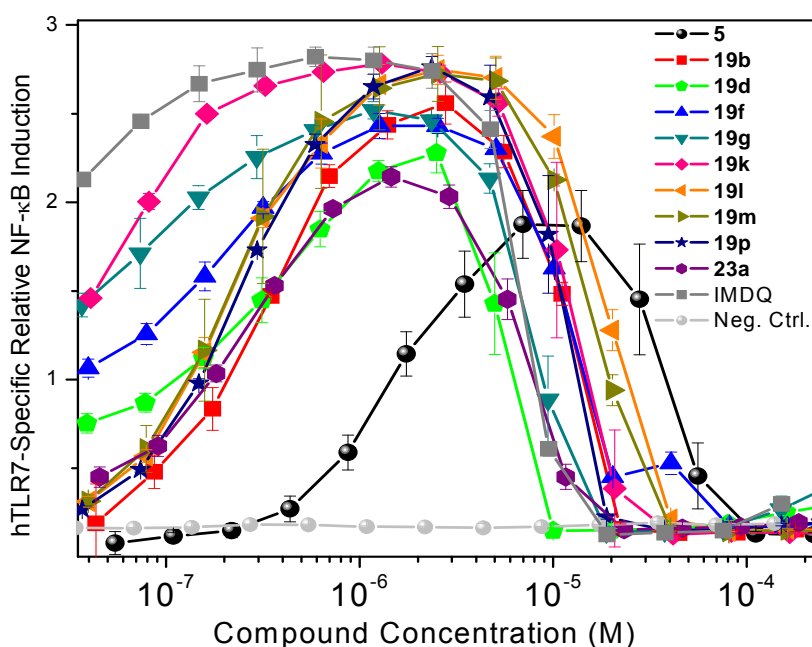


Reagents: i. For **20a-f** and **20j**, R-Boronic acid, Pd(dppf)Cl₂, Cs₂CO₃, dioxane; For **20c**, 4-Cyanophenyl boronic acid, Pd(dppf)Cl₂, Cs₂CO₃, dioxane; For **20g-i**, R-Boronic acid pinacol ester, Pd(dppf)Cl₂, Cs₂CO₃, dioxane; ii. Zn, HCOONH₄, MeOH; iii. (a) C₄H₉COCl, NEt₃, THF (b) NaOH, EtOH; iv. HCl.

In the C⁶-alkyl or -aryl analogues (Scheme 6), the SAR appeared more stringent. Whereas the C⁶-butyl compound **23a** was more active than **5**, direct aryl-aryl connections at C6 (**23b-f**) abrogated activity, but TLR7 agonistic properties were restored in the 6-benzyl (**23g**) and 6-

phenethyl analogues (**23j**). Taken together with activity data of compounds of the **19** series, we surmised that rotational constraints about the C⁶-aryl groups may hinder TLR7 occupancy. Unlike TLR2, TLR3, TLR4,¹¹⁰ and TLR5¹¹¹ for which crystal structures are available as complexes with their cognate ligands, a detailed structural characterization of the mode of binding of TLR7 ligands is not yet available to guide structure-based design of small molecule agonists of TLR7, necessitating classical SAR approaches to refine successive iterations of ligand design.

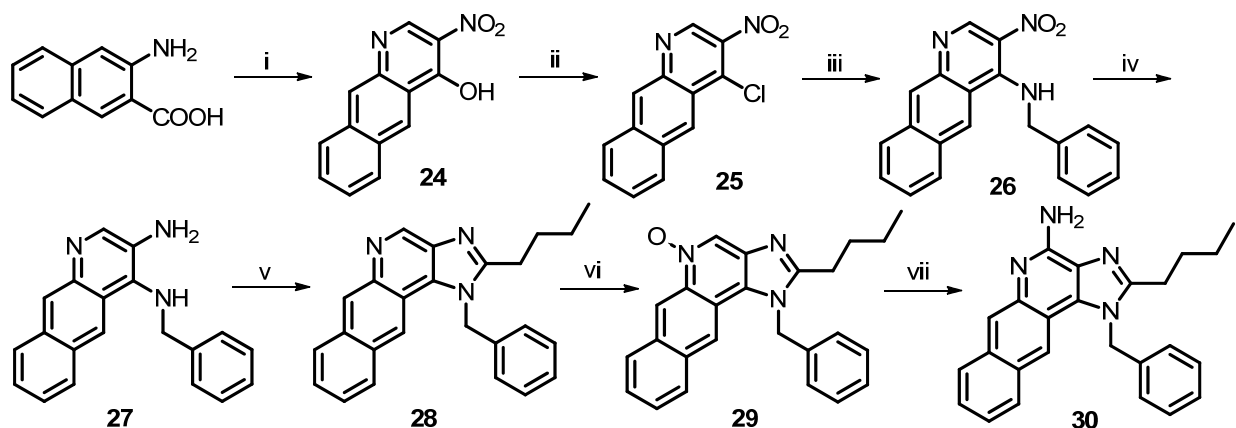
Fig. 2. TLR7 agonistic activities of imidazopyridine compounds. Data points represent means and standard deviations on quadruplicates.



The benzologue **30** was also synthesized as shown in Scheme 7. It showed substantial improvements in potency over the parent imidazopyridine **5** (Fig. 3, Table 1), but the two most potent compounds in the entire series as adjudged by primary screens were the *N*⁶-(4-

methoxybenzyl) and *N*⁶-(furan-2-ylmethyl) analogues (**19g** and **19k**, respectively), both of which were approximately twenty-fold more potent than **5** (Fig. 2, Table 1).

Scheme 7. Synthesis of benzologue 30.



Reagents: i. (a) HCl, HON=CHCH₂NO₂, H₂O (b) (CH₃CO)₂O, CH₃COOK; ii. POCl₃; iii. BnNH₂, NEt₃, CH₂Cl₂; iv. Zn, HCOONH₄, MeOH; v. (a) C₄H₉COCl, NEt₃, THF (b) NaOH, EtOH; vi. *m*CPBA, CH₂Cl₂, CHCl₃, MeOH; vii. (a) Benzoyl isocyanate, CH₂Cl₂ (b) NaOMe, MeOH.

Fig. 3. Dose-response profiles of TLR7 agonistic activity of compounds 5 and 30. Data points represent means and standard deviations on quadruplicates.

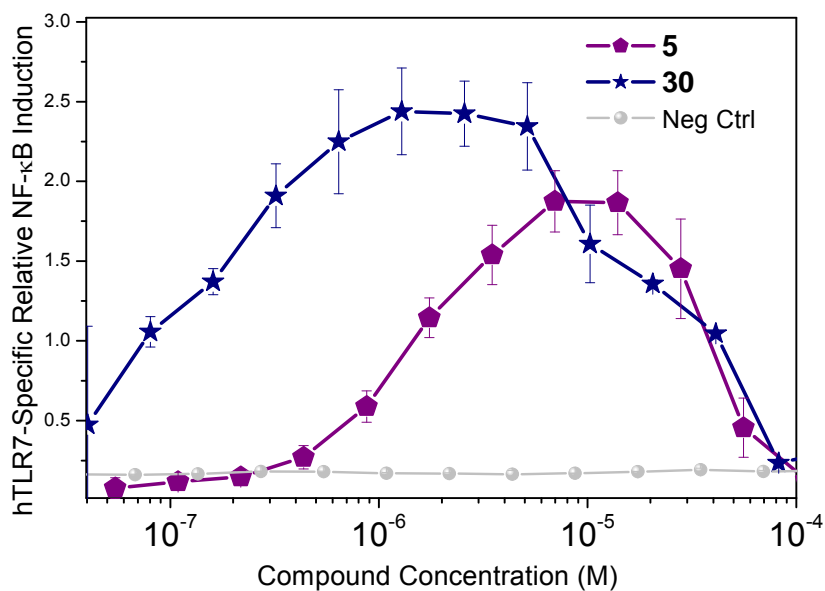
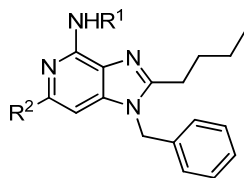


Table 1. EC₅₀ values of compounds in human TLR7/8-specific reporter gene assay.

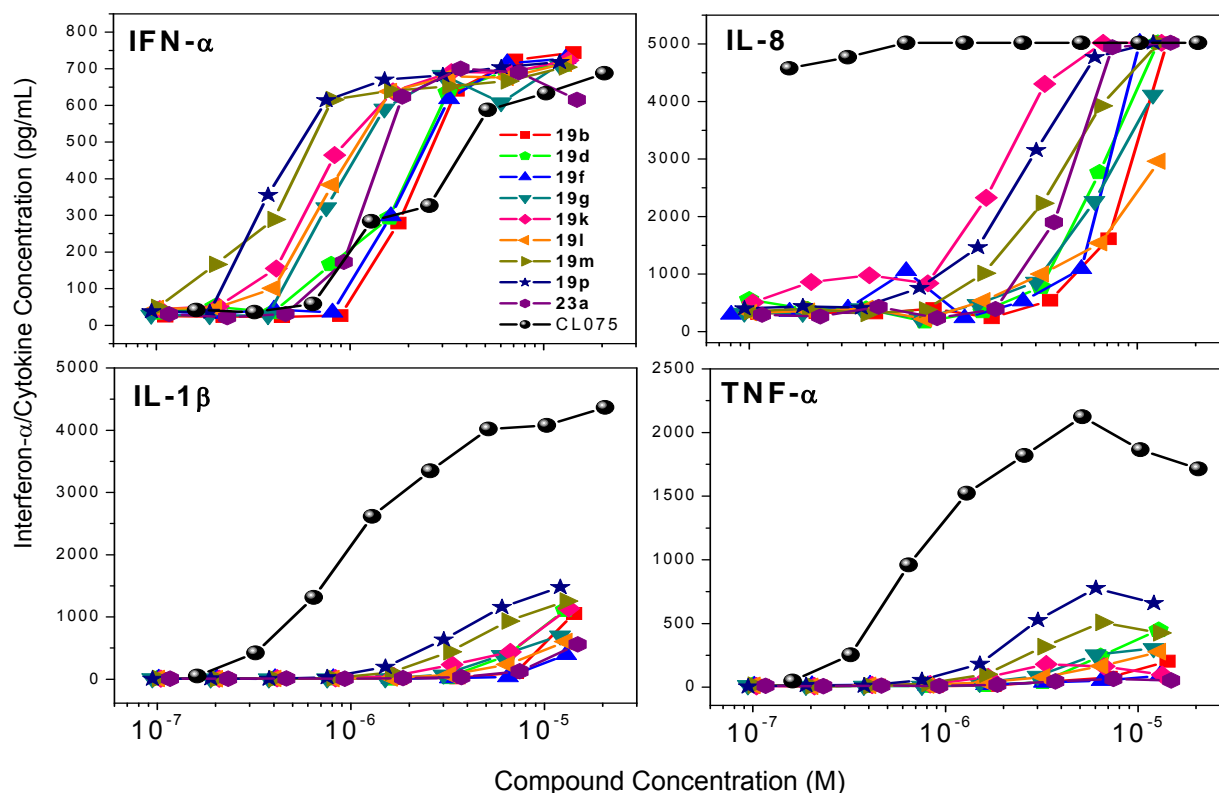


No.	R ¹	R ²	hTLR7-agonistic Activity (μM)	No.	R ¹	R ²	hTLR7-agonistic Activity (μM)
5	H	H	1.57	19n	H		Inactive
6a	COCH ₃	H	Inactive ^a	19o	H		1.09
6b	COC ₃ H ₇	H	Inactive	19p	H		0.26
11a	C ₄ H ₉	H	Inactive	19q	H		0.37
11b	CH ₂ C ₆ H ₅	H	Inactive	19r	H		1.08
17	H	Cl	Inactive	19s	H		Inactive
19a	H	NH ₂	1.25	23a	H	C ₄ H ₉	0.28
19b	H	NHC ₄ H ₉	0.34	23b	H	C ₆ H ₅	Inactive
19c	H	NHC ₇ H ₁₅	0.76	23c	H		Inactive
19d	H		0.32	23d	H		Inactive
19e	H	NHC ₆ H ₅	1.72	23e	H		Inactive
19f	H	NHCH ₂ C ₆ H ₅	0.21	23f	H		Inactive
19g	H		0.075	23g	H		0.28
19h	H		0.61	23h	H		1.80
19i	H		1.04	23i	H		Inactive
19j	H		0.64	23j	H		0.57
19k	H		0.075	30		Benzologue (Scheme 7)	0.22
19l	H		0.25				
19m	H		0.25				

^aInactive: no activity was detected up to a concentration of 500 μg/mL.

We chose the nine most active compounds (**19b**, **19d**, **19f-g**, **19k-m**, **19p**, and **23a**) for evaluation in secondary screens using IFN- α and cytokine release in human PBMCs. We used, as reference compounds, imiquimod, a known TLR7 agonist,¹¹² as well as CL075,^{45, 62} a predominantly TLR8-active agonist with an EC₅₀ of 1.32 μ M in hTLR8 assays.¹¹³

Fig. 4. Dose-response profiles of Type I interferon (IFN- α) and proinflammatory cytokine (IL-8, IL-1 β , and TNF- α) induction by selected imidazopyridine (and reference) compounds. Representative data from three independent experiments are presented.



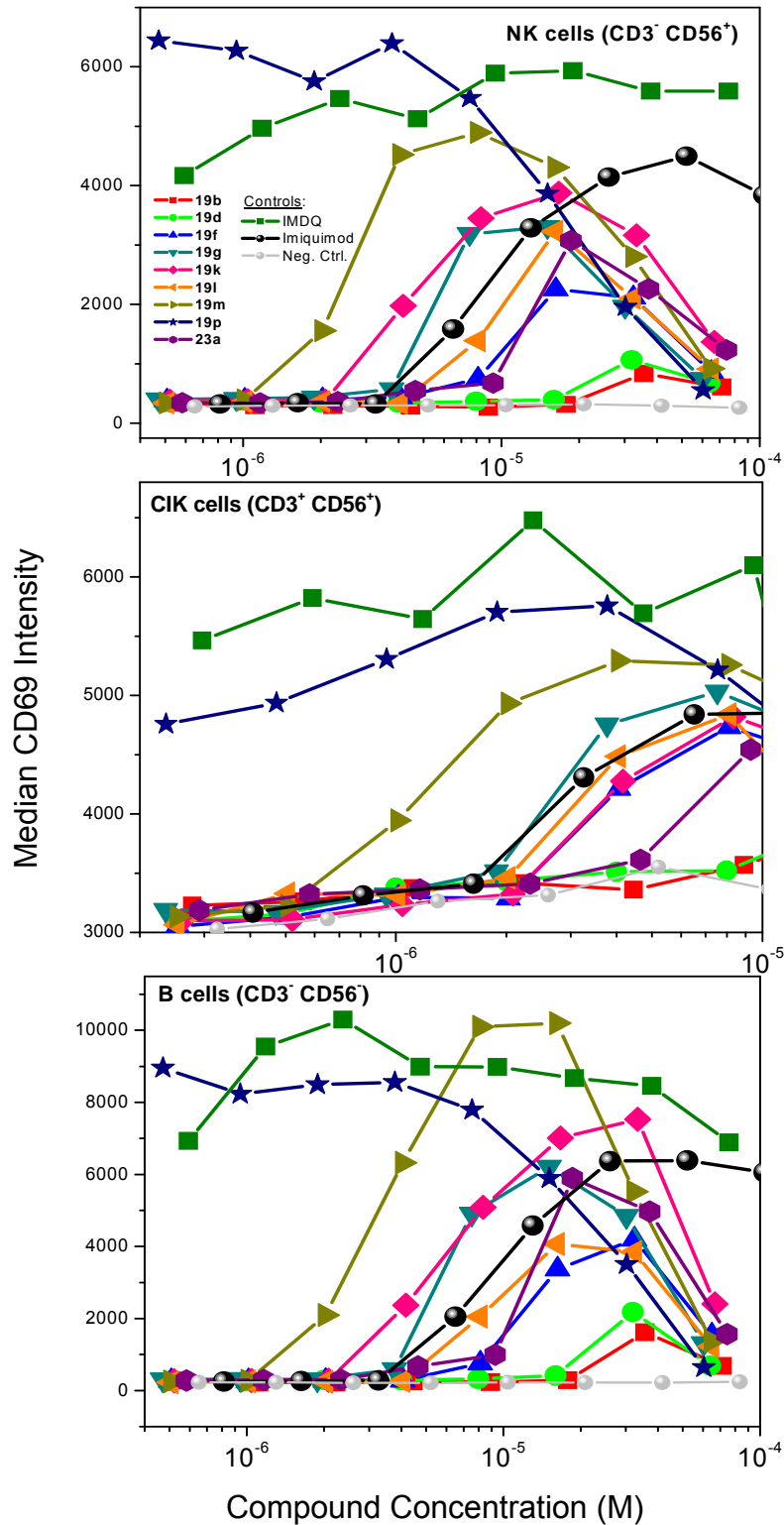
Given that the imidazopyridine compounds are pure TLR7 agonists, we expected to find prominent IFN- α induction,³⁰ and this was indeed the case, with **19p**, **19m**, and **19k** being the most potent (EC₅₀: 0.3 μ M, 0.4 μ M and 0.7 μ M, respectively; Fig. 4). CL075 was among the

least potent in IFN- α induction (EC_{50} : 2.6 μ M; Fig. 4), and as expected for a TLR8 agonist, CL075 was dramatically more active in inducing proinflammatory cytokines such as TNF- α , IL-1 β , and IL-8 (Fig. 4). We do not yet understand the basis for the slight discrepancy between rank-order potency in primary screens (**19k** \approx **19g**>**19f**>**19p**; Fig. 2, Table 1) vis-à-vis IFN- α -inducing potency in human PBMCs (**19p** \approx **19m**>**19k**; Fig. 4), and we surmise that analogues with more basic C6 substituents may allow for higher endolysosomal partitioning. The dose-response profiles show characteristic biphasic responses (dose-dependent activation, followed by apparent suppression) as we had previously observed in several chemotypes. We verified that the apparent suppression was not due to cytotoxicity using LDH release and mitochondrial redox-based assays.

We had previously shown that of all the various classes of innate immune stimuli, TLR7 agonists were extraordinarily immunostimulatory, stimulating virtually all subsets of lymphocytes (assessed by quantifying CD69 expression), and yet without inducing dominant proinflammatory cytokine responses,³⁰ and we wished to confirm the rank-order potency observed in IFN- α induction assays described above.

We observed considerable dissociation between Type I IFN induction on the one hand (Fig. 4), and CD69 upregulation in lymphocytic subsets on the other (Fig. 5). Whereas the subset of active compounds induced IFN- α with similar potencies (EC_{50} values between 0.3-2 μ M; Fig. 4), pronounced differences were observed in CD69 expression in natural killer, cytokine-induced killer and B lymphocytic subsets with **19p** being as active as the reference TLR7 agonist IMDQ, and **19d** showing virtually no activity (Fig. 5). Possible mechanisms underlying the differential activity in these two compounds are being investigated.

Fig. 5. CD69 upregulation in human natural killer (NK), cytokine-induced killer (CIK) and nominal B lymphocytes by select imidazopyridine (and reference) compounds.



5.3. Conclusions

These findings raise the possibility of utilizing these compounds in selectively targeting Type I IFN induction versus lymphocytic activation, and are being explored in greater detail. The potential advantages of strong Type I IFN inducers as candidate vaccine adjuvants have been discussed earlier. Such compounds, especially in conjunction with attenuated proinflammatory cytokines, are expected to be potently adjuvantic without inducing prominent local or systemic inflammation. As mentioned earlier, the prominent Type I IFN-inducing abilities of the imidazopyridines may also find utility as an alternative therapeutic strategy to address disease states wherein systemic IFN- α is of proven benefit. A clear delineation of structural features that confer TLR specificity not only charts a rational course for the development of effective, yet safe vaccine adjuvants, but also provides tools to understand innate immune function in greater detail.

5.4. Experimental

Chemistry. All of the solvents and reagents used were obtained commercially and used as such unless noted otherwise. Moisture- or air-sensitive reactions were conducted under nitrogen atmosphere in oven-dried (120 °C) glass apparatus. The solvents were removed under reduced pressure using standard rotary evaporators. Flash column chromatography was carried out using RediSep Rf 'Gold' high performance silica columns on CombiFlash Rf instrument unless otherwise mentioned, while thin-layer chromatography was carried out on silica gel (200 μ m) CCM pre-coated aluminum sheets. Purity for all final compounds was confirmed to be greater than 97% by LC-MS using a Zorbax Eclipse Plus 4.6 mm \times 150 mm, 5 μ m analytical reverse

phase C18 column with H₂O-isopropanol or H₂O–CH₃CN gradients and an Agilent 6520 ESI-QTOF Accurate Mass spectrometer (mass accuracy of 5 ppm) operating in the positive ion (or negative ion, as appropriate) acquisition mode.

Synthesis of compound 1: *N*-Benzyl-3-nitropyridin-4-amine. To a solution of 4-chloro-3-nitropyridine (1.0 g, 6.31 mmol) in 25 mL of CH₂Cl₂ were added triethylamine (1.32 mL, 9.47 mmol) and benzyl amine (0.83 mL, 7.57 mmol). The reaction mixture was refluxed for 18 h. The solvent was then evaporated under vacuum and H₂O was added to the residue. The solution was extracted with CH₂Cl₂ (3 × 20 mL), washed with water and dried over sodium sulfate. The solvent was evaporated and the residue was purified using silica gel column chromatography (0-5% MeOH in CH₂Cl₂) to obtain compound **1** as a yellow solid (1.4 g, 94%). ¹H NMR (500 MHz, CDCl₃) δ 9.22 (s, 1H), 8.53 (s, 1H), 8.25 (dd, *J* = 6.1, 0.6 Hz, 1H), 7.41 – 7.35 (m, 2H), 7.32 (dd, *J* = 7.2, 5.3 Hz, 3H), 6.69 (d, *J* = 6.2 Hz, 1H), 4.56 (d, *J* = 5.7 Hz, 2H). ¹³C NMR (126 MHz, CDCl₃) δ 153.38, 149.06, 148.68, 135.96, 130.04, 129.21, 128.22, 127.10, 108.25, 46.85. MS (ESI) calculated for C₁₂H₁₂N₃O₂, *m/z* 230.0924, found 230.0949 [M+H]⁺.

Synthesis of compound 2: *N*^t-Benzylpyridine-3,4-diamine. To a solution of compound **1** (1.0 g, 4.36 mmol) in 40 mL of MeOH were added zinc dust (1.4 g, 21.8 mmol) and ammonium formate (1.4 g, 21.8 mmol). The reaction mixture was stirred at room temperature for 10 min and filtered through celite. Then the solvent was evaporated and the residue was dissolved in water. This was extracted with EtOAc (3 × 20 mL), washed with water and dried over sodium sulfate. The solvent was evaporated under vacuum to obtain the compound **2** (0.8 g, 92%). ¹H NMR (500 MHz, CDCl₃) δ 7.81 (d, *J* = 5.4 Hz, 1H), 7.77 (s, 1H), 7.29 – 7.19 (m, 5H), 6.36 (d, *J* = 5.4 Hz, 1H), 4.87 (s, 1H), 4.28 (d, *J* = 5.4 Hz, 2H), 3.28 (s, 2H). ¹³C NMR (126 MHz, CDCl₃) δ

144.52, 143.51, 138.22, 137.53, 128.96, 128.79, 127.55, 127.48, 105.29, 47.22. MS (ESI) calculated for C₁₂H₁₄N₃, m/z 200.1182, found 200.1242 [M+H]⁺.

Synthesis of compound 3: 1-Benzyl-2-butyl-1*H*-imidazo[4,5-*c*]pyridine. To a solution of compound **2** (400 mg, 2.00 mmol) in 20 mL of anhydrous THF were added triethylamine (0.29 mL, 2.10 mmol) and valeryl chloride (0.27 mL, 2.20 mmol). The reaction mixture was refluxed for 2 h. The solvent was then removed under vacuum, and the residue was dissolved in EtOAc and washed with water. The EtOAc fraction was dried using sodium sulfate and evaporated under vacuum to obtain the intermediate amide compound. This was dissolved in 20 mL of EtOH and NaOH (160 mg, 4.00 mmol) in 2 mL of H₂O was added. The reaction mixture was refluxed for 4 h. The solvent was then removed under vacuum, and the residue was dissolved in EtOAc and washed with water. The organic layer was dried using sodium sulfate and evaporated and purified using column chromatography (0-5% MeOH in CH₂Cl₂) to obtain the compound **3** (210 mg, 40%). ¹H NMR (500 MHz, CDCl₃) δ 9.04 (d, *J* = 0.6 Hz, 1H), 8.34 (d, *J* = 5.6 Hz, 1H), 7.34 – 7.28 (m, 3H), 7.14 (dd, *J* = 5.6, 1.0 Hz, 1H), 7.01 (dd, *J* = 7.7, 1.8 Hz, 2H), 5.33 (s, 2H), 2.86 – 2.81 (m, 2H), 1.82 (dt, *J* = 15.5, 7.7 Hz, 2H), 1.46 – 1.36 (m, 2H), 0.91 (t, *J* = 7.4 Hz, 3H). ¹³C NMR (126 MHz, CDCl₃) δ 157.30, 142.14, 142.00, 140.48, 140.01, 135.26, 129.28, 128.37, 126.27, 105.12, 47.25, 29.44, 27.38, 22.61, 13.85. MS (ESI) calculated for C₁₇H₂₀N₃, m/z 266.1652, found 266.1715 [M+H]⁺.

Synthesis of compound 4: 1-Benzyl-2-butyl-1*H*-imidazo[4,5-*c*]pyridine 5-oxide. To a solution of compound **3** (210 mg, 0.79 mmol) in 15 mL of was added *m*-chloroperoxybenzoic acid (443 mg, 1.98 mmol), and the solution was refluxed at 45-50 °C for 1 h. The solvent was then removed and the residue was purified using column chromatography (0-10% MeOH in CH₂Cl₂) to obtain the *N*-oxide derivative (188 mg, 85%). ¹H NMR (500 MHz, CDCl₃) δ 8.71 (d, *J*

= 1.3 Hz, 1H), 8.05 (dd, $J = 7.0, 1.6$ Hz, 1H), 7.36 – 7.30 (m, 3H), 7.01 (dd, $J = 10.4, 4.3$ Hz, 3H), 5.31 (s, 2H), 2.85 – 2.80 (m, 2H), 1.79 (dt, $J = 15.4, 7.6$ Hz, 2H), 1.44 – 1.34 (m, 2H), 0.90 (t, $J = 7.4$ Hz, 3H). ^{13}C NMR (126 MHz, CDCl_3) δ 160.72, 140.89, 134.42, 134.32, 133.94, 131.52, 129.48, 128.75, 126.24, 106.63, 47.75, 29.25, 27.49, 22.52, 13.78. MS (ESI) calculated for $\text{C}_{17}\text{H}_{20}\text{N}_3\text{O}$, m/z 282.1601, found 282.1612 $[\text{M}+\text{H}]^+$.

Synthesis of compound 5: 1-Benzyl-2-butyl-1*H*-imidazo[4,5-*c*]pyridin-4-amine. To a solution of compound **4** (188 mg, 0.67 mmol) in 15 mL of CH_2Cl_2 was added benzoyl isocyanate (197 mg, 1.34 mmol) and heated at 45 °C for 2 h. The solvent was then removed under vacuum, and the residue was dissolved in 15 mL of anhydrous MeOH, followed by the addition of excess sodium methoxide. The reaction mixture was then heated at 80 °C for 1 h. The solvent was removed under vacuum and the residue was purified using column chromatography (0-7% MeOH in CH_2Cl_2) to obtain the compound **5** (56 mg, 30%). ^1H NMR (500 MHz, CDCl_3) δ 7.78 (d, $J = 5.8$ Hz, 1H), 7.34 – 7.28 (m, 3H), 7.03 (d, $J = 6.4$ Hz, 2H), 6.59 (d, $J = 5.8$ Hz, 1H), 5.27 (s, 2H), 5.15 (s, 2H), 2.83 – 2.75 (m, 2H), 1.72 (ddd, $J = 13.0, 9.0, 7.7$ Hz, 2H), 1.44 – 1.34 (m, 2H), 0.90 (t, $J = 7.4$ Hz, 3H). ^{13}C NMR (126 MHz, CDCl_3) δ 154.06, 151.00, 140.61, 140.41, 135.76, 129.21, 128.23, 126.33, 97.74, 47.52, 30.10, 27.42, 22.68, 13.89. HRMS (ESI) calculated for $\text{C}_{17}\text{H}_{21}\text{N}_4$, m/z 281.1761, found 281.1795 $[\text{M}+\text{H}]^+$.

Synthesis of compound 6a: *N*-(1-Benzyl-2-butyl-1*H*-imidazo[4,5-*c*]pyridin-4-yl)acetamide.

To a solution of compound **5** (30 mg, 0.11 mmol) in 2 mL of CH_2Cl_2 were added triethylamine (17 μL , 0.12 mmol) and acetyl chloride (8 μL , 0.11 mmol). The reaction mixture was stirred at room temperature for 3 h and purified using column chromatography (5% MeOH/ CH_2Cl_2) to obtain the compound **6a** as white solid (6 mg, 16%). ^1H NMR (500 MHz, CDCl_3) δ 11.60 (s, 1H), 8.20 (s, 1H), 7.37 (dd, $J = 7.7, 5.5$ Hz, 3H), 7.20 (d, $J = 5.6$ Hz, 1H), 7.05 (dd, $J = 6.3, 2.5$ Hz,

2H), 5.46 (s, 2H), 3.03 – 2.94 (m, 2H), 2.55 (s, 3H), 1.85 (dt, $J = 15.0, 7.6$ Hz, 2H), 1.43 (dq, $J = 14.6, 7.3$ Hz, 2H), 0.92 (t, $J = 7.3$ Hz, 3H). ^{13}C NMR (126 MHz, CDCl_3) δ 141.48, 129.64, 129.40, 129.17, 126.30, 126.25, 48.47, 29.06, 24.87, 22.44, 13.60. HRMS (ESI) calculated for $\text{C}_{19}\text{H}_{23}\text{N}_4\text{O}$, m/z 323.1866, found 323.1911 $[\text{M}+\text{H}]^+$.

Compound **6b** was synthesized similarly as compound **6a**.

6b: *N*-(1-Benzyl-2-butyl-1*H*-imidazo[4,5-*c*]pyridin-4-yl)butyramide. Butyryl chloride was used as a reagent. 4 mg, 14 %. ^1H NMR (500 MHz, CDCl_3) δ 11.31 (s, 1H), 8.30 (d, $J = 4.8$ Hz, 1H), 7.38 – 7.34 (m, 3H), 7.27 (s, 1H), 7.04 (dd, $J = 6.4, 2.6$ Hz, 2H), 5.50 (s, 2H), 2.94 (t, $J = 7.5$ Hz, 2H), 2.78 (t, $J = 7.4$ Hz, 2H), 1.80 (dp, $J = 22.1, 7.5$ Hz, 4H), 1.41 (dt, $J = 14.7, 7.4$ Hz, 2H), 1.01 (t, $J = 7.4$ Hz, 3H), 0.91 (t, $J = 7.4$ Hz, 3H). ^{13}C NMR (126 MHz, CDCl_3) δ 174.32, 141.35, 133.50, 129.69, 129.16, 126.46, 103.38, 48.58, 39.27, 29.16, 27.45, 22.55, 18.38, 13.75. HRMS (ESI) calculated for $\text{C}_{21}\text{H}_{27}\text{N}_4\text{O}$, m/z 351.2179, found 351.2240 $[\text{M}+\text{H}]^+$.

Synthesis of compound 10a: 1-Benzyl-2-butyl-4-chloro-1*H*-imidazo[4,5-*c*]pyridine. 4-Amino-2-chloropyridine (2.0 g, 15.6 mmol) was taken in 20 mL of conc. H_2SO_4 in an ice-bath to which was added 10 mL of conc. HNO_3 slowly. The reaction mixture was gradually brought to room temperature and stirred for 1 h. The reaction was quenched by pouring the reaction mixture on ice. Ammonium hydroxide solution was slowly added until a pH of 3 was reached. A white solid was obtained which was filtered, washed with water, and dried. This (*N*-nitro)aminopyridine intermediate was taken up in 10 mL of conc. H_2SO_4 and the reaction solution was heated at 90 °C for 30 min. It was cooled to room temperature and poured into ice. It was slowly neutralized with ammonium hydroxide solution until a pH of 7 and the formed yellow solid was filtered, washed with water and dried to obtain compound **7** as a mixture of 2-

chloro-3-nitropyridin-4-amine and 2-chloro-5-nitropyridin-4-amine intermediates. Sodium hydride (275 mg, 6.90 mmol) was carefully added to 20 mL of THF under N₂ and compound **7** (1.0 g, 5.76 mmol) was slowly added to the solution at 0 °C. The reaction mixture was stirred for 1 h, followed by the addition of benzyl bromide (0.75 mL, 6.34 mmol). The reaction mixture was stirred at room temperature for 2 h and poured into ice water. Then it was extracted with EtOAc (3 × 20 mL), washed with water, dried over sodium sulfate. The solvent was removed and the crude residue was purified using column chromatography (0-20% EtOAc in hexane) to obtain the compound **8** as a mixture of regioisomeric *N*-benzyl-2-chloro-3-nitropyridin-4-amine and *N*-benzyl-2-chloro-5-nitropyridin-4-amine intermediates. To this regioisomeric mixture (1.0 g, 4.2 mmol) in 20 mL of MeOH were added zinc dust (1.4 g, 21.0 mmol) and ammonium formate (1.4 g, 21.0 mmol). The reaction mixture was stirred at room temperature for 10 min and filtered through celite. Then the solvent was evaporated and the residue was dissolved in water. This was extracted with EtOAc (3 × 20 mL), washed with water and dried over sodium sulfate. The filtrate evaporated under vacuum, and chromatographed (0-20% EtOAc in hexane) to obtain the required *N*⁴-benzyl-2-chloropyridine-3,4-diamine compound **9a**. Also obtained was *N*⁴-benzyl-6-chloropyridine-3,4-diamine as a side-product. To a solution of compound **9a** (495 mg, 2.12 mmol) in 20 mL of anhydrous THF were added triethylamine (0.31 mL, 2.23 mmol) and valeryl chloride (0.28 mL, 2.33 mmol). The reaction mixture was refluxed for 1 h. The solvent was then removed under vacuum, and the residue was dissolved in 20 mL of EtOH and NaOH (170 mg, 4.24 mmol) in 2 mL of H₂O was added. The reaction mixture was refluxed for 2 h. The solvent was then removed under vacuum, and the residue was dissolved in EtOAc and washed with water. The EtOAc fraction was dried using sodium sulfate and evaporated and purified using column chromatography (0-5% MeOH in CH₂Cl₂) to obtain the compound **10a** (203 mg, 32%). ¹H NMR (500 MHz, CDCl₃) δ 8.10 (d, *J* = 5.6 Hz, 1H), 7.35 – 7.30 (m, 3H), 7.08 (d, *J* = 5.6 Hz, 1H), 7.01 (dd, *J* = 7.4, 2.0 Hz, 2H), 5.34 (s, 2H), 2.91 – 2.86 (m, 2H), 1.78 (dt, *J* = 15.7, 7.7 Hz, 2H), 1.45 – 1.36 (m, 2H), 0.90 (t, *J* = 7.4 Hz, 3H). ¹³C NMR (126 MHz, CDCl₃) δ 158.03, 141.88,

141.75, 141.12, 137.03, 134.84, 129.39, 128.58, 126.25, 105.18, 47.90, 30.04, 27.63, 22.73, 13.82. MS (ESI) calculated for C₁₇H₁₉ClN₃, m/z 300.1262, found 300.1159 [M+H]⁺.

Synthesis of compound 11a: 1-Benzyl-N,2-dibutyl-1H-imidazo[4,5-c]pyridin-4-amine. To a solution of compound **10** (50 mg, 0.17 mmol) in 1 mL of dioxane were added potassium *tert*-butoxide (57 mg, 0.51 mmol), catalytic amount of 2-dicyclohexylphosphino-2'-(*N,N*-dimethylamino)biphenyl (DavePhos) and *tris*(dibenzylideneacetone)dipalladium(0) (Pd₂(dba)₃) and butylamine (83 μL, 0.83 mmol). The reaction mixture was then heated under microwave conditions (500 W, 100 °C) in a sealed vial for 1 h. It was cooled to room temperature and filtered through celite and washed with MeOH. The solvent was removed and the crude residue was purified using column chromatography (0-5% MeOH in CH₂Cl₂) to obtain the compound **11a** (21 mg, 36%). ¹H NMR (500 MHz, CDCl₃) δ 7.84 (d, *J* = 5.9 Hz, 1H), 7.33 – 7.27 (m, 3H), 7.03 (dd, *J* = 4.5, 3.6 Hz, 2H), 6.48 (d, *J* = 5.9 Hz, 1H), 5.41 (s, 1H), 5.25 (s, 2H), 3.60 (dt, *J* = 12.9, 6.5 Hz, 2H), 2.80 – 2.74 (m, 2H), 1.73 – 1.67 (m, 4H), 1.49 (dt, *J* = 15.0, 7.4 Hz, 3H), 1.38 (dd, *J* = 15.0, 7.5 Hz, 2H), 0.96 (t, *J* = 7.4 Hz, 3H), 0.89 (t, *J* = 7.4 Hz, 3H). ¹³C NMR (126 MHz, CDCl₃) δ 153.15, 151.39, 135.95, 129.24, 129.15, 128.15, 127.25, 126.34, 126.18, 96.16, 47.43, 41.09, 32.22, 30.27, 27.41, 22.69, 20.47, 14.11, 13.89. HRMS (ESI) calculated for C₂₁H₂₉N₄, m/z 337.2387, found 337.2451 [M+H]⁺.

Compound **11b** was synthesized similarly as compound **11a**.

11b: N,1-Dibenzyl-2-butyl-1H-imidazo[4,5-c]pyridin-4-amine. Benzyl amine was used as a reagent. 33 mg, 52%. ¹H NMR (500 MHz, CDCl₃) δ 7.86 (d, *J* = 5.9 Hz, 1H), 7.45 (dd, *J* = 7.9, 0.9 Hz, 2H), 7.35 – 7.27 (m, 6H), 7.03 (d, *J* = 6.4 Hz, 2H), 6.54 (d, *J* = 5.9 Hz, 1H), 5.76 (s, 1H), 5.26 (s, 2H), 4.83 (d, *J* = 5.6 Hz, 2H), 2.79 – 2.74 (m, 2H), 1.72 – 1.67 (m, 2H), 1.37 (dq, *J* =

14.8, 7.4 Hz, 2H), 0.88 (t, $J = 7.4$ Hz, 3H). ^{13}C NMR (126 MHz, CDCl_3) δ 153.39, 150.92, 140.51, 139.81, 139.78, 135.88, 129.18, 128.62, 128.23, 128.19, 127.24, 126.36, 126.24, 96.73, 47.46, 45.40, 30.14, 27.38, 22.67, 13.88. HRMS (ESI) calculated for $\text{C}_{24}\text{H}_{27}\text{N}_4$, m/z 371.2230, found 371.2303 $[\text{M}+\text{H}]^+$.

Synthesis of compound 11c: 1-Benzyl-4-butoxy-2-butyl-1H-imidazo[4,5-c]pyridine. To a suspension of sodium hydride (48 mg, 2.00 mmol) in 2 mL of anhydrous THF was added 1-butanol (0.18 mL, 2.00 mmol). It was stirred at room temperature for 1 h, followed by the addition of compound **10** (100 mg, 0.33 mmol). The reaction mixture was heated at 60 °C for 18 h and then solvent was evaporated under vacuum. The residue was extracted with EtOAc (3 \times 10 mL), washed with water and dried over sodium sulfate. The solvent was removed and the crude residue was purified using column chromatography (0-5% MeOH in CH_2Cl_2) to obtain the compound **11c** (61 mg, 55%). ^1H NMR (500 MHz, CDCl_3) δ 7.85 (d, $J = 5.8$ Hz, 1H), 7.33 – 7.28 (m, 3H), 7.01 (dd, $J = 7.7, 1.7$ Hz, 2H), 6.77 (d, $J = 5.8$ Hz, 1H), 5.30 (s, 2H), 4.52 (t, $J = 7.0$ Hz, 2H), 2.87 – 2.82 (m, 2H), 1.90 (dd, $J = 15.0, 7.1$ Hz, 2H), 1.75 (dt, $J = 15.7, 7.7$ Hz, 2H), 1.58 – 1.48 (m, 2H), 1.38 (dq, $J = 14.7, 7.4$ Hz, 2H), 0.97 (t, $J = 7.4$ Hz, 3H), 0.88 (t, $J = 7.4$ Hz, 3H). ^{13}C NMR (126 MHz, CDCl_3) δ 156.04, 155.18, 142.02, 138.95, 135.59, 129.21, 128.27, 127.41, 126.27, 100.47, 66.25, 47.61, 31.34, 30.21, 27.44, 22.75, 19.45, 14.09, 13.85. HRMS (ESI) calculated for $\text{C}_{21}\text{H}_{28}\text{N}_3\text{O}$, m/z 338.2227, found 338.2307 $[\text{M}+\text{H}]^+$.

Synthesis of compound 12: 2,6-Dichloro-3-nitropyridin-4-amine. 4-Amino-2,6-dichloro pyridine (2.0 g, 12.27 mmol) was added to 20 mL of conc. H_2SO_4 . The mixture was cooled to 0 °C and 10 mL of conc. HNO_3 was dropwise at 0 °C. The reaction mixture was stirred at room temperature for 1 h and then poured into crushed ice. The white solid was filtered, washed with water and dried. This intermediate was dissolved in 10 mL of conc. H_2SO_4 and the reaction

solution was heated at 90 °C for 30 min. It was cooled to room temperature and poured into ice. It was slowly neutralized with ammonium hydroxide solution until a pH of 9 and the formed yellow solid was filtered, washed with water and dried to obtain compound **12** as light yellow solid. ¹H NMR (500 MHz, MeOD) δ 6.84 (s, 1H). ¹³C NMR (126 MHz, MeOD) δ 152.53, 151.18, 144.57, 111.12.

Synthesis of compound 13: *N*-Benzyl-2,6-dichloro-3-nitropyridin-4-amine. Sodium hydride (138 mg, 5.77 mmol) was carefully suspended in 10 mL of dry THF under N₂. The grey suspension was cooled to 0 °C and compound **12** (1.0 g, 4.81 mmol) was slowly added to the suspension at 0 °C. The reaction mixture was stirred for 1 h, followed by the addition of benzyl bromide (0.5 mL, 5.29 mmol). The reaction mixture was stirred at room temperature for 2 h and poured into ice water. Then it was extracted with EtOAc (3 × 20 mL), washed with water, dried over sodium sulfate. The solvent was removed and the crude residue was purified using column chromatography (0-20% EtOAc in hexane) to obtain the compound **13** as yellow solid. ¹H NMR (500 MHz, CDCl₃) δ 7.44 – 7.34 (m, 3H), 7.32 – 7.27 (m, 2H), 6.99 (s, 1H), 6.67 (s, 1H), 4.47 (d, *J* = 5.4 Hz, 2H). ¹³C NMR (126 MHz, CDCl₃) δ 152.07, 149.97, 145.68, 135.01, 129.48, 128.71, 127.32, 106.62, 47.74.

Synthesis of compound 14: *N*⁴-Benzyl-6-chloro-3-nitro-*N*²-(2,4,4-trimethylpentan-2-yl)pyridine-2,4-diamine. To a solution of compound **13** (300 mg, 1.02 mmol) in 20 mL of CH₂Cl₂ were added triethylamine (0.21 mL, 1.53 mmol) and *tert*-octylamine (0.5 mL, 3.06 mmol). The reaction mixture was refluxed for 48 h and the solvent was removed under vacuum. The crude residue was purified using column chromatography (0-20% EtOAc in hexane) to obtain the compound **14** as yellow solid (360 mg, 91%). ¹H NMR (500 MHz, CDCl₃) δ 9.57 (s, 1H), 9.51 (s, 1H), 7.39 (ddd, *J* = 7.5, 4.4, 1.3 Hz, 2H), 7.36 – 7.30 (m, 3H), 5.92 (s, 1H), 4.44 (d, *J* = 5.4 Hz,

2H), 1.95 (s, 2H), 1.56 (s, 6H), 0.98 (s, 9H). ^{13}C NMR (126 MHz, CDCl_3) δ 155.05, 154.25, 153.44, 136.10, 129.24, 128.24, 127.43, 115.80, 94.21, 57.32, 51.54, 47.64, 31.94, 31.66, 29.84. MS (ESI) calculated for $\text{C}_{20}\text{H}_{28}\text{ClN}_4\text{O}_2$, m/z 391.1895, found 391.1901 $[\text{M}+\text{H}]^+$.

Synthesis of compound 16: 1-Benzyl-2-butyl-6-chloro-*N*-(2,4,4-trimethylpentan-2-yl)-1*H*-imidazo[4,5-*c*]pyridin-4-amine. To a solution of compound **14** (260 mg, 0.66 mmol) in 20 mL of MeOH were added zinc dust (434 mg, 6.60 mmol) and ammonium formate (416 mg, 6.60 mmol). The reaction mixture was stirred at room temperature for 10 min and filtered through celite. Then the solvent was evaporated and the residue was dissolved in water. This was extracted with EtOAc (3 \times 20 mL), washed with water and dried over sodium sulfate. The solvent was removed under vacuum to obtain compound **15**, brown oil (184 mg, 77%). To a solution of compound **15** (184 mg, 0.50 mmol) in 10 mL of anhydrous THF were added triethylamine (74 μL , 0.52 mmol) and valeryl chloride (62 μL , 0.50 mmol). The reaction mixture was refluxed for 1 h. The solvent was then removed under vacuum, and the residue was dissolved in 10 mL of EtOH and NaOH (40 mg, 1.00 mmol) in 1 mL of H_2O was added. The reaction mixture was refluxed for 5 h. The solvent was then removed under vacuum, and the residue was dissolved in EtOAc and washed with water. The EtOAc fraction was dried using sodium sulfate and evaporated and purified using column chromatography (0-20% EtOAc in hexane) to obtain the compound **16** as yellow solid (120 mg, 56%). ^1H NMR (500 MHz, CDCl_3) δ 7.34 – 7.28 (m, 3H), 7.02 (d, J = 6.5 Hz, 2H), 6.42 (s, 1H), 5.38 (s, 1H), 5.16 (s, 2H), 2.76 – 2.69 (m, 2H), 2.02 (s, 2H), 1.71 – 1.65 (m, 4H), 1.60 (s, 6H), 1.37 (dd, J = 15.0, 7.5 Hz, 2H), 1.01 (s, 9H), 0.89 (t, J = 7.4 Hz, 3H). ^{13}C NMR (126 MHz, CDCl_3) δ 153.37, 149.45, 141.67, 140.77, 135.64, 129.21, 128.22, 126.31, 125.50, 93.95, 55.74, 51.42, 47.42, 31.91, 31.73, 30.12, 29.96, 27.37, 22.66, 13.87. MS (ESI) calculated for $\text{C}_{25}\text{H}_{36}\text{ClN}_4$, m/z 427.2623, found 427.2635 $[\text{M}+\text{H}]^+$.

Synthesis of compound 17: 1-Benzyl-2-butyl-6-chloro-1*H*-imidazo[4,5-*c*]pyridin-4-amine.

Compound **16** (34 mg, 0.082 mmol) was dissolved in 1 mL of HCl (4M in dioxane) and stirred at room temperature for 30 min. Then the solvent was removed under vacuum to obtain compound **17** (11 mg, 42%). ¹H NMR (500 MHz, CDCl₃) δ 7.36 – 7.30 (m, 3H), 7.01 (d, *J* = 6.4 Hz, 2H), 6.58 (s, 1H), 5.23 (s, 2H), 5.21 (s, 2H), 2.80 – 2.73 (m, 2H), 1.72 (dt, *J* = 15.5, 7.7 Hz, 2H), 1.39 (dq, *J* = 14.8, 7.4 Hz, 2H), 0.90 (t, *J* = 7.4 Hz, 3H). ¹³C NMR (126 MHz, CDCl₃) δ 154.83, 149.94, 142.31, 141.73, 135.26, 129.32, 128.57, 128.41, 126.26, 96.29, 47.59, 29.92, 27.36, 22.63, 13.87. HRMS (ESI) calculated for C₁₇H₂₀ClN₄, *m/z* 315.1371, found 315.1422 [M+H]⁺.

Synthesis of compound 19a: 1-Benzyl-2-butyl-1*H*-imidazo[4,5-*c*]pyridine-4,6-diamine. To a

solution of compound **16** (70 mg, 0.16 mmol) in 1 mL of dioxane were added potassium *tert*-butoxide (92 mg, 0.82 mmol), catalytic amount of DavePhos and Pd₂(dba)₃ and *tert*-octylamine (83 μL, 0.83 mmol). The reaction mixture was then heated under microwave conditions (500 W, 100 °C) in a sealed vial for 1 h. It was cooled to room temperature and filtered through celite and washed with MeOH. The solvent was removed and the crude residue was purified using column chromatography (0-20% EtOAc in hexane) to obtain the compound **18a**, brown solid (41 mg, 49%). Compound **18a** (33 mg, 0.063 mmol) was dissolved in 1 mL of HCl (4M in dioxane) and stirred at room temperature for 30 min. Then the solvent was removed under vacuum to obtain compound **19a** as brown solid (11 mg, 58%). ¹H NMR (500 MHz, DMSO) δ 7.37 – 7.31 (m, 2H), 7.30 – 7.25 (m, 1H), 7.09 – 7.04 (m, 2H), 6.41 (s, 2H), 5.65 (s, 1H), 5.24 (s, 2H), 2.73 – 2.67 (m, 2H), 1.59 (dt, *J* = 15.3, 7.5 Hz, 2H), 1.31 (dq, *J* = 14.7, 7.4 Hz, 2H), 0.83 (t, *J* = 7.4 Hz, 3H). ¹³C NMR (126 MHz, DMSO) δ 151.81, 147.80, 144.08, 136.91, 128.81, 128.77, 127.47, 126.29, 117.96, 76.19, 46.11, 29.27, 26.17, 21.80, 13.68. HRMS (ESI) calculated for C₁₇H₂₂N₅, *m/z* 296.1870, found 296.1906 [M+H]⁺.

Compounds **19b-19o** were synthesized similarly as compound **19a**.

19b: 1-Benzyl-*N*^{6,2}-dibutyl-1*H*-imidazo[4,5-*c*]pyridine-4,6-diamine. Butyl amine was used as a reagent. Brown solid. 23 mg, 79%. ¹H NMR (500 MHz, CDCl₃) δ 7.31 (ddd, *J* = 8.6, 6.4, 3.4 Hz, 3H), 7.05 (d, *J* = 6.7 Hz, 2H), 5.46 (s, 1H), 5.26 (s, 1H), 5.16 (s, 2H), 3.03 (t, *J* = 7.1 Hz, 2H), 2.72 – 2.66 (m, 2H), 1.68 (dd, *J* = 15.5, 7.6 Hz, 2H), 1.55 (dd, *J* = 14.8, 7.2 Hz, 2H), 1.43 – 1.33 (m, 4H), 0.90 (dt, *J* = 16.4, 7.4 Hz, 6H). ¹³C NMR (126 MHz, CDCl₃) δ 152.42, 148.50, 144.42, 135.99, 129.14, 128.06, 126.33, 74.80, 47.20, 43.09, 31.41, 30.03, 27.37, 22.66, 20.40, 14.02, 13.89. HRMS (ESI) calculated for C₂₁H₃₀N₅, *m/z* 352.2496, found 352.2515 [M+H]⁺.

18c: 1-Benzyl-2-butyl-*N*⁶-heptyl-*N*⁴-(2,4,4-trimethylpentan-2-yl)-1*H*-imidazo[4,5-*c*]pyridine-4,6-diamine. Heptylamine was used as a reagent. Brown oil. 43 mg, 65%. ¹H NMR (500 MHz, CDCl₃) δ 7.32 – 7.26 (m, 3H), 7.05 (d, *J* = 6.7 Hz, 2H), 5.39 (s, 1H), 5.13 (s, 1H), 5.11 (s, 2H), 3.13 (t, *J* = 7.2 Hz, 2H), 2.68 – 2.64 (m, 2H), 2.04 (s, 2H), 1.65 – 1.55 (m, 11H), 1.41 – 1.22 (m, 12H), 1.01 (s, 9H), 0.89 – 0.84 (m, 6H). ¹³C NMR (126 MHz, CDCl₃) δ 154.28, 150.38, 149.22, 142.39, 136.63, 128.97, 128.05, 127.76, 126.40, 120.44, 95.52, 73.57, 55.27, 51.72, 47.00, 43.63, 31.97, 31.94, 31.90, 31.79, 30.47, 30.29, 29.97, 29.32, 27.44, 27.39, 22.77, 22.71, 14.25, 13.90. MS (ESI) calculated for C₃₂H₅₂N₅, *m/z* 506.4217, found 506.4209 [M+H]⁺.

19c: 1-Benzyl-2-butyl-*N*⁶-heptyl-1*H*-imidazo[4,5-*c*]pyridine-4,6-diamine. Light brown solid. 24 mg, 80%. ¹H NMR (500 MHz, DMSO) δ 8.03 (s, 2H), 7.38 – 7.33 (m, 2H), 7.32 – 7.28 (m, 1H), 7.12 (d, *J* = 7.2 Hz, 2H), 6.84 (s, 1H), 5.98 (s, 1H), 5.39 (s, 2H), 3.08 (t, *J* = 7.0 Hz, 2H), 2.73 – 2.68 (m, 2H), 1.59 (dt, *J* = 15.3, 8.2 Hz, 2H), 1.50 (dd, *J* = 14.3, 7.2 Hz, 2H), 1.33 – 1.21 (m, 12H), 0.85 (t, *J* = 7.0 Hz, 3H), 0.81 (t, *J* = 7.4 Hz, 3H). ¹³C NMR (126 MHz, DMSO) δ 154.62, 145.66, 145.15, 136.32, 128.96, 128.86, 127.73, 126.64, 126.55, 74.21, 46.34, 42.24,

31.25, 28.78, 28.42, 28.09, 26.34, 26.18, 22.07, 21.71, 13.98, 13.62. HRMS (ESI) calculated for $C_{24}H_{36}N_5$, m/z 394.2965, found 394.3001 $[M+H]^+$.

18d: 1-Benzyl-2-butyl- N^6 -(cyclohexylmethyl)- N^4 -(2,4,4-trimethylpentan-2-yl)-1*H*-imidazo[4,5-*c*]pyridine-4,6-diamine. *N*-Cyclohexylmethylamine was used as a reagent. Yellow solid. 50 mg, 62%. 1H NMR (500 MHz, $CDCl_3$) δ 7.32 – 7.27 (m, 3H), 7.06 (d, $J = 6.7$ Hz, 2H), 5.37 (s, 1H), 5.10 (s, 2H), 2.99 (d, $J = 6.7$ Hz, 2H), 2.69 – 2.64 (m, 2H), 2.04 (s, 2H), 1.79 (d, $J = 13.2$ Hz, 2H), 1.73 – 1.60 (m, 9H), 1.58 (s, 6H), 1.35 (dd, $J = 15.0, 7.5$ Hz, 2H), 1.27 – 1.13 (m, 4H), 1.01 (s, 9H), 0.98 – 0.91 (m, 2H), 0.86 (t, $J = 7.4$ Hz, 3H). ^{13}C NMR (126 MHz, $CDCl_3$) δ 154.37, 150.36, 149.19, 142.41, 136.65, 128.97, 127.76, 126.44, 120.35, 73.62, 55.26, 51.67, 50.18, 47.02, 37.88, 31.91, 31.80, 31.48, 30.51, 30.31, 27.46, 26.80, 26.17, 22.72, 13.91. MS (ESI) calculated for $C_{32}H_{50}N_5$, m/z 504.4061, found 504.41 $[M+H]^+$.

19d: 1-Benzyl-2-butyl- N^6 -(cyclohexylmethyl)-1*H*-imidazo[4,5-*c*]pyridine-4,6-diamine. Light brown. 28 mg, 80%. 1H NMR (500 MHz, DMSO) δ 7.35 (t, $J = 7.3$ Hz, 2H), 7.31 – 7.27 (m, 1H), 7.10 (d, $J = 7.2$ Hz, 2H), 6.34 (d, $J = 3.1$ Hz, 1H), 5.85 (s, 1H), 5.33 (s, 2H), 2.92 (t, $J = 6.1$ Hz, 2H), 2.71 – 2.66 (m, 2H), 1.75 – 1.64 (m, 4H), 1.57 (dt, $J = 15.3, 7.6$ Hz, 3H), 1.49 (dtd, $J = 11.2, 7.4, 3.7$ Hz, 1H), 1.30 (dt, $J = 14.8, 7.4$ Hz, 2H), 1.21 – 1.09 (m, 4H), 0.91 (dd, $J = 22.3, 10.5$ Hz, 2H), 0.81 (t, $J = 7.4$ Hz, 3H). ^{13}C NMR (126 MHz, DMSO) δ 153.32, 146.28, 145.05, 136.69, 128.79, 127.61, 126.53, 116.94, 74.21, 48.49, 46.22, 36.76, 30.47, 29.02, 26.21, 26.05, 25.43, 21.75, 13.65. HRMS (ESI) calculated for $C_{24}H_{34}N_5$, m/z 392.2809, found 392.2806 $[M+H]^+$.

18e: 1-Benzyl-2-butyl- N^6 -phenyl- N^4 -(2,4,4-trimethylpentan-2-yl)-1*H*-imidazo[4,5-*c*]pyridine-4,6-diamine. Aniline was used as a reagent. Yellow solid. 51 mg, 55%. 1H NMR (500 MHz,

CDCl₃) δ 7.31 (dt, *J* = 16.5, 5.5 Hz, 3H), 7.22 (t, *J* = 7.8 Hz, 2H), 7.16 (d, *J* = 7.6 Hz, 2H), 7.05 (d, *J* = 6.7 Hz, 2H), 6.90 (t, *J* = 6.9 Hz, 1H), 6.16 (s, 1H), 6.02 (s, 1H), 5.23 (s, 1H), 5.12 (s, 2H), 2.74 – 2.67 (m, 2H), 2.03 (s, 2H), 1.66 (dd, *J* = 15.8, 8.2 Hz, 4H), 1.60 (s, 6H), 1.38 (dd, *J* = 15.0, 7.5 Hz, 2H), 1.02 (s, 9H), 0.89 (t, *J* = 7.4 Hz, 3H). ¹³C NMR (126 MHz, CDCl₃) δ 151.49, 149.42, 149.11, 142.46, 141.51, 136.32, 129.16, 129.06, 127.93, 126.53, 121.98, 120.91, 118.83, 55.42, 51.80, 47.26, 31.93, 31.80, 30.44, 30.19, 27.46, 22.71, 13.91. MS (ESI) calculated for C₃₁H₄₂N₅, *m/z* 484.3435, found 484.3459 [M+H]⁺.

19e: 1-Benzyl-2-butyl-N⁶-phenyl-1*H*-imidazo[4,5-*c*]pyridine-4,6-diamine. Light yellow solid. 28 mg, 76%. ¹H NMR (500 MHz, DMSO) δ 9.10 (s, 1H), 8.08 (s, 1H), 7.39 – 7.35 (m, 2H), 7.33 – 7.28 (m, 3H), 7.11 (t, *J* = 7.3 Hz, 4H), 7.01 (t, *J* = 7.3 Hz, 1H), 6.41 (s, 1H), 5.44 (s, 2H), 2.82 (t, *J* = 7.5 Hz, 2H), 1.63 (dt, *J* = 15.3, 7.6 Hz, 2H), 1.33 (dd, *J* = 14.9, 7.4 Hz, 2H), 0.84 (t, *J* = 7.4 Hz, 3H). ¹³C NMR (126 MHz, DMSO) δ 146.34, 140.41, 136.06, 129.52, 128.92, 127.84, 126.69, 122.44, 118.87, 46.68, 28.89, 26.15, 21.72, 13.63. HRMS (ESI) calculated for C₂₃H₂₆N₅, *m/z* 372.2183, found 372.2219 [M+H]⁺.

18f: N^{6,1}-Dibenzyl-2-butyl-N⁴-(2,4,4-trimethylpentan-2-yl)-1*H*-imidazo[4,5-*c*]pyridine-4,6-diamine. Benzyl amine was used as a reagent. Light brown solid. 30 mg, 46%. ¹H NMR (500 MHz, CDCl₃) δ 7.35 (d, *J* = 7.4 Hz, 2H), 7.26 (dddd, *J* = 9.4, 7.2, 6.1, 1.6 Hz, 6H), 7.03 (d, *J* = 6.8 Hz, 2H), 5.44 (s, 1H), 5.17 (s, 1H), 5.07 (s, 2H), 4.42 (s, 2H), 2.70 – 2.64 (m, 2H), 1.67 – 1.60 (m, 2H), 1.55 (s, 6H), 1.35 (dq, *J* = 14.7, 7.4 Hz, 2H), 1.02 – 0.94 (m, 9H), 0.87 (t, *J* = 7.4 Hz, 3H). ¹³C NMR (126 MHz, CDCl₃) δ 153.83, 150.58, 149.20, 142.27, 140.52, 136.49, 128.98, 128.56, 127.80, 127.68, 126.97, 126.46, 126.39, 74.17, 55.29, 51.62, 47.59, 47.07, 31.87, 31.76, 30.45, 30.28, 30.20, 27.42, 22.70, 13.90. MS (ESI) calculated for C₃₂H₄₄N₅, *m/z* 498.3591, found 498.3599 [M+H]⁺.

19f: *N*^{6,1}-Dibenzyl-2-butyl-1*H*-imidazo[4,5-*c*]pyridine-4,6-diamine. White solid. 22 mg, 85%. ¹H NMR (500 MHz, DMSO) δ 8.07 (s, 2H), 7.38 – 7.35 (m, 2H), 7.34 – 7.29 (m, 5H), 7.29 – 7.25 (m, 1H), 7.07 (d, *J* = 6.3 Hz, 2H), 6.06 (s, 1H), 5.33 (s, 2H), 4.38 (s, 2H), 2.75 – 2.69 (m, 2H), 1.58 (dt, *J* = 15.3, 7.6 Hz, 2H), 1.30 (dt, *J* = 14.8, 7.4 Hz, 2H), 0.81 (t, *J* = 7.4 Hz, 3H). ¹³C NMR (126 MHz, DMSO) δ 154.68, 145.29, 137.99, 136.12, 128.85, 128.45, 127.78, 127.51, 127.23, 126.74, 75.08, 46.43, 45.67, 28.76, 26.16, 21.70, 13.62. HRMS (ESI) calculated for C₂₄H₂₈N₅, *m/z* 386.2339, found 386.2389 [M+H]⁺.

19g: 1-Benzyl-2-butyl-*N*⁶-(4-methoxybenzyl)-1*H*-imidazo[4,5-*c*]pyridine-4,6-diamine. 4-Methoxy-benzylamine was used as a reagent. Light yellow solid. 22 mg, 69%. ¹H NMR (500 MHz, DMSO) δ 8.07 (s, 2H), 7.34 – 7.28 (m, 5H), 7.08 (d, *J* = 6.4 Hz, 2H), 6.87 (d, *J* = 8.7 Hz, 2H), 6.04 (s, 1H), 5.34 (s, 2H), 4.29 (s, 2H), 3.72 (s, 3H), 2.75 – 2.70 (m, 2H), 1.58 (dt, *J* = 15.3, 7.6 Hz, 2H), 1.29 (dd, *J* = 14.9, 7.4 Hz, 2H), 0.81 (t, *J* = 7.4 Hz, 3H). ¹³C NMR (126 MHz, DMSO) δ 158.48, 154.67, 145.28, 145.27, 136.13, 129.73, 128.92, 128.84, 127.78, 126.74, 113.82, 75.11, 55.08, 46.43, 45.18, 28.76, 26.16, 21.71, 13.62. HRMS (ESI) calculated for C₂₅H₃₀N₅O, *m/z* 416.2445, found 416.2490 [M+H]⁺.

19h: 1-Benzyl-2-butyl-*N*⁶-(3-methoxybenzyl)-1*H*-imidazo[4,5-*c*]pyridine-4,6-diamine. 3-Methoxy-benzylamine was used as a reagent. Brown solid. 27 mg, 69%. ¹H NMR (500 MHz, DMSO) δ 7.32 – 7.27 (m, 3H), 7.23 (t, *J* = 7.9 Hz, 1H), 7.06 (d, *J* = 6.1 Hz, 2H), 6.94 (dd, *J* = 12.3, 4.8 Hz, 2H), 6.83 (dd, *J* = 8.1, 2.2 Hz, 1H), 6.03 (s, 1H), 5.31 (s, 2H), 4.33 (d, *J* = 5.8 Hz, 2H), 3.71 (s, 3H), 2.70 (t, *J* = 7.6 Hz, 2H), 1.57 (dt, *J* = 15.3, 7.6 Hz, 2H), 1.29 (dd, *J* = 14.9, 7.4 Hz, 2H), 0.81 (t, *J* = 7.4 Hz, 3H). ¹³C NMR (126 MHz, DMSO) δ 159.37, 136.32, 129.52, 128.80, 127.72, 126.70, 119.55, 113.13, 112.50, 75.05, 55.00, 46.33, 45.63, 40.11, 40.02, 39.94, 28.89,

26.21, 21.72, 13.63. HRMS (ESI) calculated for C₂₅H₃₀N₅O, m/z 416.2445, found 416.2506 [M+H]⁺.

19i: 1-Benzyl-2-butyl-N⁶-(4-(trifluoromethyl)benzyl)-1H-imidazo[4,5-c]pyridine-4,6-diamine.

4-(Trifluoromethyl)benzylamine was used as a reagent. Brown solid. 17 mg, 77%. ¹H NMR (500 MHz, DMSO) δ 7.60 (d, *J* = 8.2 Hz, 2H), 7.51 (d, *J* = 8.1 Hz, 2H), 7.29 – 7.21 (m, 3H), 7.02 (d, *J* = 6.7 Hz, 2H), 6.23 (s, 1H), 5.70 (s, 2H), 5.57 (s, 1H), 5.15 (s, 2H), 4.41 (d, *J* = 6.3 Hz, 2H), 2.69 – 2.63 (m, 2H), 1.56 (dt, *J* = 15.3, 7.5 Hz, 2H), 1.29 (dd, *J* = 14.9, 7.4 Hz, 2H), 0.82 (t, *J* = 7.4 Hz, 3H). ¹³C NMR (126 MHz, DMSO) δ 153.45, 150.32, 149.41, 146.48, 143.12, 137.24, 128.58, 127.82, 127.31, 126.51, 124.88, 124.85, 118.91, 75.32, 46.04, 44.94, 29.43, 26.19, 21.82, 13.69. HRMS (ESI) calculated for C₂₅H₂₇F₃N₅, m/z 454.2213, found 454.2284 [M+H]⁺.

19j: 1-Benzyl-2-butyl-N⁶-(4-chlorobenzyl)-1H-imidazo[4,5-c]pyridine-4,6-diamine.

4-Chlorobenzylamine was used as a reagent. Yellow solid. 15 mg, 63%. ¹H NMR (500 MHz, DMSO) δ 7.33 – 7.25 (m, 8H), 7.02 (d, *J* = 6.6 Hz, 2H), 6.18 (s, 1H), 5.83 (s, 2H), 5.59 (s, 1H), 5.16 (s, 2H), 4.30 (d, *J* = 6.0 Hz, 2H), 2.68 – 2.64 (m, 2H), 1.56 (dt, *J* = 15.3, 7.5 Hz, 2H), 1.29 (dd, *J* = 14.9, 7.4 Hz, 2H), 0.82 (t, *J* = 7.4 Hz, 3H). ¹³C NMR (126 MHz, DMSO) δ 150.57, 149.14, 143.25, 140.18, 137.18, 130.77, 129.08, 128.63, 127.96, 127.37, 126.56, 118.72, 75.34, 46.06, 44.71, 40.11, 40.02, 39.94, 29.40, 26.20, 21.82, 13.69. HRMS (ESI) calculated for C₂₄H₂₇ClN₅, m/z 420.1950, found 420.1976 [M+H]⁺.

18k: 1-Benzyl-2-butyl-N⁶-(furan-2-ylmethyl)-N⁴-(2,4,4-trimethylpentan-2-yl)-1H-imidazo[4,5-

c]pyridine-4,6-diamine. Furfurylamine was used as a reagent. Yellow oil. 53 mg, 54%. ¹H NMR (500 MHz, CDCl₃) δ 7.30 (ddd, *J* = 10.9, 4.6, 1.1 Hz, 4H), 7.04 (d, *J* = 6.6 Hz, 2H), 6.28 (dd, *J* = 3.2, 1.9 Hz, 1H), 6.15 (dd, *J* = 3.2, 0.6 Hz, 1H), 5.50 (s, 1H), 5.10 (s, 2H), 4.43 (s, 2H), 2.72 –

2.64 (m, 2H), 2.03 (s, 2H), 1.68 – 1.59 (m, 4H), 1.58 (s, 6H), 1.35 (dt, $J = 14.7, 7.4$ Hz, 2H), 1.00 (s, 9H), 0.87 (t, $J = 7.4$ Hz, 3H). ^{13}C NMR (126 MHz, CDCl_3) δ 153.92, 153.28, 150.77, 149.15, 142.19, 141.69, 136.47, 129.00, 127.83, 126.42, 110.36, 106.53, 74.85, 55.32, 51.68, 47.09, 40.78, 31.89, 31.77, 30.47, 30.31, 27.43, 22.71, 13.90. MS (ESI) calculated for $\text{C}_{30}\text{H}_{42}\text{N}_5\text{O}$, m/z 488.3384, found 488.3446 $[\text{M}+\text{H}]^+$.

19k: 1-Benzyl-2-butyl- N^6 -(furan-2-ylmethyl)-1*H*-imidazo[4,5-*c*]pyridine-4,6-diamine. Brown solid. 21 mg, 55%. ^1H NMR (500 MHz, DMSO) δ 7.55 (s, 1H), 7.34 (t, $J = 7.3$ Hz, 2H), 7.31 – 7.27 (m, 1H), 7.10 (d, $J = 7.3$ Hz, 2H), 6.36 (dd, $J = 3.0, 1.9$ Hz, 1H), 6.29 (d, $J = 2.6$ Hz, 1H), 5.99 (s, 1H), 5.31 (s, 2H), 4.35 (d, $J = 5.8$ Hz, 2H), 2.73 – 2.67 (m, 2H), 1.58 (dt, $J = 15.2, 7.6$ Hz, 2H), 1.30 (dd, $J = 14.9, 7.4$ Hz, 2H), 0.82 (t, $J = 7.4$ Hz, 3H). ^{13}C NMR (126 MHz, DMSO) δ 142.17, 136.66, 128.79, 127.62, 126.61, 110.39, 107.43, 75.34, 60.19, 46.26, 38.71, 29.07, 26.21, 21.76, 13.65. HRMS (ESI) calculated for $\text{C}_{22}\text{H}_{26}\text{N}_5\text{O}$, m/z 376.2132, found 376.2184 $[\text{M}+\text{H}]^+$.

18l: 1-Benzyl-2-butyl- N^6 -(pyridin-4-ylmethyl)- N^4 -(2,4,4-trimethylpentan-2-yl)-1*H*-imidazo[4,5-*c*]pyridine-4,6-diamine. 4-Picolylamine was used as a reagent. Yellow solid. 25 mg, 31%. ^1H NMR (500 MHz, CDCl_3) δ 8.48 (dd, $J = 4.5, 1.6$ Hz, 2H), 7.29 – 7.25 (m, 3H), 7.24 (dd, $J = 4.5, 1.5$ Hz, 2H), 7.01 (d, $J = 6.1$ Hz, 2H), 5.40 (s, 1H), 5.06 (s, 2H), 4.49 (s, 2H), 2.70 – 2.64 (m, 2H), 1.92 (s, 2H), 1.63 (dt, $J = 15.5, 7.7$ Hz, 2H), 1.48 (s, 6H), 1.36 (dt, $J = 14.9, 7.4$ Hz, 2H), 0.95 (s, 9H), 0.87 (t, $J = 7.4$ Hz, 3H). ^{13}C NMR (126 MHz, CDCl_3) δ 149.83, 136.31, 129.01, 127.89, 126.40, 122.20, 74.67, 55.25, 51.56, 47.13, 46.09, 31.81, 31.75, 31.71, 30.44, 30.23, 27.41, 22.69, 13.89. MS (ESI) calculated for $\text{C}_{31}\text{H}_{43}\text{N}_6$, m/z 499.3544, found 499.3475 $[\text{M}+\text{H}]^+$.

19l: 1-Benzyl-2-butyl-*N*⁶-(pyridin-4-ylmethyl)-1*H*-imidazo[4,5-*c*]pyridine-4,6-diamine. Brown solid. 7 mg, 47%. ¹H NMR (500 MHz, DMSO) δ 8.43 (dd, *J* = 4.5, 1.5 Hz, 2H), 7.27 (ddd, *J* = 9.7, 6.8, 4.4 Hz, 5H), 7.03 (d, *J* = 6.7 Hz, 2H), 6.50 – 6.28 (m, 2H), 5.65 (s, 1H), 5.18 (s, 2H), 4.37 (d, *J* = 6.3 Hz, 2H), 2.69 – 2.65 (m, 2H), 1.57 (dt, *J* = 15.3, 7.5 Hz, 2H), 1.30 (dd, *J* = 14.9, 7.4 Hz, 2H), 0.81 (d, *J* = 7.4 Hz, 3H). ¹³C NMR (126 MHz, DMSO) δ 149.28, 137.09, 130.51, 128.65, 127.43, 126.53, 122.35, 113.97, 75.37, 46.09, 44.38, 29.34, 26.19, 21.80, 13.68. HRMS (ESI) calculated for C₂₃H₂₇N₆, *m/z* 387.2292, found 387.2299 [M+H]⁺.

19m: 1-Benzyl-2-butyl-*N*⁶-(pyridin-3-ylmethyl)-1*H*-imidazo[4,5-*c*]pyridine-4,6-diamine. 3-Picolylamine was used as a reagent. Light brown solid. 33 mg, 63%. ¹H NMR (500 MHz, DMSO) δ 8.92 (s, 1H), 8.80 (d, *J* = 5.3 Hz, 1H), 8.46 (d, *J* = 8.0 Hz, 1H), 8.12 (s, 2H), 7.94 (dd, *J* = 7.9, 5.7 Hz, 1H), 7.69 (s, 1H), 7.33 – 7.25 (m, 3H), 7.04 (d, *J* = 6.9 Hz, 2H), 6.03 (s, 1H), 5.32 (s, 2H), 4.64 (s, 2H), 2.72 (t, *J* = 7.6 Hz, 2H), 1.56 (dt, *J* = 15.2, 7.6 Hz, 2H), 1.28 (dd, *J* = 14.9, 7.4 Hz, 2H), 0.80 (t, *J* = 7.4 Hz, 3H). ¹³C NMR (126 MHz, DMSO) δ 154.65, 145.80, 145.01, 143.55, 141.29, 141.12, 138.17, 136.10, 128.83, 127.76, 126.68, 126.52, 75.49, 46.45, 42.51, 28.77, 26.12, 21.68, 13.60. HRMS (ESI) calculated for C₂₃H₂₇N₆, *m/z* 387.2292, found 387.2296 [M+H]⁺.

19n: 1-Benzyl-2-butyl-*N*⁶-(naphthalen-1-ylmethyl)-1*H*-imidazo[4,5-*c*]pyridine-4,6-diamine. 1-Naphthylmethylamine was used as a reagent. Light brown solid. 28 mg, 70%. ¹H NMR (500 MHz, DMSO) δ 12.12 (s, 1H), 8.10 (d, *J* = 8.0 Hz, 1H), 8.04 (s, 2H), 7.99 – 7.96 (m, 1H), 7.88 (d, *J* = 8.2 Hz, 1H), 7.61 – 7.53 (m, 3H), 7.45 (dd, *J* = 8.1, 7.1 Hz, 1H), 7.33 – 7.28 (m, 3H), 7.08 (d, *J* = 6.4 Hz, 2H), 6.22 (s, 1H), 5.35 (s, 2H), 4.83 (s, 2H), 2.74 – 2.68 (m, 2H), 1.58 (dt, *J* = 15.3, 7.6 Hz, 2H), 1.29 (dd, *J* = 14.9, 7.4 Hz, 2H), 0.81 (t, *J* = 7.4 Hz, 3H). ¹³C NMR (126 MHz, DMSO) δ 154.69, 145.51, 145.31, 136.23, 133.44, 132.90, 130.92, 128.83, 128.63, 127.99,

127.76, 126.67, 126.39, 125.97, 125.49, 125.43, 123.63, 74.91, 46.39, 43.99, 28.80, 26.20, 21.71, 13.62. HRMS (ESI) calculated for C₂₈H₃₀N₅, m/z 436.2496, found 436.2549 [M+H]⁺.

19o: **N⁶-([1,1'-Biphenyl]-4-ylmethyl)-1-benzyl-2-butyl-1*H*-imidazo[4,5-*c*]pyridine-4,6-diamine.** [1,1'-biphenyl]-4-yl methane amine was used as a reagent. Light brown solid. 21 mg, 51%. ¹H NMR (500 MHz, DMSO) δ 12.36 (s, 1H), 8.04 (s, 2H), 7.63 (dd, *J* = 12.4, 7.8 Hz, 4H), 7.50 – 7.42 (m, 4H), 7.40 – 7.33 (m, 1H), 7.28 (t, *J* = 7.3 Hz, 2H), 7.23 (t, *J* = 7.2 Hz, 1H), 7.07 (d, *J* = 7.3 Hz, 2H), 6.07 (s, 1H), 5.33 (s, 2H), 4.42 (s, 2H), 2.71 (t, *J* = 7.6 Hz, 2H), 1.57 (dt, *J* = 15.2, 7.7 Hz, 2H), 1.29 (dq, *J* = 14.6, 7.3 Hz, 2H), 0.81 (t, *J* = 7.3 Hz, 3H). ¹³C NMR (126 MHz, DMSO) δ 154.65, 145.40, 145.35, 139.80, 139.07, 137.24, 136.17, 128.95, 128.80, 128.06, 127.67, 127.43, 126.71, 126.69, 126.57, 75.11, 46.38, 45.31, 28.81, 26.18, 21.69, 13.61. HRMS (ESI) calculated for C₃₀H₃₂N₅, m/z 462.2652, found 462.2698 [M+H]⁺.

Synthesis of compound 19p and 19r: N⁶-(4-(aminomethyl)benzyl)-1-benzyl-2-butyl-1*H*-imidazo[4,5-*c*]pyridine-4,6-diamine. To a solution of compound **16** (70 mg, 0.16 mmol) in 1 mL of dioxane were added potassium *tert*-butoxide (90 mg, 0.80 mmol), catalytic amount of DavePhos and Pd₂(dba)₃ and *p*-xylylenediamine (109 mg, 0.80 mmol). The reaction mixture was then heated under microwave conditions (500 W, 100 °C) in a sealed vial for 1 h. It was cooled to room temperature and filtered through celite and washed with MeOH. The solvent was removed and the crude residue was purified using column chromatography (0-20% EtOAc in hexane) to obtain the compounds **18p** and **18r**. Compound **18p** (33 mg, 0.063 mmol) was dissolved in 1 mL of HCl (4M in dioxane) and stirred at room temperature for 30 min. Then the solvent was removed under vacuum to obtain compound **19p** as light yellow solid (5 mg, 63%). ¹H NMR (500 MHz, DMSO) δ 8.37 (s, 2H), 8.06 (s, 2H), 7.42 (q, *J* = 8.5 Hz, 4H), 7.36 – 7.30 (m, 3H), 7.08 (d, *J* = 6.8 Hz, 2H), 6.08 (s, 1H), 5.34 (s, 2H), 4.40 (s, 2H), 3.98 (q, *J* = 5.8 Hz, 2H),

2.75 – 2.67 (m, 2H), 1.57 (dt, $J = 15.3, 7.6$ Hz, 2H), 1.28 (dd, $J = 14.9, 7.4$ Hz, 2H), 0.80 (t, $J = 7.4$ Hz, 3H). ^{13}C NMR (126 MHz, DMSO) δ 154.71, 145.41, 145.34, 138.43, 136.19, 132.98, 129.02, 128.89, 127.79, 127.75, 126.65, 46.40, 45.31, 41.89, 28.78, 26.18, 21.70, 13.62. HRMS (ESI) calculated for $\text{C}_{25}\text{H}_{31}\text{N}_6$, m/z 415.2605, found 415.2606 $[\text{M}+\text{H}]^+$.

19r: $N^6, N^{6'}$ -(1,4-phenylenebis(methylene))bis(1-benzyl-2-butyl-1*H*-imidazo[4,5-*c*]pyridine-4,6-diamine). Compound **18r** (35 mg, 0.038 mmol) was dissolved in 1 mL of HCl (4M in dioxane) and stirred at room temperature for 30 min. Then the solvent was removed under vacuum to obtain compound **19r** as light yellow solid (12 mg, 45%). ^1H NMR (500 MHz, MeOD) δ 7.27 (s, 4H), 7.21 – 7.17 (m, 6H), 7.02 – 6.98 (m, 4H), 5.20 (s, 4H), 4.33 (s, 4H), 2.78 – 2.73 (m, 4H), 1.67 (dt, $J = 15.3, 7.6$ Hz, 4H), 1.37 (dd, $J = 15.0, 7.5$ Hz, 4H), 0.89 (t, $J = 7.4$ Hz, 6H). ^{13}C NMR (126 MHz, MeOD) δ 155.94, 150.96, 148.16, 146.47, 138.77, 137.12, 130.00, 129.03, 128.70, 127.70, 118.63, 48.01, 47.26, 30.28, 27.76, 23.29, 14.05. HRMS (ESI) calculated for $\text{C}_{42}\text{H}_{49}\text{N}_{10}$, m/z 693.4136, found 693.4331 $[\text{M}+\text{H}]^+$.

Compounds **19q** and **19s** were synthesized similarly as compounds **19p** and **19r**.

19q: N^6 -(3-(aminomethyl)benzyl)-1-benzyl-2-butyl-1*H*-imidazo[4,5-*c*]pyridine-4,6-diamine. *m*-Xylylenediamine was used as a reagent. Light yellow solid. ^1H NMR (500 MHz, MeOD) δ 7.49 (s, 1H), 7.41 (dd, $J = 3.9, 1.5$ Hz, 2H), 7.39 – 7.35 (m, 1H), 7.32 – 7.28 (m, 3H), 7.05 – 7.02 (m, 2H), 5.31 (s, 2H), 4.44 (s, 2H), 4.07 (s, 2H), 2.79 – 2.75 (m, 2H), 1.70 (dt, $J = 15.3, 7.6$ Hz, 2H), 1.38 (dq, $J = 14.8, 7.4$ Hz, 2H), 0.89 (t, $J = 7.4$ Hz, 3H). ^{13}C NMR (126 MHz, MeOD) δ 157.36, 147.23, 146.79, 140.00, 136.86, 134.96, 130.63, 130.12, 129.26, 129.19, 129.14, 129.00, 127.62, 48.10, 47.15, 44.18, 30.00, 27.75, 23.24, 14.03. HRMS (ESI) calculated for $\text{C}_{25}\text{H}_{31}\text{N}_6$, m/z 415.2605, found 415.2610 $[\text{M}+\text{H}]^+$.

19s: N^6, N^6' -(1,3-phenylenebis(methylene))bis(1-benzyl-2-butyl-1*H*-imidazo[4,5-*c*]pyridine-4,6-diamine). Light yellow solid. ^1H NMR (500 MHz, DMSO) δ 12.38 (s, 2H), 8.04 (s, 4H), 7.38 (s, 1H), 7.30 – 7.22 (m, 9H), 7.04 (d, J = 6.8 Hz, 4H), 6.01 (s, 2H), 5.28 (s, 4H), 4.34 (s, 4H), 2.73 – 2.68 (m, 4H), 1.56 (dd, J = 15.3, 7.7 Hz, 4H), 1.29 (dd, J = 14.9, 7.4 Hz, 4H), 0.81 (t, J = 7.4 Hz, 6H). ^{13}C NMR (126 MHz, DMSO) δ 154.62, 145.36, 145.31, 138.22, 136.15, 128.80, 128.61, 127.72, 126.66, 126.56, 126.38, 46.36, 45.73, 28.80, 26.19, 21.71, 13.62. HRMS (ESI) calculated for $\text{C}_{42}\text{H}_{49}\text{N}_{10}$, m/z 693.4136, found 693.4131 $[\text{M}+\text{H}]^+$.

Synthesis of compound 23a: To a solution of compound **14** (120 mg, 0.31 mmol) in 1 mL of dioxane were added cesium carbonate (303 mg, 0.93 mmol) in H_2O (0.5 mL), [1,1'-bis(diphenylphosphino)ferrocene]dichloropalladium(II) ($\text{Pd}(\text{dppf})\text{Cl}_2$) (15 mg, 0.019 mmol) and *n*-butylboronic acid (98 μL , 0.46 mmol) under N_2 . The reaction mixture was then heated at 90 $^\circ\text{C}$ in a sealed vial for 18 h. It was cooled to room temperature and filtered through celite and washed with MeOH. The solvent was removed and the crude residue was purified using column chromatography (0-15% EtOAc in hexane) to obtain the compound **20a** (97mg, 76%). To a solution of compound **20a** (94 mg, 0.23 mmol) in 10 mL of MeOH were added zinc dust (149 mg, 2.30 mmol) and ammonium formate (145 mg, 2.30 mmol). The reaction mixture was stirred at room temperature for 10 min and filtered through celite. Then the solvent was evaporated and the residue was dissolved in water. This was extracted with EtOAc (3 \times 20 mL), washed with water and dried over sodium sulfate. The solvent was removed under vacuum to obtain compound **21a** (45 mg, 51%). To a solution of compound **21a** (42 mg, 0.11 mmol) in 7 mL of anhydrous THF were added triethylamine (16 μL , 0.12 mmol) and valeryl chloride (13 μL , 0.11 mmol). The reaction mixture was refluxed for 1 h. The solvent was then removed under vacuum, and the residue was dissolved in 5 mL of EtOH and NaOH (10 mg, 0.22 mmol) in 1 mL of H_2O was added. The reaction mixture was refluxed for 18 h. The solvent was then removed under

vacuum, and the residue was dissolved in EtOAc and washed with water. The EtOAc fraction was dried using sodium sulfate and evaporated and purified using column chromatography (0-20% EtOAc in hexane) to obtain the compound **22a** (25 mg, 51%). Compound **22a** (22 mg, 0.049 mmol) was dissolved in 1 mL of HCl (4M in dioxane) and stirred at room temperature for 30 min. Then the solvent was removed under vacuum to obtain compound **23a** (11 mg, 69%).

20a: *N*⁴-Benzyl-6-butyl-3-nitro-*N*²-(2,4,4-trimethylpentan-2-yl)pyridine-2,4-diamine. Yellow oil. 97 mg, 76%. ¹H NMR (500 MHz, CDCl₃) δ 9.51 (t, *J* = 4.4 Hz, 1H), 9.40 (s, 1H), 7.37 (ddd, *J* = 7.1, 4.4, 1.6 Hz, 2H), 7.34 – 7.30 (m, 3H), 5.74 (s, 1H), 4.45 (d, *J* = 5.4 Hz, 2H), 2.44 (t, *J* = 7.5 Hz, 2H), 2.01 (s, 2H), 1.67 – 1.61 (m, 2H), 1.30 (dd, *J* = 15.0, 7.4 Hz, 2H), 0.96 (s, 9H), 0.89 (t, *J* = 7.4 Hz, 3H). ¹³C NMR (126 MHz, CDCl₃) δ 166.49, 154.69, 152.58, 136.94, 129.07, 127.92, 127.42, 115.70, 94.41, 56.59, 51.17, 47.44, 38.87, 31.95, 31.64, 30.61, 30.19, 22.43, 14.11. MS (ESI) calculated for C₂₄H₃₇N₄O₂, *m/z* 413.2911, found 413.3267 [M+H]⁺.

23a: 1-Benzyl-2,6-dibutyl-1*H*-imidazo[4,5-*c*]pyridin-4-amine. White solid. 11 mg, 69%. ¹H NMR (500 MHz, CDCl₃) δ 7.37 – 7.31 (m, 3H), 7.10 (d, *J* = 6.9 Hz, 2H), 6.81 (s, 1H), 5.47 (s, 2H), 2.85 (t, 2H), 2.72 (t, 2H), 1.74 (dd, *J* = 15.3, 7.6 Hz, 2H), 1.67 (ddd, *J* = 15.3, 10.4, 7.0 Hz, 2H), 1.38 (ddq, *J* = 14.8, 10.2, 7.4 Hz, 4H), 0.94 (t, *J* = 7.4 Hz, 3H), 0.90 (t, *J* = 7.4 Hz, 3H). ¹³C NMR (126 MHz, CDCl₃) δ 157.75, 150.13, 143.74, 137.10, 130.16, 129.22, 127.59, 124.62, 97.63, 35.61, 32.84, 30.27, 27.85, 23.31, 23.22, 14.12, 14.04. HRMS (ESI) calculated for C₂₁H₂₉N₄, *m/z* 337.2387, found 337.2476 [M+H]⁺.

Compounds **23b-23j** were synthesized similarly as compound **23a**.

20b: *N*⁴-Benzyl-3-nitro-6-phenyl-*N*²-(2,4,4-trimethylpentan-2-yl)pyridine-2,4-diamine.

Phenylboronic acid was used as a reagent. Yellow solid. 28 mg, 57%. ¹H NMR (500 MHz, CDCl₃) δ 9.68 (s, 1H), 9.54 (s, 1H), 7.92 (ddd, *J* = 4.4, 2.5, 1.4 Hz, 2H), 7.45 – 7.42 (m, 3H), 7.40 – 7.38 (m, 3H), 7.34 – 7.31 (m, 1H), 7.26 (s, 1H), 6.39 (s, 1H), 4.58 (d, *J* = 5.4 Hz, 2H), 2.09 (s, 2H), 1.64 (s, 6H), 0.99 (s, 9H). ¹³C NMR (126 MHz, CDCl₃) δ 159.01, 154.74, 153.13, 138.88, 136.87, 130.20, 129.19, 128.66, 128.06, 127.50, 127.44, 92.16, 56.72, 51.69, 47.62, 32.02, 31.74, 30.15. MS (ESI) calculated for C₂₆H₃₃N₄O₂, *m/z* 433.2598, found 433.2615 [M+H]⁺.

22b: 1-Benzyl-2-butyl-6-phenyl-*N*-(2,4,4-trimethylpentan-2-yl)-1*H*-imidazo[4,5-*c*]pyridin-4-

amine. Yellow solid. 31 mg, 47%. ¹H NMR (500 MHz, CDCl₃) δ 8.02 (dd, *J* = 8.3, 1.2 Hz, 2H), 7.39 (t, *J* = 7.7 Hz, 2H), 7.34 – 7.27 (m, 4H), 7.07 (d, *J* = 6.7 Hz, 2H), 6.94 (s, 1H), 5.34 (s, 1H), 5.28 (s, 2H), 2.79 – 2.73 (m, 2H), 2.18 (s, 2H), 1.73 – 1.66 (m, 8H), 1.39 (dd, *J* = 15.0, 7.5 Hz, 2H), 1.03 (s, 9H), 0.89 (t, *J* = 7.4 Hz, 3H). ¹³C NMR (126 MHz, CDCl₃) δ 153.22, 150.01, 148.43, 141.28, 140.32, 136.16, 129.61, 129.42, 129.15, 128.41, 128.07, 127.67, 127.54, 126.72, 126.36, 126.28, 126.22, 91.77, 55.45, 51.63, 47.28, 31.98, 31.81, 30.33, 30.25, 27.50, 22.72, 13.90. MS (ESI) calculated for C₃₁H₄₁N₄, *m/z* 469.3326, found 469.3350 [M+H]⁺.

23b: 1-Benzyl-2-butyl-6-phenyl-1*H*-imidazo[4,5-*c*]pyridin-4-amine. White solid. 13 mg, 73%.

¹H NMR (500 MHz, CDCl₃) δ 7.91 (d, *J* = 7.2 Hz, 2H), 7.54 – 7.44 (m, 3H), 7.42 – 7.34 (m, 3H), 7.05 (dd, *J* = 6.4, 1.1 Hz, 2H), 6.83 (s, 1H), 5.37 (s, 2H), 2.88 – 2.78 (m, 2H), 1.78 (dd, *J* = 15.2, 7.8 Hz, 2H), 1.42 (dq, *J* = 14.7, 7.4 Hz, 2H), 0.93 (t, *J* = 7.3 Hz, 3H). ¹³C NMR (126 MHz, CDCl₃) δ 157.54, 149.18, 142.11, 141.93, 134.08, 132.07, 130.82, 129.68, 129.66, 129.01, 127.38, 126.25, 95.25, 48.13, 29.31, 27.40, 22.52, 13.84. HRMS (ESI) calculated for C₂₃H₂₅N₄, *m/z* 357.2074, found 357.2155 [M+H]⁺.

20c: 4-(4-(Benzylamino)-5-nitro-6-((2,4,4-trimethylpentan-2-yl)amino)pyridin-2-yl)benzonitrile. 4-Cyanophenylboronic acid was used as a reagent. Yellow solid. 30 mg, 55%. ¹H NMR (500 MHz, CDCl₃) δ 9.72 (s, 1H), 9.51 (s, 1H), 7.97 (d, *J* = 8.6 Hz, 2H), 7.72 (d, *J* = 8.6 Hz, 2H), 7.44 – 7.31 (m, 5H), 6.38 (s, 1H), 4.59 (d, *J* = 5.4 Hz, 2H), 2.06 (s, 2H), 1.63 (s, 6H), 0.99 (s, 9H). ¹³C NMR (126 MHz, CDCl₃) δ 156.75, 154.69, 153.26, 143.14, 136.53, 132.50, 129.28, 128.23, 127.93, 127.35, 118.79, 113.38, 93.05, 56.87, 51.72, 47.68, 32.01, 31.72, 30.10. MS (ESI) calculated for C₂₇H₃₂N₅O₂, *m/z* 458.2551, found 458.2571 [M+H]⁺.

22c: 4-(1-Benzyl-2-butyl-4-((2,4,4-trimethylpentan-2-yl)amino)-1*H*-imidazo[4,5-*c*]pyridin-6-yl)benzamide. Cyano group was converted into amide in the basic condition. Yellow solid. 22 mg, 41%. ¹H NMR (500 MHz, CDCl₃) δ 8.10 (d, *J* = 8.5 Hz, 2H), 7.84 (d, *J* = 8.5 Hz, 2H), 7.34 – 7.28 (m, 3H), 7.08 – 7.04 (m, 2H), 6.99 (s, 1H), 6.14 (s, 1H), 5.79 (s, 1H), 5.41 (s, 1H), 5.29 (s, 2H), 2.81 – 2.74 (m, 2H), 2.17 (s, 2H), 1.72 – 1.66 (m, 8H), 1.43 – 1.33 (m, 2H), 1.03 (s, 9H), 0.89 (t, *J* = 7.4 Hz, 3H). ¹³C NMR (126 MHz, CDCl₃) δ 169.46, 153.74, 150.08, 147.00, 144.87, 140.11, 135.97, 131.83, 129.20, 128.15, 127.62, 126.76, 126.74, 126.31, 92.63, 55.50, 51.55, 47.31, 31.95, 31.79, 30.25, 30.17, 27.46, 22.69, 13.89. MS (ESI) calculated for C₃₂H₄₂N₅O, *m/z* 512.3384, found 512.3408 [M+H]⁺.

23c: 4-(4-Amino-1-benzyl-2-butyl-1*H*-imidazo[4,5-*c*]pyridin-6-yl)benzamide. White solid. 11 mg, 79%. ¹H NMR (500 MHz, MeOD) δ 8.09 – 8.05 (m, 2H), 7.89 – 7.85 (m, 2H), 7.51 (s, 1H), 7.41 – 7.32 (m, 3H), 7.17 (d, *J* = 7.0 Hz, 2H), 5.62 (s, 2H), 3.76 – 3.72 (m, 1H), 3.68 – 3.64 (m, 1H), 3.58 (dd, *J* = 7.0, 2.7 Hz, 1H), 2.94 – 2.89 (m, 2H), 1.78 (dt, *J* = 15.3, 7.6 Hz, 2H), 1.42 (dd, *J* = 15.0, 7.5 Hz, 2H), 0.92 (t, *J* = 7.4 Hz, 3H). ¹³C NMR (126 MHz, MeOD) δ 171.03, 159.91, 149.79, 143.90, 141.45, 137.23, 136.75, 136.73, 130.29, 129.74, 129.43, 128.43, 127.76,

125.80, 98.94, 73.57, 72.45, 62.18, 43.73, 30.01, 27.99, 23.28, 14.04. HRMS (ESI) calculated for C₂₄H₂₆N₅O, m/z 400.2132, found 400.2177 [M+H]⁺.

20d: N⁴-Benzyl-5-nitro-N⁶-(2,4,4-trimethylpentan-2-yl)-[2,3'-bipyridine]-4,6-diamine. 4-Pyridinylboronic acid was used as a reagent. Orange solid. 135 mg, 82%. ¹H NMR (500 MHz, CDCl₃) δ 9.74 (t, *J* = 5.1 Hz, 1H), 9.54 (s, 1H), 9.10 (dd, *J* = 2.2, 0.6 Hz, 1H), 8.65 (dd, *J* = 4.8, 1.6 Hz, 1H), 8.21 – 8.16 (m, 1H), 7.42 – 7.36 (m, 5H), 7.35 – 7.31 (m, 1H), 6.38 (s, 1H), 4.59 (d, *J* = 5.5 Hz, 2H), 2.07 (s, 2H), 1.63 (s, 6H), 0.99 (s, 9H). ¹³C NMR (126 MHz, CDCl₃) δ 156.52, 154.78, 153.22, 150.86, 148.93, 136.60, 134.75, 134.36, 129.26, 128.17, 127.35, 123.54, 116.37, 92.38, 56.86, 51.65, 47.65, 32.01, 31.72, 30.11. MS (ESI) calculated for C₂₅H₃₂N₅O₂, m/z 434.2551, found 434.2563 [M+H]⁺.

23d: 1-Benzyl-2-butyl-6-(pyridin-3-yl)-1*H*-imidazo[4,5-*c*]pyridin-4-amine. Light yellow solid. 10 mg, 72%. ¹H NMR (500 MHz, MeOD) δ 9.28 (d, *J* = 1.9 Hz, 1H), 8.94 (dd, *J* = 5.5, 1.2 Hz, 1H), 8.83 (d, *J* = 8.2 Hz, 1H), 8.11 (ddd, *J* = 8.2, 5.6, 0.5 Hz, 1H), 7.72 (s, 1H), 7.40 – 7.32 (m, 3H), 7.18 (d, *J* = 6.9 Hz, 2H), 5.65 (s, 2H), 2.98 – 2.91 (m, 2H), 1.78 (dd, *J* = 15.3, 7.7 Hz, 2H), 1.42 (dd, *J* = 15.0, 7.5 Hz, 2H), 0.92 (t, *J* = 7.4 Hz, 3H). ¹³C NMR (126 MHz, MeOD) δ 150.19, 143.97, 143.57, 143.11, 136.48, 130.41, 130.32, 129.52, 128.03, 127.74, 127.73, 100.47, 48.55, 29.93, 27.90, 23.26, 14.02. HRMS (ESI) calculated for C₂₂H₂₄N₅, m/z 358.2026, found 358.2067 [M+H]⁺.

20e: N⁴-Benzyl-6-(furan-3-yl)-3-nitro-N²-(2,4,4-trimethylpentan-2-yl)pyridine-2,4-diamine. 3-Furylboronic acid was used as a reagent. Yellow solid. 95 mg, 70%. ¹H NMR (500 MHz, CDCl₃) δ 9.68 (t, *J* = 4.8 Hz, 1H), 9.49 (s, 1H), 7.95 (dd, *J* = 1.5, 0.8 Hz, 1H), 7.45 (t, *J* = 1.7 Hz, 1H), 7.41 – 7.34 (m, 4H), 7.34 – 7.30 (m, 1H), 6.69 (dd, *J* = 1.9, 0.8 Hz, 1H), 6.07 (s, 1H), 4.53 (d, *J*

= 5.4 Hz, 2H), 2.05 (s, 2H), 1.60 (s, 6H), 0.98 (s, 9H). ^{13}C NMR (126 MHz, CDCl_3) δ 154.88, 153.66, 153.09, 143.99, 143.68, 136.85, 129.19, 128.06, 127.39, 127.36, 108.83, 91.66, 56.68, 51.51, 47.61, 31.99, 31.71, 30.13. MS (ESI) calculated for $\text{C}_{24}\text{H}_{31}\text{N}_4\text{O}_3$, m/z 423.2391, found 423.2401 $[\text{M}+\text{H}]^+$.

22e: **1-Benzyl-2-butyl-6-(furan-3-yl)-*N*-(2,4,4-trimethylpentan-2-yl)-1*H*-imidazo[4,5-*c*]pyridin-4-amine.** Brown oil. 30 mg, 41%. ^1H NMR (500 MHz, CDCl_3) δ 7.94 (dd, $J = 1.6, 0.7$ Hz, 1H), 7.41 (t, $J = 1.7$ Hz, 1H), 7.34 – 7.27 (m, 3H), 7.05 (d, $J = 6.6$ Hz, 2H), 6.76 (dd, $J = 1.8, 0.8$ Hz, 1H), 6.61 (s, 1H), 5.30 (s, 1H), 5.24 (s, 2H), 2.76 – 2.71 (m, 2H), 2.13 (s, 2H), 1.70 – 1.65 (m, 2H), 1.64 (s, 6H), 1.36 (dt, $J = 14.7, 7.4$ Hz, 2H), 1.02 (s, 9H), 0.88 (t, $J = 7.4$ Hz, 3H). ^{13}C NMR (126 MHz, CDCl_3) δ 152.80, 150.15, 143.24, 142.70, 140.71, 140.01, 136.16, 129.15, 128.83, 128.06, 126.33, 125.88, 108.87, 91.20, 55.44, 51.45, 47.25, 31.93, 31.79, 30.29, 30.16, 27.45, 22.71, 13.90. MS (ESI) calculated for $\text{C}_{29}\text{H}_{39}\text{N}_4\text{O}$, m/z 459.3118, found 459.3168 $[\text{M}+\text{H}]^+$.

23e: 1-Benzyl-2-butyl-6-(furan-3-yl)-1*H*-imidazo[4,5-*c*]pyridin-4-amine. Light yellow solid. 12 mg, 64%. ^1H NMR (500 MHz, MeOD) δ 8.23 – 8.19 (m, 1H), 7.73 – 7.70 (m, 1H), 7.42 (s, 1H), 7.40 – 7.32 (m, 3H), 7.15 (d, $J = 6.9$ Hz, 2H), 6.97 (dd, $J = 2.0, 0.9$ Hz, 1H), 5.58 (s, 2H), 2.90 – 2.85 (m, 2H), 1.75 (dt, $J = 15.3, 7.6$ Hz, 2H), 1.40 (dq, $J = 14.8, 7.4$ Hz, 2H), 0.91 (t, $J = 7.4$ Hz, 3H). ^{13}C NMR (126 MHz, MeOD) δ 159.50, 149.42, 146.46, 144.24, 142.92, 136.72, 135.38, 130.27, 129.41, 127.69, 124.89, 121.45, 109.21, 96.82, 48.27, 29.95, 27.91, 23.26, 14.03. HRMS (ESI) calculated for $\text{C}_{21}\text{H}_{23}\text{N}_4\text{O}$, m/z 347.1866, found 347.1921 $[\text{M}+\text{H}]^+$.

20f: ***N*¹-Benzyl-3-nitro-6-(thiophen-3-yl)-*N*²-(2,4,4-trimethylpentan-2-yl)pyridine-2,4-diamine.** 3-Thienylboronic acid was used as a reagent. Yellow solid. 107 mg, 76%. ^1H NMR (500 MHz, CDCl_3) δ 9.69 (s, 1H), 9.52 (s, 1H), 7.89 (dd, $J = 3.0, 1.2$ Hz, 1H), 7.49 (dd, $J = 5.1,$

1.2 Hz, 1H), 7.42 – 7.30 (m, 6H), 6.26 (s, 1H), 4.56 (d, $J = 5.4$ Hz, 2H), 2.08 (s, 2H), 1.63 (s, 6H), 0.99 (s, 9H). ^{13}C NMR (126 MHz, CDCl_3) δ 154.88, 154.61, 153.25, 142.21, 136.90, 129.19, 128.05, 127.38, 126.59, 126.56, 126.28, 91.99, 56.68, 51.59, 47.61, 32.02, 31.72, 30.16. MS (ESI) calculated for $\text{C}_{24}\text{H}_{31}\text{N}_4\text{O}_2\text{S}$, m/z 439.2162, found 439.2183 $[\text{M}+\text{H}]^+$.

22f: 1-Benzyl-2-butyl-6-(thiophen-3-yl)-*N*-(2,4,4-trimethylpentan-2-yl)-1*H*-imidazo[4,5-*c*]pyridin-4-amine. Brown solid. 25 mg, 35%. ^1H NMR (500 MHz, CDCl_3) δ 7.79 (dd, $J = 3.1, 1.2$ Hz, 1H), 7.58 (dd, $J = 5.0, 1.2$ Hz, 1H), 7.33 – 7.27 (m, 4H), 7.06 (d, $J = 6.6$ Hz, 2H), 6.79 (s, 1H), 5.35 (s, 1H), 5.25 (s, 2H), 2.78 – 2.70 (m, 2H), 2.17 (s, 2H), 1.70 (dd, $J = 8.7, 7.0$ Hz, 3H), 1.67 (s, 6H), 1.38 (dq, $J = 14.7, 7.4$ Hz, 2H), 1.26 (dd, $J = 8.7, 5.6$ Hz, 1H), 1.02 (s, 9H), 0.89 (t, $J = 7.4$ Hz, 3H). ^{13}C NMR (126 MHz, CDCl_3) δ 153.04, 150.02, 144.89, 144.32, 140.11, 136.13, 129.14, 128.07, 126.45, 126.34, 125.94, 125.41, 121.55, 91.54, 55.43, 51.49, 50.96, 47.26, 31.96, 31.80, 30.26, 30.21, 27.46, 22.71, 13.89. MS (ESI) calculated for $\text{C}_{29}\text{H}_{39}\text{N}_4\text{S}$, m/z 475.2890, found 475.2922 $[\text{M}+\text{H}]^+$.

23f: 1-Benzyl-2-butyl-6-(thiophen-3-yl)-1*H*-imidazo[4,5-*c*]pyridin-4-amine. White solid. 9 mg, 53%. ^1H NMR (500 MHz, MeOD) δ 8.04 (dd, $J = 2.9, 1.4$ Hz, 1H), 7.66 (dd, $J = 5.1, 2.9$ Hz, 1H), 7.58 (dd, $J = 5.1, 1.4$ Hz, 1H), 7.48 (s, 1H), 7.41 – 7.32 (m, 3H), 7.17 (d, $J = 6.9$ Hz, 2H), 5.59 (s, 2H), 2.94 – 2.86 (m, 2H), 1.76 (dt, $J = 15.3, 7.6$ Hz, 2H), 1.41 (dq, $J = 14.8, 7.4$ Hz, 2H), 0.91 (t, $J = 7.4$ Hz, 3H). ^{13}C NMR (126 MHz, MeOD) δ 159.63, 149.38, 144.24, 137.90, 136.73, 135.24, 130.28, 129.42, 129.31, 127.74, 126.73, 126.03, 124.88, 97.21, 49.07, 29.96, 27.94, 23.26, 14.03. HRMS (ESI) calculated for $\text{C}_{21}\text{H}_{23}\text{N}_4\text{S}$, m/z 363.1638, found 363.1686 $[\text{M}+\text{H}]^+$.

20g: *N*^{4,6}-Dibenzyl-3-nitro-*N*²-(2,4,4-trimethylpentan-2-yl)pyridine-2,4-diamine. Benzyl boronic acid pinacol ester was used as a reagent. Orange oil. 135 mg, 91%. ^1H NMR (500 MHz,

CDCl₃) δ 9.54 (t, *J* = 5.0 Hz, 1H), 9.37 (s, 1H), 7.36 (ddd, *J* = 7.4, 4.5, 1.4 Hz, 2H), 7.31 (dt, *J* = 9.8, 4.4 Hz, 1H), 7.27 (ddd, *J* = 6.7, 3.3, 1.4 Hz, 5H), 7.22 – 7.18 (m, 3H), 5.75 (s, 1H), 4.40 (d, *J* = 5.4 Hz, 2H), 3.75 (s, 2H), 1.89 (s, 2H), 1.49 (s, 6H), 0.90 (s, 9H). ¹³C NMR (126 MHz, CDCl₃) δ 164.70, 154.68, 152.84, 138.77, 136.80, 129.45, 129.07, 128.54, 127.91, 127.46, 126.50, 124.96, 115.72, 94.56, 56.63, 51.05, 47.44, 45.61, 31.87, 31.60, 30.09, 24.86. MS (ESI) calculated for C₂₇H₃₅N₄O₂, *m/z* 447.2755, found 447.2737 [M+H]⁺.

22g: 1,6-Dibenzyl-2-butyl-*N*-(2,4,4-trimethylpentan-2-yl)-1*H*-imidazo[4,5-*c*]pyridin-4-amine.

Light brown solid. 55 mg, 60%. ¹H NMR (500 MHz, CDCl₃) δ 7.33 – 7.27 (m, 5H), 7.24 (t, *J* = 7.6 Hz, 2H), 7.14 (t, *J* = 7.3 Hz, 1H), 7.01 (d, *J* = 6.4 Hz, 2H), 6.31 (s, 1H), 5.22 (s, 1H), 5.16 (s, 2H), 3.96 (s, 2H), 2.74 – 2.67 (m, 2H), 2.02 (s, 2H), 1.66 – 1.61 (m, 2H), 1.56 (s, 6H), 1.35 (dd, *J* = 15.0, 7.5 Hz, 2H), 0.93 (s, 9H), 0.86 (t, *J* = 7.4 Hz, 3H). ¹³C NMR (126 MHz, CDCl₃) δ 152.37, 151.90, 150.06, 141.57, 140.10, 136.28, 129.31, 129.06, 128.21, 127.95, 126.38, 125.78, 124.94, 93.59, 55.35, 50.98, 47.19, 45.39, 31.85, 31.68, 30.41, 30.27, 27.42, 22.67, 13.87. MS (ESI) calculated for C₃₂H₄₃N₄, *m/z* 483.3482, found 483.3526 [M+H]⁺.

23g: 1,6-Dibenzyl-2-butyl-1*H*-imidazo[4,5-*c*]pyridin-4-amine. White solid. 23 mg, 58%. ¹H NMR (500 MHz, DMSO) δ 13.63 (s, 1H), 8.27 (s, 2H), 7.37 – 7.29 (m, 7H), 7.27 – 7.23 (m, 1H), 7.15 (s, 1H), 7.11 (d, *J* = 6.9 Hz, 2H), 5.52 (s, 2H), 4.08 (s, 2H), 2.86 – 2.79 (m, 2H), 1.61 (dt, *J* = 15.3, 7.6 Hz, 2H), 1.31 (dt, *J* = 14.9, 7.4 Hz, 2H), 0.81 (t, *J* = 7.4 Hz, 3H). ¹³C NMR (126 MHz, DMSO) δ 156.72, 148.03, 142.12, 141.72, 137.39, 135.93, 128.96, 128.72, 128.70, 127.92, 126.98, 126.63, 123.29, 97.60, 46.84, 40.11, 38.20, 28.89, 26.28, 21.69, 13.61. HRMS (ESI) calculated for C₂₄H₂₇N₄, *m/z* 371.2230, found 371.2285 [M+H]⁺.

20h: *N*⁴-Benzyl-6-(4-methylbenzyl)-3-nitro-*N*²-(2,4,4-trimethylpentan-2-yl)pyridine-2,4-diamine. 4-Methyl benzylboronic acid pinacol ester was used as a reagent. Yellow oil. 130 mg, 91%. ¹H NMR (500 MHz, CDCl₃) δ 9.52 (t, *J* = 5.0 Hz, 1H), 9.37 (s, 1H), 7.37 – 7.30 (m, 3H), 7.28 – 7.24 (m, 3H), 7.10 – 7.03 (m, 7H), 5.74 (s, 1H), 4.39 (d, *J* = 5.4 Hz, 2H), 3.70 (s, 2H), 2.31 (s, 3H), 1.90 (s, 2H), 1.51 (s, 6H), 0.90 (s, 9H). ¹³C NMR (126 MHz, CDCl₃) δ 165.00, 154.68, 152.83, 136.82, 135.98, 135.70, 135.50, 134.26, 129.28, 129.23, 129.12, 129.05, 128.98, 127.89, 127.47, 115.70, 94.47, 83.50, 56.63, 51.03, 47.44, 45.22, 31.87, 31.57, 30.12, 24.87, 21.19, 21.11. MS (ESI) calculated for C₂₈H₃₇N₄O₂, *m/z* 461.2911, found 461.3003 [M+H]⁺.

23h: 1-Benzyl-2-butyl-6-(4-methylbenzyl)-1*H*-imidazo[4,5-*c*]pyridin-4-amine. White solid. 19 mg, 66%. ¹H NMR (500 MHz, MeOD) δ 7.38 – 7.32 (m, 3H), 7.16 (d, *J* = 7.9 Hz, 2H), 7.13 – 7.08 (m, 4H), 6.89 (s, 1H), 5.49 (s, 2H), 4.08 (s, 2H), 2.92 – 2.87 (m, 2H), 2.32 (s, 3H), 1.76 (dt, *J* = 15.3, 7.6 Hz, 2H), 1.40 (dt, *J* = 14.8, 7.4 Hz, 2H), 0.91 (t, *J* = 7.4 Hz, 3H). ¹³C NMR (126 MHz, MeOD) δ 159.11, 149.35, 144.27, 143.93, 138.37, 136.53, 134.52, 130.68, 130.25, 129.85, 129.42, 127.74, 124.41, 99.41, 39.40, 30.01, 27.84, 23.26, 21.08, 14.03. HRMS (ESI) calculated for C₂₅H₂₉N₄, *m/z* 385.2387, found 385.2451 [M+H]⁺.

20i: *N*⁴-Benzyl-3-nitro-6-(4-(trifluoromethoxy)benzyl)-*N*²-(2,4,4-trimethylpentan-2-yl)pyridine-2,4-diamine. 4-(Trifluoromethoxy)benzylboronic acid pinacol ester was used as a reagent. Yellow solid. 115 mg, 70%. ¹H NMR (500 MHz, CDCl₃) δ 9.57 (t, *J* = 5.0 Hz, 1H), 9.37 (s, 1H), 7.38 – 7.29 (m, 3H), 7.28 (t, *J* = 1.8 Hz, 2H), 7.21 – 7.17 (m, 2H), 7.10 (d, *J* = 7.9 Hz, 2H), 5.74 (s, 1H), 4.43 (d, *J* = 5.5 Hz, 2H), 1.83 (s, 2H), 1.45 (s, 6H), 0.88 (s, 9H). ¹³C NMR (126 MHz, CDCl₃) δ 163.87, 154.70, 152.91, 137.54, 136.71, 130.77, 129.10, 127.95, 127.33, 121.09, 115.75, 94.57, 56.63, 50.96, 47.44, 44.69, 31.82, 31.55, 30.02. MS (ESI) calculated for C₂₈H₃₄F₃N₄O₃, *m/z* 531.2578, found 531.2738 [M+H]⁺.

23i: 1-Benzyl-2-butyl-6-(4-(trifluoromethoxy)benzyl)-1*H*-imidazo[4,5-*c*]pyridin-4-amine.

White solid. 21 mg, 47%. ¹H NMR (500 MHz, CDCl₃) δ 7.37 – 7.29 (m, 5H), 7.21 (d, *J* = 8.0 Hz, 2H), 7.08 (d, *J* = 6.5 Hz, 2H), 6.79 (s, 1H), 5.45 (s, 2H), 4.09 (s, 2H), 2.87 (dd, *J* = 9.3, 6.1 Hz, 2H), 1.74 (dt, *J* = 15.3, 7.6 Hz, 2H), 1.41 (dt, *J* = 15.0, 7.4 Hz, 2H), 0.91 (t, *J* = 7.4 Hz, 3H). ¹³C NMR (126 MHz, MeOD) δ 157.96, 150.50, 149.43, 149.42, 143.48, 138.54, 136.96, 131.59, 130.16, 129.25, 127.66, 124.97, 122.37, 99.02, 40.76, 30.29, 27.86, 23.31, 14.05. HRMS (ESI) calculated for C₂₅H₂₆F₃N₄O, *m/z* 455.2053, found 455.2131 [M+H]⁺.

20j: *N*⁴-Benzyl-3-nitro-6-phenethyl-*N*²-(2,4,4-trimethylpentan-2-yl)pyridine-2,4-diamine. 2-

Phenylethylboronic acid was used as a reagent. Yellow oil. 85 mg, 59%. ¹H NMR (500 MHz, CDCl₃) δ 9.52 (t, *J* = 4.9 Hz, 1H), 9.43 (s, 1H), 7.36 (t, *J* = 7.2 Hz, 2H), 7.33 – 7.28 (m, 4H), 7.27 – 7.25 (m, 3H), 7.19 (d, *J* = 7.3 Hz, 1H), 7.17 (d, *J* = 7.0 Hz, 2H), 5.69 (s, 1H), 4.39 (d, *J* = 5.4 Hz, 2H), 2.99 (dd, *J* = 9.1, 6.8 Hz, 2H), 2.75 (dd, *J* = 9.1, 6.8 Hz, 2H), 2.04 (s, 2H), 1.58 (s, 6H), 0.98 (s, 9H). ¹³C NMR (126 MHz, CDCl₃) δ 165.06, 154.74, 152.65, 141.77, 136.85, 129.09, 128.52, 128.49, 127.95, 127.39, 126.10, 115.78, 94.52, 56.68, 51.35, 47.41, 40.87, 34.61, 31.97, 31.69, 30.20. MS (ESI) calculated for C₂₈H₃₇N₄O₂, *m/z* 461.2911, found 461.3096 [M+H]⁺.

23j: 1-Benzyl-2-butyl-6-phenethyl-1*H*-imidazo[4,5-*c*]pyridin-4-amine. Yellow solid. 11 mg,

42%. ¹H NMR (500 MHz, CDCl₃) δ 7.36 – 7.30 (m, 3H), 7.23 – 7.18 (m, 2H), 7.13 (ddd, *J* = 5.7, 3.7, 1.5 Hz, 3H), 7.02 (d, *J* = 6.5 Hz, 2H), 6.68 (s, 1H), 5.38 (s, 2H), 2.99 (s, 4H), 2.85 – 2.79 (m, 2H), 1.69 (ddd, *J* = 13.2, 8.5, 6.7 Hz, 2H), 1.37 (dq, *J* = 14.8, 7.4 Hz, 2H), 0.89 (t, *J* = 7.4 Hz, 3H). ¹³C NMR (126 MHz, MeOD) δ 157.35, 150.48, 148.64, 143.39, 141.89, 137.14, 130.14, 129.53, 129.43, 129.16, 127.59, 127.22, 124.68, 97.93, 48.17, 38.42, 36.84, 30.28, 27.83, 23.31, 14.03. HRMS (ESI) calculated for C₂₅H₂₉N₄, *m/z* 385.2387, found 385.2446 [M+H]⁺.

Synthesis of compound 24: 3-Nitrobenzo[g]quinolin-4-ol. Nitromethane (0.96 mL, 18 mmol) was added dropwise to a solution of NaOH (2.2 g, 54 mmol) in water (5 mL), at 0 °C. The mixture was then warmed to 40 °C and nitromethane (0.96 mL, 18 mmol) was again added slowly at 40-45 °C. The temperature was maintained until a clear solution was obtained. The reaction mixture was then heated to 55 °C for 2-5 minutes, cooled to 30 °C, poured onto crushed ice and acidified with conc. HCl (5 mL). The resultant solution of methazoic acid was added immediately to a filtered solution of 3-amino-2-naphtholic acid (3 g, 16 mmol) and conc. HCl (1 mL) in water (20 mL). The reaction mixture was allowed to stand at room temperature for 12 h. After filtration, the residue obtained was washed with water, and dried (1.1 g, 90%). A solution of intermediate (2 g, 7.75 mmol) in acetic anhydride (10 mL) was placed in a 2-neck flask fitted with a reflux condenser. It was stirred and heated to 105 °C until a clear solution was obtained. Heating was then discontinued and potassium acetate (0.77 g, 7.90 mmol) was added. The mixture was then refluxed for 15 min with vigorous stirring, until a solid started to precipitate. The reaction mixture was then slowly cooled to room temperature. The residue was filtered, washed with glacial acetic acid until the washings were colorless, then suspended in water, filtered, washed with water and dried at 110 °C to get compound **24** (0.93 g, 50%). ¹H NMR (500 MHz, DMSO) δ 13.12 (s, 1H), 9.28 (s, 1H), 8.95 (s, 1H), 8.27 – 8.21 (m, 2H), 8.11 (d, *J* = 8.4 Hz, 1H), 7.69 (t, *J* = 7.1 Hz, 1H), 7.61 (t, *J* = 7.1 Hz, 1H). ¹³C NMR (126 MHz, DMSO) δ 168.61, 144.40, 135.05, 134.63, 130.14, 129.54, 128.94, 128.71, 127.46, 127.41, 126.65, 126.48, 116.78. MS (ESI) calculated for C₁₃H₈N₂O₃, *m/z* 240.05, found 263.04 [M+Na]⁺.

Synthesis of compound 25: 4-Chloro-3-nitrobenzo[g]quinoline. A suspension of compound **24** (2.0 g, 8.30 mmol) in phosphorus(V) oxychloride was placed in a pressure vessel and it was heated at 150 °C. After a clear solution was obtained, the reaction mixture was kept at 150 °C for 1 h. Then it was slowly cooled to room temperature and the solvent was evaporated under

vacuum. The residue was poured over crushed ice while stirring and the formed solid was filtered, washed with water and dried to obtain compound **25** (1.95 g, 91%). ¹H NMR (500 MHz, DMSO) δ 13.34 (d, *J* = 6.9 Hz, 1H), 9.26 (d, *J* = 7.3 Hz, 1H), 8.95 (s, 1H), 8.25 (d, *J* = 9.4 Hz, 2H), 8.11 (d, *J* = 8.4 Hz, 1H), 7.72 – 7.67 (m, 1H), 7.61 (ddd, *J* = 8.1, 6.8, 1.1 Hz, 1H). ¹³C NMR (126 MHz, DMSO) δ 168.64, 144.23, 134.96, 134.64, 130.16, 129.56, 128.98, 128.70, 127.48, 127.43, 126.69, 126.48, 116.74.

Synthesis of compound 26: *N*-Benzyl-3-nitrobenzo[*g*]quinolin-4-amine. To a solution of compound **25** (1.0 g, 3.90 mol) in 20 mL of CH₂Cl₂ was added triethylamine (0.81 mL, 5.80 mmol) and benzylamine (0.50 mL, 4.60 mmol). The reaction mixture was refluxed for 2 h. The solvent was then evaporated under vacuum and H₂O was added to the residue. The solution was extracted with CH₂Cl₂ (3 × 20 mL), washed with water and dried over sodium sulfate. The solvent was evaporated and the residue was purified using silica gel column chromatography (0-5% MeOH in CH₂Cl₂) to obtain compound **26** as a yellow solid (1.1 g, 88%). ¹H NMR (500 MHz, CDCl₃) δ 10.57 (s, 1H), 9.41 (s, 1H), 8.87 (s, 1H), 8.50 (s, 1H), 8.02 (d, *J* = 8.4 Hz, 1H), 7.83 (d, *J* = 8.4 Hz, 1H), 7.65 – 7.60 (m, 1H), 7.55 – 7.51 (m, 1H), 7.50 – 7.47 (m, 4H), 7.42 (ddd, *J* = 11.0, 5.4, 3.0 Hz, 1H), 5.28 (d, *J* = 5.9 Hz, 2H). ¹³C NMR (126 MHz, CDCl₃) δ 152.50, 147.73, 145.88, 136.85, 135.48, 130.53, 129.64, 129.12, 129.03, 128.98, 128.83, 128.11, 128.04, 127.29, 126.86, 124.21, 118.09, 53.19. MS (ESI) calculated for C₂₀H₁₆N₃O₂, *m/z* 330.1237, found 330.1304 [M+H]⁺.

Synthesis of compound 30: 1-Benzyl-2-butyl-1*H*-benzo[*g*]imidazo[4,5-*c*]quinolin-4-amine.

To a solution of compound **26** (300 mg, 0.91 mmol) in 20 mL of MeOH were added zinc dust (594 mg, 9.10 mmol) and ammonium formate (574 mg, 9.10 mmol). The reaction mixture was stirred at room temperature for 30 min and filtered through celite. Then the solvent was

evaporated and the residue was dissolved in water. This was extracted with EtOAc (3 × 20 mL), washed with water and dried over sodium sulfate. The solvent was removed under vacuum to obtain compound **27** (100 mg, 37%). To a solution of compound **27** (98 mg, 0.33 mmol) in 10 mL of anhydrous THF were added triethylamine (48 μL, 0.35 mmol) and valeryl chloride (40 μL, 0.33 mmol). The reaction mixture was refluxed for 2 h. The solvent was then removed under vacuum, and the residue was dissolved in 10 mL of EtOH and NaOH (26 mg, 0.66 mmol) in 1 mL of H₂O was added. The reaction mixture was refluxed for 2 h. The solvent was then removed under vacuum, and the residue was dissolved in EtOAc and washed with water. The EtOAc fraction was dried using sodium sulfate and evaporated and purified using column chromatography (0-10% MeOH in CH₂Cl₂) to obtain the compound **28** (76 mg, 63%). To a solution of compound **28** (76 mg, 0.21 mmol) in a solvent mixture of MeOH:CH₂Cl₂:CHCl₃ (1:10:10) was added 3-chloroperoxy benzoic acid (443 mg, 1.98 mmol), and the solution was refluxed at 45-50 °C for 1 h. The solvent was then removed and the residue was purified using column chromatography (0-10% MeOH in CH₂Cl₂) to obtain the *N*-oxide derivative **29** (64 mg, 80%). To a solution of compound **29** (64 mg, 0.17 mol) in 10 mL of CH₂Cl₂ was added benzoyl isocyanate (37 mg, 0.25 mmol) and heated at 45 °C for 18 h. The solvent was then removed under vacuum, and the residue was dissolved in 15 mL of anhydrous MeOH, followed by the addition of excess sodium methoxide. The reaction mixture was then heated at 80 °C for 2 h. The solvent was removed under vacuum and the residue was purified using column chromatography (0-10% MeOH in CH₂Cl₂) to obtain the compound **30** (20 mg, 30%). ¹H NMR (500 MHz, DMSO) δ 8.40 (s, 1H), 8.05 (s, 1H), 7.88 (d, *J* = 8.3 Hz, 1H), 7.77 (d, *J* = 8.3 Hz, 1H), 7.38 (d, *J* = 7.2 Hz, 1H), 7.33 (dd, *J* = 12.9, 5.2 Hz, 3H), 7.24 (d, *J* = 7.4 Hz, 1H), 7.16 (d, *J* = 7.4 Hz, 2H), 6.91 (s, 2H), 6.02 (s, 2H), 3.00 – 2.92 (m, 2H), 1.74 (dt, *J* = 15.4, 7.6 Hz, 2H), 1.40 (dd, *J* = 14.9, 7.4 Hz, 2H), 0.88 (t, *J* = 7.4 Hz, 3H). ¹³C NMR (126 MHz, DMSO) δ 136.73, 131.80,

128.91, 127.99, 127.81, 127.46, 126.82, 125.81, 123.63, 118.72, 48.20, 29.71, 26.27, 21.85, 13.69. HRMS (ESI) calculated for C₂₅H₂₅N₄, m/z 381.2074, found 381.2089 [M+H]⁺.

Human TLR-7/-8 reporter gene assays (NF- κ B induction). As described in Chapter 2.

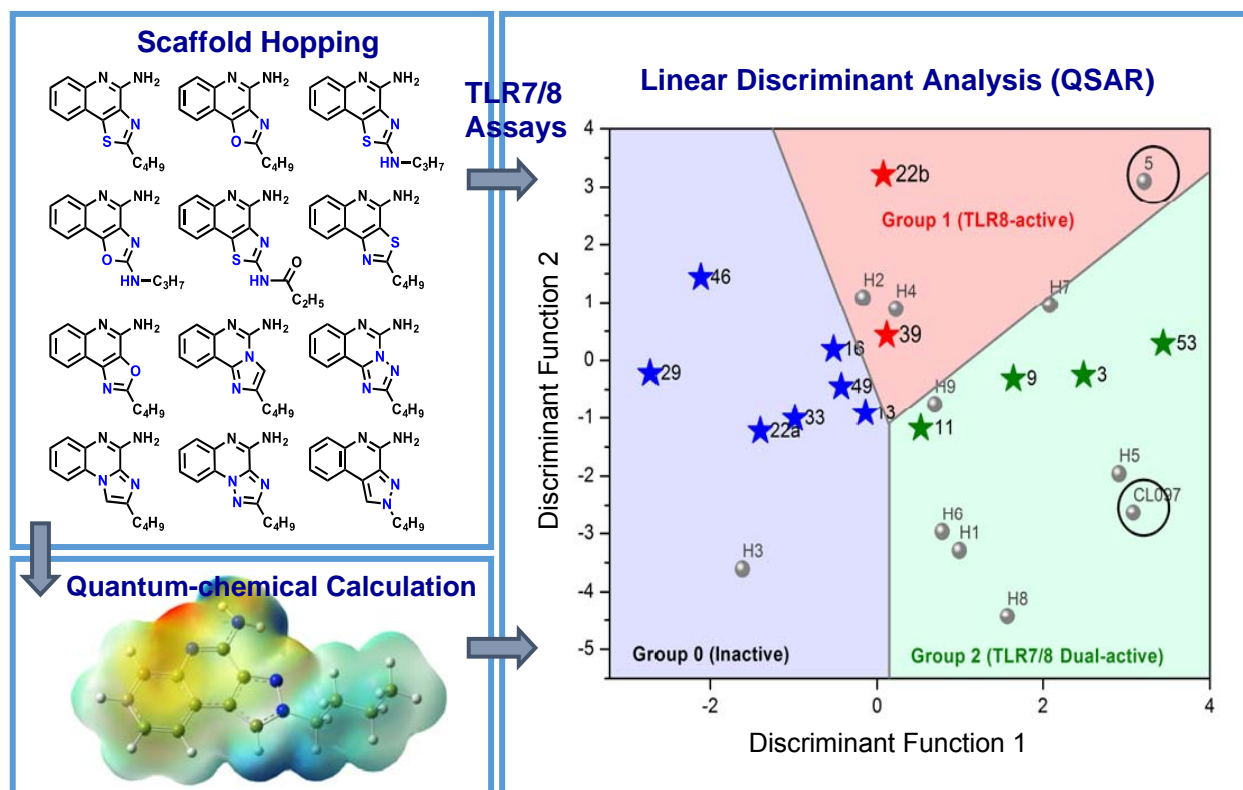
Immunoassays for Interferon (IFN)- α , and cytokines. As described in Chapter 2.

Flow-cytometric immunostimulation experiments. CD69 upregulation was determined by flow cytometry using protocols published by us previously,³⁰ and modified for rapid-throughput. Briefly, heparin-anticoagulated whole blood samples were obtained by venipuncture from healthy human volunteers with informed consent and as per guidelines approved by the University of Kansas Human Subjects Experimentation Committee. Serial dilutions of selected imidazopyridine compounds (and imiquimod, used as a reference compound) were performed using a Bio-Tek Precision 2000 XS liquid handler in sterile 96-well polypropylene plates, to which were added 100 μ L aliquots of anticoagulated whole human blood. The plates were incubated at 37°C for 16.5 h. Negative (endotoxin free water) controls were included in each experiment. Following incubation, fluorochrome-conjugated antibodies (CD3-PE, CD56-APC, CD69-PE-Cy7, 10 μ L of each antibody, Becton-Dickinson Biosciences, San Jose, CA) were added to each well with a liquid handler, and incubated at 37 °C in the dark for 30 min. Following staining, erythrocytes were lysed and leukocytes fixed by mixing 200 μ L of the samples in 2 mL pre-warmed Whole Blood Lyse/Fix Buffer (Becton-Dickinson Biosciences, San Jose, CA) in 96 deep-well plates. After washing the cells twice at 200 g for 8 minutes in saline, the cells were transferred to a 96-well plate. Flow cytometry was performed using a BD FACSAarray instrument in the tri-color mode (tri-color flow experiment) and two-color mode (two-

color flow experiment) for acquisition on 100,000 gated events. Compensation for spillover was computed for each experiment on singly-stained samples. CD69 activation in the major lymphocytic populations, viz., natural killer lymphocytes (NK cells: CD3⁻CD56⁺), cytokine-induced killer phenotype (CIK cells: CD3⁺CD56⁺), B lymphocytes (B cells: CD3⁻CD19⁺).

Chapter 6.

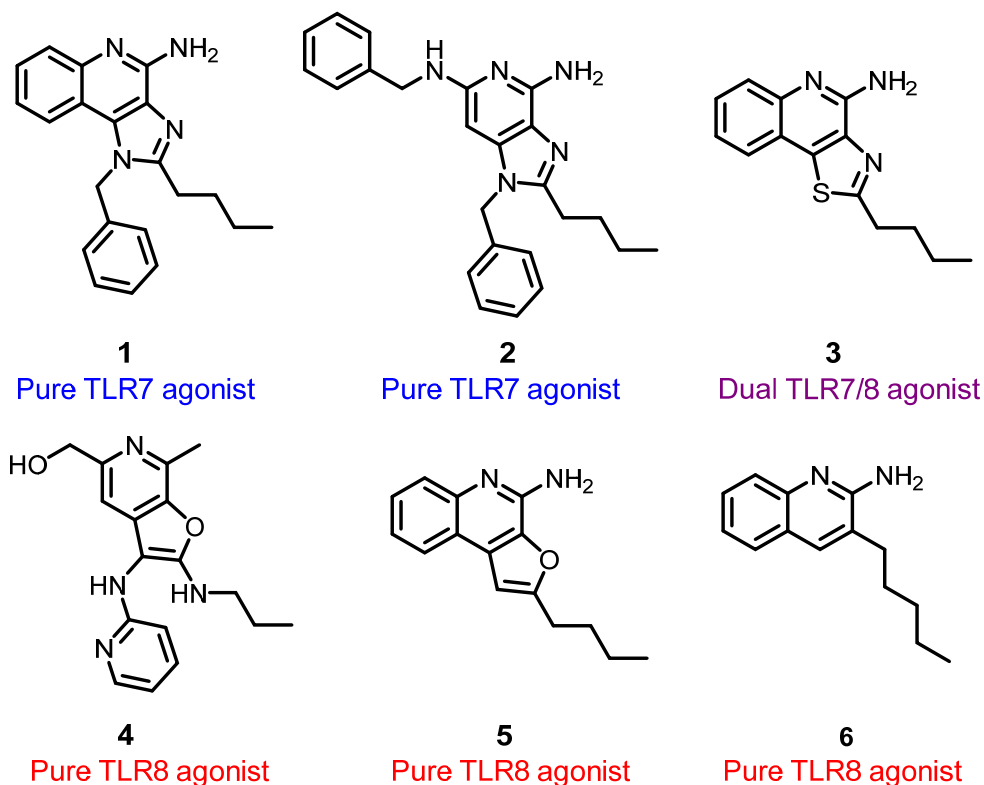
Determinants of activity at human TLR7 and 8: QSAR of diverse heterocyclic scaffolds



6.1. Introduction

Extensive SARs on several TLR7/8-agonistic scaffolds such as imidazo[4,5-*c*]quinolines,^{55b, 69} thiazolo[4,5-*c*]quinolines (Chapter 2),¹¹³ furo[2,3-*c*]pyridines (Chapter 3),¹¹⁴ imidazo[4,5-*c*]pyridines (Chapter 5),¹¹⁵ and furo[2,3-*c*]quinolines¹¹⁶ have been reported from our laboratory (Fig. 1). Recently, a C2-butyl furo[2,3-*c*]quinoline (**5**) having pure TLR8 agonistic activity was cocrystallized with the human TLR8 ectodomain.¹¹⁷ This served as the point of departure toward a focused structure-based ligand design study, leading to the identification of 3-pentylquinoline-2-amine (**6**, Fig. 1) as a novel, structurally simple, and highly potent human TLR8-specific agonist.¹¹⁸

Fig. 1. Structures of representative TLR7 and TLR8 agonists.



Our SAR investigations in several of these scaffolds, while continuing to incrementally improve our understanding of the structural features required for the TLR7/8 activity, pointed strongly also to the strict dependence of the selectivity for TLR7 vis-à-vis TLR8 on the electronic configurations of the heterocyclic systems, the nuances of which we desired to examine quantitatively with the goal of developing 'heuristics' to clearly define structural requisites governing activity at TLR7 and/or TLR8. In order to systematically examine the effect of electronic properties on the activity profiles, we undertook a scaffold hopping approach,¹¹⁹ which entailed the syntheses and biological evaluations of thirteen different chemotypes including oxazolo[4,5-*c*]quinoline, thiazolo/oxazolo[4,5-*c*]quinolin-2-amines, thiazolo/oxazolo[5,4-*c*]quinolines, imidazo[1,2-*c*]quinazoline, [1,2,4]triazolo[1,5-*c*]quinazoline, imidazo[1,2-*a*]quinoxaline, [1,2,4]triazolo[1,5-*a*]quinoxaline, [1,2,4]-triazolo[4,3-*a*]quinoxaline, and pyrazolo[3,4-*c*]quinoline.

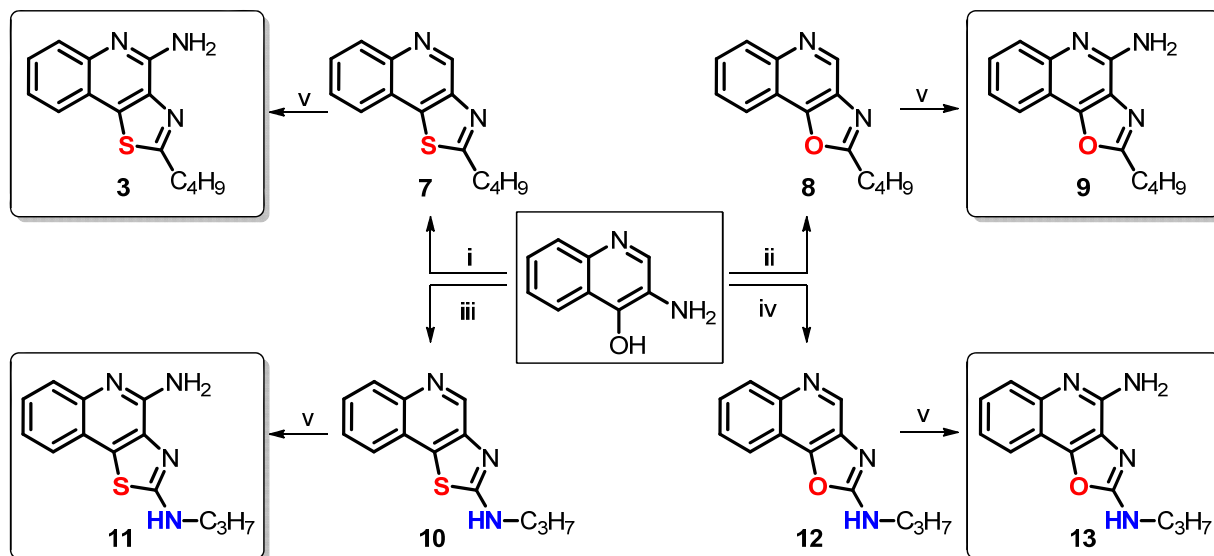
Crystal structures of TLR8 in complex with two most active compounds confirmed important binding interactions playing a key role in ligand occupancy and biological activity. Reasoning that stereo-electronic effects of heterocyclic ring systems could have a profound effect on the biological activity of TLR7/8 modulators, we undertook studies of three-dimensional molecular electrostatic potential (MESP) in an effort to obtain complementary and/or mechanistic information in characterizing active molecules.¹²⁰ Density functional theory (DFT) based quantum chemical calculations and linear discriminant analyses were therefore performed. These studies allowed, for the first time, a clear delineation of inactive, TLR8-active and TLR7/8 dual active compounds, confirming the critical role of partial charges in determining biological activity.

6.2. Results and Discussion

As mentioned earlier, a number of leads including pure TLR7 agonists (**1** and **2**), dual TLR7/8 agonist (**3**), and pure TLR8 agonists (**4**, **5**, and **6**) are undergoing preclinical evaluation as vaccine adjuvants in our laboratory. Our earlier structure-activity relationship studies on the imidazo[4,5-*c*]quinolines,^{55b, 69} thiazolo[4,5-*c*]quinolines,¹¹³ furo[2,3-*c*]pyridines,¹¹⁴ as well as furo[2,3-*c*]quinolines¹¹⁶ had all converged on the optimal chain length for the C2 alkyl substituent being butyl. Our goal was therefore to examine the electronic effects of heterocyclic modifications, while holding the substituent at the C2 position invariant at 4 atoms.

We envisioned that a reagent-based diversification approach¹²¹ could allow us to access to several different heterocyclic scaffolds (including the thiazolo[4,5-*c*]quinolines) with substantial variations in the electronic configurations (Scheme 1). Employing this diversification strategy, the previously described 2-butylthiazolo[4,5-*c*]quinoline was synthesized from aminoquinolin-4-ol and valeroyl chloride via a one-pot, sequential reaction involving acylation and subsequent microwave-accelerated (120 °C, 600 W) cyclization using P₂S₅ (**7**, Scheme 1), while replacement of P₂S₅ with P₂O₅ in this reaction resulted in its congener **8** (2-butyloxazolo[4,5-*c*]quinoline) in moderate yield. Microwave-assisted cyclization also yielded *N*-propylthiazolo[4,5-*c*]quinolin-2-amine **10** using propyl isothiocyanate, whereas conventional heating was unsuccessful. The synthesis of *N*-propyloxazolo[4,5-*c*]quinolin-2-amine **12** using P₂O₅ led to the formation of a mixture of compounds with very poor yields; substituting *N*-(3-dimethylamino propyl)-*N'*-ethylcarbodiimide (EDC) for P₂O₅ in this reaction not only worked as a sulfur scavenger, but greatly enhanced yields of the desired oxazolo analog **12** (Scheme 1). The C4 amine functionality was then installed using conventional methods^{69, 113} to furnish the 2-butyloxazolo[4,5-*c*]quinolin-4-amine **9**, the *N*-propylthiazolo[4,5-*c*]quinoline-2,4-diamine **11**, and the *N*-propyloxazolo[4,5-*c*]quinoline-2,4-diamine **13**.

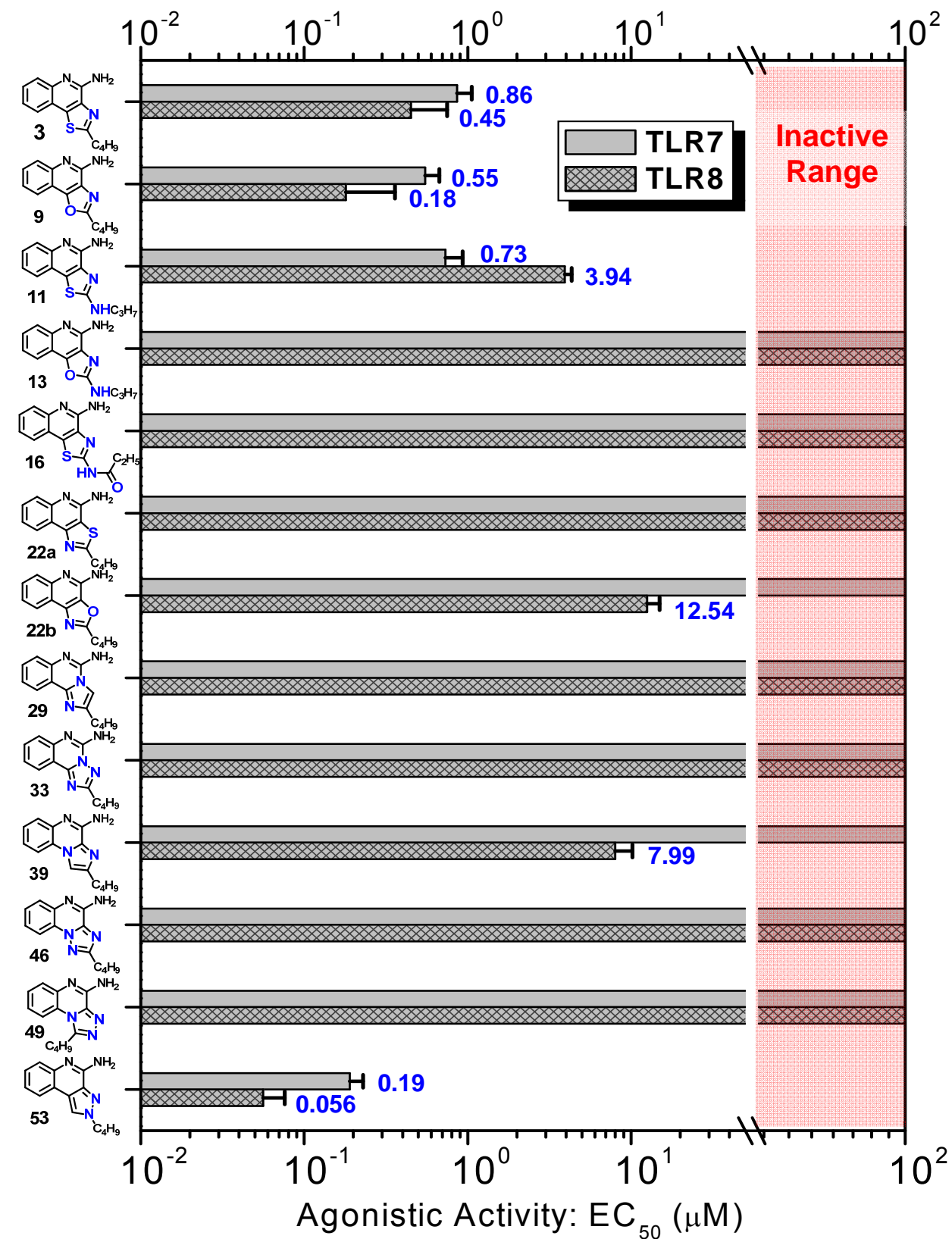
Scheme 1. Synthesis of thiazolo/oxazolo[4,5-*c*]quinolin-4-amines using reagent-based diversification.



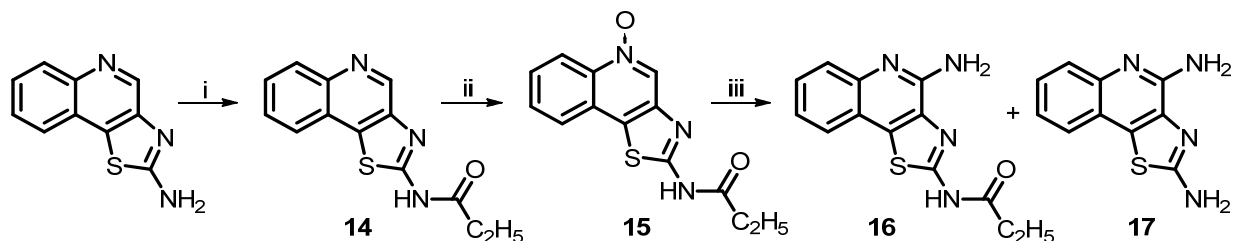
Reagents and conditions: i. (a) C_4H_9COCl , Pyridine, 50 °C, 1 h (b) P_2S_5 , 120 °C, MW, 1 h; ii. (a) C_4H_9COCl , Pyridine, 50 °C, 1h (b) P_2O_5 , 120 °C, MW, 1 h; iii. (a) C_3H_7NCS , Pyridine, 50 °C, 30 min (b) P_2S_5 , 120 °C, MW, 30 min; iv. (a) C_3H_7NCS , Pyridine, 50 °C, 30 min (b) EDC, 120 °C, MW, 30 min; v. (a) *m*CPBA, $CHCl_3$, 25 °C, 4 h (b) Benzoyl isocyanate, CH_2Cl_2 , 45 °C, 1.5 h (c) CH_3ONa , MeOH, 70 °C, 30 min.

The 2-butyl-oxazolo[4,5-*c*]quinolin-4-amine **9** displayed more potent dual TLR7/8-agonistic activity compared to the thiazolo[4,5-*c*]quinolin-4-amine **3**, with EC_{50} values of 0.55 μ M and 0.18 μ M in TLR7 and TLR8 assays, respectively (Fig. 2). The *N*-propylthiazolo[4,5-*c*]quinoline-2,4-diamine **11**, however, exhibited comparable TLR7-agonistic activity (EC_{50} : 0.73 μ M), but a ten-fold reduction in TLR8 potency (EC_{50} : 3.94 μ M). Astonishingly, the *N*-propyl-oxazolo[4,5-*c*]quinolin-2,4-diamines **13** was entirely devoid of any detectable TLR7- or TLR8-agonistic activity. The C2 *N*-acyl derivative, *N*-(4-aminothiazolo[4,5-*c*]quinolin-2-yl)propionamide **16** and its des-acyl analog **17** were synthesized from commercially-available thiazolo[4,5-*c*]quinolin-2-amine (Scheme 2). These compounds were also found to be inactive in cell based assays (Fig. 2).

Fig. 2. TLR7- and TLR8-agonistic potencies (EC_{50} values) of the compounds determined in TLR-specific reporter gene assays. Means and standard deviations on quadruplicate samples are depicted.



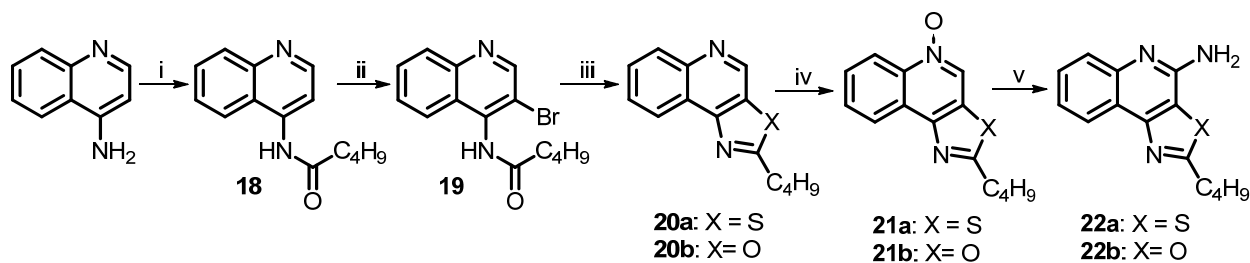
Scheme 2. Synthesis of C2 N-acyl derivative **16** and its des-acyl analog **17**.



Reagents and conditions: i. $\text{C}_2\text{H}_5\text{COCl}$, Pyridine, 25 °C, 1 h; ii. *m*CPBA, CHCl_3 , 25 °C, 4 h; iii. (a) Benzoyl isocyanate, CH_2Cl_2 , 45 °C, 1.5 h (b) CH_3ONa , MeOH, 70 °C, 30 min.

The dramatic (and rather unexpected) differences in activity profiles of the closely-related congeners warranted a detailed investigation of analogues with variable electronic properties. We first synthesized and evaluated the regioisomeric 2-butylthiazolo[5,4-*c*]quinolin-4-amine **22a** and 2-butylloxazolo[5,4-*c*]quinolin-4-amine **22b** (Scheme 3). The thiazolo[5,4-*c*]quinoline derivative (**22a**) was completely inactive in both TLR7 and TLR8 agonism assays and the oxazolo[5,4-*c*]quinoline derivative (**22b**) was found to possess negligibly low TLR8-agonistic activity. This result, too, was unexpected, given that we had observed prominent and selective TLR8 agonism in the 2-butylfuro[2,3-*c*]quinolin-4-amine **5**,¹¹⁶ but further strengthened the case for a systematic exploration of the role of electron densities in the heterocyclic core in determining TLR7/8 activity.

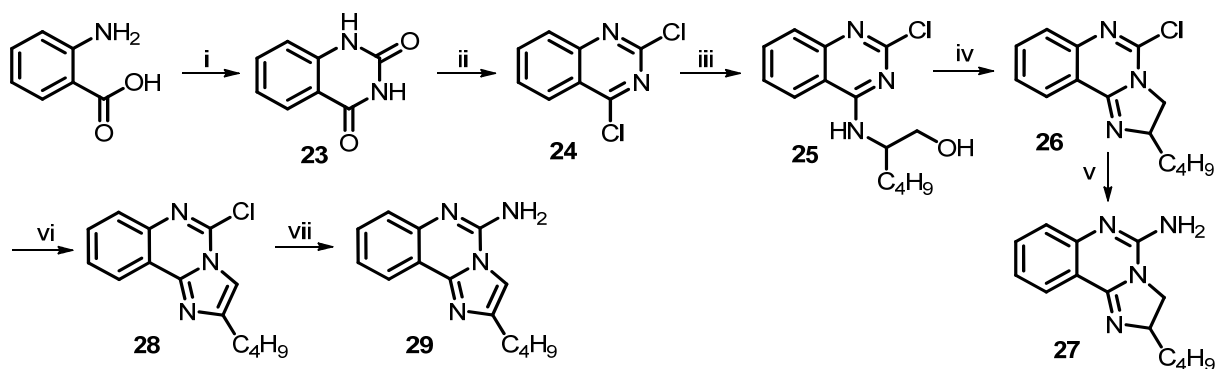
Scheme 3. Synthesis of regioisomeric thiazolo/oxazolo[5,4-*c*]quinolin-4-amines.



Reagents and conditions: i. $\text{C}_4\text{H}_9\text{COCl}$, Pyridine, 65 °C, 1.5 h; ii. NBS, AIBN, Benzene, 85 °C, 5 h; iii. For **a**, Lawesson's reagent, Pyridine, MW, 140 °C, 35 min; For **b**, CuI , K_2CO_3 , Pyridine, MW, 140 °C, 35 min; iv. *m*CPBA, CH_2Cl_2 , 25 °C, 4 h; v. (a) Benzoyl isocyanate, CH_2Cl_2 , 45 °C, 3 h (b) CH_3ONa , CH_3OH , 70 °C, 8 h.

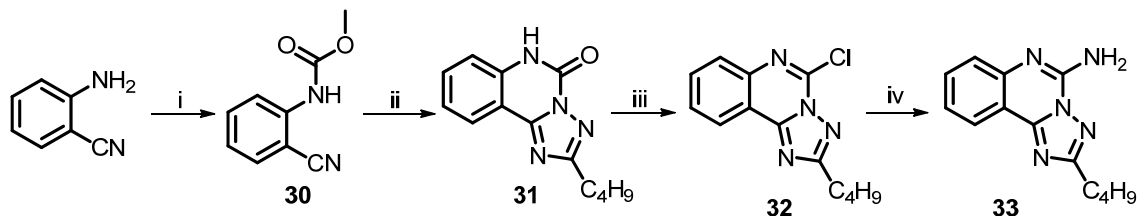
Further scaffold modifications were therefore carried out based on the pure TLR7-agonistic lead molecule 1-benzyl-2-butyl-1*H*-imidazo[4,5-*c*]quinolin-4-amine **1** (Fig.1). ‘Repositioning’ of the nitrogen atoms in the imidazole ring as well as triazole analogues were designed and synthesized (Schemes 4-8).¹²² The novel analogues 2,3-dihydroimidazo[1,2-*c*]quinazoline **27** and imidazo[1,2-*c*]quinazoline **29**, with an altered imidazole fused ring (Scheme 4) were entirely inactive (Fig. 2). We sought to examine if activity could be restored by incorporating an additional nitrogen atom in ring system, but the triazole analogue **33** (2-butyl-[1,2,4]triazolo[1,5-*c*]quinazolin-5-amine, Scheme 5) was also inactive. On the other hand, the 1,2-dihydroimidazo[1,2-*a*]quinoxaline **37** and the imidazo[1,2-*a*]quinoxaline **39** shown in Scheme 6 were found to be selective TLR8 agonists with EC₅₀ values of 3.05 μM and 7.99 μM, respectively (Fig. 2).

Scheme 4. Synthesis of imidazo[1,2-*c*]quinazolines.



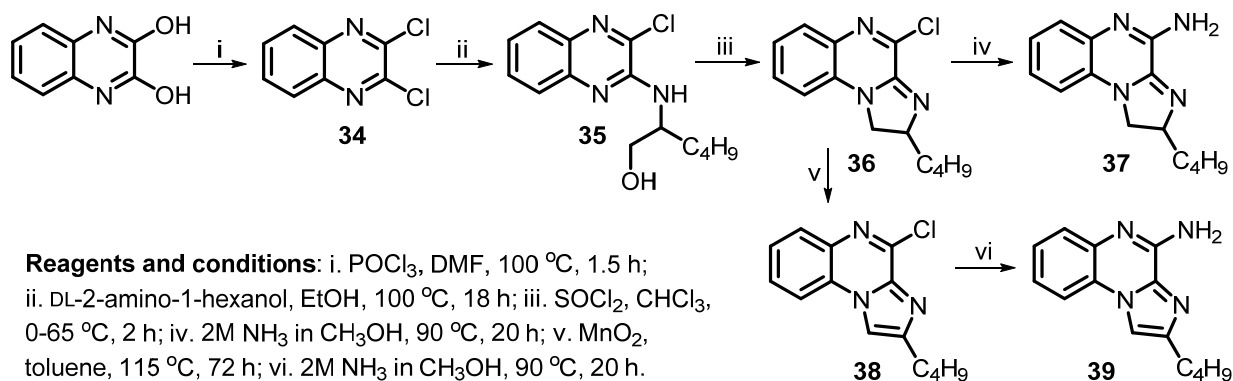
Reagents: i. Urea; ii. DIPEA, POCl₃; iii. DL-2-amino-1-hexanol, DMAP, DIPEA, DMF; iv. NEt₃, CH₃SO₂Cl, CH₂Cl₂; v. 2M NH₃ in CH₃OH; vi. MnO₂, toluene; vii. 2M NH₃ in CH₃OH.

Scheme 5. Synthesis of [1,2,4]triazolo[1,5-*c*]quinazoline.



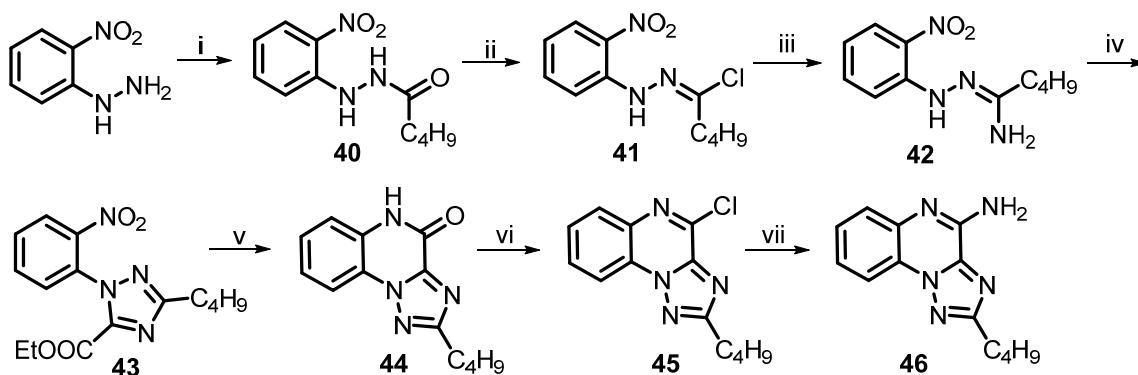
Reagents: i. Methyl chloroformate, Na₂CO₃; ii. Valeric acid hydrazide, NMP; iii. DIPEA, POCl₃; iv. 2M NH₃ in CH₃OH.

Scheme 6. Synthesis of imidazo[1,2-*a*]quinoxalines.

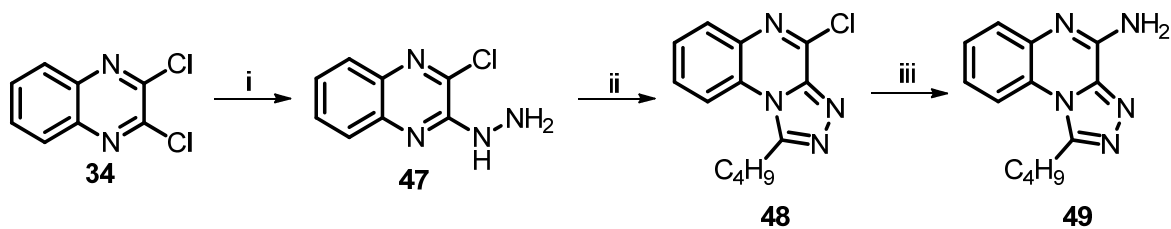


Transitioning from the imidazo[1,2-*a*]quinoxaline scaffold to two other triazolo analogues (**46** in Scheme 7 and **49** in Scheme 8) also resulted in complete loss of activity.

Scheme 7. Synthesis of [1,2,4]triazolo[1,5-*a*]quinoxaline.

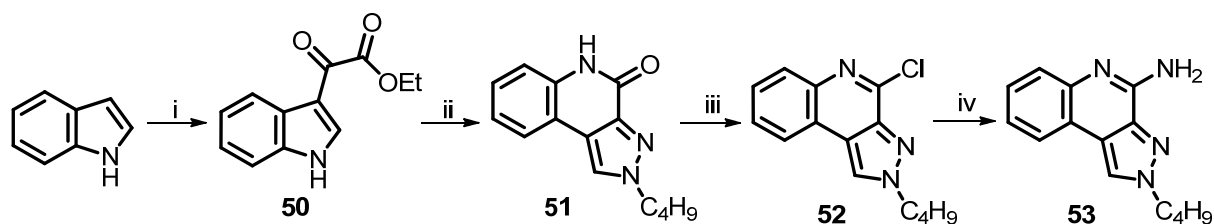


Scheme 8. Synthesis of [1,2,4]triazolo[4,3-*a*]quinoxaline.



Our scaffold-hopping approach also led us to synthesize 2-butyl-2*H*-pyrazolo[3,4-*c*]quinolin-4-amine **53** (Scheme 9). Compound **53** was found to be extraordinarily potent as a TLR7 agonist (EC_{50} : 0.19 μ M), significantly greater than that of the thiazoloquinoline **3** (EC_{50} : 0.86 μ M), the oxazoloquinoline **9** (EC_{50} : 0.55 μ M), and the aminothiazoloquinoline **11** (EC_{50} : 0.73 μ M), and approaching that of our best-in-class, pure TLR7 agonistic imidazoquinoline **1** (EC_{50} : 0.059 μ M). Furthermore, the pyrazolo[3,4-*c*]quinoline **53** was also found to be the most potent in TLR8 agonism assays (EC_{50} : 0.056 μ M) among all TLR8-active compounds that we had hitherto characterized (Fig. 2).

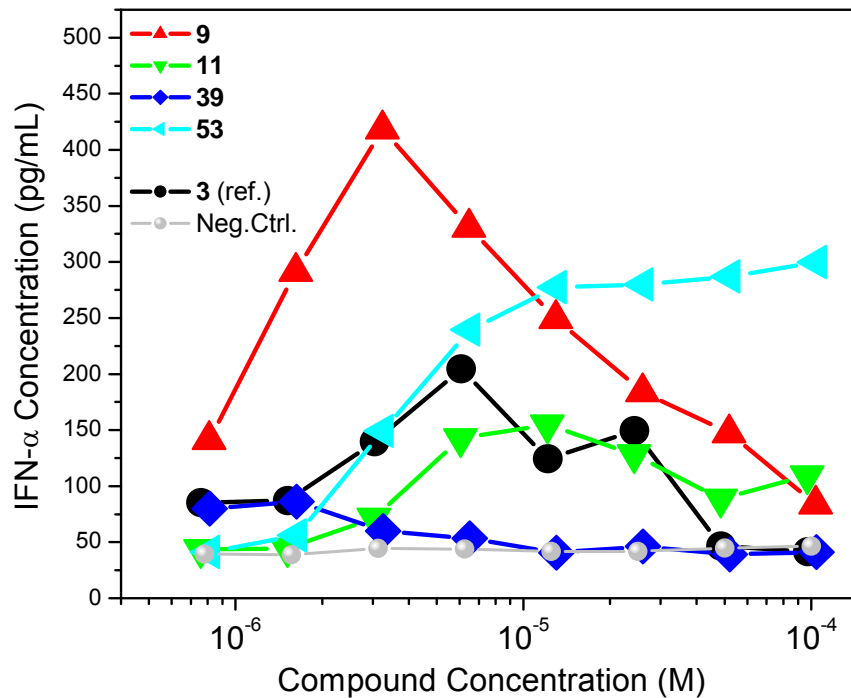
Scheme 9. Synthesis of pyrazolo[3,4-*c*]quinoline.



Reagents: i. Ethyl chlorooxoacetate, pyridine, Et_2O ; ii. Butylhydrazine.HCl, EtOH, CH_3COOH ; iii. PCl_5 , $POCl_3$; iv. 2M NH_3 in CH_3OH .

We confirmed TLR7/8 selectivity and potency of the active compounds in secondary screens including cytokine-inducing properties in human PBMCs, as well as cellular activation in ex vivo whole human blood. In IFN- α induction assays, as expected and in accordance with our previous SAR, compounds with TLR7 agonistic activity (**9**, **11**, and **53**) showed IFN- α inducing ability and the TLR8 selective compound **39** did not (Fig. 3).

Fig. 3. Dose-response profiles of IFN- α induction by the active compounds in human PBMCs. Means on triplicate samples of a representative experiment are shown.



We also found strong Type II IFN (IFN- γ), cytokine (IL-1 α , IL-1 β , IL-6, IL-10, TNF- α), and chemokine (IP-10/CXCL-10, MCP-1, MIP-1 β) induction by the active compounds consistent with their TLR7/8 selectivity profiles (Fig. 4). The extraordinary potency of **53** was also manifested in CD69 expression in whole blood assays, showing dramatically enhanced expression in cytokine-induced killer-, natural killer-, T-, and B-lymphocytic subsets (Fig. 5).

Fig. 4. Cytokine and chemokine induction profiles in human PBMCs stimulated with 10 μ M of select compounds. Means on triplicate samples of a representative experiment are shown.

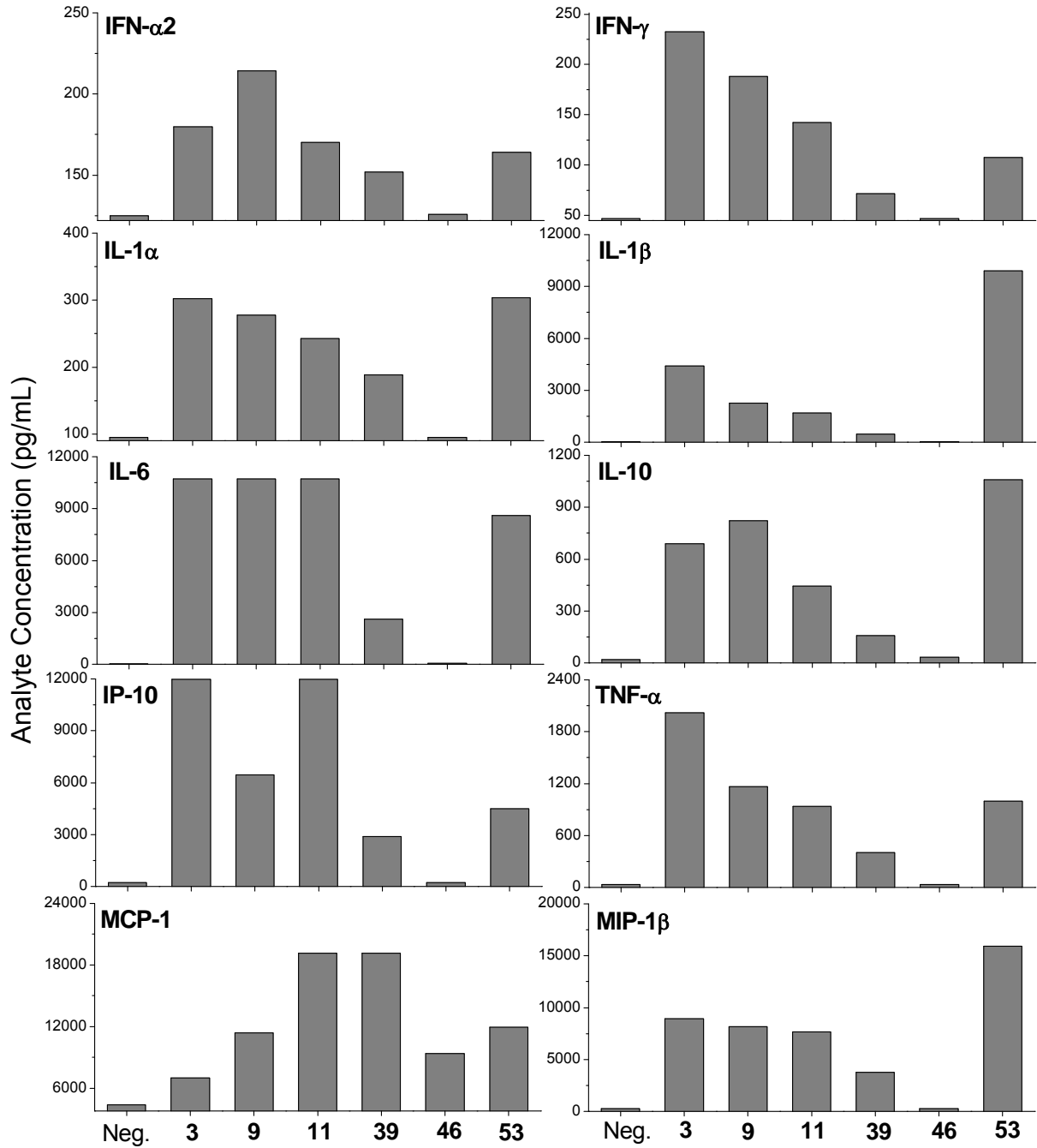
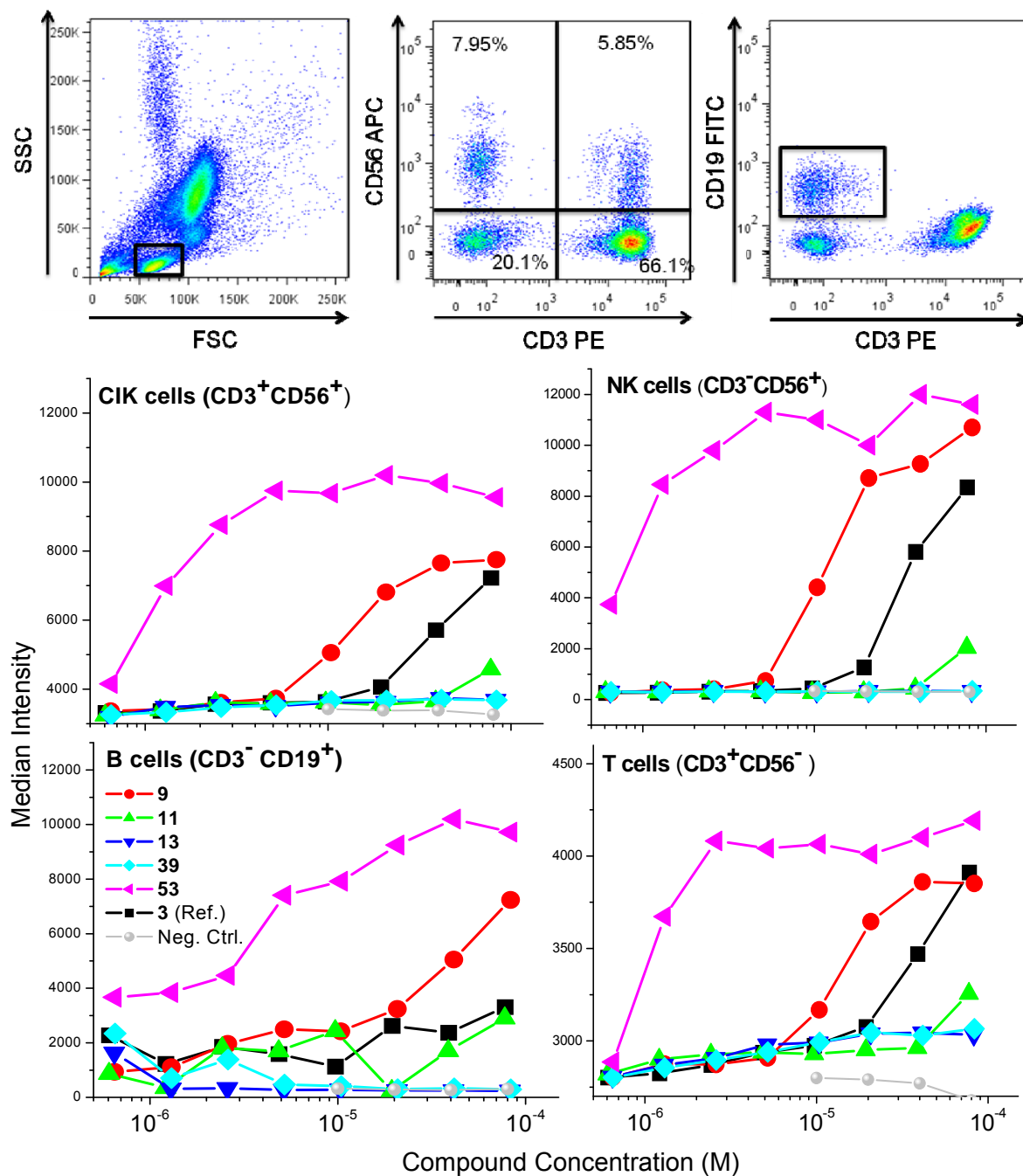


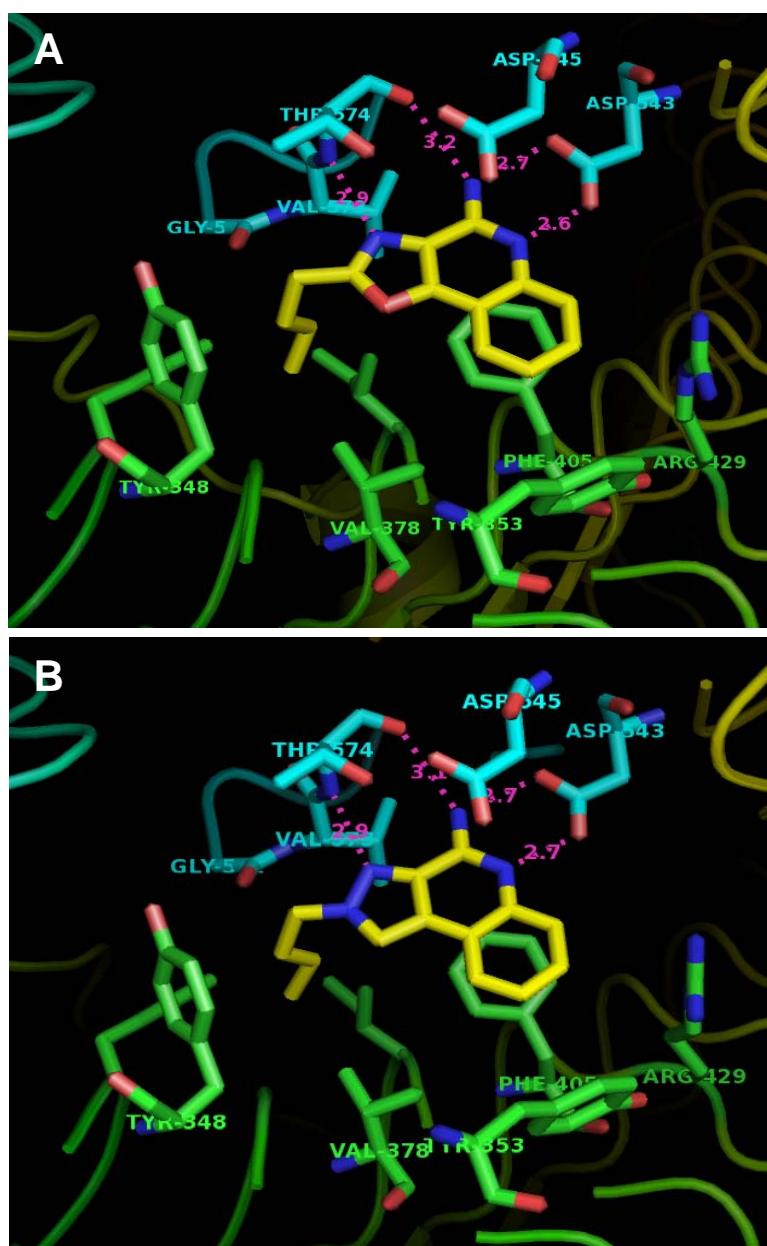
Fig. 5. CD69 upregulation in human lymphocytic subsets by active analogues.



We were fortunate in also being able to obtain the crystal structures of TLR8 in complex with the two most active compounds: the oxazoloquinoline **9** and the pyrazoloquinoline **53**. An examination of TLR8 liganded with **9** and **53** confirmed near-identical binding geometries of the

two compounds (Fig. 6). Major interactions include hydrogen bonding of the amidine group with Asp543 and the N atom of the oxazole/pyrazole ring with Thr574, π - π interactions of the quinoline ring with Phe405, and hydrophobic interactions of the alkyl chain in a pocket formed by Tyr348, Val378, and Phe405.

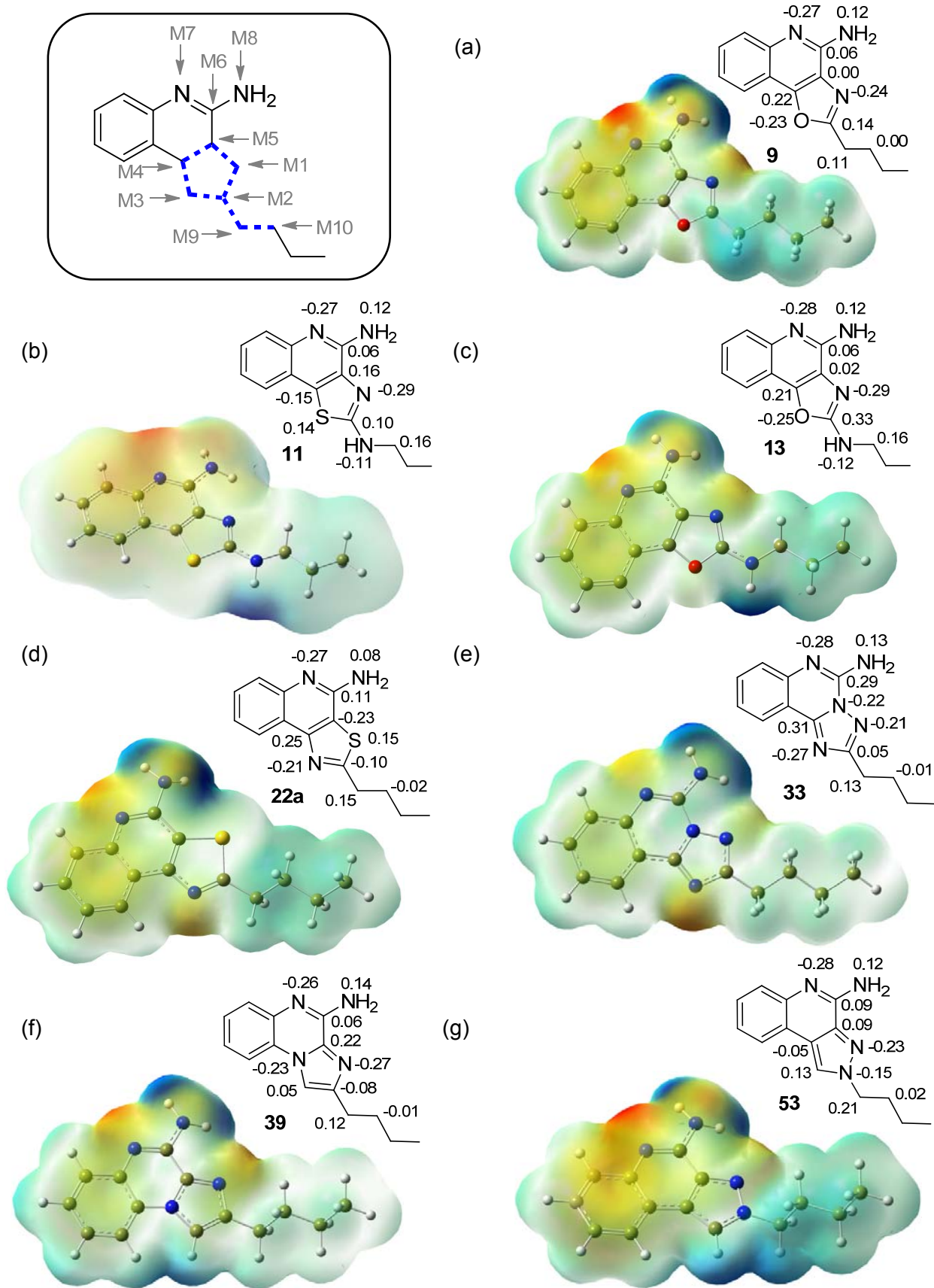
Fig. 6. Crystal structures of human TLR8 ectodomain complexed with compound **9** (Panel A) and compound **53** (Panel B), showing key interactions in the binding pocket. PDB codes for compounds **9** and **53** are, respectively, 4QBZ and 4QC0.



Whereas the steric properties of most of these analogues are very similar, their activity profiles are considerably different and the data, taken together, strongly pointed to electronic densities of ring system(s) being dominant determinants of occupancy and activation of TLR7 and TLR8 by these analogues. We therefore undertook quantum chemical calculations of electron densities and of Mulliken atomic charges with the objective of obtaining insights into the properties of these molecules, which we hoped would lead to quantitative predictors of selectivity and potency at TLR7 and TLR8.

As described earlier, the crystal structures of TLR8 complexed with active analogues showed key H-bonds between the amidine group of the quinoline moiety with the side chain of Asp543, and the N atoms of the oxazole or pyrazole moieties of compounds **9** and **53**, respectively, with Thr574, providing major contributions to overall binding interactions (Fig. 6). Consistent with our expectation that the strength and geometry of the H-bonds are modulated by electron densities and Mulliken charges on appropriate heteroatoms, we observed clear differences in atoms known to be involved in H-bonding interactions. The active compounds **3**, **9**, **11**, **39**, and **53** (Fig. 7) display pronounced negative charges (-0.24, -0.24, -0.29, -0.27, and -0.23 electron units, respectively) at position M1 of the five-membered ring. Compounds that do not have the electronegative atom at position M1 (**22a** and **29**; +0.15, 0.0) were found to be inactive. We also noticed a higher partial positive charge at the M2 position in the oxazolo[4,5-c]quinoline-2,4-diamine **13** (0.33 electron unit, Fig. 7c) compared to other compounds, attributable to adjacent electronegative heteroatoms (N and O), possibly explaining the lack of activity. The quinazoline analogues **29** and **33** were unique in that the presence of an additional electronegative nitrogen atom at position M5 (-0.25 and -0.22, respectively) resulted in strong positive charge at position M6 (+0.26 and +0.29 electron units, respectively), again correlating with absence of agonistic activities.

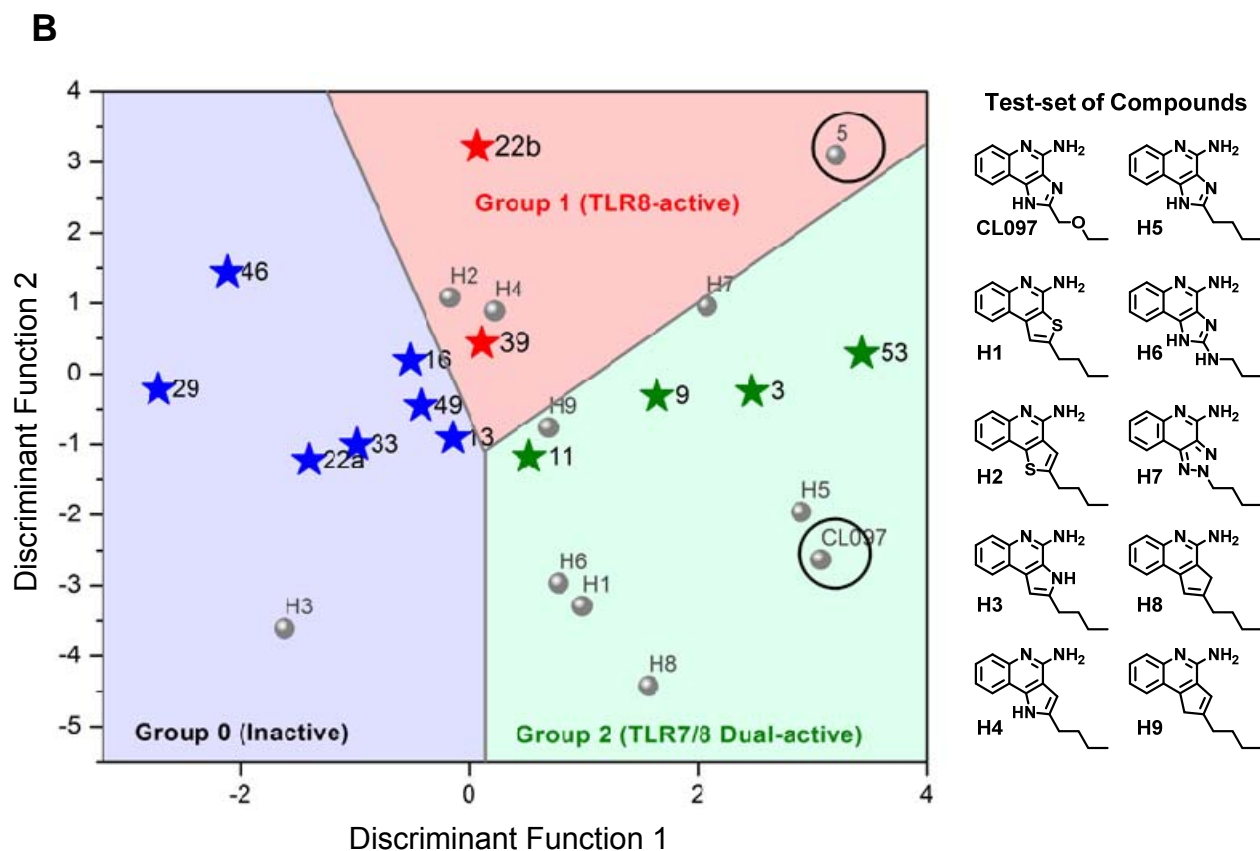
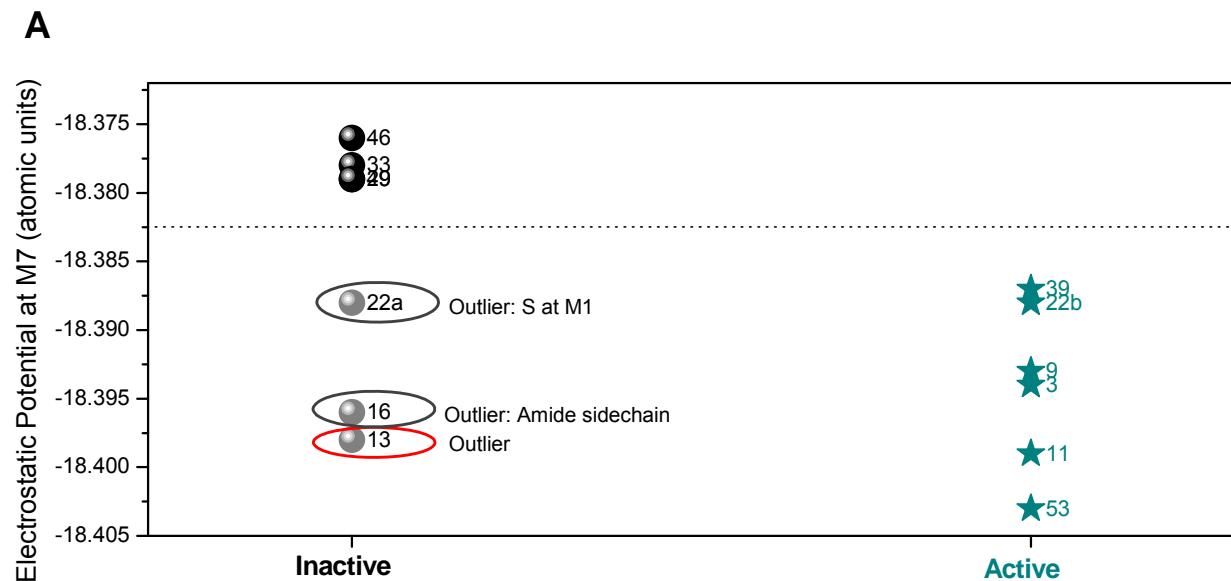
Fig. 7. Molecular electrostatic potential surfaces of selected compounds.



Given the importance of hydrogen bonding of the amidine group with Asp543, we examined electrostatic potentials at M7. Active compounds could be differentiated from inactive compounds (Fig. 8A) with three exceptions: compounds **13**, **16** and **22a**. The absence of TLR7/8-agonistic activity in **16** and **22a** could be explained readily; the presence of a polar amide sidechain in **16** is expected to disfavor interactions in the hydrophobic pocket, while the regio-isomeric thiazoloquinoline **22a** possesses a bulky sulfur atom at M1. The misclassification of **13** as an active compound may, as mentioned earlier, be related to the higher partial positive charge at the M2 position.

The availability of electron density and charge parameters for all atoms in all of the analogues prompted us to examine if a formal classification of active vis-à-vis inactive compounds could be arrived at, with our goal of being able to utilize such methodology in prospectively designing 'bespoke' compounds with predefined selectivity. Stepwise linear discriminant analyses were performed with the 13 compounds shown in Fig. 2 as a training set. A linear combination of the variables corresponding to M1-M6 explained 100% of the variance in two dimensions (Discriminant Functions 1 and 2, see Fig. 8B), allowing a clear-cut classification of inactive (coded '0'), TLR8-active (coded '1'), and TLR7/8 dual-active (coded '2') compounds (Fig. 8B). The discriminant functions were utilized to examine a test set of compounds which included **5**¹¹⁶ (Fig. 1), CL097,^{43a} as well as nine 'hypothetical' compounds (Fig. 8B). Compound **5** and CL097 were correctly classified as being TLR8 (Group 1) and TLR7/8 dual-active (Group 2). All of the proposed analogues with the exception of **H3** were predicted to be active. It is noteworthy that the isomeric compounds **H8** and **H9** (2-butyl-cyclopentaquinolin-4-amines) could be considered as conformationally-constrained analogues of 3-alkyl-quinoline-2-amines¹¹⁸ (Fig. 1) which we have recently designed and characterized as pure TLR8 agonists. The thienoquinolines **H1** and **H2** as well as the pyrroloquinolines **H3** and **H4** are of particular interest, and we are currently evaluating such analogues.

Fig. 8. A: Classification of inactive and active compounds based on electrostatic potentials at M7. **B:** Linear discriminant analysis. Demarcation of Group 0 (inactive), Group 1 (TLR8-specific), and Group 2 (TLR7/8-dual active) compounds obtained via linear discriminant analyses of Mulliken charges.



6.3. Conclusion

We undertook a scaffold-hopping approach, which entailed the syntheses and biological evaluations of 13 different chemotypes. Density functional theory based quantum chemical calculations on these compounds followed by linear discriminant analyses permitted the classification of inactive, TLR8-active, and TLR7/8 dual-active compounds, confirming the critical role of partial charges in determining biological activity. The question as to why the activity profiles of the oxazoloquinoline **9** and its 2-amino analogue **13** are completely divergent remains unclear, however, crystallographic observations of the complex of **9** with TLR8 even in conjunction with electronic structure calculations only allow us to speculate at the present time as to the role of the water molecule by virtue of its permanent dipole moment and polarizability on stabilizing (or destabilizing interactions) depending on electron densities around the five-membered ring. We are gratified, nonetheless, that quantum chemical calculations in conjunction with rigorous multivariate analyses may afford an empirical, but accessible means to evaluating analogues de novo.

6.4. Experimental

Chemistry. All of the solvents and reagents used were obtained commercially and used as such unless noted otherwise. Moisture- or air-sensitive reactions were conducted under nitrogen atmosphere in oven-dried (120 °C) glass apparatus. The solvents were removed under reduced pressure using standard rotary evaporators. Flash column chromatography was carried out using RediSep Rf “Gold” high performance silica columns on CombiFlash Rf instrument unless otherwise mentioned, while thin-layer chromatography was carried out on silica gel CCM precoated aluminum sheets. Purity for all final compounds was confirmed to be greater than

97% by LC-MS using a Zorbax Eclipse Plus 4.6 mm × 150 mm, 5 μm analytical reverse phase C18 column with H₂O-CH₃CN gradients and an Agilent 6520 ESIQTOF Accurate Mass spectrometer (mass accuracy of 5 ppm) operating in the positive ion acquisition mode.

Synthesis of compound 7: 2-Butylthiazolo[4,5-c]quinoline. To a solution of 3-aminoquinolin-4-ol (12 mg, 0.075 mmol) in pyridine (0.5 mL) was added valeroyl chloride (11 μL, 0.09 mmol) and the resulting mixture was heated in a sealed vial at 50 °C for 1 h. P₂S₅ (33 mg) was added and the mixture was heated at 120 °C for 1 h under microwave irradiation. The solvents were removed and the crude residue was purified by flash chromatography (SiO₂, 0-5% MeOH in CH₂Cl₂) to give compound **7** (13.4 mg, 79%) as reddish brown solid. [¹H NMR (500 MHz, CDCl₃) δ 9.44 (s, 1H), 8.24 (d, *J* = 8.4 Hz, 1H), 7.96 (dd, *J* = 8.1, 0.9 Hz, 1H), 7.73 (ddd, *J* = 8.4, 5.4, 1.4 Hz, 1H), 7.63 (ddd, *J* = 8.1, 7.1, 1.1 Hz, 1H), 3.25–3.19 (m, 2H), 1.97–1.89 (m, 2H), 1.55–1.46 (m, 2H), 1.00 (t, *J* = 7.4 Hz, 3H). ¹³C NMR (126 MHz, CDCl₃) δ 173.0, 147.9, 145.8, 144.2, 140.6, 130.6, 128.8, 128.8, 127.6, 125.0, 123.6, 34.2, 32.0, 22.4, 13.9. MS (ESI-TOF, *m/z*): calculated for C₁₄H₁₄N₂S 243.0950; found 243.0976 [M+H]⁺ (Data from *Org. Biomol. Chem.* 2013, 11, 1179)].

Synthesis of compound 8: 2-Butyloxazolo[4,5-c]quinolone. To a solution of 3-aminoquinolin-4-ol (12 mg, 0.075 mmol) in pyridine (0.5 mL) was added valeroyl chloride (11 μL, 0.09 mmol) and the resulting mixture was heated in a sealed vial at 50 °C for 1 h. P₂O₅ (22 mg) was added and the resulting mixture was heated at 120 °C for 1 h under microwave irradiation. The solvents were removed and the crude residue was purified by flash chromatography (SiO₂, 0-5% MeOH in CH₂Cl₂) to give compound **8** as pale yellow solid (11.5 mg, 63%). ¹H NMR (500 MHz, CDCl₃) δ 9.27 (s, 1H), 8.25 (d, *J* = 8.4 Hz, 1H), 8.20 (ddd, *J* = 8.1, 1.5, 0.6 Hz, 1H), 7.75 (ddd, *J* = 8.5, 7.0, 1.5 Hz, 1H), 7.68 (ddd, *J* = 8.1, 7.0, 1.1 Hz, 1H), 3.08 (dd, *J* = 9.0, 6.3 Hz,

2H), 1.96 (ddd, $J = 15.2, 7.6, 6.0$ Hz, 2H), 1.51 (dt, $J = 14.8, 7.4$ Hz, 2H), 1.01 (t, $J = 7.4$ Hz, 3H). ^{13}C NMR (126 MHz, CDCl_3) δ 167.5, 152.1, 145.9, 143.9, 134.9, 130.1, 128.7, 127.3, 120.1, 116.3, 28.9, 28.4, 22.3, 13.7. MS (ESI-TOF, m/z): calculated for $\text{C}_{14}\text{H}_{14}\text{N}_2\text{O}$ 227.1179; found 227.1216 $[\text{M}+\text{H}]^+$.

Synthesis of 2-Butyloxazolo[4,5-*c*]quinoline 5-oxide. To a solution of compound **8** (68 mg, 0.30 mmol) in CHCl_3 (5 mL), was added *m*-CPBA ($\leq 77\%$, 100 mg, 0.45 mmol) and the reaction mixture was stirred at room temperature for 4 h. The solvent was removed under reduced pressure and the crude residue was purified by flash chromatography (SiO_2 , 0-5% MeOH in CH_2Cl_2) to give 2-butyloxazolo[4,5-*c*]quinoline 5-oxide. ^1H NMR (500 MHz, CDCl_3) δ 8.97 (s, 1H), 8.92 – 8.87 (m, 1H), 8.18 (ddd, $J = 6.4, 2.2, 0.6$ Hz, 1H), 7.83 – 7.77 (m, 2H), 3.06 (dd, $J = 9.0, 6.3$ Hz, 2H), 1.97 – 1.90 (m, 2H), 1.55 – 1.47 (m, 2H), 1.01 (t, $J = 7.4$ Hz, 3H). ^{13}C NMR (126 MHz, CDCl_3) δ 169.5, 144.3, 139.8, 134.6, 130.0, 129.7, 129.6, 121.5, 120.8, 116.6, 28.8, 28.4, 22.3, 13.7. MS (ESI-TOF, m/z): calculated for $\text{C}_{14}\text{H}_{14}\text{N}_2\text{O}_2$ 243.1128; found 243.1146 $[\text{M}+\text{H}]^+$.

Synthesis of compound 9: 2-Butyloxazolo[4,5-*c*]quinolin-4-amine. 2-Butyloxazolo[4,5-*c*]quinoline 5-oxide (60 mg, 0.25 mmol) was dissolved in anhydrous CH_2Cl_2 (2 mL). Benzoyl isocyanate (74 mg, 0.50 mmol) was added and the resulting mixture was refluxed for 1.5 h. The solvent was removed and the residue was dissolved in anhydrous methanol (2 mL). Sodium methoxide (27 mg, 0.50 mmol) was added and the resulting mixture was refluxed for 30 min. The solvent was removed under reduced pressure and the crude residue was purified by flash chromatography (SiO_2 , 0-10% MeOH in CH_2Cl_2) to give compound **9** as white solid (37 mg, 61%). ^1H NMR (500 MHz, MeOD) δ 7.95 (ddd, $J = 8.0, 1.5, 0.5$ Hz, 1H), 7.70 – 7.65 (m, 1H), 7.56 (ddd, $J = 8.5, 7.0, 1.5$ Hz, 1H), 7.35 (ddd, $J = 8.1, 7.0, 1.1$ Hz, 1H), 3.09 – 3.03 (m, 2H),

1.92 (ddd, $J = 13.7, 8.2, 6.9$ Hz, 2H), 1.55 – 1.46 (m, 2H), 1.02 (t, $J = 7.4$ Hz, 3H). ^{13}C NMR (126 MHz, MeOD) δ 168.0, 154.0, 152.9, 146.4, 130.2, 126.3, 125.6, 124.0, 121.1, 114.3, 30.0, 28.9, 23.3, 14.0. MS (ESI-TOF, m/z): calculated for $\text{C}_{14}\text{H}_{15}\text{N}_3\text{O}$ 242.1288; found 242.1313 $[\text{M}+\text{H}]^+$.

Synthesis of compound 10: *N*-Propylthiazolo[4,5-*c*]quinolin-2-amine. To a solution of 3-aminoquinolin-4-ol (32 mg, 0.20 mmol) in pyridine (1 mL) was added propyl isothiocyanate (31 μL , 0.30 mmol) and the resulting mixture was heated in a sealed vial at 50 °C for 30 min. P_2S_5 (89 mg) was added and the resulting mixture was heated at 120 °C for 1 h under microwave irradiation. The solvent was removed and the crude residue was purified by flash chromatography (SiO_2 , 0-5% MeOH in CH_2Cl_2) to give compound **10** as pale brown solid (34 mg, 70%). ^1H NMR (400 MHz, CDCl_3) δ 9.12 (s, 1H), 8.15 (dd, $J = 8.3, 0.8$ Hz, 1H), 7.78 – 7.71 (m, 1H), 7.60 (ddd, $J = 8.4, 7.0, 1.7$ Hz, 1H), 7.55 (ddd, $J = 8.2, 7.0, 1.4$ Hz, 1H), 5.85 (s, 1H), 3.47 (dd, $J = 11.7, 7.0$ Hz, 2H), 1.78 (dd, $J = 14.4, 7.3$ Hz, 2H), 1.06 (t, $J = 7.4$ Hz, 3H). ^{13}C NMR (126 MHz, CDCl_3) δ 168.3, 147.0, 143.1, 143.1, 134.0, 130.3, 127.1, 127.0, 123.7, 123.6, 47.8, 22.7, 11.4. MS (ESI-TOF, m/z): calculated for $\text{C}_{13}\text{H}_{13}\text{N}_3\text{S}$ 244.0903; found 244.0946 $[\text{M}+\text{H}]^+$.

11: *N*²-Propylthiazolo[4,5-*c*]quinoline-2,4-diamine. ^1H NMR (500 MHz, MeOD) δ 7.57 (d, $J = 8.4$ Hz, 1H), 7.50 (d, $J = 8.0$ Hz, 1H), 7.42 – 7.36 (m, 1H), 7.26 – 7.19 (m, 1H), 3.42 (t, $J = 7.0$ Hz, 2H), 1.72 (h, $J = 7.3$ Hz, 2H), 1.02 (t, $J = 7.4$ Hz, 3H). ^{13}C NMR (126 MHz, MeOD) δ 169.3, 152.0, 143.2, 137.6, 133.7, 128.3, 125.8, 124.4, 123.9, 121.0, 47.8, 23.5, 11.8. MS (ESI-TOF, m/z): calculated for $\text{C}_{13}\text{H}_{14}\text{N}_4\text{S}$ 259.1012; found 259.1054 $[\text{M}+\text{H}]^+$.

Synthesis of compound 12: *N*-Propyloxazolo[4,5-*c*]quinolin-2-amine. To a solution of 3-aminoquinolin-4-ol (32 mg, 0.20 mmol) in pyridine (1 mL) was added propyl isothiocyanate (31 μ L, 0.30 mmol) and the resulting mixture was heated in a sealed vial at 50 °C for 30 min. EDC (77 mg, 0.4 mmol) was added and the resulting mixture was heated at 120 °C for 30 min under microwave irradiation. The solvent was removed and the crude residue was purified by flash chromatography (SiO₂, 0-5% MeOH in CH₂Cl₂) to give compound **12** as brown solid (25 mg, 59%). ¹H NMR (500 MHz, MeOD) δ 8.83 (s, 1H), 8.06 – 8.02 (m, 1H), 8.01 – 7.97 (m, 1H), 7.67 – 7.58 (m, 2H), 3.42 (t, *J* = 7.1 Hz, 2H). ¹³C NMR (126 MHz, MeOD) δ 164.7, 150.1, 145.1, 141.2, 137.8, 129.7, 128.7, 128.6, 120.2, 116.7, 45.9, 23.6, 11.6. MS (ESI-TOF, *m/z*): calculated for C₁₃H₁₃N₃O 228.1131; found 228.1164 [M+H]⁺.

2-(Propylamino)oxazolo[4,5-*c*]quinoline 5-oxide. ¹H NMR (500 MHz, DMSO-*d*₆) δ 8.83 (s, 1H), 8.58 (t, *J* = 5.8 Hz, 1H), 8.56 (d, *J* = 8.8 Hz, 1H), 7.97 (dd, *J* = 8.3, 0.6 Hz, 1H), 7.75 (ddd, *J* = 8.2, 6.9, 1.1 Hz, 1H), 7.69 – 7.64 (m, 1H), 3.36 – 3.30 (m, 10H), 1.69 – 1.59 (m, 2H), 0.94 (t, *J* = 7.4 Hz, 3H). ¹³C NMR (126 MHz, DMSO-*d*₆) δ 163.8, 139.3, 137.2, 136.8, 129.4, 127.7, 127.3, 120.5, 119.6, 115.3, 44.4, 22.0, 11.3. MS (ESI-TOF, *m/z*): calculated for C₁₃H₁₃N₃O₂ 244.1081; found 244.0974 [M+H]⁺.

13: *N*²-Propyloxazolo[4,5-*c*]quinoline-2,4-diamine. ¹H NMR (500 MHz, DMSO-*d*₆) δ 11.96 (s, 1H), 8.16 (dd, *J* = 8.0, 1.2 Hz, 1H), 7.50 – 7.45 (m, 1H), 7.44 (dd, *J* = 8.2, 1.0 Hz, 1H), 7.16 (ddd, *J* = 8.1, 6.6, 1.5 Hz, 1H), 7.06 (t, *J* = 5.9 Hz, 1H), 3.24 (dd, *J* = 14.1, 6.3 Hz, 2H), 1.63 – 1.48 (m, 2H), 0.90 (t, *J* = 7.4 Hz, 3H). ¹³C NMR (126 MHz, DMSO-*d*₆) δ 161.7, 155.7, 150.2, 137.4, 129.0, 124.9, 124.0, 120.2, 117.0, 112.8, 43.9, 22.6, 11.3. MS (ESI-TOF, *m/z*): calculated for C₁₃H₁₄N₄O 243.1240; found 243.1141 [M+H]⁺.

Synthesis of compound 15: 2-Propionamidothiazolo[4,5-c]quinoline 5-oxide. To a solution of thiazolo[4,5-c]quinolin-2-amine (100 mg, 0.497 mmol) in pyridine (2 mL) was added propionyl chloride (54 μ L, 0.62 mmol) and the resulting mixture was stirred at room temperature for 1 h. The solvent was removed and the crude residue was purified by flash chromatography (SiO₂, 0-5% MeOH in CH₂Cl₂) to give compound *N*-(thiazolo[4,5-c]quinolin-2-yl)propionamide **14** as impure solid, which was dissolved in CHCl₃ (4 mL). *m*-CPBA (\leq 77%, 224 mg, 1.0 mmol) was added and the reaction mixture was stirred at room temperature for 4 h and then concentrated. The crude residue was purified by flash chromatography (SiO₂, 0-5% MeOH in CH₂Cl₂) to give compound **15** as white solid (98 mg, 72%). ¹H NMR (500 MHz, DMSO-*d*₆) δ 12.75 (s, 1H), 9.11 (s, 1H), 8.68 – 8.62 (m, 1H), 8.24 – 8.17 (m, 1H), 7.86 – 7.76 (m, 2H), 2.56 (q, *J* = 7.5 Hz, 2H), 1.14 (t, *J* = 7.5 Hz, 3H). ¹³C NMR (126 MHz, DMSO-*d*₆) δ 173.3, 160.0, 142.9, 137.8, 129.8, 129.7, 128.7, 125.1, 124.6, 123.6, 120.3, 28.4, 8.8. MS (ESI-TOF, *m/z*): calculated for C₁₃H₁₁N₃O₂S 274.0645; found 274.0667 [M+H]⁺.

Synthesis of compound 16: *N*-(4-Aminothiazolo[4,5-c]quinolin-2-yl)propionamide. Compound **15** (55 mg, 0.20 mmol) was dissolved in anhydrous CH₂Cl₂ (2 mL). Benzoyl isocyanate (59 mg, 0.40 mmol) was added and the resulting mixture was refluxed for 1.5 h. The solvent was removed under reduced pressure and the residue was dissolved in anhydrous MeOH (2 mL). Sodium methoxide (22 mg, 0.40 mmol) was added and the reaction mixture was refluxed for 30 min. The solvent was removed and the crude residue was purified by flash chromatography (SiO₂, 0-10% MeOH in CH₂Cl₂) to give compound **16** as white solid (41 mg, 79%). ¹H NMR (500 MHz, DMSO-*d*₆) δ 12.53 (s, 1H), 7.80 (dd, *J* = 8.0, 1.0 Hz, 1H), 7.61 (dd, *J* = 8.3, 0.6 Hz, 1H), 7.48 (ddd, *J* = 8.4, 7.0, 1.4 Hz, 1H), 7.26 (ddd, *J* = 8.1, 7.0, 1.2 Hz, 1H), 2.55 (q, *J* = 7.5 Hz, 2H), 1.14 (t, *J* = 7.5 Hz, 3H). ¹³C NMR (126 MHz, DMSO-*d*₆) δ 173.1, 157.0, 151.5, 144.2, 133.8, 133.1, 127.8, 125.9, 123.7, 122.2, 119.1, 28.3, 9.0. MS (ESI-TOF, *m/z*):

calculated for C₁₃H₁₂N₄OS 273.0805; found 273.0832 [M+H]⁺. The sodium methoxide solvolysis also resulted in small amount of thiazolo[4,5-c]quinoline-2,4-diamine **17** which was isolated from the crude mixture as white solid (4 mg, 9%). ¹H NMR (500 MHz, MeOD) δ 7.58 (ddd, *J* = 8.4, 1.0, 0.5 Hz, 1H), 7.52 (ddd, *J* = 8.0, 1.4, 0.5 Hz, 1H), 7.41 (ddd, *J* = 8.4, 7.0, 1.5 Hz, 1H), 7.24 (ddd, *J* = 8.1, 7.1, 1.1 Hz, 1H). ¹³C NMR (126 MHz, MeOD) δ 169.6, 152.0, 143.6, 137.3, 134.7, 128.4, 126.0, 124.4, 123.9, 121.1. MS (ESI-TOF, *m/z*): calculated for C₁₀H₈N₄S 217.0542; found 217.0569 [M+H]⁺.

Synthesis of compound 18: *N*-(Quinolin-4-yl)valeramide. To a solution of 4-aminoquinoline (302 mg, 2.1 mmol) in pyridine (6 mL) was added valeroyl chloride (0.28 mL, 2.4 mmol). The mixture was heated at 65 °C for 90 min and then concentrated. The crude residue was purified by flash chromatography (SiO₂, 0-10% MeOH in CH₂Cl₂) to give compound **18** as a dark brown solid (382 mg, 80%). ¹H NMR (500 MHz, DMSO-*d*₆) δ 11.11 (s, 1H), 9.07 (d, *J* = 6.5 Hz, 1H), 8.95 (dd, *J* = 8.7, 1.1 Hz, 1H), 8.70 (d, *J* = 6.4 Hz, 1H), 8.32 (dd, *J* = 8.5, 1.1 Hz, 1H), 8.12 (ddd, *J* = 8.4, 6.9, 1.1 Hz, 1H), 7.93 (ddd, *J* = 8.4, 6.9, 1.1 Hz, 1H), 2.80 (t, *J* = 7.4 Hz, 2H), 1.66 (tt, *J* = 7.5 Hz, 2H), 1.39 (tq, *J* = 7.4 Hz, 2H), 0.94 (t, *J* = 7.4 Hz, 3H). ¹³C NMR (126 MHz, DMSO-*d*₆) δ 174.2, 149.6, 145.0, 139.0, 133.8, 128.1, 123.8, 121.2, 119.0, 108.9, 36.4, 26.6, 21.6, 13.7. MS (ESI-TOF, *m/z*): calculated for C₁₄H₁₆N₂O 229.1341; found 229.1306 [M+H]⁺.

Synthesis of compound 19: *N*-(3-Bromoquinolin-4-yl)valeramide. To a suspension of compound **18** (151 mg, 0.66 mmol) in benzene (anhydrous, 10 mL) was added *N*-bromosuccinimide (NBS, 143 mg, 0.81 mmol) and azobisisobutyronitrile (AIBN, 99 mg, 0.60 mmol). The mixture was refluxed for 5 h and then concentrated. The crude residue was purified by flash chromatography (SiO₂, 0-30% EtOAc in hexane) to give compound **19** as a light brown solid (86 mg, 42%). ¹H NMR (500 MHz, DMSO-*d*₆) δ 10.31 (s, 1H), 9.05 (s, 1H), 8.08 (dd, *J*=

8.5, 1.2 Hz, 1H), 7.95 (dd, $J = 8.4, 1.4$ Hz, 1H), 7.84 (ddd, $J = 8.4, 6.9, 1.5$ Hz, 1H), 7.70 (ddd, $J = 8.2, 6.8, 1.3$ Hz, 1H), 2.54-2.46 (m, 2H), 1.68 (quin, $J = 7.5$ Hz, 2H), 1.43 (sex, $J = 7.4$ Hz, 2H), 0.95 (t, $J = 7.4$ Hz, 3H). ^{13}C NMR (126 MHz, DMSO- d_6) δ 171.4, 152.1, 147.1, 141.5, 130.2, 129.1, 127.8, 126.6, 123.8, 116.8, 35.2, 27.3, 21.9, 13.8. MS (ESI-TOF, m/z): calculated for $\text{C}_{14}\text{H}_{15}\text{BrN}_2\text{O}$ 307.0446; found 307.0254 $[\text{M}+\text{H}]^+$.

Synthesis of compound 20a: 2-Butylthiazolo[5,4-c]quinoline. To a solution of compound **19** (60.8 mg, 0.20 mmol) in pyridine (4 mL) was added Lawesson's reagent (234 mg, 0.58 mmol). The resulting mixture was heated in a sealed vial under microwave irradiation (500 W, 140 °C) for 35 min and then concentrated. The crude residue was purified by flash chromatography (SiO_2 , 0-10% EtOAc in hexanes) to give compound **20a** as brown oil (15 mg, 31%). ^1H NMR (500 MHz, CDCl_3) δ 9.33 (s, 1H), 8.71 (dd, $J = 8.1, 1.5$ Hz, 1H), 8.22 (brd, $J = 8.3$ Hz, 1H), 7.76 (ddd, $J = 8.3, 7.0, 1.5$ Hz, 1H), 7.70 (ddd, $J = 8.1, 7.0, 1.2$ Hz, 1H), 3.27 (t, $J = 7.7$ Hz, 2H), 1.95 (tt, $J = 7.6, 7.7$ Hz, 2H), 1.52 (qt, $J = 7.3, 7.4$ Hz, 2H), 1.01 (t, $J = 7.4$ Hz, 3H). ^{13}C NMR (126 MHz, CDCl_3) δ 177.3, 154.9, 145.9, 143.8, 129.4, 128.7, 127.8, 127.2, 123.6, 123.4, 34.3, 32.0, 22.3, 13.8. MS (ESI-TOF, m/z): calculated for $\text{C}_{14}\text{H}_{14}\text{N}_2\text{S}$ 243.0956; found 243.1019 $[\text{M}+\text{H}]^+$.

Synthesis of compound 21a: 2-Butylthiazolo[5,4-c]quinoline 5-oxide. To a solution of compound **20a** (14.5 mg, 0.060 mmol) in CH_2Cl_2 (1 mL) was added *m*-CPBA ($\leq 77\%$, 35.2 mg). The reaction mixture was stirred at room temperature for 2.5 h and then concentrated. The crude residue was purified by flash chromatography (SiO_2 , MeOH in CH_2Cl_2 : 0 to 5%) to give compound **21a** (13.5 mg, 87%) as brown oil. ^1H NMR (500 MHz, CDCl_3) δ 9.04 (s, 1H), 8.90-8.76 (m, 1H), 8.78-8.58 (m, 1H), 7.95-7.72 (m, 2H), 3.25 (t, $J = 7.7$ Hz, 2H), 1.94 (tt, $J = 7.6, 7.7$ Hz, 2H), 1.63-1.44 (m, 2H), 1.02 (t, 3H, $J = 7.3$ Hz). ^{13}C NMR (126 MHz, CDCl_3) δ 176.4, 147.8,

140.1, 134.3, 132.6, 130.0, 129.5, 128.0, 124.4, 120.3, 34.1, 31.9, 22.3, 13.8. MS (ESI-TOF, m/z): calculated for $C_{14}H_{14}N_2OS$ 259.0827; found 259.0755 $[M+H]^+$.

Synthesis of compound 22a: 2-Butylthiazolo[5,4-c]quinolin-4-amine. To a solution of compound **21a** (10.1 mg, 0.039 mmol) in CH_2Cl_2 (0.2 mL) was added benzoyl isocyanate (13.2 mg, 0.090 mmol). The mixture was heated to reflux for 3 h and then concentrated. The crude residue was purified by flash chromatography (SiO_2 , 0-15% EtOAc in hexanes) to give intermediate as light brown oil (8.8 mg, 63%). Benzamide (8.8 mg, 0.024 mmol) was dissolved in NaOMe solution (0.5 mL, 0.5 M in MeOH). The mixture was heated to reflux overnight and then concentrated. The crude residue was purified by flash chromatography (SiO_2 , 0-5% MeOH in CH_2Cl_2) to give compound **22a** as a yellow solid (5.6 mg, 89%). 1H NMR (500 MHz, $CDCl_3$) δ 8.50 (dd, $J = 8.1, 1.2$ Hz, 1H), 7.82 (brd, $J = 8.4$ Hz, 1H), 7.62 (ddd, $J = 8.4, 7.0, 1.5$ Hz, 1H), 7.44 (ddd, $J = 8.0, 7.0, 1.1$ Hz, 1H), 5.15 (brs, 2H), 3.25 (t, $J = 7.7$ Hz, 2H), 2.00-1.87 (m, 2H), 1.61-1.43 (m, 2H), 1.02 (t, $J = 7.4$ Hz, 3H). ^{13}C NMR (126 MHz, $CDCl_3$) δ 175.7, 157.0, 150.9, 145.8, 129.2, 125.7, 123.6, 123.5, 120.2, 116.7, 34.2, 32.0, 22.3, 13.8. MS (ESI-TOF, m/z): calculated for $C_{14}H_{15}N_3S$ 258.1065; found 258.0964 $[M+H]^+$.

Synthesis of compound 20b: 2-Butyloxazolo[5,4-c]quinoline. To a solution of compound **19** (50.4 mg, 0.16 mmol) in pyridine (2 mL) was added CuI (66 mg, 0.35 mmol) and K_2CO_3 (47 mg, 0.34 mmol). The resulting mixture was heated in a sealed vial under microwave irradiation (500 W, 140 °C) for 35 min and then concentrated. The crude residue was purified by flash chromatography (SiO_2 , 0-10% EtOAc in hexanes) to give compound **20b** as a brown solid (28 mg, 76%). 1H NMR (500 MHz, $CDCl_3$) δ 9.20 (bs, 1H), 8.46 (bs, 1H), 8.25 (bs, 1H), 7.76 (bt, $J = 6.0$ Hz, 1H), 7.72 – 7.64 (m, 1H), 3.09 (t, $J = 7.6$ Hz, 2H), 2.00 – 1.91 (m, 2H), 1.55 – 1.43 (m, 2H), 1.00 (t, $J = 7.4$ Hz, 3H). ^{13}C NMR (126 MHz, $CDCl_3$) δ 169.8, 145.5, 143.7, 135.1, 129.9,

128.3, 127.4, 122.2, 29.0, 28.7, 22.3, 13.7. MS (ESI-TOF, m/z): calculated for $C_{14}H_{14}N_2O$ 227.1184; found 227.1051 $[M+H]^+$.

Synthesis of compound 21b: 2-Butyloxazolo[5,4-c]quinoline 5-oxide. To a solution of compound **20b** (28 mg, 0.124 mmol) in CH_2Cl_2 (2 mL) was added *m*-CPBA ($\leq 77\%$, 83.5 mg). The reaction mixture was stirred at room temperature for 4 h and then concentrated. The crude residue was purified by flash chromatography (SiO_2 , 0-5% MeOH in CH_2Cl_2) to give compound **21b** as a red solid (22 mg, 73%). 1H NMR (500 MHz, $CDCl_3$) δ 8.93 (s, 1H), 8.87-8.79 (m, 1H), 8.46-8.41 (m, 1H), 7.84-7.75 (m, 2H), 3.06 (t, $J = 7.6$ Hz, 2H), 1.93 (tt, $J = 7.7, 7.6$ Hz, 2H), 1.50 (qt, $J = 7.4, 7.3$ Hz, 2H), 1.01 (t, $J = 7.4$ Hz, 3H). ^{13}C NMR (126 MHz, $CDCl_3$) δ 169.9, 143.9, 140.1, 135.7, 129.6, 129.3, 123.6, 122.8, 121.8, 120.8, 28.9, 28.5, 22.3, 13.7. MS (ESI-TOF, m/z): calculated for $C_{14}H_{14}N_2O_2$ 243.1134; found 243.1032 $[M+H]^+$.

Synthesis of compound 22b: 2-Butyloxazolo[5,4-c]quinolin-4-amine. To a solution of compound **21b** (17.8 mg, 0.073 mmol) in CH_2Cl_2 (0.5 mL) was added benzoyl isocyanate (38.4 mg, 0.26 mmol). The mixture was heated to reflux for 4 h and then concentrated. The crude residue was purified by flash chromatography (SiO_2 , 0-20% EtOAc in hexanes) to give intermediate as colorless oil (8.7 mg, 34%). Benzamide (6 mg, 0.017 mmol) was dissolved in NaOMe solution (0.5 mL, 0.5 M in MeOH). The mixture was heated to reflux for 8 h and then concentrated. The crude residue was purified by flash chromatography (SiO_2 , 0-5% MeOH in CH_2Cl_2) to give compound **22b** as a yellow solid (3.3 mg, 79%). 1H NMR (500 MHz, $CDCl_3$) δ 8.22 (dd, $J = 8.2, 1.5$ Hz, 1H), 7.80 (dd, $J = 8.7, 1.5$ Hz, 1H), 7.59 (ddd, $J = 8.5, 7.0, 1.6$ Hz, 1H), 7.42 (ddd, $J = 8.2, 7.0, 1.1$ Hz, 1H), 5.15 (bs, 2H), 3.05 (t, $J = 7.7$ Hz, 2H), 2.01-1.85 (m, 2H), 1.58-1.43 (m, 2H), 1.00 (t, $J = 7.4$ Hz, 3H). ^{13}C NMR (126 MHz, $CDCl_3$) δ 168.6, 144.9, 144.0,

135.2, 128.5, 127.3, 126.2, 123.5, 122.0, 119.0, 29.2, 28.6, 22.3, 13.7. MS (ESI-TOF, m/z): calculated for $C_{14}H_{15}N_3O$ 242.1293; found 242.1240 $[M+H]^+$.

Synthesis of compound 23: Quinazoline-2,4(1H,3H)-dione. The mixture of anthranilic acid (500 mg, 3.65 mmol) and urea (2.2 g, mol) was heated at 150 °C for 6 h. The reaction mixture was cooled to room temperature and then water (50 mL) was added to quench the reaction. The crude product was obtained by filtration, and then washed with water (20 mL \times 3). The residue was dissolved in hot aq. NaOH and cooled to 0 °C and pH was adjusted to 5-6 using dilute HCl and stirred for 30 min. The crude mixture was filtered and washed with water and dried under vacuum to yield compound **23** as white solid (500 mg, 85%). 1H NMR (500 MHz, DMSO- d_6) δ 11.28 (s, 1H), 11.14 (s, 1H), 7.88 (dd, J = 7.8, 1.1 Hz, 1H), 7.65 – 7.60 (m, 1H), 7.17 (ddd, J = 8.2, 6.1, 1.8 Hz, 2H). ^{13}C NMR (126 MHz, DMSO- d_6) δ 162.9, 150.3, 140.9, 135.0, 127.0, 122.4, 115.3, 114.4. MS (ESI-TOF, m/z): calculated for $C_8H_6N_2O_2$ 163.0502; found 163.0491 $[M+H]^+$.

Synthesis of compound 25: 2-((2-Chloroquinazolin-4-yl)amino)hexan-1-ol. POCl₃ (5 mL) and DIPEA (430 μ L, 2.47 mmol) were added to compound **23** (200 mg, 1.23 mmol) and the reaction mixture was heated to reflux for 4 h. The excess POCl₃ was removed by evaporation. The residue was dissolved in ice water, and then the suspension was filtered and washed with water to afford compound **24** as white solid (220 mg, 90%). To a solution of compound **24** (200 mg, 1 mmol) in DMF (5 mL), was added DL-2-amino-1-hexanol (194 μ L, 1.5 mmol), the resulting mixture was heated at 100 °C for 1 h, and allowed to cool, and concentrated. The residue was purified by flash chromatography (SiO₂, 0-50% EtOAc in Hexane) to give compound **25** as a yellow solid (95 mg, 34 %). 1H NMR (500 MHz, DMSO- d_6) δ 8.37 (dd, J = 8.4, 0.8 Hz, 1H), 8.24 (d, J = 8.4 Hz, 1H), 7.78 (ddd, J = 8.3, 7.0, 1.3 Hz, 1H), 7.60 (dd, J = 8.3, 0.8 Hz, 1H), 7.52 (ddd, J = 8.2, 7.0, 1.2 Hz, 1H), 4.80 (t, J = 5.7 Hz, 1H), 4.35 (qd, J = 5.7, 10.6 Hz, 1H), 3.56 –

3.46 (m, 2H), 1.74 – 1.65 (m, 1H), 1.62 – 1.52 (m, 1H), 1.29 (dddd, $J = 14.8, 10.3, 8.2, 3.2$ Hz, 4H), 0.85 (t, $J = 6.7$ Hz, 3H). ^{13}C NMR (126 MHz, DMSO- d_6) δ 161.4, 157.1, 150.4, 133.6, 126.6, 125.8, 123.5, 113.6, 62.8, 52.9, 30.1, 27.8, 22.1, 14.0. MS (ESI-TOF, m/z): calculated for $\text{C}_{14}\text{H}_{18}\text{ClN}_3\text{O}$ 280.1211; found 280.1279 $[\text{M}+\text{H}]^+$.

Synthesis of compound 27: 2-Butyl-2,3-dihydroimidazo[1,2-c]quinazolin-5-amine. To a solution of compound **25** (50 mg, 0.18 mmol) in CH_2Cl_2 (2 mL) was added triethylamine (38 μL , 0.27 mmol) and methanesulfonyl chloride (17 μL , 0.22 mmol) and the resulting mixture was stirred at room temperature overnight. CH_2Cl_2 (20 mL) was added and the organic layer was washed with water (10 mL x 2), dried over anhydrous sodium sulfate and evaporated to furnish the crude residue of compound **26** (45 mg, 96% crude yield). Ammonia in methanol (2M, 1 mL) was added to compound **26** (10 mg, 38 μmol) and the reaction mixture was heated at 80 $^\circ\text{C}$ for 2 h and concentrated. The residue was purified by flash chromatography (SiO_2 , 0-10% MeOH in CH_2Cl_2) to give compound **27** as a yellow solid (6 mg, 66%). ^1H NMR (500 MHz, MeOD) δ 7.88 (dd, $J = 8.0, 1.2$ Hz, 1H), 7.53 (ddd, $J = 8.5, 7.2, 1.5$ Hz, 1H), 7.20 (d, $J = 8.0$ Hz, 1H), 7.12 (ddd, $J = 8.1, 7.2, 1.0$ Hz, 1H), 4.42 – 4.35 (m, 1H), 4.21 (t, $J = 10.4$ Hz, 1H), 3.77 (dd, $J = 10.3, 7.6$ Hz, 1H), 1.87 – 1.78 (m, 1H), 1.66 (ddd, $J = 11.0, 6.6, 3.7$ Hz, 1H), 1.50 – 1.37 (m, 4H), 0.97 (t, $J = 7.1$ Hz, 3H). ^{13}C NMR (126 MHz, MeOD) δ 156.9, 151.8, 150.6, 135.4, 126.5, 124.6, 123.6, 113.2, 64.5, 51.9, 37.3, 28.6, 23.7, 14.4. MS (ESI-TOF, m/z): calculated for $\text{C}_{14}\text{H}_{18}\text{N}_4$ 243.1604; found 243.1589 $[\text{M}+\text{H}]^+$.

Synthesis of compound 29: 2-Butylimidazo[1,2-c]quinazolin-5-amine. To a solution of compound **26** (28 mg, 0.11 mmol) in toluene (2 mL) was added MnO_2 (47 mg, 0.54 mmol) and heated at reflux for 20 h. Additional MnO_2 was added and the reaction mixture was refluxed for another 48 h. The mixture was allowed to cool, filtered and purified by column chromatography

(SiO₂, 0-50% EtOAc in Hexane) to obtain compound **28** as a pale yellow solid (12 mg, 41%). Compound **28** (10 mg) in ammonia solution (2M in ammonia, 1 mL) was heated at 80 °C for 2 h, concentrated and purified by column chromatography (SiO₂, 0-10% MeOH in CH₂Cl₂) to obtain compound **29** as a pale yellow solid (4 mg, 36%). ¹H NMR (500 MHz, MeOD) δ 8.28 (dd, *J* = 8.0, 0.9 Hz, 1H), 7.70 (s, 1H), 7.58 – 7.51 (m, 2H), 7.35 (ddd, *J* = 8.1, 6.8, 1.5 Hz, 1H), 2.84 – 2.78 (m, 2H), 1.79 (ddd, *J* = 13.1, 8.5, 6.6 Hz, 2H), 1.48 (dq, *J* = 14.8, 7.4 Hz, 2H), 1.01 (t, *J* = 7.4 Hz, 3H). ¹³C NMR (126 MHz, MeOD) δ 131.5, 125.5, 124.7, 123.5, 108.3, 32.4, 29.1, 23.5, 14.2. MS (ESI-TOF, *m/z*): calculated for C₁₄H₁₆N₄ 241.1448; found 241.1466 [M+H]⁺.

Synthesis of compound 30: Methyl (2-cyanophenyl)carbamate. 2-Aminobenzonitrile (200 mg, 1.69 mmol) and sodium carbonate (359 mg, 3.39 mmol) was heated to reflux in methyl chloroformate (7 mL) for 4 h. The reaction mixture was concentrated and purified by column chromatography (SiO₂, 0-20% EtOAc in Hexane) to obtain compound **30** as a white solid (276 mg, 93%). ¹H NMR (500 MHz, DMSO-*d*₆) δ 9.77 (s, 1H), 7.79 (dd, *J* = 7.8, 1.3 Hz, 1H), 7.67 (ddd, *J* = 8.2, 7.6, 1.6 Hz, 1H), 7.52 (d, *J* = 8.1 Hz, 1H), 7.33 (td, *J* = 7.6, 1.1 Hz, 1H), 3.69 (s, 3H). ¹³C NMR (126 MHz, DMSO-*d*₆) δ 154.5, 140.5, 133.9, 133.3, 125.5, 125.2, 116.8, 107.3, 52.2. MS (ESI-TOF, *m/z*): calculated for C₉H₈N₂O₂ 177.0659; found 177.0694 [M+H]⁺.

Synthesis of compound 31: 2-Butyl-[1,2,4]triazolo[1,5-*c*]quinazolin-5(6*H*)-one. To a solution of compound **30** (200 mg, 1.14 mmol) in *N*-methyl-2-pyrrolidone (NMP, 5 mL) was added valeric acid hydrazide (158 mg, 1.36 mmol) and the reaction mixture was heated at 180 °C for 3 h. Crushed ice was added to the reaction mixture and the solid obtained was filtered and purified by column chromatography (SiO₂, 0-50% EtOAc in hexanes) to obtain compound **31** as white solid (270 mg, 98%). ¹H NMR (500 MHz, DMSO-*d*₆) δ 12.21 (s, 1H), 8.11 (dd, *J* = 7.9, 1.1 Hz, 1H), 7.69 – 7.64 (m, 1H), 7.41 (d, *J* = 8.2 Hz, 1H), 7.39 – 7.33 (m, 1H), 2.82 (t, *J* =

7.6 Hz, 2H), 1.79 – 1.72 (m, 2H), 1.43 – 1.33 (m, 2H), 0.92 (t, $J = 7.4$ Hz, 3H). ^{13}C NMR (126 MHz, $\text{DMSO-}d_6$) δ 166.5, 152.7, 143.8, 136.9, 132.6, 124.0, 123.5, 116.0, 110.3, 29.6, 27.7, 21.8, 13.7. MS (ESI-TOF, m/z): calculated for $\text{C}_{13}\text{H}_{14}\text{N}_4\text{O}$ 243.1240; found 243.1350 $[\text{M}+\text{H}]^+$.

Synthesis of compound 32: 2-Butyl-5-chloro-[1,2,4]triazolo[1,5-c]quinazoline. To a suspension of compound **31** (18 mg, 74 μmol) in POCl_3 (1 mL) was added DIPEA (29 μL , 0.15 mmol) and the resulting mixture was heated at 110 $^\circ\text{C}$ for 18 h. The mixture was cooled to room temperature and concentrated. The residue was purified by flash chromatography (SiO_2 , 0-30% EtOAc in hexane) to give compound **32** as a pale yellow solid (15 mg, 79%). ^1H NMR (500 MHz, $\text{DMSO-}d_6$) δ 8.41 (d, $J = 8.0$ Hz, 1H), 7.99 (d, $J = 8.3$ Hz, 1H), 7.94 (t, $J = 7.7$ Hz, 1H), 7.82 (t, $J = 7.5$ Hz, 1H), 2.93 (t, $J = 7.6$ Hz, 2H), 1.84 – 1.76 (m, 2H), 1.47 – 1.37 (m, 2H), 0.94 (t, $J = 7.4$ Hz, 3H). ^{13}C NMR (126 MHz, $\text{DMSO-}d_6$) δ 167.0, 152.0, 142.3, 135.3, 132.7, 129.1, 127.6, 123.6, 116.8, 29.7, 27.8, 21.8, 13.7. MS (ESI-TOF, m/z): calculated for $\text{C}_{13}\text{H}_{13}\text{ClN}_4$ 261.0902; found 261.1021 $[\text{M}+\text{H}]^+$.

Synthesis of compound 33: 2-Butyl-[1,2,4]triazolo[1,5-c]quinazolin-5-amine. Compound **32** (10 mg, 38 μmol) was treated with 2M ammonia in methanol (1 mL), heated at 80 $^\circ\text{C}$ for 20 h and concentrated. The residue was purified by flash chromatography (SiO_2 , 0-10% MeOH in CH_2Cl_2) to give compound **33** as a white solid (5 mg, 55%). ^1H NMR (500 MHz, MeOD) δ 8.21 (ddd, $J = 8.0, 1.5, 0.5$ Hz, 1H), 7.65 (ddd, $J = 8.5, 7.1, 1.5$ Hz, 1H), 7.57 (dd, $J = 8.4, 0.5$ Hz, 1H), 7.37 (ddd, $J = 8.1, 7.1, 1.1$ Hz, 1H), 2.97 – 2.89 (m, 2H), 1.86 (dt, $J = 15.3, 7.6$ Hz, 2H), 1.50 – 1.38 (m, 2H), 0.98 (t, $J = 7.4$ Hz, 3H). ^{13}C NMR (126 MHz, MeOD) δ 167.9, 153.1, 146.3, 146.1, 133.4, 126.0, 124.8, 124.5, 114.4, 31.4, 29.2, 23.4, 14.1. MS (ESI-TOF, m/z): calculated for $\text{C}_{13}\text{H}_{15}\text{N}_5$ [242.1400; found 242.1399 $\text{M}+\text{H}]^+$.

Synthesis of compound 34: 2,3-Dichloroquinoxaline. Quinoxaline-2,3-diol (500 mg, 3.08 mmol) and POCl₃ (5 mL) in DMF (5 mL) were heated at 100 °C for 1.5 h, allowed to cool, and concentrated. The residue was treated with ice water and filtered to give compound **34** as off white solid (418 mg, 68%). ¹H NMR (500 MHz, DMSO-*d*₆) δ 8.10 – 8.06 (m, 2H), 7.96 – 7.91 (m, 2H). ¹³C NMR (126 MHz, DMSO-*d*₆) δ 144.7, 140.1, 131.8, 128.0. MS (ESI-TOF, *m/z*): calculated for C₈H₄Cl₂N₂ 198.9824; found 198.9853 [M+H]⁺.

Synthesis of compound 35: 2-((3-Chloroquinoxalin-2-yl)amino)hexan-1-ol. To a solution of compound **34** (200 mg, 1 mmol) in EtOH (5 mL), was added DL-2-amino-1-hexanol (194 μL, 1.5 mmol) in EtOH (3 mL), heated at 90 °C for 18 h, allowed to cool, and concentrated. The residue was purified by flash chromatography (SiO₂, 0-20% EtOAc in Hexane) to give compound **35** as a yellow solid (160 mg, 57%). ¹H NMR (500 MHz, CDCl₃) δ 7.80 (dd, *J* = 8.2, 1.0 Hz, 1H), 7.66 (dd, *J* = 8.3, 0.9 Hz, 1H), 7.58 (ddd, *J* = 8.4, 7.0, 1.4 Hz, 1H), 7.40 (ddd, *J* = 8.3, 7.0, 1.4 Hz, 1H), 5.65 (d, *J* = 6.6 Hz, 1H), 4.30 – 4.22 (m, 1H), 3.90 (dd, *J* = 11.1, 2.8 Hz, 1H), 3.76 (dd, *J* = 11.1, 6.3 Hz, 1H), 3.60 (s, 1H), 1.78 – 1.64 (m, 2H), 1.48 – 1.35 (m, 4H), 0.93 (t, *J* = 7.1 Hz, 3H). ¹³C NMR (126 MHz, CDCl₃) δ 148.5, 140.6, 138.1, 136.6, 130.5, 128.1, 125.7, 125.4, 66.8, 54.6, 31.3, 28.5, 22.7, 14.1. MS (ESI-TOF, *m/z*): calculated for C₁₄H₁₈ClN₃O 280.1211; found 280.1296 [M+H]⁺.

Synthesis of compound 36: 2-Butyl-4-chloro-1,2-dihydroimidazo[1,2-*a*]quinoxaline. To a solution of compound **35** (100 mg, 0.36 mmol) in CHCl₃ (1 mL), was added thionyl chloride (1 mL) at 0 °C, and heated to reflux for 2 h. The mixture was cooled to room temperature and concentrated. The residue was purified by flash chromatography (SiO₂, 0-10% MeOH in CH₂Cl₂) to give compound **36** as a yellow solid (75 mg, 80%). ¹H NMR (500 MHz, DMSO-*d*₆) δ 8.02 (dd, *J* = 8.1, 0.7 Hz, 1H), 7.94 – 7.89 (m, 1H), 7.67 (dd, *J* = 14.6, 7.6 Hz, 2H), 4.90 (m, 1H), 4.62 –

4.51 (m, 2H), 1.90 – 1.82 (m, 1H), 1.78 – 1.70 (m, 1H), 1.47 – 1.33 (m, 4H), 0.92 (t, $J = 7.1$ Hz, 3H). ^{13}C NMR (126 MHz, $\text{DMSO-}d_6$) δ 147.5, 136.5, 134.3, 133.3, 129.0, 128.8, 126.8, 115.5, 57.2, 53.4, 33.9, 26.3, 21.9, 13.9. MS (ESI-TOF, m/z): calculated for $\text{C}_{14}\text{H}_{16}\text{ClN}_3$ 262.1106; found 262.1173 $[\text{M}+\text{H}]^+$.

Synthesis of compound 37: 2-Butyl-1,2-dihydroimidazo[1,2-a]quinoxalin-4-amine.

Compound **36** (29 mg, 0.11 mmol) was dissolved in 2 M ammonia in methanol (1 mL) and heated in a sealed vial at 90 °C for 20 h and concentrated. The residue was purified by flash chromatography (SiO_2 , 0-10% MeOH in CH_2Cl_2) to give compound **37** as a yellow solid (18 mg, 67%). ^1H NMR (500 MHz, MeOD) δ 7.25 (dd, $J = 7.9, 1.2$ Hz, 1H), 7.13 (td, $J = 7.9, 1.4$ Hz, 1H), 7.00 (td, $J = 7.8, 1.3$ Hz, 1H), 6.85 (dd, $J = 8.0, 1.2$ Hz, 1H), 4.38 – 4.30 (m, 1H), 4.26 – 4.20 (m, 1H), 3.76 (dd, $J = 10.3, 8.6$ Hz, 1H), 1.79 – 1.71 (m, 1H), 1.68 – 1.57 (m, 1H), 1.53 – 1.37 (m, 4H), 0.95 (t, $J = 7.1$ Hz, 3H). ^{13}C NMR (126 MHz, MeOD) δ 149.4, 147.7, 134.7, 130.9, 125.9, 125.2, 123.0, 112.8, 65.8, 52.8, 37.8, 28.9, 23.8, 14.4. MS (ESI-TOF, m/z): calculated for $\text{C}_{14}\text{H}_{18}\text{N}_4$ 243.1604; found 243.1677 $[\text{M}+\text{H}]^+$.

Synthesis of compound 38: 2-Butyl-4-chloroimidazo[1,2-a]quinoxaline. To a solution of compound **37** (357 mg, 1.36 mmol) in toluene (15 mL) was added MnO_2 (593 mg, 6.82 mmol) and heated to reflux for 24 h. Additional MnO_2 (593 mg, 6.82 mmol) was added and after another 48 h, the mixture was allowed to cool and filtered. The solvent was evaporated and the crude product was purified by flash chromatography (SiO_2 , 0-50% EtOAc in hexane) to give compound **38** as a yellow solid (99 mg, 28%). ^1H NMR (500 MHz, $\text{DMSO-}d_6$) δ 8.73 (s, 1H), 8.33 (dd, $J = 8.3, 0.9$ Hz, 1H), 7.97 (dd, $J = 8.2, 1.2$ Hz, 1H), 7.78 – 7.73 (m, 1H), 7.67 – 7.62 (m, 1H), 2.80 (t, $J = 7.6$ Hz, 2H), 1.72 (dd, $J = 15.2, 7.6$ Hz, 2H), 1.44 – 1.34 (m, 2H), 0.94 (t, $J = 7.4$ Hz, 3H). ^{13}C NMR (126 MHz, $\text{DMSO-}d_6$) δ 158.1, 150.8, 144.0, 143.5, 138.8, 138.4, 136.3,

136.3, 125.5, 122.8, 40.3, 37.6, 31.4, 23.3. MS (ESI-TOF, m/z): calculated for $C_{14}H_{14}ClN_3$ 260.0949; found 260.0900 $[M+H]^+$.

Synthesis of compound 39: 2-Butylimidazo[1,2-a]quinoxalin-4-amine. Compound **38** (70 mg, 0.27 mmol) was dissolved in 2M ammonia in methanol (2 mL), heated in a sealed vial at 90 °C for 20 h and concentrated. The residue was purified by flash chromatography (SiO_2 , 0-100% EtOAc in hexane) to give compound **39** as a pale yellow solid (21 mg, 33%). 1H NMR (500 MHz, MeOD) δ 8.18 (s, 1H), 7.94 (dd, $J = 8.1, 1.2$ Hz, 1H), 7.60 (dd, $J = 8.1, 1.2$ Hz, 1H), 7.46 – 7.41 (m, 1H), 7.36 (ddd, $J = 8.5, 7.3, 1.4$ Hz, 1H), 2.86 – 2.80 (m, 2H), 1.80 (ddd, $J = 13.1, 8.4, 6.7$ Hz, 2H), 1.47 (dd, $J = 15.0, 7.5$ Hz, 2H), 1.00 (t, $J = 7.4$ Hz, 3H). ^{13}C NMR (126 MHz, MeOD) δ 149.5, 148.1, 137.3, 132.9, 127.7, 126.7, 125.8, 125.0, 116.2, 112.2, 32.8, 29.2, 23.5, 14.2. MS (ESI-TOF, m/z): calculated for $C_{14}H_{16}N_4$ 241.1448; found 241.1462 $[M+H]^+$.

Synthesis of compound 40: *N*-(2-Nitrophenyl)pentanehydrazide. To a solution of (2-nitrophenyl)hydrazine (500 mg, 3.26 mmol) in CH_2Cl_2 (10 mL) was added *N*-methylmorpholine (298 μ L, 4.24 mmol), followed by valeroyl chloride (415 μ L, 3.43 mmol). The reaction was stirred at room temperature for 1 h and concentrated. The residue was purified by flash chromatography (SiO_2 , 0-10% MeOH in CH_2Cl_2) to give compound **40** as a yellow solid (564 mg, 73%). 1H NMR (500 MHz, $DMSO-d_6$) δ 10.10 (s, 1H), 9.21 (s, 1H), 8.09 (dd, $J = 8.5, 1.5$ Hz, 1H), 7.61 – 7.56 (m, 1H), 7.05 (dd, $J = 8.6, 1.1$ Hz, 1H), 6.85 (ddd, $J = 8.4, 7.0, 1.3$ Hz, 1H), 2.23 (t, $J = 7.5$ Hz, 2H), 1.56 (dt, $J = 15.0, 7.5$ Hz, 2H), 1.33 (dq, $J = 14.6, 7.4$ Hz, 2H), 0.90 (t, $J = 7.4$ Hz, 3H). ^{13}C NMR (126 MHz, $DMSO-d_6$) δ 171.9, 145.5, 136.5, 131.6, 125.8, 117.7, 114.6, 33.0, 27.0, 21.8, 13.7. MS (ESI-TOF, m/z): calculated for $C_{11}H_{15}N_3O_3$ 238.1186; found 238.1189 $[M+H]^+$.

Synthesis of compound 41: *N*-(2-Nitrophenyl)pentanehydrazonoyl chloride. Compound **40** (82 mg, 0.35 mmol) in POCl₃ (3 mL) was heated at 110 °C for 2 h. The mixture was cooled to room temperature and concentrated. The residue was treated with ice water and extracted with CH₂Cl₂. The organic layer was washed with brine, dried over Na₂SO₄, concentrated and the crude product was purified by flash chromatography (SiO₂, 0-10% EtOAc in hexane) to give compound **41** as yellow oil (68 mg, 76%). ¹H NMR (500 MHz, DMSO-*d*₆) δ 10.82 (s, 1H), 8.15 (dt, *J* = 8.6, 0.9 Hz, 1H), 7.71 (dd, *J* = 4.5, 1.0 Hz, 2H), 7.03 – 6.99 (m, 1H), 2.76 – 2.71 (m, 2H), 1.68 (dt, *J* = 20.6, 7.5 Hz, 2H), 1.42 – 1.32 (m, 2H), 0.92 (t, *J* = 7.4 Hz, 3H). ¹³C NMR (126 MHz, DMSO-*d*₆) δ 140.1, 137.0, 134.1, 131.4, 125.9, 119.5, 115.8, 37.9, 28.1, 21.1, 13.6.

Synthesis of compound 42: *N*-(2-Nitrophenyl)pentanehydrazonamide. Compound **41** (60 mg, 0.23 mmol) was treated with 2 M ammonia in methanol (1 mL) and stirred at room temperature for 20 h. The residue was concentrated to give compound **42** as a red solid (38 mg, 70%). ¹H NMR (500 MHz, DMSO-*d*₆) δ 9.73 (s, 1H), 8.11 (dd, *J* = 8.5, 1.4 Hz, 1H), 7.61 (ddd, *J* = 8.5, 7.2, 1.4 Hz, 1H), 7.22 (d, *J* = 8.5 Hz, 1H), 6.89 (t, *J* = 7.6 Hz, 1H), 2.44 (t, *J* = 7.6 Hz, 2H), 1.71 – 1.62 (m, 2H), 1.38 (dt, *J* = 14.7, 7.4 Hz, 2H), 0.93 (t, *J* = 7.4 Hz, 3H). ¹³C NMR (126 MHz, DMSO-*d*₆) δ 142.5, 136.4, 125.9, 118.1, 114.5, 30.8, 28.6, 21.6, 13.6. MS (ESI-TOF, *m/z*): calculated for C₁₁H₁₆N₄O₂ 237.1346; found 237.1344 [M+H]⁺.

Synthesis of compound 43: Ethyl 3-butyl-1-(2-nitrophenyl)-1*H*-1,2,4-triazole-5-carboxylate. To a solution of compound **42** (78 mg, 0.33 mmol) in ether (3 mL) was added dropwise ethyl oxalyl chloride (110 μL, 0.99 mmol) in ether (2 mL). Toluene (5 mL) was added, and the mixture was heated at 110 °C for 3 h, and concentrated. The residue was purified by flash chromatography (SiO₂, 0-50% EtOAc in hexane) to give compound **43** as yellow oil (60 mg, 57%). ¹H NMR (500 MHz, DMSO-*d*₆) δ 8.26 (dd, *J* = 8.5, 1.4 Hz, 1H), 7.94 (ddd, *J* = 8.0,

7.4, 1.5 Hz, 1H), 7.87 – 7.83 (m, 2H), 4.20 (q, $J = 7.1$ Hz, 2H), 2.73 (t, $J = 7.4$ Hz, 2H), 1.71 – 1.64 (m, 2H), 1.37 – 1.29 (m, 2H), 1.13 (t, $J = 7.1$ Hz, 3H), 0.90 (t, $J = 7.4$ Hz, 3H). ^{13}C NMR (126 MHz, DMSO- d_6) δ 164.6, 161.0, 156.5, 144.2, 134.6, 131.5, 131.2, 130.1, 125.3, 62.1, 29.6, 27.1, 21.5, 13.8, 13.6. MS (ESI-TOF, m/z): calculated for $\text{C}_{15}\text{H}_{18}\text{N}_4\text{O}_4$ 319.1401; found 319.1410 $[\text{M}+\text{H}]^+$.

Synthesis of compound 44: 2-Butyl-[1,2,4]triazolo[1,5-*a*]quinoxalin-4(5*H*)-one. To a solution of compound **43** (58 mg, 0.18 mmol) in acetic acid (2 mL) was added iron powder (100 mg). The mixture was heated at 90 °C for 1 h, allowed to cool, filtered, and concentrated. The residue was purified by flash chromatography (SiO_2 , 0-10% MeOH in CH_2Cl_2) to give compound **44** as a white solid (19 mg, 43%). ^1H NMR (500 MHz, DMSO- d_6) δ 12.31 (s, 1H), 8.04 (dd, $J = 8.2, 1.0$ Hz, 1H), 7.50 – 7.43 (m, 2H), 7.36 (ddd, $J = 8.5, 7.1, 1.6$ Hz, 1H), 2.90 – 2.83 (m, 2H), 1.76 (ddd, $J = 13.3, 8.4, 6.7$ Hz, 2H), 1.39 (dq, $J = 14.7, 7.4$ Hz, 2H), 0.93 (t, $J = 7.4$ Hz, 3H). ^{13}C NMR (126 MHz, DMSO- d_6) δ 166.0, 152.2, 144.3, 128.6, 127.8, 123.5, 122.4, 116.6, 115.4, 29.9, 27.6, 21.7, 13.7. MS (ESI-TOF, m/z): calculated for $\text{C}_{13}\text{H}_{14}\text{N}_4\text{O}$ 243.1240; found 243.1227 $[\text{M}+\text{H}]^+$.

Syntheses of compounds **45** and **46** were carried out as reported for **32** and **33**, respectively.

45: 2-Butyl-4-chloro-[1,2,4]triazolo[1,5-*a*]quinoxaline. ^1H NMR (500 MHz, DMSO- d_6) δ 8.35 (dd, $J = 8.3, 1.0$ Hz, 1H), 8.13 (dd, $J = 8.2, 1.0$ Hz, 1H), 7.90 (ddd, $J = 8.4, 7.3, 1.4$ Hz, 1H), 7.79 (ddd, $J = 8.5, 7.3, 1.4$ Hz, 1H), 3.00 – 2.93 (m, 2H), 1.81 (ddd, $J = 13.3, 8.4, 6.7$ Hz, 2H), 1.47 – 1.36 (m, 2H), 0.94 (t, $J = 7.4$ Hz, 3H). ^{13}C NMR (126 MHz, DMSO- d_6) δ 167.0, 142.7, 140.3, 134.7, 130.9, 129.1, 128.0, 127.5, 115.3, 29.9, 27.8, 21.8, 13.7. MS (ESI-TOF, m/z): calculated for $\text{C}_{13}\text{H}_{13}\text{ClN}_4$ 261.0902; found 261.1890 $[\text{M}+\text{H}]^+$.

46: 2-Butyl-[1,2,4]triazolo[1,5-a]quinoxalin-4-amine. ^1H NMR (500 MHz, MeOD) δ 8.17 (dd, J = 8.2, 1.0 Hz, 1H), 7.68 (dd, J = 8.2, 1.0 Hz, 1H), 7.54 – 7.50 (m, 1H), 7.44 (ddd, J = 8.5, 7.3, 1.3 Hz, 1H), 3.00 – 2.97 (m, 2H), 1.88 (dt, J = 15.2, 7.6 Hz, 2H), 1.48 (dq, J = 14.8, 7.4 Hz, 2H), 1.00 (t, J = 7.4 Hz, 3H). ^{13}C NMR (126 MHz, MeOD) δ 167.8, 149.1, 140.2, 137.9, 128.6, 126.8, 126.5, 125.6, 116.0, 31.6, 29.2, 23.4, 14.1. MS (ESI-TOF, m/z): calculated for $\text{C}_{13}\text{H}_{15}\text{N}_5$ 242.1400; found 242.1391 $[\text{M}+\text{H}]^+$.

Synthesis of compound 47: 2-Chloro-3-hydrazinylquinoxaline. To a solution of 2,3-dichloroquinoxaline **34** (160 mg, 0.81 mmol) in MeOH (4 mL), hydrazine hydrate (100 μL , 3.24 mmol) was added and the reaction mixture was stirred at room temperature overnight. The solvent was evaporated to obtain compound **47** as a pale yellow solid (148 mg, 95%). ^1H NMR (500 MHz, MeOD) δ 7.78 – 7.71 (m, 2H), 7.61 (ddd, J = 8.4, 7.1, 1.5 Hz, 1H), 7.42 (ddd, J = 8.4, 7.1, 1.3 Hz, 1H). ^{13}C NMR (126 MHz, MeOD) δ 150.9, 142.2, 138.3, 137.7, 131.4, 128.6, 126.7, 126.3. MS (ESI-TOF, m/z): calculated for $\text{C}_8\text{H}_7\text{ClN}_4$ 195.0432; found 195.0344 $[\text{M}+\text{H}]^+$.

Synthesis of compound 48: 1-Butyl-4-chloro-[1,2,4]triazolo[4,3-a]quinoxaline. Trimethyl orthovalerate (0.5 mL) was added to compound **47** (50 mg, 0.257 mmol) and the resulting mixture was heated at 100 $^\circ\text{C}$ for 1 h. The solvent was removed and the product obtained was purified by flash chromatography to obtain compound **48** as a white solid (38 mg, 57%). ^1H NMR (500 MHz, CDCl_3) δ 8.12 (dd, J = 8.4, 1.1 Hz, 1H), 8.09 (dd, J = 8.0, 1.4 Hz, 1H), 7.74 (ddd, J = 8.4, 7.4, 1.7 Hz, 1H), 7.68 (ddd, J = 7.9, 7.4, 1.3 Hz, 1H), 3.53 – 3.45 (m, 2H), 2.08 – 1.99 (m, 2H), 1.67 – 1.54 (m, 2H), 1.04 (t, J = 7.4 Hz, 3H). ^{13}C NMR (126 MHz, CDCl_3) δ 152.8, 143.3, 142.9, 135.8, 130.6, 130.0, 128.1, 126.4, 115.6, 28.8, 28.5, 22.6, 13.9. MS (ESI-TOF, m/z): calculated for $\text{C}_{13}\text{H}_{13}\text{ClN}_4$ 261.0902; found 261.1004 $[\text{M}+\text{H}]^+$.

Synthesis of compound 49: 1-Butyl-[1,2,4]triazolo[4,3-a]quinoxalin-4-amine. Compound **48** (25 mg, 0.096 mmol) was dissolved in ammonia solution (2M in methanol, 1 mL) and heated in a sealed vial at 60 °C for 4 h. Concentration and purification by column chromatography (SiO₂, 0-5% MeOH in CH₂Cl₂) to give compound **49** as a white solid (16 mg, 70%). ¹H NMR (500 MHz, CDCl₃) δ 7.96 (dd, *J* = 8.4, 1.1 Hz, 1H), 7.71 (dd, *J* = 8.1, 1.4 Hz, 1H), 7.53 – 7.47 (m, 1H), 7.38 (ddd, *J* = 8.7, 7.3, 1.5 Hz, 1H), 5.87 (bs, 2H), 3.48 – 3.39 (m, 2H), 2.07 – 1.98 (m, 2H), 1.60 (dq, *J* = 14.8, 7.4 Hz, 2H), 1.04 (t, *J* = 7.4 Hz, 3H). ¹³C NMR (126 MHz, CDCl₃) δ 152.3, 147.1, 139.9, 137.6, 127.7, 127.4, 124.6, 124.5, 115.4, 28.8, 28.4, 22.6, 13.9. MS (ESI-TOF, *m/z*): calculated for C₁₃H₁₅N₅ 242.1400; found 242.1426 [M+H]⁺.

Synthesis of compound 50: Ethyl 2-(1*H*-indol-3-yl)-2-oxoacetate. To a solution of indole (1.01 g, 8.66 mmol) in anhydrous Et₂O (17 mL) and pyridine (0.95 mL, 11.7 mmol) was added a solution of ethyl chlorooxoacetate (1.2 mL, 10.7 mmol) in anhydrous Et₂O (3 mL) at 0 °C over a period of 15 min. The reaction mixture was stirred at 0 °C for 2 h and filtered. The resulting solid was then wash with cold Et₂O and water, dried over high vacuum to give compound **50** as a pale yellow powder (1.52 g, 81%). ¹H NMR (500 MHz, DMSO-*d*₆) δ 12.39 (bs, 1H), 8.42 (d, *J* = 3.3 Hz, 1H), 8.18-8.13 (m, 1H), 7.57-7.53 (m, 1H), 7.32-7.24 (m, 2H), 4.36 (q, *J* = 7.1 Hz, 2H), 1.34 (t, *J* = 7.1 Hz, 3H). ¹³C NMR (126 MHz, DMSO-*d*₆) δ 179.1, 163.6, 138.3, 136.7, 125.5, 123.9, 122.9, 121.1, 112.8, 112.4, 61.6, 14.0. MS (ESI-TOF, *m/z*): calculated for C₁₂H₁₁NO₃ 218.0812; found 218.0796 [M+H]⁺.

Synthesis of compound 51: 2-Butyl-2*H*-pyrazolo[3,4-*c*]quinolin-4(5*H*)-one. To a solution of butylhydrazine hydrochloride salt (288 mg, 2.31 mmol) in absolute EtOH (20 mL) was added compound **50** (352 mg, 1.62 mmol) and acetic acid (0.4 mL). The reaction mixture was heated to reflux and stirred for 24 h, cooled to room temperature and concentrated. The crude product

was purified by flash chromatography (SiO₂, 0-3% MeOH in CH₂Cl₂) to give compound **51** as a grey powder (243 mg, 62%). ¹H NMR (500 MHz, DMSO-*d*₆) δ 11.32 (s, 1H), 8.69 (s, 1H), 7.85 (d, *J* = 7.8 Hz, 1H), 7.36-7.29 (m, 2H), 7.17 (m, 1H), 4.37 (t, *J* = 7.0 Hz, 2H), 1.94-1.80 (m, 2H), 1.35-1.20 (m, 2H), 0.91 (t, *J* = 7.4 Hz, 3H). ¹³C NMR (126 MHz, DMSO-*d*₆) δ 157.0, 139.9, 135.9, 127.2, 125.5, 123.5, 122.0, 121.2, 115.9, 115.3, 52.5, 31.8, 19.2, 13.4. MS (ESI-TOF, *m/z*): calculated for C₁₄H₁₅N₃O 242.1288; found 242.1272 [M+H]⁺.

Synthesis of compound 52: 2-Butyl-4-chloro-2H-pyrazolo[3,4-*c*]quinoline. To a mixture of compound **51** (163 mg, 0.675 mmol) and PCl₅ (33.3 mg, 0.160 mmol) was added POCl₃ (3 mL). The reaction mixture was heated to reflux, stirred for 2 h and then concentrated. The residue was diluted with CH₂Cl₂ and washed with saturated NaHCO₃, dried over Na₂SO₄, filtered and concentrated. The crude product was purified by flash chromatography (0-20% EtOAc in Hexanes) to give compound **52** as a yellow solid (152 mg, 86%). ¹H NMR (500 MHz, CDCl₃) δ 8.31 (s, 1H), 8.08-8.04 (m, 1H), 8.02-7.98 (m, 1H), 7.63-7.55 (m, 2H), 4.53 (t, *J* = 7.3 Hz, 2H), 2.12-2.00 (m, 2H), 1.46-1.37 (m, 2H), 0.99 (t, *J* = 7.4 Hz, 3H). ¹³C NMR (126 MHz, CDCl₃) δ 143.4, 142.1, 141.3, 129.4, 127.4, 127.4, 123.5, 123.1, 122.5, 121.9, 54.3, 32.7, 19.9, 13.6. MS (ESI-TOF, *m/z*): calculated for C₁₄H₁₄ClN₃ 260.0949; found 260.0989 [M+H]⁺.

Synthesis of compound 53: 2-Butyl-2H-pyrazolo[3,4-*c*]quinolin-4-amine. Ammonia solution (2M in MeOH, 1 mL) was added to compound **52** (60 mg, 0.23 mmol) and the reaction mixture was heated in a sealed vial at 100 °C for overnight and then concentrated. The crude product was purified by flash chromatography (0-10% MeOH in CH₂Cl₂) to give compound **53** as a pale yellow powder (27 mg, 48%). ¹H NMR (500 MHz, DMSO-*d*₆) δ 8.82 (s, 1H), 7.95 (dd, *J* = 7.8 Hz, *J* = 1.5 Hz, 1H), 7.53 (dd, *J* = 8.2, 1.2 Hz, 1H), 7.39 (ddd, *J* = 8.3, 7.1, 1.5 Hz, 1H), 7.29-7.22 (m, 1H), 4.46 (t, *J* = 7.0 Hz, 2H), 3.42 (s, 2H), 2.00-1.84 (m, 2H), 1.37-1.24 (m, 2H), 0.92 (t, *J* =

7.4 Hz, 3H). ¹³C NMR (126 MHz, DMSO-*d*₆) δ 150.1, 140.3, 135.5, 126.9, 125.3, 123.4, 123.3, 122.5, 120.6, 118.1, 52.8, 32.0, 19.2, 13.5. MS (ESI-TOF, *m/z*): calculated for C₁₄H₁₆N₄ 241.1448; found 241.1470 [M+H]⁺.

Human TLR-7/-8 reporter gene assays (NF-κB induction). As described in Chapter 2.

Immunoassays for Interferon (IFN)-α and cytokines. As described in Chapter 2.

Flow-cytometric immunostimulation experiments. As described in Chapter 5.

Protein expression, purification and crystallization. The extracellular domain of human TLR8 (hTLR8, residues 27–827) was prepared as described previously,¹¹³ and was concentrated to 16 mg/mL in 10 mM MES (pH 5.5), 50 mM NaCl. The protein solutions for the crystallization of hTLR8/compound complexes contained hTLR8 (8.5 mg/mL) and compound (protein: compound molar ratio of 1:10) in a crystallization buffer containing 7 mM MES (pH 5.5), 35 mM NaCl. Crystallization experiments were performed with sitting-drop vapor-diffusion methods at 293K. Crystals of hTLR8/compound were obtained with reservoir solutions containing 9-12% (w/v) PEG3350, 0.3 M potassium formate, and 0.1 M sodium citrate (pH 4.8-5.2).

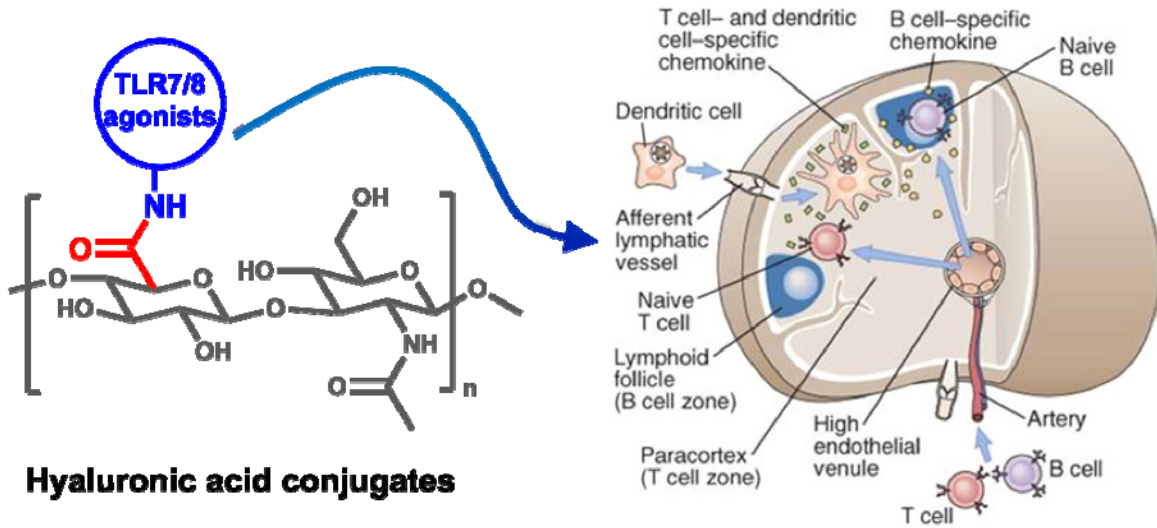
Data collection and structure determination. Diffraction datasets were collected on beamlines PF-AR NE3A (Ibaraki, Japan) and SPring-8 BL41XU under cryogenic conditions at 100 K. Crystals of hTLR8/compound were soaked into a cryoprotectant solution containing 15% (w/v) PEG3350, 0.23 M potassium formate, 75 mM sodium citrate pH 4.8-5.2, 7.5 mM MES pH 5.5, 38 mM NaCl, and 25% glycerol. Datasets were processed using the HKL2000 package¹¹⁹

or imosflm.¹²⁰ hTLR8/compound structures were determined by the molecular replacement method using the Molrep program¹²¹ with the hTLR8/CL097 structure (PDB ID: 3W3J) as a search model. The model was further refined with stepwise cycles of manual model building using the COOT program¹²² and restrained refinement using REFMAC¹²³ until the R factor was converged. Compound molecule, *N*-glycans, and water molecules were modeled into the electron density maps at the latter cycles of the refinement. The quality of the final structure was evaluated with PROCHECK.¹²⁴ The figures representing structures were prepared with PyMOL.¹²⁵ Coordinates have been deposited in the Protein Data Bank of the Research Collaboratory for Structural Bioinformatics; PDB codes for compounds **9** and **53** are, respectively, 4QBZ and 4QC0.

Quantum chemical computations and linear discriminant analyses. Calculations were performed using the NWChem¹²⁶ quantum chemical software for the electronic structure, electrostatic charge and property calculations. All the compounds were fully optimized at the density functional theory (DFT) level of theory using the M06-2X¹²⁷ functional and correlation consistent cc-pVDZ basis set. The optimized structures were verified as minima by calculating the second-order Hessian matrices. The molecular electrostatic potentials were calculated on the DFT-optimized geometries and superimposed onto a constant electron density (0.002 e/Å³) to provide a measure of the electrostatic potential at roughly the van der Waals surface of the molecules using the Gauss View03 software. The color-coded surface provides a location of the positive (blue, positive) and negative (red, negative) electrostatic potentials. The regions of positive charge indicate relative electron deficiency, and regions of negative potential indicate areas of excess negative charge. Fisher's linear discriminant analyses were performed using SPSS v22 (IBM, Armonk, NY); classification function coefficients.

Chapter 7.

Hyaluronic acid conjugation of TLR7/8 agonists for lymphoid tissue delivery



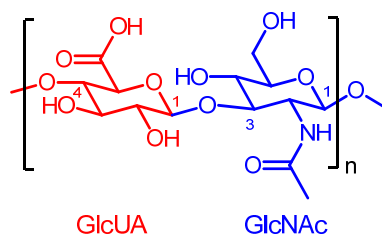
7.1. Introduction

The lymphatic system provides for unidirectional transport for interstitial fluid and proteins exiting microcirculation due to hydrostatic pressure, and returning then back to blood circulation. Lymphatic fluid drains from the initial lymphatics or lymphatic capillaries first into lymph nodes, which are highly organized secondary lymphoid tissues specialized in immune surveillance of the contents of afferent lymph.¹²³ Immune cells located in specialized zones within lymph nodes not only respond to antigens arriving from distal sites of infection, but also receive and orchestrate appropriate immune responses to migrating antigen-presenting cells (APCs) bearing antigenic epitopes. This is of particular relevance in immunization, wherein, peripheral APCs, such as dendritic cells (DCs) and macrophages capture antigens from the injection site and then migrate into the lymphoid tissues to trigger downstream T- and B-lymphocyte activation as well as memory cell differentiation.¹²⁴ The lymph nodes also contain a large number of resident APCs, which can actively process antigens and serve as major reservoir for long-lived memory B cells and central memory T cells, therefore playing a crucial role in generating long-term immunological memory.¹²⁵

The flow of interstitial fluid also brings fragments of extracellular matrix (ECM) macromolecules into lymph.¹²⁶ Important among the constituents of ECM is hyaluronic acid (hyaluronan, HA), a linear glycosaminoglycan polymer with a molecular weight that can reach 10^7 Daltons, and composed of repeating polymeric disaccharides of D-glucuronic acid (GlcUA) and *N*-acetyl glucosamine (GlcNAc) linked by β -1,4 and β -1,3 glucosidic bonds (Fig. 1).¹²⁷ HA serves to maintain a hydrated and stable extracellular space, not only by virtue of its ability to absorb a large amount of water expanding up to 1000 times its solid volume, but also due to its distinct hydrodynamic properties, such as very high viscosity. Depending on the molecular size, HA shows the capacity to interact with many different binding proteins and important group of

receptors.¹²⁸ The two most abundant of these receptors are CD44, which is a single chain, transmembrane glycoprotein expressed on leukocytes that traffic through the lymphatics,¹²⁹ and lymphatic vessel endothelial hyaluronan receptor-1 (LYVE-1), which is expressed almost exclusively on lymphatic endothelium.¹³⁰ CD44–HA interaction is known to be involved in a variety of cellular functions, including cell–cell interactions, receptor-mediated internalization/ degradation of HA, and cell migration. LYVE-1 participates in HA-mediated leukocyte trafficking, adhesion, and transmigration.^{126b}

Fig. 1. Chemical structure of hyaluronic acid.

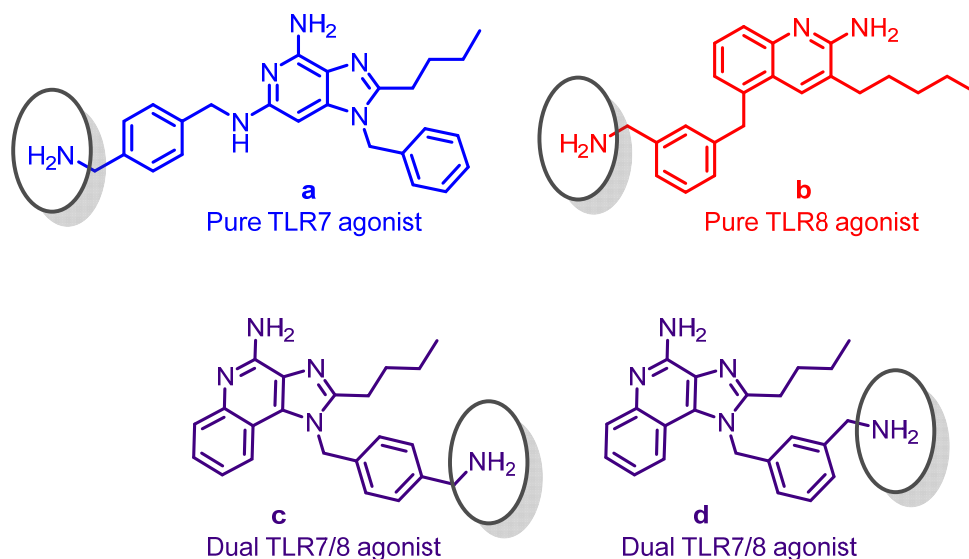


The efficient delivery of antigen/adjuvant has been a major challenge in the development of subunit vaccines, and enhancing vaccine delivery to secondary lymphoid organs might be a promising approach for improving vaccine efficacy.^{124, 131} Several studies have addressed enhanced or targeted delivery of antigens to secondary lymphoid tissue, including the use of depot-forming adjuvants,¹³² nanoparticulate carriers that are preferentially internalized by APCs,¹³³ or intralymphatic immunization,^{125a} but strategies that could use well-defined molecular conjugates would be more attractive. We envisioned that we could take advantage of the characteristics of HA — biodegradability, biocompatibility, high potential loading, and most of all, selective interaction with receptors — for targeted delivery¹³⁴ of small molecule Toll-like receptor (TLR) agonists to lymph nodes.

A number of lead adjuvants including the pure TLR7 agonist (**a**, Chapter 5),¹¹⁵ the pure TLR8 agonist (**b**) and the dual TLR7/8 agonists (**c**, **d**)^{56, 58} are undergoing preclinical evaluation as

vaccine adjuvants in our laboratory (Fig. 2). The approach of targeted delivery of these adjuvants may also serve to minimize systemic exposure of these small molecules with molecular properties that portend a large volume of distribution. For proof-of-concept studies, we selected these four compounds with an amine functional group (Fig. 2) that can be utilized in a straightforward manner for direct coupling with carboxylic acid group on HA. There are numerous methods that have been reported for HA conjugation;¹²⁷ we eschewed methods entailing harsh reaction conditions such as strongly alkaline or acidic pH, prolonged heating, or conditions calling for ultra-sound or microwave irradiation which are all known to potentially induce significant HA degradation, and elected to use the recently-reported triazine-activated amidation strategy, since it allows for a highly controlled substitution under aqueous/mixed-solvent conditions, at room temperature, and at neutral pH.¹³⁵

Fig. 2. Chemical structures of TLR7 and TLR8 agonists used for hyaluronic acid conjugation.

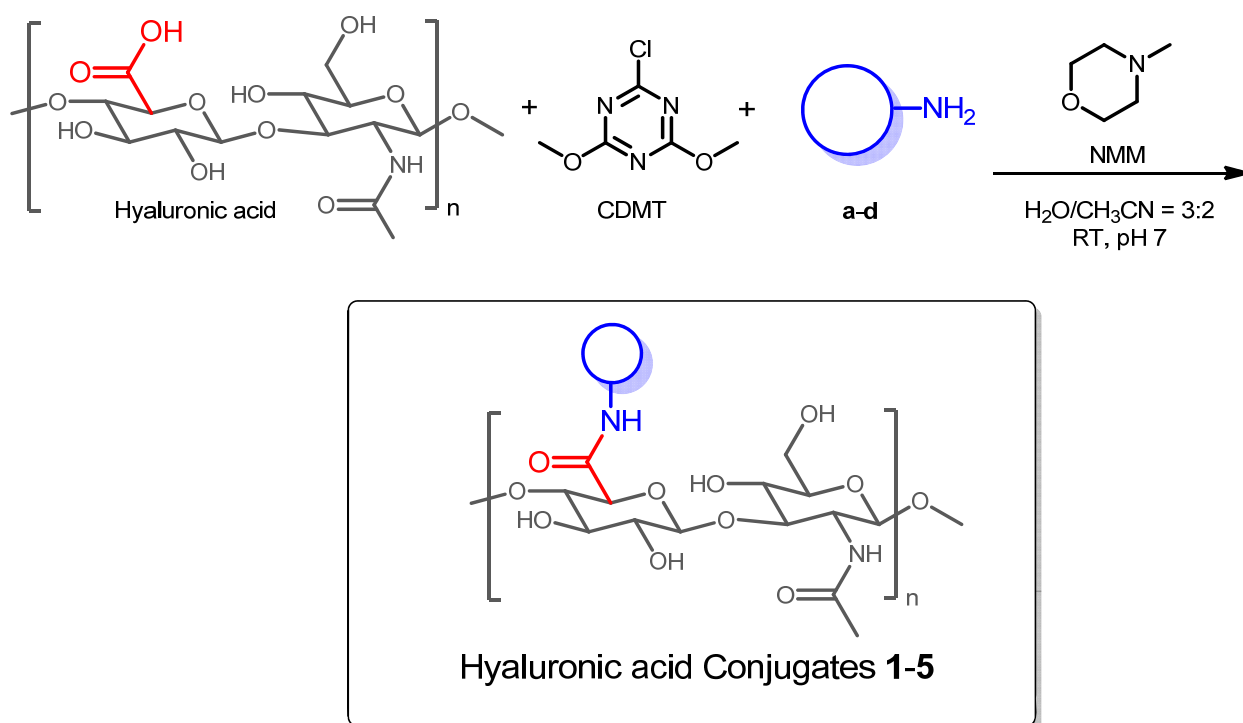


The conjugation reactions proceeded uneventfully, and spectroscopic and analytical characterization of the products suggested efficient hyaluronic acid conjugation with small molecules, as described below.

7.2. Results and Discussion

The reaction of 2-chloro-4,6-dimethoxy-1,3,5-triazine (CDMT) with carboxylic acids of HA and amines of small molecule TLR agonists in the presence of *N*-methylmorpholine (NMM) proceeded smoothly as reported in the literature¹³⁵ (Scheme 1).

Scheme 1.

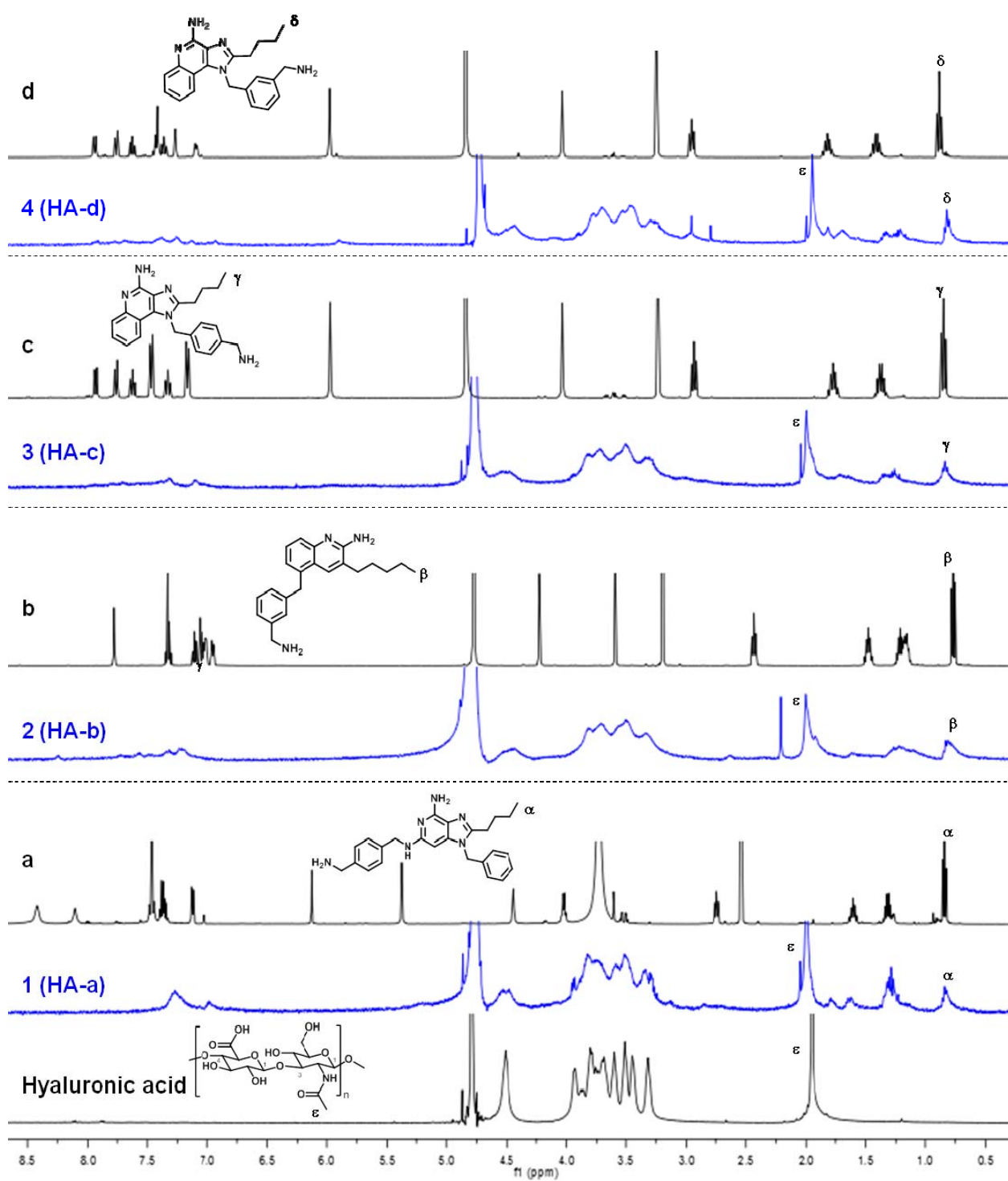


All reactants were soluble in a mixture of water and acetonitrile (3:2) and the pH values of the reaction mixtures after addition of all reactants were about 7~8. After overnight stirring at room temperature, the reaction mixtures were treated with Dowex ion exchange resin before dialysis to remove the morpholinium species, as well as unreacted amines which could otherwise act as counter-ions in their protonated form toward non-modified carboxylic acid groups of HA. Dialysis against 0.1 N NaCl solutions also helped eliminate electrostatically bound amines from anionic

polymers. As could be expected, the benzylic amine, and not the amidine amine participates in the formation of the amide bond, since the reaction with analogues that do not have the benzylic amine group did not yield detectable substitution (such as compound **6** in Chapter 6; data not shown). In addition to coupling the individual TLR7-, TLR8-, and TLR7/8-agonistic compounds on HA (HA-**a**, HA-**b**, HA-**c**, respectively), we also carried out the simultaneous coupling of HA with a mixture of three amine compounds — (HA-**a+b+c**) with the aim being to examine the relative adjuvanticity of a construct carrying multiple TLR agonists (conjugate **5**). The product yields were calculated based on the average molecular weight of the disaccharide repeating units considering the degree of substitution and found similar between the products ranging 71–75% (Table 1).

All products were characterized using ^1H NMR spectroscopy and the spectra for products **1-4**, as well as that of native hyaluronic acid and of the small molecules **a-d** are presented in Fig. 3. The poorly-resolved broad multiplet between c.a. 3.2 – 4.0 ppm corresponds to the resonances of the protons in the sugar ring of HA; a broad peak at 4.5 ppm could be assigned to the two anomeric protons attached to the carbons adjacent to two oxygen atoms, and the CH_3 protons of the *N*-acetyl group of HA could be readily identified at 1.95 ppm (Fig. 3). New peaks associated with aliphatic (butyl or pentyl chain) protons at 0.8 – 3.0 ppm and aromatic protons at 7.0 – 8.5 ppm, both of which are diagnostic of the conjugated small molecules, were observed. The degrees of substitution (DS) were determined by comparing integrated signals of the $\omega\text{-CH}_3$ resonance of the butyl/pentyl side chain of the small molecules (triplet, 0.86 ppm, shown as $\alpha\text{-}\delta$ in Fig. 3); this resonance could be clearly resolved from that of the CH_3 signal arising from the *N*-acetylglucosamine moiety (singlet, 1.95 ppm, shown as ε in Fig. 3) of native HA. As shown in Table 1, the DS ranged from 29 to 39%. The slight difference in the observed DS could be attributable to differential steric accessibility of the amines and/or solubility.

Fig. 3. ^1H NMR spectra of hyaluronic acid, small molecules **a-d**, and conjugates **1-4**.



While the ratios of peak integrals by ^1H NMR spectroscopy showed high batch-to-batch repeatability and consistency, we were mindful of the broad signals due to highly viscous sample solutions, as well as sample microheterogeneity, we sought to quantify the ‘loading’ also using spectroscopic measurements at 260 nm. All the TLR7/8 agonistic small molecules used for conjugation exhibit a distinct and intense absorption profile in the UV spectral region, and it was therefore straightforward to measure small molecule loading. The highest loading amount was found in conjugate **3** and the lowest in conjugate **2** (31% and 10%, respectively, Table 1).

Table 1. Properties of the conjugates.

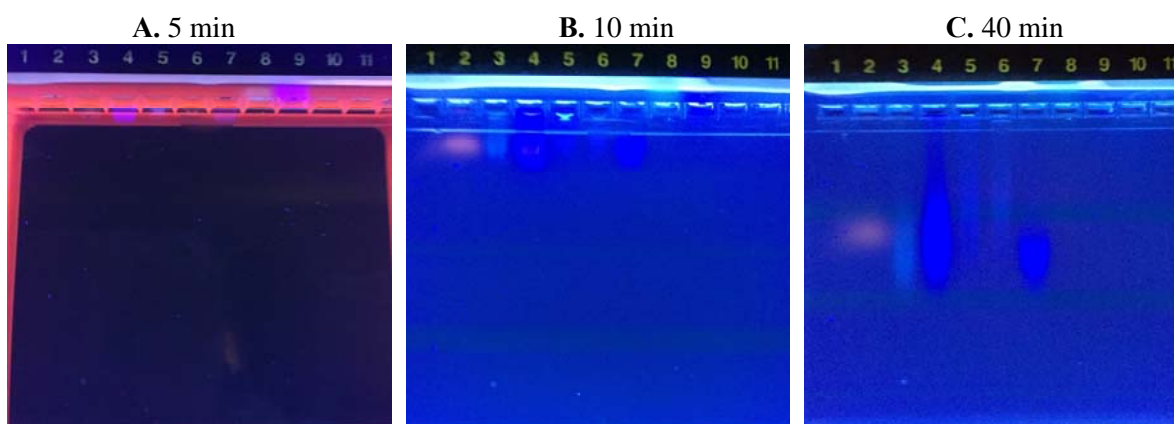
Conjugate No.	TLR agonist (SM)	Yield (%)	DS (%)	SM Content (w/w %)
1	a	75	29	21
2	b	75	35	10
3	c	71	39	31
4	d	74	36	21
5	a + b + c	N/A	N/A	N/A

DS, degree of substitution; SM, small molecule

Taking advantage of the UV absorptivity of compounds, the conjugates were also analyzed by gel electrophoresis. Samples were loaded on agarose gel and visualized by UV illumination. After a few minutes of running, we noticed that free small molecules (**a** and **b**) tend to travel toward the cathode due to its positive charges of the protonated amine (Figs. 4A and 4B; Lanes 8 and 9), which was not observed from conjugate samples. The conjugates **1-5**, on the other hand, clearly showed UV-absorbing bands (Fig. 4; Lanes 3-7), indicating covalent conjugation of the small molecules with hyaluronic acid, with an apparent molecular weight corresponding to 500 kDa, as adjudged by comparing the electrophoretic mobility of rhodamine-labeled HA (Fig.

4C, Lane 2). This technique was particularly useful in characterizing conjugate **5** (HA–**a+b+c**; Lane 7 in Fig. 4), which was not amenable to quantification of the loading either by ^1H NMR, or spectrophotometry owing to degeneracy of signals and spectral overlaps, respectively.

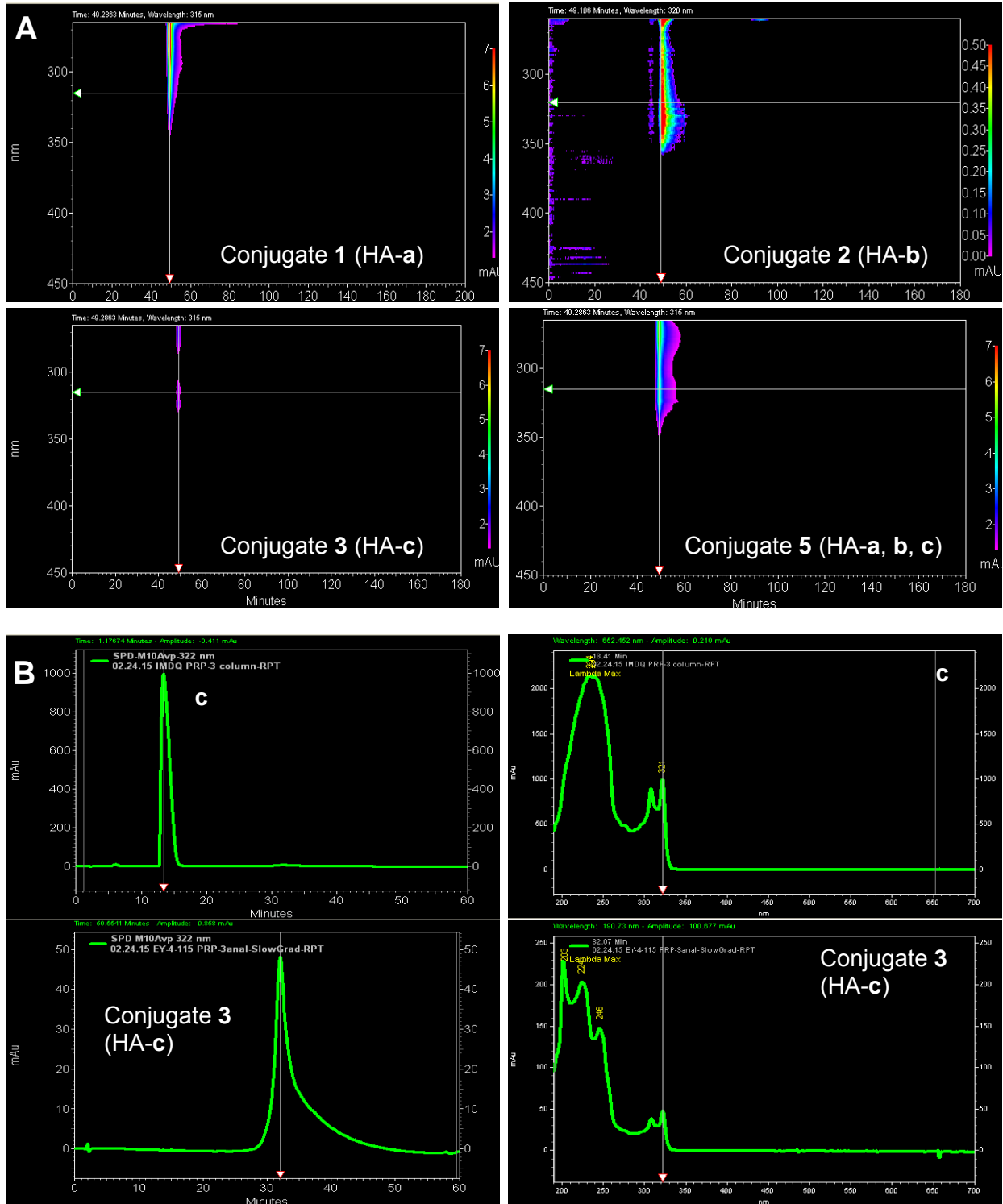
Fig. 4. Agarose gel electrophoresis. Lane 1: HA; Lane 2: rhodamine-labeled HA; Lane 3: conjugate **1** (HA–**a**); Lane 4: conjugate **2** (HA–**b**); Lane 5: conjugate **3** (HA–**c**); Lane 6: conjugate **4** (HA–**d**); Lane 7: conjugate **5** (HA–**a+b+c**); Lane 8: **a**; Lane 9: **b**; Lane 10: **c**; Lane 11: **d**.



The conjugates were also confirmed by size exclusion chromatography (SEC) analysis as shown in Fig. 5A. HA has no significant absorption in the UV and the conjugates were clearly observed to elute with a retention time of 50 min.

Reverse-phase HPLC analyses were also carried out to ensure the purity of conjugates. With a polymeric PRP-3 column, conjugate **3**, for example, eluted at 32 min, while that of its corresponding small molecule **c** appeared at a retention time of 14 min. Again, the spectroscopic signatures of the small molecules enabled unambiguous identification of the conjugates and, importantly, verified that no unconjugated small molecules were detected in the conjugate samples (Fig. 5B).

Fig. 5. A: Size exclusion chromatography. **B:** Reverse-phase HPLC with polymeric PRP-3 column. Shown below are detected at 320 nm.

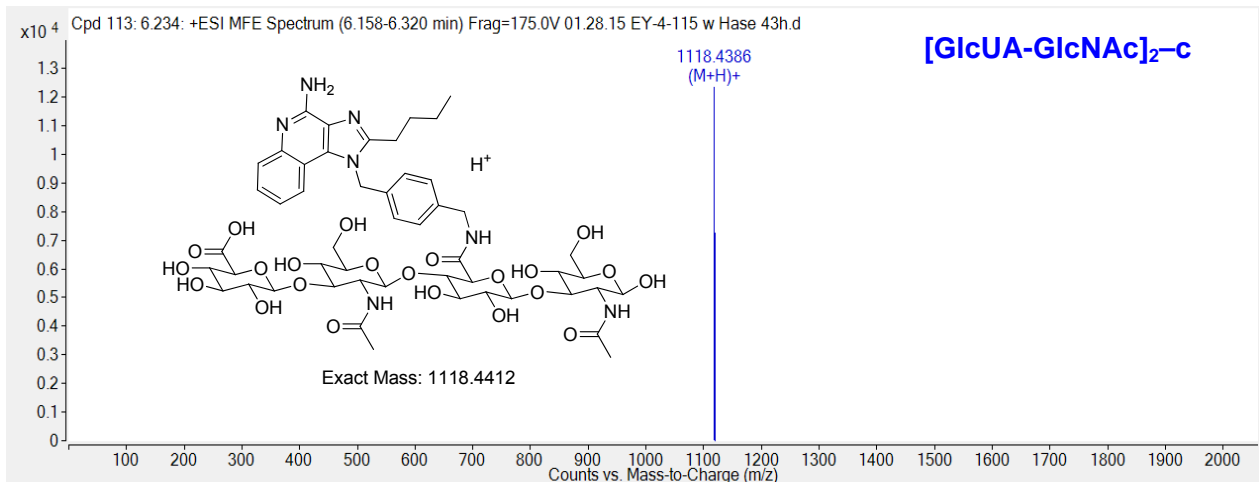
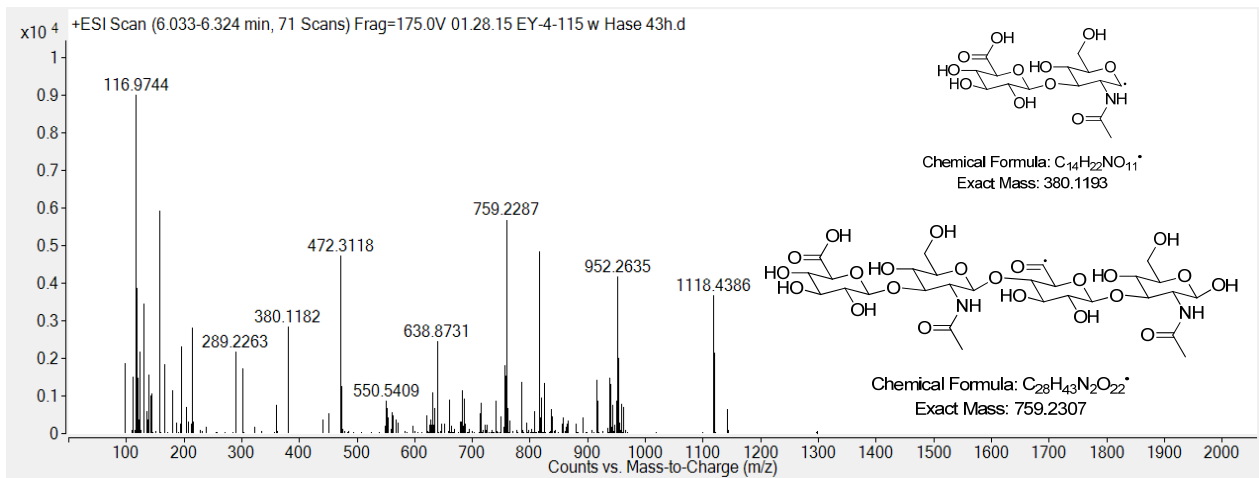
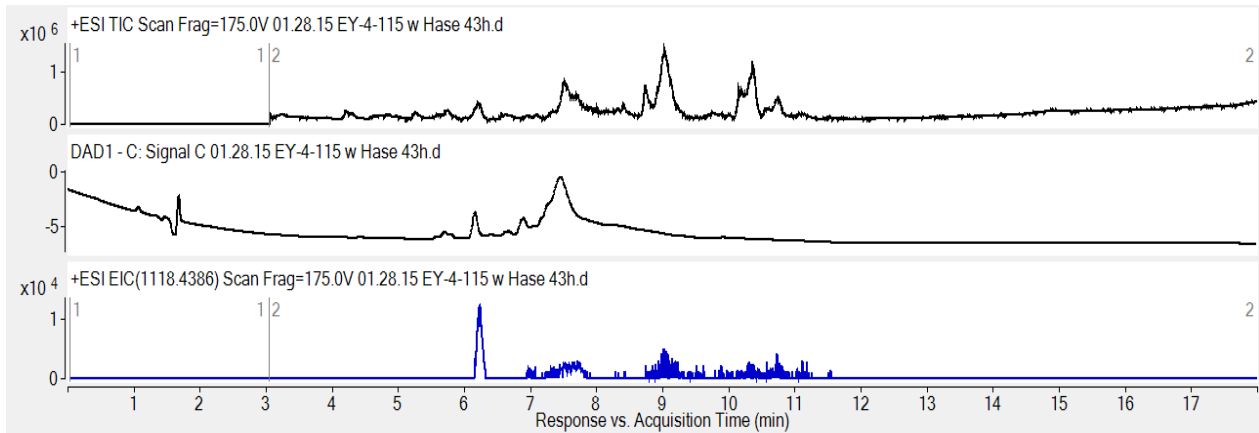


In vitro enzymatic degradation was performed using hyaluronidase (HAase) from bovine testes (400-1000 units/mg), and analyzed by LC-MS. After 45 h incubation of conjugates with hyaluronidase, oligosaccharides of HA covalently adducted with the small molecules were identified. Common major oligosaccharide species throughout the conjugates are tetra- and decasaccharides with one small molecule and dodecasaccharides with two small molecules on them (Table 2). From the HAase treated conjugate **5**, these major oligosaccharides with each small molecule as well as with the combination of different small molecules were found.

Table 2. Major oligosaccharide species found by LC-MS analysis after in vitro hyaluronidase enzymatic degradation of hyaluronic acid conjugates.

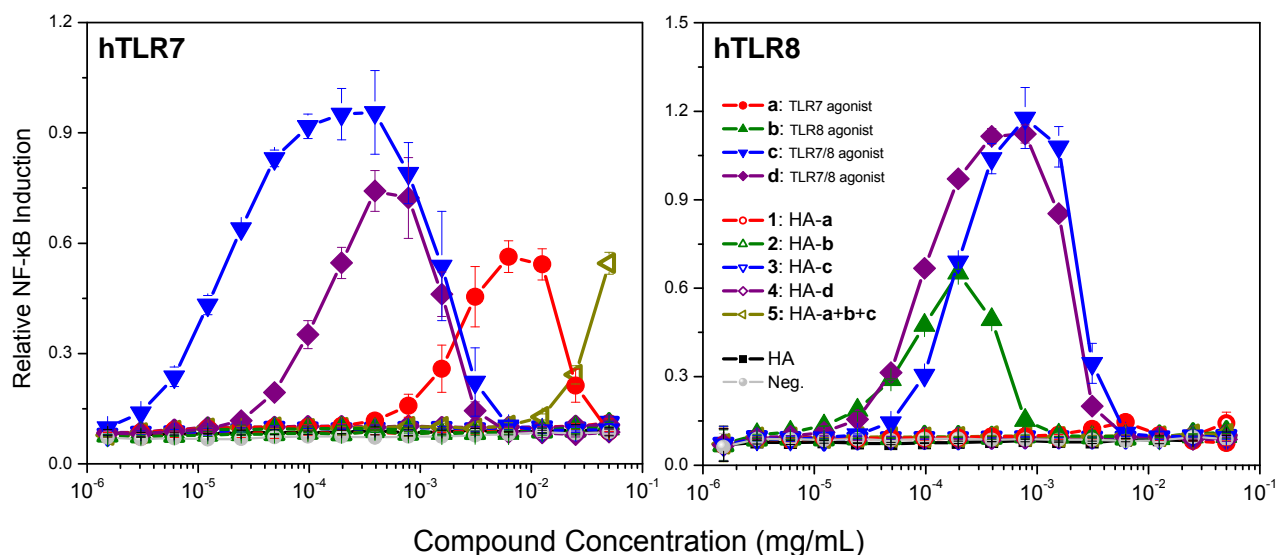
Conjugate No.	RT (min)	Species	Conjugate No.	RT (min)	Species
Conjugate 1 (HA-a)	7.262	[GlcUA-GlcNAc] ₅ -a	Conjugate 3 (HA-c)	6.234	[GlcUA-GlcNAc] ₂ -c
	7.927	[GlcUA-GlcNAc] ₂ -a		6.965	[GlcUA-GlcNAc] ₆ -[c] ₂
	8.885	[GlcUA-GlcNAc] ₆ -[a] ₂		7.549	[GlcUA-GlcNAc] ₅ -c
Conjugate 2 (HA-b)	6.966	[GlcUA-GlcNAc] ₂ -b	Conjugate 4 (HA-d)	6.059	[GlcUA-GlcNAc] ₂ -d
	7.759	[GlcUA-GlcNAc] ₆ -[b] ₂		6.830	[GlcUA-GlcNAc] ₆ -[d] ₂
	8.505	[GlcUA-GlcNAc] ₅ -b		7.247	[GlcUA-GlcNAc] ₅ -d
Conjugate 5 (HA-a, b, c)	6.243	[GlcUA-GlcNAc] ₂ -c	Conjugate 5 (HA-a, b, c)	7.900	[GlcUA-GlcNAc] ₆ -[a][c]
	6.977	[GlcUA-GlcNAc] ₂ -b		7.911	[GlcUA-GlcNAc] ₂ -a
	7.278	[GlcUA-GlcNAc] ₅ -[b][c]		8.161	[GlcUA-GlcNAc] ₈ - [a][b][c]
	7.376	[GlcUA-GlcNAc] ₆ -[b][c]		8.293	[GlcUA-GlcNAc] ₆ -[a][b]
	7.517	[GlcUA-GlcNAc] ₅ -c		8.528	[GlcUA-GlcNAc] ₅ -b

Fig. 6. LC-MS spectra of hyaluronidase treated conjugate 3.



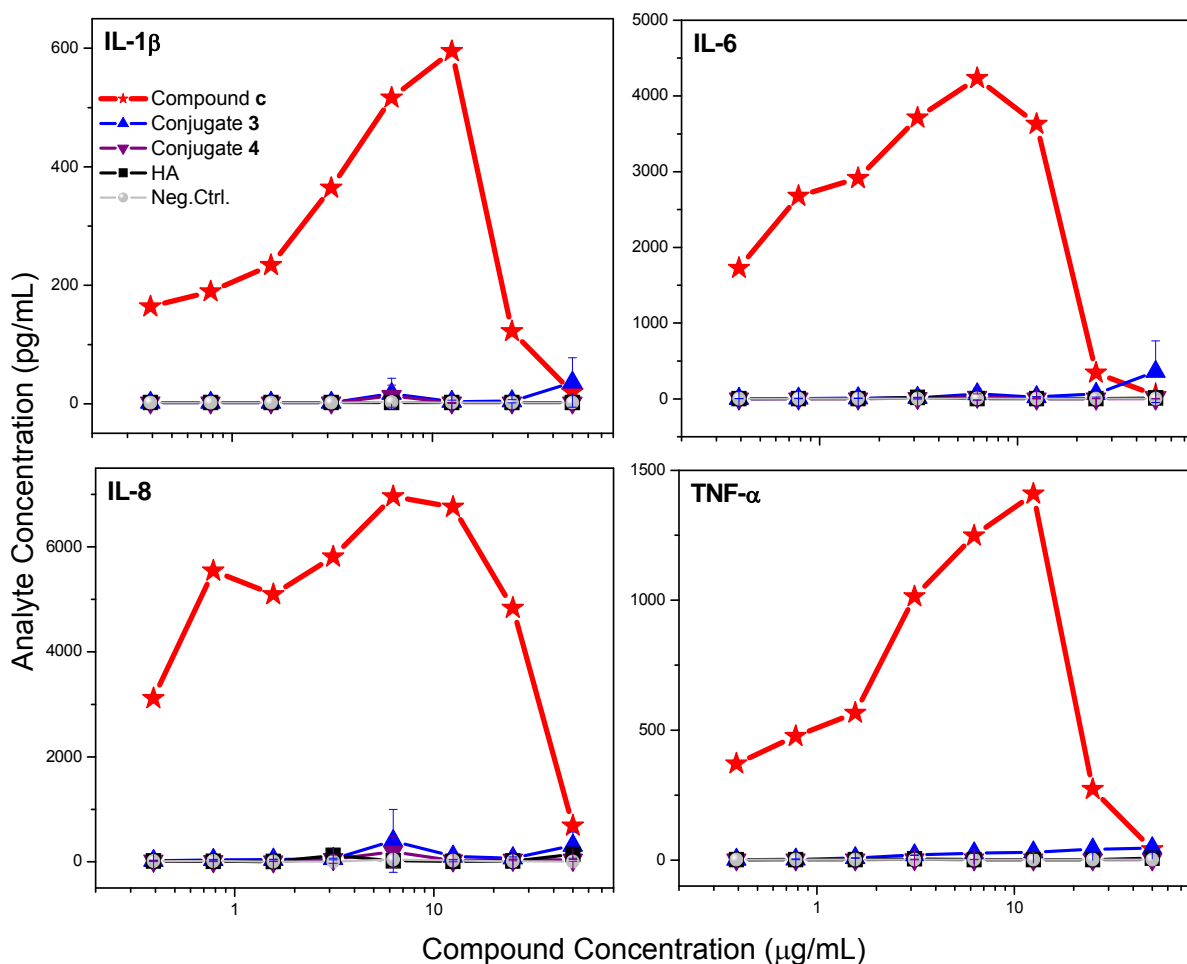
Next, the conjugates were screened in NF- κ B reporter gene assays specific for human TLR7 and TLR8. Whereas all small molecule TLR-7 and/or -8 agonists (**a-d**) showed, as expected, agonistic activities, the HA conjugates did not display any detectable NF- κ B induction up to concentrations of 50 μ g/mL in both TLR7 and TLR8 agonism assays. Hyaluronic acid (used as control) was also verified to be quiescent in these assays (Fig. 7).

Fig. 7. Dose-response profiles of TLR7/8 agonism.



We examined the cytokine/chemokine-inducing properties of these conjugates using human PBMCs and they did not show any proinflammatory cytokine induction (represented by IL-1 β , IL-6, IL-8, and TNF- α in Fig. 8). It is important to note that the hyaluronic acid conjugates become “silent”, presumably because the polyanionic character of the conjugates precludes significant internalization and access to the endolysosomal compartment. These results, importantly, augur very weak (if any) reactogenicity for the HA conjugates vis-à-vis the unconjugated agonists and, therefore, are predicted to have a very high safety profile in addition to their being highly adjuvantic.

Fig. 8. Dose-response profiles of cytokine induction in hPBMCs by the selected conjugates and controls.



The adjuvantic activities of these conjugates were evaluated in New Zealand White rabbits and compared to a variety of candidate adjuvants under evaluation in our laboratory in a standardized manner. All candidate adjuvants were designed to be entirely water soluble, with a purity of at least 99.5% as judged by LC-MS profiles. The adjuvant dose was held constant at 100 μg/dose. The antigen used was Diphtheria toxoid (CRM197) at 10 μg/dose. The vaccine construct was formulated under excipient-free conditions in sterile, pyrogen-free saline. Rabbits (n = 4 per cohort) were pre-bled on Day 0 for estimation of preimmune titers, and then primed with the first dose of vaccine. Animals were boosted on Days 15 and 28, and bled on Days 25 (for Immune-1 sera) and 38 (for Immune-2 sera), respectively. All ELISA assays were carried

out in a 384-well plate format with automated liquid handling instrumentation as described in the Experimental Section. Reference hyperimmune sera were used in each plate for quality control purposes.

As shown in Fig. 9, conjugates **3** and **4** were found to be highly adjuvantic in evoking high antigen-specific IgG titers even after a single boost; titers were higher than that obtained using the corresponding unconjugated small molecule TLR7/8 agonist **c** (Fig. 9B). Particularly, conjugate **4** was shown to be most adjuvantic among all TLR active compounds that we had characterized in our laboratory with a rise-in-titer values of >1000 (Fig. 10, overleaf). Considering very small dose of the TLR agonist in the conjugate, the strong adjuvantic activity of the conjugate after a single boost, coupled with the complete lack of proinflammatory cytokine induction in ex vivo models, as mentioned earlier, presages a highly effective and safe vaccine adjuvant.

Fig. 9. Adjuvantic activities of HA conjugates after a single boost. Antigen: Diphtheria toxoid (CRM197), 10 µg/dose; Adjuvant: 100 µg/dose in NZ rabbits; Formulation: excipient-free saline. **A.** Antigen-specific titers in HA conjugate-adjuvanted rabbits. Preimmune values are in open symbols. **B.** Box-and-whisker plots of ratios of immune/preimmune titers yielding absorbance values of 1.0.

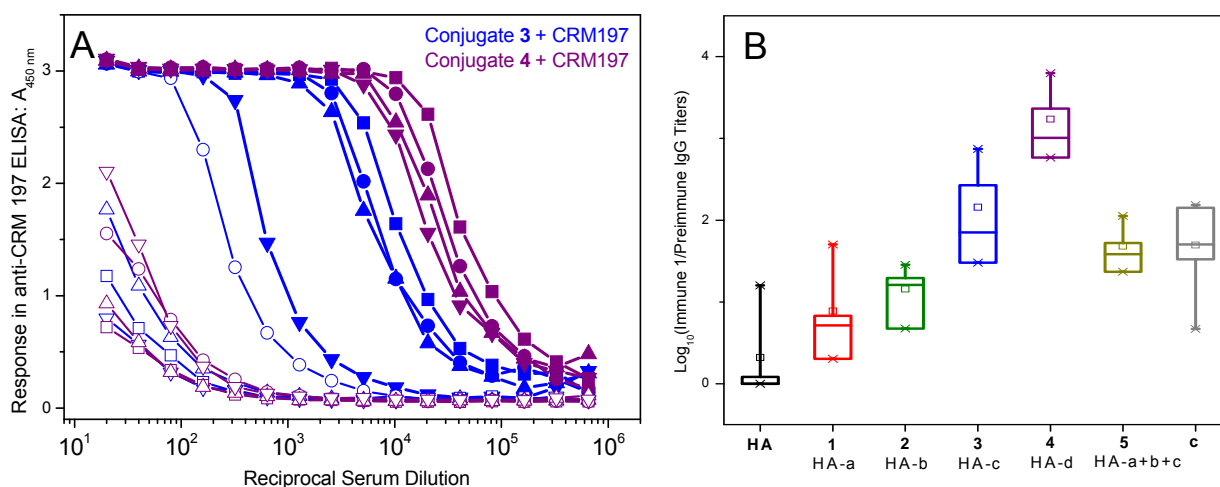
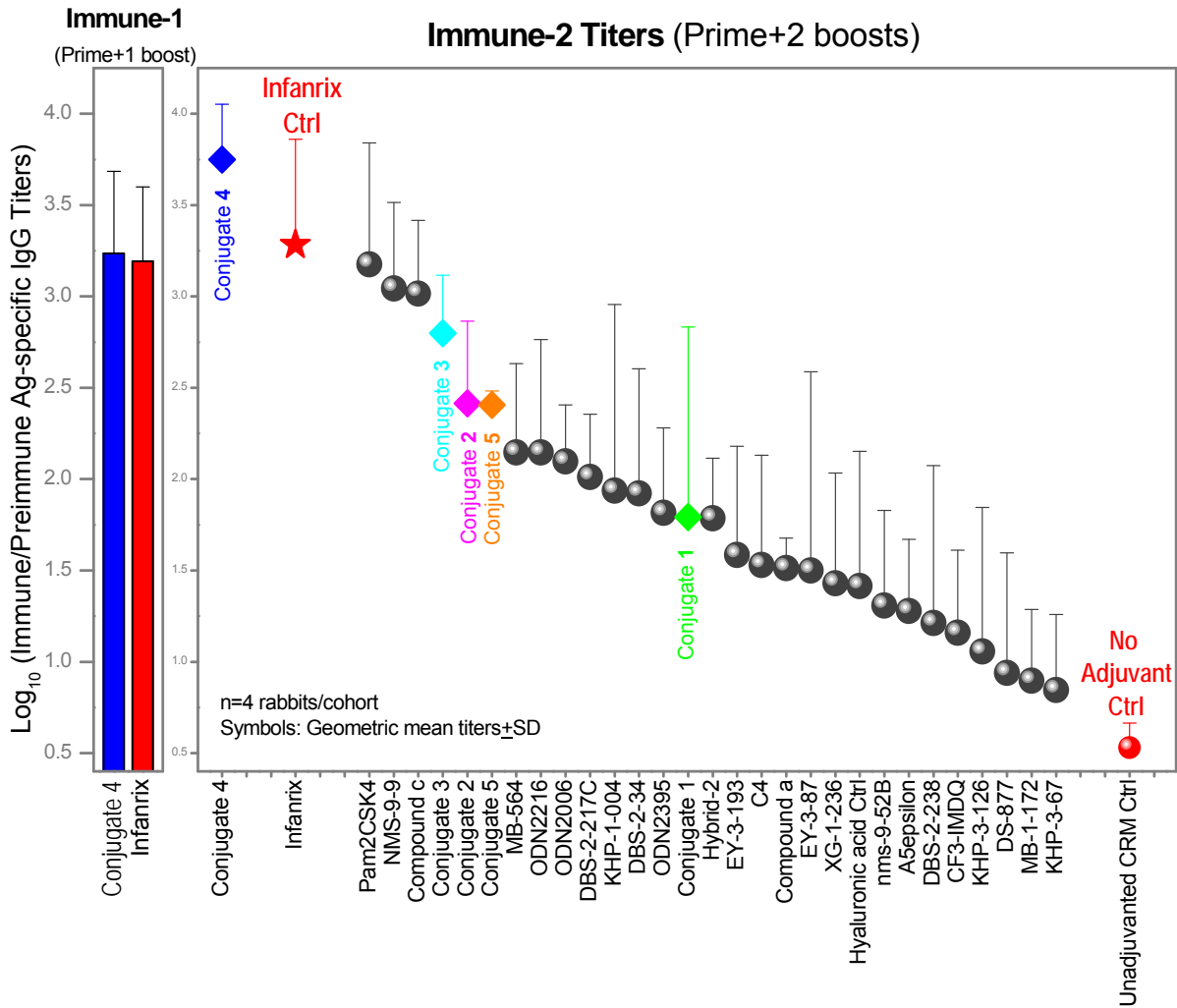


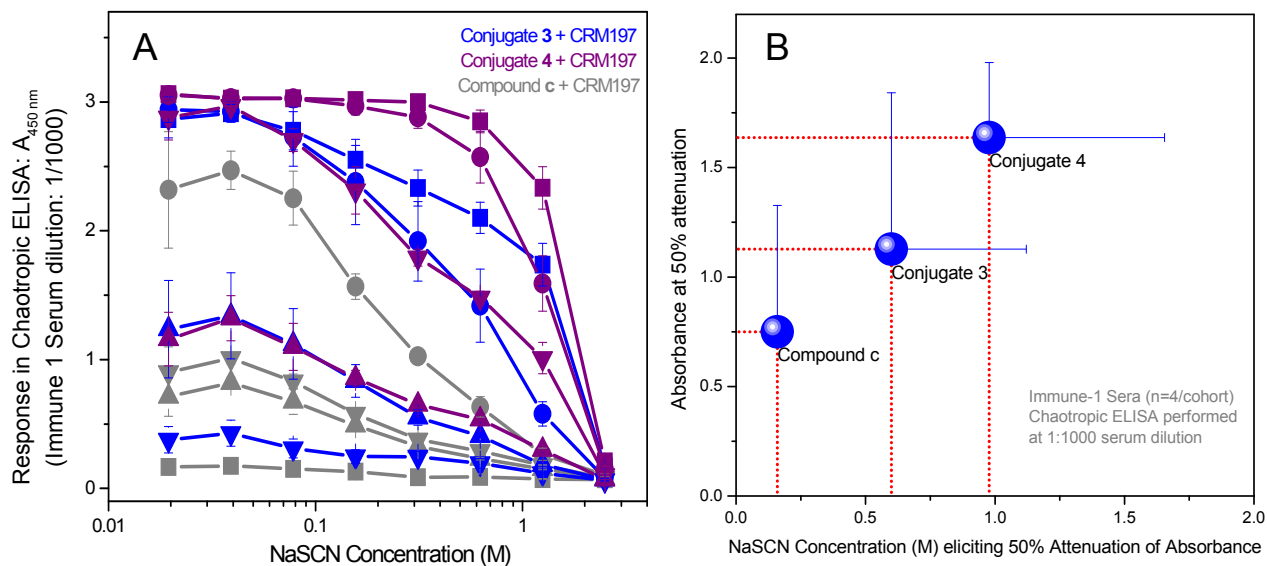
Fig. 10. Induction of high anti-CRM197 IgG levels after a single boost (Immune-1 sera) by HA conjugate 4 and Infanrix (left panel), compared to titers after two boosts (Immune-2 sera) for the HA conjugates, as well as a variety of experimental, candidate adjuvants. Also shown in red are titers obtained by immunization with a full human dose of Infanrix and unadjuvanted controls (right panel).



Whilst measurements of serum antibody titers employing an immunoassay such as ELISA serve to quantify antigen-specific antibody concentrations, antibody ‘avidity’ (functional affinity; the sum of affinities of multiple antigen-binding sites in polyclonal antibodies simultaneously interacting with their cognate antigenic epitopes) is an important characteristic of protective

immune responses.¹³⁶ In order to also assess the quality of antibody, the strength of the interaction between CRM197 and antigen-specific IgG antibodies obtained 10 days after a single boost (Immune-1) was determined using the chaotropic ELISA.¹³⁷ Replicate wells containing antibody bound to antigens were exposed to increasing concentrations of the chaotropic thiocyanate ion that disrupts antibody-antigen complexes and the concentration of sodium thiocyanate (NaSCN) that decreases antibody binding by 50% was used as the measurement of avidity. As shown in Fig. 11B, the highest avidity was found in the conjugate 4-
 adjuvanted sera with 50% attenuation of absorbance elicited at 1.0 M NaSCN. This result unambiguously indicates higher quality IgG elicited by the hyaluronic acid conjugates.

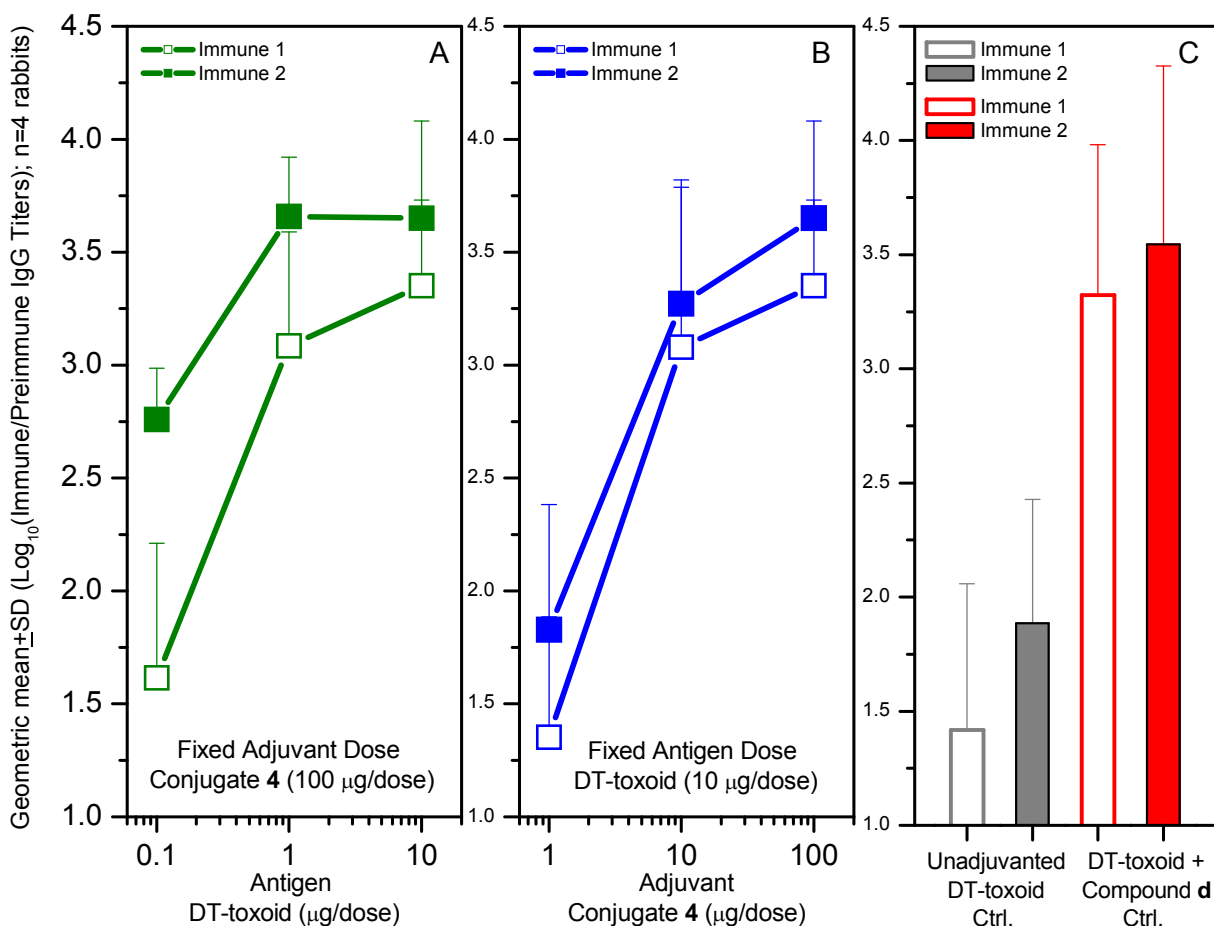
Fig. 11. A. Chaotropic ELISA with increasing concentration of sodium thiocyanate (NaSCN) after a single boost (Immune-1 sera). **B.** Quantitation of antibody avidity in chaotropic ELISAs with NaSCN concentration eliciting 50% attenuation of absorbance.



The observation of extraordinary adjuvantic potency completely dissociated with biomarkers of inflammation and reactogenicity is unprecedented in the field, and warranted confirmation. In an

independent experiment, cohorts of rabbits (n=4 per group) were immunized with either graded doses of antigen (human vaccine-grade formalin-inactivated Diphtheria toxoid, Statens Serum Institute, Denmark) with a fixed dose of conjugate 4 to examine dose-sparing effects, or graded doses of adjuvant with a fixed dose of Diphtheria toxoid. As shown in Fig. 12A, conjugate 4 elicits very high titers even at an antigen concentration of 1 $\mu\text{g}/\text{dose}$, confirming the excellent dose-sparing effect of the adjuvant. Although 100 $\mu\text{g}/\text{dose}$ of conjugate 4 is optimal, robust humoral responses are observed even with 10 μg of conjugate 4, as depicted in Fig. 12B.

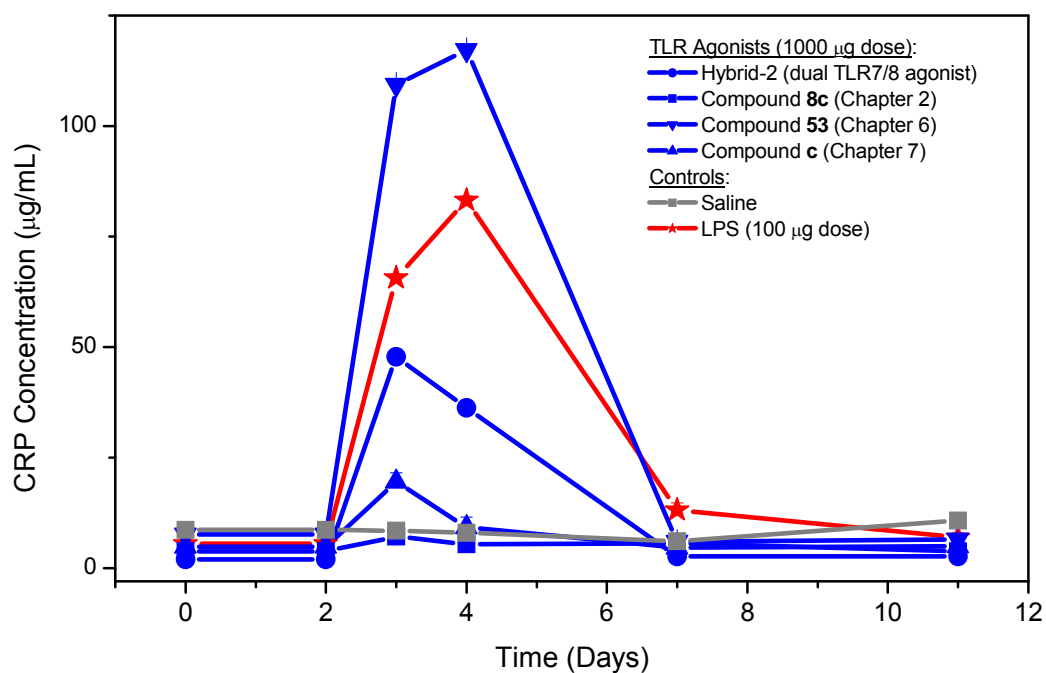
Fig. 12. Dose-sparing effects of conjugate 4 as adjuvant in rabbits (n=4 per group) immunized with: Graded doses of formalin-inactivated Diphtheria toxoid with fixed dose (100 $\mu\text{g}/\text{dose}$) of conjugate 4 (A); graded doses of conjugate 4 with fixed dose (10 $\mu\text{g}/\text{dose}$) of antigen (B); unadjuvanted and compound d- adjuvanted (100 $\mu\text{g}/\text{dose}$) controls (C).



7.3. Conclusion

A potential drawback in using small molecule TLR agonists as vaccine adjuvants is their propensity to diffuse out of the vaccination site into systemic circulation, thereby not only limiting their adjuvantic properties, but perhaps also enhancing the risk of systemic reactogenicity. The administration of R-848 (Chapter 1) was poorly tolerated in human preclinical trials, with systemic side effects including fever, headache, malaise, and myalgia,^{42, 138} likely due to systemic immune activation. Indeed, intravenous injections of large doses of TLR7/8 agonists (described in earlier chapters; listed in Fig. 13) as a bolus in rabbits induce C-reactive protein, an acute-phase bio-marker of systemic inflammation (Fig. 13).¹³⁹

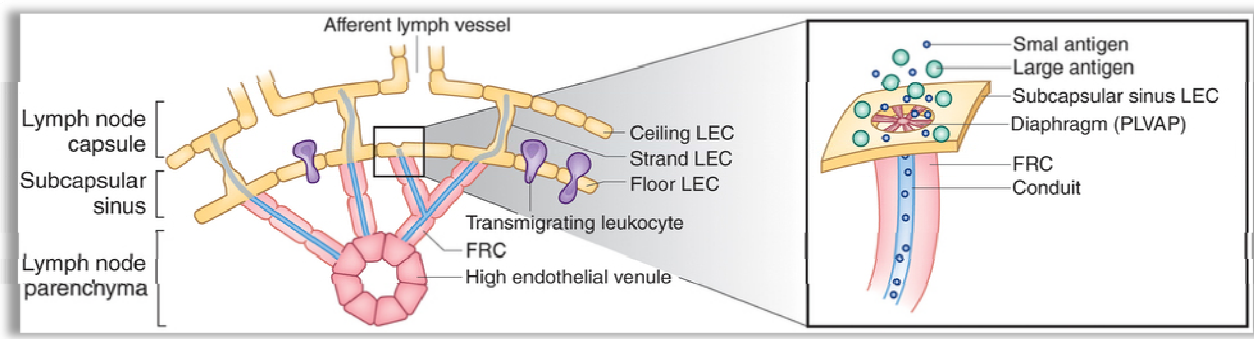
Fig. 13. Induction of C-reactive protein (CRP) in New Zealand White Rabbits ($n=5$ per cohort) by TLR7/8 agonists. Animals were bled two days before challenge to obtain baseline CRP levels, and were injected with either 1 mg of candidate adjuvant (or 100 μg of LPS, used as control) formulated in saline intravenously as a bolus, into the marginal vein of the ear, on Day 0. Successive bleeds were performed on Day 1, 2, 5 and 9 after injection. Rabbit CRP-specific ELISAs were performed to quantify CRP in the sera.



Limiting systemic exposure has recently been addressed by adsorbing small molecules incorporating phosphonate groups on ‘alum’ [Al(OH)₃].¹⁴⁰ Whilst alum has been the mainstay of vaccines since the 1920s, aluminum exposure has been implicated in neurotoxicity,¹⁴¹ especially in the preterm¹⁴² and infant populations and our understanding of innate immune signaling may have reached a threshold as to allow considering rational alternatives.

Targeted delivery of the TLR agonists to secondary lymphoid organs using molecular conjugation to HA was therefore evaluated to simultaneously enhance selective delivery to draining lymph nodes while limiting systemic exposure. As mentioned earlier, both CD44 and LYVE-1 are known to interact with HA. Soluble antigens in the interstitial fluid are carried by bulk lymphatic via afferent lymphatic ducts into the subcapsular sinus of the draining lymph node.¹⁴³ Recent studies on the microanatomic architecture of the subcapsular sinus of the lymph node receiving afferent lymphatic fluid show that in the subcapsular sinus, plasmalemma vesicle-associated protein (PLVAP; also known as PV-1, PAL-E or MECA-32 antigen) forms a physical sieve that limits the entry of molecules smaller than 70 kDa from accessing lymph node parenchyma, and confining such large molecules to the sinus (Fig. 14).¹⁴⁴

Fig. 14. The subcapsular sinus of the lymph node, lined by lymphatic endothelial cells, is directly connected to the afferent lymphatic vessels. The fibroblastic reticular cells (FRCs) constitute a network interconnecting the subcapsular sinus and vasculature, forming a conduit system for direct egress of fluid and small molecules arriving from the subcapsular sinus to the blood circulation. Molecules of size >70 kDa are retained by a diaphragm made up of PLVAP, which forms a cartwheel structure. Adapted from: *The lymph node filter revealed. M. Hons & M. Sixt, Nature Immunology 16, 338–340 (2015).*



Sinus-lining macrophages are known to transfer antigens from the sinus lumen to the B cell follicles.¹⁴⁵ Given that the size of HA that was used in these studies is approximately 500 kDa, we speculate that the retention of the HA conjugates in the subcapsular sinus may facilitate and enhance sampling by the sinus-resident macrophages, augment localized innate immune signaling, and marshal subsequent adaptive immune responses in a spatiotemporally far more efficient manner.

As noted earlier, the hyaluronic acid conjugates entirely lose their TLR-agonistic activities, both in respect to TLR recognition as probed by the reporter gene assays, as well as in their ability to induce cytokines in secondary screens. One of these 'silent' conjugates has, however, yielded the best adjuvant, capable of evoking, with a single boost regimen, affinity-matured high-avidity immunoglobulins whose titers rival and surpass all of the best-in-class small molecule adjuvants that have been examined to date. As mentioned earlier, significant hyaluronidase activity is associated with macrophages,¹⁴⁶ possibly rendering the conjugate into small oligosaccharide fragments bearing the TLR agonist(s). The high adjuvanticity observed with several of the conjugates tested perhaps additionally implies that amidases in the subcapsular macrophage may release the free agonist, which may act in the milieu where the antigen is also being sampled. These are questions yet to be formally addressed. Studies, for instance, have already begun on conjugates obtained with carboxymethylcellulose to probe the contribution of the receptor-mediated 'uptake' of hyaluronic acid vis-à-vis passive, but contemporaneous delivery of antigen and adjuvant via bulk lymphatic flow. Finally, the superior adjuvanticity observed with conjugate **4** suggests that HA conjugates bearing dual TLR7/8 agonists may be necessary for optimal innate immune signaling and subsequent adaptive immune recruitment, since neither conjugate **1** (bearing a pure TLR7 agonist), nor conjugate **2** (decorated with a pure TLR8 agonist) were found to be as strongly adjuvantic as conjugate **4**. These results, made possible by extensive SAR on a variety of chemotypes described in the preceding chapters, have laid the

foundation and point the way forward for many other experimental approaches designed to probe the consequences of rational, targeted vaccine delivery that take into consideration not only the medicinal chemistry and immunology of small molecule innate immune stimuli, but also incorporate elements of the microanatomical organization and physiology of the immune system.

7.4. Experimental

Materials

Sodium hyaluronate (HA) from *Streptococcus equi* (bacterial glycosaminoglycan polysaccharide) was purchased from Sigma-Aldrich (USA) and used as received. All other reagents and solvents including 2-chloro-4,6-dimethoxy-1,3,5-triazine (CDMT, 97%), *N*-methylmorpholine (NMM, 99%), as well as Dowex[®]50WX8 ion exchange resin (hydrogen form, 50-100 mesh) were purchased from Sigma-Aldrich. Hyaluronate Rhodamine (500 kDa) was purchased from Creative PEGWorks (USA). Hyaluronidase from bovine testes (55 kDa, 400-1000 units/mg) was purchased from Sigma-Aldrich and used for enzymatic degradation. For dialysis, Slide-A-Lyzer G2 Dialysis Cassettes, 3.5 K MWCO (Thermo Scientific) were used.

Synthesis of hyaluronic acid conjugates

General procedure for triazine-activated amidation of hyaluronic acid (HA). Sodium hyaluronate (1.0 eq., 100.0 mg, 0.25 mmol $-\text{COO}^-$) was dissolved in 20 mL of water under gentle stirring. The solution was cooled in an ice bath and 14 mL of acetonitrile were added dropwise. 2-Chloro-4,6-dimethoxy-1,3,5-triazine (1.0 eq., 44 mg, 0.25 mmol) and *N*-methylmorpholine (1.5 eq., 41 μL , 0.38 mmol) were added to the solution and the mixture was subsequently allowed to come to room temperature and was stirred for 1 h. Thereafter the

amine compound (1.0 eq., 0.25 mmol) was added and the mixture was stirred at room temperature overnight. The crude mixture was stirred with Dowex[®]50WX8 ion exchange resin (1 g) for 1 h, then filtered and dialyzed (3.5 kDa MW cutoff) against aq. NaCl (0.1 N) for 2 days and against dH₂O for 3 days and lyophilized. The solids obtained were thoroughly washed with acetone. The product yields were calculated based on the average molecular weight of the disaccharide repeating units considering the degree of substitution.

For the synthesis of conjugate **5**, the mixture of small molecules **a**, **b** and **c** (each 0.4 eq., 0.1 mmol) was used.

Characterization of HA conjugates

Proton nuclear magnetic resonance spectroscopy (¹H NMR). ¹H NMR spectra of the samples (5 mg/mL in D₂O) were recorded on a Bruker Advance 400 MHz spectrometer. The chemical shifts are given in parts per million (ppm) and are calibrated relative to the residual solvent protons (HDO: 4.79 ppm). Degrees of substitution (DS) were calculated from comparing the integrals of the methyl protons (1.95 ppm) of the *N*-acetylglucosamine moiety of HA and distinctive peaks of the introduced methyl group of small molecules (0.86 ppm) and are given in % per 100 disaccharide units.

Size exclusion chromatography (SEC). A Shimadzu analytical HPLC system was used with HiPrep 16/60 Sephacryl S-200 HR (GE Healthcare, PA, USA) size exclusion chromatography (SEC) column for analytical characterization. Samples of the conjugates (1 mg/mL, 50 μL) were injected using PBS (pH 7.4) buffer containing 0.05% NaN₃ as a mobile phase at a flow rate of 1.5 mL/min.

High performance liquid chromatography (HPLC). A Shimadzu analytical gradient reversed-phase HPLC system was used with PRP-3 (cross-linked polystyrene/poly-divinylbenzene

polymeric stationary phase, Hamilton Laboratory Products, Reno, NV) column for analytical characterization. Gradient elution was carried out at constant flow of 1 mL/min, from 90% A to 50% A (corresponding to 10% B to 50% B) for 50 min and from 50% A to 0% A (corresponding to 50% B to 100% B) for 5 min followed by an isocratic elution at 100% B for 5 min. Mobile phase compositions were (A) water with 0.1% TFA and (B) acetonitrile with 0.1% TFA.

Quantification of small molecule loading in HA conjugates. The compound (TLR7/8 agonist; **a, b, c, d**) stock solutions at a concentration of 1 mg/mL were used to prepare standard solutions with concentrations of 0.78, 1.56, 3.125, 6.25, 12.5, 25, 50, and 100 $\mu\text{g/mL}$, respectively. The conjugate solutions were also prepared by dissolving 100 μg of each conjugate sample in 1 mL of water. Percentage of small molecule loading was determined by UV measurement at 260 nm by correlating with the standard curve.

Gel electrophoresis. Samples were subjected to electrophoresis using 1.2% Clear E-Gel[®] agarose gel (Life Technologies). 20 μl of prepared samples (1mg/mL) were loaded into each well and gel was run for 40 min. Bands were visualized in the gel by UV illumination. The size of the oligosaccharides was compared with rhodamine labeled, commercially available HA of defined size (500 kDa).

In vitro enzymatic degradation. The reaction solutions were prepared by mixing 200 μL of HA conjugates (1 mg/mL in H_2O) with 200 μL of hyaluronidase solution (HAase, 400-1000 U/mL in H_2O). The solutions were incubated at 37 °C for 48 h then analyzed by LC-MS.

Human TLR-7/-8 reporter gene assays (NF- κB Induction). As described in Chapter 2.

Immunoassays for cytokines. As described in Chapter 2.

Rabbit immunization and antigen-specific ELISA. All experiments were performed at Harlan Laboratories (Indianapolis, IN) in accordance with institutional guidelines (University of Kansas IACUC permit # 119-06). Adult New Zealand White rabbits are immunized intramuscularly in the flank region with (a) 10 μ g of antigen (CRM197) in 0.2 mL saline (n = 4 for unadjuvanted, antigen+saline control cohort), or (b) 10 μ g of antigen plus 100 μ g of adjuvant in 0.2 mL saline (n = 4 for antigen+adjuvant test cohorts). Pre-immune test-bleeds were first obtained via venipuncture of the marginal vein of the ear on Day 1. Animals are immunized on Days 1, 15 and 28. A test-bleed is performed via the marginal vein of the ear on Days 25 and 38. Sera are banked at -80 °C for antigen-specific IgG quantitation by ELISA.

C-reactive protein (CRP) measurements. Cohorts of New Zealand White Rabbits (n=5 per cohort) were bled two days before administration of the test compounds to obtain baseline CRP levels. Animals were injected with either 1 mg of candidate adjuvant (or 100 μ g of LPS, used as control) formulated in saline intravenously as a bolus, into the marginal vein of the ear, on Day 0. Successive bleeds were performed on Day 1, 2, 5 and 9 after injection. Sera were stored at -80 °C until used and rabbit CRP-specific ELISAs were performed to obtain the concentrations of CRP in the sera samples.

References

1. Plotkin, S. A., Vaccines: the fourth century. *Clinical and vaccine immunology : CVI* **2009**, *16* (12), 1709-19.
2. (a) Bergmann-Leitner, E.; Leitner, W., Adjuvants in the Driver's Seat: How Magnitude, Type, Fine Specificity and Longevity of Immune Responses Are Driven by Distinct Classes of Immune Potentiators. *Vaccines* **2014**, *2* (2), 252-296; (b) Hunter, R. L., Overview of vaccine adjuvants: present and future. *Vaccine* **2002**, *20 Suppl 3*, S7-12; (c) Ulmer, J. B.; Valley, U.; Rappuoli, R., Vaccine manufacturing: challenges and solutions. *Nature biotechnology* **2006**, *24* (11), 1377-83.
3. (a) O'Hagan, D. T.; Valiante, N. M., Recent advances in the discovery and delivery of vaccine adjuvants. *Nature reviews. Drug discovery* **2003**, *2* (9), 727-35; (b) Mosca, F.; Tritto, E.; Muzzi, A.; Monaci, E.; Bagnoli, F.; Iavarone, C.; O'Hagan, D.; Rappuoli, R.; De Gregorio, E., Molecular and cellular signatures of human vaccine adjuvants. *Proceedings of the National Academy of Sciences of the United States of America* **2008**, *105* (30), 10501-6; (c) McKee, A. S.; Munks, M. W.; Marrack, P., How do adjuvants work? Important considerations for new generation adjuvants. *Immunity* **2007**, *27* (5), 687-90.
4. Wiley, S. R.; Raman, V. S.; Desbien, A.; Bailor, H. R.; Bhardwaj, R.; Shakri, A. R.; Reed, S. G.; Chitnis, C. E.; Carter, D., Targeting TLRs expands the antibody repertoire in response to a malaria vaccine. *Science translational medicine* **2011**, *3* (93), 93ra69.
5. (a) Reed, S. G.; Orr, M. T.; Fox, C. B., Key roles of adjuvants in modern vaccines. *Nature medicine* **2013**, *19* (12), 1597-608; (b) Coffman, R. L.; Sher, A.; Seder, R. A., Vaccine adjuvants: putting innate immunity to work. *Immunity* **2010**, *33* (4), 492-503.
6. (a) O'Hagan, D. T.; De Gregorio, E., The path to a successful vaccine adjuvant--'the long and winding road'. *Drug discovery today* **2009**, *14* (11-12), 541-51; (b) Guy, B., The perfect mix: recent progress in adjuvant research. *Nature reviews. Microbiology* **2007**, *5* (7), 505-17.
7. Clements, C. J.; Griffiths, E., The global impact of vaccines containing aluminium adjuvants. *Vaccine* **2002**, *20 Suppl 3*, S24-33.
8. De Gregorio, E.; Tritto, E.; Rappuoli, R., Alum adjuvanticity: unraveling a century old mystery. *European journal of immunology* **2008**, *38* (8), 2068-71.
9. Lambrecht, B. N.; Kool, M.; Willart, M. A.; Hammad, H., Mechanism of action of clinically approved adjuvants. *Current opinion in immunology* **2009**, *21* (1), 23-9.
10. (a) Seubert, A.; Monaci, E.; Pizza, M.; O'Hagan, D. T.; Wack, A., The adjuvants aluminum hydroxide and MF59 induce monocyte and granulocyte chemoattractants and enhance monocyte differentiation toward dendritic cells. *Journal of immunology (Baltimore, Md.*

- : 1950) **2008**, *180* (8), 5402-12; (b) O'Hagan, D. T.; Ott, G. S.; De Gregorio, E.; Seubert, A., The mechanism of action of MF59 - an innately attractive adjuvant formulation. *Vaccine* **2012**, *30* (29), 4341-8.
11. de Bruijn, I. A.; Nauta, J.; Cramer, W. C.; Gerez, L.; Palache, A. M., Clinical experience with inactivated, virosomal influenza vaccine. *Vaccine* **2005**, *23 Suppl 1*, S39-49.
12. Garcon, N.; Chomez, P.; Van Mechelen, M., GlaxoSmithKline Adjuvant Systems in vaccines: concepts, achievements and perspectives. *Expert review of vaccines* **2007**, *6* (5), 723-39.
13. Vandepapeliere, P.; Horsmans, Y.; Moris, P.; Van Mechelen, M.; Janssens, M.; Koutsoukos, M.; Van Belle, P.; Clement, F.; Hanon, E.; Wettendorff, M.; Garcon, N.; Leroux-Roels, G., Vaccine adjuvant systems containing monophosphoryl lipid A and QS21 induce strong and persistent humoral and T cell responses against hepatitis B surface antigen in healthy adult volunteers. *Vaccine* **2008**, *26* (10), 1375-86.
14. (a) Agrawal, S.; Agrawal, A.; Doughty, B.; Gerwitz, A.; Blenis, J.; Van Dyke, T.; Pulendran, B., Cutting edge: different Toll-like receptor agonists instruct dendritic cells to induce distinct Th responses via differential modulation of extracellular signal-regulated kinase-mitogen-activated protein kinase and c-Fos. *Journal of immunology (Baltimore, Md. : 1950)* **2003**, *171* (10), 4984-9; (b) Dillon, S.; Agrawal, A.; Van Dyke, T.; Landreth, G.; McCauley, L.; Koh, A.; Maliszewski, C.; Akira, S.; Pulendran, B., A Toll-like receptor 2 ligand stimulates Th2 responses in vivo, via induction of extracellular signal-regulated kinase mitogen-activated protein kinase and c-Fos in dendritic cells. *Journal of immunology (Baltimore, Md. : 1950)* **2004**, *172* (8), 4733-43.
15. (a) Janeway, C. A., Jr.; Medzhitov, R., Innate immune recognition. *Annual review of immunology* **2002**, *20*, 197-216; (b) Pulendran, B.; Ahmed, R., Immunological mechanisms of vaccination. *Nat Immunol* **2011**, *12* (6), 509-17.
16. (a) Iwasaki, A.; Medzhitov, R., Regulation of adaptive immunity by the innate immune system. *Science* **2010**, *327* (5963), 291-5; (b) Medzhitov, R.; Janeway, C. A., Jr., Innate immune recognition and control of adaptive immune responses. *Seminars in immunology* **1998**, *10* (5), 351-3.
17. Sansonetti, P. J., The innate signaling of dangers and the dangers of innate signaling. *Nat Immunol* **2006**, *7* (12), 1237-42.
18. (a) Akira, S.; Uematsu, S.; Takeuchi, O., Pathogen recognition and innate immunity. *Cell* **2006**, *124* (4), 783-801; (b) Kumagai, Y.; Takeuchi, O.; Akira, S., Pathogen recognition by innate receptors. *Journal of infection and chemotherapy : official journal of the Japan Society of*

- Chemotherapy* **2008**, *14* (2), 86-92; (c) Kawai, T.; Akira, S., The role of pattern-recognition receptors in innate immunity: update on Toll-like receptors. *Nat Immunol* **2010**, *11* (5), 373-84.
19. Loo, Y. M.; Gale, M., Jr., Immune signaling by RIG-I-like receptors. *Immunity* **2011**, *34* (5), 680-92.
20. (a) Kersse, K.; Bertrand, M. J.; Lamkanfi, M.; Vandenabeele, P., NOD-like receptors and the innate immune system: coping with danger, damage and death. *Cytokine & growth factor reviews* **2011**, *22* (5-6), 257-76; (b) Clarke, T. B.; Weiser, J. N., Intracellular sensors of extracellular bacteria. *Immunological reviews* **2011**, *243* (1), 9-25.
21. (a) Hoving, J. C.; Wilson, G. J.; Brown, G. D., Signalling C-type lectin receptors, microbial recognition and immunity. *Cellular microbiology* **2014**, *16* (2), 185-94; (b) Kutikhin, A. G.; Yuzhalin, A. E.; Tsitko, E. A.; Brusina, E. B., Pattern recognition receptors and DNA repair: starting to put a jigsaw puzzle together. *Frontiers in immunology* **2014**, *5*, 343; (c) Kawai, T.; Akira, S., The roles of TLRs, RLRs and NLRs in pathogen recognition. *International immunology* **2009**, *21* (4), 317-37.
22. (a) Krishnan, J.; Lee, G.; Choi, S., Drugs targeting Toll-like receptors. *Archives of pharmacal research* **2009**, *32* (11), 1485-502; (b) Manavalan, B.; Basith, S.; Choi, S., Similar Structures but Different Roles - An Updated Perspective on TLR Structures. *Frontiers in physiology* **2011**, *2*, 41; (c) Song, D. H.; Lee, J. O., Sensing of microbial molecular patterns by Toll-like receptors. *Immunological reviews* **2012**, *250* (1), 216-29; (d) Kang, J. Y.; Lee, J. O., Structural biology of the Toll-like receptor family. *Annual review of biochemistry* **2011**, *80*, 917-41.
23. (a) Takeda, K.; Akira, S., Toll-like receptors. *Current protocols in immunology / edited by John E. Coligan ... [et al.]* **2007**, *Chapter 14*, Unit 14 12; (b) Yu, L.; Wang, L.; Chen, S., Endogenous toll-like receptor ligands and their biological significance. *Journal of cellular and molecular medicine* **2010**, *14* (11), 2592-603.
24. (a) Shizuo Akira, K. T., Tsuneyasu Kaisho, Toll-like receptors- critical proteins linking innate and acquired immunity. *Nature Immunology* **2001**, *2* (8), 675-680; (b) Cottalorda, A.; Vershelde, C.; Marçais, A.; Tomkowiak, M.; Musette, P.; Uematsu, S.; Akira, S.; Marvel, J.; Bonnefoy-Berard, N., TLR2 engagement on CD8 T cells lowers the threshold for optimal antigen-induced T cell activation. *European journal of immunology* **2006**, *36* (7), 1684-93; (c) Kaisho, T.; Akira, S., Toll-like receptors as adjuvant receptors. *Biochimica et biophysica acta* **2002**, *1589* (1), 1-13.
25. (a) Warshakoon, H. J.; Hood, J. D.; Kimbrell, M. R.; Malladi, S.; Wu, W. Y.; Shukla, N. M.; Agnihotri, G.; Sil, D.; David, S. A., Potential adjuvant properties of innate immune stimuli.

- Human vaccines* **2009**, 5 (6), 381-94; (b) Duthie, M. S.; Windish, H. P.; Fox, C. B.; Reed, S. G., Use of defined TLR ligands as adjuvants within human vaccines. *Immunological reviews* **2011**, 239 (1), 178-96; (c) Mastelic, B.; Ahmed, S.; Egan, W. M.; Del Giudice, G.; Golding, H.; Gust, I.; Neels, P.; Reed, S. G.; Sheets, R. L.; Siegrist, C. A.; Lambert, P. H., Mode of action of adjuvants: implications for vaccine safety and design. *Biologicals : journal of the International Association of Biological Standardization* **2010**, 38 (5), 594-601.
26. Dougan, G.; Hormaeche, C., How bacteria and their products provide clues to vaccine and adjuvant development. *Vaccine* **2006**, 24 Suppl 2, S2-13-9.
27. (a) Tagliabue, A.; Rappuoli, R., Vaccine adjuvants: the dream becomes real. *Human vaccines* **2008**, 4 (5), 347-9; (b) Mata-Haro, V.; Cekic, C.; Martin, M.; Chilton, P. M.; Casella, C. R.; Mitchell, T. C., The vaccine adjuvant monophosphoryl lipid A as a TRIF-biased agonist of TLR4. *Science* **2007**, 316 (5831), 1628-32.
28. Poltorak, A.; He, X.; Smirnova, I.; Liu, M. Y.; Van Huffel, C.; Du, X.; Birdwell, D.; Alejos, E.; Silva, M.; Galanos, C.; Freudenberg, M.; Ricciardi-Castagnoli, P.; Layton, B.; Beutler, B., Defective LPS signaling in C3H/HeJ and C57BL/10ScCr mice: mutations in Tlr4 gene. *Science* **1998**, 282 (5396), 2085-8.
29. (a) Johnson, A. G.; Tomai, M.; Solem, L.; Beck, L.; Ribi, E., Characterization of a nontoxic monophosphoryl lipid A. *Reviews of infectious diseases* **1987**, 9 Suppl 5, S512-6; (b) Tomai, M. A.; Solem, L. E.; Johnson, A. G.; Ribi, E., The adjuvant properties of a nontoxic monophosphoryl lipid A in hyporesponsive and aging mice. *Journal of biological response modifiers* **1987**, 6 (2), 99-107; (c) Johnson, A. G.; Tomai, M. A., A study of the cellular and molecular mediators of the adjuvant action of a nontoxic monophosphoryl lipid A. *Advances in experimental medicine and biology* **1990**, 256, 567-79.
30. Hood, J. D.; Warshakoon, H. J.; Kimbrell, M. R.; Shukla, N. M.; Malladi, S. S.; Wang, X.; David, S. A., Immunoprofiling toll-like receptor ligands: Comparison of immunostimulatory and proinflammatory profiles in ex vivo human blood models. *Human vaccines* **2010**, 6 (4), 322-35.
31. (a) Lee, J.; Chuang, T. H.; Redecke, V.; She, L.; Pitha, P. M.; Carson, D. A.; Raz, E.; Cottam, H. B., Molecular basis for the immunostimulatory activity of guanine nucleoside analogs: activation of Toll-like receptor 7. *Proceedings of the National Academy of Sciences of the United States of America* **2003**, 100 (11), 6646-51; (b) Diebold, S. S.; Kaisho, T.; Hemmi, H.; Akira, S.; Reis e Sousa, C., Innate antiviral responses by means of TLR7-mediated recognition of single-stranded RNA. *Science* **2004**, 303 (5663), 1529-31; (c) Crozat, K.; Beutler, B., TLR7: A new sensor of viral infection. *Proceedings of the National Academy of Sciences of the United*

- States of America* **2004**, 101 (18), 6835-6; (d) Diebold, S. S., Recognition of viral single-stranded RNA by Toll-like receptors. *Advanced drug delivery reviews* **2008**, 60 (7), 813-23.
32. Heil, F.; Hemmi, H.; Hochrein, H.; Ampenberger, F.; Kirschning, C.; Akira, S.; Lipford, G.; Wagner, H.; Bauer, S., Species-specific recognition of single-stranded RNA via toll-like receptor 7 and 8. *Science* **2004**, 303 (5663), 1526-9.
33. (a) Takeda, K.; Akira, S., TLR signaling pathways. *Seminars in immunology* **2004**, 16 (1), 3-9; (b) Akira, S.; Takeda, K., Toll-like receptor signalling. *Nature reviews. Immunology* **2004**, 4 (7), 499-511; (c) Desmet, C. J.; Ishii, K. J., Nucleic acid sensing at the interface between innate and adaptive immunity in vaccination. *Nature reviews. Immunology* **2012**, 12 (7), 479-91.
34. (a) Dockrell, D. H.; Kinghorn, G. R., Imiquimod and resiquimod as novel immunomodulators. *The Journal of antimicrobial chemotherapy* **2001**, 48 (6), 751-5; (b) Garland, S. M., Imiquimod. *Current opinion in infectious diseases* **2003**, 16 (2), 85-9; (c) Miller, R. L.; Meng, T. C.; Tomai, M. A., The antiviral activity of Toll-like receptor 7 and 7/8 agonists. *Drug news & perspectives* **2008**, 21 (2), 69-87.
35. (a) Pope, B. L.; Chourmouzis, E.; Sigindere, J.; Capetola, R. J.; Lau, C. Y., In vivo enhancement of murine natural killer cell activity by 7-allyl-8-oxoguanosine (loxoribine). *International journal of immunopharmacology* **1992**, 14 (8), 1375-82; (b) Reitz, A. B.; Goodman, M. G.; Pope, B. L.; Argentieri, D. C.; Bell, S. C.; Burr, L. E.; Chourmouzis, E.; Come, J.; Goodman, J. H.; Klaubert, D. H.; et al., Small-molecule immunostimulants. Synthesis and activity of 7,8-disubstituted guanosines and structurally related compounds. *Journal of medicinal chemistry* **1994**, 37 (21), 3561-78; (c) Gupta, S.; Vayuvegula, B.; Gollapudi, S., Substituted guanine ribonucleosides as B cell activators. *Clinical immunology and immunopathology* **1991**, 61 (2 Pt 2), S21-7.
36. (a) Wierenga, W.; Skulnick, H. I.; Stringfellow, D. A.; Weed, S. D.; Renis, H. E.; Eidson, E. E., 5-substituted 2-amino-6-phenyl-4(3H)-pyrimidinones. Antiviral- and interferon-inducing agents. *Journal of medicinal chemistry* **1980**, 23 (3), 237-9; (b) Li, L. H.; Wallace, T. L.; Wierenga, W.; Skulnick, H. I.; DeKoning, T. F., Antitumor activity of pyrimidinones, a class of small-molecule biological response modifiers. *Journal of biological response modifiers* **1987**, 6 (1), 44-55; (c) Hamilton, R. D.; Wynalda, M. A.; Fitzpatrick, F. A.; Teagarden, D. L.; Hamdy, A. H.; Snider, B. G.; Weed, S. D.; Stringfellow, D. A., Comparison between circulating interferon and drug levels following administration of 2-amino-5-bromo-6-phenyl-4(3H)-pyrimidinone (ABPP) to different animal species. *Journal of interferon research* **1982**, 2 (3), 317-27.

37. Gerster, J. F.; Lindstrom, K. J.; Miller, R. L.; Tomai, M. A.; Birmachu, W.; Bomersine, S. N.; Gibson, S. J.; Imbertson, L. M.; Jacobson, J. R.; Knafla, R. T.; Maye, P. V.; Nikolaidis, N.; Oneyemi, F. Y.; Parkhurst, G. J.; Pecore, S. E.; Reiter, M. J.; Scribner, L. S.; Testerman, T. L.; Thompson, N. J.; Wagner, T. L.; Weeks, C. E.; Andre, J. D.; Lagain, D.; Bastard, Y.; Lupu, M., Synthesis and structure-activity-relationships of 1H-imidazo[4,5-c]quinolines that induce interferon production. *Journal of medicinal chemistry* **2005**, *48* (10), 3481-91.
38. Miller, R. L.; Gerster, J. F.; Owens, M. L.; Slade, H. B.; Tomai, M. A., Imiquimod applied topically: a novel immune response modifier and new class of drug. *International journal of immunopharmacology* **1999**, *21* (1), 1-14.
39. Testerman, T. L.; Gerster, J. F.; Imbertson, L. M.; Reiter, M. J.; Miller, R. L.; Gibson, S. J.; Wagner, T. L.; Tomai, M. A., Cytokine induction by the immunomodulators imiquimod and S-27609. *Journal of leukocyte biology* **1995**, *58* (3), 365-72.
40. (a) Bernstein, D. I.; Harrison, C. J.; Tomai, M. A.; Miller, R. L., Daily or weekly therapy with resiquimod (R-848) reduces genital recurrences in herpes simplex virus-infected guinea pigs during and after treatment. *The Journal of infectious diseases* **2001**, *183* (6), 844-9; (b) Schon, M. P.; Schon, M., TLR7 and TLR8 as targets in cancer therapy. *Oncogene* **2008**, *27* (2), 190-9.
41. Imbertson, L. M.; Beaurline, J. M.; Couture, A. M.; Gibson, S. J.; Smith, R. M.; Miller, R. L.; Reiter, M. J.; Wagner, T. L.; Tomai, M. A., Cytokine induction in hairless mouse and rat skin after topical application of the immune response modifiers imiquimod and S-28463. *The Journal of investigative dermatology* **1998**, *110* (5), 734-9.
42. Pockros, P. J.; Guyader, D.; Patton, H.; Tong, M. J.; Wright, T.; McHutchison, J. G.; Meng, T. C., Oral resiquimod in chronic HCV infection: safety and efficacy in 2 placebo-controlled, double-blind phase IIa studies. *Journal of hepatology* **2007**, *47* (2), 174-82.
43. (a) Salio, M.; Speak, A. O.; Shepherd, D.; Polzella, P.; Illarionov, P. A.; Veerapen, N.; Besra, G. S.; Platt, F. M.; Cerundolo, V., Modulation of human natural killer T cell ligands on TLR-mediated antigen-presenting cell activation. *Proceedings of the National Academy of Sciences of the United States of America* **2007**, *104* (51), 20490-5; (b) Velasquez, L. S.; Hjelm, B. E.; Arntzen, C. J.; Herbst-Kralovetz, M. M., An intranasally delivered Toll-like receptor 7 agonist elicits robust systemic and mucosal responses to Norwalk virus-like particles. *Clinical and vaccine immunology : CVI* **2010**, *17* (12), 1850-8.
44. Dummer, R.; Hauschild, A.; Becker, J. C.; Grob, J. J.; Schadendorf, D.; Tebbs, V.; Skalsky, J.; Kaehler, K. C.; Moosbauer, S.; Clark, R.; Meng, T. C.; Urosevic, M., An exploratory study of systemic administration of the toll-like receptor-7 agonist 852A in patients with

refractory metastatic melanoma. *Clinical cancer research : an official journal of the American Association for Cancer Research* **2008**, *14* (3), 856-64.

45. Gorden, K. B.; Gorski, K. S.; Gibson, S. J.; Kedl, R. M.; Kieper, W. C.; Qiu, X.; Tomai, M. A.; Alkan, S. S.; Vasilakos, J. P., Synthetic TLR agonists reveal functional differences between human TLR7 and TLR8. *Journal of immunology (Baltimore, Md. : 1950)* **2005**, *174* (3), 1259-68.

46. Horsmans, Y.; Berg, T.; Desager, J. P.; Mueller, T.; Schott, E.; Fletcher, S. P.; Steffy, K. R.; Bauman, L. A.; Kerr, B. M.; Averett, D. R., Isatoribine, an agonist of TLR7, reduces plasma virus concentration in chronic hepatitis C infection. *Hepatology (Baltimore, Md.)* **2005**, *42* (3), 724-31.

47. Fletcher, S.; Steffy, K.; Averett, D., Masked oral prodrugs of toll-like receptor 7 agonists: a new approach for the treatment of infectious disease. *Current opinion in investigational drugs (London, England : 2000)* **2006**, *7* (8), 702-8.

48. Kang, S. S.; Kauls, L. S.; Gaspari, A. A., Toll-like receptors: applications to dermatologic disease. *Journal of the American Academy of Dermatology* **2006**, *54* (6), 951-83; quiz 983-6.

49. Tei, Y.; Matsuyama, H.; Wada, T.; Kurisu, H.; Tahara, M.; Naito, K., In vitro antitumor activity of broprimine against urinary bladder tumor cells. *Anticancer research* **2002**, *22* (3), 1667-71.

50. (a) Wysocka, M.; Newton, S.; Benoit, B. M.; Introcaso, C.; Hancock, A. S.; Chehimi, J.; Richardson, S. K.; Gelfand, J. M.; Montaner, L. J.; Rook, A. H., Synthetic imidazoquinolines potently and broadly activate the cellular immune response of patients with cutaneous T-cell lymphoma: synergy with interferon-gamma enhances production of interleukin-12. *Clinical lymphoma & myeloma* **2007**, *7* (8), 524-34; (b) Goodman, M. G., A new approach to vaccine adjuvants. Immunopotentialiation by intracellular T-helper-like signals transmitted by loxoribine. *Pharmaceutical biotechnology* **1995**, *6*, 581-609.

51. (a) Rajagopal, D.; Paturel, C.; Morel, Y.; Uematsu, S.; Akira, S.; Diebold, S. S., Plasmacytoid dendritic cell-derived type I interferon is crucial for the adjuvant activity of Toll-like receptor 7 agonists. *Blood* **2010**, *115* (10), 1949-57; (b) Kastenmuller, K.; Wille-Reece, U.; Lindsay, R. W.; Trager, L. R.; Darrah, P. A.; Flynn, B. J.; Becker, M. R.; Udey, M. C.; Clausen, B. E.; Igyarto, B. Z.; Kaplan, D. H.; Kastenmuller, W.; Germain, R. N.; Seder, R. A., Protective T cell immunity in mice following protein-TLR7/8 agonist-conjugate immunization requires aggregation, type I IFN, and multiple DC subsets. *The Journal of clinical investigation* **2011**, *121* (5), 1782-96.

52. (a) Bracci, L.; La Sorsa, V.; Belardelli, F.; Proietti, E., Type I interferons as vaccine adjuvants against infectious diseases and cancer. *Expert review of vaccines* **2008**, *7* (3), 373-

- 81; (b) Tovey, M. G.; Lallemand, C.; Thyphronitis, G., Adjuvant activity of type I interferons. *Biological chemistry* **2008**, *389* (5), 541-5; (c) Berenson, L. S.; Ota, N.; Murphy, K. M., Issues in T-helper 1 development--resolved and unresolved. *Immunological reviews* **2004**, *202*, 157-74.
53. (a) Gately, M. K.; Brunda, M. J., Interleukin-12: a pivotal regulator of cell-mediated immunity. *Cancer treatment and research* **1995**, *80*, 341-66; (b) Scott, P.; Trinchieri, G., IL-12 as an adjuvant for cell-mediated immunity. *Seminars in immunology* **1997**, *9* (5), 285-91.
54. (a) Eberl, M.; Beck, E.; Coulson, P. S.; Okamura, H.; Wilson, R. A.; Mountford, A. P., IL-18 potentiates the adjuvant properties of IL-12 in the induction of a strong Th1 type immune response against a recombinant antigen. *Vaccine* **2000**, *18* (19), 2002-8; (b) Marshall, D. J.; Rudnick, K. A.; McCarthy, S. G.; Mateo, L. R.; Harris, M. C.; McCauley, C.; Snyder, L. A., Interleukin-18 enhances Th1 immunity and tumor protection of a DNA vaccine. *Vaccine* **2006**, *24* (3), 244-53.
55. (a) Shukla, N. M.; Malladi, S. S.; Day, V.; David, S. A., Preliminary evaluation of a 3H imidazoquinoline library as dual TLR7/TLR8 antagonists. *Bioorganic & medicinal chemistry* **2011**, *19* (12), 3801-11; (b) Shukla, N. M.; Kimbrell, M. R.; Malladi, S. S.; David, S. A., Regioisomerism-dependent TLR7 agonism and antagonism in an imidazoquinoline. *Bioorganic & medicinal chemistry letters* **2009**, *19* (8), 2211-4.
56. Shukla, N. M.; Lewis, T. C.; Day, T. P.; Mutz, C. A.; Ukani, R.; Hamilton, C. D.; Balakrishna, R.; David, S. A., Toward self-adjuvanting subunit vaccines: model peptide and protein antigens incorporating covalently bound toll-like receptor-7 agonistic imidazoquinolines. *Bioorganic & medicinal chemistry letters* **2011**, *21* (11), 3232-6.
57. Shukla, N. M.; Salunke, D. B.; Balakrishna, R.; Mutz, C. A.; Malladi, S. S.; David, S. A., Potent adjuvanticity of a pure TLR7-agonistic imidazoquinoline dendrimer. *PloS one* **2012**, *7* (8), e43612.
58. Shukla, N. M.; Mutz, C. A.; Ukani, R.; Warshakoon, H. J.; Moore, D. S.; David, S. A., Syntheses of fluorescent imidazoquinoline conjugates as probes of Toll-like receptor 7. *Bioorganic & medicinal chemistry letters* **2010**, *20* (22), 6384-6.
59. (a) Stringfellow, D. A.; Glasgow, L. A., Tilorone hydrochloride: an oral interferon-inducing agent. *Antimicrobial agents and chemotherapy* **1972**, *2* (2), 73-8; (b) Stringfellow, D. A., Comparison interferon- inducing and antiviral properties of 2-amino-5-bromo-6-methyl-4-pyrimidinol (U-25,166), tilorone hydrochloride, and polyinosinic-polycytidylic acid. *Antimicrobial agents and chemotherapy* **1977**, *11* (6), 984-92.
60. (a) Gerster, J. F.; Lindstrom, K. J.; Marszalek, G. J.; Merrill, B. A.; Mickelson, J. W.; Rice, M. J., Oxazolo, thiazolo and selenazolo[4,5-c]-quinolin-4-amines and analogs thereof.

- World Patent* **2000**, WO00/06577, 1-102; (b) Prince, R. B.; Rice, M. J.; Wurst, J. R.; Merrill, B. A.; Kshirsagar, T. A.; Heppner, P. D., Aryloxy and arylalkyleneoxy substituted thiazoloquinolines and thiazolonaphthyridines. *World Patent* **2006**, WO 2006/009826 A1, 1-104.
61. Jurk, M.; Heil, F.; Vollmer, J.; Schetter, C.; Krieg, A. M.; Wagner, H.; Lipford, G.; Bauer, S., Human TLR7 or TLR8 independently confer responsiveness to the antiviral compound R-848. *Nat Immunol* **2002**, 3 (6), 499.
62. Gorski, K. S.; Waller, E. L.; Bjornton-Severson, J.; Hanten, J. A.; Riter, C. L.; Kieper, W. C.; Gordon, K. B.; Miller, J. S.; Vasilakos, J. P.; Tomai, M. A.; Alkan, S. S., Distinct indirect pathways govern human NK-cell activation by TLR-7 and TLR-8 agonists. *International immunology* **2006**, 18 (7), 1115-26.
63. Levy, O.; Suter, E. E.; Miller, R. L.; Wessels, M. R., Unique efficacy of Toll-like receptor 8 agonists in activating human neonatal antigen-presenting cells. *Blood* **2006**, 108 (4), 1284-90.
64. van den Berg, J. P.; Westerbeek, E. A.; van der Klis, F. R.; Berbers, G. A.; van Elburg, R. M., Transplacental transport of IgG antibodies to preterm infants: a review of the literature. *Early human development* **2011**, 87 (2), 67-72.
65. Kollmann, T. R.; Crabtree, J.; Rein-Weston, A.; Blimkie, D.; Thommai, F.; Wang, X. Y.; Lavoie, P. M.; Furlong, J.; Fortuno, E. S., 3rd; Hajjar, A. M.; Hawkins, N. R.; Self, S. G.; Wilson, C. B., Neonatal innate TLR-mediated responses are distinct from those of adults. *Journal of immunology (Baltimore, Md. : 1950)* **2009**, 183 (11), 7150-60.
66. (a) PrabhuDas, M.; Adkins, B.; Gans, H.; King, C.; Levy, O.; Ramilo, O.; Siegrist, C. A., Challenges in infant immunity: implications for responses to infection and vaccines. *Nat Immunol* **2011**, 12 (3), 189-94; (b) Siegrist, C. A., The challenges of vaccine responses in early life: selected examples. *Journal of comparative pathology* **2007**, 137 Suppl 1, S4-9.
67. Corbett, N. P.; Blimkie, D.; Ho, K. C.; Cai, B.; Sutherland, D. P.; Kallos, A.; Crabtree, J.; Rein-Weston, A.; Lavoie, P. M.; Turvey, S. E.; Hawkins, N. R.; Self, S. G.; Wilson, C. B.; Hajjar, A. M.; Fortuno, E. S., 3rd; Kollmann, T. R., Ontogeny of Toll-like receptor mediated cytokine responses of human blood mononuclear cells. *PLoS one* **2010**, 5 (11), e15041.
68. (a) Levy, O., Innate immunity of the newborn: basic mechanisms and clinical correlates. *Nature reviews. Immunology* **2007**, 7 (5), 379-90; (b) Wood, N.; Siegrist, C. A., Neonatal immunization: where do we stand? *Current opinion in infectious diseases* **2011**, 24 (3), 190-5.
69. Shukla, N. M.; Malladi, S. S.; Mutz, C. A.; Balakrishna, R.; David, S. A., Structure-activity relationships in human toll-like receptor 7-active imidazoquinoline analogues. *Journal of medicinal chemistry* **2010**, 53 (11), 4450-65.

70. Nguyen, T. B.; Kumar, E. V.; Sil, D.; Wood, S. J.; Miller, K. A.; Warshakoon, H. J.; Datta, A.; David, S. A., Controlling plasma protein binding: structural correlates of interactions of hydrophobic polyamine endotoxin sequestrants with human serum albumin. *Molecular pharmaceutics* **2008**, *5* (6), 1131-7.
71. Prince, R. B.; Merrill, B. A.; Heppner, P. D.; Kshirsagar, T. A.; Wurst, J. R.; Manske, K. J.; Rice, M. J., Alkyloxy substituted thiazoloquinolines and thiazolonaphthyridines. *World Patent* **2006**, *WO 2006/086449*, 1-193.
72. (a) Alexopoulou, L.; Desnues, B.; Demaria, O., [Toll-like receptor 8: the awkward TLR]. *Medecine sciences : M/S* **2012**, *28* (1), 96-102; (b) Govindaraj, R. G.; Manavalan, B.; Basith, S.; Choi, S., Comparative analysis of species-specific ligand recognition in Toll-like receptor 8 signaling: a hypothesis. *PloS one* **2011**, *6* (9), e25118; (c) Gorden, K. K.; Qiu, X. X.; Binsfeld, C. C.; Vasilakos, J. P.; Alkan, S. S., Cutting edge: activation of murine TLR8 by a combination of imidazoquinoline immune response modifiers and polyT oligodeoxynucleotides. *Journal of immunology (Baltimore, Md. : 1950)* **2006**, *177* (10), 6584-7.
73. David, S. A.; Smith, M. S.; Lopez, G. J.; Adany, I.; Mukherjee, S.; Buch, S.; Goodenow, M. M.; Narayan, O., Selective transmission of R5-tropic HIV type 1 from dendritic cells to resting CD4+ T cells. *AIDS research and human retroviruses* **2001**, *17* (1), 59-68.
74. Kimbrell, M. R.; Warshakoon, H.; Cromer, J. R.; Malladi, S.; Hood, J. D.; Balakrishna, R.; Scholdberg, T. A.; David, S. A., Comparison of the immunostimulatory and proinflammatory activities of candidate Gram-positive endotoxins, lipoteichoic acid, peptidoglycan, and lipopeptides, in murine and human cells. *Immunology letters* **2008**, *118* (2), 132-41.
75. (a) Petrone, P. M.; Simms, B.; Nigsch, F.; Lounkine, E.; Kutchukian, P.; Cornett, A.; Deng, Z.; Davies, J. W.; Jenkins, J. L.; Glick, M., Rethinking molecular similarity: comparing compounds on the basis of biological activity. *ACS chemical biology* **2012**, *7* (8), 1399-409; (b) Tsunoyama, K.; Amini, A.; Sternberg, M. J.; Muggleton, S. H., Scaffold hopping in drug discovery using inductive logic programming. *Journal of chemical information and modeling* **2008**, *48* (5), 949-57.
76. (a) Hirota, K.; Kazaoka, K.; Niimoto, I.; Kumihara, H.; Sajiki, H.; Isobe, Y.; Takaku, H.; Tobe, M.; Ogita, H.; Ogino, T.; Ichii, S.; Kurimoto, A.; Kawakami, H., Discovery of 8-hydroxyadenines as a novel type of interferon inducer. *Journal of medicinal chemistry* **2002**, *45* (25), 5419-22; (b) Isobe, Y.; Tobe, M.; Ogita, H.; Kurimoto, A.; Ogino, T.; Kawakami, H.; Takaku, H.; Sajiki, H.; Hirota, K.; Hayashi, H., Synthesis and structure-activity relationships of 2-substituted-8-hydroxyadenine derivatives as orally available interferon inducers without emetic side effects. *Bioorganic & medicinal chemistry* **2003**, *11* (17), 3641-7.

77. Shukla, N. M.; Mutz, C. A.; Malladi, S. S.; Warshakoon, H. J.; Balakrishna, R.; David, S. A., Toll-like receptor (TLR)-7 and -8 modulatory activities of dimeric imidazoquinolines. *Journal of medicinal chemistry* **2012**, *55* (3), 1106-16.
78. Baviskar, A. T.; Madaan, C.; Preet, R.; Mohapatra, P.; Jain, V.; Agarwal, A.; Guchhait, S. K.; Kundu, C. N.; Banerjee, U. C.; Bharatam, P. V., N-fused imidazoles as novel anticancer agents that inhibit catalytic activity of topoisomerase IIalpha and induce apoptosis in G1/S phase. *Journal of medicinal chemistry* **2011**, *54* (14), 5013-30.
79. Kawai, T.; Akira, S., TLR signaling. *Seminars in immunology* **2007**, *19* (1), 24-32.
80. Smirnov, D.; Schmidt, J. J.; Capecchi, J. T.; Wightman, P. D., Vaccine adjuvant activity of 3M-052: an imidazoquinoline designed for local activity without systemic cytokine induction. *Vaccine* **2011**, *29* (33), 5434-42.
81. Ukani, R.; Lewis, T. C.; Day, T. P.; Wu, W.; Malladi, S. S.; Warshakoon, H. J.; David, S. A., Potent adjuvant activity of a CCR1-agonistic bis-quinoline. *Bioorganic & medicinal chemistry letters* **2012**, *22* (1), 293-5.
82. Boucher, H. W.; Corey, G. R., Epidemiology of methicillin-resistant *Staphylococcus aureus*. *Clinical infectious diseases : an official publication of the Infectious Diseases Society of America* **2008**, *46* Suppl 5, S344-9.
83. Gould, I. M., Clinical activity of anti-Gram-positive agents against methicillin-resistant *Staphylococcus aureus*. *The Journal of antimicrobial chemotherapy* **2011**, *66* Suppl 4, iv17-iv21.
84. Warshakoon, H. J.; Burns, M. R.; David, S. A., Structure-activity relationships of antimicrobial and lipoteichoic acid-sequestering properties in polyamine sulfonamides. *Antimicrobial agents and chemotherapy* **2009**, *53* (1), 57-62.
85. Peterson, L. R.; Shanholtzer, C. J., Tests for bactericidal effects of antimicrobial agents: technical performance and clinical relevance. *Clinical microbiology reviews* **1992**, *5* (4), 420-32.
86. (a) Nikaido, H.; Vaara, M., Molecular basis of bacterial outer membrane permeability. *Microbiological reviews* **1985**, *49* (1), 1-32; (b) Vaara, M.; Vaara, T., Polycations sensitize enteric bacteria to antibiotics. *Antimicrobial agents and chemotherapy* **1983**, *24* (1), 107-13.
87. (a) Kimura, Y.; Matsunaga, H.; Vaara, M., Polymyxin B octapeptide and polymyxin B heptapeptide are potent outer membrane permeability-increasing agents. *The Journal of antibiotics* **1992**, *45* (5), 742-9; (b) Vaara, M., Agents that increase the permeability of the outer membrane. *Microbiological reviews* **1992**, *56* (3), 395-411; (c) Viljanen, P.; Matsunaga, H.; Kimura, Y.; Vaara, M., The outer membrane permeability-increasing action of deacylpolymyxins. *The Journal of antibiotics* **1991**, *44* (5), 517-23.

88. Balakrishna, R.; Wood, S. J.; Nguyen, T. B.; Miller, K. A.; Suresh Kumar, E. V.; Datta, A.; David, S. A., Structural correlates of antibacterial and membrane-permeabilizing activities in acylpolyamines. *Antimicrobial agents and chemotherapy* **2006**, *50* (3), 852-61.
89. Al-Tel, T. H.; Al-Qawasmeh, R. A., Post Groebke-Blackburn multicomponent protocol: synthesis of new polyfunctional imidazo[1,2-a]pyridine and imidazo[1,2-a]pyrimidine derivatives as potential antimicrobial agents. *European journal of medicinal chemistry* **2010**, *45* (12), 5848-55.
90. Edwards, A. D.; Diebold, S. S.; Slack, E. M.; Tomizawa, H.; Hemmi, H.; Kaisho, T.; Akira, S.; Reis e Sousa, C., Toll-like receptor expression in murine DC subsets: lack of TLR7 expression by CD8 alpha+ DC correlates with unresponsiveness to imidazoquinolines. *European journal of immunology* **2003**, *33* (4), 827-33.
91. (a) Krug, A.; Luker, G. D.; Barchet, W.; Leib, D. A.; Akira, S.; Colonna, M., Herpes simplex virus type 1 activates murine natural interferon-producing cells through toll-like receptor 9. *Blood* **2004**, *103* (4), 1433-7; (b) Lund, J.; Sato, A.; Akira, S.; Medzhitov, R.; Iwasaki, A., Toll-like receptor 9-mediated recognition of Herpes simplex virus-2 by plasmacytoid dendritic cells. *The Journal of experimental medicine* **2003**, *198* (3), 513-20.
92. Isaacs, A.; Lindenmann, J., Virus interference. I. The interferon. *Proceedings of the Royal Society of London. Series B, Biological sciences* **1957**, *147* (927), 258-67.
93. Iwasaki, A.; Medzhitov, R., Toll-like receptor control of the adaptive immune responses. *Nat Immunol* **2004**, *5* (10), 987-95.
94. Le Bon, A.; Etchart, N.; Rossmann, C.; Ashton, M.; Hou, S.; Gewert, D.; Borrow, P.; Tough, D. F., Cross-priming of CD8+ T cells stimulated by virus-induced type I interferon. *Nat Immunol* **2003**, *4* (10), 1009-15.
95. Le Bon, A.; Schiavoni, G.; D'Agostino, G.; Gresser, I.; Belardelli, F.; Tough, D. F., Type I interferons potently enhance humoral immunity and can promote isotype switching by stimulating dendritic cells in vivo. *Immunity* **2001**, *14* (4), 461-70.
96. (a) Durali, D.; de Goer de Herve, M. G.; Giron-Michel, J.; Azzarone, B.; Delfraissy, J. F.; Taoufik, Y., In human B cells, IL-12 triggers a cascade of molecular events similar to Th1 commitment. *Blood* **2003**, *102* (12), 4084-9; (b) Lund, F. E.; Randall, T. D., Effector and regulatory B cells: modulators of CD4+ T cell immunity. *Nature reviews. Immunology* **2010**, *10* (4), 236-47.
97. de Goer de Herve, M. G.; Durali, D.; Dembele, B.; Giuliani, M.; Tran, T. A.; Azzarone, B.; Eid, P.; Tardieu, M.; Delfraissy, J. F.; Taoufik, Y., Interferon-alpha triggers B cell effector 1 (Be1) commitment. *PloS one* **2011**, *6* (4), e19366.

98. Sareneva, T.; Matikainen, S.; Kurimoto, M.; Julkunen, I., Influenza A virus-induced IFN-alpha/beta and IL-18 synergistically enhance IFN-gamma gene expression in human T cells. *Journal of immunology (Baltimore, Md. : 1950)* **1998**, *160* (12), 6032-8.
99. Horscroft, N. J.; Pryde, D. C.; Bright, H., Antiviral applications of Toll-like receptor agonists. *The Journal of antimicrobial chemotherapy* **2012**, *67* (4), 789-801.
100. Bergman, S. J.; Ferguson, M. C.; Santanello, C., Interferons as therapeutic agents for infectious diseases. *Infectious disease clinics of North America* **2011**, *25* (4), 819-34.
101. Weigel, B. J.; Cooley, S.; DeFor, T.; Weisdorf, D. J.; Panoskaltis-Mortari, A.; Chen, W.; Blazar, B. R.; Miller, J. S., Prolonged subcutaneous administration of 852A, a novel systemic toll-like receptor 7 agonist, to activate innate immune responses in patients with advanced hematologic malignancies. *American journal of hematology* **2012**, *87* (10), 953-6.
102. Kurimoto, A.; Ogino, T.; Ichii, S.; Isobe, Y.; Tobe, M.; Ogita, H.; Takaku, H.; Sajiki, H.; Hirota, K.; Kawakami, H., Synthesis and evaluation of 2-substituted 8-hydroxyadenines as potent interferon inducers with improved oral bioavailabilities. *Bioorganic & medicinal chemistry* **2004**, *12* (5), 1091-9.
103. Kurimoto, A.; Hashimoto, K.; Nakamura, T.; Norimura, K.; Ogita, H.; Takaku, H.; Bonnert, R.; McNally, T.; Wada, H.; Isobe, Y., Synthesis and biological evaluation of 8-oxoadenine derivatives as toll-like receptor 7 agonists introducing the antedrug concept. *Journal of medicinal chemistry* **2010**, *53* (7), 2964-72.
104. Xiang, A. X.; Webber, S. E.; Kerr, B. M.; Rueden, E. J.; Lennox, J. R.; Haley, G. J.; Wang, T.; Ng, J. S.; Herbert, M. R.; Clark, D. L.; Banh, V. N.; Li, W.; Fletcher, S. P.; Steffy, K. R.; Bartkowski, D. M.; Kirkovsky, L. I.; Bauman, L. A.; Averett, D. R., Discovery of ANA975: an oral prodrug of the TLR-7 agonist isatoribine. *Nucleosides, nucleotides & nucleic acids* **2007**, *26* (6-7), 635-40.
105. Brummer, E.; Antonysamy, M. A.; Bythadka, L.; Gullikson, G. W.; Stevens, D. A., Effect of 3M-003, an imidazoquinoline, on phagocyte candidacidal activity directly and via induction of peripheral blood mononuclear cell cytokines. *FEMS immunology and medical microbiology* **2010**, *59* (1), 81-9.
106. Lindstrom, K. J.; Nikolaidis, N., Imidazo[4,5-c]pyridin-4-amines. *World Patent* **1995**, *WO 95/02597*.
107. Kshirsagar, T. A.; Merril, B. A.; Langer, S. E.; Lindstrom, K. J.; Johannessen, S. C.; Marszalek, G. J.; Wurst, J. R.; Manske, K. J.; Niwas, S.; Lundquist Jr., G. D.; Heppner, P. D.; Griesgraber, G. W.; Danielson, M. E., Method of preferentially inducing the biosynthesis of interferon. *World Patent* **2006**, *WO 2006/091467 A2[1]*.

108. Kshirsagar, T. A.; Lundquist Jr., G. D.; Dellaria Jr., J. F.; Radmer, M. R.; Zimmermann, B. M., Oxime and hydroxylamine substituted imidazo[4,5-c] ring compounds and methods. *World Patent* **2006**, WO 2006/086634.
109. Dellaria, J. F.; Haraldson, G. A.; Heppner, P. D.; Lindstrom, K. J.; Merrill, B. A., Sulfonamido substituted imidazopyridines. **2003**, US 6,525,064 B1, 1-35.
110. Jin, M. S.; Lee, J. O., Structures of TLR-ligand complexes. *Current opinion in immunology* **2008**, 20 (4), 414-9.
111. Yoon, S. I.; Kurnasov, O.; Natarajan, V.; Hong, M.; Gudkov, A. V.; Osterman, A. L.; Wilson, I. A., Structural basis of TLR5-flagellin recognition and signaling. *Science* **2012**, 335 (6070), 859-64.
112. (a) Hemmi, H.; Kaisho, T.; Takeuchi, O.; Sato, S.; Sanjo, H.; Hoshino, K.; Horiuchi, T.; Tomizawa, H.; Takeda, K.; Akira, S., Small anti-viral compounds activate immune cells via the TLR7 MyD88-dependent signaling pathway. *Nat Immunol* **2002**, 3 (2), 196-200; (b) Kaisho, T.; Akira, S., Toll-like receptor function and signaling. *The Journal of allergy and clinical immunology* **2006**, 117 (5), 979-87; quiz 988.
113. Kokatla, H. P.; Yoo, E.; Salunke, D. B.; Sil, D.; Ng, C. F.; Balakrishna, R.; Malladi, S. S.; Fox, L. M.; David, S. A., Toll-like receptor-8 agonistic activities in C2, C4, and C8 modified thiazolo[4,5-c]quinolines. *Organic & biomolecular chemistry* **2013**, 11 (7), 1179-98.
114. Salunke, D. B.; Yoo, E.; Shukla, N. M.; Balakrishna, R.; Malladi, S. S.; Serafin, K. J.; Day, V. W.; Wang, X.; David, S. A., Structure-activity relationships in human Toll-like receptor 8-active 2,3-diamino-furo[2,3-c]pyridines. *Journal of medicinal chemistry* **2012**, 55 (18), 8137-51.
115. Yoo, E.; Crall, B. M.; Balakrishna, R.; Malladi, S. S.; Fox, L. M.; Hermanson, A. R.; David, S. A., Structure-activity relationships in Toll-like receptor 7 agonistic 1H-imidazo[4,5-c]pyridines. *Organic & biomolecular chemistry* **2013**, 11 (38), 6526-45.
116. Kokatla, H. P.; Sil, D.; Malladi, S. S.; Balakrishna, R.; Hermanson, A. R.; Fox, L. M.; Wang, X.; Dixit, A.; David, S. A., Exquisite selectivity for human toll-like receptor 8 in substituted furo[2,3-c]quinolines. *Journal of medicinal chemistry* **2013**, 56 (17), 6871-85.
117. Tanji, H.; Ohto, U.; Shibata, T.; Miyake, K.; Shimizu, T., Structural reorganization of the Toll-like receptor 8 dimer induced by agonistic ligands. *Science* **2013**, 339 (6126), 1426-9.
118. Kokatla, H. P.; Sil, D.; Tanji, H.; Ohto, U.; Malladi, S. S.; Fox, L. M.; Shimizu, T.; David, S. A., Structure-based design of novel human Toll-like receptor 8 agonists. *ChemMedChem* **2014**, 9 (4), 719-23.
119. (a) Sun, H.; Tawa, G.; Wallqvist, A., Classification of scaffold-hopping approaches. *Drug discovery today* **2012**, 17 (7-8), 310-24; (b) Böhm, H.-J.; Flohr, A.; Stahl, M., Scaffold hopping.

- Drug Discovery Today: Technologies* **2004**, 1 (3), 217-224; (c) Lloyd, D. G.; Buenemann, C. L.; Todorov, N. P.; Manallack, D. T.; Dean, P. M., Scaffold hopping in de novo design. Ligand generation in the absence of receptor information. *Journal of medicinal chemistry* **2004**, 47 (3), 493-6.
120. (a) Murray, J. S.; Politzer, P., The Use of the Molecular Electrostatic Potential in Medicinal Chemistry. *Quantum Medicinal Chemistry. Wiley-VCH Verlag GmbH & Co* **2003**, 17, 233-54; (b) Höltje, H.-D.; Höltje, M., Applications of Quantum Chemical Methods in Drug Design. *Quantum Medicinal Chemistry. Wiley-VCH Verlag GmbH & Co* **2003**, 17, 255-74.
121. Lai, J. J.; Salunke, D. B.; Sun, C. M., Multistep microwave-assisted divergent synthesis of indolo-fused pyrazino-/diazepinoquinoxalinones on PEG support. *Organic letters* **2010**, 12 (10), 2174-7.
122. Borchardt, A. J.; Beauregard, D.; Cook, T.; Davis, R. L.; Gamache, D. A.; Yanni, J. M., Heterocyclic inhibitors of histamine receptors for the treatment of disease. *World Patent* **2006**, WO 2010/030785 A2.
123. Liao, S.; von der Weid, P. Y., Lymphatic system: An active pathway for immune protection. *Seminars in cell & developmental biology* **2014**.
124. Swartz, M. A.; Hubbell, J. A.; Reddy, S. T., Lymphatic drainage function and its immunological implications: from dendritic cell homing to vaccine design. *Seminars in immunology* **2008**, 20 (2), 147-56.
125. (a) Waeckerle-Men, Y.; Bruffaerts, N.; Liang, Y.; Jurion, F.; Sander, P.; Kundig, T. M.; Huygen, K.; Johansen, P., Lymph node targeting of BCG vaccines amplifies CD4 and CD8 T-cell responses and protection against Mycobacterium tuberculosis. *Vaccine* **2013**, 31 (7), 1057-64; (b) Pal, I.; Ramsey, J. D., The role of the lymphatic system in vaccine trafficking and immune response. *Advanced drug delivery reviews* **2011**, 63 (10-11), 909-22.
126. (a) Jiang, D.; Liang, J.; Noble, P. W., Hyaluronan as an immune regulator in human diseases. *Physiol Rev* **2011**, 91, 221; (b) Jackson, D. G., Immunological functions of hyaluronan and its receptors in the lymphatics. *Immunol Rev* **2009**, 230 (1), 216-31.
127. Schanté, C. E.; Zuber, G.; Herlin, C.; Vandamme, T. F., Chemical modifications of hyaluronic acid for the synthesis of derivatives for a broad range of biomedical applications. *Carbohydrate Polymers* **2011**, 85 (3), 469-89.
128. Mero, A.; Campisi, M., Hyaluronic acid bioconjugates for the delivery of bioactive molecules. *Polymers* **2014**, 6 (2), 346-69.

129. Misra, S.; Heldin, P.; Hascall, V. C.; Karamanos, N. K.; Skandalis, S. S.; Markwald, R. R.; Ghatak, S., Hyaluronan-CD44 interactions as potential targets for cancer therapy. *The FEBS journal* **2011**, *278* (9), 1429-43.
130. Jackson, D. G., Biology of the lymphatic marker LYVE-1 and applications in research into lymphatic trafficking and lymphangiogenesis. *APMIS* **2004**, *112*, 526-538.
131. (a) Wang, C.; Liu, P.; Zhuang, Y.; Li, P.; Jiang, B.; Pan, H.; Liu, L.; Cai, L.; Ma, Y., Lymphatic-targeted cationic liposomes: a robust vaccine adjuvant for promoting long-term immunological memory. *Vaccine* **2014**, *32* (42), 5475-83; (b) Liu, H.; Moynihan, K. D.; Zheng, Y.; Szeto, G. L.; Li, A. V.; Huang, B.; Van Egeren, D. S.; Park, C.; Irvine, D. J., Structure-based programming of lymph-node targeting in molecular vaccines. *Nature* **2014**, *507* (7493), 519-22.
132. Gupta, R. K., Aluminum compounds as vaccine adjuvants. *Advanced drug delivery reviews* **1998**, *32* (3), 155-172.
133. (a) Bachmann, M. F.; Jennings, G. T., Vaccine delivery: a matter of size, geometry, kinetics and molecular patterns. *Nature reviews. Immunology* **2010**, *10* (11), 787-96; (b) De Temmerman, M. L.; Rejman, J.; Demeester, J.; Irvine, D. J.; Gander, B.; De Smedt, S. C., Particulate vaccines: on the quest for optimal delivery and immune response. *Drug discovery today* **2011**, *16* (13-14), 569-82; (c) Reddy, S. T.; van der Vlies, A. J.; Simeoni, E.; Angeli, V.; Randolph, G. J.; O'Neil, C. P.; Lee, L. K.; Swartz, M. A.; Hubbell, J. A., Exploiting lymphatic transport and complement activation in nanoparticle vaccines. *Nature biotechnology* **2007**, *25* (10), 1159-64.
134. Oh, E. J.; Park, K.; Kim, K. S.; Kim, J.; Yang, J. A.; Kong, J. H.; Lee, M. Y.; Hoffman, A. S.; Hahn, S. K., Target specific and long-acting delivery of protein, peptide, and nucleotide therapeutics using hyaluronic acid derivatives. *Journal of controlled release : official journal of the Controlled Release Society* **2010**, *141* (1), 2-12.
135. (a) Bergman, K.; Elvingson, C.; Hilborn, J.; Svensk, G.; Bowden, T., Hyaluronic acid derivatives prepared in aqueous media by triazine-activated amidation. **2007**, *8* (7), 2190-5; (b) Borke, T.; Winnik, F. M.; Tenhu, H.; Hietala, S., Optimized triazine-mediated amidation for efficient and controlled functionalization of hyaluronic acid. *Carbohydr Polym* **2015**, *116*, 42-50.
136. Bachmann, M. F.; Kalinke, U.; Althage, A.; Freer, G.; Burkhart, C.; Roost, H.; Aguet, M.; Hengartner, H.; Zinkernagel, R. M., The role of antibody concentration and avidity in antiviral protection. *Science* **1997**, *276* (5321), 2024-7.
137. (a) Pullen, G. R.; Fitzgerald, M. G.; Hosking, C. S., Antibody avidity determination by ELISA using thiocyanate elution. *Journal of immunological methods* **1986**, *86* (1), 83-7; (b) Harris, S. L.; Tsao, H.; Ashton, L.; Goldblatt, D.; Fernsten, P., Avidity of the immunoglobulin G

response to a *Neisseria meningitidis* group C polysaccharide conjugate vaccine as measured by inhibition and chaotropic enzyme-linked immunosorbent assays. *Clinical and vaccine immunology : CVI* **2007**, *14* (4), 397-403.

138. (a) Sauder, D. N.; Smith, M. H.; Senta-McMillian, T.; Soria, I.; Meng, T. C., Randomized, single-blind, placebo-controlled study of topical application of the immune response modulator resiquimod in healthy adults. *Antimicrobial agents and chemotherapy* **2003**, *47* (12), 3846-52; (b) Szeimies, R. M.; Bichel, J.; Ortonne, J. P.; Stockfleth, E.; Lee, J.; Meng, T. C., A phase II dose-ranging study of topical resiquimod to treat actinic keratosis. *The British journal of dermatology* **2008**, *159* (1), 205-10.

139. (a) Taylor, D. N.; Treanor, J. J.; Sheldon, E. A.; Johnson, C.; Umlauf, S.; Song, L.; Kavita, U.; Liu, G.; Tussey, L.; Ozer, K.; Hofstaetter, T.; Shaw, A., Development of VAX128, a recombinant hemagglutinin (HA) influenza-flagellin fusion vaccine with improved safety and immune response. *Vaccine* **2012**, *30* (39), 5761-9; (b) Christian, L. M.; Iams, J. D.; Porter, K.; Glaser, R., Inflammatory responses to trivalent influenza virus vaccine among pregnant women. *Vaccine* **2011**, *29* (48), 8982-7.

140. Wu, T. Y.; Singh, M.; Miller, A. T.; De Gregorio, E.; Doro, F.; D'Oro, U.; Skibinski, D. A.; Mbow, M. L.; Bufali, S.; Herman, A. E.; Cortez, A.; Li, Y.; Nayak, B. P.; Tritto, E.; Filippi, C. M.; Otten, G. R.; Brito, L. A.; Monaci, E.; Li, C.; Aprea, S.; Valentini, S.; Calabromicron, S.; Laera, D.; Brunelli, B.; Caproni, E.; Malyala, P.; Panchal, R. G.; Warren, T. K.; Bavari, S.; O'Hagan, D. T.; Cooke, M. P.; Valiante, N. M., Rational design of small molecules as vaccine adjuvants. *Science translational medicine* **2014**, *6* (263), 263ra160.

141. Bishop, N. J.; Morley, R.; Day, J. P.; Lucas, A., Aluminum neurotoxicity in preterm infants receiving intravenous-feeding solutions. *The New England journal of medicine* **1997**, *336* (22), 1557-61.

142. (a) Fanni, D.; Ambu, R.; Gerosa, C.; Nemolato, S.; Iacovidou, N.; Van Eyken, P.; Fanos, V.; Zaffanello, M.; Faa, G., Aluminum exposure and toxicity in neonates: a practical guide to halt aluminum overload in the prenatal and perinatal periods. *World journal of pediatrics : WJP* **2014**, *10* (2), 101-7; (b) Bohrer, D.; Oliveira, S. M.; Garcia, S. C.; Nascimento, P. C.; Carvalho, L. M., Aluminum loading in preterm neonates revisited. *Journal of pediatric gastroenterology and nutrition* **2010**, *51* (2), 237-41.

143. Lammermann, T.; Sixt, M., The microanatomy of T-cell responses. *Immunological reviews* **2008**, *221*, 26-43.

144. (a) Rantakari, P.; Auvinen, K.; Jappinen, N.; Kapraali, M.; Valtonen, J.; Karikoski, M.; Gerke, H.; Iftakhar, E. K. I.; Keuschnigg, J.; Umemoto, E.; Tohya, K.; Miyasaka, M.; Elima, K.;

Jalkanen, S.; Salmi, M., The endothelial protein PLVAP in lymphatics controls the entry of lymphocytes and antigens into lymph nodes. *Nat Immunol* **2015**, *16* (4), 386-96; (b) Hons, M.; Sixt, M., The lymph node filter revealed. *Nat Immunol* **2015**, *16* (4), 338-40.

145. (a) Junt, T.; Moseman, E. A.; Iannacone, M.; Massberg, S.; Lang, P. A.; Boes, M.; Fink, K.; Henrickson, S. E.; Shayakhmetov, D. M.; Di Paolo, N. C.; van Rooijen, N.; Mempel, T. R.; Whelan, S. P.; von Andrian, U. H., Subcapsular sinus macrophages in lymph nodes clear lymph-borne viruses and present them to antiviral B cells. *Nature* **2007**, *450* (7166), 110-4; (b) Phan, T. G.; Grigorova, I.; Okada, T.; Cyster, J. G., Subcapsular encounter and complement-dependent transport of immune complexes by lymph node B cells. *Nat Immunol* **2007**, *8* (9), 992-1000.

146. Cantor, J. O.; Cerreta, J. M.; Armand, G.; Osman, M.; Turino, G. M., The pulmonary matrix, glycosaminoglycans and pulmonary emphysema. *Connective tissue research* **1999**, *40* (2), 97-104.